

2450



EMSC-D152738
17 JAN 1972
SS-1187

CC 115583

VOLUME II
FINAL REPORT
SPACE SHUTTLE
THERMAL PROTECTION SYSTEM
DEVELOPMENT
DESIGN METHODOLOGY

Contract NAS9-12083

National Aeronautics and Space Administration
Manned Spacecraft Center

OFFICE OF PRIME RESPONSIBILITY

Reproduced by
NATIONAL TECHNICAL
INFORMATION SERVICE
US Department of Commerce
Springfield, VA. 22151

LOCKHEED MISSILES & SPACE COMPANY

(NASA-CR-~~115583~~) SPACE SHUTTLE THERMAL PROTECTION SYSTEM DEVELOPMENT. VOLUME 2: DESIGN METHODOLOGY Final Report (Lockheed Missiles and Space Co.) 411 p. N75-70147
Unclas
00/98 49931


VOLUME II - DESIGN METHODOLOGY
FINAL REPORT

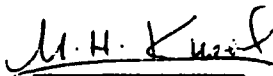
SPACE SHUTTLE
THERMAL PROTECTION SYSTEM
DEVELOPMENT

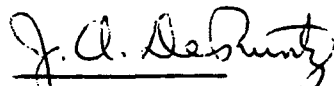
17 January 1972

National Aeronautics and Space Administration
Manned Spacecraft Center
Houston, Texas


Prepared by:


R. P. Banas
Thermodynamics


M. H. Kural
Structures


J. A. DeRuntz
Structural Mechanics,
Task 2 Leader

Approved by


R. D. Buttram
Project Leader

FOREWORD

This is Volume II of the final report prepared by Lockheed Missiles and Space Company, Inc. (LMSC) for NASA Contract NAS 9-12083, Space Shuttle Thermal Protection System Development.

Documented in this volume are the LMSC design efforts performed under this contract for the National Aeronautics and Space Administration Manned Spacecraft Center, under the direction of the Thermal Technology Branch of the Structures and Mechanics Division, D. J. Tillian, COR.

This volume, subtitled Design Methodology, delineates the work performed under Task 2.0. Per agreement with the COR, this separate volume satisfies the Data Requirements List twelfth item: DESIGN METHODS REPORT. A short summary of this work has been included in Section 2.0 of Vol I.

The following individuals have participated in this effort and deserve recognition for accomplishing the program objectives:

R. P. Banas
A. B. Burns
A. J. Chinn
J. A. DeRuntz
M. H. Kural
R. Lambert
J. R. Ritz
B. Van West
J. T. Woneis

PRECEDING PAGE BLANK NOT FILMED

CONTENTS

Section		Page
	FOREWORD	iii
	SUMMARY	vii
1	INTRODUCTION	1. 1-1
	1.1 Criteria Requirements and Environments	1. 1-1
	1.2 Design Methods	1. 2-1
2	RSI METHODS OF ANALYSIS	2. 0-1
	2.1 Thermal Analysis	2. 1-1
	2.2 Structural Considerations for LI-1500 Substrates	2. 2-1
	2.3 RSI Stress Analysis and Modeling	2. 3-1
	2.4 Dynamic Analysis	2. 4-1
	2.5 Comparison of Methods with Experimental Results	2. 5-1
3	PARAMETRIC STUDIES	3. 0-1
	3.1 Thermophysical/Mechanical Property/Variations	3. 1-1
	3.2 Design Details Variations	3. 2-1
	3.3 Environmental Variations	3. 3-1
	3.4 Conclusions - Parametric Studies	3. 4-1
4	OPTIMIZATION STUDIES	4. 0-1
	4.1 Selection of Optimum Subpanel Configuration	4. 1-1
	4.2 Selection of Optimum Primary Structure Configuration	4. 2-1
	4.3 Thermal/Structural Optimization of 1-Atmosphere Test Panels	4. 3-1
	4.4 Thermal/Structural Optimization for Flight Panels	4. 4-1

CONTENTS (CONT'D)

Section		Page
5	ATTACHMENT METHODS	5.0-1
	5.1 Bonding Attachment (Baseline)	5.1-1
	5.2 Mechanical Attachment	5.2-1
	5.3 Partial Tile Support	5.3-1
	5.4 Removal of Bonded LI-1500	5.4-1
6	PROTOTYPE PANEL DESIGN/ANALYSIS	6.0-1
	6.1 Prototype Panel Design Conditions	6.1-1
	6.2 TPS System Design Properties	6.2-1
	6.3 Thermal Analysis	6.3-1
	6.4 Design and Analysis of Prototype Panel Substrates	6.4-1
	6.5 RSI Tile Analysis	6.5-1
	6.6 Dynamic Analyses	6.6-1
	6.7 Critical Failure Modes	6.7-1
	6.8 TPS Cost Study	6.8-1
	6.9 Comparison of LI-1500 Panel Designs vs Metallic Heat Shield Designs	6.9-1
	6.10 Prototype Panels	6.10-1
	Appendixes	6.10-1
A	Design and Analysis of Candidate Primary Structure Configurations	A-1
B	Stress Analysis of Substrate for Prototype Panel No. 1	B-1
C	Stress Analysis of Substrates for Prototype Panel No. 2 through 4	C-1
D	Dynamic Analysis of Prototype Panel Substrates	D-1
E	Venting Characteristics of LI-1500 Tiles with Strain Isolation	E-1

SUMMARY

Design methodology developed by LMSC for the shuttle TPS – including analysis, verification, and design techniques – allows detailed definition of design applications of LI-1500. Although such methodology is applied to LMSC-developed RSI material in the design of four deliverable prototype panels, the design/analysis logic applies to other RSI material systems as well. This study has considered RSI for application to primary structure and subpanels. Optimization methods have been developed which result in minimum weight/cost systems that are refurbishable. Strength/stiffness requirements and failure criteria are identified for LI-1500 RSI system components and metallic substrate materials and configurations. Fastener concepts and tile bonding methods have been studied and textured coating systems evaluated.

Design methods and groundrules were established to carry out parametric studies and evaluate alternate design concepts. The impact of unique LI-1500 thermophysical properties on RSI panel design was ascertained and conclusions as to design validity have been drawn. Finally, cost and weight comparisons with competing TPS concepts have been made. These items are discussed in detail in this volume of the report and are summarized here.

Design/Analysis Methods:

- RSI stress analysis requires fine-mesh, double-precision finite element codes.
- TPS design should utilize sophisticated 2-D and 3-D analysis techniques developed or modified specifically for RSI panels.
- Rational design/analysis should incorporate orthotropic LI-1500 properties.
- Combined stress-failure mode of RSI is recognized as a possibility.
- Experimental results validate analysis techniques.
- Design of substrate should incorporate no skin buckling in lieu of test data.

Optimization Studies:

- Heat sink effect of bond indicates lower TPS system weight than mechanical fasteners.
- Bond weight is not a significant driver on lower surface.
- Bond weight is a major driver on upper surface.
- Primary panel structure should be optimized, using nonlinear beam-column analysis.
- Zee-stiffeners are optimum for panel designs compared with other configurations of similar cost/manufacturing complexity.
- Panel designs should be based on thermal/structural optimization.

Design Details Evaluation:

- Orbital cold-soak condition (-200°F) negates strain isolation properties of RTV-560 leading to unacceptable LI-1500 stress levels.
- Strain arrestor plate can offer strain isolation at -200°F orbital cold-soak condition as well as allowing use of larger tiles.
- Coating stresses are well within allowables, even on sides of tile.
- Discontinuous bond between tiles keeps LI-1500 stress levels down.
- Low-density filler block in baseline joint does not appreciably perturb LI-1500 temperature distribution.
- Based on preliminary studies, lightweight core concept shows no apparent advantage.
- Textured and discontinuous coatings offer no advantage.

Attachment Studies:

- Beryllium subpanel concept with direct-bonded LI-1500 leads to largest (12 in. x 12 in.) tile size.
- Mechanical fasteners show promise.
- LMSC has feasible refurbishment scheme for bonded tiles.

LI-1500 Advantages:

- Reduced conductivity of LI-1500 under reentry pressure environment results in lighter TPS system than competitive materials.
- Low LI-1500 coefficient of expansion limits thermal stresses and reduces required external gaps.
- Degradation effects on resulting RSI stress levels due to repeated thermal cycling of LI-1500 offer no problem.

Cost/Weight Comparisons:

- LI-1500 TPS system is indicated to be lighter and less costly than comparable metallic heatshield.
- LI-1500 TPS system is indicated to be less costly than ablative heat shield.

Section 1 INTRODUCTION

The development of rigidized surface insulation for space shuttle application includes the establishment of rationale, methods of analyses, techniques, and design details. This key contract task defines the criteria/methodology required for shuttle usage of LI-1500 RSI. The effort is divided into two subtasks.

- The first defines the criteria, requirements, and environments applicable to the shuttle TPS. The specific point design requirements for the prototype panels are given in Section 6 of this volume.
- The second concerns design applications and methodology establishment which culminates in the design of the deliverable panels.

1.1 CRITERIA REQUIREMENTS AND ENVIRONMENTS

Space shuttle requirements applicable to the design of the Thermal Protection Systems (TPS) have been delineated in a separate document,⁽¹⁻¹⁾ together with design criteria and primary design conditions to be utilized in the development of the TPS. Applicable loads and thermal environments are provided for both the orbiter and booster, based on the vehicle design data available at the time of the study. Requirements and criteria for accomplishing "proof of design" also are included. These data are briefly summarized in the following subsections.

The results of the study summarized herein are considered to represent a basis for initiating TPS detail design/analysis efforts in a Phase C Space Shuttle development program. In the course of the present TPS technology development program, and other concurrent space shuttle studies, some changes to requirements and design criteria will naturally evolve. These are not expected to be extensive in scope and, in most cases, of only minor consequence to the designs.

(1-1) LMSC-A991379/SS-1108, "Design Criteria for Space Shuttle Thermal Protection System Development," dated 1 Sep 1971

In other areas, considerable changes can be expected due to improved knowledge of the environments to be encountered and the time-dependent thermal effects within the TPS. Changed space shuttle configuration and detail analyses of the TPS subsystems and of the detail design areas within each subsystem will also introduce their iterations. Finally, improved knowledgeability of material-characteristics effects and related implications on the design criteria will affect final TPS configurations.

A major element of TPS design criteria, which is dependent upon specific Space Shuttle System concepts and baseline mission presumptions, is the definition of the optimization criteria between TPS weight and cost. To this end, relative cost and weight analyses of competing concepts are provided in Section 6.8.

The criteria and loads specified by NASA/MSFC for prototype panel design are included in Section 6.1.

Objectives and Scope.

Thermal protection systems for the space shuttle must protect the primary vehicle substructure and other vehicle subsystems during various phases of mission environments. The TPS on the orbiter, and (where required) on the booster, must perform this function with a high level of reliability. Extensive failure of the TPS systems is likely to lead to loss of, or major damage to, the vehicle system. In that sense, TPS is somewhat like a pressure vessel wherein structural integrity of all its elements is essential to achieve normal or safe operation. It has one major handicap compared to a pressure vessel, in that pressure vessels can readily be proof-tested, even on a flight article, whereas the total TPS cannot. On the orbiter, it must be capable of successfully performing its function in 100 operational missions.

The high level of reliability must be achieved while minimizing weight and cost. On the orbiter, a typical total weight of the TPS can lie between 20,000 and 30,000 pounds, with weight uncertainties on the order of 5,000 pounds. For the O4OA orbiter with a 270 nm mission, this uncertainty represents approximately 25 percent of the total payload. Thus, the system is quite weight-critical as well as being reliability sensitive.

A primary objective of the space shuttle program is - "development of an economical general purpose transportation system." Development and operation of the TPS of the orbiter vehicle system is roughly estimated to represent 5 to 10 percent of total orbiter program costs. Thus, the TPS has major influence on total-program economy, and at the same time technologically represents one of the most critical subsystems in the Space Shuttle System. Minimizing cost, therefore, is a primary consideration during the TPS design selection process. Since a major portion of TPS program costs is expected to be encountered in the maintenance and refurbishment operational activities, the TPS life-cycle costs must be utilized as the cost basis for trade-study comparisons.

Requirements and criteria that influence design/development of the TPS are defined in a variety of NASA and contractor documents. The criteria elements (summarized and identified by the sources by reference to the applicable documents in Ref 1-1) are as follows:

- Space shuttle program requirements and criteria applicable to TPS
- Space shuttle structural design criteria applicable to TPS
- Design/development optimization criteria applicable to TPS
- Spacecraft criteria and standards applicable to TPS
- Loads and thermal environment data applicable to orbiter and booster TPS.

The "applicable documents" are: (1) primary applicable space shuttle directives or documents, (2) related space shuttle design criteria studies, and (3) space vehicle or other potentially applicable design documents. The documents listed in these three groupings are identified in the text of Ref 1-1, where applicable. The same requirement/criterion items often appear in two or more cited references.

Design Requirements.

Space Shuttle System requirements applicable to the TPS have been extracted primarily from the Space Shuttle draft "Statement of Work" and its technical requirement Appendices. These are described in Ref 1-1, in the fullest detail available as determined from the applicable studies and documents resulting therefrom, under the following groupings: (1) System Requirements, (2) General Technical Requirements, (3) Thermal Protection and Control, (4) Natural Environment Design Requirements, and (5) Manned Spacecraft Criteria and Standards.

Requirements that are especially pertinent to this development program are listed below.

- The combined storage and operational service life of the Space Shuttle System shall be a minimum of 10 years after the first manned orbital flight. Each Space Shuttle System flight article shall be capable, with a cost-effective level of refurbishment and maintenance, of a minimum operational lifetime of 100 missions.
- The Space Shuttle System flight hardware turn-around time from landing at the launch facility to launch readiness shall be less than 14 calendar days.
- The orbiter vehicle and booster vehicle shall be insensitive to weather conditions during pad preparations and standby periods.
- All TPS materials/systems will sustain 100 design missions. TPS design for all missions shall assure crew safety for worst case abort entry.
- The TPS shall be designed to the same criteria as the primary structure of the airframe.
- External thermal coatings shall have a reuse capability of 100 flights without significant deterioration or degradation. Coating systems requiring refurbishment shall be consistent with other repair/replacement/maintenance requirements.
- The space shuttle shall be designed for 0.95 probability of no puncture during the maximum total time-in-orbit, using the meteoroid model defined in par. 2.5.1 of TM-X-53957.

1.1-4

4<

Structural Design Criteria.

The basic structural design criteria applicable to the space shuttle TPS are specified in the draft Space Shuttle Statement-of-Work, Appendix B, and explained (at least in part) in NASA SP 8057. These criteria have been extracted and set forth in the fullest detail available in Ref 1-1 under the following groupings: (1) Strength Requirements, (2) Strength Allowables, (3) Design Load Criteria, (4) Rigidity Criteria, and (5) Optimization Criteria. Structural criteria which are especially pertinent to this development program are listed below.

- Combined Stresses. The structural design shall exclude the use of pressure-stabilized structures, with the exception of main propulsion tanks when exposed to ascent flight loads. When the stresses due to internal pressure and thermal conditions are additive to the external flight loads, the ultimate external load will be combined with the maximum regulated internal pressure and the thermally induced load, times a factor of 1.5. When the stresses due to internal pressure and thermal conditions are relieving (subtractive) the external flight loads, the minimum thermally induced load and the minimum regulated pressure (or zero pressure, if the operational capability of the vehicle is not affected by the loss of pressure) will be combined with the ultimate external load. No load conditions outside the crew safety envelope shall be considered. In no case shall the ratios of allowable stress to combined limit stress be less than 1.35.
- The design loads used for final vehicle design shall be based on a Monte Carlo analysis in which the vehicle is flown analytically through a sufficient number of profiles to statistically define the 99 percentile loads.
- Aeroelasticity. Static and dynamic structural deformations and responses under all conditions and environments shall not cause (1) a structural failure or system malfunction, (2) impair the stability and control characteristics of the vehicle, or (3) cause unintentional contact between adjacent bodies.
- Dynamic Aeroelasticity. The orbiter vehicle shall be free from classical flutter, stall flutter, and control-surface buzz at dynamic pressures up to 1.32 times the maximum dynamic pressure expected during flight. External

panels shall be free of panel flutter at 1.5 times the local dynamic pressure at the appropriate temperature and Mach number for all flight regimes including aborts.

- **Basic Optimization Criteria.** Three primary value elements are involved in design-optimization and development-program-optimization of the TPS: (1) structural integrity reliability, (2) system weight, and (3) life-cycle costs. All three of these have major influence on the Space Shuttle System total cost-effectiveness. Trade studies invariably must involve two of the three elements, and very often all three.
- A level of structural integrity reliability comparable to that achieved in a commercial air transport is essential. Therefore, this element is presumed constant, and at a level, which to all intents and purposes, is equal to 1.0. Design-configuration and program optimizations, therefore, are not concerned about the numerical value of reliability, but rather the cost in dollars and weight to achieve it. Safe-life designs may be traded off against fail-safe designs to determine which produces the required level of structural integrity assurance at the best combination of weight and cost.
- To achieve a balanced design, the dollars expended to reduce weight enough for increasing payload by one pound should be the same for all elements of the Space Shuttle Vehicle Systems, provided that the technological (and cost) uncertainties are essentially equivalent. If payload can be increased by weight reductions in primary airframe (by use of exotic materials) at the same cost as for a comparable change in the TPS, but with less uncertainty, then the trade is in favor of the change in the airframe. Also, quite obviously, if it requires 6 pounds of weight removed from the booster to increase payload by 1 pound, and it requires only 1 pound off of the orbiter to do the same thing, then six times as much money can be spent for weight reduction on the orbiter than on the booster.

Environmental Data.

Environmental data are presented in the following categories: ascent trajectory, entry trajectory, peak temperature isotherms, differential pressures, and vibration/acoustics.

Attachment of RSI directly to primary structure may be the final TPS design. In this application, the strains and deflections of the structure will dictate the TPS attachment design. Strains and deflections are dependent on vehicle loadings and configurations as well as structural geometry. Primary vehicle loadings are not included due to this dependence. Design for this application will be based on representative strains and deflections derived from specific configurations and loading conditions, which do not differ appreciably for the various vehicles and environments currently proposed.

Design environments for the prototype panels are not included in this section. These conditions are presented in Section 6.1.

Ascent trajectories for the mated system booster and orbiter are shown in Ref 1-1 for the LMSC, MDAC, and NAR configurations, respectively. All trajectories result in orbiter injection to a 50 x 100 nm orbit with an inclination-angle of 28.5 deg. The final design reference orbit was a circular orbit at 270 nm with an inclination-angle of 55 deg.

Orbiter entry trajectories from a 270-nm orbit (LMSC) and a 100-nm polar orbit (MDAC and NAR) are shown in Ref 1-1. The LMSC orbiter shown is a delta-body configuration, while both the NAR and MDAC orbiters are of the delta-wing category. All trajectories generate about 1,100 nm of aerodynamic crossrange, but the LMSC trajectory takes 1,350 sec to reach 100,000 ft while the MDAC and NAR trajectories take about 2,100 sec. The impact of longer reentry time is to increase the insulation requirements of the TPS. All trajectories were generated under what essentially appears to be the same philosophy. A choice of TPS material is made and heating boundaries are generated for the orbiter lower centerline based on the temperature capability of the chosen TPS material(s). An entry trajectory is generated using the appropriate aerodynamic characteristics for each orbiter. The trajectory is maintained above the heating boundary by use of bank angle and angle-of-attack modulation while attaining 1,100 nm of aerodynamic crossrange. Orbiter peak-temperature isotherms corresponding to the entry trajectories are depicted for the LMSC, MDAC, NAR and GAC orbiters in Ref 1-1.

The orbiter shell differential pressures have been obtained for three critical flight phases for the delta-body orbiter maximum αq on ascent, during a 2.5 g subsonic maneuver. These pressures are shown in Ref 1-1. To account for venting uncertainties, ± 0.25 psi has been added to the differential pressures shown in this document.

The orbiter and booster thermal protection system will be subjected to various acoustic and aerodynamic buffeting as well as mechanically induced random-vibration responses during the mission profile. During liftoff, intense acoustic pressures are generated by the booster engine exhaust turbulence. During transonic and maximum dynamic pressure portion of flight, high unsteady aerodynamic pressures are experienced due to turbulent boundary layer noise, separated flow, oscillating shock waves, and interaction of shock waves and boundary layer. During reentry, both hypersonic and low-speed aerodynamic noise is present. Acoustic environments encountered by flight test vehicles during takeoff, landing, cruise, and maneuvers must also be considered. The acoustic environments presented in Ref 1-1 are for launch, maximum dynamic pressure, and reentry phases of the mission.

Typical booster entry trajectories, peak temperatures, and design loads are shown in a series of six figures in Ref 1-1.

Proof of Design.

A properly balanced development program will include some combination of the following engineering activities: analysis, design, development testing, qualification testing, acceptance testing, operational (flight and ground) testing, and/or special testing. The scope of work undertaken in each of these activities influences to some extent the level-of-effort warranted in the other activities, to achieve adequate proof of design. Therefore, definition of the basic requirements for proof of design is an integral part of design criteria. The responsibility for planning proof of design overall rests with the vehicle contractor. Proof of structural adequacy of the TPS under all anticipated loads and environmental conditions shall be provided by appropriate analyses and tests.

Reports shall be prepared on analyses and tests conducted to verify the structural adequacy of the design. Assumptions, methods, and data used shall be defined. An integrated plan, early in the Phase C Space Shuttle Program, shall describe the total plan for verifying structural adequacy and shall include schedules for accomplishment. The plan shall be revised as necessary to reflect changes in schedules, requirements, objectives, design characteristics, and operational usage.

Reports shall be prepared to provide the following information concerning the TPS: operating restrictions (limitations on preparation testing and operational use), inspection and repair, and operational-usage measurements (systems for evaluating structural adequacy during operational usage).

Analyses in the areas listed below shall be performed to verify structural adequacy in compliance with the design criteria defined in previous sections. Where adequate theoretical analysis does not exist or where experimental correlation with theory is inadequate, the analysis shall be supplemented by tests.

- Design criteria (i. e., Ref 1-1 and its subsequent revisions)
- Design loads
- Thermal analysis
- Stress analysis

The stress analyses shall verify structural adequacy in terms of the optimization criteria defined in a previous subsection, Structural Design Criteria. Tests shall be conducted to assist in defining or verifying static and dynamic design loads, pressures, and environments that the TPS will encounter through its service life.

When structural material characteristics, including physical and allowable mechanical properties and failure mechanisms, are not available in NASA-approved references, tests shall be performed to characterize the materials in accordance with the specified design criteria.

Development tests, represented in part by the present program, shall be performed as necessary to:

- Evaluate design concepts
- Verify analytical techniques
- Evaluate structural modifications for achieving desirable structural characteristics
- Obtain data for reliability predictions
- Determine failure modes or causes of failure.

Qualification tests shall be conducted on flight-quality hardware to demonstrate structural adequacy under more stringent loads than the worst expected loads. In defining the number and types of qualification tests, the highest practical level of assembly shall be used. Test conditions shall be selected to demonstrate clearly that all elements of the structure satisfy design criteria. Tests shall be performed on representative sections of each of the TPS subsystems, to verify the following:

- Detrimental deflections do not occur under deformation-critical combined limit-load/limit pressure and thermal conditions
- Rupture or collapse does not occur under critical combined ultimate-load/ultimate-pressure and thermal conditions
- Neither detrimental deflections nor rupture occur under limit-load/thermal exposure to specified life-cycle criteria.

The foregoing tests shall demonstrate, as closely as is practicable, the structural integrity for the primary design conditions, including demonstrations of cumulative damage tolerance where applicable.

Acceptance tests shall be conducted on flight hardware to verify that the materials, manufacturing processes, and workmanship meet design specifications.

Flight tests conducted for purposes of structural integrity evaluation shall include verification of limit-load/thermal conditions used in the design of the TPS and in the

test conditions used in the TPS qualification tests. These tests shall specifically include tests, with appropriate instrumentation, to collect data permitting evaluation of at least critical heating and of refurbishment techniques. Prior to or in conjunction with these tests, techniques for inspection of the TPS subsystems shall be developed to locate hidden defects, deteriorations, and fatigue effects.

1.2 DESIGN METHODS

The objective of this task is to develop a logical design path through the TPS system variables and, thereby, arrive at an optimum thermal/structural design. The methods of analysis have been identified and relationships between the RSI/booster/orbiter parameters established. Detail guidelines are presented to substantiate the design of the prototype panels fabricated and delivered under this contract. The effect of atmospheric testing on RSI systems is important, i. e., LI-1500 heat conductivity is strongly dependent upon environmental pressure. The so-called "test" (1 ATM) and "flight" (reduced pressure) prototypes are defined; these differ in required LI-1500 thickness. Both sets of point designs have been analyzed in the midterm report.⁽¹⁻²⁾ Per NASA/ MSC direction, the deliverable panels are being fabricated using LI-1500 thickness sized to be tested at reentry pressure levels, hence only the flight panels have been reassessed in this report.

In establishing the design methods, effort has been concentrated on:

- Metallic substrate design
- Thermal sizing of RSI
- RSI tile stress analysis
- RSI attachment methods

Based on these studies, prototype panels designed to NASA specified conditions are compared with metallic heat shield designs. Flutter and acoustic analyses are also presented for the prototype panels.

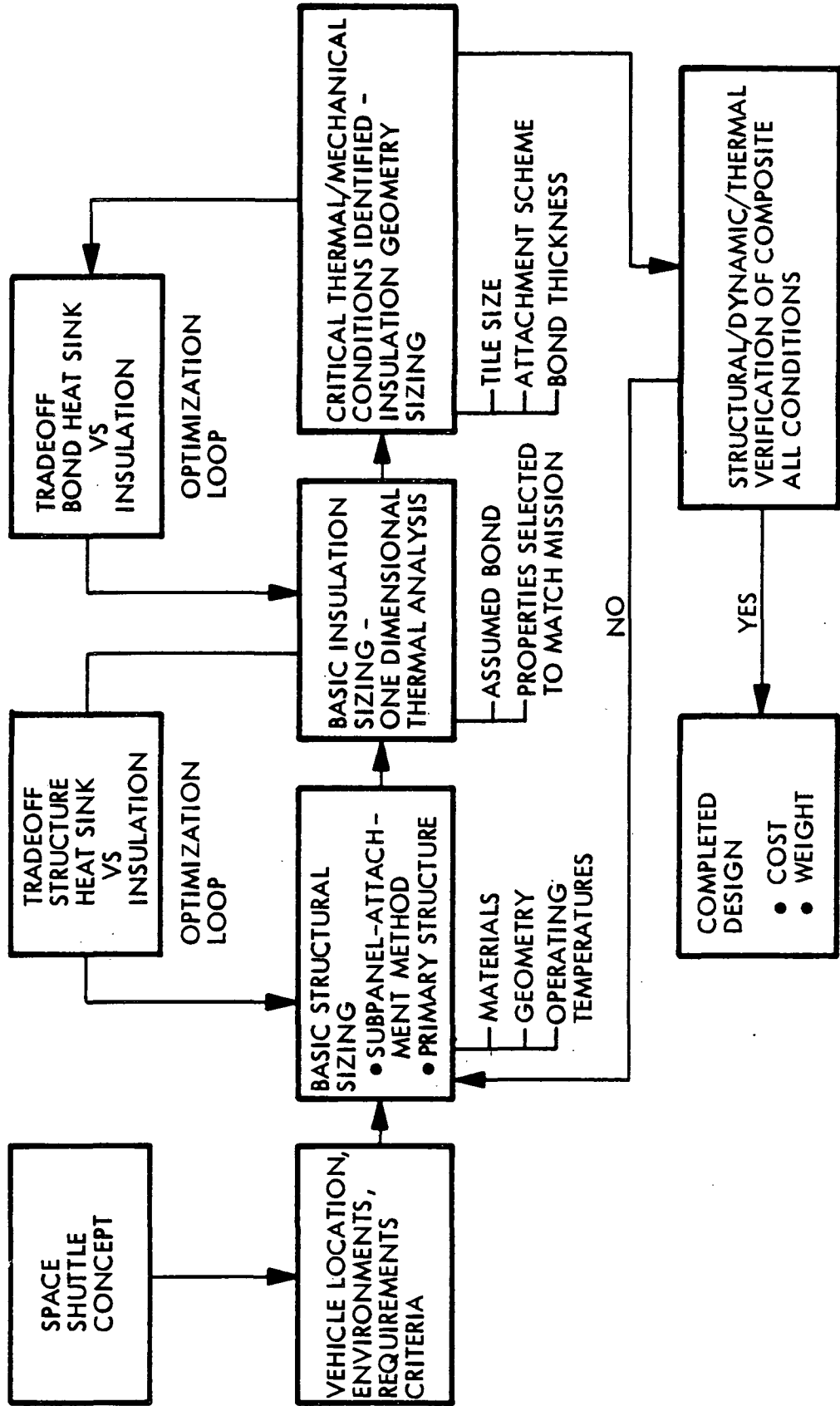
The design sequence is best illustrated in Fig. 1.2-1. First, the basic structural sizing is done in conjunction with a thermal analysis that establishes required RSI thickness. This optimization loop considers the tradeoff between heat sink effect of structure versus insulation thickness. Next, the RSI system stress levels are determined through a second optimization loop in which bond thickness is varied to ensure acceptable RSI stress levels under the environmental design conditions. Finally, a complete verification of the design is made.

(1-2) LMSC-A997045, "Midterm Summary Report, Space Shuttle Thermal Protection System Development," NAS 9-12083, 12 Nov 1971

Since the methodology employed is highly computer-oriented, the results cannot be summarized at this time in a set of "design curves" which would permit the selection of all important TPS system parameters using this report alone. Rather, the work presented here identifies the behavior of the TPS system under design load and heating conditions and defines what constitutes critical conditions. This report outlines the approach and required analytical tools which together can be employed to arrive at rational near-optimum designs for the flight and operational conditions.



LOGIC SEQUENCE - PROTOTYPE PANEL DESIGN



1.2-3

14A

Fig. 1.2-1

Section 2
RSI METHODS OF ANALYSIS

This section presents descriptions of the analytical techniques for the following:

- Thermal Analysis: Defining temperature distributions as a function of time, vehicle location, and flight environment
- Substrate Analysis: Subpanels and primary structure
- Two-Dimensional and Three-Dimensional Analysis: Coating, RSI, bond, and substrate composite
- Dynamic Analysis: Sonic fatigue and flutter stability
- Comparison of Methods with Experimental Results

In this report, reference is frequently made to the prototype panels designed and fabricated under this contract. As mentioned previously, the so-called "flight" and "test" panels differ only in LI-1500 thickness, due to its reduced thermal conductivity at low pressure. Thus, LI-1500 thickness for a flight panel is determined by using actual reentry pressure levels, while that for a test panel is sized for 1 ATM. Panel designs numbered 1, 2, and 4 represent three alternatives for one vehicle location, while panel no. 3 applies to a different area of the orbiter. The loading and environmental conditions for these designs are discussed in detail in Section 6. It should be noted that LI-1500 and bond thicknesses for a specific panel designation in some of the following discussions may not agree with final designs as presented in Section 6, since these seemingly inconsistent values represent parametric studies and/or preliminary designs.

2.1 THERMAL ANALYSIS

Lockheed's THERM computer code was used to define temperature distributions in the RSI panel. This code utilizes finite difference techniques to solve the transient conduction equation for a one-, two-, or three-dimensional problem and has an automatic plotting routine available to the user. The code handles other modes of heat transfer such as convection and radiation.

The heat balance at each node, as programmed in the computer code, is given by:

$$\Delta V \rho C_P \frac{\partial T_i}{\partial \theta} = \dot{q}_{in} - \dot{q}_{out} = \sum_{j=1}^n \left(\frac{T_i - T_j}{R_{i-j}} \right)$$

where:

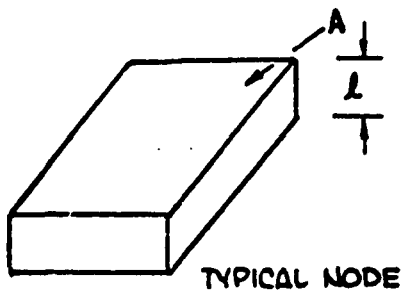
ΔV	=	node volume
ρ	=	density
C_P	=	specific heat
T	=	temperature
θ	=	time
q	=	heat rate
R_{i-j}	=	thermal resistance between nodes i and j
i, j	=	node numbers

\dot{q}_{in} is the heat conducted to the node from adjacent higher temperature nodes and \dot{q}_{out} is the heat lost by conduction to adjacent lower temperature nodes. The temperature of the surface node is driven to follow the temperature history of the desired orbiter location.

The expressions for determining resistor and capacitor values are shown in Table 2.1-1. These equations are evaluated during each computer iteration, thereby changing resistor and capacitor values as the node temperatures change to allow for temperature/pressure dependent material properties. The resulting values are then used to calculate the temperature response of the network for the next iteration.

Table 2.1-1
THERMAL RESISTOR AND CAPACITOR METHODOLOGY

TYPE	VALUE	COMMENTS
RESISTOR DESCRIPTION		
Conduction	$R = \ell/kA$	$k = f(\text{Temp, Pressure})$
Radiation	$R = \frac{1}{\sigma(\text{RADK})(T_i^2 + T_j^2)(T_i + T_j)}$ <p>Where:</p> $\text{RADK} = \epsilon_{ij} A_i F_i$ <p>and:</p> $\epsilon_{ij} = \frac{1}{\frac{1}{\epsilon_i} + \frac{1}{\epsilon_j} - 1}$	<p>T in °R</p> <p>Parallel Plate View Factor</p>
Air Convection	$R = \frac{1}{hA}$	$h = \frac{0.14k_{\text{air}}}{\ell} (G_R P_R)^{1/3}$
CAPACITOR DESCRIPTION		
All	$C = \rho \ell A C_P$	$C_P = f(\text{Temp})$



ℓ = Depth or length of conduction path

A = Area of node perpendicular to conduction path

σ = 0.478×10^{-12} Btu/ft²-sec °R⁴

ϵ = emittance

G_R = Grashof number

P_R = Prandtl number

The following groundrules and assumptions were used in conjunction with the THERM code for the basic insulation sizing of the prototype panel:

- One-dimensional analysis
- Radiation equilibrium temperature used as a surface-temperature boundary condition
- Adiabatic substrate
- No ground cart cooling of substrate in either primary structure application or subpanel application
- Thermal model including a node for adhesive

Thermal models considered for the sizing were divided into seven nodes as shown in Fig. 2.1-1. The effect of lumping both the adhesive and substrate as one node was investigated. It was found that for adhesive thickness (with RTV-560 conductivity of $0.18 \text{ Btu/ft-hr-}^{\circ}\text{F}$) up to 0.20 in., the maximum transient difference between the LI-1500 adhesive interface temperature and the adhesive substrate interface temperature is about 20°F . Since it was desirable to compare transient temperature differences between interfaces, the thermal model with the adhesive and substrate modelled individually was used. For adhesives with lower thermal conductivity or thicknesses greater than 0.20 in., the adhesive node should be included in the thermal model.

Effect of LI-1500 Sizing With Two-Dimensional Thermal Models

To check the adequacy of the one-dimensional LI-1500 sizing and to obtain transient temperature differences for various elements of the TPS, two-dimensional thermal models were generated. LI-1500 sizing was performed with the THERM computer code.

The thermal model used for test panels Nos. 2 and 4 is shown in Fig. 2.1-2. Dimensions shown are for the titanium panel. The thermal model for the beryllium test panel is shown in Fig. 2.1-3. The LI-1500 thickness can be easily changed for

THERMAL MODEL CONSIDERED FOR LI-1500 SIZING

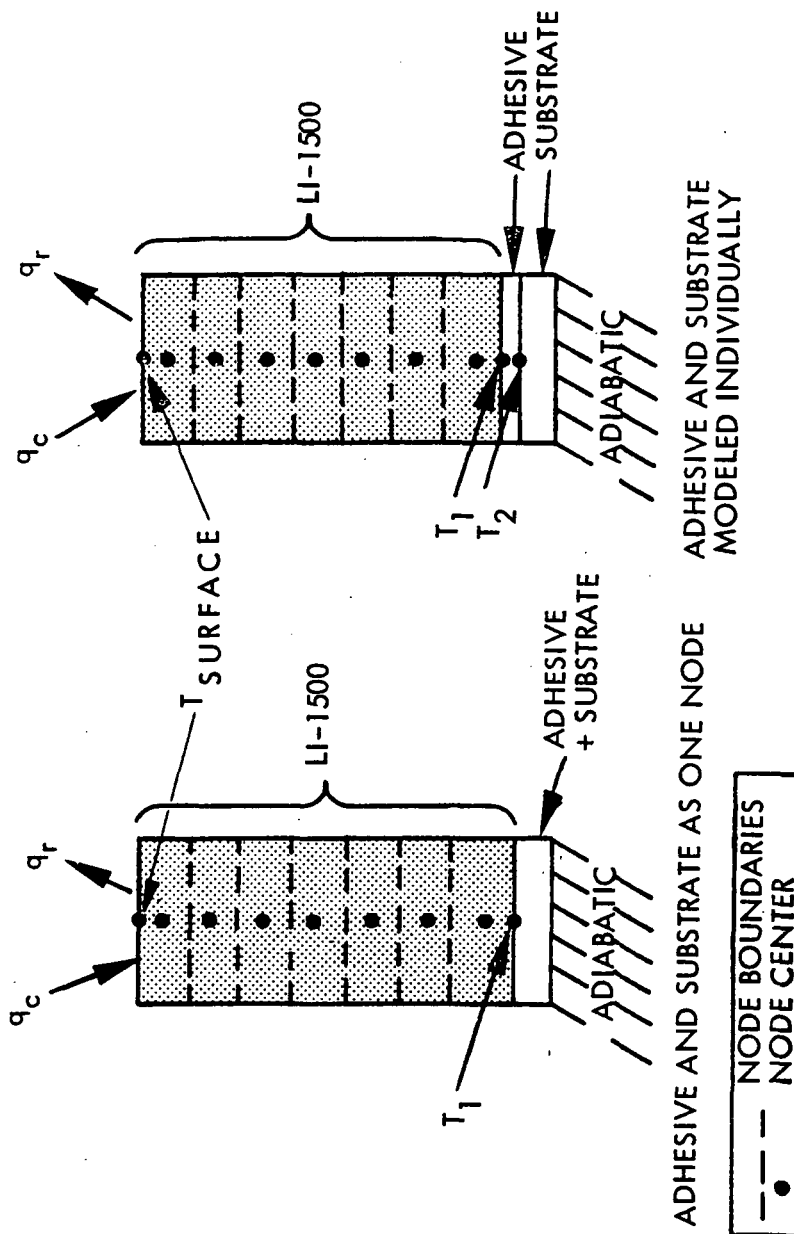
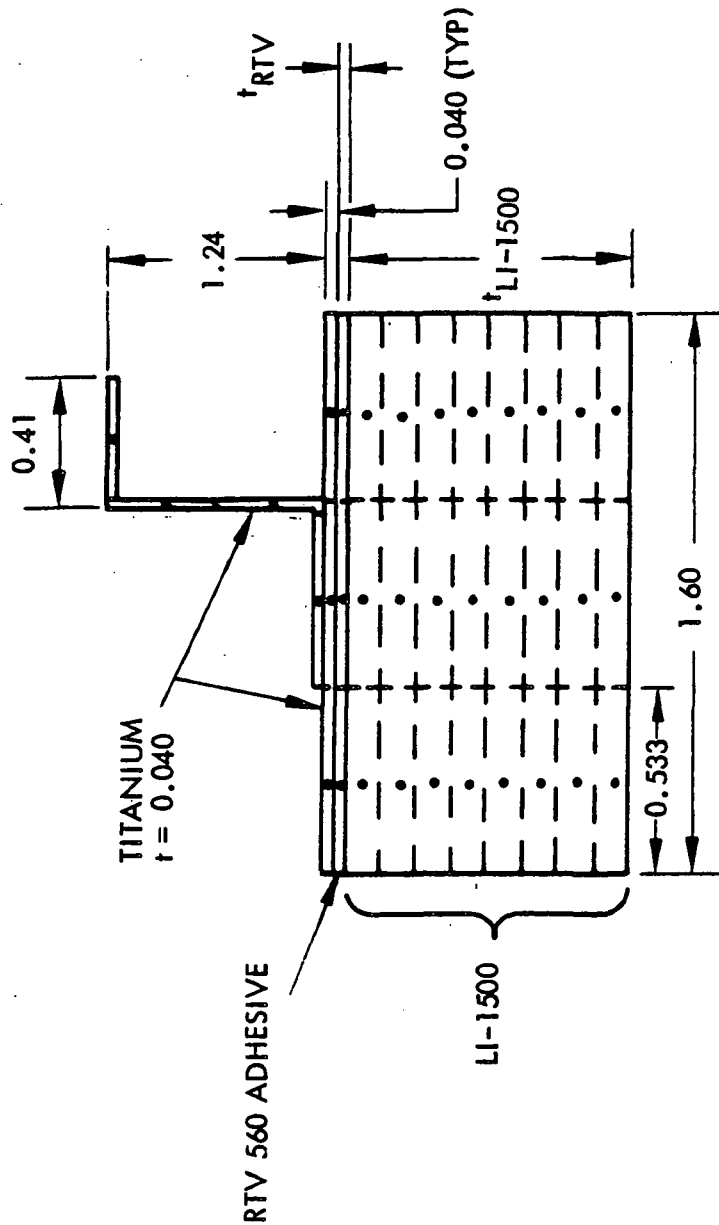


Fig. 2.1-1



TWO-DIMENSIONAL THERMAL MODEL FOR TITANIUM AND ALUMINUM PANEL



LMSC-D152738
Vol II

DIMENSIONS SHOWN ARE FOR
PANEL 4 TITANIUM

BOND AND LI-1500 THICKNESS DETERMINED
BY OPTIMIZATION STUDY

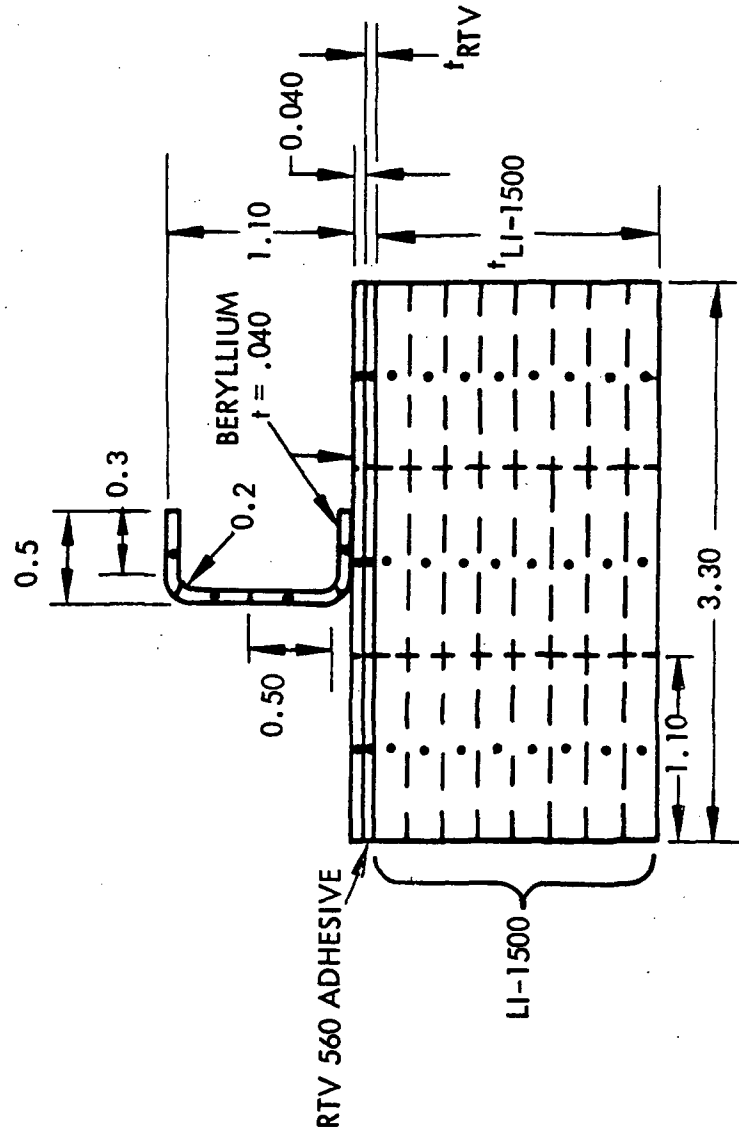
DO6096 (1)

Fig. 2.1-2

TWO-DIMENSIONAL THERMAL MODEL FOR BERYLLIUM PANEL



• NODE CENTERS
- - - NODE BOUNDARIES



BOND AND LI-1500 THICKNESS DETERMINED BY OPTIMIZATION STUDY

Fig. 2.1-3

DO6095 (1)

consecutive computer runs. As in the one-dimensional sizing discussed previously, an adiabatic boundary condition was used. An isotropic thermal conductivity for 1 ATM air was used for this model. The thermal conductivity and specific heat values for LI-1500 are given in Section 6.2.

A comparison of the LI-1500 thermal sizing between a one- and two-dimensional thermal model for the titanium test panel with a 0.030 bond is shown in Fig. 2.1-4 (as discussed later, the final design thickness is 0.090 in.). The results are shown with a plot of maximum titanium face-sheet temperature versus LI-1500 thickness. The results indicate that the one-dimensional model is conservative, but there is a negligible difference in LI-1500 thickness (0.10 in.) at the titanium design temperature of 600^oF. Larger adhesive thickness than that shown will not change the results, since the LI-1500 thickness will be reduced in accordance with a tradeoff factor which will be discussed in Section 4. Temperature histories for the titanium face sheet and stiffener are shown in Fig. 2.1-5. Large transient temperature differences are indicated (50-75^oF), but these eventually decrease as the TPS approaches its maximum values. These transient temperatures are used to determine temperature-induced bending loads in the panels.

A comparison of results between the one- and two-dimensional thermal models for the aluminum test Panel 2 is shown in Fig. 2.1-6. The maximum backface temperatures are nearly identical, which ascertains the adequacy of the one-dimensional thermal model for the TPS sizing studies on the aluminum panel.

The effect of the thermal model on the maximum substrate temperature for the beryllium test panel is shown in Fig. 2.1-7. These results indicate the one-dimensional thermal model is adequate for insulation sizing.

Also, the results show the effect of backface boundary conditions on the maximum panel temperature. If the panel is sized with an adiabatic boundary condition for a 600^oF temperature and tested with a nonadiabatic boundary condition, the maximum temperature will be about 490^oF. The same result is shown in Fig. 6.3-14 for the one-dimensional model. The same comparison between the one- and two-dimensional thermal models would exist for the flight panels with either adiabatic or nonadiabatic assumed boundary conditions.

EFFECTS OF THERMAL MODEL ON
TPS SIZING RESULTS

TEST PANEL NO. 4

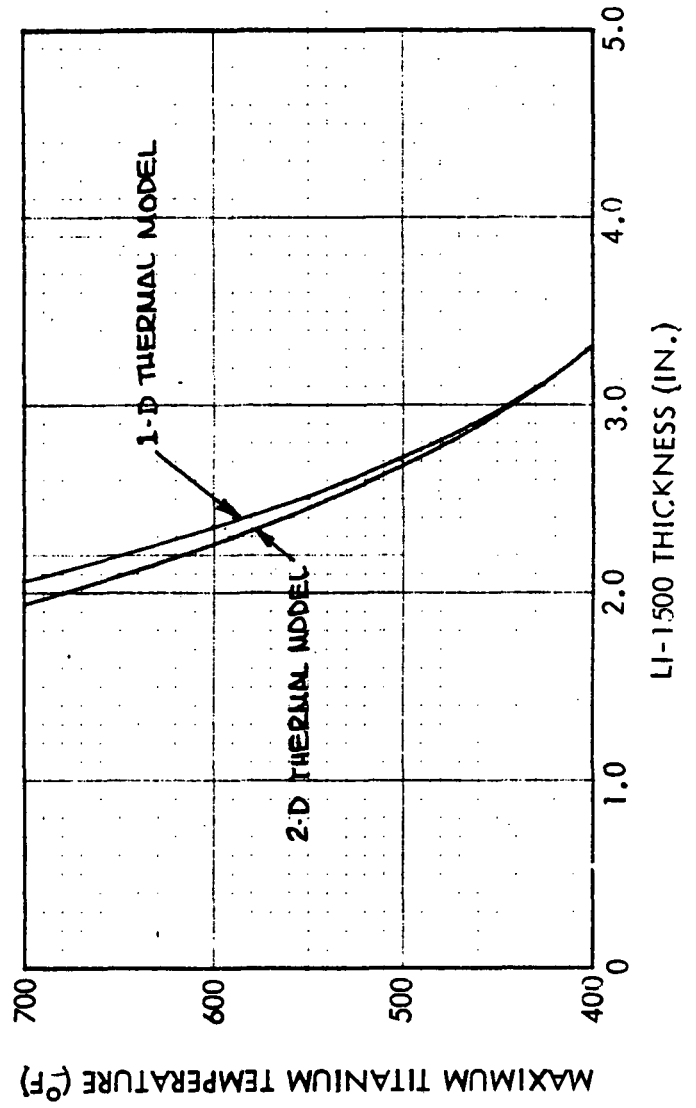
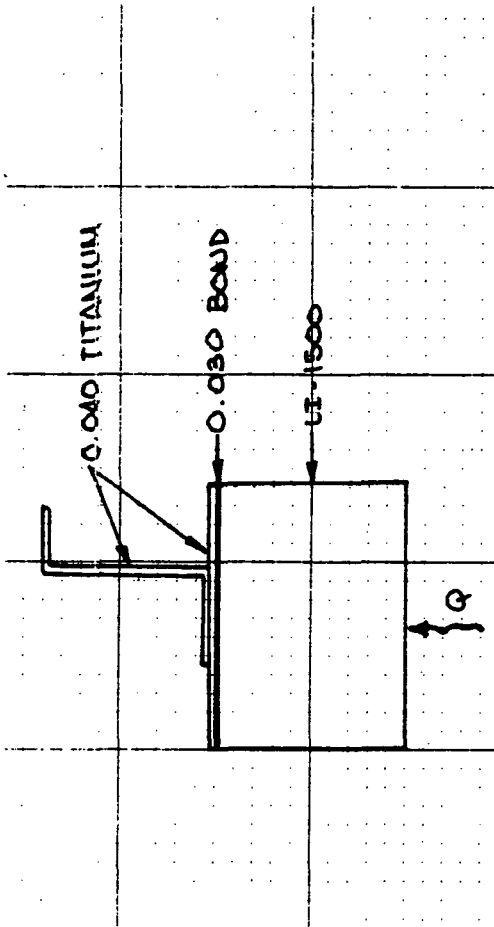


Fig. 2.1-4

DO6092



TEMPERATURE HISTORIES FOR A TITANIUM
TEST PANEL



TWO-DIMENSIONAL THERMAL MODEL

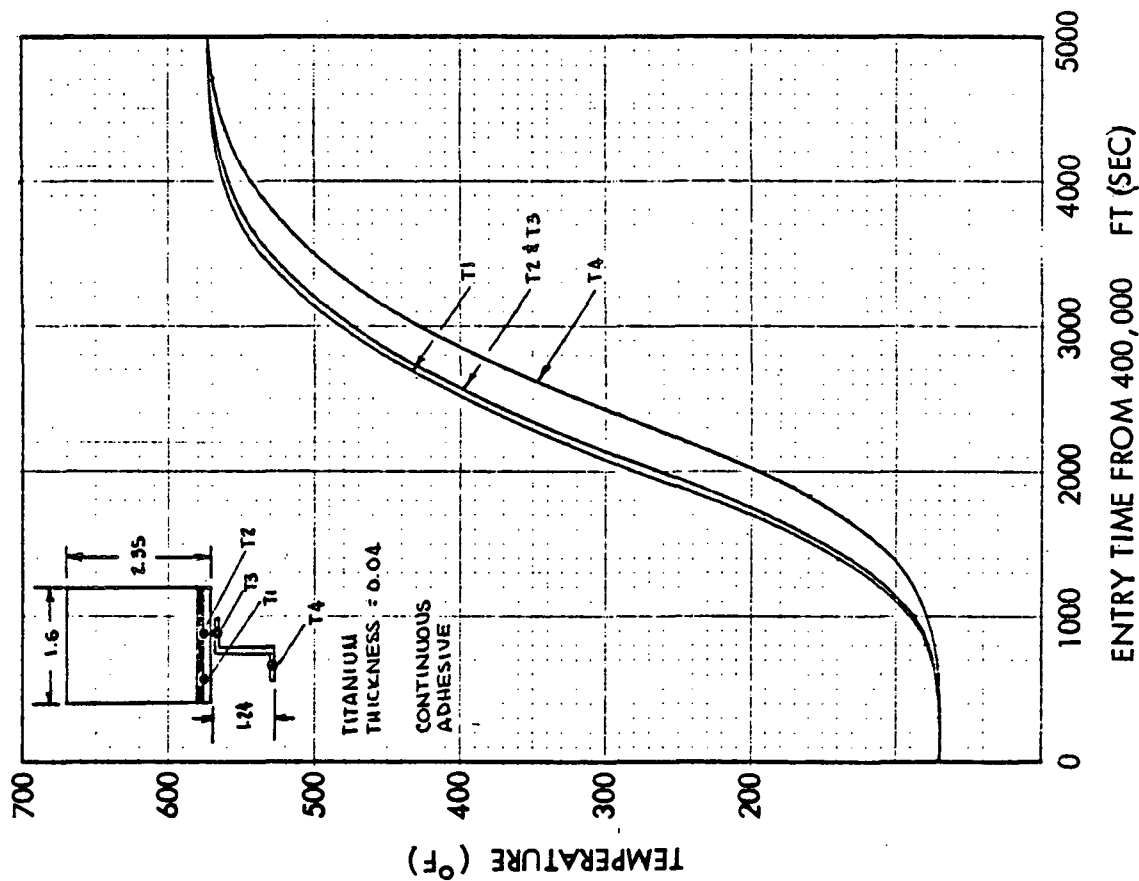


Fig. 2.1-5

DO6100

VARIATION OF MAXIMUM SUBSTRATE TEMPERATURE
WITH LI-1500 THICKNESS TEST PANEL NO. 2

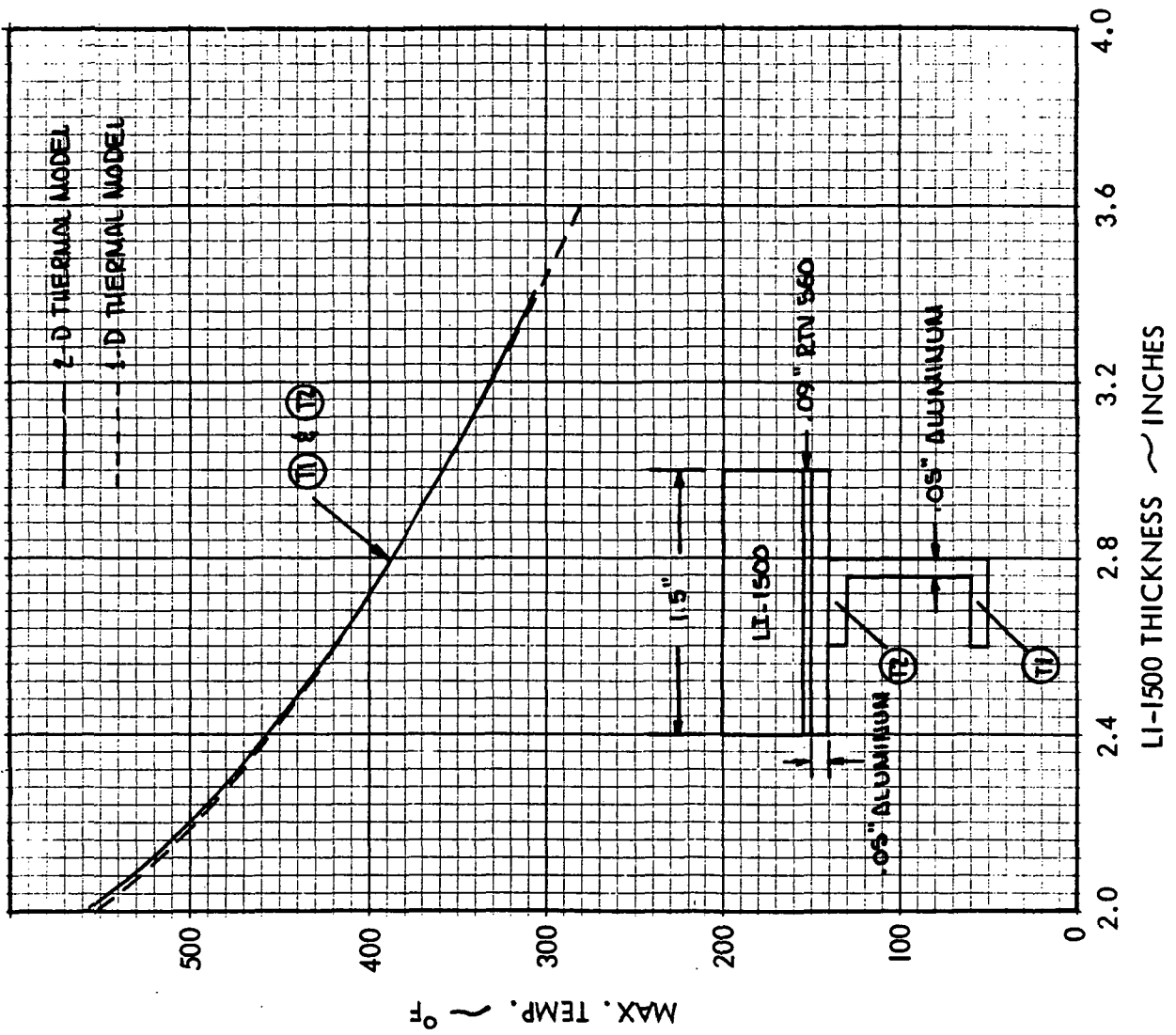
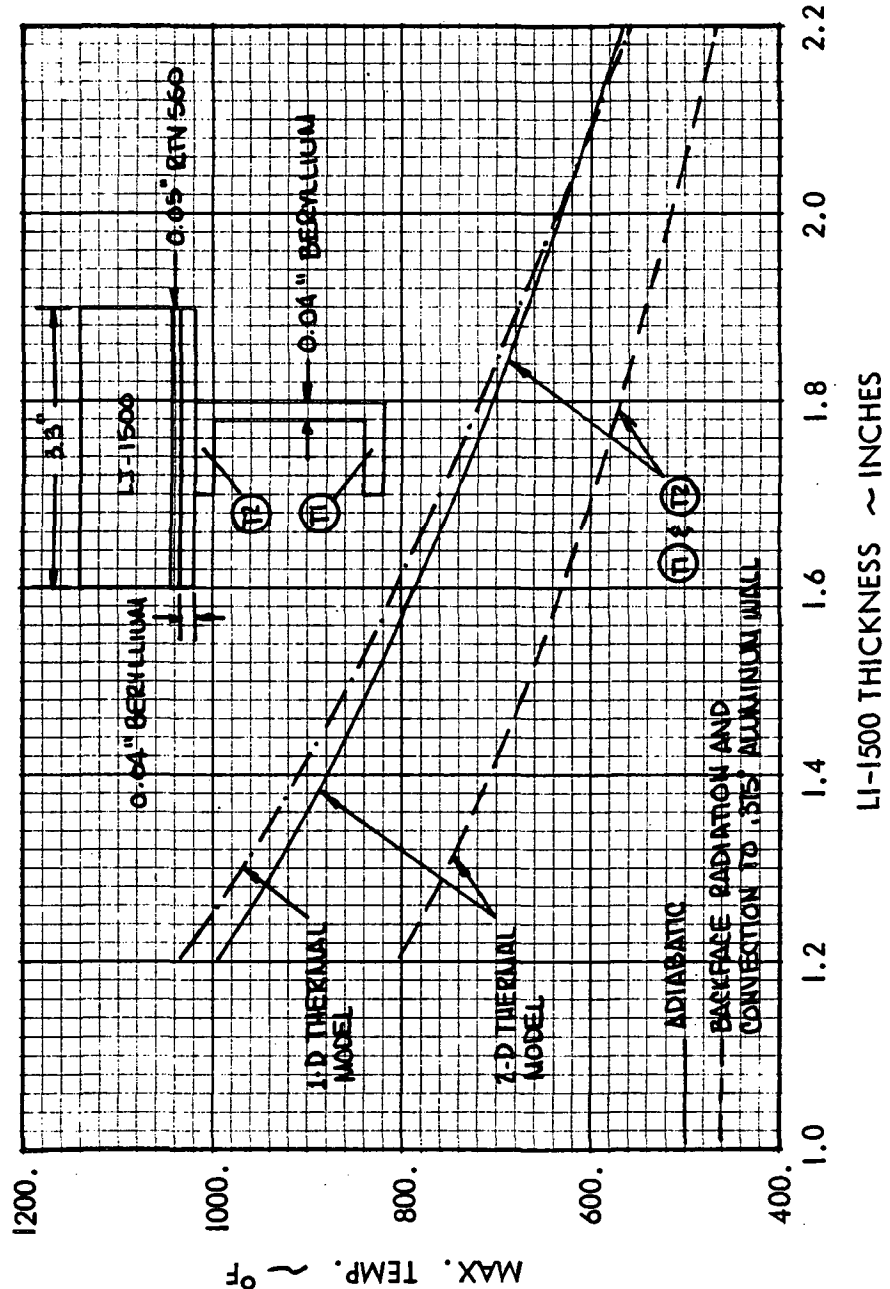


Fig. 2.1-6

DO6028

VARIATION OF MAXIMUM BERYLLIUM TEMPERATURE WITH LI-1500 THICKNESS - TEST PANEL NO. I



305999

Fig. 2.1-7

2.2 STRUCTURAL CONSIDERATIONS FOR LI-1500 SUBSTRATES

Methods of Optimization and Analysis

Subpanels. In this TPS concept, easily removable units called subpanels are mounted above the vehicle primary structure. These subpanels, which are covered with LI-1500 tiles, are designed to carry only airloads over spans which generally correspond to major frame or rib spacings. Because only minor support is provided at the panel edges that are perpendicular to the frames or ribs, simple beam analysis is used in the design and analysis. Bending stresses obtained in this manner based on simply supported edge conditions, are compared with local instability allowables for the extreme fiber elements in compression and with the material ultimate tensile properties for the extreme fiber elements in tension. Also, attention is directed to the maximum deflection of the panel and the effect of this deflection upon the design of the LI-1500 tiles.

Panel designs somewhat lighter than those developed here could be achieved if local instability criteria on the skin were relaxed. This could be done to some extent, since the bond and the LI-1500 tile act to stabilize the skin. However, the extent of stabilization is likely to be small and would involve an added analysis effort as well as one more optimization loop in the overall TPS design. In addition, further testing would be required. At this time, LMSC does not consider possible skin buckling to be compatible with a substructure that must maintain close tolerance tile alignments to prevent local increases in heating and erosion.

This type of analysis is easily coded for the computer to perform structural optimization studies. LMSC has developed a code, called SUBPAN, which has been used in the present program. The code may be used to optimize several subpanel material/configuration combinations. Mechanical properties for a number of materials are stored in the program as a function of temperature. These materials include titanium, beryllium, graphite-epoxy, and aluminum. Alternately, mechanical properties for other materials may be read in. The configurations that may be called include zee-stiffened subpanels, trapezoidal corrugation-stiffened subpanels, honeycomb-sandwich subpanels, integral L-stiffened subpanels, and plane trapezoidal corrugated subpanels.

Data needed to operate this code include panel length, design temperature, and pressure (burst and/or collapse), plus definition of the practical restraints involved and the selection of material and configuration. The practical restraints generally include specification of the minimum gages permissible and the widths of section elements that are fixed by practical considerations (e.g., zee-stiffener attach-flange width).

The code is patterned after work reported in the literature on the optimization of beams, which has shown that, for practical designs, the analysis must be set in terms of both permissible deflection and permissible bending stress. Beams optimized to a deflection criterion alone tend to be deep with thin sections, while beams optimized to a stress criterion alone tend to be shallow and flexible. In the LMSC code, the deflection criterion is stated as a maximum permitted at the center of the panel, under the application of limit loads, and it may be varied as desired. Because the subpanels must have a capability for carrying burst pressures as well as collapse pressures, and some configurations are unsymmetrical, both tensile and compressive outer-fiber stresses are computed on either side of the neutral axis to ensure that allowable stresses are not exceeded. The search for the lightest design meeting the criteria established, while satisfying the constraints imposed, is limited to standard sheet gages. Also, properties for a number of standard commercially available honeycomb cores have been stored in the program to ensure this standardization feature for honeycomb-sandwich subpanel optimization.

Primary Structure. LI-1500 is also proposed for direct application to primary structure. These panels carry direct axial loads, both tension and compression, in addition to airloads. For the purposes of this program, the primary structure panels are considered to be flat and very wide in comparison to their length; therefore, the conditions along the unloaded edges are not important and the panels may be analyzed as beam columns. An appropriate closed-form solution for uniformly loaded, simply supported, beam columns of uniform cross-section may be found in Timoshenko's "Theory of Elastic Stability." This type of edge support is probably conservative for most applications, particularly those in which the panels are continuous over intermediate supports. However, the use of more realistic edge conditions depends upon the detail definition of the intermediate supports and their resistance to rotation under load.

Stresses applied to the cross-section are equal to the sum of the direct stress plus bending stress due to the beam-column action. These stresses are compared with compressive and tensile stress allowables at the section outer fibers as described above for subpanels. In a similar way, the effect of deflection due to beam-column action upon the LI-1500 tile design also is considered.

Data for use in the design of beam-columns are shown in Figs. 2.2-1 and 2. These figures yield stiffness requirements as a function of the uniformly applied pressure p , axial line load P , and the maximum deflection Δ_{\max} . Intercept points along the ordinate correspond to Euler-column stiffness values; the bottom curve represents a beam subject to uniform lateral pressure alone. Although the beam-column analysis itself is nonlinear, these curves are extremely close to being linear. Hence, the required stiffness can be very closely approximated as the sum of that necessary to limit the deflection due to the pressure and that required to resist column buckling, i.e.,

$$EI_{\text{reqd}} \approx \frac{5 p l^4}{384 \Delta_{\max}} + \frac{Pl^2}{\pi^2}$$

Beam-column analysis has been computerized at LMSC and used in the design and analysis of the prototype panels. This code, PRIPAN, has been integrated into the existing computer program for the structural optimization of subpanels by merely redefining the stiffness requirements for the section and utilizing the existing search techniques. Before this work was completed, structural optimization of primary structure panels was performed using wide-column minimum weight solutions that were perturbed according to a fixed interaction equation to account for pressure effects. Beam-column analysis checks subsequently were performed to verify and/or modify the resulting designs.

Comparative results between the two methods are shown in Table 2.2-1 for the three deliverable panels. In each case, the attach flange dimension, a_z , was specified and held constant through the optimization process. The designs labeled (a) represent the wide-column optimum, whereas the designs identified by (b) were generated by the

BEAM COLUMN REQUIRED STIFFNESS
FOR DEFLECTION CRITERION

24-IN. PANEL LENGTH

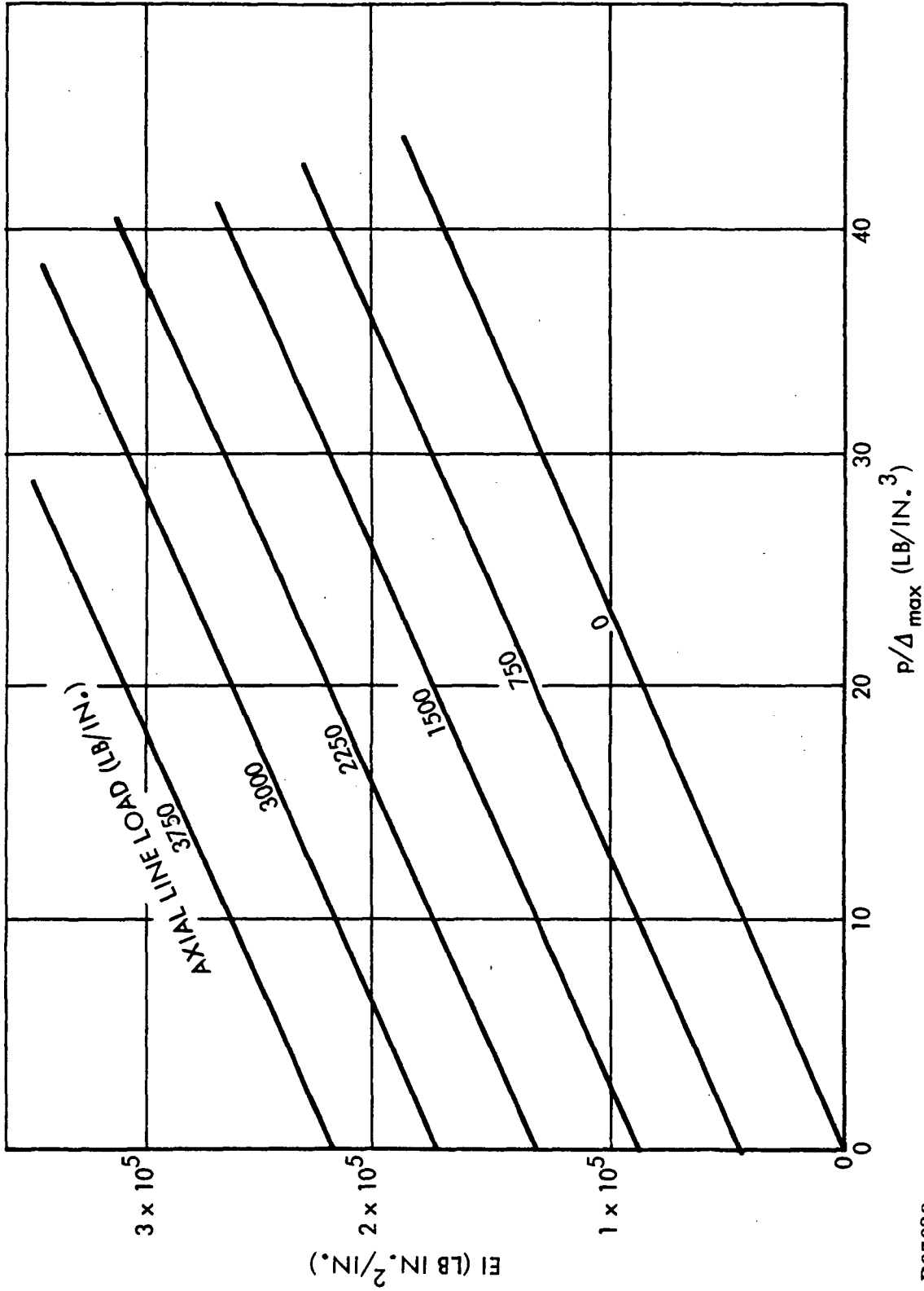


Fig. 2.2-1

D07029



BEAM COLUMN REQUIRED STIFFNESS
FOR DEFLECTION CRITERION

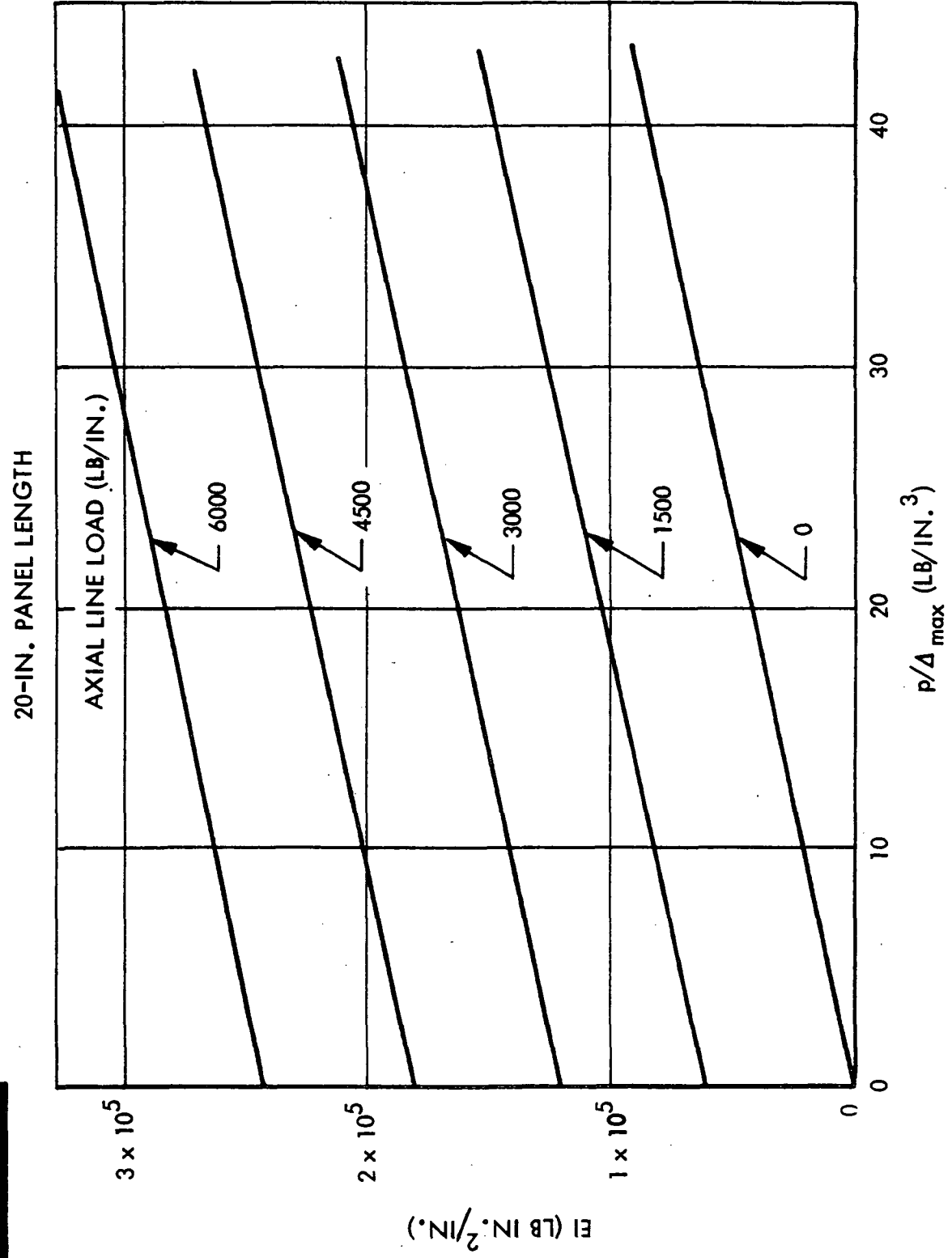
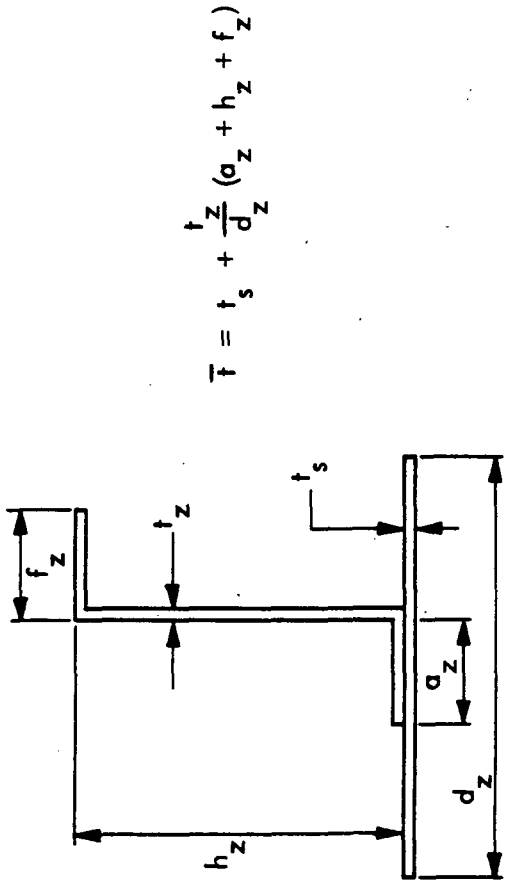


Fig. 2.2-2

DO7030

Table 2.2-1

COMPARISON OF OPTIMUM CONFIGURATIONS
WIDE-COLUMN AND PRIPAN ANALYSIS



PANEL	\bar{f}	d_z	t_s	t_z	a_z	h_z	f_z
2 - a	0.1144	1.60	0.050	0.050	0.40	1.36	0.40
b	0.1201	1.55	0.050	0.050	0.40	1.25	0.52
b	0.1144	0.99	0.032	0.040	0.40	1.24	0.39
3 - a	0.1431	1.60	0.063	0.063	0.48	1.20	0.48
b	0.1436	1.67	0.063	0.063	0.48	1.24	0.42
b	0.1415	1.05	0.040	0.050	0.48	1.27	0.38
4 - a	0.0895	1.60	0.040	0.040	0.41	1.24	0.41
b	0.1056	1.08	0.040	0.040	0.41	0.98	0.38
b	0.1038	1.35	0.050	0.040	0.41	1.03	0.38



beam-column optimization analysis. It is interesting to see that the latter method produces a design very close to that from the wide-column method (except for panel 4) but that a lighter (smaller \bar{t}) design exists with thinner gauges and a closer zee-spacing. Although \bar{t} is less, the rivet weight has not been included in the calculation, and it may well be that the additional rivets needed would offset the expected reduction in weight. As it is, the close zee-spacing would preclude the use of such a design, since it would be difficult to insert the rivets. In addition, the number of stiffeners would be increased for a given panel, resulting in a cost increase.

For panel 4, the results seem to indicate that the design obtained originally is not conservative. Comparing this design with the results from the optimization computer code (the 'b' designs), it appears that the skin b/t ratio is too large. Reexamination of the analysis for this design shows that skin buckling has been based on an assumption of greater-than-simple support of the skin at the stiffeners. This was considered acceptable, because the stresses are due to pressure loads that are assumed to force an inward buckle pattern between stiffeners in all bays. In the optimization computer code, simply supported edge conditions are assumed in order to eliminate any uncertainty on this point. As a result, higher \bar{t} 's are obtained, which are probably more realistic for vehicle hardware designs.

2.3 RSI STRESS ANALYSIS AND MODELING

The work described here is an outline of the development of a linearized two-dimensional model to approximate the behavior of the RSI panel under combined mechanical and thermal loads. Included is a discussion of the two-dimensional (2-D) finite element code, WILSON, and its subsequent application to modeling of the panel. This method represents the baseline analytical technique used for the RSI stress analysis. The three-dimensional (3-D) program, SAP, which is being used to verify the validity of a 2-D analysis, also is discussed, and comparisons of the two methods are presented. The manner of temperature-profile modeling through the RSI thickness is discussed as well as the effect of using isotropic material properties for LI-1500 early in the program before data were available to show the orthotropic nature of the material. Finally, nonlinear beam-column effects are discussed.

2-D WILSON Program

This code is a two-dimensional finite element program, capable of performing either plane-stress or plane-strain analyses for orthotropic temperature-dependent material properties. The version in use incorporates double precision arithmetic to account for the wide range of elastic and geometric properties of the materials in the TPS panel design. Program parameters are given in Table 2.3-1.

2-D RSI System Model

The way in which one half of the TPS panel is modeled for the WILSON code is shown in Fig. 2.3-1 where it is noted that the panel is assumed to be simply supported. The substrate stiffeners and skin are replaced by an effective substructure material whose elastic properties are those of the substrate but with thickness based on the bending stiffness of the actual panel substrate*. As seen in the model, two layers of elements are used for the effective substructure, one layer for the bond, eight for the LI-1500, and one layer for the coating. The reason for different size elements in the LI-1500 is that if the coating is lapped over the edges, numerical inaccuracies can occur due to elastic and geometric property mismatch. The effect of element aspect ratio also has been studied to minimize these sources of inaccuracy.

*This is the thickness listed with all stress analysis results in this report, in contrast to an effective thickness based on weight which is used for thermal analyses.

Table 2.3-1

SUMMARY OF WILSON AND SAP CODE PARAMETERS



TWO-DIMENSIONAL ANALYSIS (WILSON CODE)

NUMBER OF ELEMENTS = 1092
 NUMBER OF NODES = 1196
 DEGREES OF FREEDOM = 2392
 RUN TIME (TYPICAL PROBLEM) 1108 0.03: 16 HRS CPU
 0.01: 18 HRS I/O

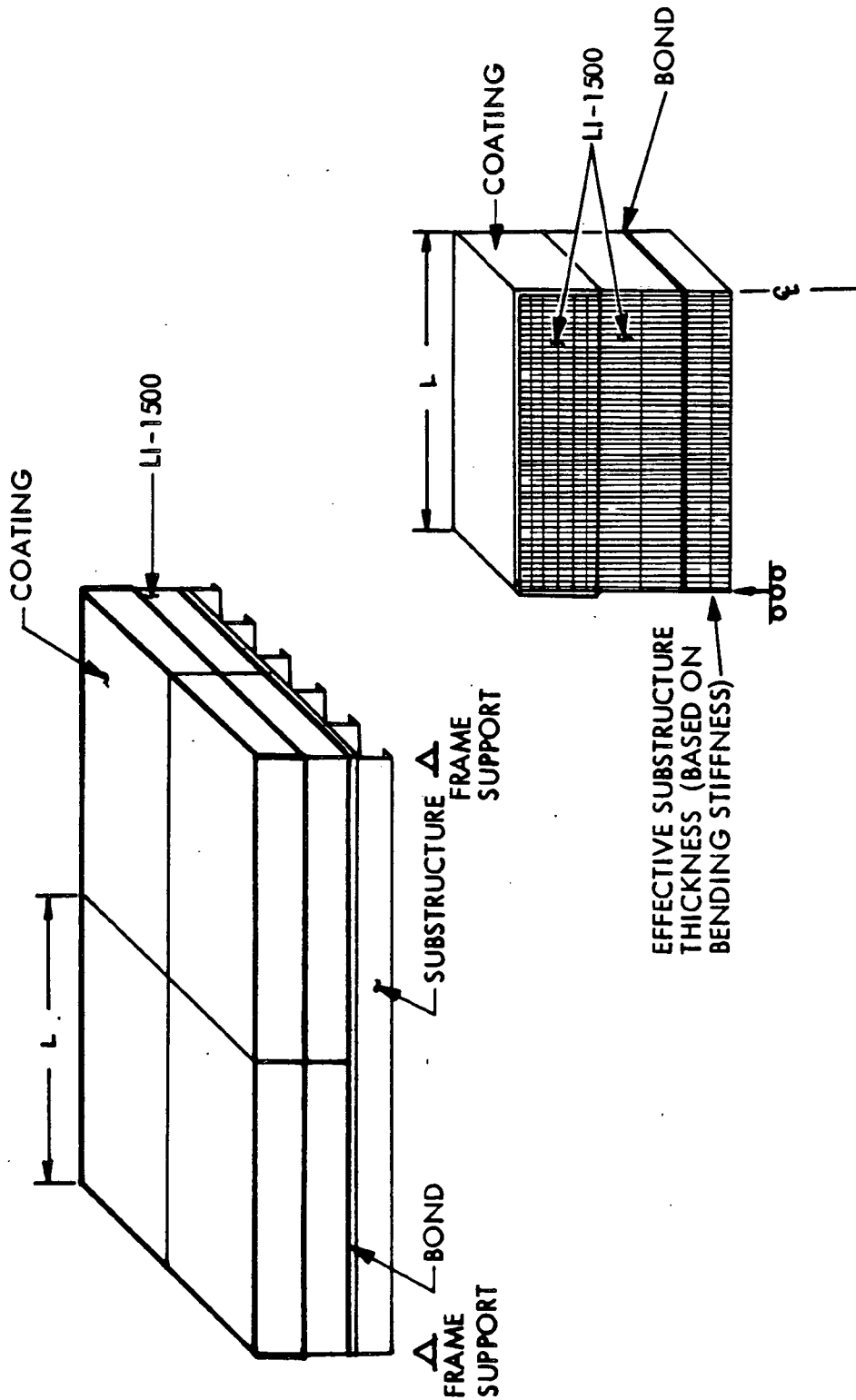
THREE-DIMENSIONAL ANALYSIS (SAP CODE)

NUMBER OF 3-D ELEMENTS = 960
 NUMBER OF QM5 PLATE ELEMENTS = 204
 NUMBER OF NODES = 1638
 BANDWIDTH = 362
 DEGREES-OF-FREEDOM = 3968
 RUN TIME (TYPICAL PROBLEM) 1108 = 1:45 HRS CPU

OLD VERSION CDC 0:37 HRS CPU
 0:33 HRS I/O

SPEED UP VERSION (NEW) CDC 0:10 HRS CPU
 0:15 HRS I/O

TWO DIMENSIONAL MODELS OF TPS PANELS



2.3-3

36

Fig. 2.3-1

To determine stress variations in the direction perpendicular to the stiffeners, a different model for the WILSON code is necessary (see Fig. 2.3-2). Here the discrete stiffeners are replaced by springs having the stiffness associated with bending of the actual stiffeners at midspan.

Due to mechanical and thermal loads, the panel experiences bending, but it is found that the in-plane strain of the substrate is the primary source of RSI stressing. It has been ascertained that the effective thickness model has negligible effects on the location of the neutral axis of the overall RSI system model in the bending mode. In-plane line loads in the primary structure panels are proportioned to the effective thickness so that in-plane substructure stress and strain levels are those of the actual panel.

Effect of Orthotropic LI-1500 Material Properties

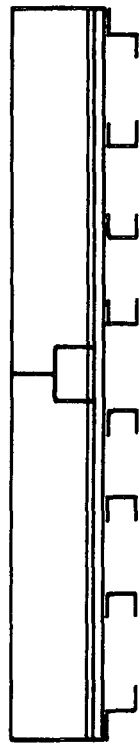
Isotropic elastic moduli were assumed for initial parametric studies. After the orthotropic data were obtained, a comparison was drawn to see what effect the use of isotropic data would have on the early parametric studies. The results of this check are shown in Table 2.3-2, which presents the RSI system stress levels of interest. Maximum effects are noted in coating stresses that go down markedly, but some LI-1500 stress components do go up somewhat. Although stress magnitudes are dependent upon anisotropic effects, the general conclusions of the initial parametric studies carried out with isotropic data continue to hold; all subsequent studies and prototype panel verification calculations utilize orthotropic property data.

Plane Stress/Plane Strain Comparison

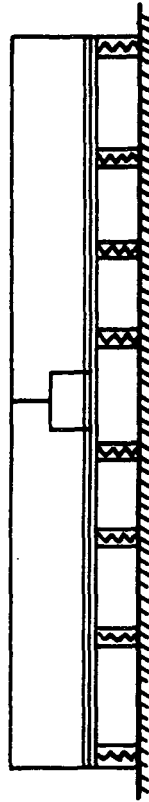
Plane-stress analyses were used to accomplish initial studies in the TPS program; however, a plane-strain solution was used for direct comparison. The case studied is for a beryllium subpanel with 600^oF backface temperature and a 1.14 burst pressure. The analysis assumed isotropic LI-1500 elastic properties with $E = 60,000$ psi, and the expansion coefficients of each material in the third direction have been set to zero. The comparisons are shown in Table 2.3-3, where it is noted that there is very little



TRANSVERSE DIRECTION WILSON MODEL



ACTUAL PANEL



EQUIVALENT PANEL

Fig. 2.3-2

D07028



**ORTHOTROPIC-ISOTROPIC LI-1500 MATERIAL
PROPERTIES COMPARISON**

BERYLLIUM FUSELAGE PANEL (SHORT TRAJECTORY)

P = 1.14 PSI BURST

T_{Be} = 600°F, T_{COATING} = 75°F

STRESS COMPARISON

	<u>ORTHOTROPIC</u>	<u>ISOTROPIC</u>
MAX LI-1500	153.2	130.4
MIN LI-1500	- 10.4	- 8.4
SHEAR LI-1500	54.6	67.6
LONG. LI-1500	153.2	124.8
PEEL LI-1500	56.5	65.8
MAX RTV-560	107.8	118.2
MIN RTV-560	- 48.3	- 53.2
SHEAR RTV-560	54.9	67.9
LONG. RTV-560	- 19.3	- 21.1
PEEL RTV-560	79.1	77.1
MAX COATING	1647.8	3723
MIN COATING	-129.4	-290.0
	E _{LONG} = 60,000	E = 60,000
	E _{NORMAL} = 6,000	G = 24,000
	G = 4,150	

ALL STRESS AND MODULUS VALUES IN PSI

difference in the two solutions except, of course, for the normal stress in the third direction, σ_T . This stress is due to the restraint of Poisson effects in the third direction and would apply only for a tile infinitely long in that direction. Hence, Poisson effects can be bounded by the two solutions, although it is expected that they are of less importance than other three-dimensional effects.

Linear/Nonlinear Temperature Study

Temperature distributions through the LI-1500 thickness during reentry are nonlinear, while those of the ground conditions are linear. To determine what effect the nonlinear distribution has on the RSI stress levels, the most nonlinear case has been compared with a linear distribution joining the same surface and backface temperatures. These results are reported in Table 2.3-4, where it is seen that all stress levels are within 5 percent, with the exception of coating stresses, which are greater in the linear case, although they are not critical. These results do not affect present stress analyses, since the actual temperature distributions are used. However, Table 2.3-4 indicates that a linear approximation could be made without impacting RSI panel designs.

3-D SAP Program

The program used for the three-dimensional analysis of the thermal protection system test panels is a version of SAP, a general finite element program developed by E. Wilson of the University of California at Berkeley.⁽²⁻¹⁾ Two types of elements are available in this version: a four-node numerically integrated plane stress quadrilateral (QM5) and an eight-node isoparametric hexahedral element (BRICK8). The BRICK8 element, was modified to include a general temperature distribution within the element. Although the program may be run on either the UNIVAC 1108 or the CDC 6600 computer, increased numerical accuracy due to a larger word size makes CDC the first choice.

⁽²⁻¹⁾SAP, A General Structural Analysis Program, E. L. Wilson, Report to Walla Walla District's U. S. Engineer's Office, Structural Engineering Laboratory, University of California, Berkeley, California, Sep 1970

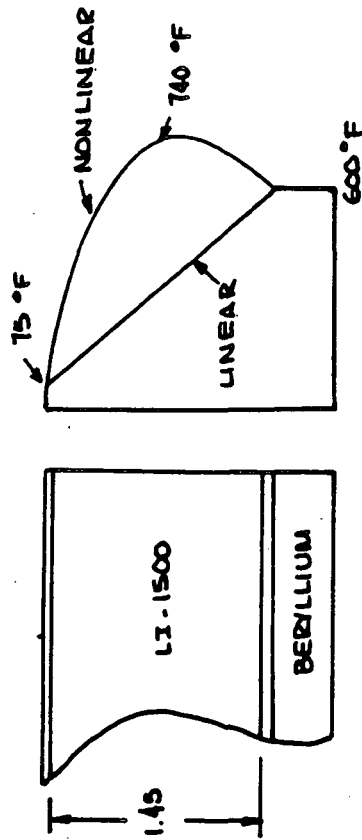
Table 2.3-3

LOKNEED PLANE-STRESS/PLANE-STRAIN COMPARISON, ISOTROPIC ANALYSIS

	PLANE-STRESS SOLUTION	PLANE-STRAIN SOLUTION
<u>MAX. LI-1500 STRESS (PSI)</u>		
PRINCIPAL TENSILE	77.3	79.1
PRINCIPAL COMPRESSIVE	-89.1	-92.4
SHEAR	64.9	63.5
LONGITUDINAL	73.9 (T)	75.8 (T)
NORMAL	26.8 (T)	27.8 (T)
σ_T^*	0.0	21.9 (T)
<u>MAX. RTV-560 STRESS (PSI)</u>		
PRINCIPAL TENSILE	48.9	52.1
PRINCIPAL COMPRESSIVE	-31.6	-33.3
SHEAR	37.8	38.4
LONGITUDINAL	-19.3 (C)	-22.0 (C)
NORMAL	30.0 (T)	32.1 (T)
<u>COATING (0025) STRESS (PSI)</u>		
PRINCIPAL TENSILE	1793	1759
PRINCIPAL COMPRESSIVE	-274	-269

* σ_T IS PERPENDICULAR TO LONGITUDINAL AND NORMAL STRESSES

Table 2.3-4
BERYLLIUM SUBPANEL - 6-IN. TILE LINEAR -
NONLINEAR TEMPERATURE COMPARISON



TEMPERATURE DISTRIBUTION

MAXIMUM STRESSES IN PANEL

QUANTITY	LINEAR	NONLINEAR
PRINCIPAL TENSILE	57.7	60.4
PRINCIPAL COMPRESSIVE	-4.3	-3.8
SHEAR	17.3	17.2
LONG.	57.7	60.4
PEEL	8.9	8.8
PRINCIPAL TENSILE	20.6	20.1
PRINCIPAL COMPRESSIVE	-23.4	-23.6
SHEAR	16.8	16.6
LONG.	-18.5	-19.2
PEEL	11.7	11.5
PRINCIPAL TENSILE	0.1	7.0
PRINCIPAL COMPRESSIVE	-160.4	-52.9

ORTHOTROPIC
ANALYSIS

LI-1500

RTV

COATING

D05168 (1)

3-D RSI System Model

The case chosen for analysis is a 24 x 24 in. beryllium subpanel. Since the panel is symmetrical in two directions about its center, only one quarter of the panel was modeled. Each panel is composed of four 12 x 12 in. LI-1500 tiles, so only the beryllium substructure is assumed continuous across the symmetry planes and the panel is simply supported along its unstiffened edge. Six layers of BRICK8 elements are used in the model - four layers through the LI-1500 insulation, one layer through the bond, and one layer through the beryllium. Along the stiffened edge of the panel, an additional layer of BRICK8 elements is used to model the edge stiffener base. Plane stress QM5 elements are used to model the coating on the outside of the LI-1500 and the longitudinal beryllium stiffeners. The completed model is illustrated in Fig. 2.3-3 with a view looking up under the panel. SAP code parameters for this model are summarized in Table 2.3-1.

Temperature for the problem was assumed to be 600°F throughout the beryllium and the bond, and decreasing linearly from 600°F to 75°F through the LI-1500 with the stress-free temperature being 75°F. A burst pressure of 1.14 psi was applied to the beryllium panel.

2-D, 3-D Stress Analysis Comparisons

Results of a 3-D SAP analysis of the RSI panel are given in Figs. 2.3-4 through 2.3-9 with comparisons from the 2-D WILSON analysis using the model of Fig. 2.3-1 for stress variations in the direction of the stiffeners and that of Fig. 2.3-2 for stress variation in the direction transverse to the stiffeners. The maximum longitudinal stress in the LI-1500 is shown in Fig. 2.3-4 where it is seen that the 2-D analysis tends to underestimate that of the 3-D analysis. This is not unexpected as the 2-D results represent some averaged behavior of the panel, whereas the 3-D results shown are maximums at the center of the tile. In addition, the 2-D analysis cannot represent the temperature effects in the third direction and, of course, this comment applies to comparison of other stress components as well. Although the results for the stiffener

THREE DIMENSIONAL MODEL OF TPS PANELS

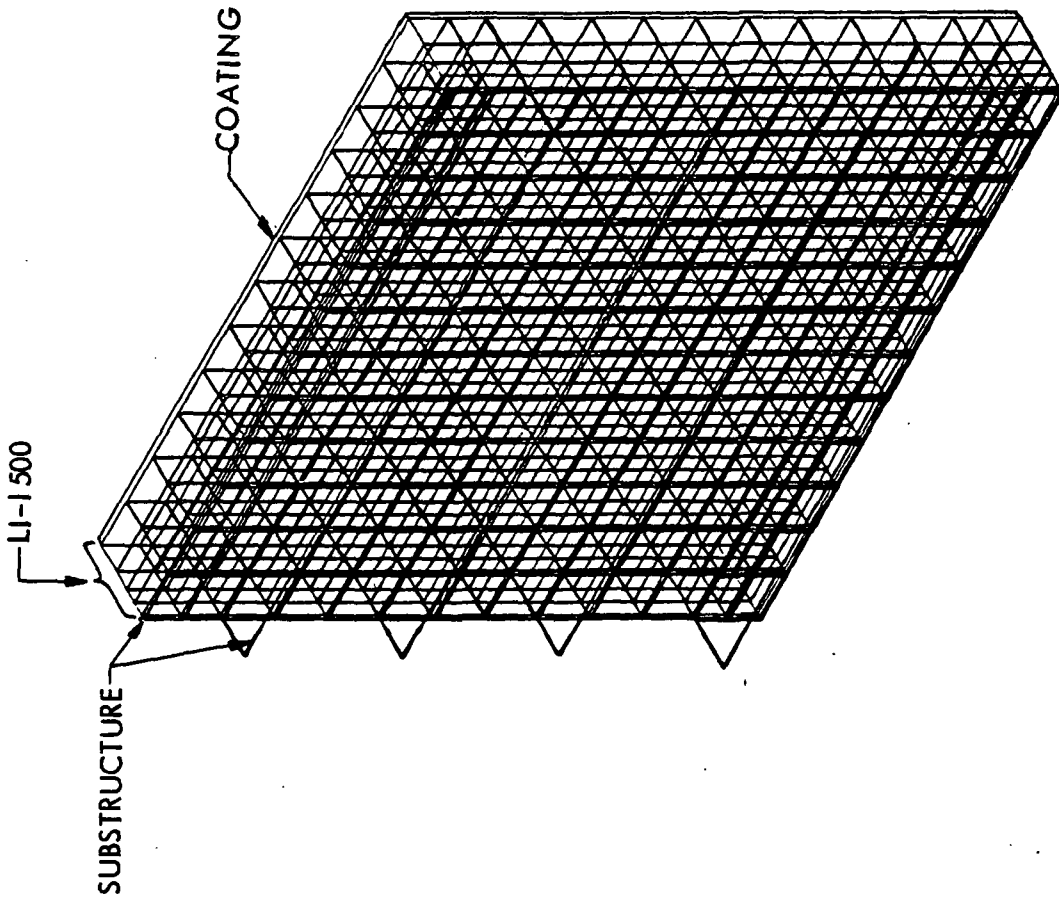
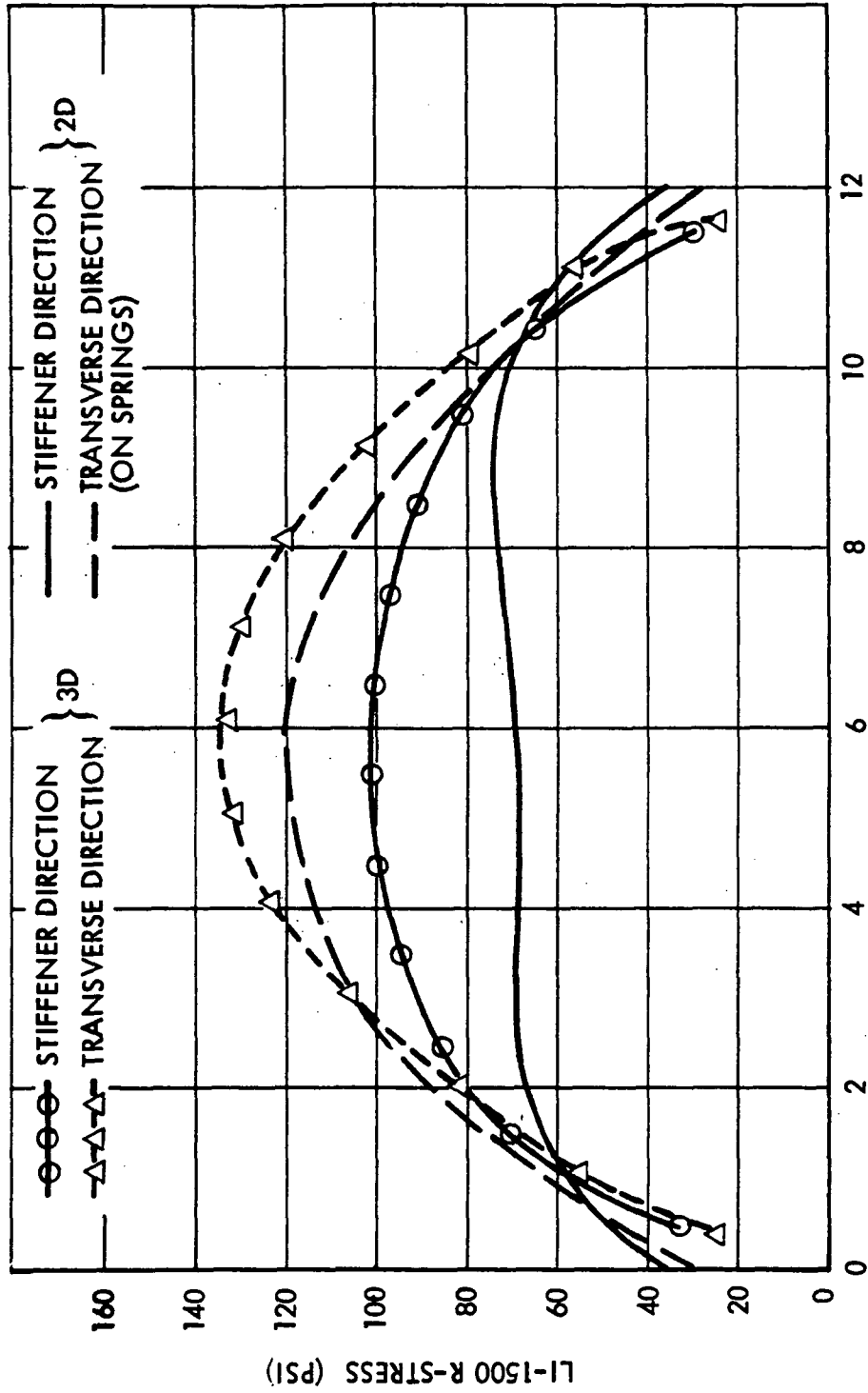


Fig. 2.3-3

D04998

LI-1500 LONGITUDINAL STRESS



DISTANCE ALONG TILE (IN.)

Fig. 2.3-4

D07032



LI-1500 SHEAR STRESS

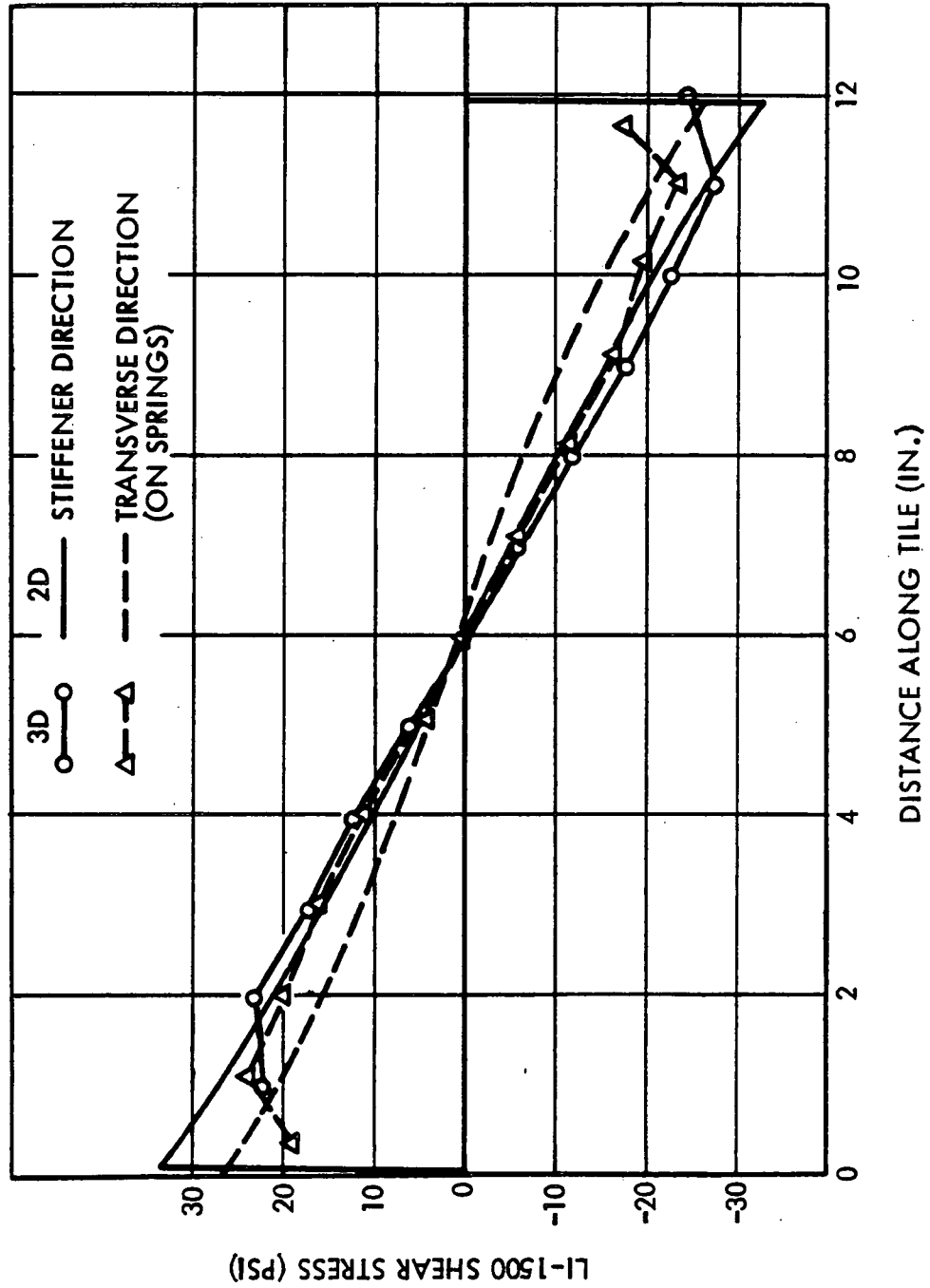


Fig. 2.3-5

D07033 (1)

LI-1500 PEEL STRESS

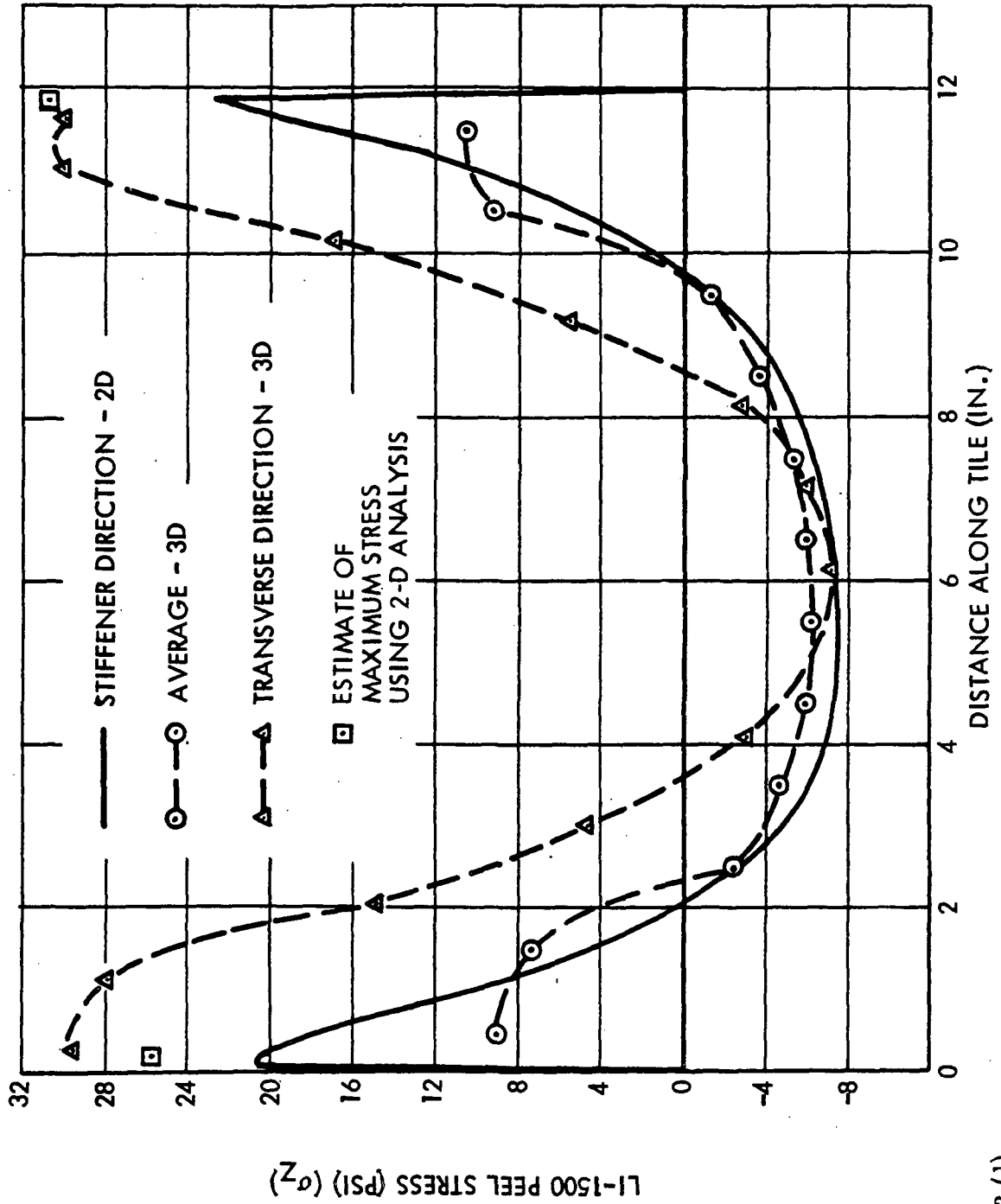


Fig. 2.3-6

D07043 (1)



PEEL STRESS IN LI-1500 AT BOND-LINE - 3D ANALYSIS

LMSC-D152738
Vol II

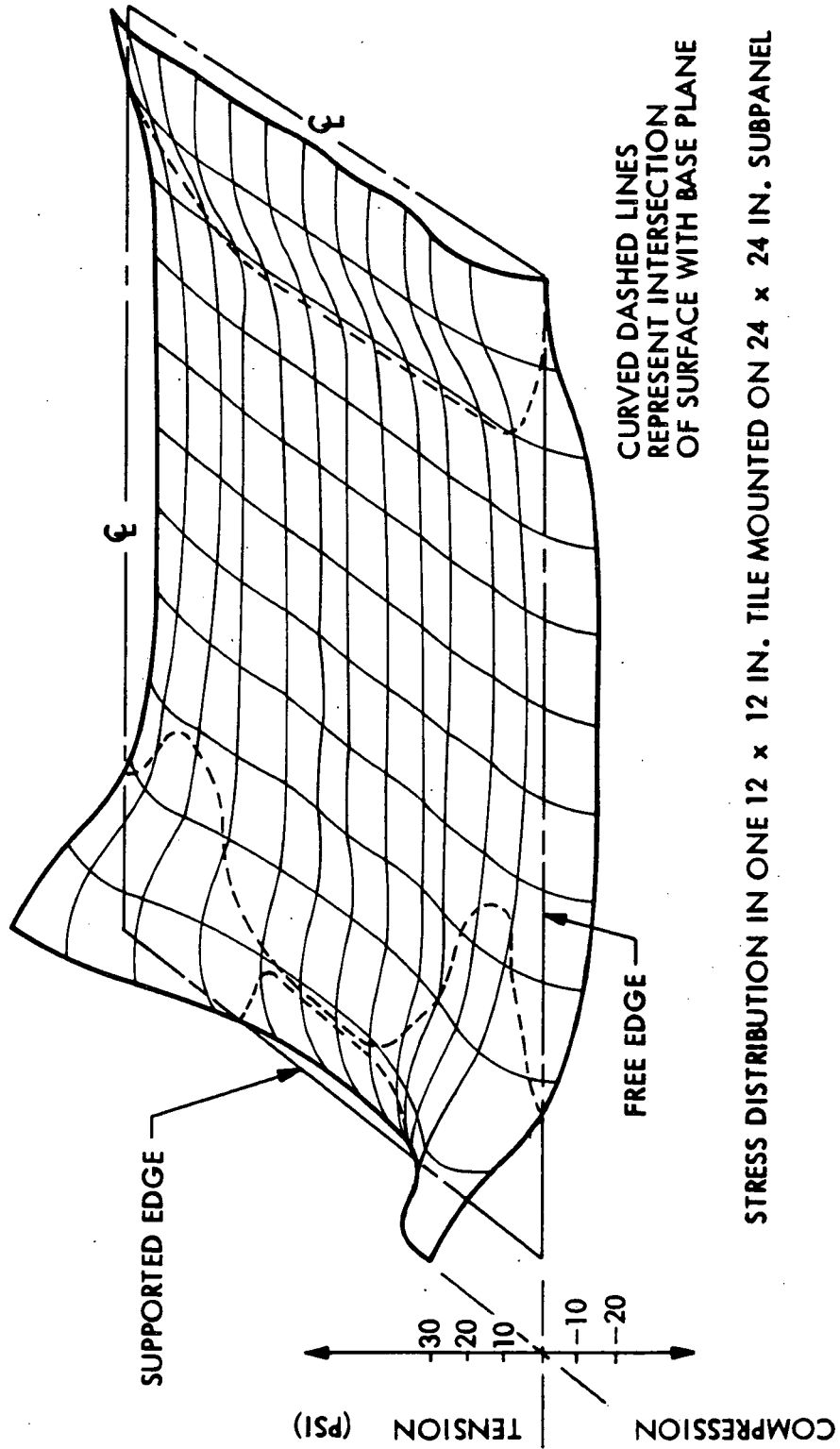


Fig. 2.3-7

COATING STRESS

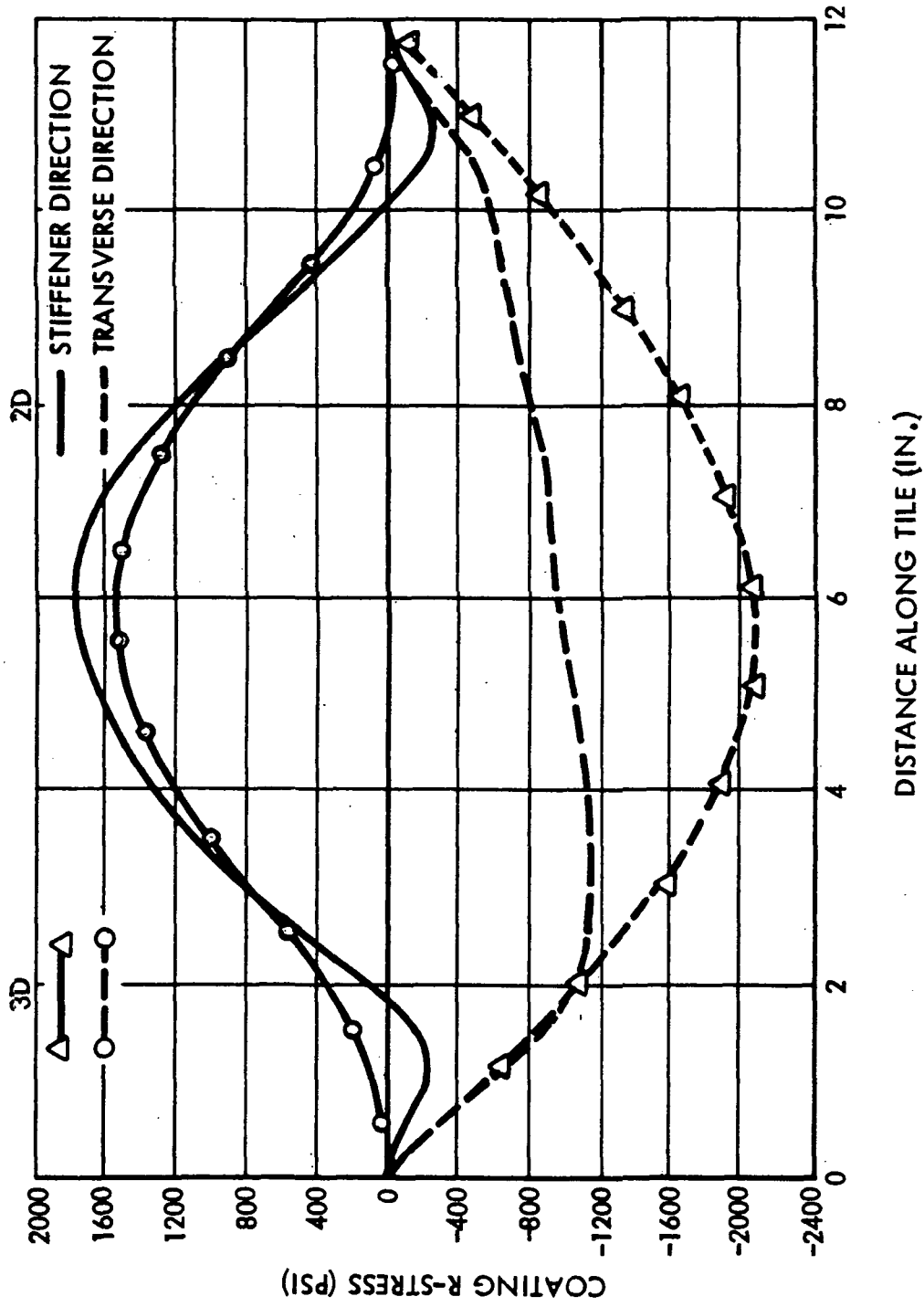


Fig. 2.3-8

D07036

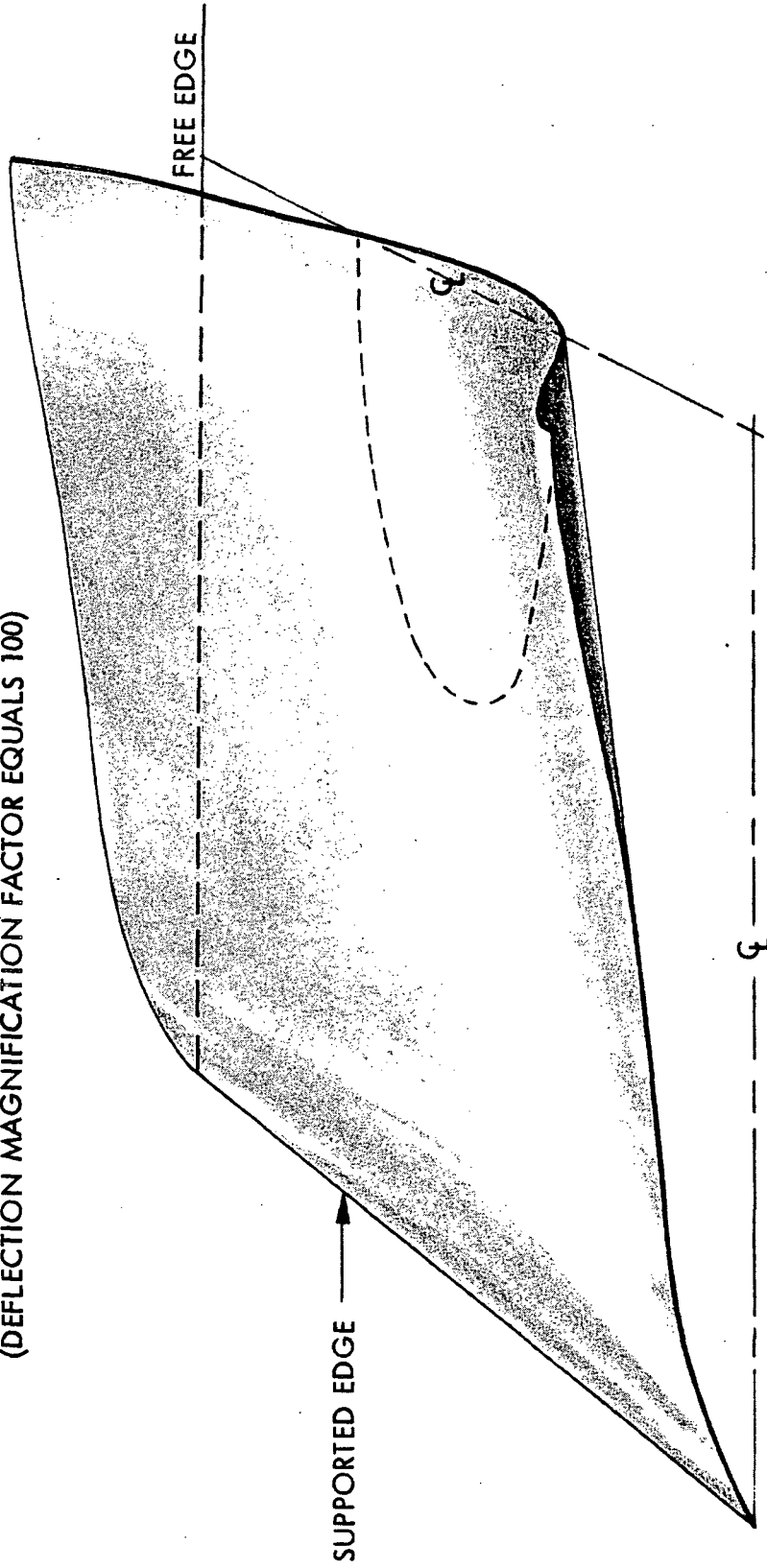




PANEL DEFLECTION

(ONLY ONE-FOURTH OF PANEL SHOWN)

(DEFLECTION MAGNIFICATION FACTOR EQUALS 100)



CURVED DASHED LINES
REPRESENT INTERSECTION
OF SURFACE WITH BASE PLANE

direction differ to a greater extent than those for the transverse direction, this difference does not affect panel designs, because the maximum LI-1500 longitudinal stresses occur in the transverse direction and the 2-D and 3-D results are much closer here.

LI-1500 shear stress is presented in Fig. 2.3-5 where it is noted that the results are in good agreement and that the 2-D analysis tends to overestimate the maximum shear, hence lending some conservatism to the panel designs since the LI-1500 shear stress is a critical design quantity. This overestimate is typical as stress singularities in two dimensions are stronger than in three dimensions, because there is an extra dimension in which the stress can decay in this case.

LI-1500 peel stress (i.e., the normal stress component perpendicular to the plate) is shown in Fig. 2.3-6. The three curves in this figure cannot rigorously be compared with one another as will be explained; however, they provide a means of assessing 2-D analysis methods as applied to the RSI plate. The solid curve represents the 2-D analysis in the stiffened direction while that indicated by circles is for the same direction but is an average taken in the transverse direction of the 3-D results. Hence, this represents some mean or uniform behavior which is what a 2-D analysis should predict. As can be seen, the curves agree reasonably well except at the ends where 2-D analysis overestimates this average 3-D behavior. However, the maximum peel stresses that occur at the ends of the tile are greater than the 2-D results and the curve marked with triangles shows the variation along one edge of a tile in the transverse rather than the stiffener direction. Thus, 2-D analysis underestimates the maximum peel stress.

Since the peel stress arises due to equilibrium conditions involving shear stresses that occur in both the stiffened and transverse directions of the panel, the total peel stress at a corner is actually due to shear components in both these directions. Therefore, a 2-D analysis in the transverse direction will produce peel stresses which should be additive in some way at the corner to the 2-D results from a stiffened direction analysis. This sum is shown as the two points marked with squares in Fig. 2.3-6 at either end of the tile; as can be seen, the correlation is relatively good. Although 2-D analysis is not capable of determining the actual variation of peel stress across the

2.3-18

51<

0.2

panel in both directions shown in Fig. 2.3-7 (as determined from the 3-D analysis), the 2-D method is apparently able to estimate maximum values reasonably well for this stress component.

Comparisons of coating stresses are given in Fig. 2.3-8, where it is noted that 2-D and 3-D results agree quite well for the stiffener direction. The discrepancy in the transverse direction is due to the sensitivity of the spring-mounted model of Fig. 2.3-2. The springs tend to perturb some stress components near the center of the tile leading to dubious values there. To correct the situation, a means of improving this 2-D model is being sought.

A final result of the 3-D analysis is the deflected shape of a quarter panel shown in Fig. 2.3-9 where a magnification of 100 has been applied to the deformation field.

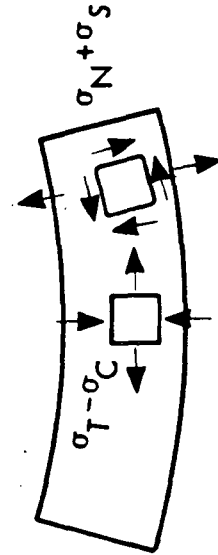
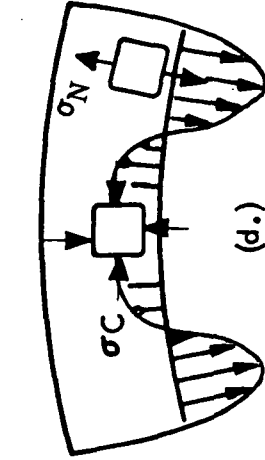
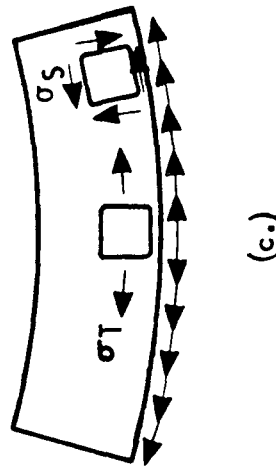
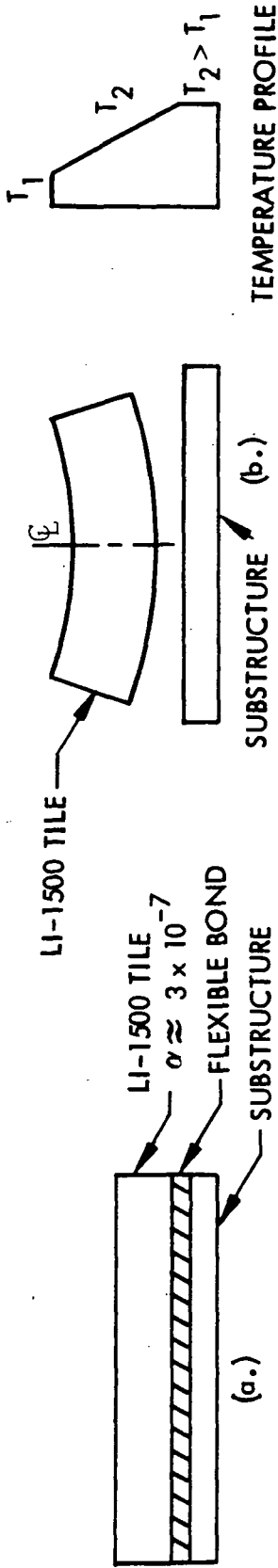
The thermal expansion interaction with bonded tiles and unequal panel stiffness in the two directions leads to an anticlastic surface which is not determinable by 2-D methods. On the other hand, 2-D methods would apply if only mechanical pressure and axial loads were to act, to the exclusion of the temperature field. Hence, 2-D analyses must be conducted in both directions to ensure adequate TPS panel designs, since the substrate experiences significant temperature increases.

RSI Panel Response to Substrate Strain

This section considers the physical behavior of an RSI panel which experiences thermal straining of the substrate. Referring to the series of sketches in Fig. 2.3-10, the unloaded panel is shown in (a.). Under the temperature rise from ambient given in (b.), the tile and substrate would expand in a stress-free manner if the bond were not present. One affect of the bond causes the tile to be loaded by shear stresses along its lower edge and leads to longitudinal tensile stresses, σ_T , which are maximum at the center of the tile near the bondline as shown in (c.). The shear stresses are maximum near the ends of the tile. To conform with the lack of curvature in the expanded substructure, self-equilibrating normal stresses develop and are transmitted through the bond, causing a reverse bending of the tile as shown in (d.). These are also maximum near the ends of the tile. This reverse bending gives rise to longitudinal



RSI PANEL RESPONSE



compressive stress, σ_C , at the bondline. The total state of stress in the tile is then a summation of (c.) and (d.) as shown in (e.).

The resultant longitudinal stress is always tensile and maximum at the bondline for the temperature distribution shown in (b.). The reverse bending due to normal stresses merely reduces the intensity of the longitudinal stresses.

It is important to note the role of the bending stiffness of the substructure on this final state of stress. For very small EI values, the substrate would conform to the tile curvature with little normal stress arising; hence, the maximum longitudinal stress would not be reduced and this stress component would be a driving parameter on tile designs. On the other hand, for very high EI values, the tile would be pulled back to conform with the undeformed substrate, causing large normal stresses which would reduce the magnitude of the longitudinal tensile stress. Since maximum shear stresses in the LI-1500 are due mainly to the differential expansion of the panel components and not on the substructure bending stiffness to any marked degree, this case would lead to critical states of shear and normal stress near the ends of the tile. Hence, two failure modes of the tile are possible:

- Stiff substrate conducive to combined normal stress/shear stress failure mode near ends of the tile
- Flexible substrate conducive to longitudinal tensile stress/normal compressive stress failure mode at center of the tile

Each of these possible modes must be considered in rational TPS panel design. This is particularly important, since the designs incorporate stiffening in one direction only, thus lending a preference to one failure mode or another depending upon direction in the plane of the panel.

A comparative 2-D WILSON study showing these effects is given in Table 2.3-5. The panel geometry is that used for the 2-D, 3-D comparisons discussed earlier. The first case in Table 2.3-5 represents the panel in the stiffener direction while the second case considers only the plate thickness ($t = 0.040$ in.) of the substructure



Table 2.3-5

BERYLLIUM PANEL - TWO DIMENSIONAL WILSON CODE STUDY

ISOTROPIC ANALYSIS

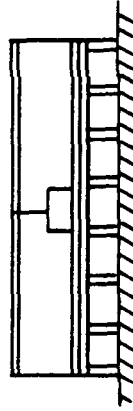
t_{LI-1500} = 1.6 IN.
 t_{RTV-560} = 0.060 IN.

T_{COAT} = 75°F
 T_{Be} = 600°F

LINEAR DISTRIBUTION
 TO BONDLINE

MAXIMUM LI-1500 STRESSES

	CASE 1	CASE 2	CASE 3
STRESSES (PSI)	STIFFENER DIRECTION t _{Be} = 0.376 IN.	TRANSVERSE DIRECTION t _{Be} = 0.040 IN.	TRANSVERSE DIRECTION t _{Be} = 0.040 IN. WITH SPRING SUPPORT
PRINCIPAL TENSILE	77	140	122
PRINCIPAL COMPRESSIVE	-89	-100	-24
SHEAR	39	31	30
LONGITUDINAL NORMAL TENSION	74	140	122
	27	3	11



55 A

(an extreme case for the transverse direction). A more realistic third case in this direction was analyzed which considered the spring supports provided by the longitudinal stiffeners.

A final comment must be made on these results and their associated failure modes. The presence of a small normal compressive stress at the same location as a large longitudinal tensile stress as shown in Fig. 2.3-10e would not be expected to affect LI-1500 allowables so that the uniaxial strong-direction tensile allowable given in Table 6.2-1 could be used for design. However, this conclusion does not necessarily apply to the combined normal stress/shear stress state near the ends of the tile; hence, combined stress testing is necessary to establish the interactive effect of these stress components on LI-1500 failure. Preliminary results of such testing are discussed in Section 2.5.

Beam-Column Effect on RSI Stresses

To account for the magnification of deflections and bending moments in the RSI panel when a compressive in-plane load acts in conjunction with a uniform pressure field, several runs were made for the worst case shown in Table 2.3-6. This is panel No. 3 for which a linear analysis predicts a maximum deflection of 0.016 in., whereas the nonlinear beam-column solution shows that this value is actually amplified by a factor of 5.2 giving a result of 0.087 in. To account for this increase in deflection in the 2-D linear WILSON analysis of the RSI tile, several runs were made in which the pressure applied to the panel was multiplied by this factor. Clearly, such a procedure would lead to higher than actual stress levels; however, as seen from Table 2.3-5, the stress levels are still very low and indicate that beam-column bending effects on the RSI tile are overshadowed by the in-plane strain effects.

Table 2.3-6

SIMULATED BEAM COLUMN DEFLECTION

ALUMINUM TEST PANEL NO. 3, AREA 1

	P = 6000 PPI		
	P = 11.7 COLL	P = 11.7 BURST	P = 2.25 BURST
LI-1500 MAX STRESSES (PSI)			
PRINCIPAL TENSION	13	15	14
PRINCIPAL COMPRESSION	-37	-45	-35
SHEAR (RZ)	15	8	9
MAX SHEAR	16	20	17
LONG. (TENSION)	11	15	13
LONG. (COMPR)	-28	-45	-35
PEEL	6	13	5
RTV-560 MAX STRESSES (PSI)			
PRINCIPAL TENSION	8	13	8
PRINCIPAL COMPRESSION	-25	-6	-10
SHEAR (RZ)	12	8	9
MAX SHEAR	13	8	9
LONG. (TENSION)	2	4	0
PEEL	7	-3	0
MAX COATING STRESSES (PSI)			
PRINCIPAL TENSION	16	434	196
PRINCIPAL COMPRESSION	-154	0	0



2.4 DYNAMIC ANALYSIS

Sonic-fatigue and flutter stability analyses are required to verify TPS panel integrity under flight loading/environment criteria. RMS stress levels are found for panel substrates due to acoustic excitation of the lowest structural mode. The methodology employed is discussed in Appendix D where results for the deliverable panels are developed.

Also, flutter analyses, with results, are presented in Appendix D. These consider both the complete panel mode as well as the inter-stiffener flutter case.

2.5 COMPARISON OF METHODS WITH EXPERIMENTAL RESULTS

Thermal Analysis

Temperature predictions were performed for the 100-cycle LI-1500 tests described in Section 3, Volume I, of this report using the following groundrules and assumptions:

- a. THERM computer code
- b. One-dimensional thermal model
- c. Variation of thermal conductivity and specific heat from Tables 6.2-5 and 6.2-6, density = 15 lb/ft³
- d. Input measured surface temperature as boundary condition
- e. Adiabatic substrate
- f. 0.030 in. RTV-560 adhesive between LI-1500 and aluminum substrate

The measured temperature histories are shown in Figs. 2.5-1a, b, c, and d for the instrumented LI-1500 specimen with the 0042 coating (TT-42-6). Data are plotted for the 4th, 47th, 75th and 100th thermal cycles. The consistency and repeatability of the measured temperature data are noted in these figures. Also, the repeatability demonstrates the thermal stability of the LI-1500.

Fig. 2.5-1a shows a comparison of measured and predicted temperatures at various locations within the LI-1500. Since the specimens were bonded to 0.125 in. aluminum substrates, which were placed on a second piece of 0.125 in. aluminum, the predictions were made for two substrate thicknesses. As shown, the effect of the substrate upon the predicted temperature becomes negligible at depths between 1.3 and 2.09 in. The effect is small at a depth of 2.09 in. The predictions also were complicated by the fact that the contact resistance between the two 0.125 in. aluminum plates was not known and the adiabatic boundary condition was not met.

A summary of the peak-predicted and measured temperatures for the 4th, 47th, 75th, and 100th cycles is shown in Fig. 2.5-2., showing excellent overall correlation.

TEMPERATURE HISTORIES FOR SPECIMEN TT 42-6
DURING 100 CYCLE TESTS

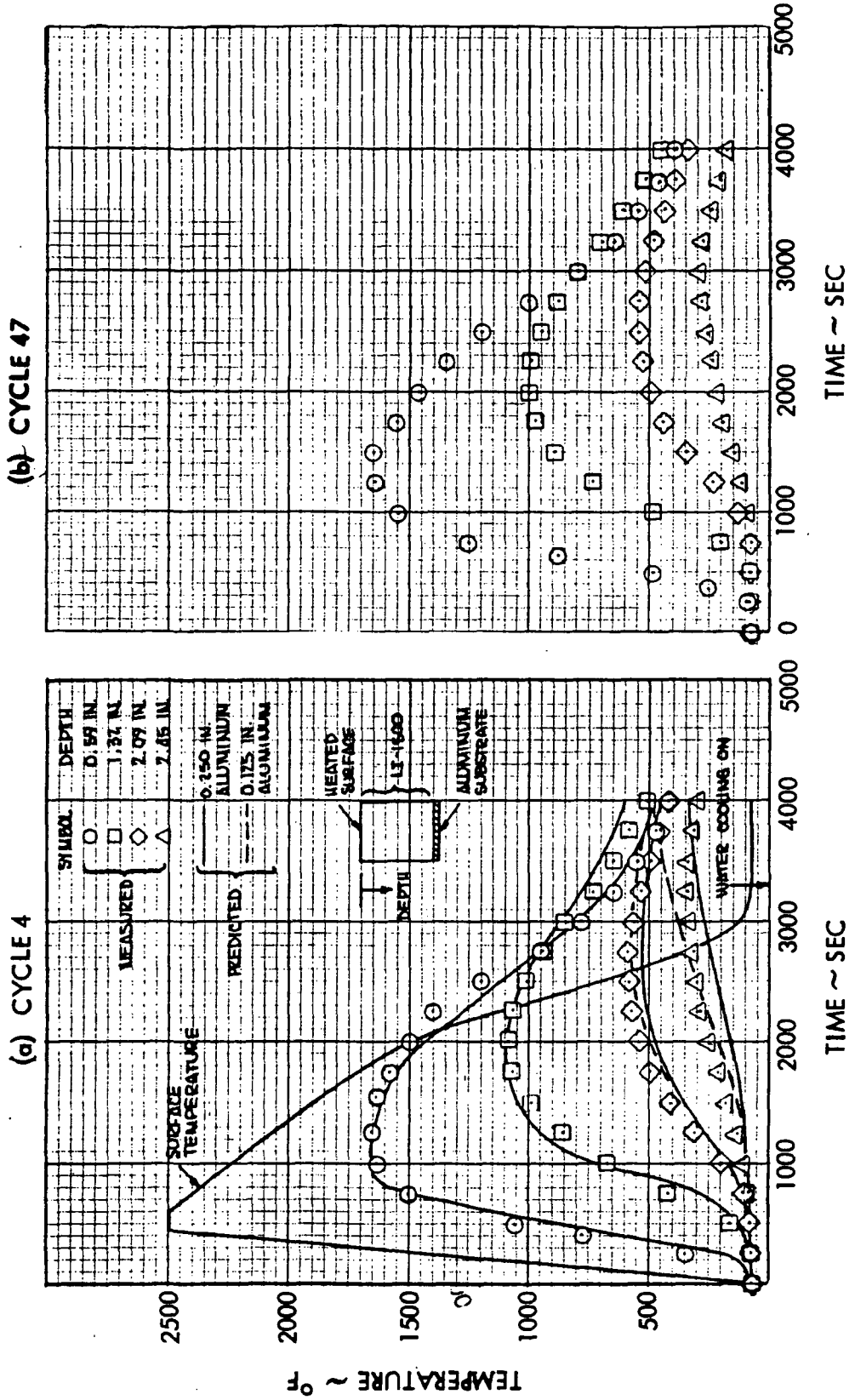


Fig. 2.5-1

DO6156

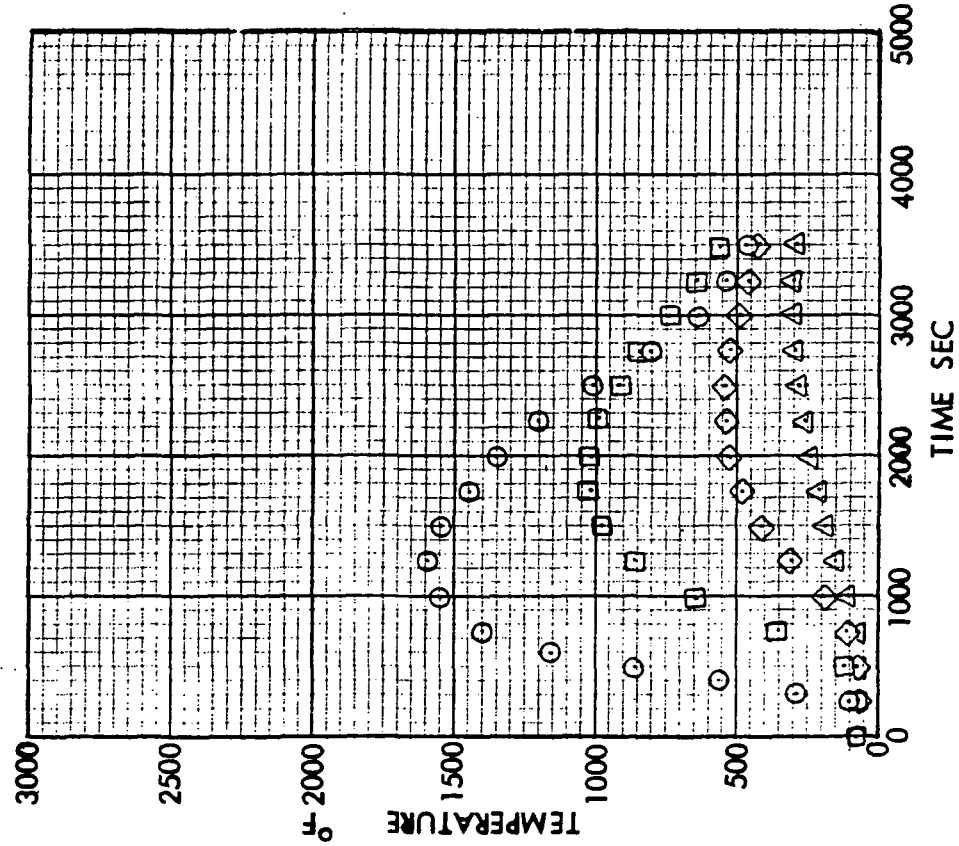
60

2.5-2

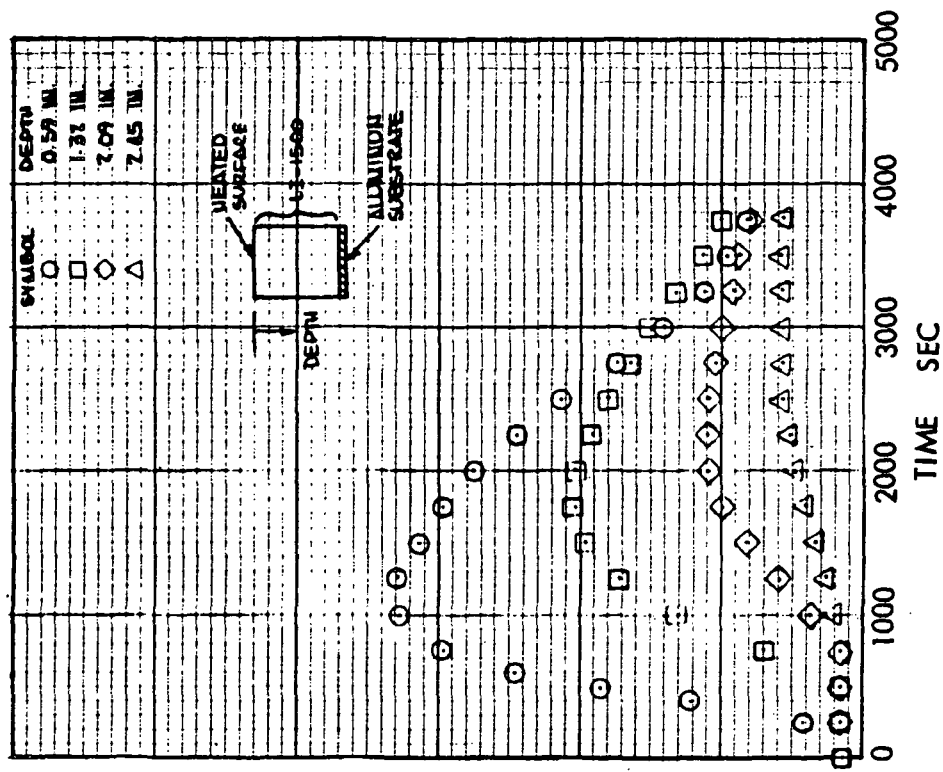
TEMPERATURE HISTORIES FOR SPECIMEN TT 42-6
DURING 100 CYCLE TESTS



(c) CYCLE 75



(d) CYCLE 100



DO6160

Fig. 2.5-1 (Cont'd)

COMPARISON OF MEASURED AND PREDICTED PEAK TEMPERATURES FOR 100 CYCLE TESTS - SPECIMEN TT 42-6

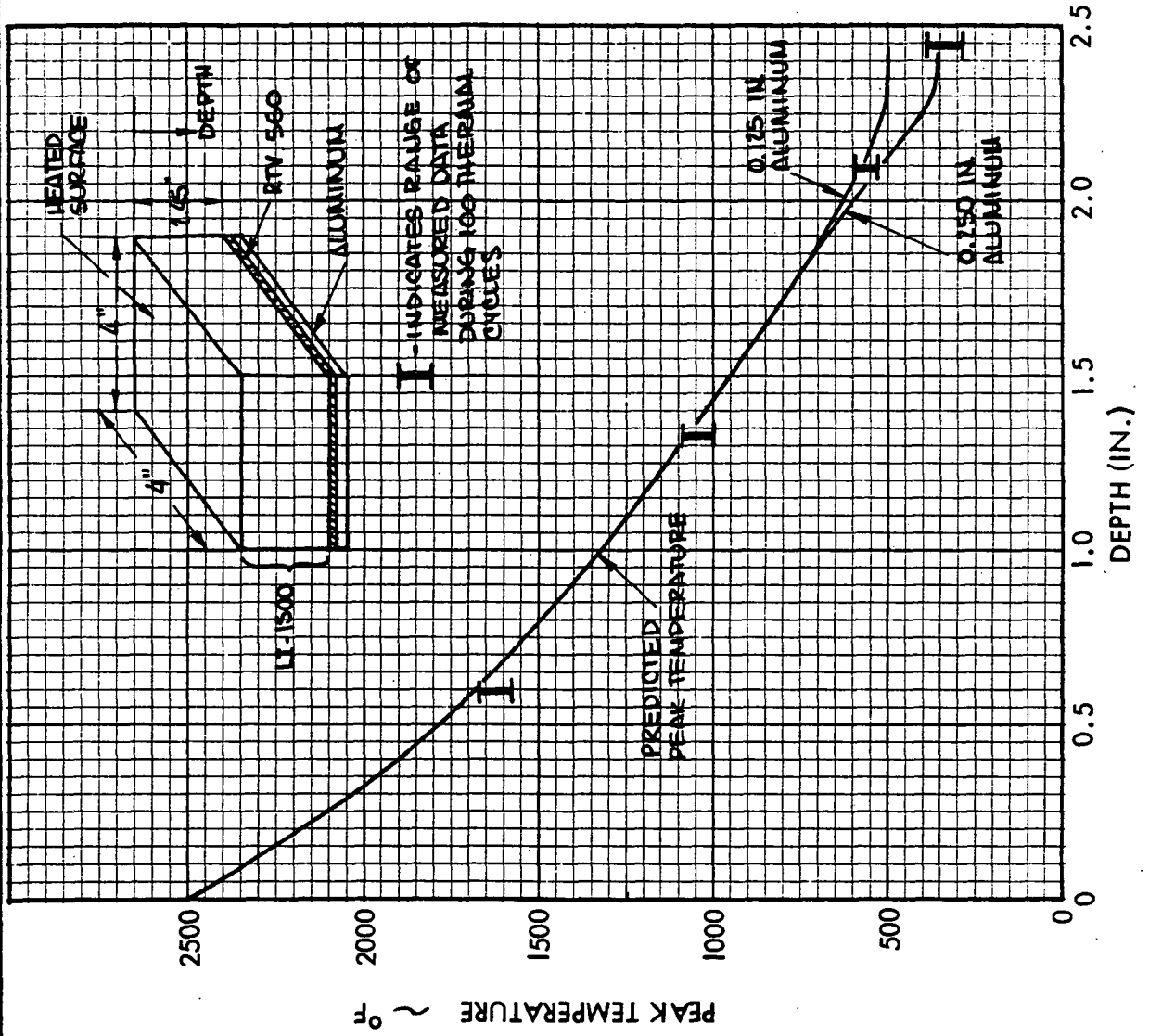


Fig. 2.5-2

Figs. 2.5-3a, b, c, and d show measured temperature histories for specimens TT-42-4, the integral silicon-carbide coated specimen, for the 4th, 47th, 75th, and 100th cycles. The first thermocouple failed sometime after the 47th cycle, and no data are shown for the 75th and 100th cycles.

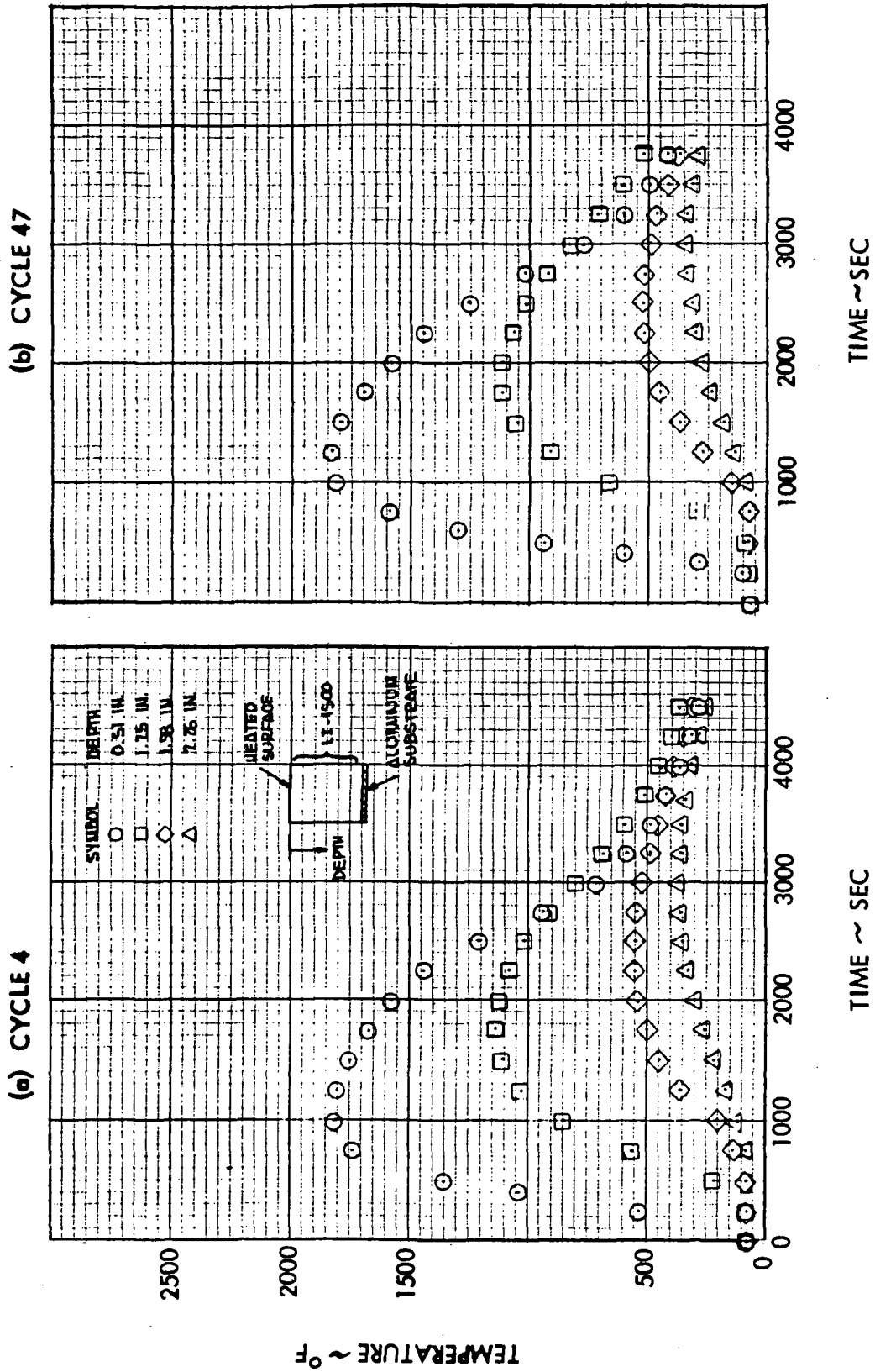
The excellent repeatability of the measured data is also shown in Fig. 2.5-4 where the peak measured temperatures for the 4th, 47th, 75th, and 100th cycles are compared to the predicted values.

Even after 83.3 hours of accumulated thermal exposure with about 4.17 hours at the peak temperature of 2500°F and 14 hours above 2300°F, the use of the as-fabricated thermal conductivity values results in good agreement between the measured and predicted temperatures for both instrumented specimens TT-42-4 and TT-42-6.

RSI Failure Analysis

Potential failure mode characteristics of the LI-1500 coating and attachments are to be identified through both testing efforts and analytical investigations. The efforts performed under this task have concentrated on the overstress mechanical and thermal loading of the composite TPS as a primary failure mode. However, under actual flight conditions, the LI-1500 will be subjected to combined stresses, and the value of uniaxial allowable results are somewhat questionable for the actual use conditions. To become fully acquainted with a new material's capabilities, it is necessary to first establish its uniaxial properties. Once these properties are established, combined stress states must be investigated. Although LMSC is not completely satisfied with the uniaxial results and realizes more data points are required, a series of combined shear and tension tests have been performed in an effort to determine the allowables in the weak shear/tension directions (i. e., shear parallel to the fiber-orientation direction and tension normal to the fiber-orientation direction). This particular combination of stress components is one critical design condition and occurs near the ends of a tile. Room temperature tests were performed in the torsion tester (described in Section 4 of Vol I) through a modification of the test fixture that allowed a predetermined tension load to be put on the shear specimens prior to application of the torque load.

TEMPERATURE HISTORIES FOR SPECIMEN TT 42-4 DURING 100 CYCLE TESTS



DO6154

Fig. 2.5-3

TEMPERATURE HISTORIES FOR SPECIMEN TT 42-4
DURING 100 CYCLE TESTS (CONTINUED)

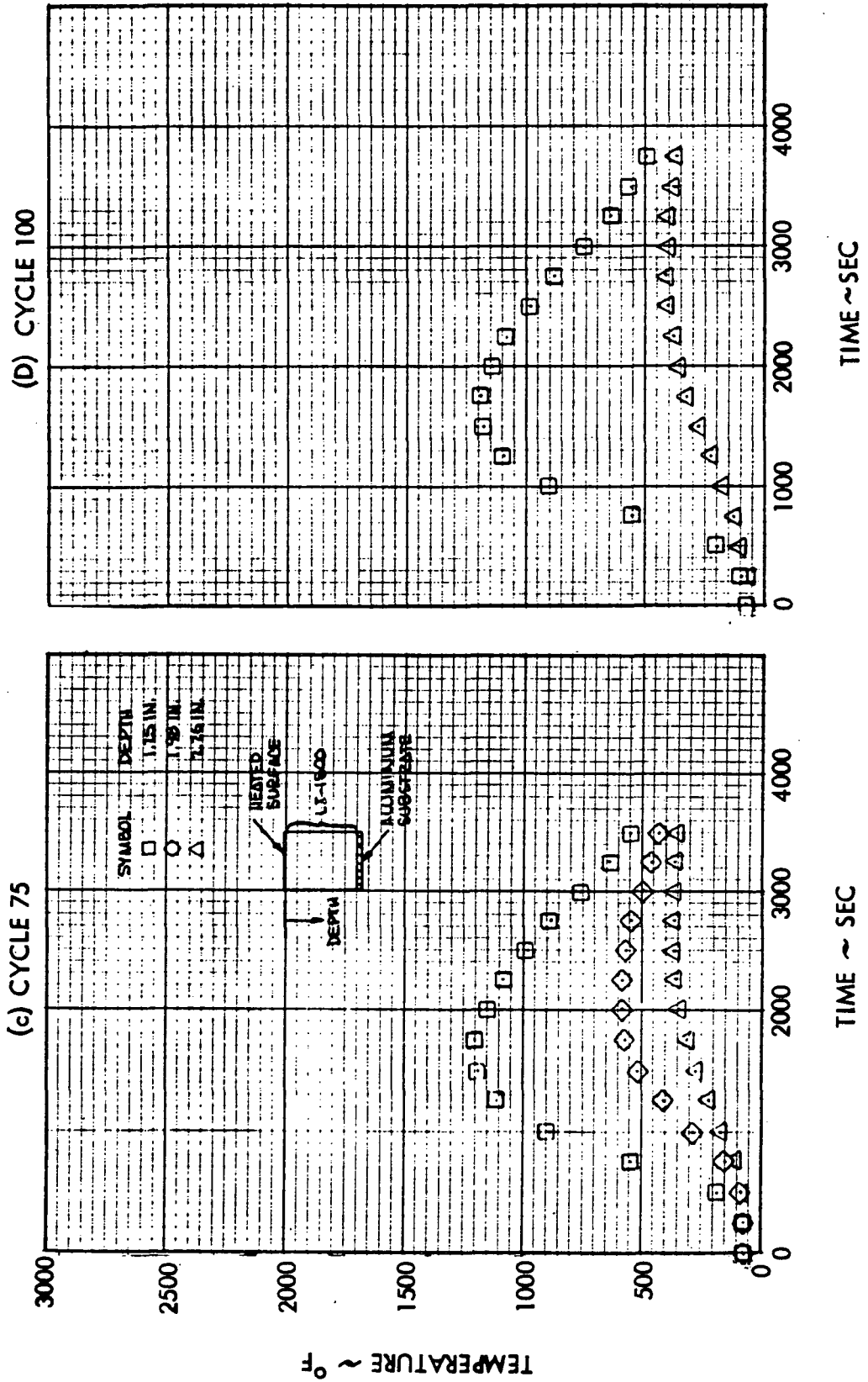


Fig. 2.5-3 (Cont'd)

COMPARISON OF MEASURED AND PREDICTED PEAK TEMPERATURES FOR 100 CYCLE TESTS - SPECIMEN TT42-4

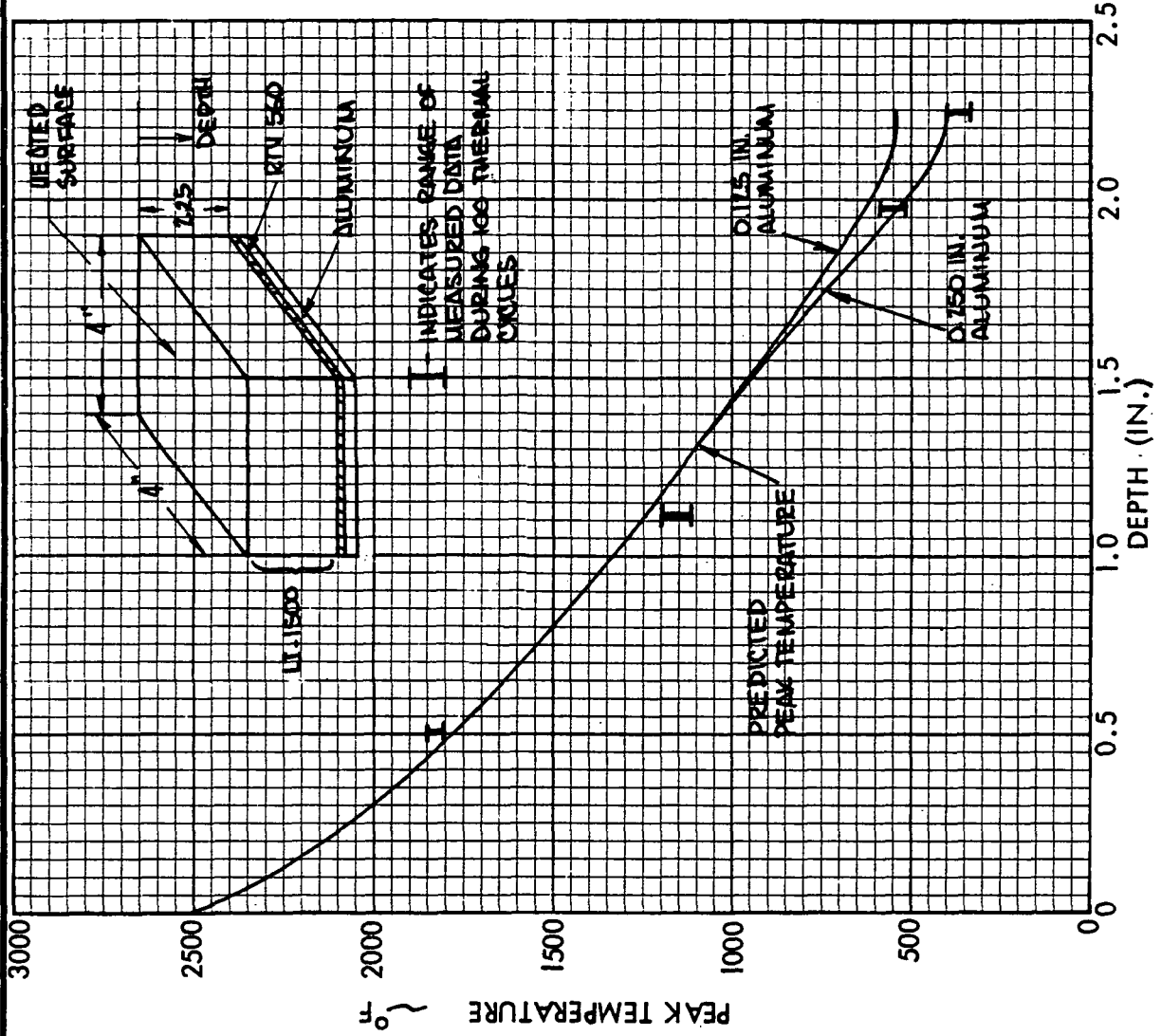


Fig. 2.5-4



DO6097

66<

Of course, the results of these tests suffer from the same conditions of nonuniformity of the state-of-stress as discussed in Section 4 of Vol I. However, the results provide lower bounds on the failure envelope and offer preliminary guidelines for future work.

Ideally, such tests should be carried out on thin-walled cylinders in a combined tension-torsion mode; however, due to basic LI-1500 characteristics, such cylinders would have to be at least 4-in. long with a 3 to 4 in. outer diameter and a 3/8-in. wall thickness, minimum. Such dimensions would require large quantities of LI-1500, and the close tolerance machining required for meaningful data might not be practical.

The results of preliminary testing are summarized in Fig. 2.5-5 and Table 2.5-1. These apply to LI-1500 of various densities for a restricted range of weak direction tension σ , which was dictated by test apparatus limitations for the denser materials. The data appear to correspond to a linear failure criterion, which is not precluded by any theoretical considerations but seems to indicate a large degree of interaction between these stress components. By way of contrast, no interaction would be characterized by a rectangular profile joining the uniaxial allowables.

To demonstrate the combined shear/normal stress failure mode and verify analytical techniques, a test specimen has been fabricated and tested. Fig. 2.5-6 shows a schematic of the test specimen, which consists of two small LI-1500 tiles (with the 0042 coating) bonded to an aluminum substrate. The bonding agent is RTV-560 and was sized to 0.020-in. thickness to ensure LI-1500 overstress conditions at loads below the aluminum yield.

A stress analysis was performed, using the methods discussed in Section 2.3 for tensile loads in the aluminum plate. The specimen was then pulled to a load sufficient to severely damage the LI-1500, and the results of this test are shown in Fig. 2.5-7.

Photographs of the specimen (before and after) are shown in Fig. 2.5-8a and b, while acoustic emission data for the test are shown in Fig. 2.5.9. The spike in the center

PRELIMINARY INTERACTION DATA

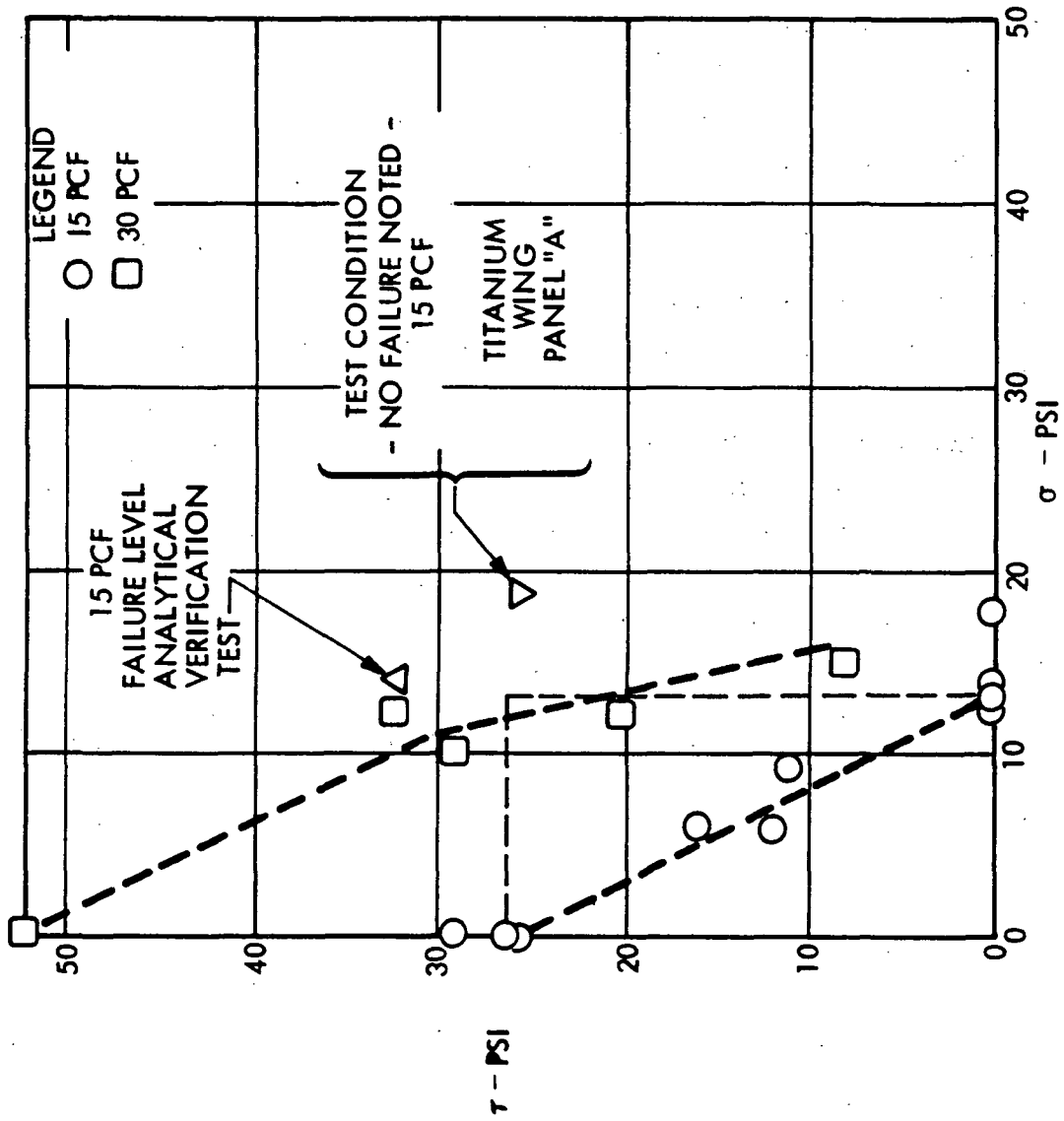


Fig. 2.5-5



DO6024

Table 2.5-1
RESULTS OF LIMITED BIAXIAL TESTING



LI-1500 Density	σ_{ult} (psi)	τ_{ult} (psi)
15 pcf	0	25
	0	26
	0	29
	6	16
	6	12
	9	11
	13	0
	14	0
	14	0
30 pcf	18	0
	0	52
	10	29
	12	32
	12	20
55 pcf	15	8
	10	100
	15	80
	20	76
	20	96
60 pcf	20	92
	15	58

ANALYTICAL VERIFICATION MODEL

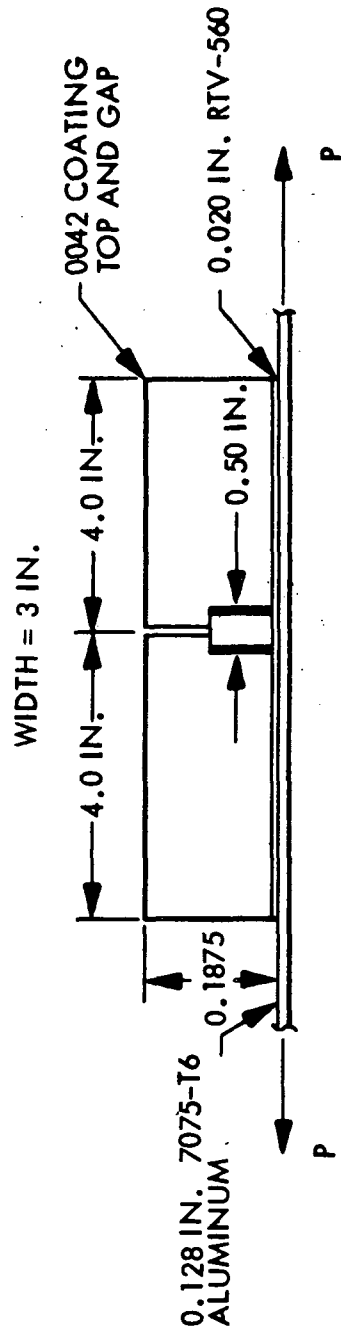


Fig. 2.5-6

D07138





LI-1500 STRESSES AS A FUNCTION OF LOAD - ANALYTICAL VERIFICATION TEST

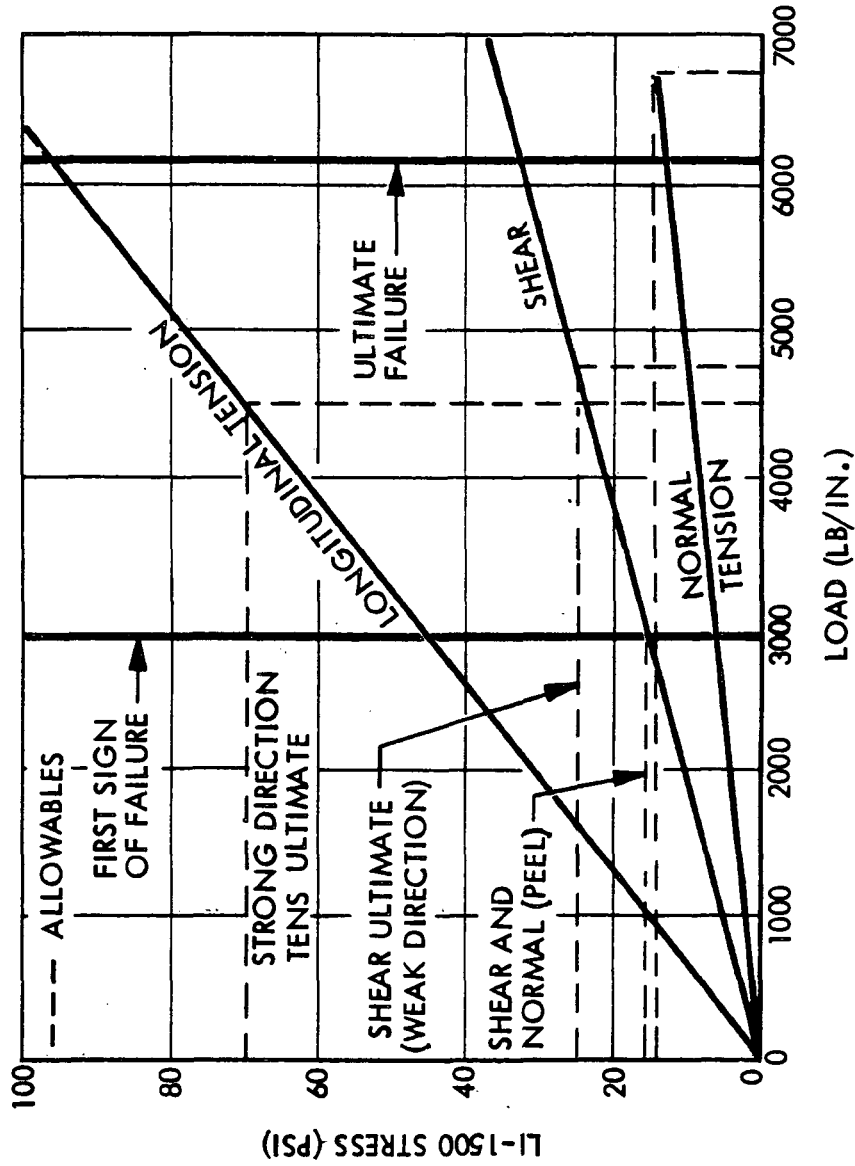
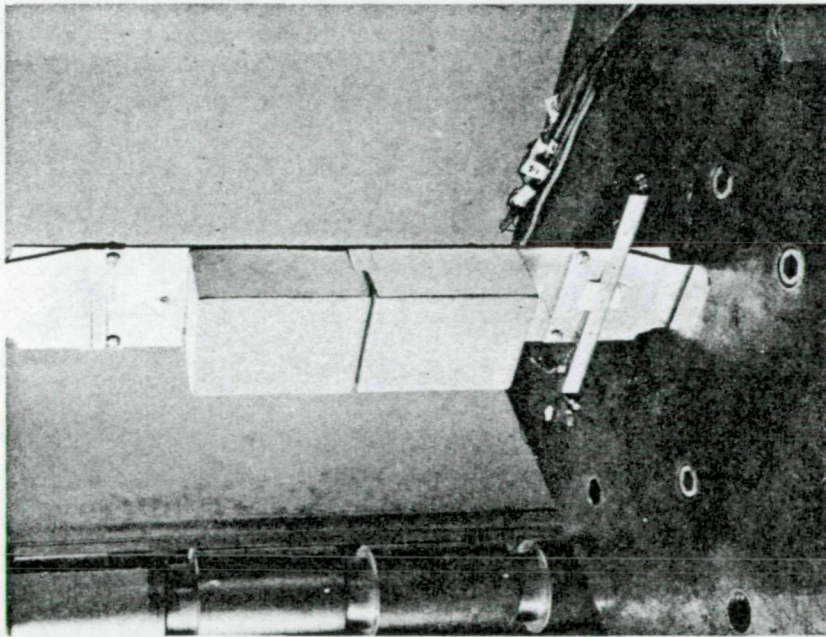


Fig. 2.5-7

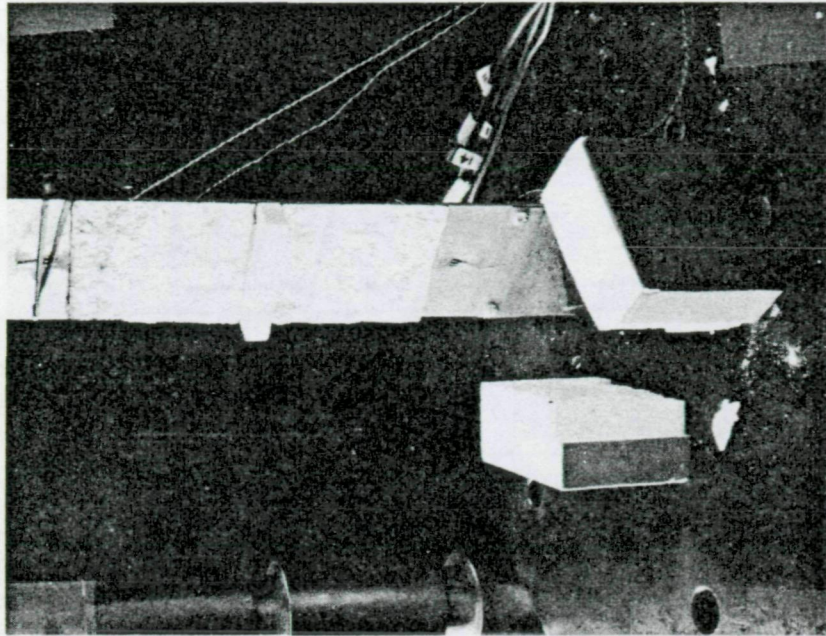


TEST OF ANALYTICAL VERIFICATION MODEL



ANALYTICAL VERIFICATION
TEST PANEL

(a)



FAILURE MODE OF ANALYTICAL
VERIFICATION MODEL

(b)

72<



ACOUSTIC EMISSION DATA
FOR ANALYTICAL VERIFICATION MODEL

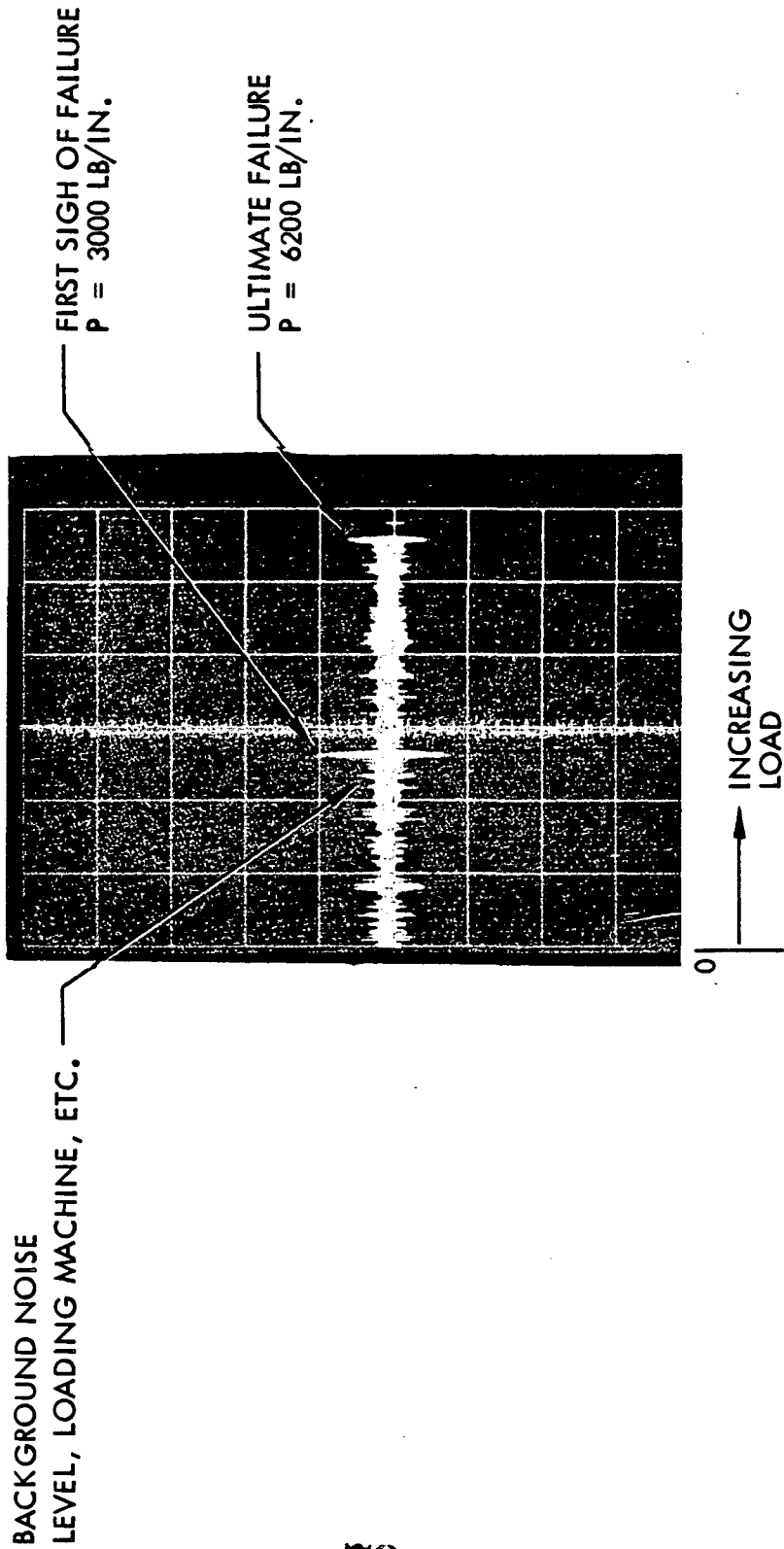


Fig. 2.5-9

of the oscilloscope trace represents the first sign of failure although no visual cracking was noted. This phenomenon was audible to test observers. As seen from Fig. 2.5-7, this spike occurred at a load corresponding to the combined shear and normal stress criterion, although the ultimate strength was not reached until twice this load. Stress levels at ultimate are recorded in Table 2.5-2, while the combined stress-failure point is shown in Fig. 2.5-5.

The test results seem to substantiate the analytical predictions in that some initial cracking evidently occurred at the predicted combined shear and peel stress allowable cutoff. However, it is rather difficult to draw conclusions on the basis of only one test.

Similar results have also been noted concerning a titanium wing panel designed under the preceding contract (NAS 9-11222). This panel withstood an axial line load equivalent to 60,000 psi with a backface temperature of 320^oF without experiencing the failure mode discussed here. ⁽²⁻¹⁾ Stress levels computed for this test are summarized in Table 2.5-3, and the state of combined stress is also shown in Fig. 2.5-5 as the point not only outside the linear interaction curve but the no-interaction curve as well.

A final example of analysis/experimental comparison concerns Aluminum Flight Panel No. 2 discussed in Section 5.1 of Volume I. The panel was safely subjected to a thermal environment alone and the corresponding maximum stress levels predicted by a 2-D WILSON analysis are shown in Table 2.5-4. Comparison of the shear/normal stresses of this table with the linear interaction curve of Fig. 2.5-5 shows that the associated stress point falls inside the line in this case.

It is concluded that more testing must be conducted for analytical verification and failure mode analysis.

⁽²⁻¹⁾ Data according to NASA document ES65-9/2/71-099 supplied by ES6/Chief, Structural Test Branch, G. E. Griffith



Table 2.5-2

ANALYTICAL VERIFICATION TESTS

SUMMARY OF ANALYTICAL PREDICTIONS
RESULTS OBTAINED BY TWO-DIMENSIONAL WILSON CODE

LOADING = 48,400 PSI (6200 LB/IN.)

MAX. LI-1500 STRESSES

PRINCIPAL TENSION = 97 PSI
PRINCIPAL COMPRESSION = -13 PSI
SHEAR (COMPONENT) = 32 PSI
MAX. SHEAR = 50 PSI
LONGITUDINAL (TENSION) = 97 PSI
NORMAL (TENSION) = 12 PSI

MAX. RTV-560 STRESSES

PRINCIPAL TENSION = 46 PSI
PRINCIPAL COMPRESSION = -23 PSI
SHEAR (COMPONENT) = 32 PSI
MAX. SHEAR = 32 PSI
LONGITUDINAL (TENSION) = 10 PSI
NORMAL (TENSION) = 18 PSI

MAT. PROPERTIES USED IN THE ANALYSIS:

	E ₁ (PSI)	E ₂ (PSI)	μ	G (PSI)
LI-1500	60,000	6000	.3	4150
RTV-560	300	300	.5	100
7075-AL	10.5 x 10 ⁶	10.5 x 10 ⁶	.3	4.2 x 10 ⁶



Table 2.5-3
CALCULATED STRESS LEVELS IN TITANIUM WING PANEL*

TILE SIZE	6 IN.	SHEAR LI-1500	26
TEMPERATURE SURFACE	75°F	LONGITUDINAL LI-1500	74
TEMPERATURE TI	320°F	σ Z (TENS) LI-1500	19
AXIAL LOAD	60,000 (TENS)	σ Z (COMP) LI-1500	-4
PRESSURE	0	MAXIMUM RTV	34
E_{COAT}	3.5×10^6 PSI	MINIMUM RTV	-19
$T_{LI-1500}$	0.71 IN.	SHEAR RTV	22
T_{RTV}	0.056 IN.	LONGITUDINAL RTV	-9
T_{TI}	0.19 IN.	PEEL RTV	19
MAXIMUM LI-1500	74	MAXIMUM COATING	594
MINIMUM LI-1500	-3	MINIMUM COATING	-50

* ALL STRESS VALUES IN PSI



12-IN. TITLE, ALUMINUM FLIGHT PANEL NO. 2

LOADING: GROUND CONDITION (BACKFACE TEMP = 300°F)

MAX STRESSES (PSI)

<u>LI-1500</u>	
PRINCIPAL TENSION	40
PRINCIPAL COMPRESSION	-26
SHEAR	12
LONGITUDINAL TENSION	40
LONGITUDINAL COMP	-26
NORMAL TENSION	7
NORMAL COMPRESSION	-4
<u>RTV-560</u>	
PRINCIPAL TENSION	14
PRINCIPAL COMPRESSION	-12
SHEAR (R2)	11
PRINCIPAL SHEAR	12
LONGITUDINAL	-7
NORMAL TENSION	6
<u>COATING (E = 9.1 x 10⁹)</u>	
PRINCIPAL TENSION	4
PRINCIPAL COMPRESSION	-354

Section 3
PARAMETRIC STUDIES

Variables of both material and application must be considered in the methodology effort. This section presents the studies performed by LMSC considering the variables expected to influence TPS design. Variations due to the following parameters are presented:

- Thermophysical/Mechanical Property Variations
 - a. Substrate Material Parametric Studies
 - b. Effect of LI-1500 Conductivity on Required LI-1500 Thickness
 - c. Coating Modulus Effects on RSI Stress Levels
 - d. Effect of LI-1500 Modulus on RSI Stress Levels
 - e. Effects of Bond Moduli Variation on RSI Stress Levels
 - f. Integral Coating Concept
 - g. Effects of Thermal Cycling on LI-1500
- Design Details Variations
 - a. Substrate Configuration Parametric Studies
 - b. Effect of Bond Thickness on Required LI-1500 Thickness
 - c. Effect of Coating Thickness on RSI Stress Levels
 - d. Stress Variations due to LI-1500 Thickness
 - e. Bond Thickness Effects on Stress Levels
 - f. Gap and Joint Studies
 - g. Effects of Coating Texturing and Discontinuities on RSI Stress Levels
 - h. Effects of Partial Bonding and Bond Discontinuities on RSI Stress Levels
 - i. Mechanical Fastener Study

- j. Tile Size Influence on RSI Stress Levels
 - k. Effects of Different Coating Configurations on RSI Stress Levels
 - l. RSI Tile Bonded to Corrugated Substrate
 - m. Effect of Tile Size on Coating Weight
 - n. Strain Arrestor Plate
 - o. Lightweight Core Concept
 - p. Effect of Contact Conductance on Stiffener Temperatures
 - q. Effect of Discontinuous Bond on Substrate Temperatures
 - r. Thermal Analysis of FI-600 Filler Strip
- Environmental Variations
 - a. Coating Stress During Reentry
 - b. Orbital Cold Soak Condition

It should be noted that substrate thicknesses listed with stress analyses in the studies are based on the bending stiffness of the substrate. This is in contrast to the effective thickness based on weight which is used in the thermal analyses.

Application of RSI to both subpanels and primary structure is considered. The important variables examined here are listed in Table 3.0-1 while the results of the studies are summarized in Section 3.4.

Table 3.0-1

PARAMETRIC VARIABLES



- SUBSTRATE
- MATERIAL/TEMPERATURE
- CONFIGURATION
- SIZE/SPAN
- LOADS
- WEIGHT
- JOINTS
- GAP SIZE
- JOINT TYPE
- SURFACE COATING
- MATERIALS/PROPERTIES
- TEXTURING
- DISCONTINUITIES
- THICKNESS
- WEIGHT
- ATTACHMENT
- MECHANICAL/BONDING
- PROPERTIES
- LOADS
- WEIGHT
- LI-1500
- PROPERTIES
- TILE SIZE
- TILE THICKNESS
- TILE/ATTACHMENT INTEGRATION
- LOADS
- WEIGHT

3.0-3



3.1 THERMOPHYSICAL/MECHANICAL PROPERTY VARIATIONS

Substrate Material Parametric Studies

To provide insight into the selection of materials for optimum subpanels and primary structure weight, ratios can be presented in the form:

$$\frac{W_x}{W_i} = \frac{\rho_x}{\rho_i} \left(\frac{\bar{\eta} \cdot E_i}{\eta \cdot E_x} \right)^{\frac{1}{n}}$$

where

W = $\bar{t} \cdot \rho$ = weight per unit surface area

\bar{t} = weight - equivalent flat - plate thickness

ρ = material density

$\bar{\eta}$ = E_T/E

E_T is the tangent modulus at a stress level corresponding to a given constant axial line load. The value of the exponent n is usually 2.0 for conventionally stiffened configurations composed of straight elements but is smaller for configurations with curved elements.

This equation, which corresponds to wide column structural optimization data (see Section 3.2), may be rewritten using beryllium as the base material:

$$\frac{W_x}{W_{Be}} = \frac{\rho_x}{\rho_{Be}} \left(\frac{E_{T_{Be}}}{E_{T_x}} \right)^{\frac{1}{n}}$$

Beryllium has been used for convenience in presenting the results as it turns out to be a lower bond for the other materials considered. The above form of the equation permits the comparison of a number of materials in both the elastic and plastic stress ranges for a given value of n . Using $n = 2$, the results shown in Figs. 3.1-1 and 3.1-2 are obtained. These figures have been developed for room temperature and 600°F material properties, respectively.



BERYLLIUM - BASED WEIGHT RATIOS FOR ELASTIC-PLASTIC CONVENTIONALLY STIFFENED WIDE COLUMNS AT ROOM TEMPERATURE

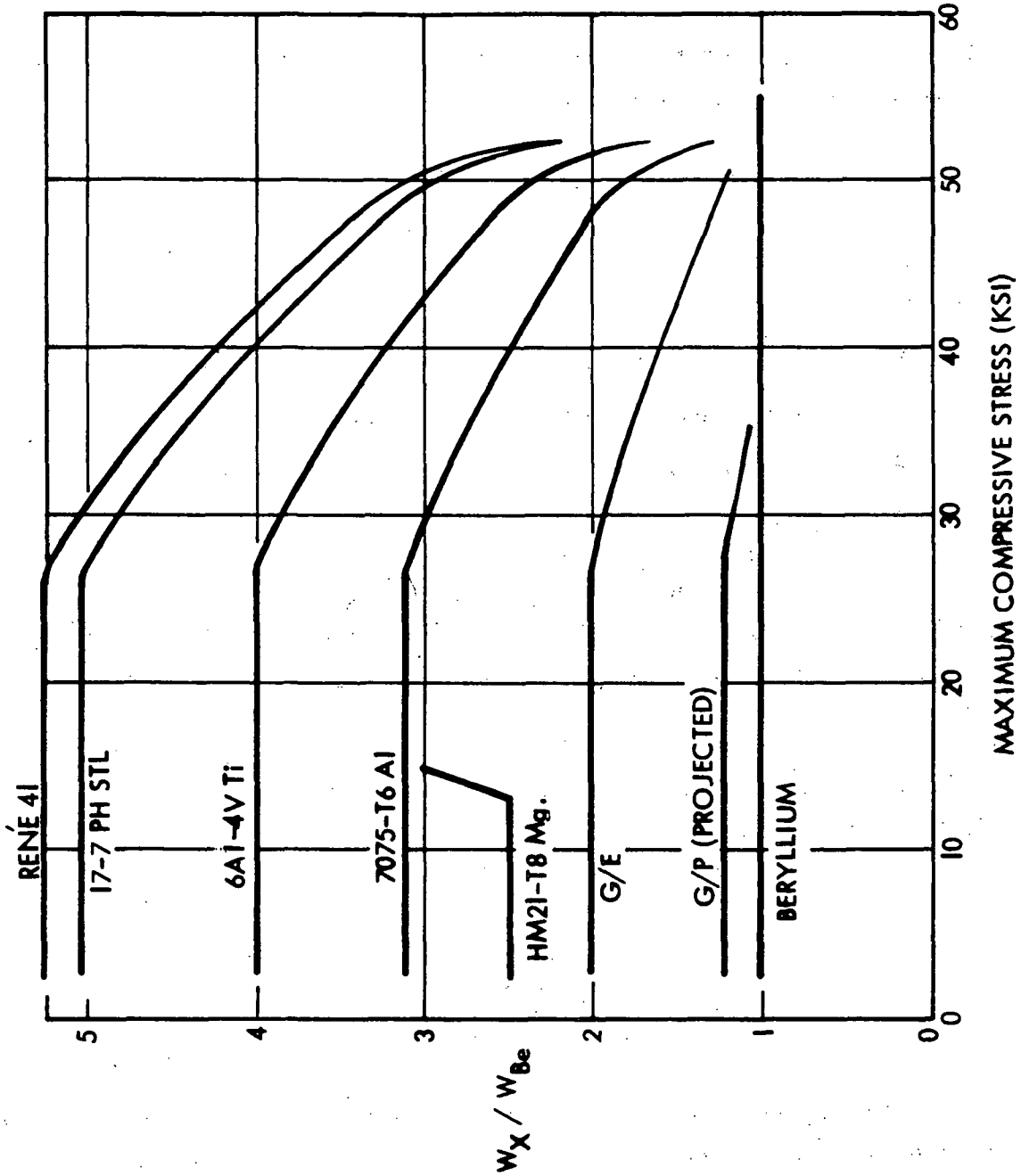


Fig. 3.1-1

DO6027

BERYLLIUM - BASED WEIGHT RATIOS FOR ELASTIC-
PLASTIC CONVENTIONALLY STIFFENED WIDE COLUMNS
AT 600°F

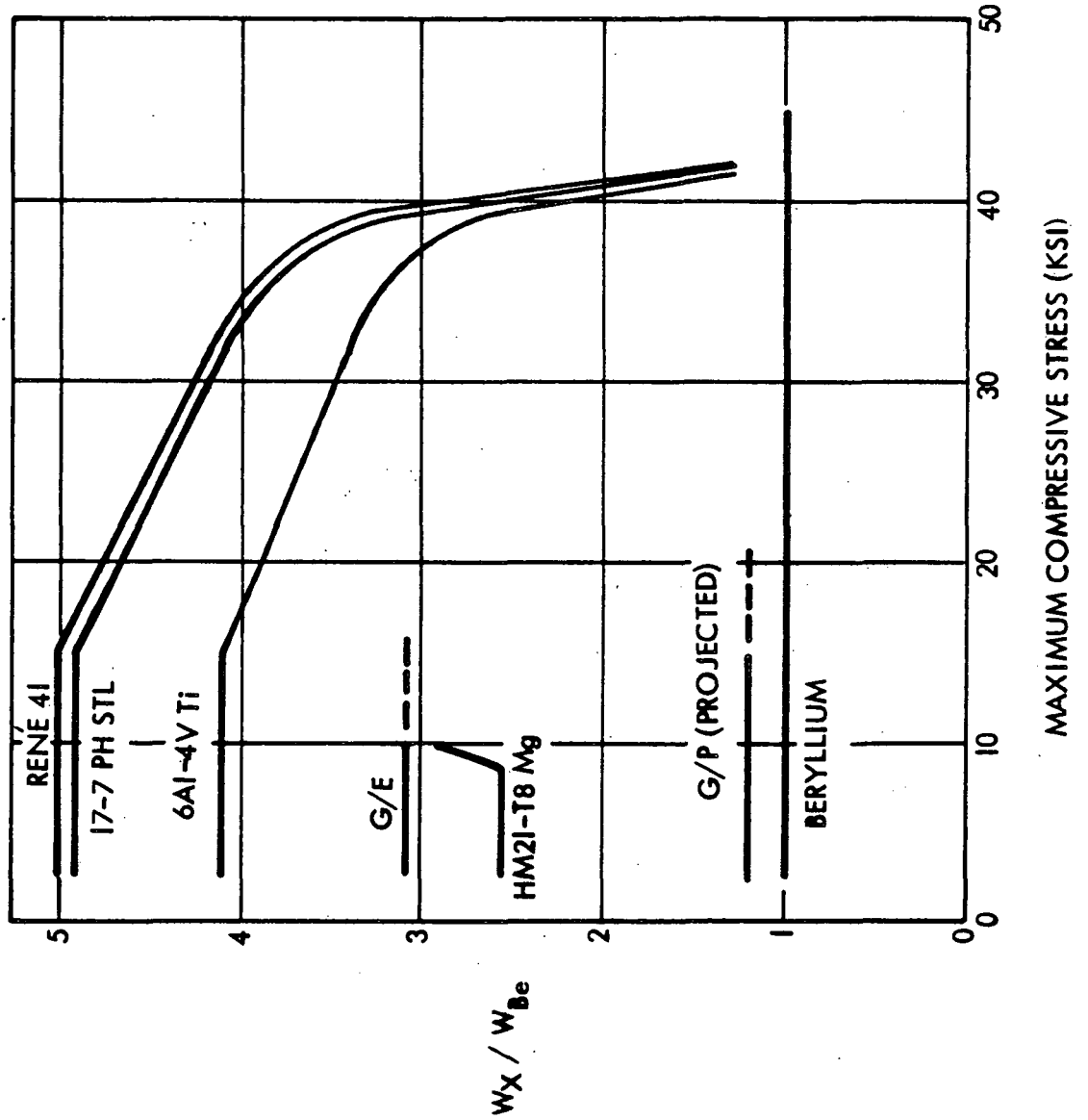


Fig. 3.1-2

Parallel lines in the figures represent complimentary areas of elasticity in the materials while curved lines represent plasticity effects. The majority of the curved lines are in a downward direction indicating plasticity in the beryllium. The lone exception is HM21A-T8 magnesium, curving upward, indicating plasticity in the magnesium at corresponding stresses in the beryllium which are elastic. It is clear from the figures that beryllium is the most efficient material among those studied when the optimum stress is below the proportional limit for beryllium. At optimum stresses above this point, beryllium's advantage drops off rather rapidly.

The data of Figs. 3.1-1 and 3.1-2 must of course be interpreted qualitatively inasmuch as subpanels and primary structure panels are not classed as wide columns. However, in primary structure panels the difference lies only in the added bending due to air loads; thus, it would seem logical to view these figures in terms of the maximum outer fiber compressive stress rather than a uniform compressive stress. The same analogy may be applied to subpanels.

In the case of primary structure panels under moderate axial loads (1500-3000 ppi), the stress corresponding to optimum design for panel lengths of about 25 in. is above the proportional limit for beryllium. The additional compressive stress due to bending under air loads essentially eliminates beryllium from consideration due to the high degree of plasticity. Figure 3.1-1 shows that fibrous graphite systems are better candidates in these applications at room temperature, followed by aluminum, titanium, and steels in that order. For immediate design use, aluminum and titanium are prime choices.

The situation with regard to subpanels is different in that the total compressive stress is due to bending from airloads. In this case, stresses for optimum design, while usually in the plastic range for beryllium, are sufficiently low that beryllium is the best choice of material. The stress level for optimum design is controlled to some degree by the constraint on maximum deflection which prevents shallow, highly stressed designs. The curves in Figs. 3.1-1 and 3.1-2 show that graphite polyimide is projected to be very competitive with beryllium in this application; however, LMSC does not consider G/P to be a production material at the present time due to lack of test data and problems of quality control.

3.1-4

84<

it is of interest to note that charts of this type show greater spread between curves when drawn to represent more efficient structural configurations. ⁽³⁻¹⁾ Thus, the position of beryllium in the elastic stress range improves relative to other materials for configurations without flat sheets (see Fig. 3.2-1).

Effect of LI-1500 Conductivity on Required LI-1500 Thickness

As noted from Fig. 3.1-3, at 2000^oF the vacuum thermal conductivity of LI-1500 is about 45 percent of the 1 ATM value. Hence, the sizing for flight panels assumes that the pressure within the LI-1500 during entry equals the local static pressure at the edge of the boundary layer (see Section 6.3). During entry, a pressure lag will probably exist, allowing the actual pressure within the LI-1500 to lag the local static pressure; therefore, use of the local static pressure will result in conservative LI-1500 thickness requirements.

Figure 3.1-4 shows a comparison of the LI-1500 thickness requirements for a beryllium flight and 1 ATM test panel. The flight panel results were obtained using the temperature and pressure histories for Area 2 (shown in Fig. 6.3-5) to determine the thermal conductivity of LI-1500. The test panel results utilized the 1-ATM thermal conductivity values.

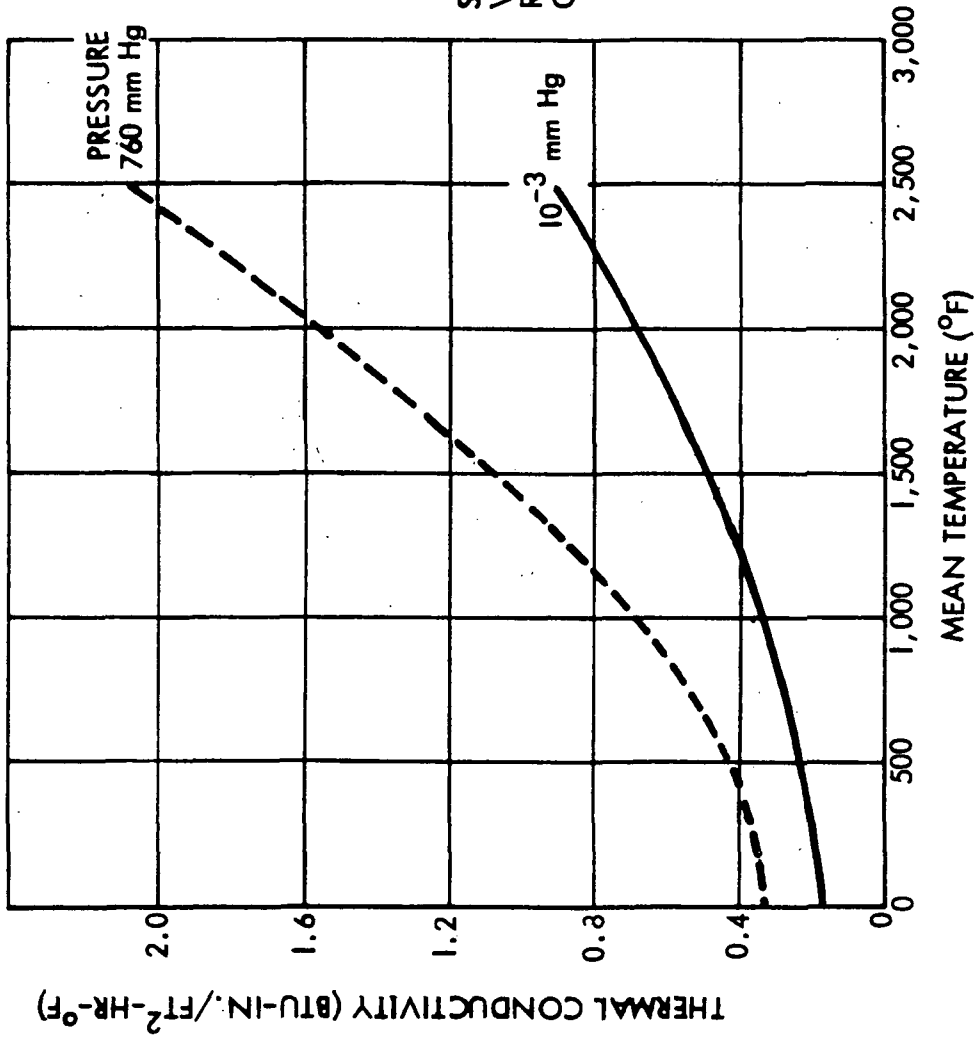
For example, with a maximum substrate temperature of 600^oF, the LI-1500 requirements are reduced about 31 percent from 2.1 to 1.45 in. of LI-1500, as seen from Fig. 3.1-4. Similar reductions can be obtained for the other three flight panels.

Table 3.1-1 shows a comparison of LI-1500 thickness and unit weight between the flight and test panels. In all cases, the flight panels require about 24 to 38 percent less LI-1500 and are 10 to 17 percent lighter in unit weight than the 1 ATM test panels.

⁽³⁻¹⁾ Crawford, R. F. and Burns, A.B., "Strength, Efficiency, and Design Data for Beryllium Structures", ASD TR 61-692, February 1962



LI-1500 THERMAL CONDUCTIVITY DESIGN DATA



SEE SECTION 4.1.3 OF
VOLUME I OF THIS
REPORT FOR SOURCE
OF DATA

Fig. 3.1-3



COMPARISON OF LI-1500 THICKNESS BETWEEN FLIGHT AND TEST PANEL

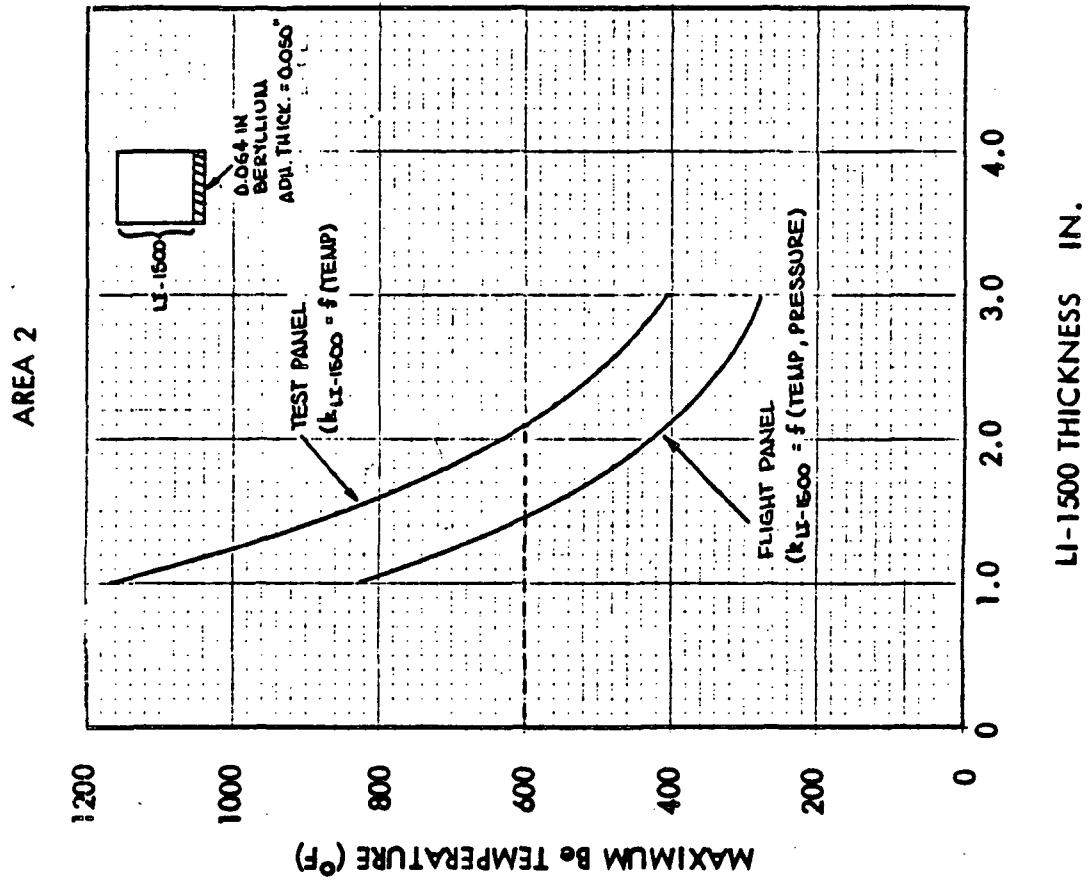


Fig. 3.1-4

Table 3.1-1

COMPARISON OF PROTOTYPE PANELS FOR TEST AND FLIGHT

Panel No.	Description	Orbiter Area	Panel Design Temp	LI-1500 Thickness~in.		Panel Unit Weight~lb/ft ²	
				Test ¹ Panel	Flight ² Panel	Test ¹	Flight ²
1	Beryllium Subpanel Application $\bar{t} = 0.064$ in., 0.090 in., RTV-560 Adhesive	2	600 ^o F	1.89	1.25	3.6 (5.2)*	2.8 (4.6)*
2	Aluminum Primary Structure Application $\bar{t} = 0.125$ in., 0.090 in., RTV-560 Adhesive	2	300 ^o F	3.34	2.52	6.6	5.7
3	Aluminum Primary Structure Application $\bar{t} = 0.154$ in., 0.090 in., RTV-560 Adhesive	1	300 ^o F	1.85	1.40	5.2	4.8
4	Titanium Primary Structure Application $\bar{t} = 0.097$ in., 0.090 in., RTV-560 Adhesive	2	600 ^o F	2.00	1.35	5.4	4.7

¹LI-1500 thermal conductivity is a function of temperature only (pressure = 1 atm)

²LI-1500 thermal conductivity is a function of temperature and pressure

*Value includes the weight of a $\bar{t} = 0.114$ in. aluminum primary structure

Coating Modulus Effects on RSI Stress Levels

Variations of coating modulus are primarily reflected in coating stress levels. The results of this study are summarized in Fig. 3.1-5 for a beryllium subpanel using an isotropic plane stress WILSON analysis. From these curves, it is apparent that the "driver" is principally the thermal loading, although the direction of the applied pressure is important. In effect, the temperature rise induces a tensile field in the coating while bending effects due to the pressure field either add or subtract from the thermal effect. These general conclusions are also representative of other panel configurations.

Effect of LI-1500 Modulus on RSI Stress Levels

The effect of varying Young's modulus for an assumed isotropic LI-1500 material is summarized in Figs. 3.1-6 through 3.1-9. These studies were carried out early in the program before anisotropic data on LI-1500 were available. Some comparisons of isotropic versus anisotropic analysis are presented in Section 2.3. The curves show increasing LI-1500 stress with increasing modulus, which is consistent with the substrate strain being the driving variable. On the other hand, the RTV-560 peel stress appears insensitive to LI-1500 modulus. As might be expected, coating stress decreases as the LI-1500 and the coating moduli tend toward each other. Finally, the maximum principal tensile stress and the maximum shear in the RTV are seen to increase with increasing LI-1500 modulus. A beryllium subpanel with a 600° F backface temperature and a 1.14-psi burst pressure was chosen for this study.

Effect of Bond Moduli Variation on RSI Stress Levels

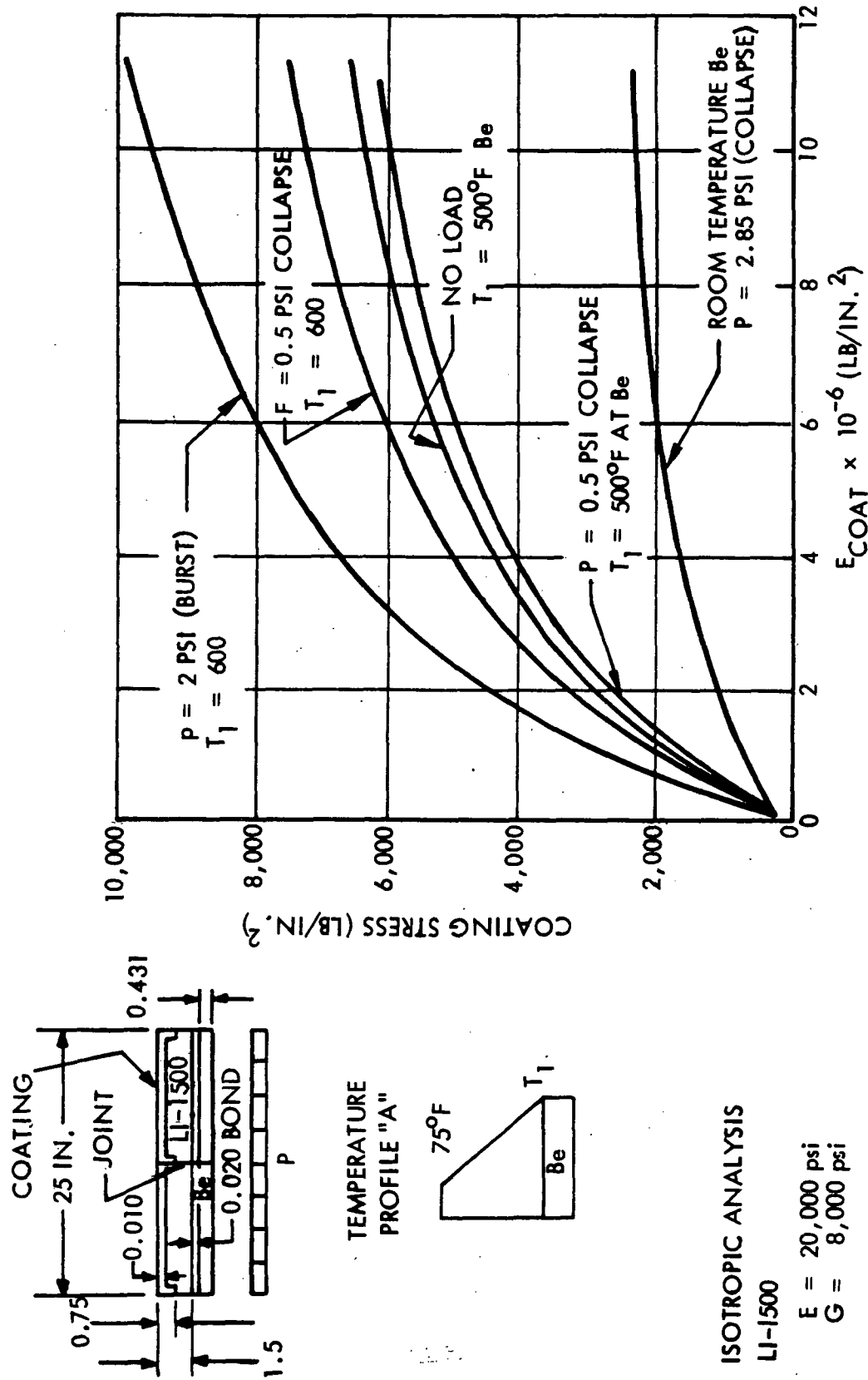
The sensitivity of RSI stresses to variations of Young's modulus, E_{RTV} , and Poisson's ratio, μ_{RTV} , are summarized in Tables 3.1-2 and 3.1-3. As would be expected, lower values of E_{RTV} provide more effective strain isolation as seen in Table 3.1-2, indicating a factor of approximately 2 in LI-1500 stresses for the values investigated. These changes amount to about 20 percent when Poisson's ratio is varied over the range chosen. It is expected that μ_{RTV} for RTV-560 is closer to 0.5, which is the

3.1-9

89<



VARIATION OF COATING STRESSES WITH COATING MODULUS



ISOTROPIC ANALYSIS
LI-1500

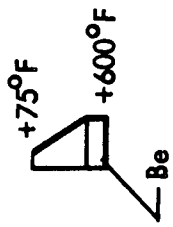
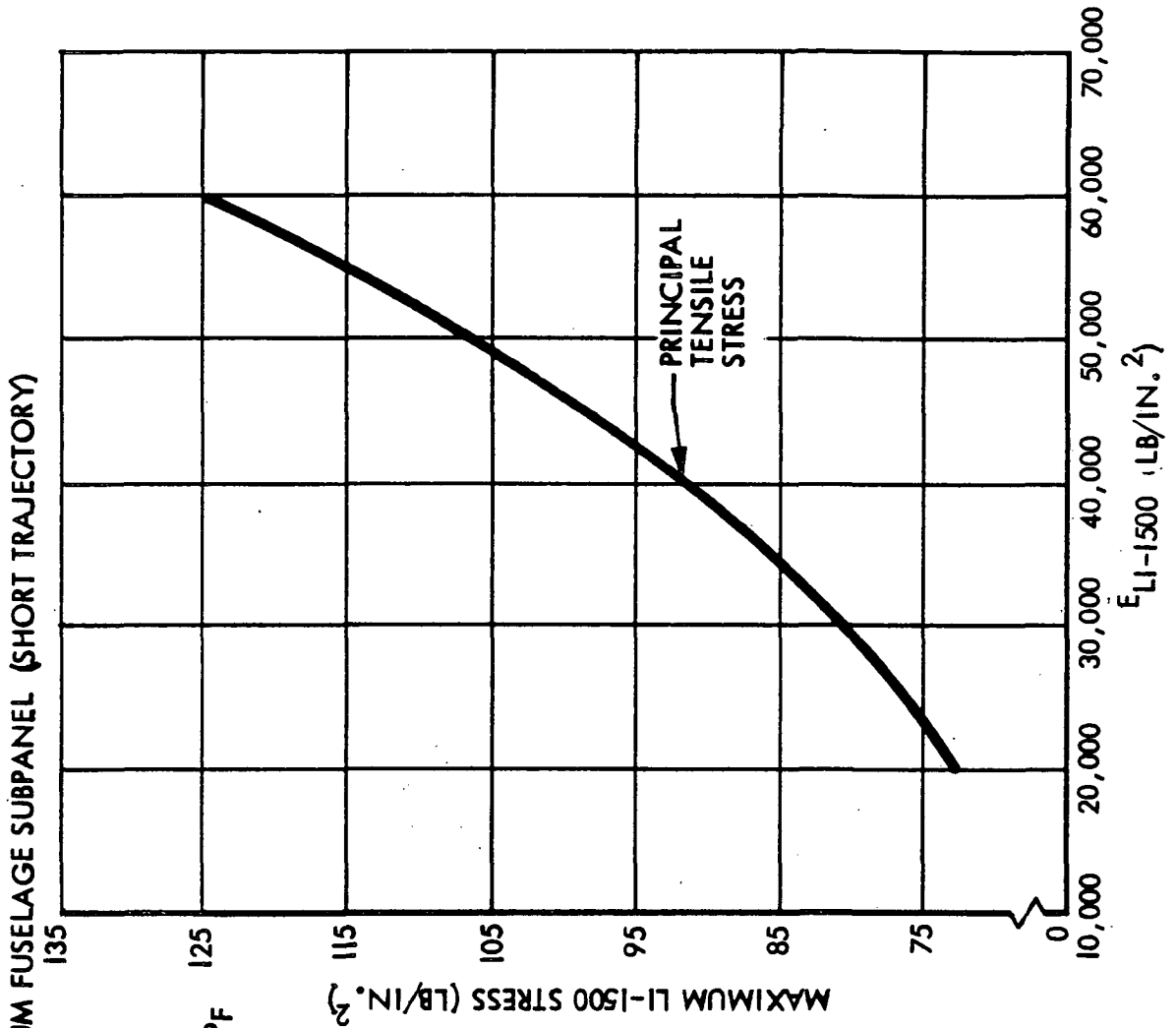
$E = 20,000$ psi
 $G = 8,000$ psi

D04956 (1)

Fig. 3.1-5



VARIATION OF LI-1500 STRESSES WITH LI-1500 ELASTIC MODULUS



TEMPERATURE PROFILE

- $t_{LI-1500}$ = 1.6 IN.
- $t_{RTV-560}$ = 0.020 IN.
- $t_{COATING}$ = 0.010 IN.
- LOADING p = 1.14 PSI BURST
- $E_{RTV-560}$ = 300 PSI
- $E_{COATING}$ = 3.5×10^6 PSI
- $G_{LI-1500}$ = 0.4E

ISOTROPIC ANALYSIS

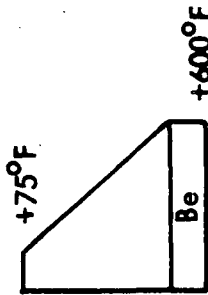
Fig. 3.1-6



VARIATION OF SHEAR AND PEEL STRESSES WITH LI-1500 ELASTIC MODULUS

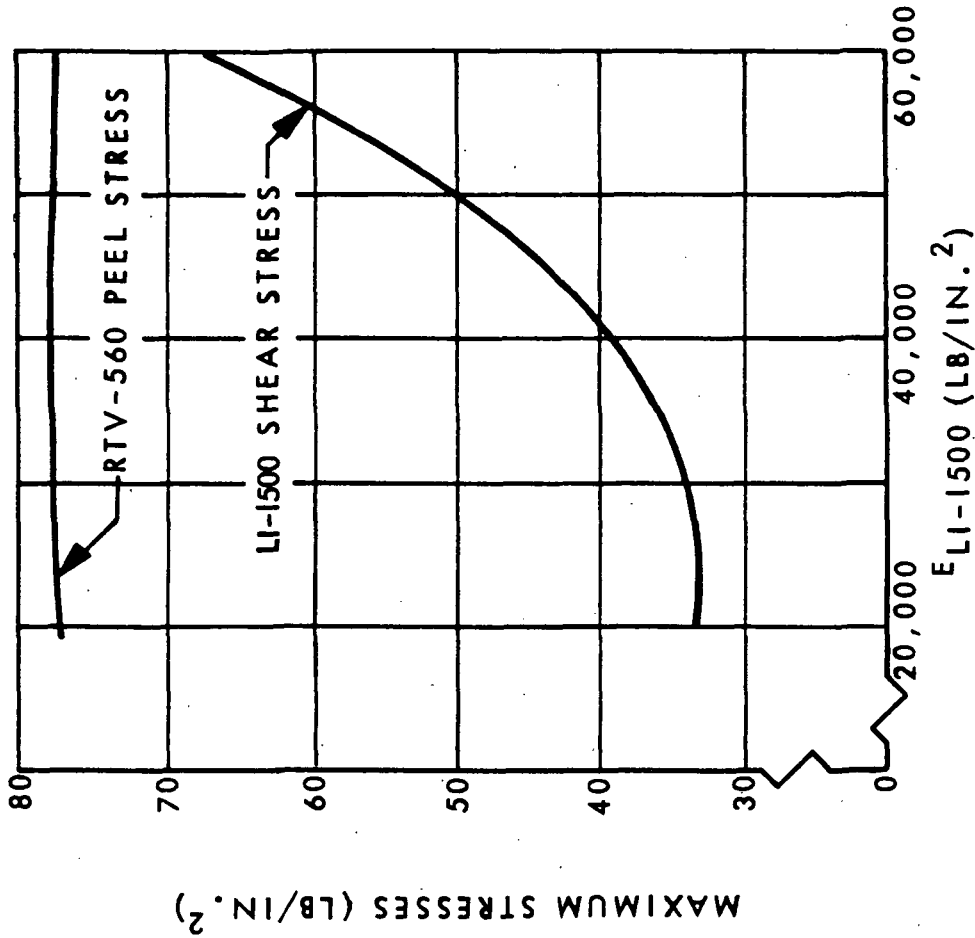
BERYLLIUM FUSELAGE SUBPANEL (SHORT TRAJECTORY)

TEMPERATURE PROFILE



- t_{LI-1500} = 1.6 IN.
- t_{RTV-560} = 0.020 IN.
- t_{COATING} = 0.010 IN.
- LOADING P = 1.14 PSI BURST
- E_{RTV-560} = 300 PSI
- E_{COATING} = 3.5 × 10⁶ PSI
- G_{LI-1500} = 0.4E

ISOTROPIC ANALYSIS



D05009(1)

Fig. 3.1-7



VARIATION OF COATING STRESS WITH LI-1500 ELASTIC MODULUS

$t_{LI-1500} = 1.6$ IN.

$t_{RTV-560} = 0.020$ IN.

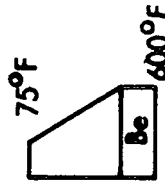
$t_{COATING} = 0.010$ IN.

$E_{RTV-560} = 300$ PSI

$E_{COATING} = 3.5 \times 10^6$ PSI

$G_{LI-1500} = 0.4E$

LOADING $p = 1.14$ PSI BURST



TEMPERATURE PROFILE

ISOTROPIC ANALYSIS

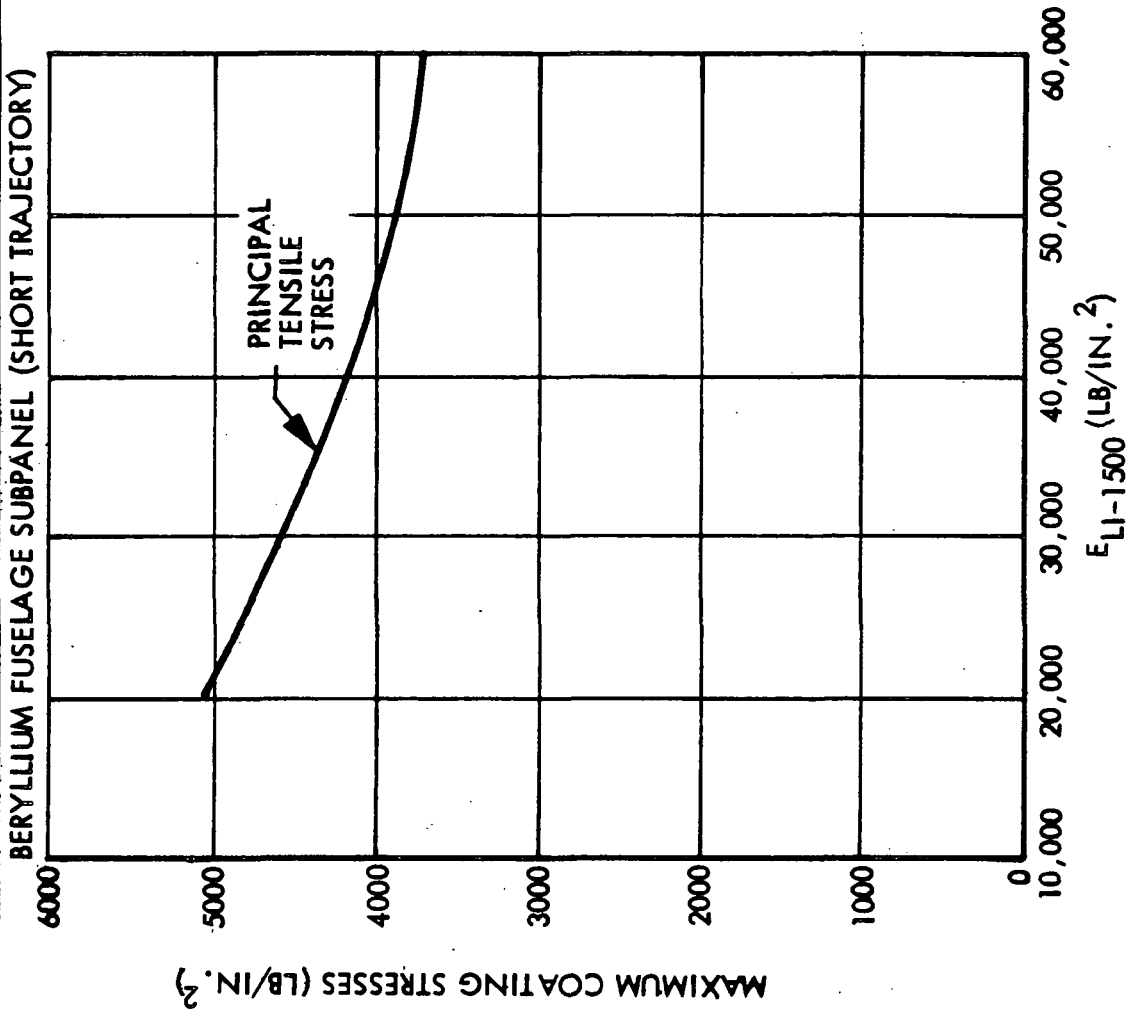
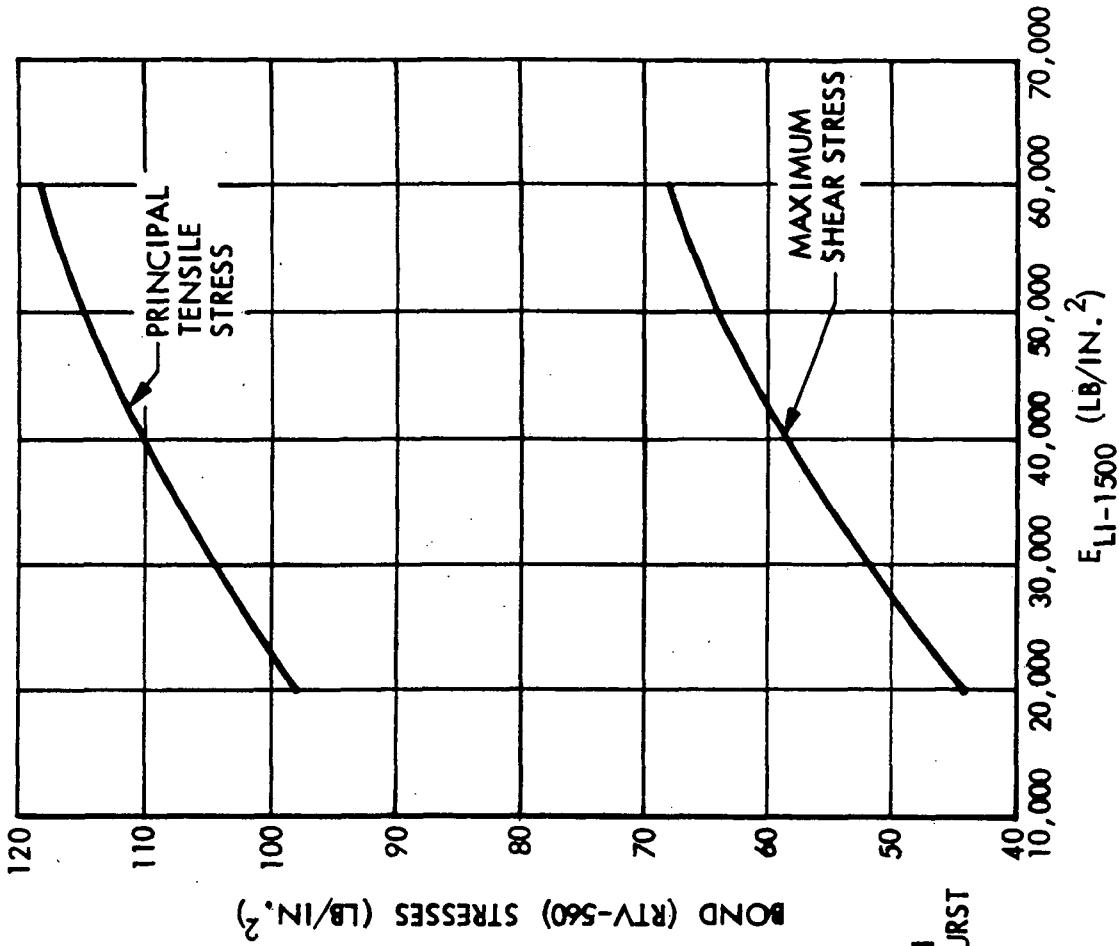


Fig. 3.1-8

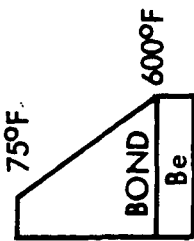
VARIATION OF BOND STRESSES WITH LI-1500 ELASTIC MODULUS



BERYLLIUM FUSELAGE SUBPANEL (SHORT TRAJECTORY)



TEMPERATURE PROFILE



- $t_{LI-1500} = 1.6$ IN.
- $t_{RTV-560} = 0.020$ IN.
- $t_{COATING} = 0.010$ IN.
- $G_{LI-1500} = 0.4$ E
- $E_{RTV-560} = 300$ PSI
- $E_{COATING} = 3.5 \times 10^6$ PSI
- LOADING: $P = 1.14$ PSI BURST

ISOTROPIC ANALYSIS

D04949 (1)

Fig. 3.1-9



Table 3.1-2

EFFECT OF BOND MODULUS OF ELASTICITY ON STRESS INTENSITY

ALUMINUM PANEL AT AREA 2 -1.5 PSI BURST,
6,000 PPI TENSION, ALUMINUM PANEL AT 250°F

STRESS (PSI)	$E_{RTV} = 300 \text{ PSI}$	$E_{RTV} = 100 \text{ PSI}$
<u>LI-1500</u>		
MAXIMUM	48.9	25.0
MINIMUM	- 8.7	- 4.8
SHEAR	15.8	7.6
LONGITUDINAL	48.9	25.0
NORMAL	5.6	2.8
<u>RTV-560</u>		
MAXIMUM	16.9	7.6
MINIMUM	-14.6	- 7.3
SHEAR	14.8	7.3
LONGITUDINAL	- 2.2	- 2.6
NORMAL	5.5	1.8
<u>COATING</u>		
MAXIMUM	20.3	23.5
MINIMUM	- 1.0	- 1.7

EFFECT OF POISSON'S RATIO OF BOND ON
TPS STRESS INTENSITY



ALUMINUM PANEL, FUSELAGE AREA NO. 2

STRESS (PSI)	PRTV = 0.3	PRTV = 0.5
<u>LI-1500</u> MAXIMUM MINIMUM SHEAR LONGITUDINAL NORMAL	58.1 -10.5 18.2 58.1 6.1	48.9 -8.7 15.8 48.9 5.6
<u>RTV-560</u> MAXIMUM MINIMUM SHEAR LONGITUDINAL NORMAL	19.0 -17.2 17.4 -5.4 5.4	16.9 -14.6 14.8 -2.2 5.5
<u>COATING</u> MAXIMUM MINIMUM	18.8 -	20.3 -1.0

PRESSURE = 1.5 PSI BURST
 AIR TEMPERATURE = 250°F
 COATING TEMPERATURE = 100°F
 AJ THICKNESS = 0.711 IN.
 RTV THICKNESS = 0.090 IN.
 LI-1500 THICKNESS = 3.4 IN.
 COATING THICKNESS = 0.010 IN.
 TILE LENGTH = 4.0 IN.
 TENSILE LINE LOAD = 6000 PPI

theoretical value for an incompressible material. These tables have been constructed with data corresponding to a critical loading case of an aluminum primary structure panel; similar results would be expected under other conditions.

Integral Coating Concept

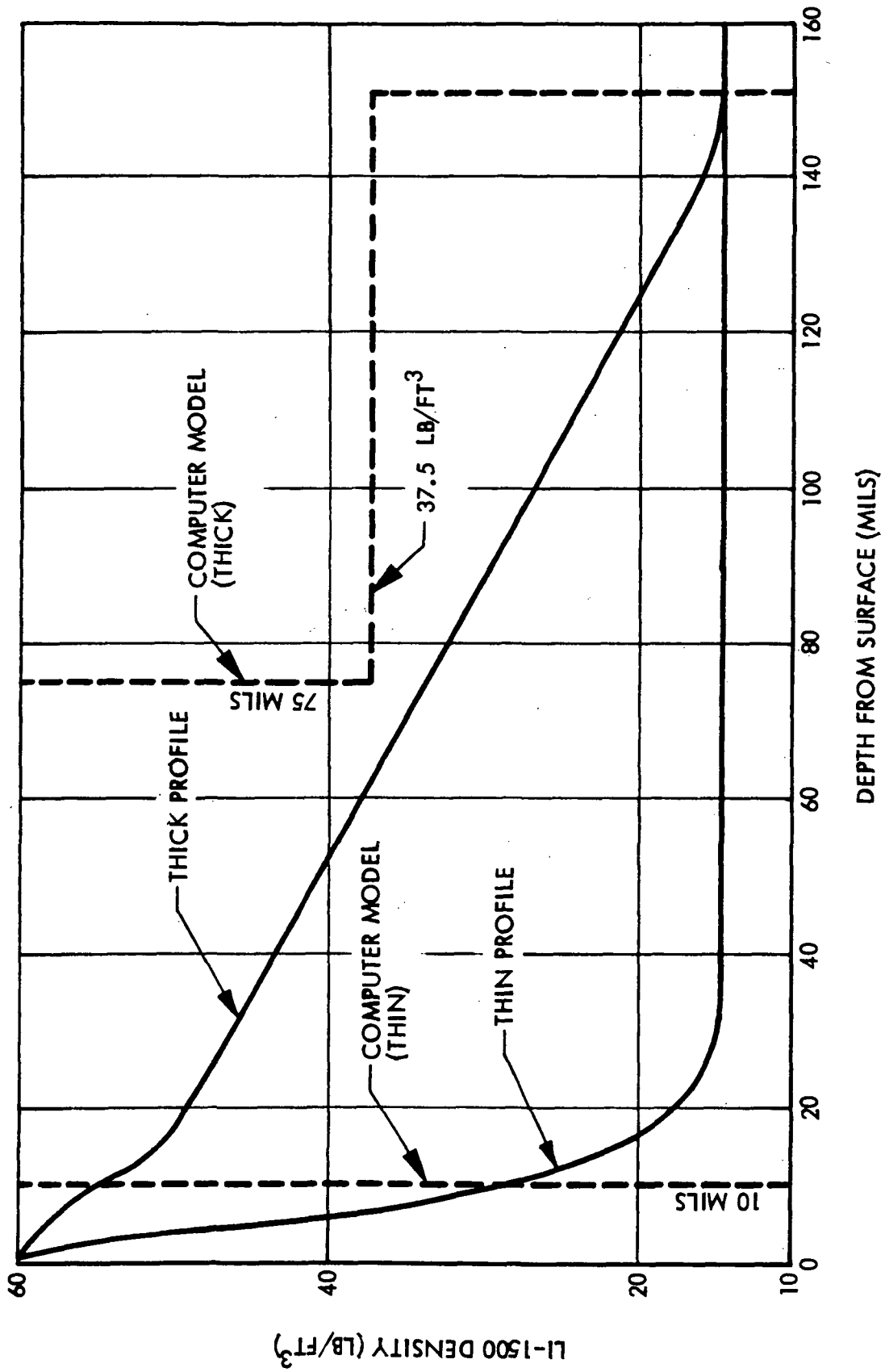
Since LI-1500 can be locally densified in a surface layer, a study was performed to ascertain what effects this might have on an RSI system design. In Fig. 3.1-10 are shown typical bounding profiles of density variation; Figs. 3.1-11 and 3.1-12 present strong direction elastic modulus and strength of LI-1500 as functions of density. Comparative results for a beryllium subpanel (Table 3.1-4) show that there is virtually no difference in stress levels for the thin or thick profile, except for the coating (densified layer) stress. It is noted that the integral coating or local densification concept results in lower coating stresses than a system with an add-on coating, in this case, chrome oxide. The large change here is due to the difference in elastic moduli. It can be tentatively concluded that a thin profile integral coating is best under the conditions presented here, offering a weight savings over the thick profile.

Effects of Thermal Cycling on LI-1500

As discussed in Section 4, Volume I, thermal cycling of LI-1500 apparently leads to a higher modulus in LI-1500. The effect of these changes in a thin layer under the coating was investigated for an aluminum fuselage panel and compared with results for virgin LI-1500. These are summarized in Table 3.1-5, where it is noted that there is little change in stress level and that the cycled LI-1500 experiences little or no stress. From this example, it may be tentatively concluded that the thermal cycling to maximum surface temperatures of a thin layer underneath the coating does not degrade the mechanical capability of the RSI system.



LI-1500 INTEGRAL COATING DENSITY PROFILES



D04984(1)

Fig. 3.1-10

LI-1500 STRONG DIRECTION
ELASTIC MODULUS VS SPECIMEN DENSITY

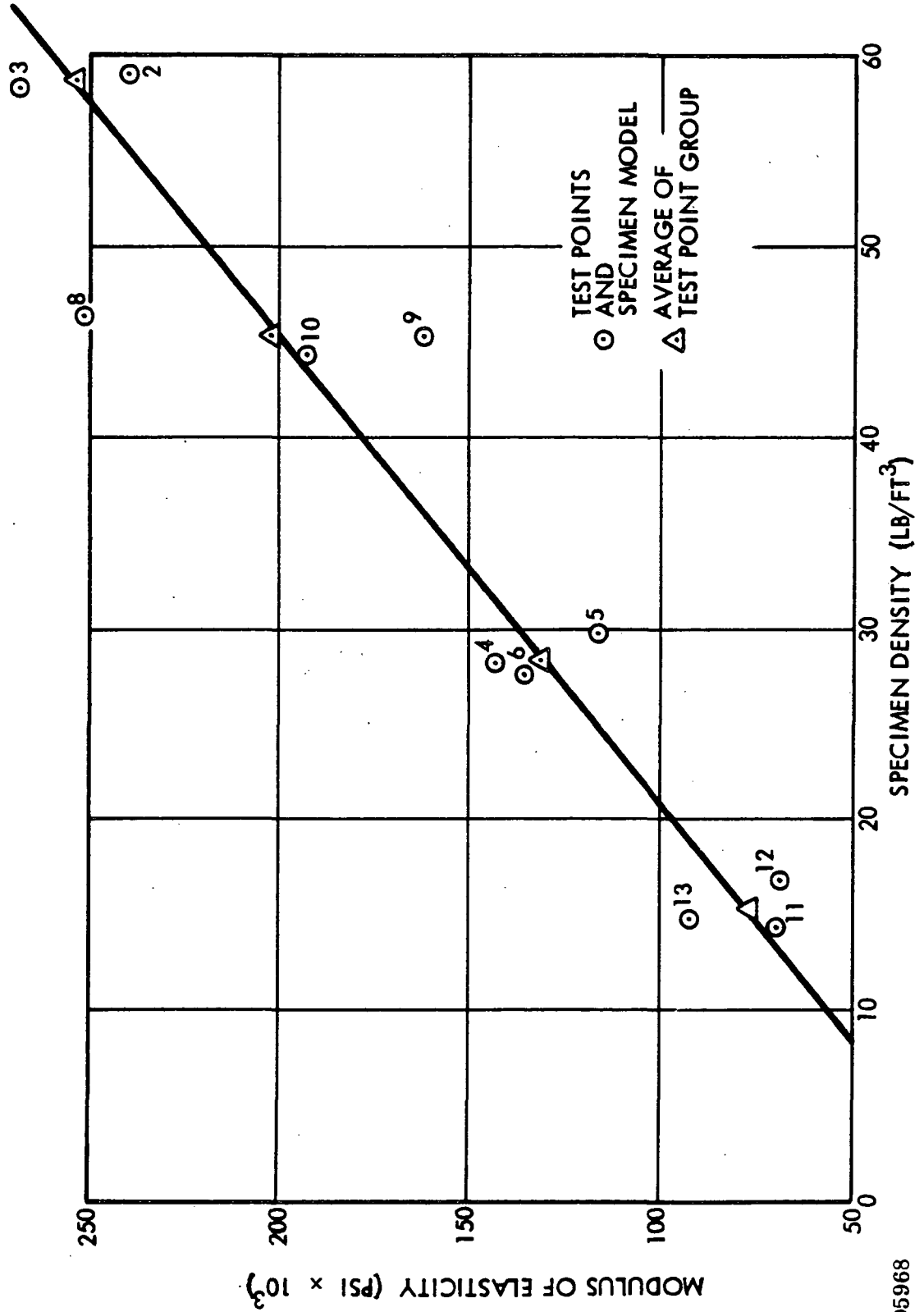
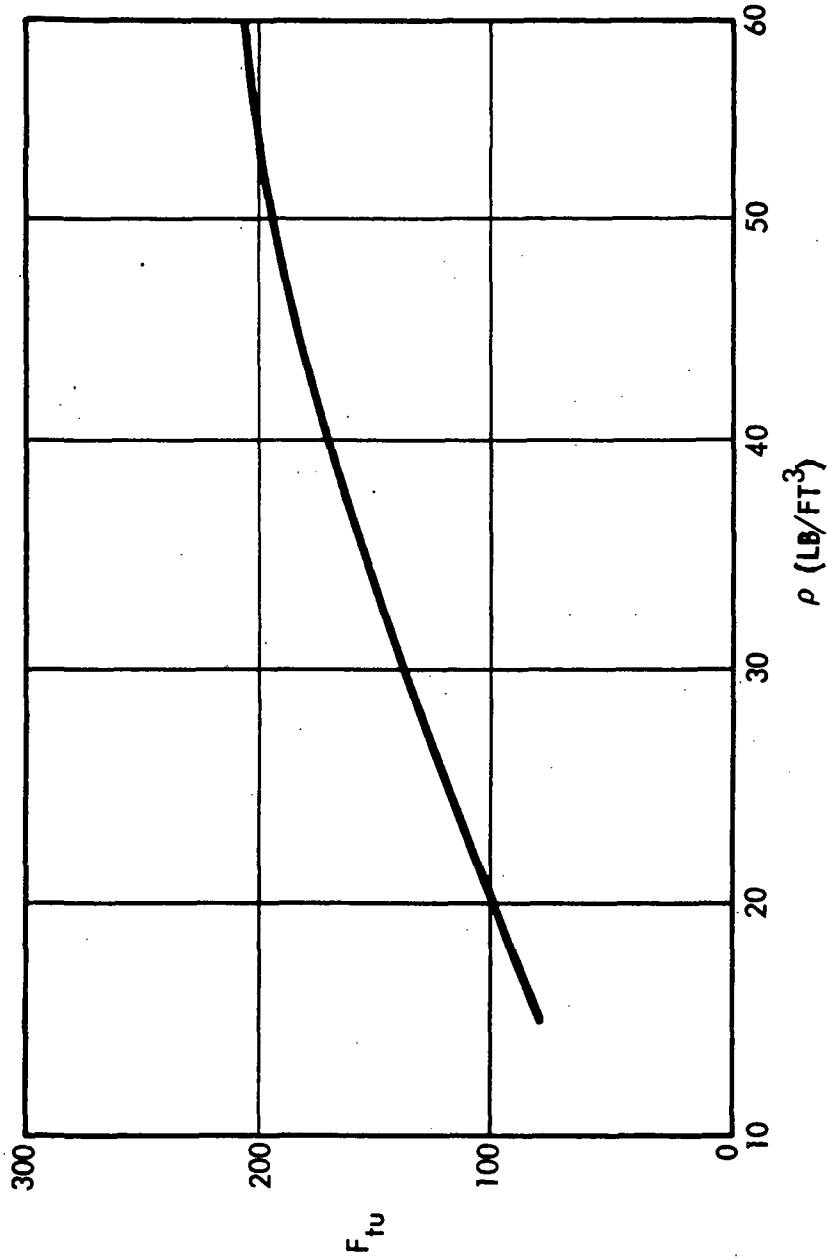


Fig. 3.1-11

DO5968



LI-1500 DENSITY - STRENGTH CURVE (TEST RESULTS)
STRONG DIRECTION



3.1-20

100<

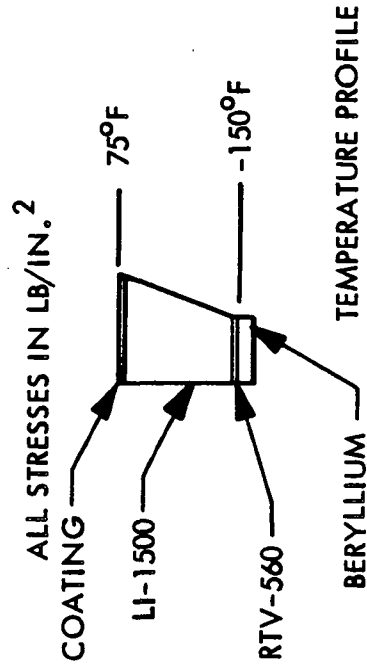
Fig. 3.1-12

DO5967

Table 3.1-4

STRUCTURAL COMPARISON OF COATING CONCEPTS

	STRESS (PSI)	ADD-ON COATING	INTEGRAL COATING THIN PROFILE	INTEGRAL COATING THICK PROFILE
LI-1500	MAXIMUM MINIMUM SHEAR LONGITUDINAL PEEL	13.4 - 120.4 51.5 - 68.9 11.1	13.6 -109.1 - 49.2 - 69.4 10.3	13.6 -110.2 - 49.2 - 69.5 10.8
RTV-560	MAXIMUM MINIMUM SHEAR LONGITUDINAL PEEL	48.0 - 145.5 50.8 32.5 11.5	48.6 -114.6 - 47.6 32.3 10.4	48.2 -116.0 - 47.6 32.4 10.9
COATING	THICKNESS MAXIMUM MINIMUM	t = 0.010 11.3 -1761.2	t = 0.010 14.4 -230.0	t = 0.150 6.1 -161.4



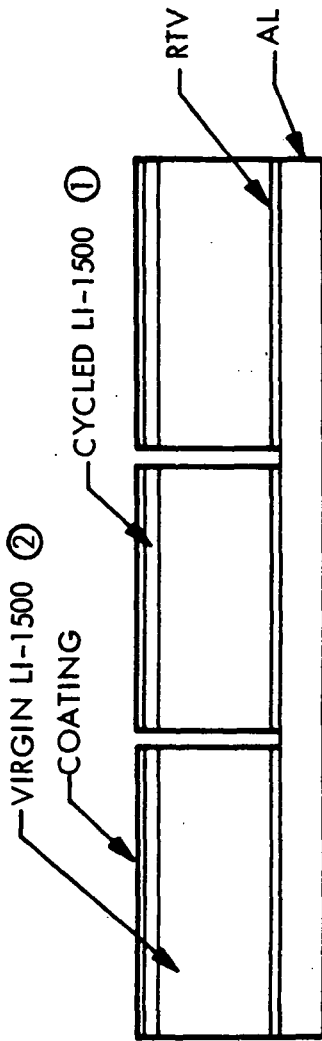
PRESSURE = 6.75 PSI COLLAPSE
 t_o BERYLLIUM = 0.4312 IN.
 t_o RTV-560 = 0.020 IN.
 t_o LI-1500 = 2.3 IN.
 t_o COATING = AS SHOWN
 LI-1500 TILE LENGTH = 12 IN.





Table 3.1-5

AL TEST PANEL NO. 2 ORBITER FUSELAGE AREA 2



	COATING	CYCLED LI-1500 (1)	VIRGIN LI-1500 (2)	RTV BOND	WITHOUT CYCLED LI-1500	
					COAT	RTV
MAX	26	1	50	17	20	17
MIN	-2	0	-9	-15	-1	-15
SHEAR		0	16	15	16	15
R-Z PRINCIP		1	25	17		
LONG		1	50	-6	49	-2
PEEL		0	6	6	6	6

T_{COAT} = 0.01
 T_{CY. LI-1500} = 0.2

4-IN. TILES

E_{COAT} = 3.5 x 10⁶
 E_{CY. LI-1500} = 90,000

LOADING CONDITION	1.5 PSI BURST 6000 LB/IN. TENS
TEMP	100°F 250°F
THICK	0.010 3.396 0.090 0.711

3.2 DESIGN DETAILS VARIATIONS

Substrate Configuration Parametric Studies

The studies performed for Contract NAS 9-11222 and for the present contract indicate that subpanel and primary structure configurations may be qualitatively compared, utilizing wide column structural optimization data that have been reported in the literature. These data are of the general form:

$$\frac{N_x}{l \bar{\eta} E} = \epsilon \left(\frac{\bar{t}}{l} \right)^n$$

$$\bar{\eta} = E_T/E$$

where

- N_x = given axial load
- ϵ = a measure of efficiency of a given configuration
- $\bar{\eta}$ = an effective plasticity reduction factor, ratio of tangent modulus at a stress level corresponding to N_x to initial modulus
- l = length of the panel
- \bar{t} = weight - equivalent flat-plate thickness

The value of the exponent n is usually 2.0 for conventionally stiffened configurations composed of straight elements but is smaller for configurations with curved elements.

Several configurations are shown in Fig. 3.2-1. Observe that the configurations without a flat sheet or skin are more efficient (lighter weight) than the others - for example, the corrugated configuration which is discussed later in Table 3.2-13. Also, configurations with curved stiffening elements are more efficient than those with straight stiffening elements. Phase B studies have indicated that manufacturability of these sections is difficult in a structure of changing dimension. In addition there is lack of adequate test data for some of the sections, hence, only those configurations that do include a flat sheet or skin are studied here. Among these configurations, the zee-stiffened configuration is most efficient. Other configurations that are more efficient than the zee-stiffened configuration may be identified - for example, the integral "L" or "T"

COMPARISON OF WIDE COLUMN CONFIGURATIONS

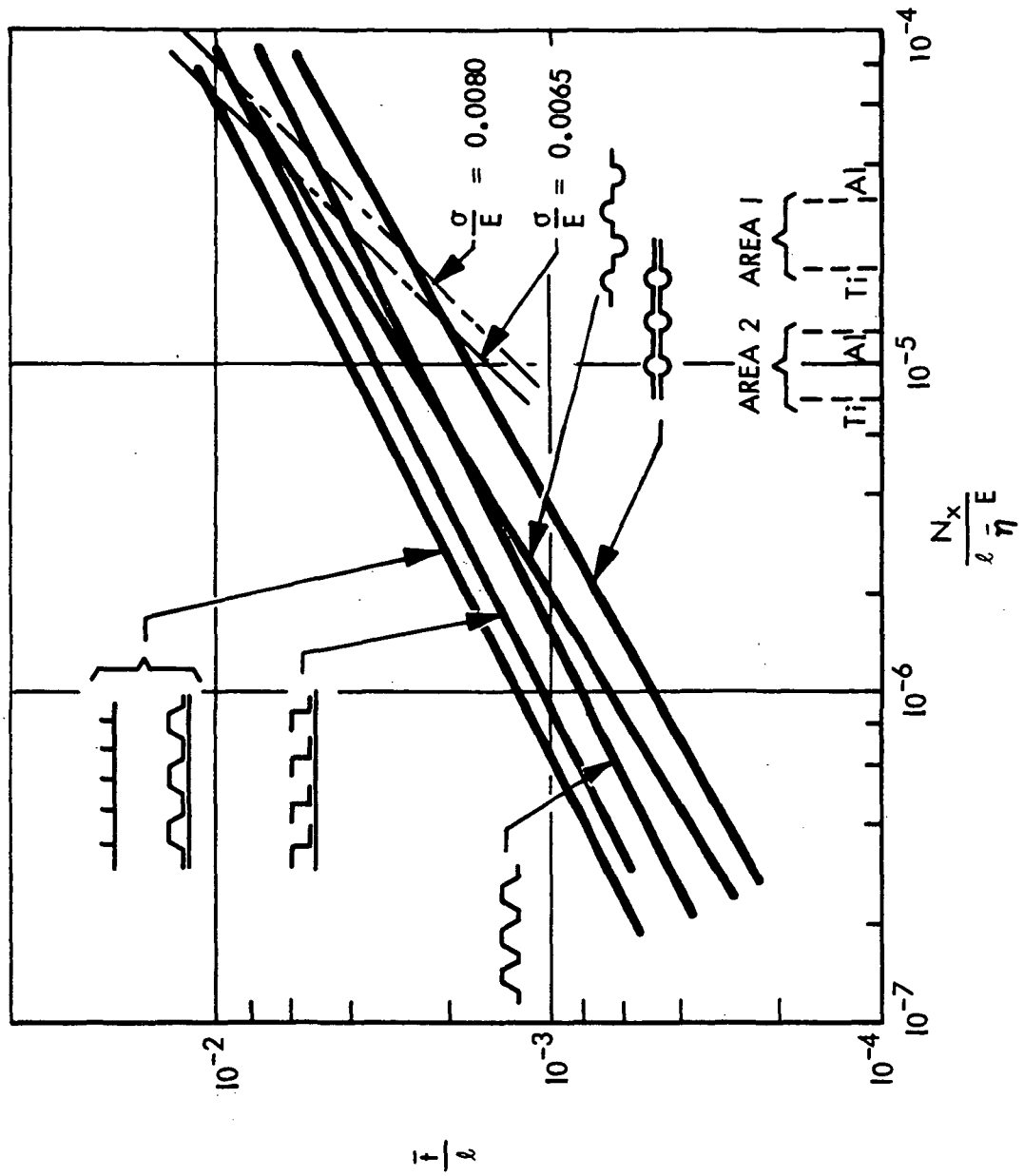


Fig. 3.2-1

configuration, but the increase in efficiency is only about 10 percent as seen from Table 3.2-1. LMSC has not pursued such configurations here; however, related programs have indicated that availability and manufacturing capabilities preclude their usage at this time. Likewise, honeycomb-sandwich construction is less efficient than zee-stiffened construction, principally because of the difference between the true optimum core weight and that which is practical to handle and fabricate.

Effect of Bond Thickness on Required LI-1500 Thickness

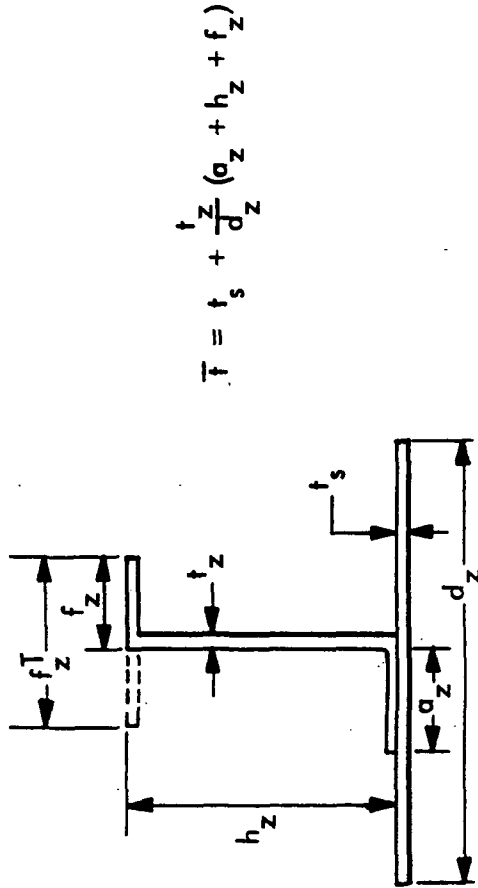
Another tradeoff in the design methodology logic is the variation of bond thickness with LI-1500 thickness. As the bond thickness is increased to produce allowable stress values within the LI-1500 or on the surface coating, the LI-1500 thickness may be reduced. This effect is shown in Fig. 3.2-2 where the variation of bond thickness with LI-1500 thickness is plotted for various beryllium effective thicknesses for a beryllium temperature of 600^oF. For the 0.064 in. beryllium (which corresponds to test panel No. 1), an increase in bond of 0.075 (from 0.025 to 0.100 in.) allows a reduction in LI-1500 thickness of 0.32 (from 2.25 to 1.93). This amounts to a thickness tradeoff of 4 to 1. For example, an increase of bond by 0.010 in. would allow a decrease of 0.040 in. in the required LI-1500 thickness.

Similar results are shown in Figs. 3.2-3 through 3.2-5 for test panels Nos. 2, 3, and 4, respectively. Tradeoff factors have been determined from computer runs that considered various adhesive thickness for a constant substrate thickness. The tradeoff factors are dependent on the density-specific heat products of the adhesive, LI-1500, and the substrate material. Approximate tradeoff factors of 4.5, 3.5, and 4.0 were determined for test panels Nos. 2, 3, and 4 from the data of these figures, respectively. Hence, an average tradeoff of about 4.0 could be used for all four test panels.



Table 3.2-1

COMPARISON OF Z, L, AND I OPTIMUM CONFIGURATIONS



$$\bar{T} = t_s + \frac{t_z}{d_z} (a_z + h_z + f_z)$$

PANEL	\bar{T}	d_z	t_s	t_z	a_z	h_z	f_z
2 Z	0.1201	1.55	0.050	0.050	0.40	1.25	0.52
L	0.1081	1.55	0.050	0.050	0.0	1.30	0.50
T	0.1178	1.46	0.050	0.050	0.0	1.00	0.98
T	0.1071	1.14	0.040	0.040	0.0	1.14	0.77
3 Z	0.1436	1.67	0.063	0.063	0.48	1.20	0.48
L	0.1327	1.51	0.063	0.063	0.0	1.27	0.40
T	0.1282	1.45	0.063	0.050	0.0	1.26	0.63
4 Z	0.1038	1.35	0.050	0.040	0.41	1.03	0.38
L	0.0933	1.35	0.050	0.040	0.0	1.08	0.38
L	0.0923	1.08	0.040	0.040	0.0	1.03	0.38
T	0.1002	1.35	0.050	0.040	0.0	0.93	0.76

D07038 (1)

VARIATION OF ADHESIVE THICKNESS WITH LI-1500 THICKNESS - TEST PANEL I



MAXIMUM BERYLLIUM TEMPERATURE = 600°F

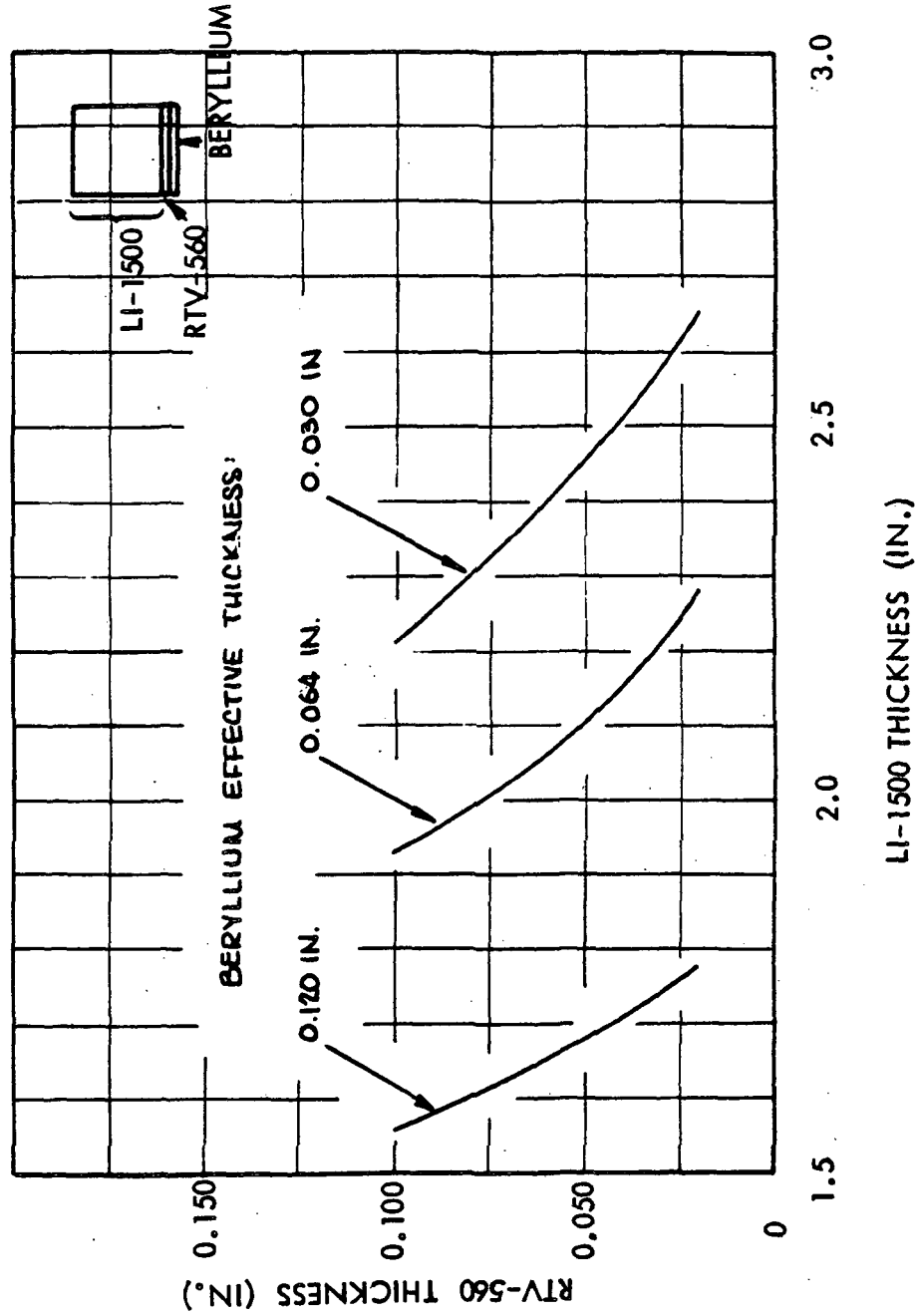


Fig. 3.2-2

DO6003



VARIATION OF ADHESIVE THICKNESS WITH LI-1500 THICKNESS - TEST PANEL NO. 2

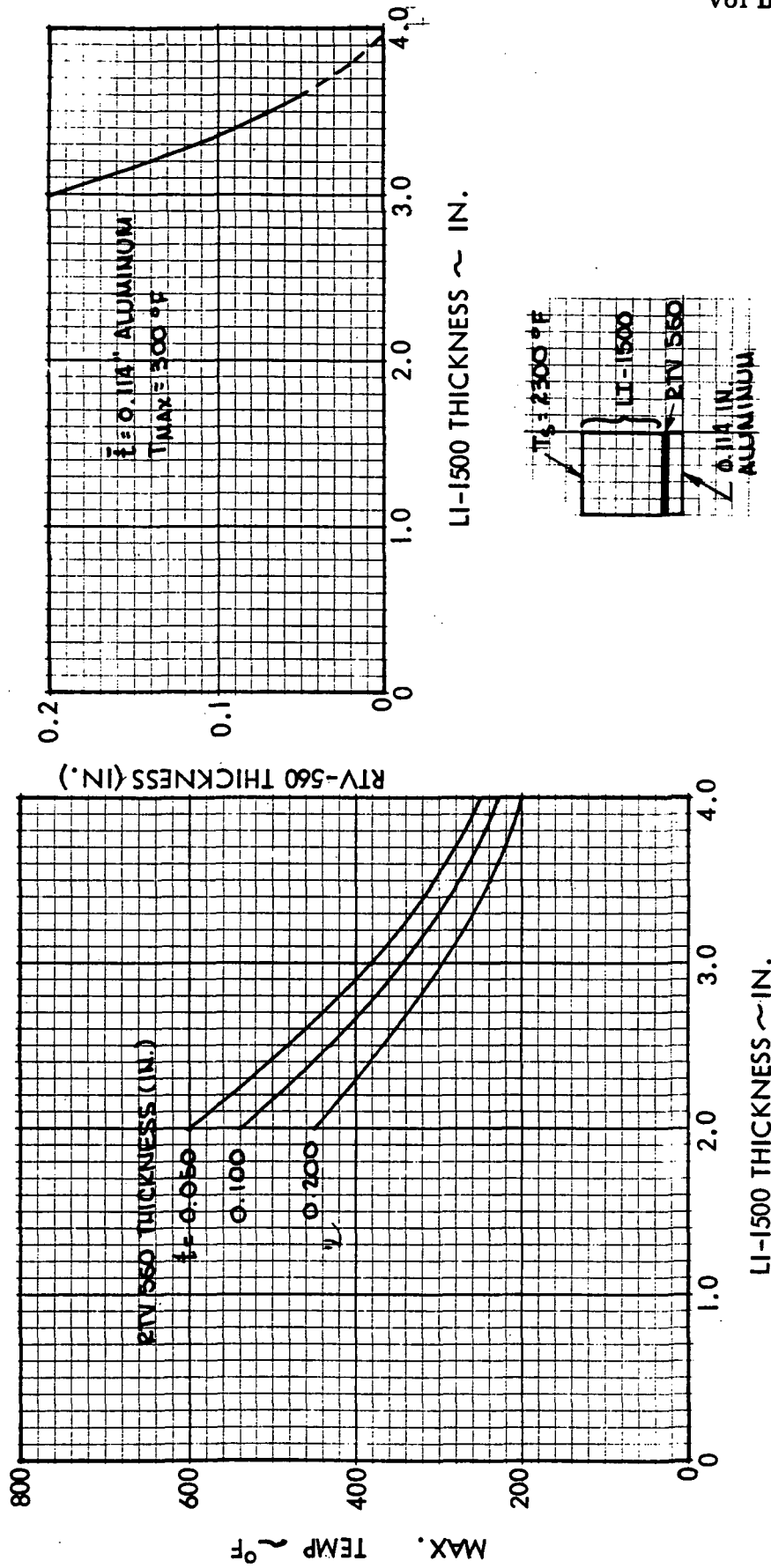


Fig. 3.2-3



VARIATION OF ADHESIVE THICKNESS WITH LI-1500 THICKNESS - TEST PANEL NO. 3

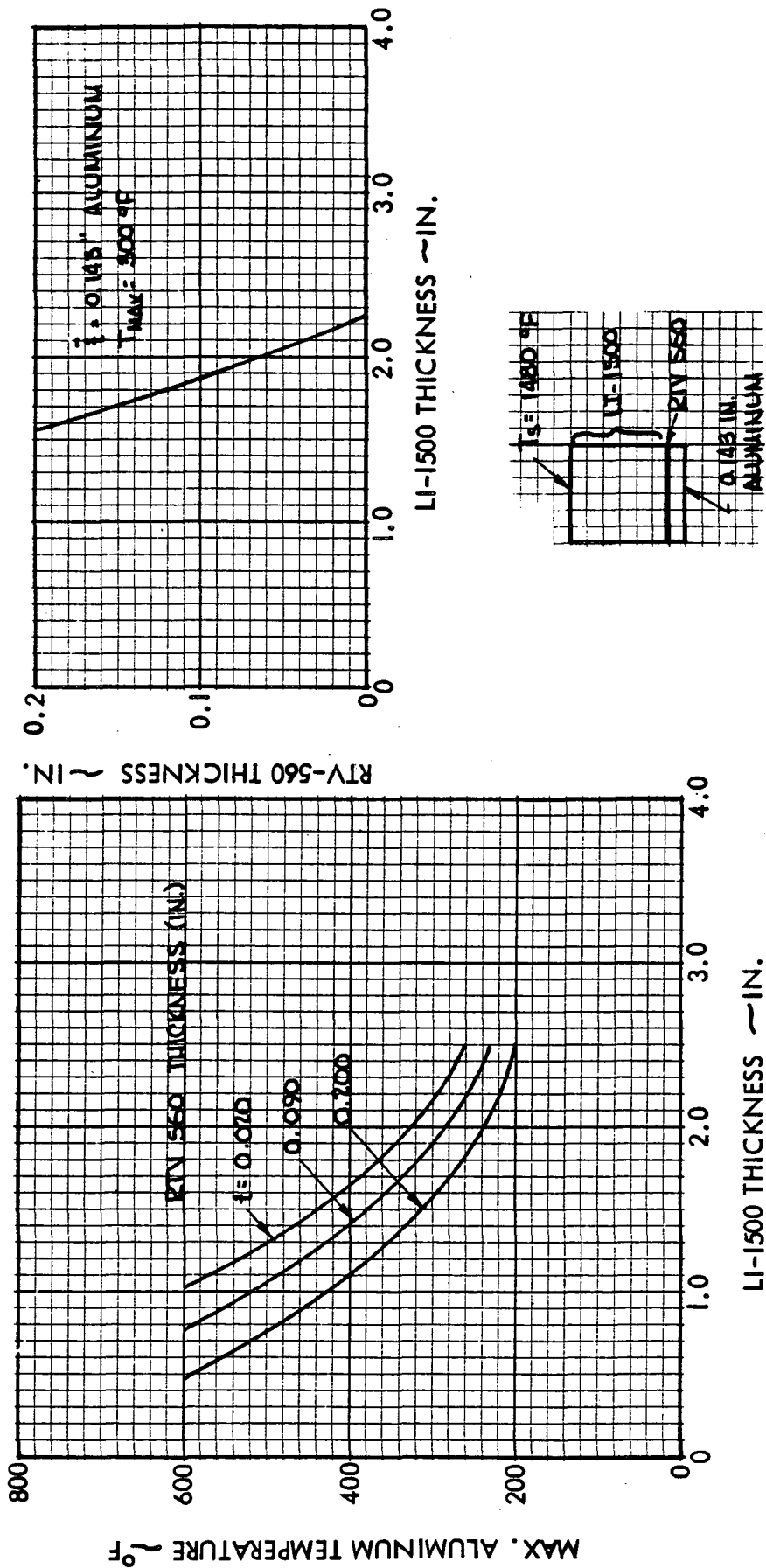


Fig. 3.2-4

VARIATION OF ADHESIVE THICKNESS WITH LI-1500 THICKNESS - TEST PANEL NO. 4

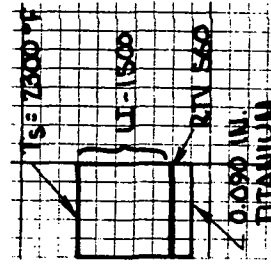
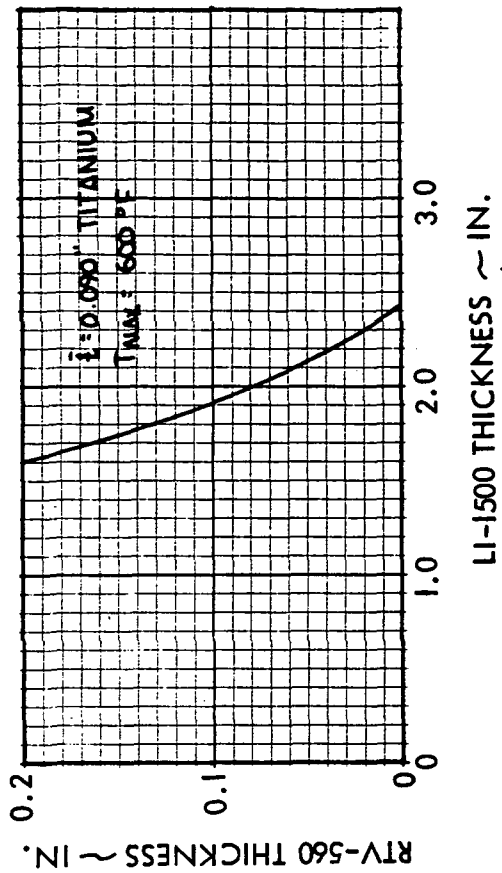
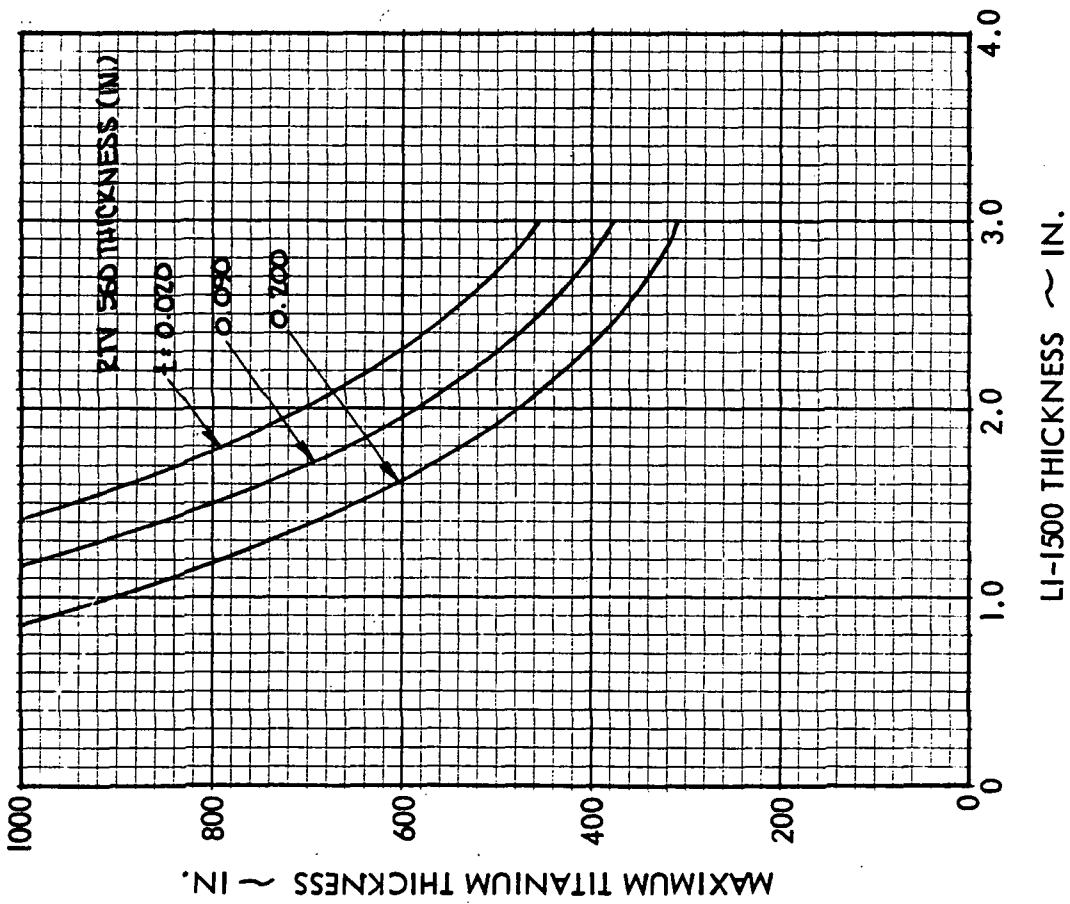


Fig. 3.2-5

DO6029

Figures 3.2-6 through 3.2-9 are tradeoff curves showing the relationships between LI-1500 and RTV-560 thickness for the four flight panels. Also parametric data used to generate the tradeoff curves are shown in these figures. Approximate tradeoff factors, based on a linear variation (of LI-1500 thickness with RTV thickness) from 0 to 0.20 in. of RTV-560 for all four panels, are 3.3, 4.1, 3.0 and 3.3 for panels 1 to 4, respectively. Use of the tradeoff curves results in a lower unit weight than would result if a constant LI-1500 thickness was used with increasing adhesive thickness. By comparing the far righthand column in Tables 3.2-2 and 3.2-3, it is seen that the use of the tradeoff factor could account for a 0.84 lb/ft² decrease in unit weight if the required adhesive thickness for strain isolation considerations increased to 0.200 in. These tables, for the aluminum flight panel No. 2, are constructed from the equation:

$$(W/A)_{\text{Total}} = (W/A)_{\text{LI-1500}} + (W/A)_{\text{RTV-560}} + (W/A)_{\text{Coating}}$$

using 0.10 lb/ft² for 0042 coating.

Table 3.2-2

UNIT WEIGHT OF TPS USING TRADEOFF CURVE

$t_{\text{RTV-560}}$ (in.)	W/A_{RTV} (lb/ft ²)	$t_{\text{LI-1500}}$ (in.)	$W/A_{\text{LI-1500}}$ (lb/ft ²)	W/A_{Total} (lb/ft ²)
0.030	0.221	2.80	3.50	3.82
0.090	0.663	2.52	3.15	3.91
0.200	1.472	2.13	2.66	4.23

Table 3.2-3

UNIT WEIGHT OF TPS WITHOUT TRADEOFF CURVE

$t_{\text{RTV-560}}$ (in.)	W/A_{RTV} (lb/ft ²)	$t_{\text{LI-1500}}$ (in.)	$W/A_{\text{LI-1500}}$ (lb/ft ²)	W/A_{Total} (lb/ft ²)
0.030	0.221	2.80	3.50	3.82
0.090	0.663	2.80	3.50	4.26
0.200	1.472	2.80	3.50	5.07

3.2-9

11<



TRADEOFF CURVES - BERYLLIUM FLIGHT PANEL NO. 1

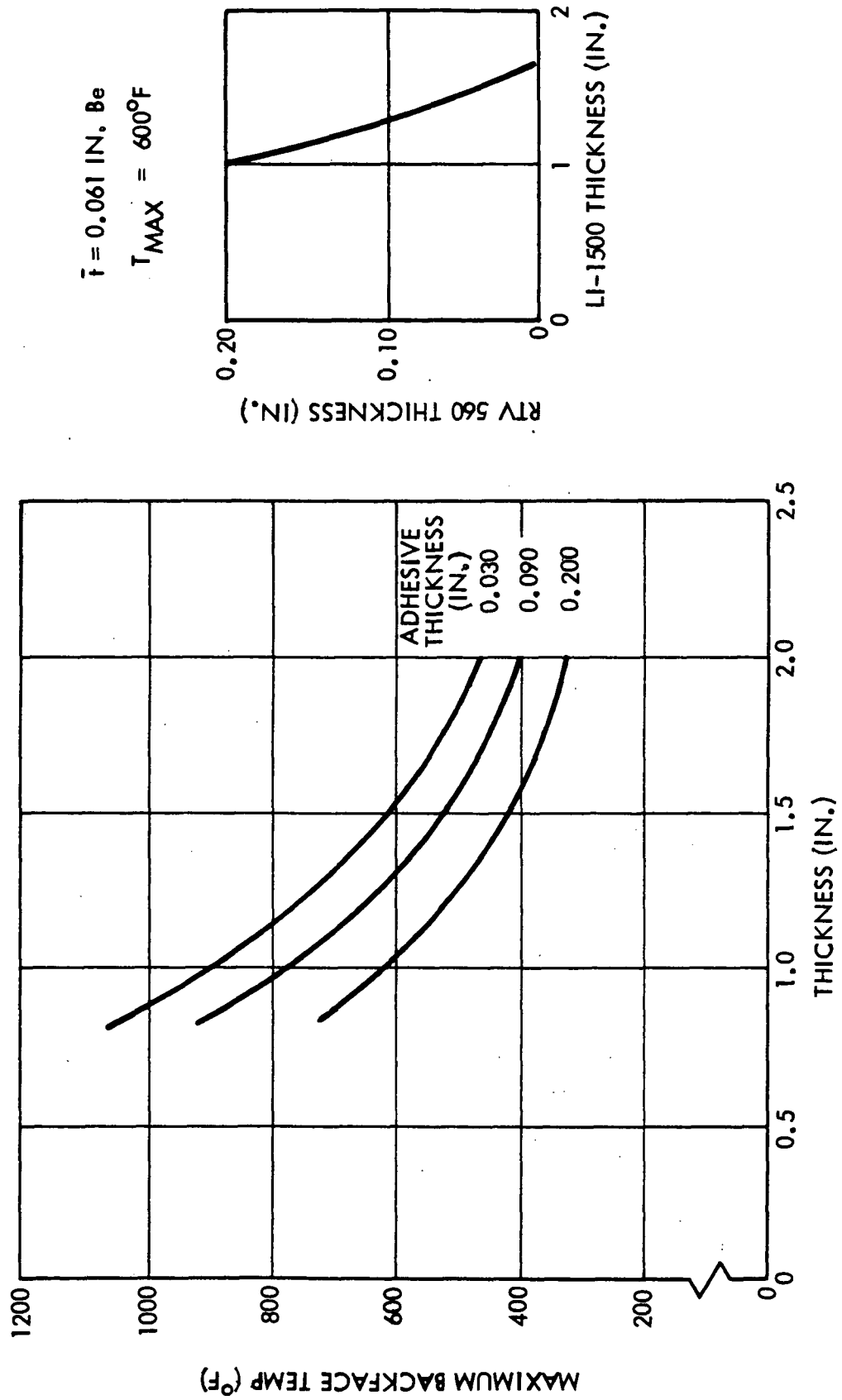


Fig. 3.2-6

DO7053

MAXIMUM BACKFACE TEMP (°F)

3.2-10



TRADEOFF CURVES - ALUMINUM FLIGHT PANEL NO. 2

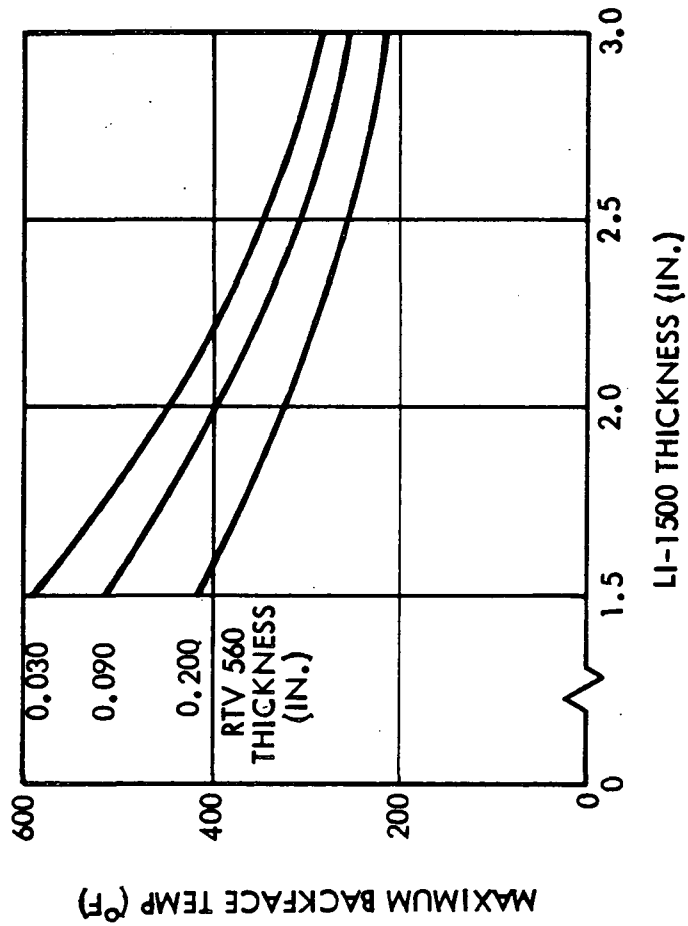
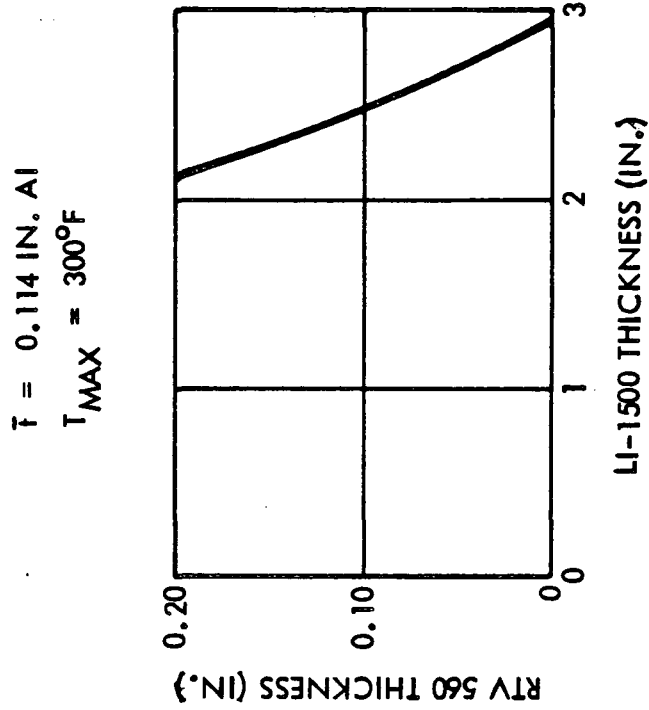


Fig. 3.2-7



TRADEOFF CURVES - ALUMINUM FLIGHT PANEL NO. 3

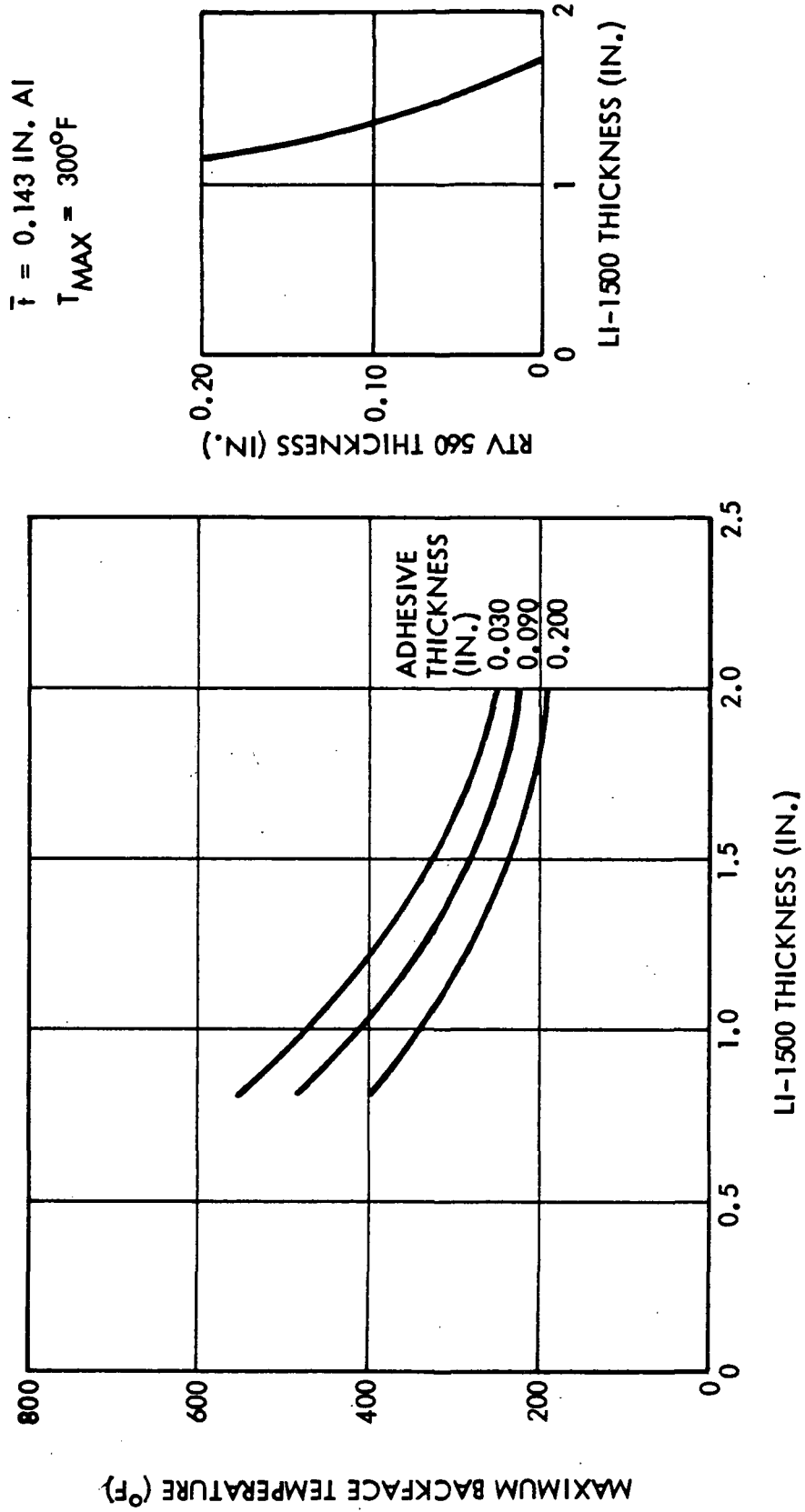


Fig. 3.2-8

DO7055



TRADEOFF CURVES - TITANIUM FLIGHT PANEL NO. 4

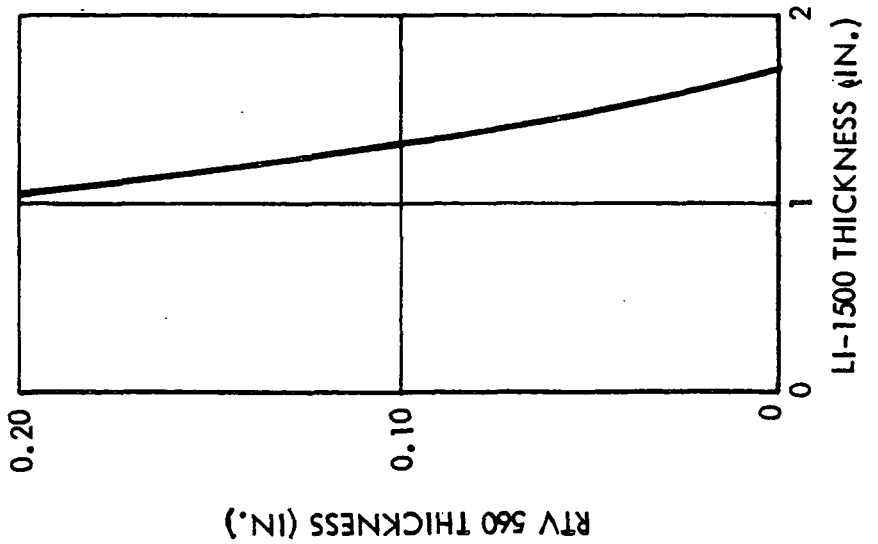
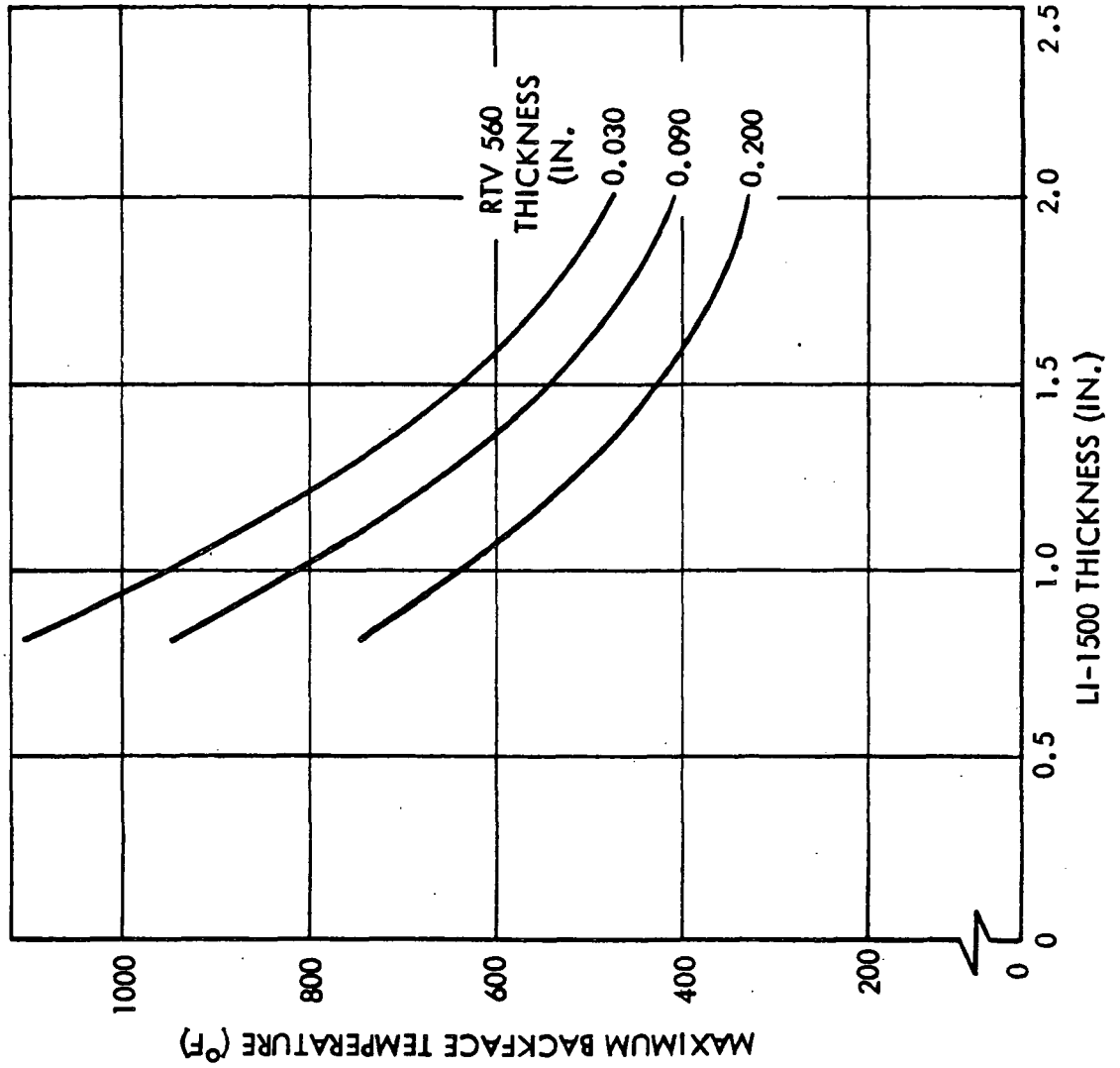


Fig. 3.2-9

In other words, if 2.80 in. of LI-1500 was required for thermal considerations to restrict the backface temperature to 300°F with an adhesive thickness of 0.030 in. and structural consideration dictated an increase in adhesive to 0.200 in., a unit weight savings of $5.07 - 4.23 = 0.84 \text{ lb/ft}^2$ could be realized by using the tradeoff factor. Use of the tradeoff factor reduces the required LI-1500 as the adhesive thickness is increased. Similar trends would apply for other panel configurations.

Effect of Coating Thickness on RSI Stress Levels

The results of this study are presented in Figs. 3.2-10 through 3.2-13 for an assumed isotropic LI-1500 material. Inspection of these curves indicates that coating thickness variation does not affect stress levels in the LI-1500 or the RTV-560 bond. However, coating stress decreases with increasing coating thickness, indicating that, although the line load carried by the coating increases with increasing thickness, it does so at a lower rate than the thickness itself. Hence, a lower coating stress is evident in this case.

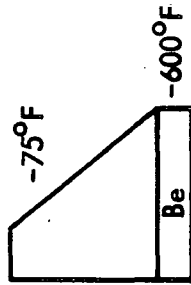
Stress Variations Due to LI-1500 Thickness

These isotropic analytical studies are summarized in Figs. 3.2-14 through 3.2-17, where bond and LI-1500 stress levels are not affected by LI-1500 thickness. However, coating stresses decrease with LI-1500 thickness for the worst possible case shown here. Essentially, thermal expansion and burst pressure induce tensile loads in the coating. In addition, the thermal load causes the substrate to bend in such a direction so as to cause a compressive stress in the coating. This latter stress is dependent upon the distance of the coating from the location of the neutral axis of bending, which is in the substrate. A thicker layer of LI-1500 thus results in higher compressive bending stresses, which have a net effect of subtracting from the dominant tensile load in the coating due to substrate expansion.



VARIATION OF LI-1500 STRESS WITH COATING THICKNESS

FUSELAGE PANEL PER LMSC-A989337 (SKW 100510)



TEMP PROFILE:

3.2-15

ISOTROPIC ANALYSIS

$$T_{LI-1500} = 1.60 \text{ IN.}$$

$$T_{RTV-560} = 0.060 \text{ IN.}$$

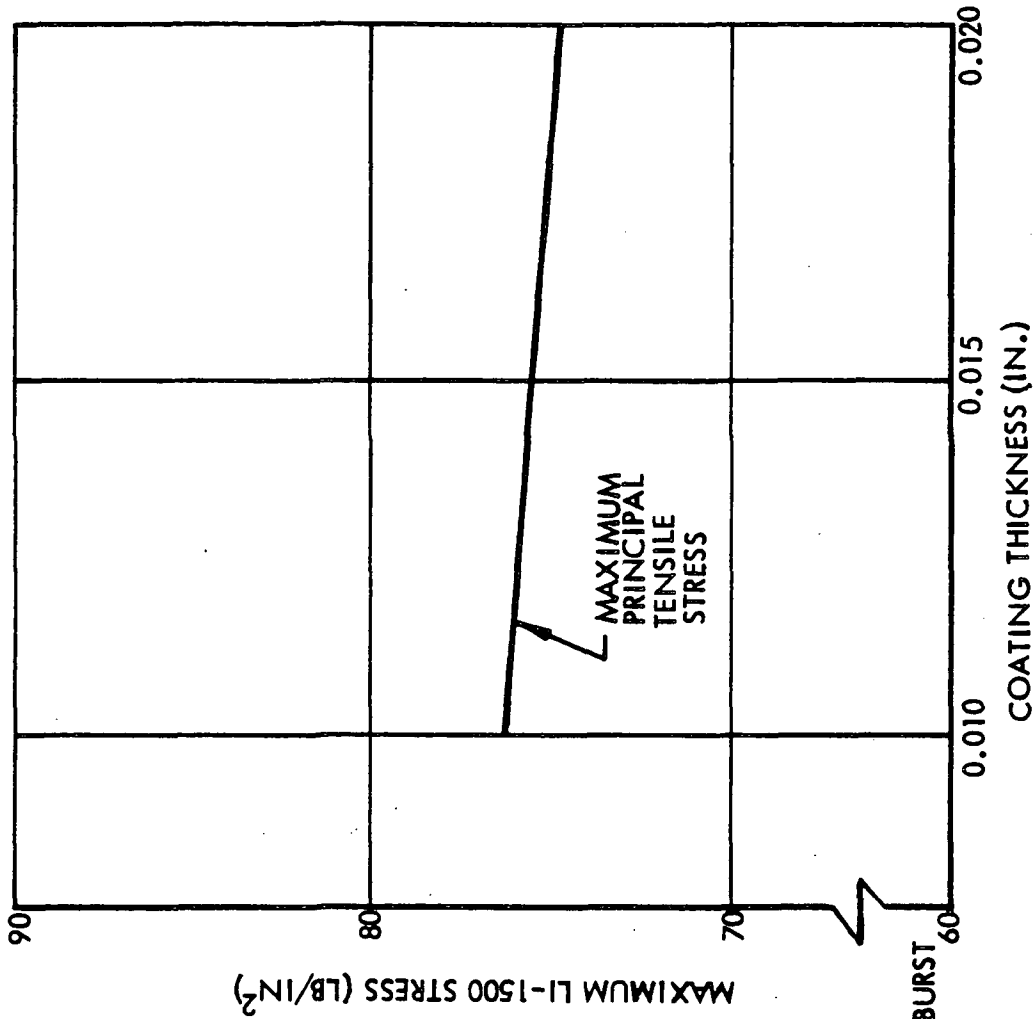
$$E_{RTV-560} = 300 \text{ PSI}$$

$$E_{COATING} = 3.5 \times 10^6 \text{ PSI}$$

$$E_{LI-1500} = 60,000 \text{ PSI}$$

$$G_{LI-1500} = 24,000 \text{ PSI}$$

LOADING: SUBSONIC CRUISE, = 1.14 PSI BURST



DO5994

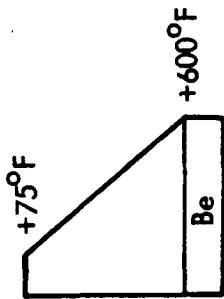
Fig. 3.2-10



VARIATION OF SHEAR AND PEEL STRESSES WITH COATING THICKNESS

BERYLLIUM FUSELAGE SUBPANEL (SHORT TRAJECTORY)

TEMPERATURE PROFILE



- $t_{LI-1500}$ = 1.60 IN.
- $E_{RTV-560}$ = 300 PSI
- $G_{LI-1500}$ = 24,000 PSI
- $t_{RTV-560}$ = 0.060 IN.
- $E_{COATING}$ = 3.5×10^6 PSI
- $E_{LI-1500}$ = 60,000 SPI
- LOADING $P = 1.14$ PSI BURST

ISOTROPIC ANALYSIS

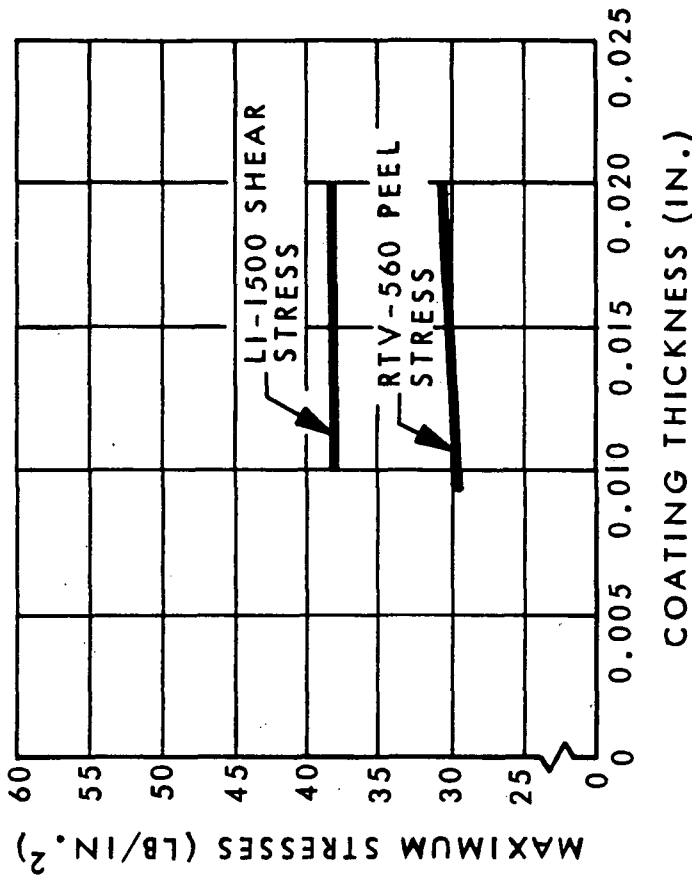


Fig. 3.2-11

VARIATION OF BOND STRESSES WITH COATING THICKNESS



BERYLLIUM FUSELAGE SUBPANEL
(SHORT TRAJECTORY)

$$t_{LI-1500} = 1.60 \text{ IN.} \quad E_{RTV-560} = 300 \text{ PSI,}$$

$$G_{LI-1500} = 24,000 \text{ PSI}$$

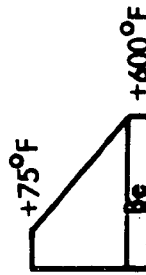
$$t_{RTV-560} = 0.060 \text{ IN.}$$

$$E_{COATING} = 3.5 \times 10^6 \text{ PSI}$$

$$E_{LI-1500} = 60,000 \text{ PSI}$$

LOADING $P = 1.14 \text{ PSI BURST}$

TEMPERATURE PROFILE



ISOTROPIC ANALYSIS

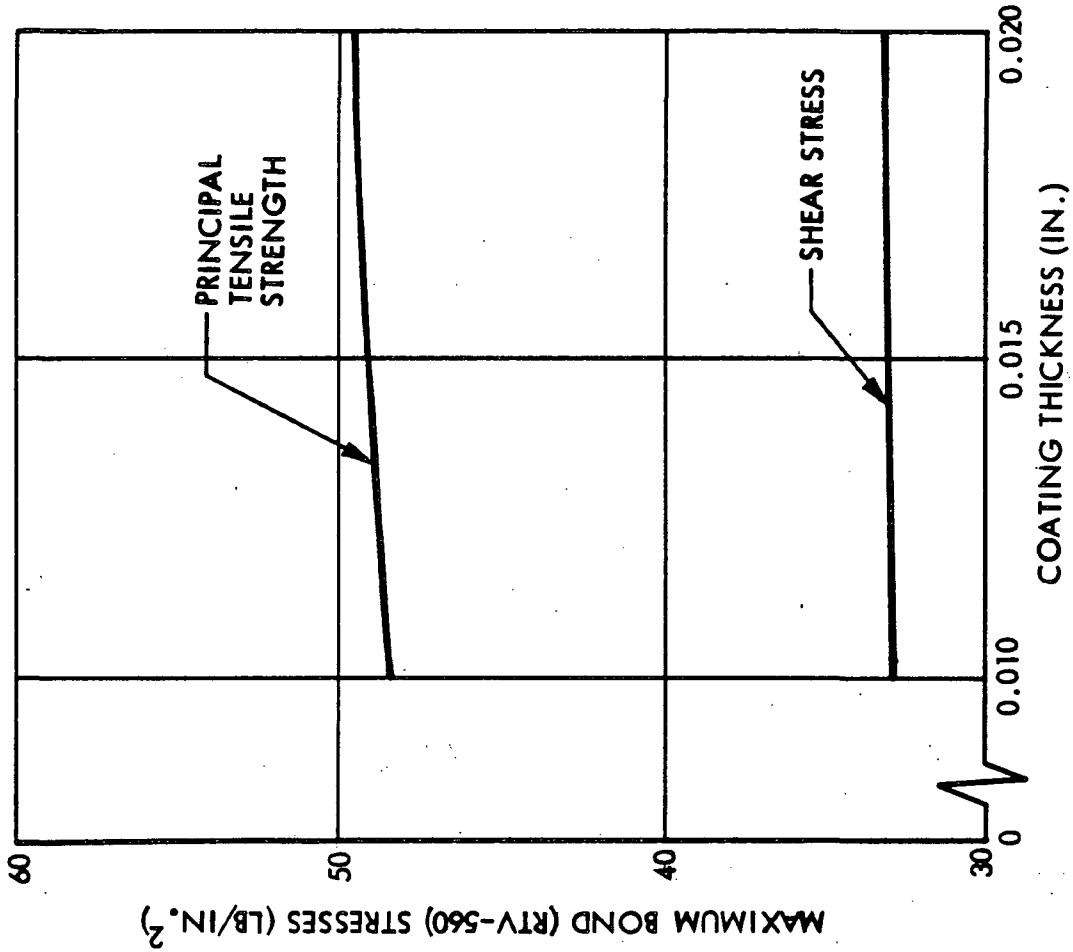
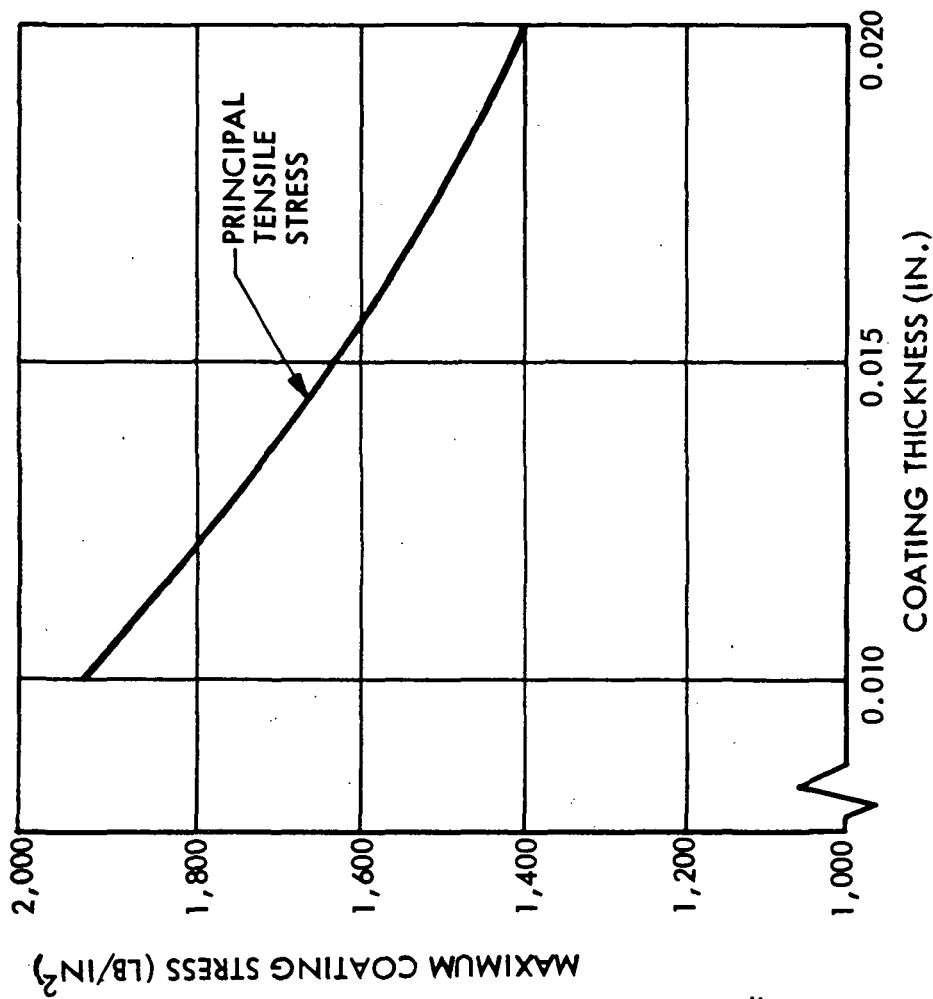


Fig. 3.2-12



VARIATION OF COATING STRESS WITH COATING THICKNESS

BERYLLIUM FUSELAGE SUBPANEL (SHORT TRAJECTORY)



$$t_{LI-1500} = 1.60 \text{ IN.}$$

$$E_{RTV-560} = 300 \text{ PSI}$$

$$G_{LI-1500} = 24,000 \text{ PSI}$$

$$t_{RTV-560} = 0.060 \text{ IN.}$$

$$E_{COATING} = 3.5 \times 10^6 \text{ PSI}$$

$$E_{LI-1500} = 60,000 \text{ PSI}$$

$$\text{LOADING } P = 1.14 \text{ PSI BURST}$$



ISOTROPIC ANALYSIS

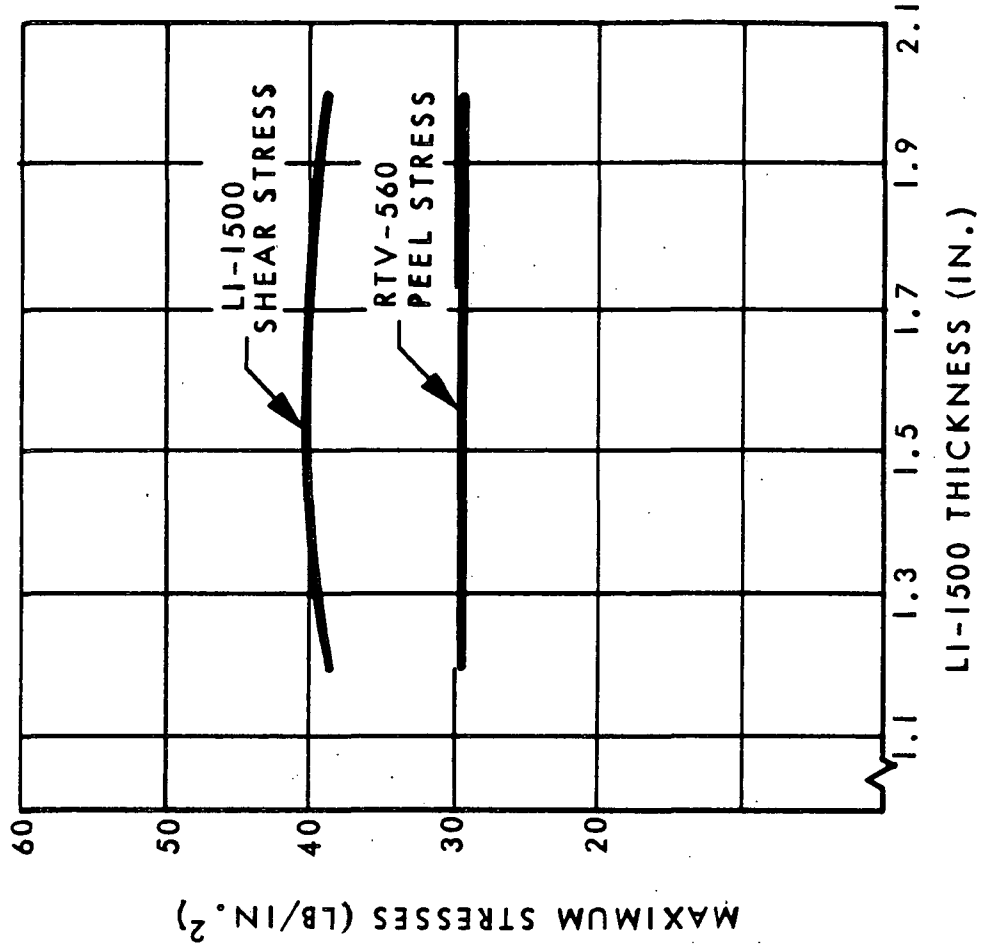
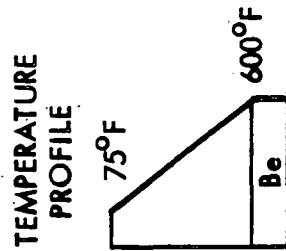
Fig. 3.2-13



VARIATION OF SHEAR AND PEEL STRESSES WITH LI-1500 THICKNESS

BERYLLIUM FUSELAGE SUBPANEL (SHORT TRAJECTORY)

- t_{COATING} = 0.010 IN.
- t_{RTV-560} = 0.060 IN.
- E_{RTV-560} = 300 PSI
- G_{LI-1500} = 24,000 PSI
- E_{COATING} = 3.5×10^6 PSI
- E_{LI-1500} = 60,000 PSI
- LOADING: p = 1.14 PSI BURST



ISOTROPIC ANALYSIS

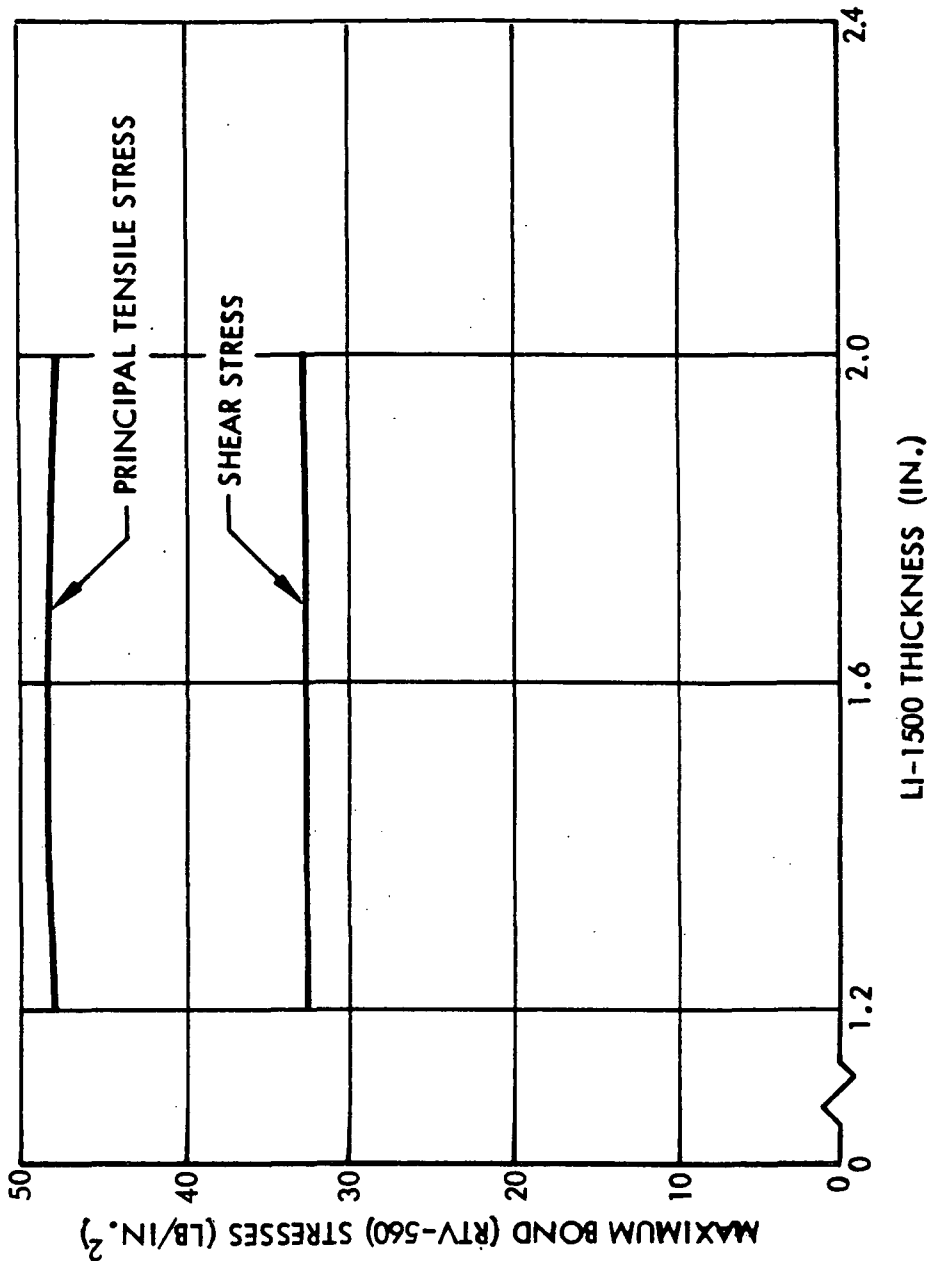
D05010(1)

Fig. 3.2-14



VARIATION OF BOND STRESSES WITH LI-1500 THICKNESS

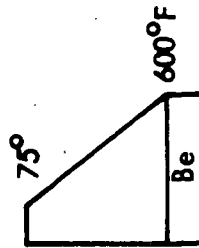
BERYLLIUM FUSELAGE SUBPANEL (SHORT TRAJECTORY)



- $t_{COATING} = 0.010$ IN.
- $t_{RTV-560} = 0.060$ IN.
- $E_{RTV-560} = 300$ PSI,
- $G_{LI-1500} = 24,000$ PSI
- $E_{COATING} = 3.5 \times 10^6$ PSI
- $E_{LI-1500} = 60,000$ PSI

LOADING:
P = 1.14 PSI BURST

TEMPERATURE
PROFILE



ISOTROPIC ANALYSIS

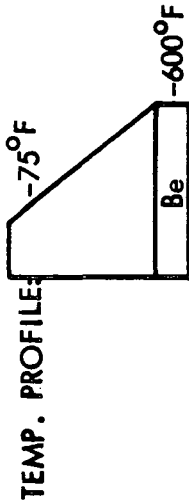
D04960 (1)

Fig. 3.2-15



VARIATION OF LI-1500 STRESS WITH LI-1500 THICKNESS

FUSELAGE PANEL PER LMSC- (SKW 100510)



$T_{COATING} = 0.010$ IN.

$T_{COATING} = 0.060$ IN.

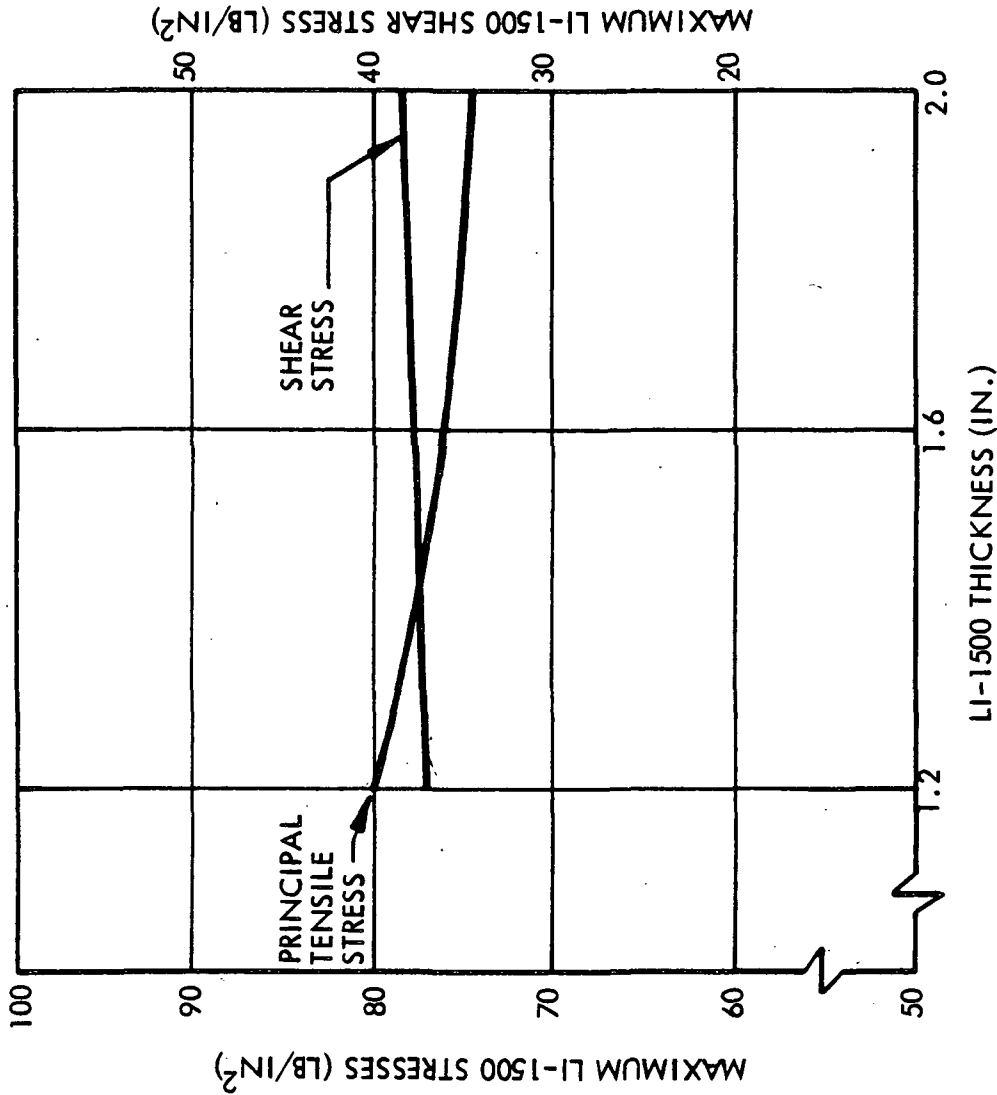
$E_{RTV-560} = 300$ PSI

$E_{COATING} = 3.5 \times 10^6$ PSI

$E_{LI-1500} = 60,000$ PSI

LOADING: SUBSONIC CRUISE

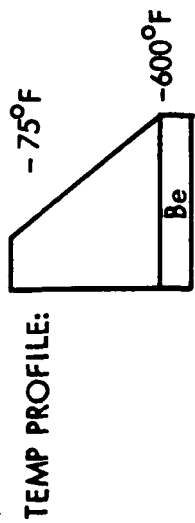
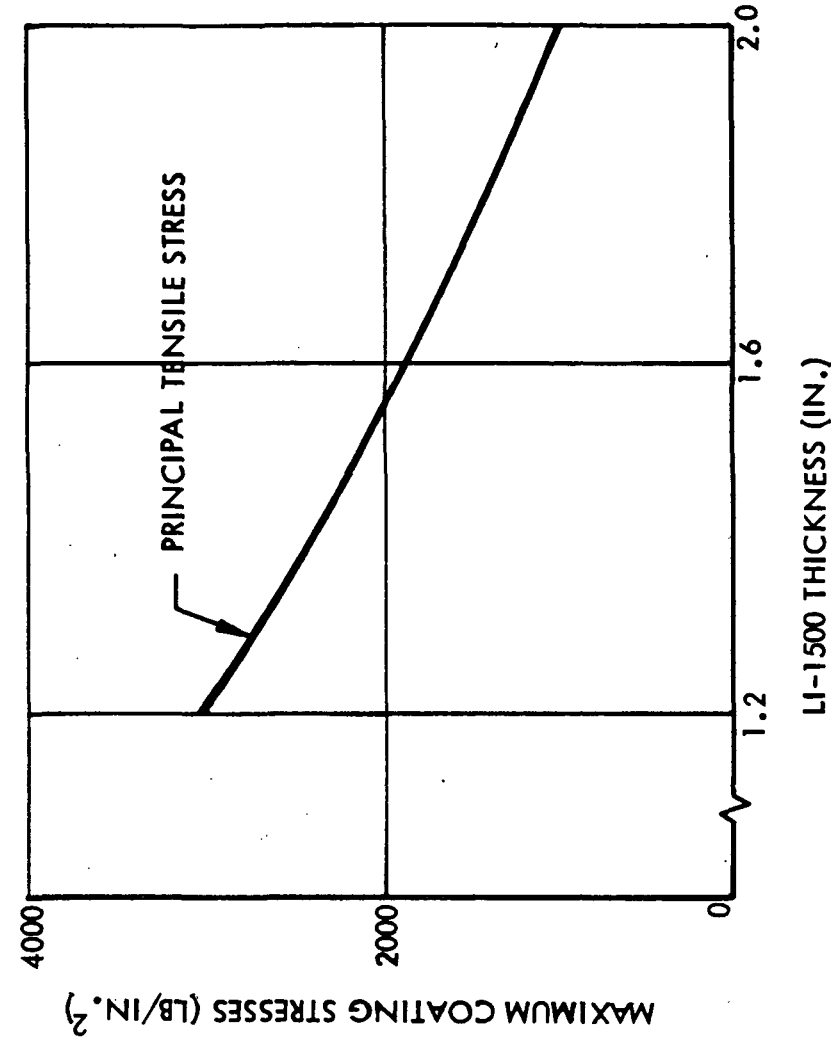
$P = 1.14$ PSI



VARIATION OF LI-1500 STRESS WITH LI-1500 THICKNESS



VARIATION OF COATING STRESSES WITH LI-1500 THICKNESS



FUSELAGE PANEL PER LMSC-A989337

$T_{COATING} = 0.010$ IN.

$T_{RTV-560} = 0.060$ IN.

$E_{RTV-560} = 300$ PSI

$E_{COATING} = 3.5 \times 10^6$ PSI

$E_{LI-1500} = 60,000$ PSI

LOADING: SUBSONIC CRUISE
P-1.14 PSI BURST

Fig. 3.2-17

Bond Thickness Effects on Stress Levels

Isotropic WILSON stress analyses using a constant LI-1500 thickness were carried out for a beryllium subpanel; the results are shown in Figs. 3.2-18 through 3.2-21. It is evident from these curves that bond thickness is a critical variable in RSI design. Effectively, a thicker bond offers more strain isolation from the deformations of the substrate than a thin bond.

A similar study is shown for the Aluminum Test Panel No. 2 in Figs. 3.2-22 through 3.2-27 although, in this case, an orthotropic WILSON analysis was used. In addition, the LI-1500 thickness was varied in accordance with previously discussed heat sink trade-off factors as the bond thickness was changed to keep the substrate temperature at 250°. The results again indicate the sensitivity of RSI stress levels on bond thickness.

Gap and Joint Studies

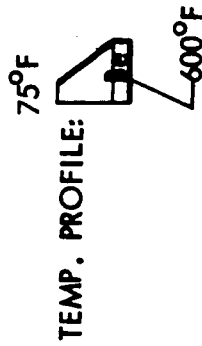
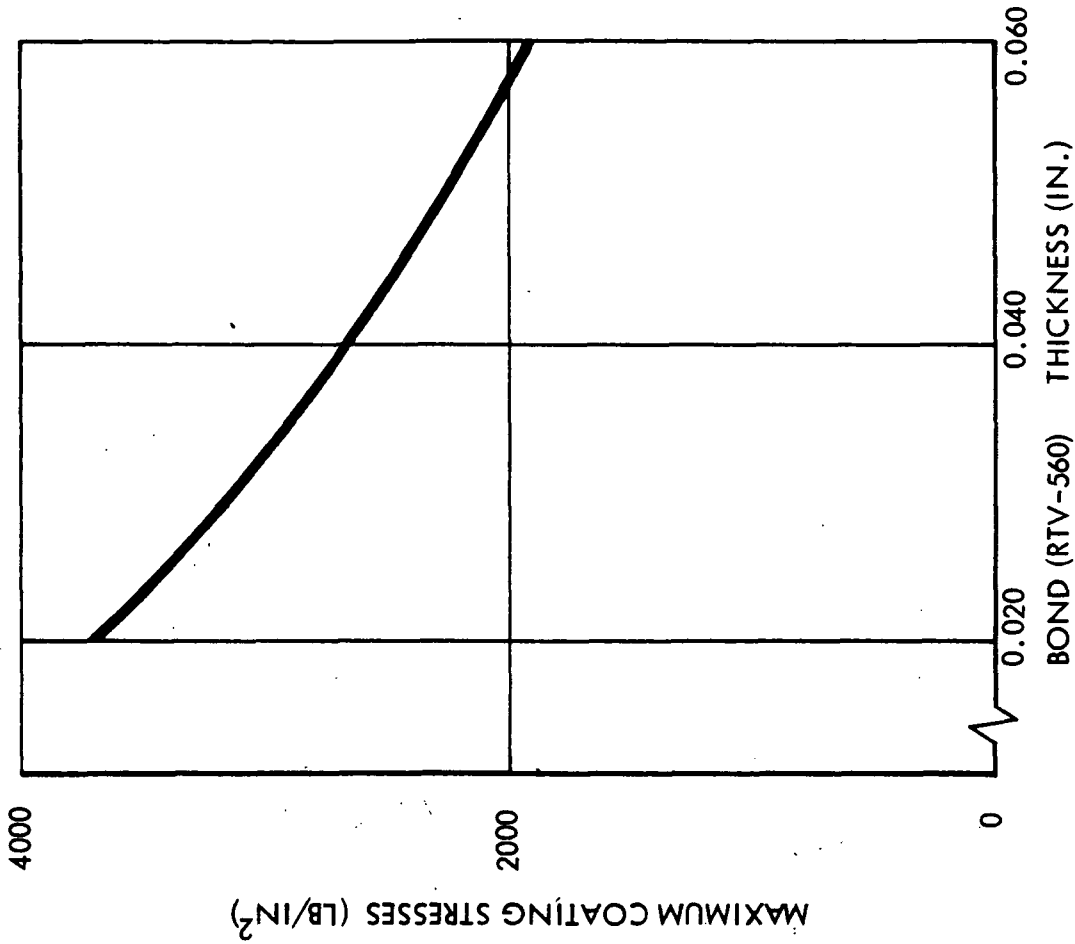
The effect of joint design on stress levels and gap dimensions between tiles has been investigated for a beryllium subpanel configuration. Table 3.2-4 summarizes a number of WILSON analyses for this study, in which the adjacent surfaces in the joint have been modeled in various ways. Case A represents a baseline configuration with surfaces never in bearing contact whereas Case B assumes that adjacent surfaces are partially continuous, due to bearing forces that lead to stress concentrations. Similar results are experienced in C. Case D represents the joint being filled with a material possessing LI-1500 elastic properties, except that the shear modulus has been assumed to be zero, simulating a frictionless joint. This case effectively behaves as a 12-in. tile, which leads to higher stress levels over the Case A baseline 6-in. tile. Case E is included for comparative purposes only, since it is not a suitable joint for other reasons as well as leading to slightly higher stress levels than the baseline joint. Case A is clearly superior, since the bonded length of tile is less than 6 inches and the stress levels are comparable to a shorter tile length. Similar results are shown in Table 3.2-5.

Studies of gap motion for an open joint during reentry are presented in Figs. 3.2-28 and 3.2-29 for a beryllium subpanel with 6-in. tiles and an aluminum primary structure panel with 4-in. panels. In the former case, high temperature conditions at the surface



VARIATION OF COATING STRESSES WITH BOND THICKNESS

FUSELAGE PANEL PER LMSC-A989337 (SKW 100510)



$t_{LI-1500} = 1.6 \text{ IN.}$

$t_{COATING} = 0.010 \text{ IN.}$

$E_{COATING} = 3.5 \times 10^6 \text{ PSI}$

LOADING: SUBSONIC CRUISE

$p = 1.14 \text{ PSI BURST}$

$E_{RTV-560} = 300 \text{ PSI}$

$E_{LI-1500} = 60,000 \text{ PSI}$

$G_{LI-1500} = 24,000 \text{ PSI}$

DO5993(1)

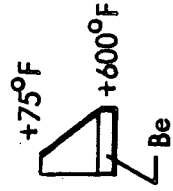
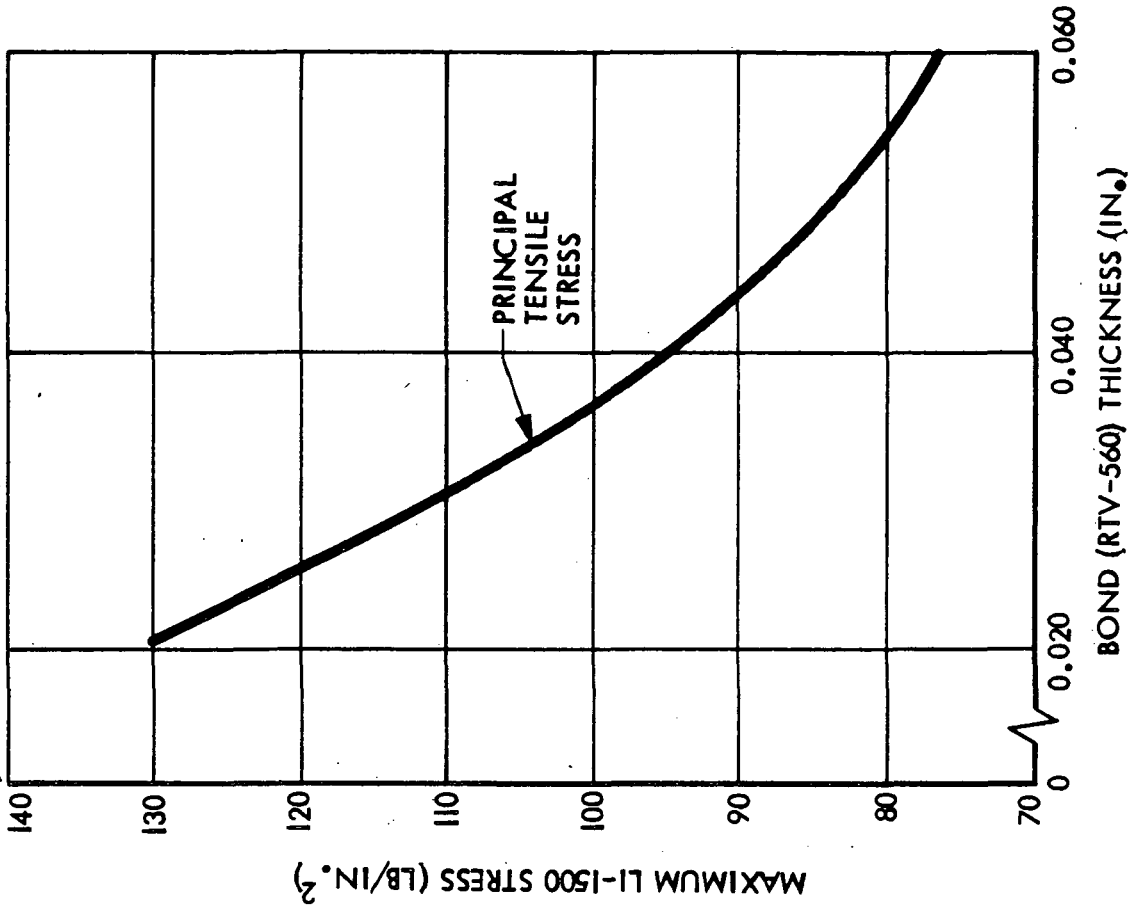
VARIATION OF COATING STRESSES WITH BOND THICKNESS

Fig. 3.2-18



VARIATION OF LI-1500 STRESSES WITH BOND THICKNESS

BERYLLIUM FUSELAGE SUBPANEL (SHORT TRAJECTORY)



TEMPERATURE PROFILE

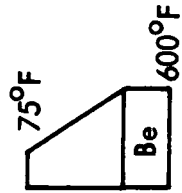
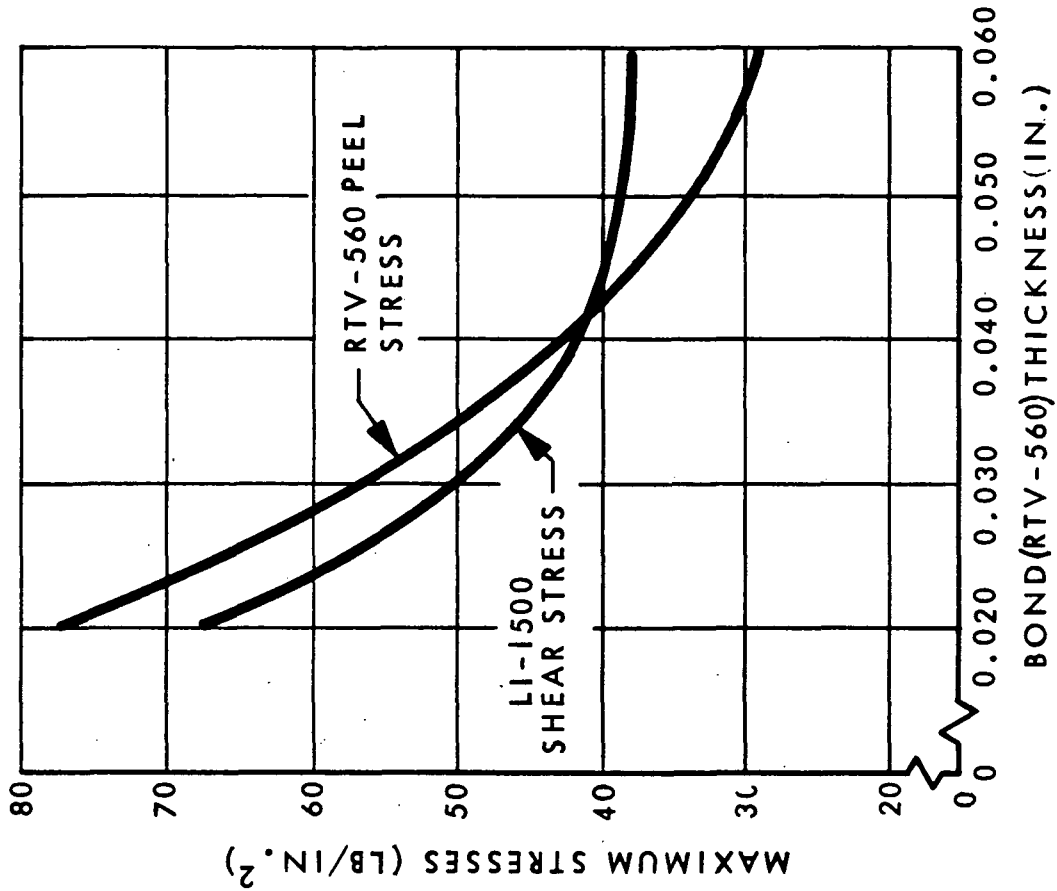
- $t_{LI-1500} = 1.6$ IN.
- $t_{COATING} = 0.010$ IN.
- $E_{COATING} = 3.5 \times 10^6$ PSI
- LOADING: $p = 1.14$ PSI BURST
- $G_{LI-1500} = 24,000$ PSI
- $E_{RTV-560} = 300$ PSI
- $E_{LI-1500} = 60,000$ PSI

ISOTROPIC ANALYSIS

Fig. 3.2-19

VARIATION OF SHEAR AND PEEL STRESSES WITH RTV-560 BOND THICKNESS

BERYLLIUM FUSELAGE SUBPANEL (SHORT TRAJECTORY)



TEMPERATURE PROFILE

- $t_{LI-1500} = 1.6 \text{ IN.}$
- $t_{COATING} = 0.010 \text{ IN.}$
- $E_{COATING} = 3.5 \times 10^6 \text{ PSI}$
- LOADING $P = 1.14 \text{ PSI BURST}$
- $G_{LI-1500} = 24,000 \text{ PSI}$
- $E_{RTV-560} = 300 \text{ PSI}$
- $E_{LI-1500} = 60,000 \text{ PSI}$

ISOTROPIC ANALYSIS

3.2-26

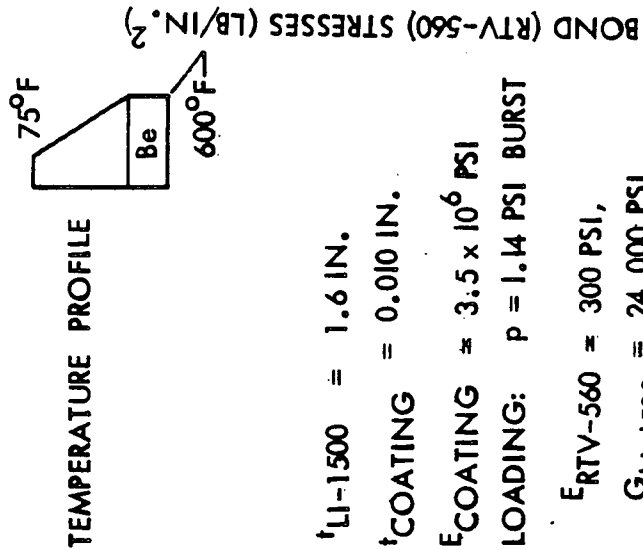
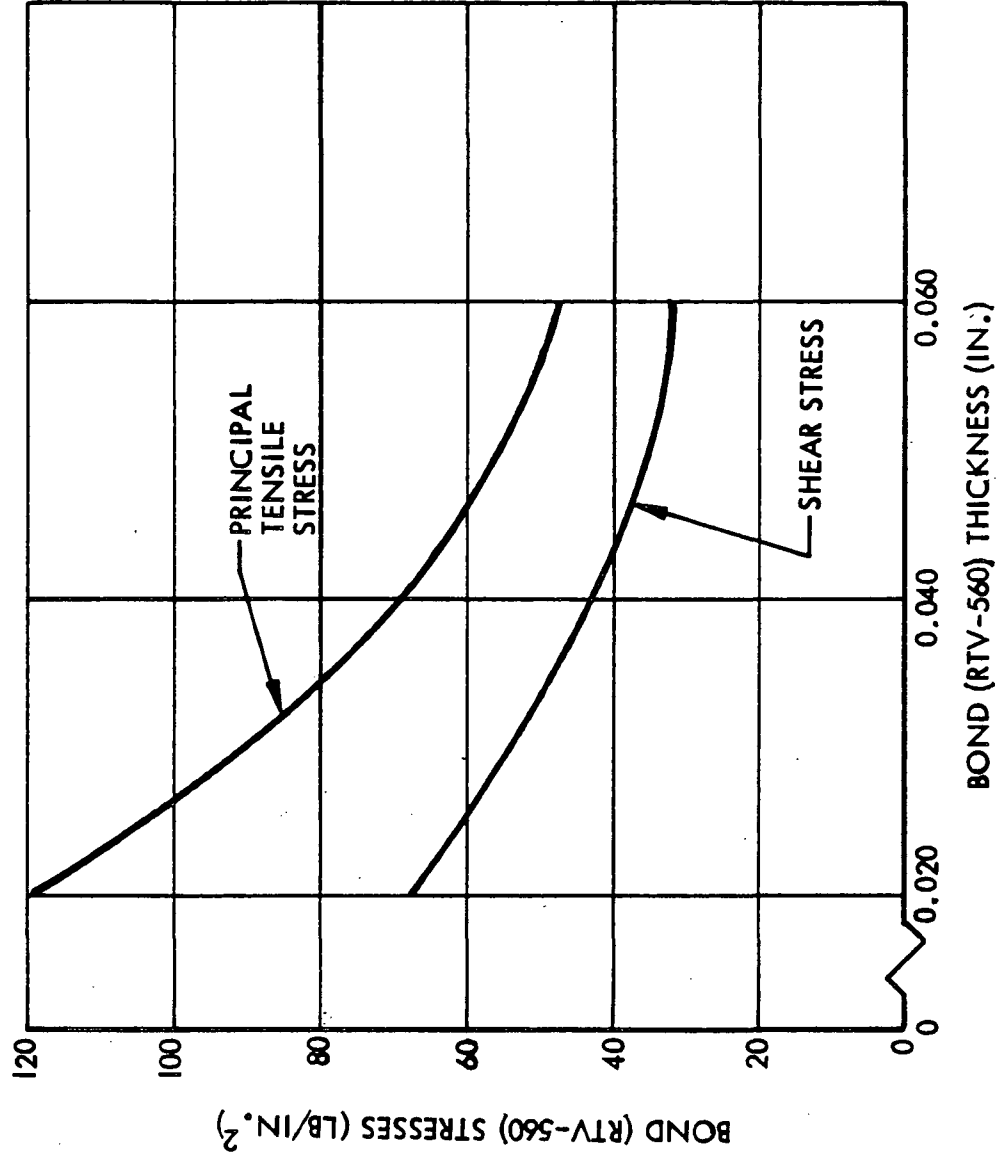
Fig. 3.2-20

D05008 (1)



VARIATION OF BOND STRESSES WITH BOND THICKNESS

BERYLLIUM FUSELAGE SUBPANEL (SHORT TRAJECTORY)



ISOTROPIC ANALYSIS

Fig. 3.2-21



VARIATION OF LI-1500 SHEAR AND PEEL STRESSES WITH BOND THICKNESS (CONSTANT BACKFACE TEMPERATURE)

ALUMINUM PRIMARY STRUCTURE NO. 2
(FUSELAGE AREA NO. 2)

† ALUMINUM = 0.711 IN.

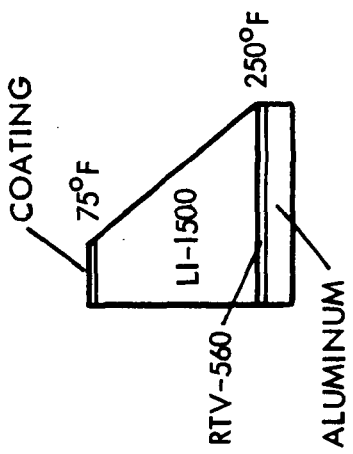
† COATING = 0.010 IN.

LI-1500 TILE LENGTH = 4 IN.

p = 1.5 PSI BURST

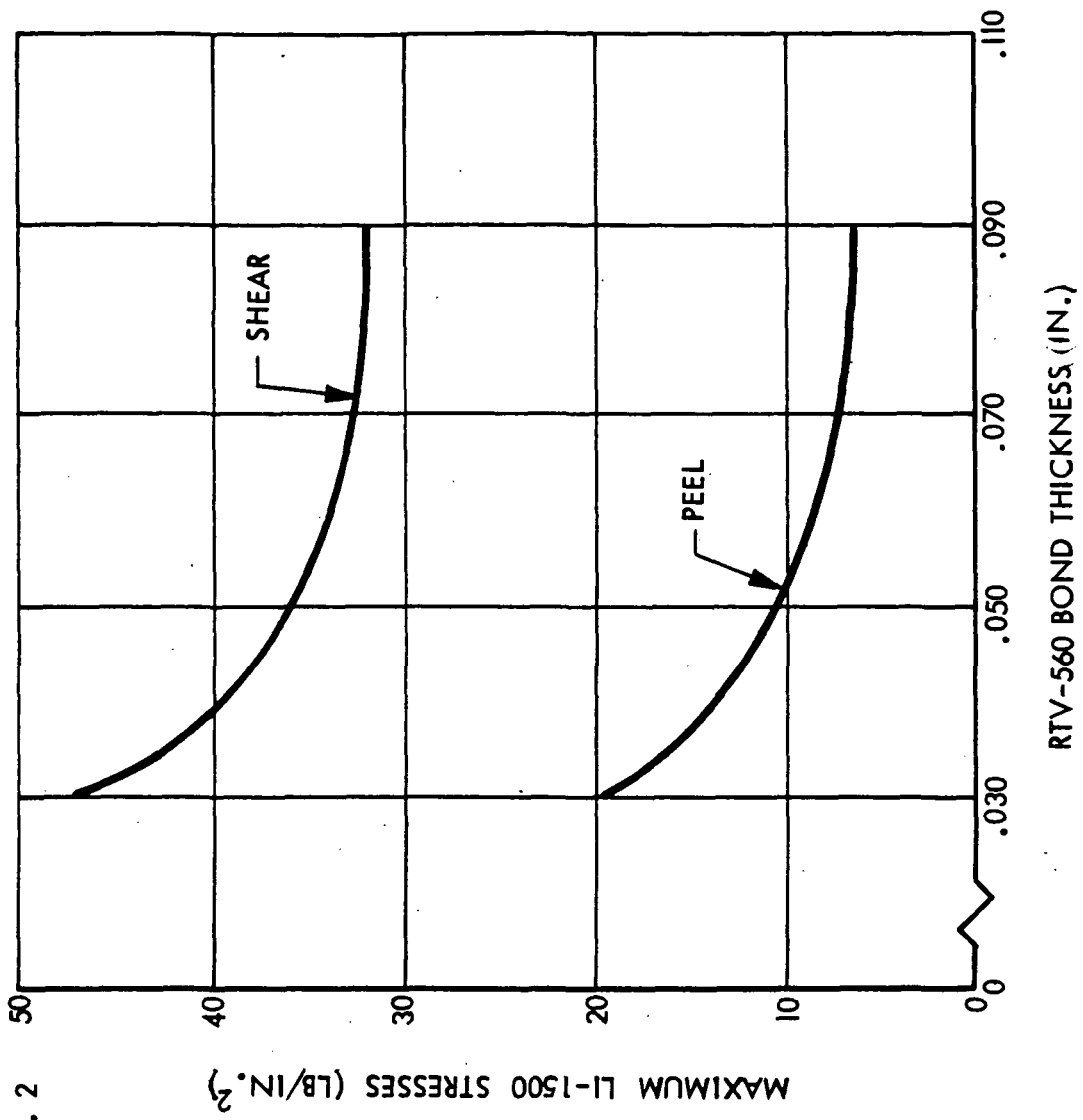
6000 PPI TENSION

130 <



TEMPERATURE PROFILE

ORTHOTROPIC ANALYSIS



DO4990 (1)

RDB

Fig. 3.2-22



VARIATION OF LI-1500 STRESS WITH BOND THICKNESS (CONSTANT BACKFACE TEMPERATURE)

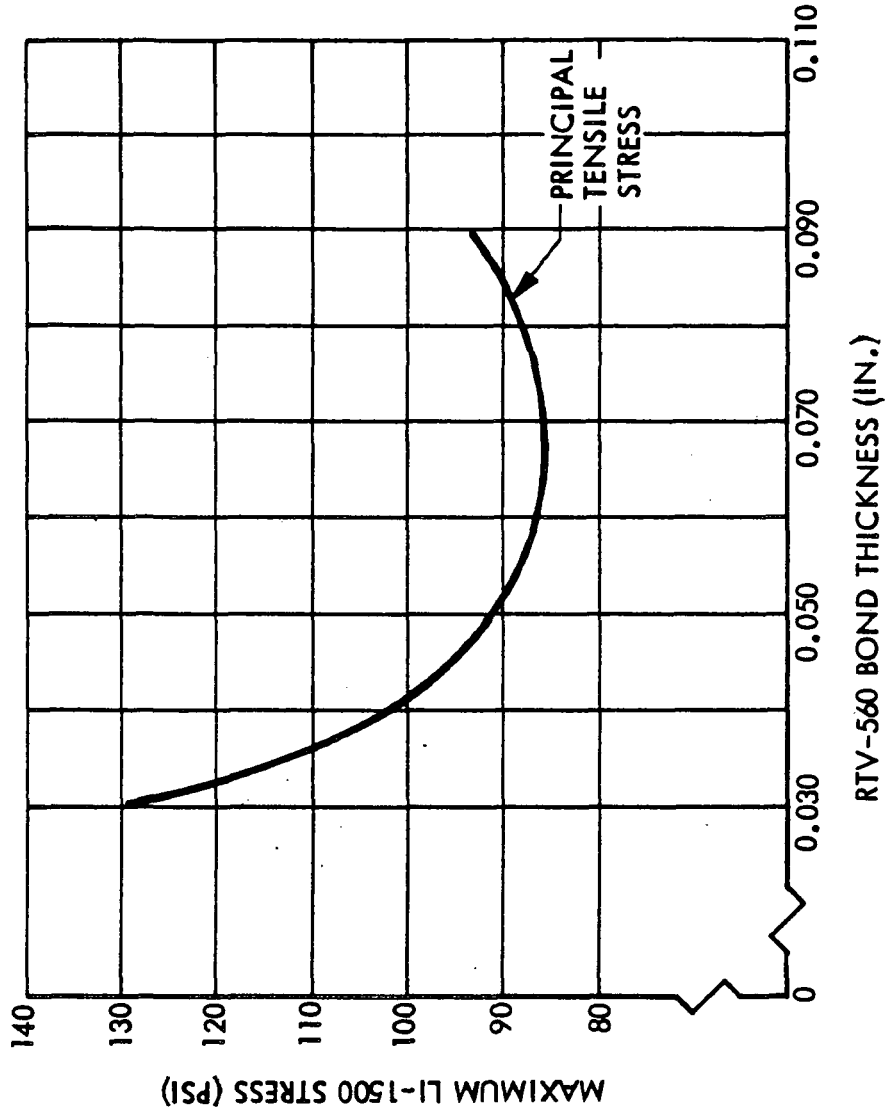
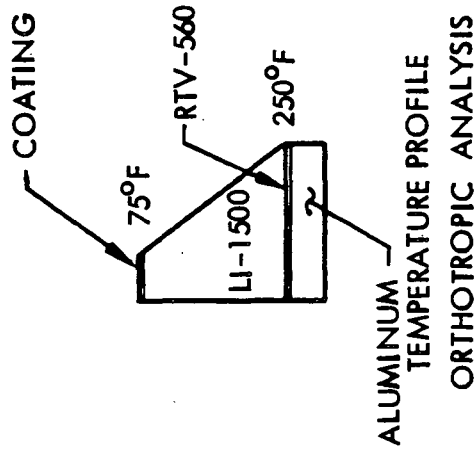
ALUMINUM PRIMARY STRUCTURE PANEL NO. 2 (FUSELAGE AREA NO. 2)

^t ALUMINUM = 0.711 IN.

^t COATING = 0.010 IN.

LI-1500 TILE LENGTH = 4 IN.

LOADING: $p = 1.5$ PSI BURST
6000 PPI TENSION

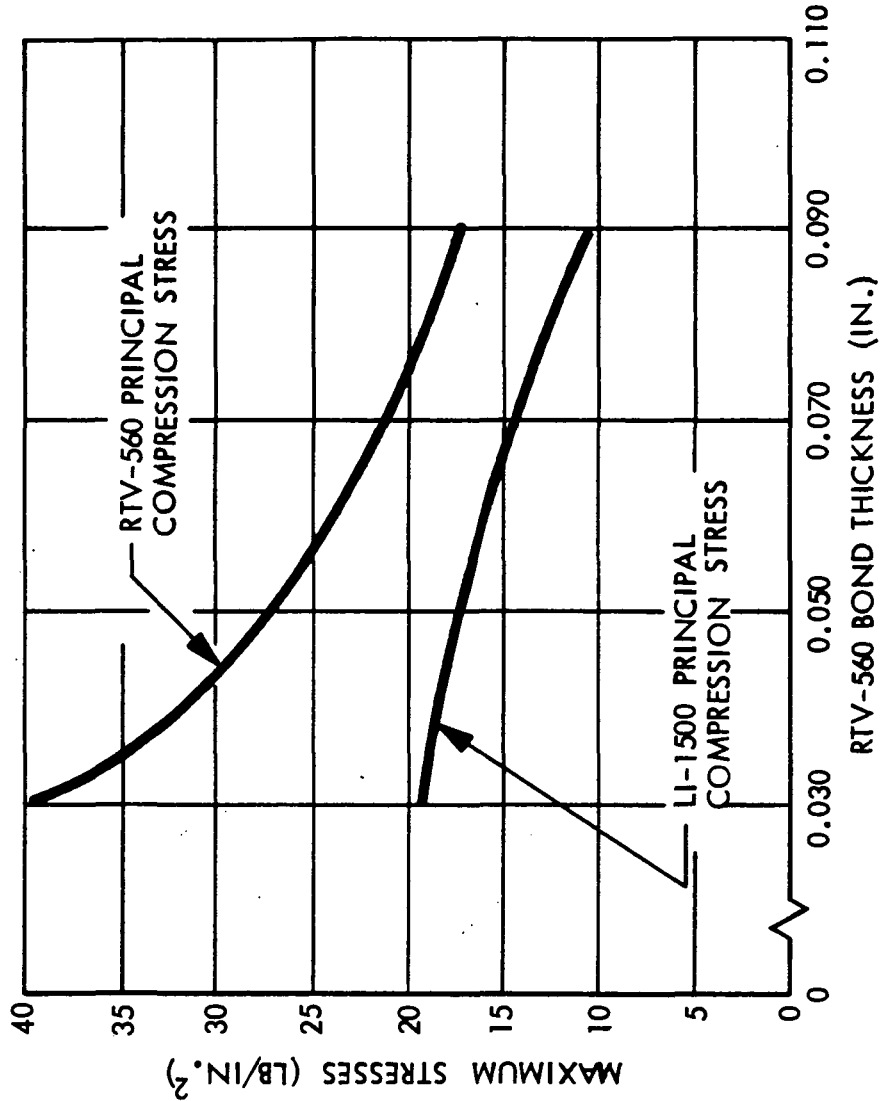
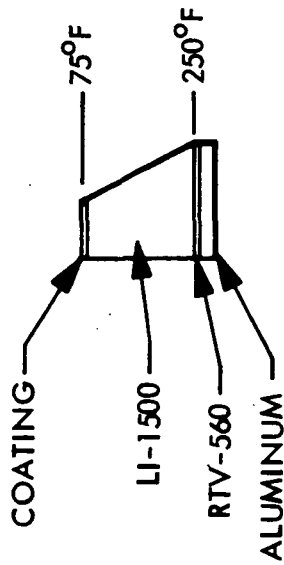




VARIATION OF LI-1500 AND RTV-560 MINIMUM STRESSES WITH BOND THICKNESS (CONSTANT BACKFACE TEMPERATURE)

ALUMINUM PRIMARY STRUCTURE PANEL NO. 2
(FUSELAGE AREA NO. 2)

t_{ALUMINUM} = 0.711 IN.
 t_{COATING} = 0.010 IN.
 LI-1500 TILE LENGTH = 4 IN.
 P = 1.5 PSI BURST
 6000 PPI TENSION

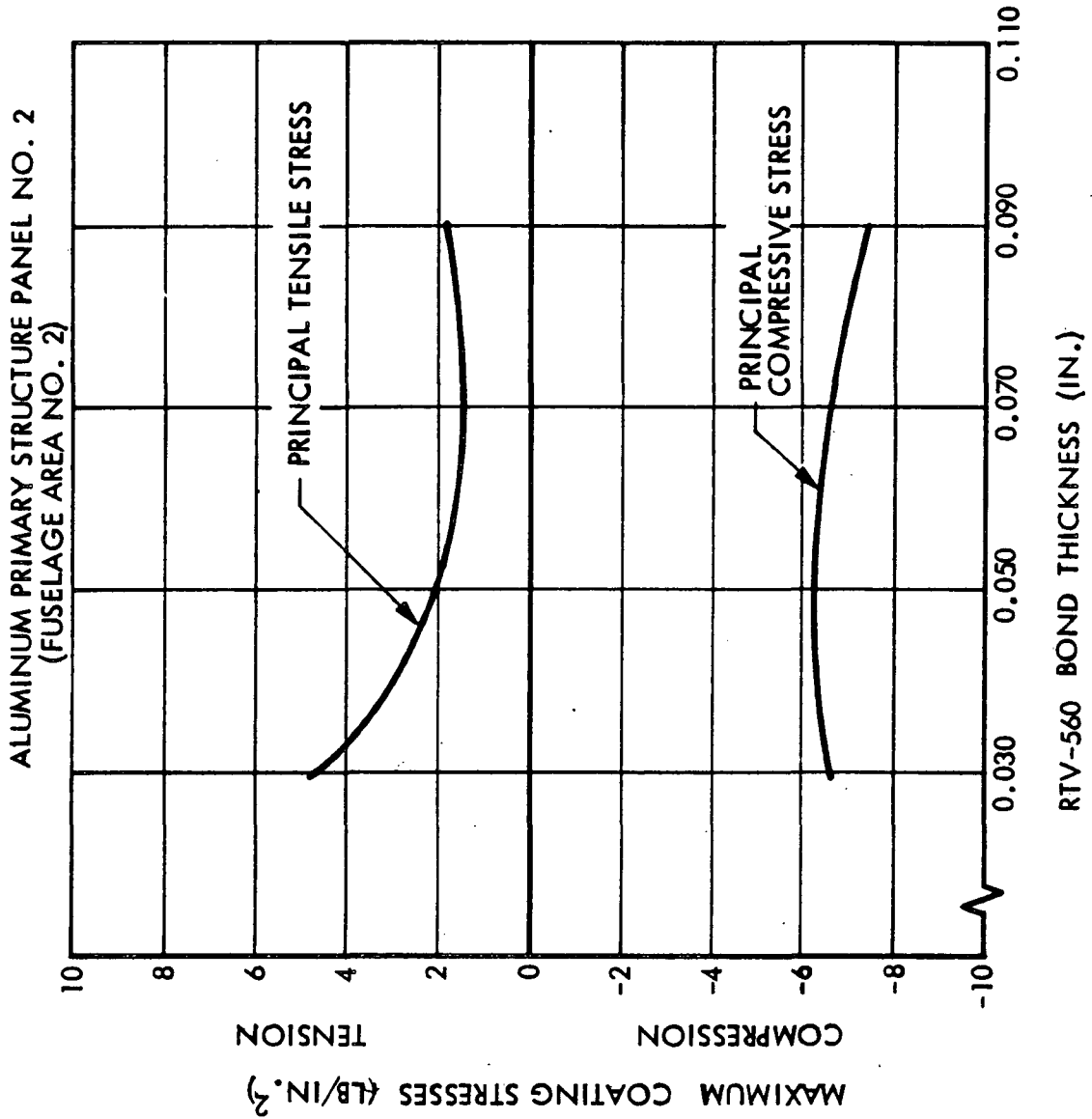


D04977 (1)

Fig. 3.2-24



VARIATION OF PRINCIPAL COATING STRESSES WITH BOND THICKNESS - CONSTANT BACKFACE TEMPERATURE

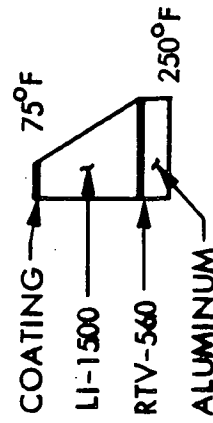


t_{ALUMINUM} = 0.711 IN.

t_{COATING} = 0.010 IN.

LOADING p = 1.5 PSI BURST
6000 PPI TENSION

LI-1500 TILE
LENGTH = 4 IN.



TEMPERATURE PROFILE
ORTHOTROPIC ANALYSIS

D05000 (1)

Fig. 3.2-25



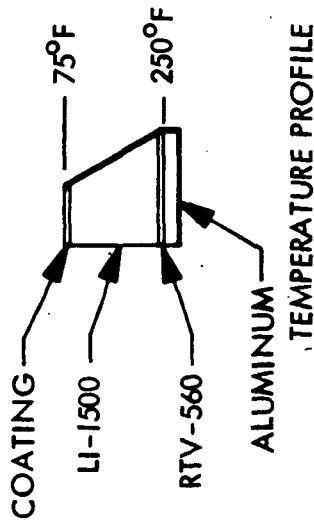
VARIATION OF RTV-560 SHEAR AND PEEL STRESSES WITH BOND THICKNESS - (CONSTANT BACKFACE TEMPERATURE)

ALUMINUM PRIMARY STRUCTURE NO. 2
(FUSELAGE AREA NO. 2)

$t_{\text{ALUMINUM}} = 0.711 \text{ IN.}$

$P = 1.5 \text{ PSI BURST}$
6000 PPI TENSION

$t_{\text{COATING}} = 0.010 \text{ IN.}$
LI-1500 TILE LENGTH = 4 IN.



ORTHOTROPIC ANALYSIS

D04999(1)

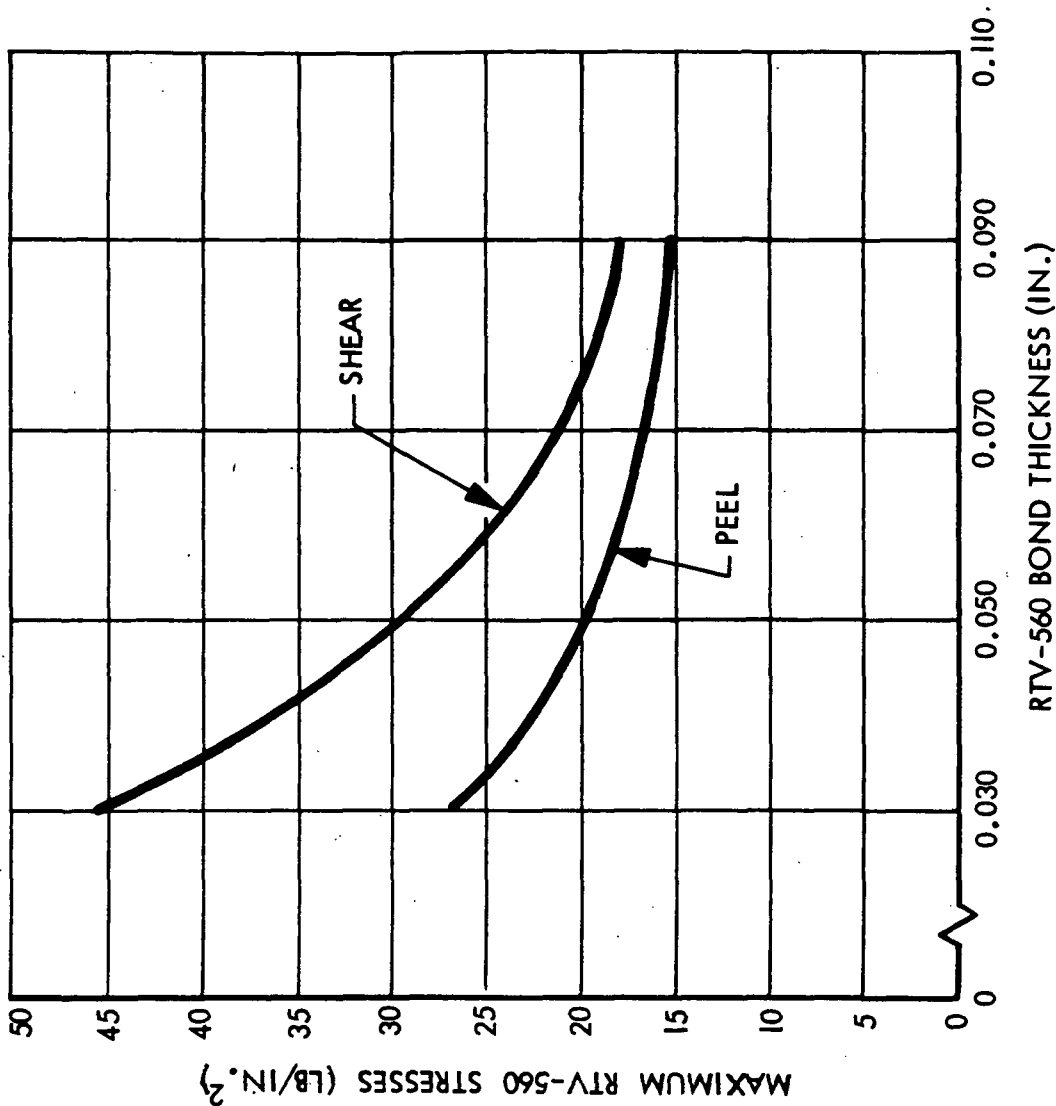


Fig. 3.2-26



VARIATION OF MAXIMUM BOND STRESS WITH BOND THICKNESS - CONSTANT BACKFACE TEMPERATURE

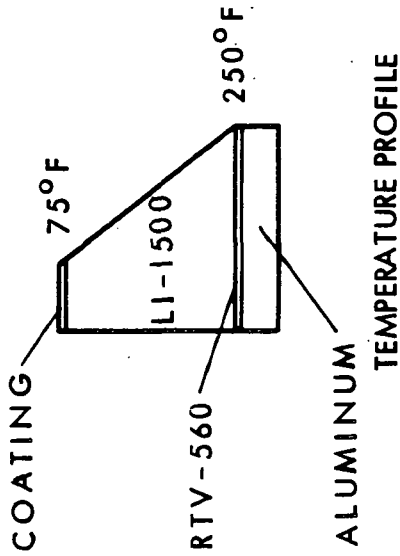
ALUMINUM PRIMARY STRUCTURE PANEL NO. 2
(FUSELAGE AREA NO. 2)

$t_{\text{ALUMINUM}} = 0.711 \text{ IN.}$

$t_{\text{COATING}} = 0.010 \text{ IN.}$

LOADING: $p = 1.5 \text{ PSI BURST}$
6000 PPI TENSION

LI-1500
TILE LENGTH = 4 IN.



ORTHOTROPIC ANALYSIS

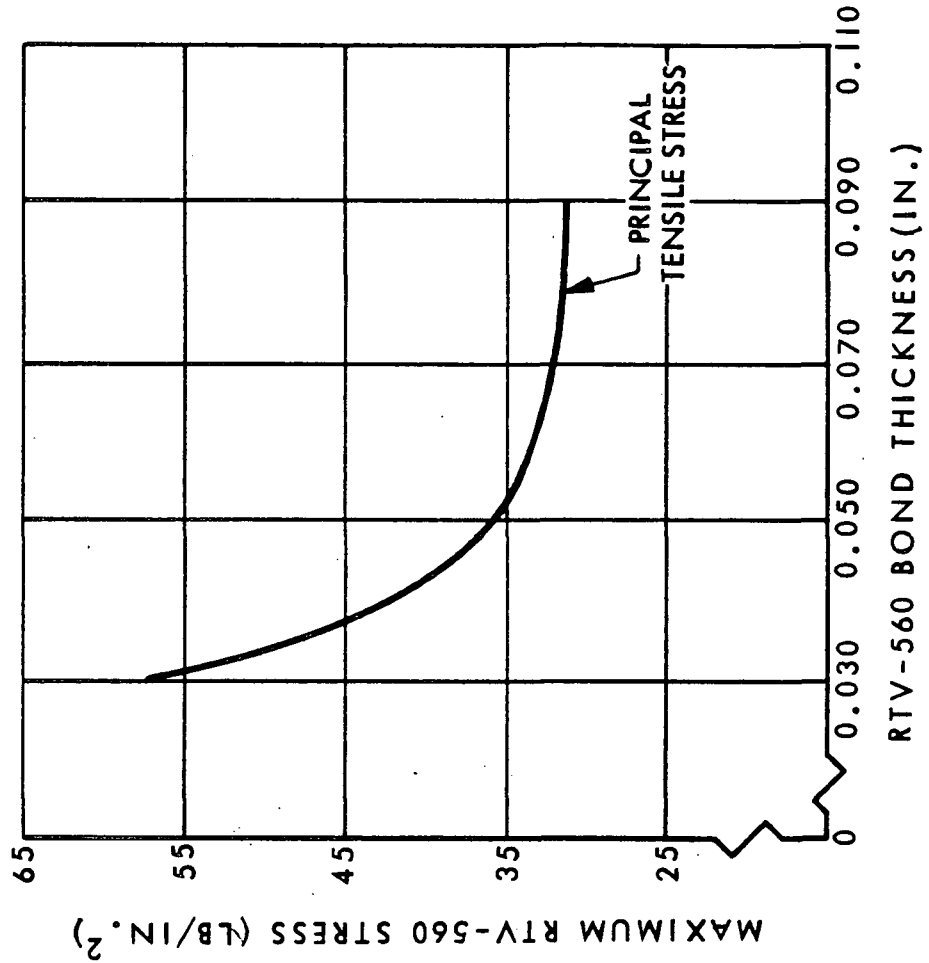


Fig. 3.2-27



Table 3.2-4

JOINT COMPARISON STUDIES

	(A)	(B)	(C)	(D)*	(E)
MAX. LI-1500	12.4	19.4	58.5	47.3	14.8
MIN. LI 1500	-8.7	-221.4	-227.1	-32.0	-10.0
SHEAR (R2) LI-1500	3.0	41.9	82.2	10.1	3.5
LONG. LI-1500	12.4	-221.4	-227.0	46.6	14.8
PEEL LI-1500	4.1	6.5	4.6	9.2	4.5
MAX. RTV-560	4.1	6.0	5.9	5.5	4.5
MIN. RTV-560	-10.0	-16.0	-15.7	-21.0	-11.4
SHEAR RTV-560	1.6	4.0	3.8	4.4	1.8
LONG. RTV-560	-4.8	-7.1	-7.0	-9.6	-5.4
PEEL RTV-560	4.1	4.6	4.6	4.2	4.5
MAX. COATING	0.4	25.6	25.2	9.2	0.3
MIN. COATING	-236.1	-395.4	-396.7	-1539.5	-333.8

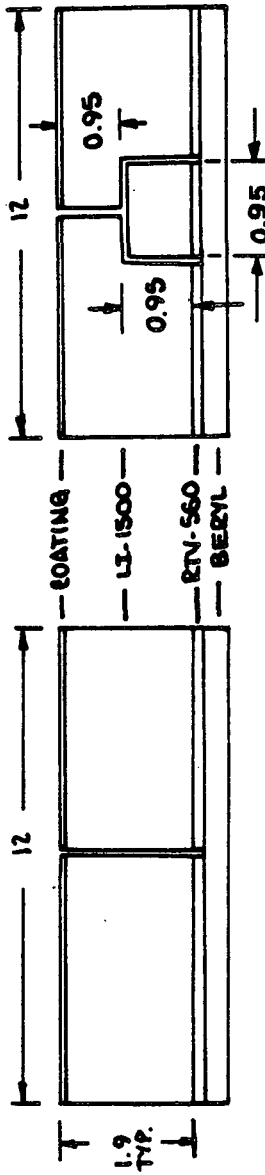
BERYLLIUM TEST PANEL 6.75 PSI COLLAPSE PRESSURE
LOADING CONDITION: 75°F. UNIFORM

- LOCATION OF MAXIMUM STRESS
- *JOINT FILLED WITH ZERO SHEAR MODULUS MATERIAL

D07081(1)

Table 3.2-5

BERYLLIUM FUSELAGE PANEL, AREA 2
JOINT CONCEPTS



MAXIMUM STRESSES

32.6
-1.5
8.4
32.5
6.1

MAXIMUM STRESSES

34.9
-1.7
9.0
34.8
7.0

9.9
-17.6
8.6
-16.9
6.7

49.9

MAX LI-1500
MIN LI-1500
SHEAR LI-1500
LONG LI-1500
PEEL LI-1500

MAX RTV-560
MIN RTV-560
SHEAR RTV-560
LONG RTV-560
PEEL RTV-560

MAX COATING
MIN COATING

LOADING

P = 1.5 PSI BURST

T_{Be} = 550°F

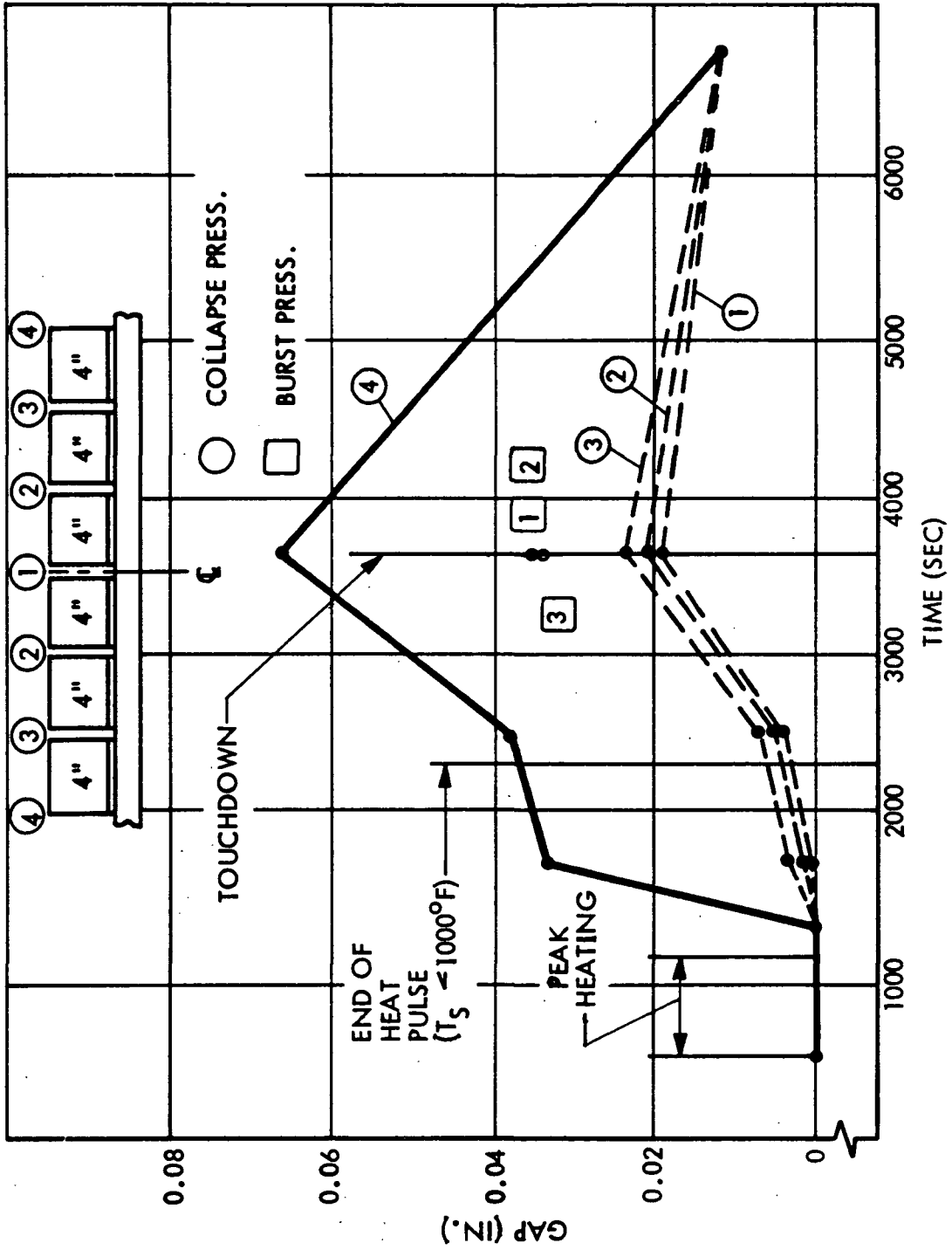
T_{COAT} = 100°F

D05138 (1)

3.2-35

137

GAP ENLARGEMENT BETWEEN TILES ON 24" ALUMINUM FLIGHT PANEL #2
AT VARIOUS TIMES AFTER START OF REENTRY



DO5973 (1)

Fig. 3.2-28



GAP ENLARGEMENT BETWEEN TILES ON 24" BERYLLIUM SUBPANEL #1
AT VARIOUS TIMES AFTER START OF REENTRY

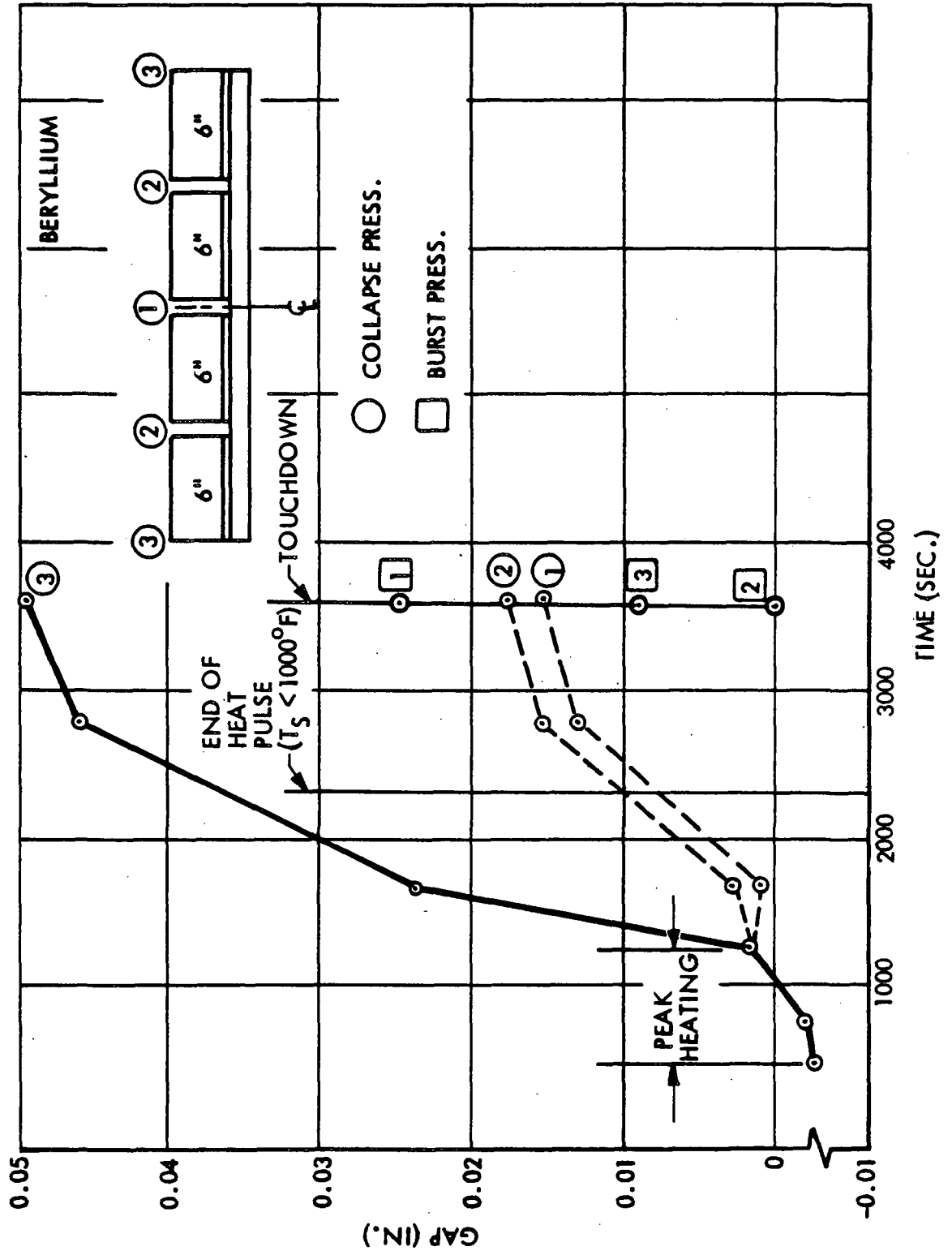


Fig. 3.2-29

initially tend to close the gap followed by domination of the substrate expansion. Maximum gap opening occurs at the panel ends, and the 50-mil enlargement (which occurs at touchdown following reentry) shown for the beryllium panel is the total opening due to both panels at the common support as shown in Fig. 3.2-30. Results for the aluminum panel are qualitatively similar, although the maximum in this case is approximately 65 mils. From these studies, it appears that the baseline joint is most desirable in that large gaps directly open to the bondline are not possible during reentry.

Initial closing of the baseline joint is presented for the beryllium subpanel in Fig. 3.2-31 where appropriate gap dimensions for zero bearing forces are deduced. Minimum required gaps for other configurations are also summarized in Table 3.2-6. Since the primary difference in test and flight panels is one of LI-1500 thickness, it is seen that gap size is linearly related to LI-1500 thickness. This is plausible since collapse pressure induces overall panel bending.

Effects of Coating Texturing and Discontinuities on RSI Stress Levels

The desirability of a waved-surface coating to reduce stress has been investigated. Results shown in Fig. 3.2-32a and b indicate wide fluctuations in coating stress, principally caused by local bending effects due to eccentric load paths through the coating. These fluctuations depend on the wave length of the texturing and, for the case shown, there is approximately a 10-percent decrease in maximum coating stress. In effect, the texturing acts to lower the overall extensional stiffness of the coating, hence there is a lower stress for a given strain.

Studies of discontinuous coatings are presented in Figs. 3.2-33 through 3.2-35. The overall effect on coating stress is essentially the same as that due to texturing, although the coating stress must go to zero at the discontinuities. However, as noted in Fig. 3.2-33, the maximum stresses in the LI-1500 at the discontinuity are magnified approximately five times over those corresponding to a continuous coating. This is clearly unacceptable, hence the use of this concept is precluded. These conclusions apply to the general case, although these studies were carried out on a specific beryllium subpanel configuration.

GAP OPENING DUE TO THERMAL EXPANSION

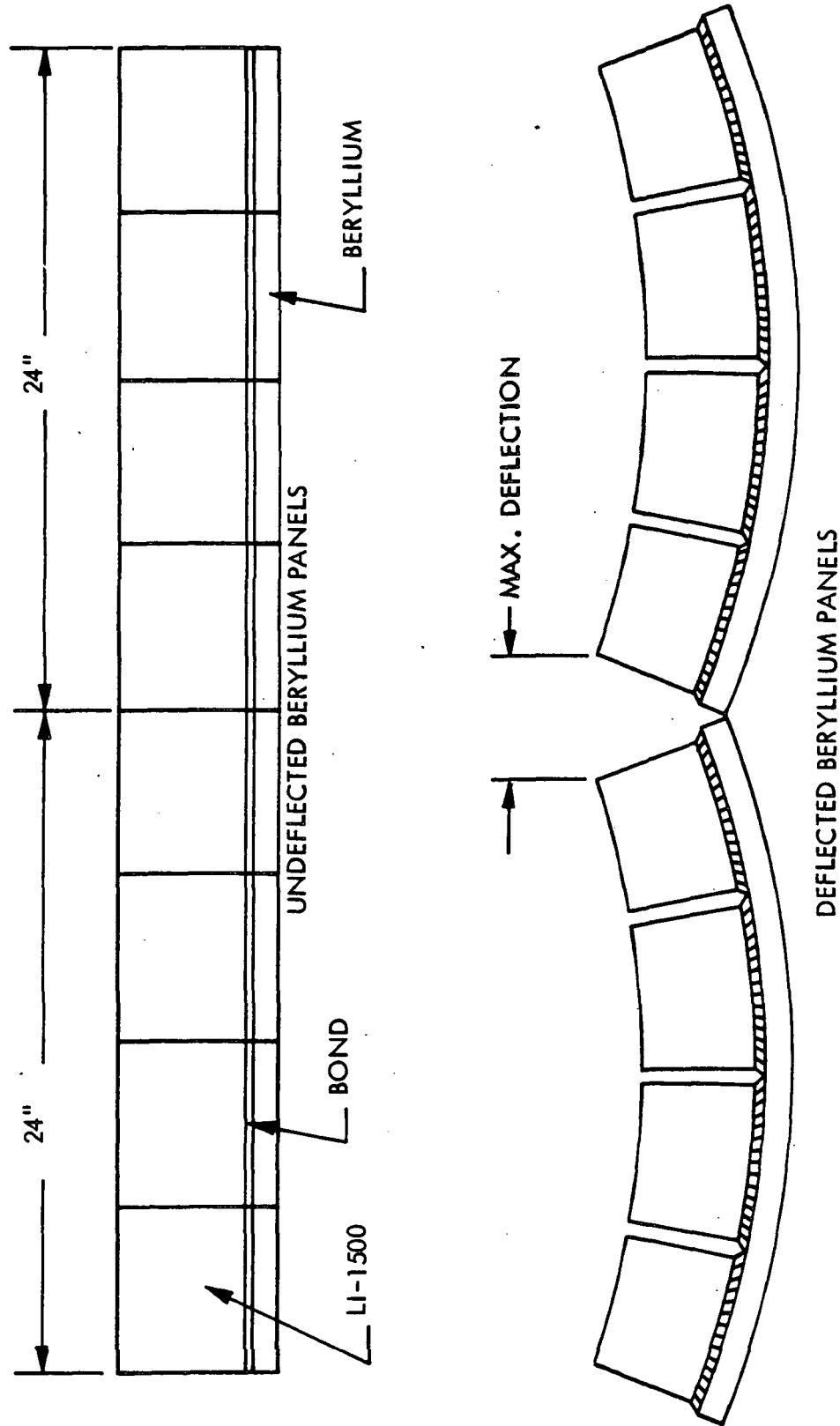
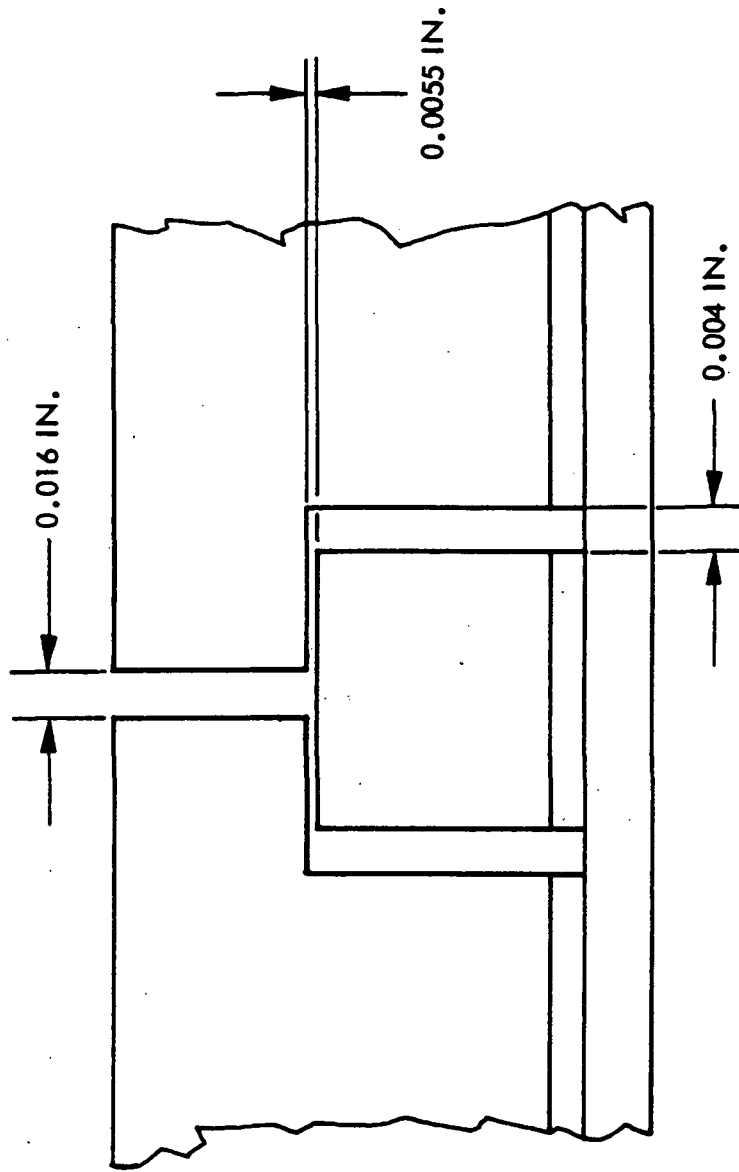


Fig. 3.2-30



MINIMUM GAPS REQUIRED IN Be PANEL JOINT



(TILE LENGTH = 6") (6.75 PSI COLLAPSE PRESSURE AT R.T.)

Fig. 3.2-31

Table 3.2-6

**MINIMUM GAPS REQUIRED AT THE
JOINTS FOR ZERO INTERFERENCE**

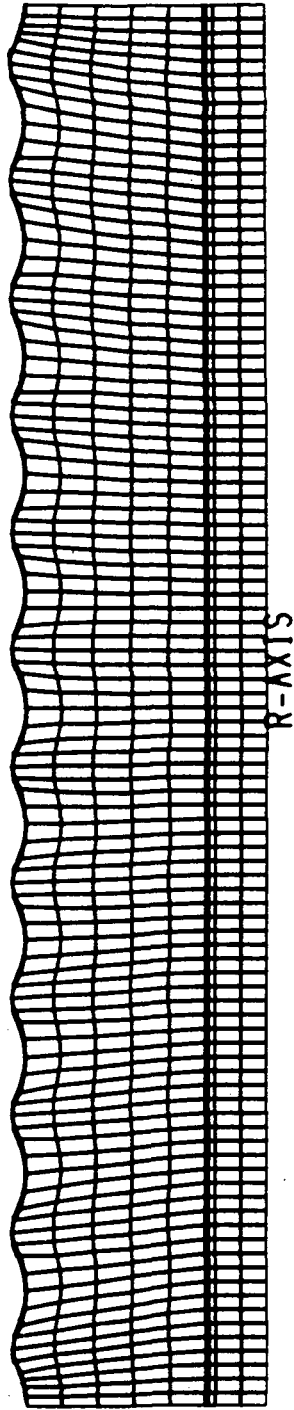
<u>PANEL</u>	<u>REQUIRED GAP</u>
BERYLLIUM TEST NO. 1	0.035
ALUMINUM TEST NO. 2	0.045
ALUMINUM TEST NO. 3	0.024
TITANIUM TEST NO. 4	0.030
BERYLLIUM FLIGHT NO. 1	0.023
ALUMINUM FLIGHT NO. 2	0.034
ALUMINUM FLIGHT NO. 3	0.018
TITANIUM FLIGHT NO. 4	0.019





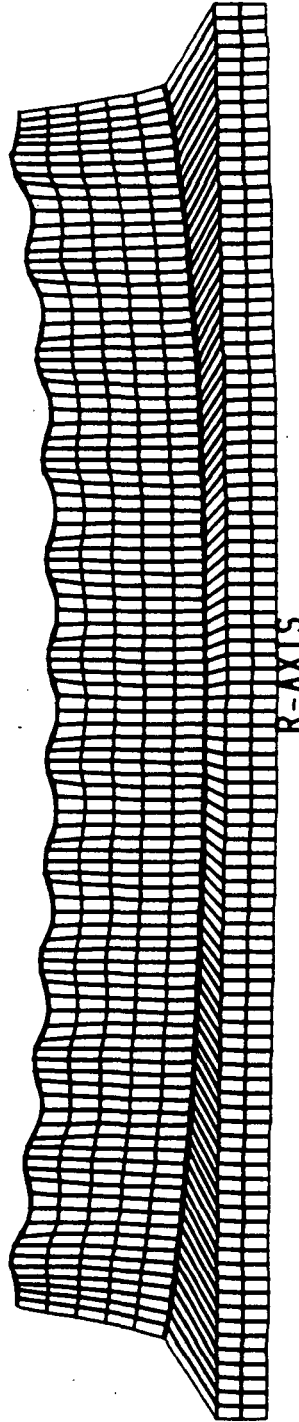
TEXTURED COATING STUDY - BERYLLIUM FUSELAGE PANEL

$P = 1.14 \text{ PSI BURST}$, $T_{Be} = 600^\circ\text{F}$, $T_{COAT} = 75^\circ\text{F}$, TILE LENGTH = 12 IN.



COMPUTER
MODEL

NO
LOAD



DURING
LOADING

Fig. 3.2-32a

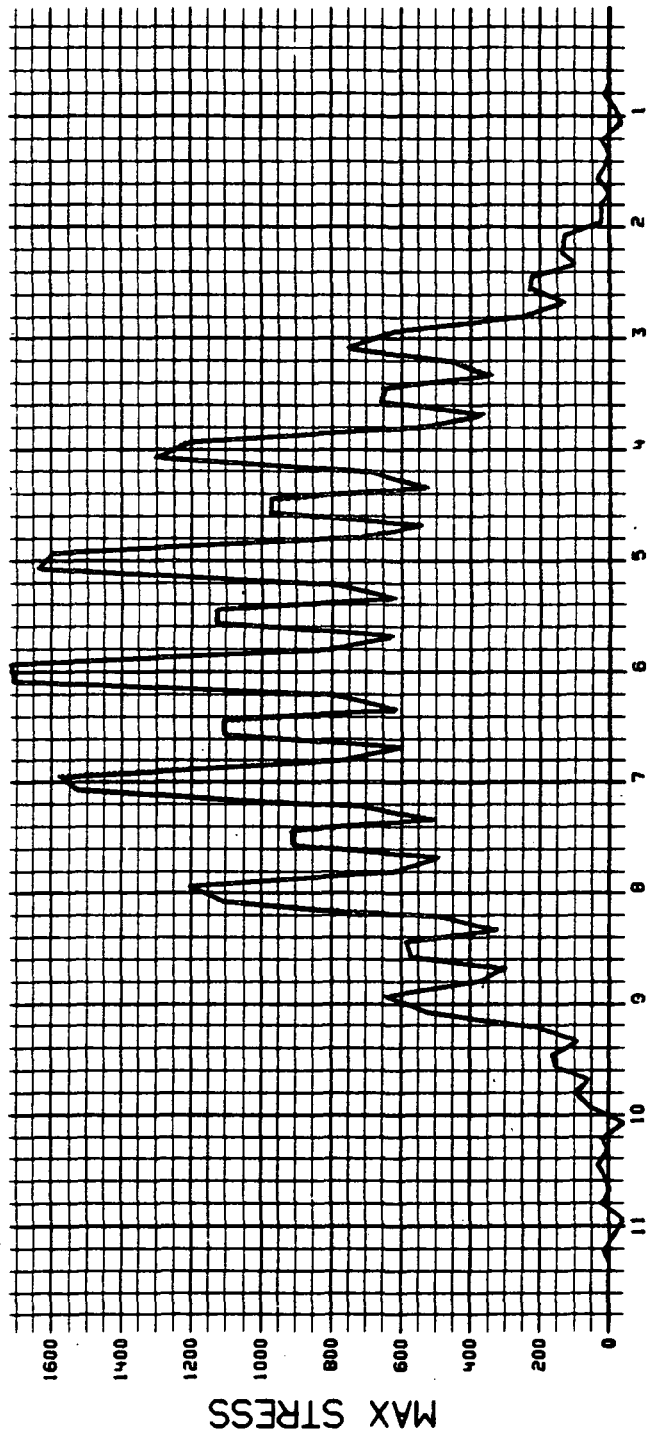
D07079



TEXTURED COATING STUDY - BERYLLIUM FUSELAGE PANEL (Cont'd)

P = 1.14 PSI BURST, $T_{Be} = 600^{\circ}F$, $T_{COAT} = 75^{\circ}F$, TILE LENGTH = 12 IN.

CASE J-TEXTURED COATING STUDY-FUS.PANEL PER LMSC-989337, E=60000 T=.06
THERMAL PROTECTION SYSTEMS



MAX TEXTURED COATING STRESS = 1718 PSI (TENSION)
MAX STRAIGHT COATING STRESS = 1950 PSI (TENSION)

145<
3.2-43

Fig. 3.2-32 b



VARIATION OF COATING STRESS WITH NUMBER OF COATING DISCONTINUITIES

SYM ABOUT

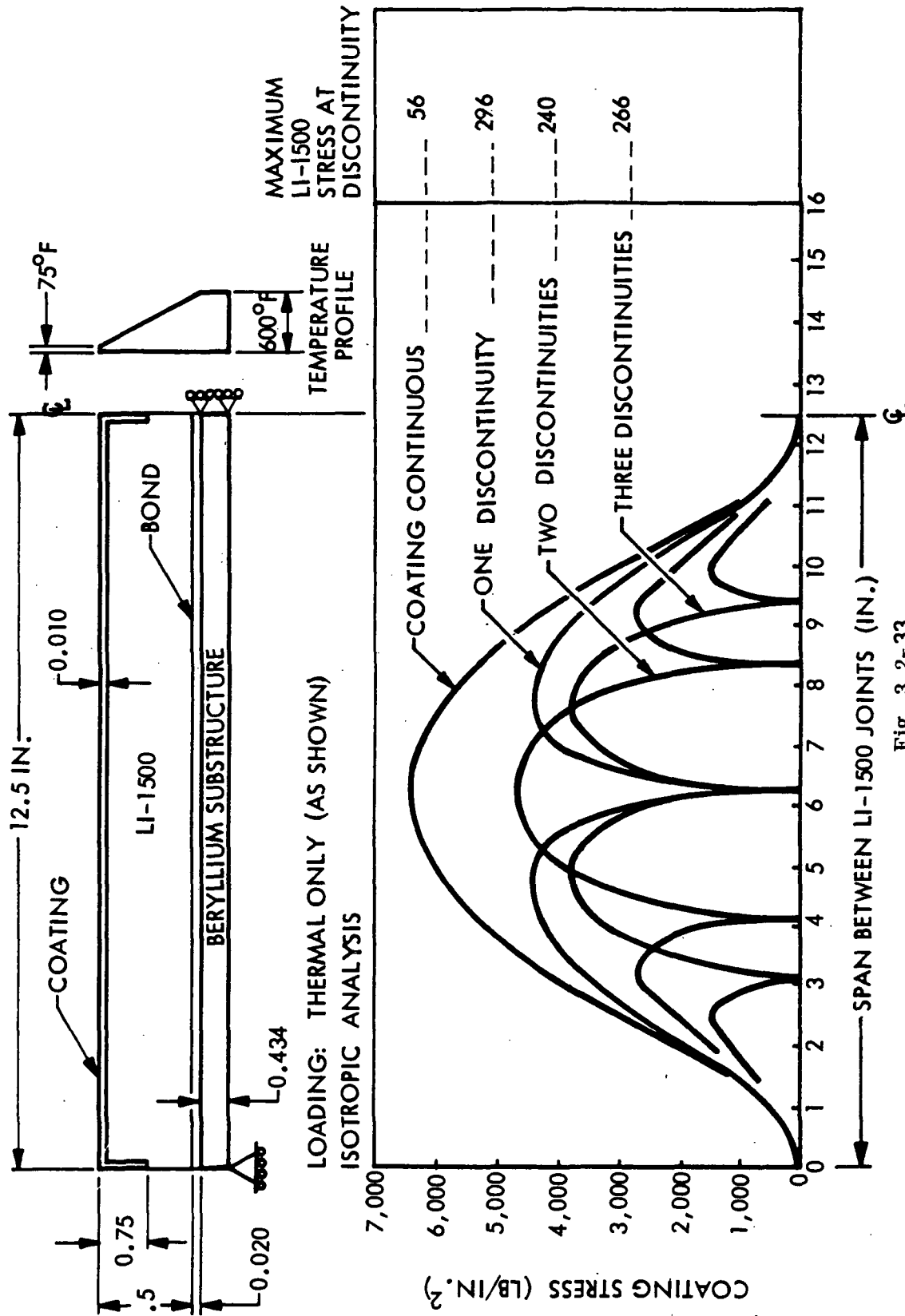


Fig. 3.2-33

D04950 (1)

VARIATION OF COATING STRESS WITH NUMBER OF COATING DISCONTINUITIES

MAXIMUM LI-1500 STRESS = 157 PSI

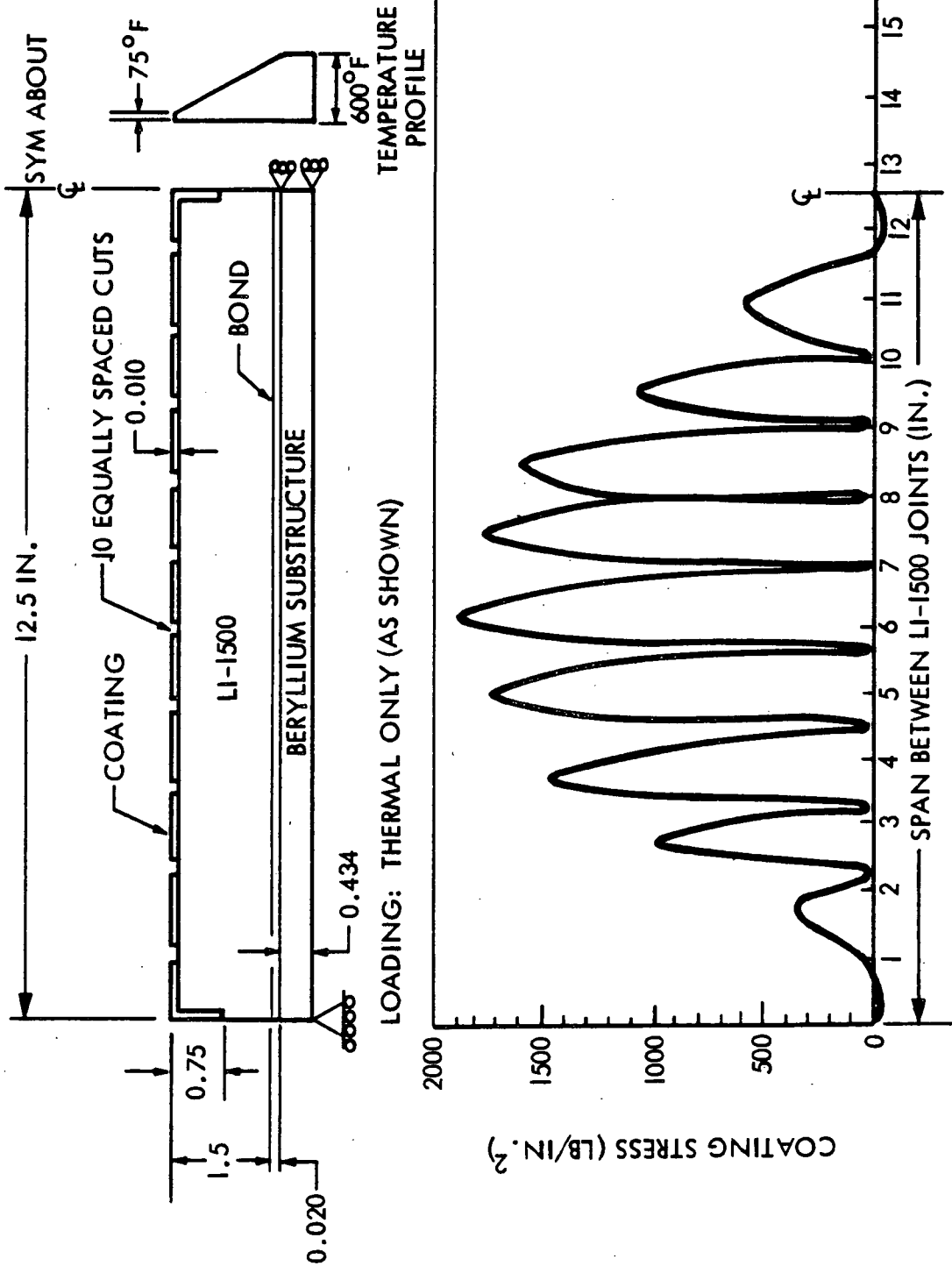
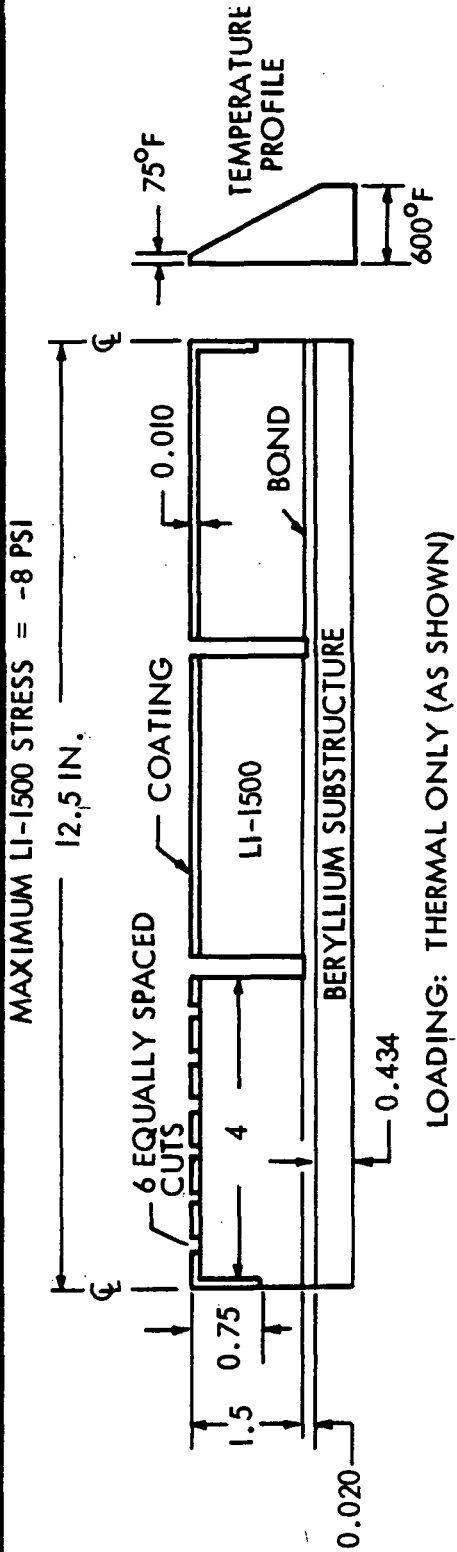


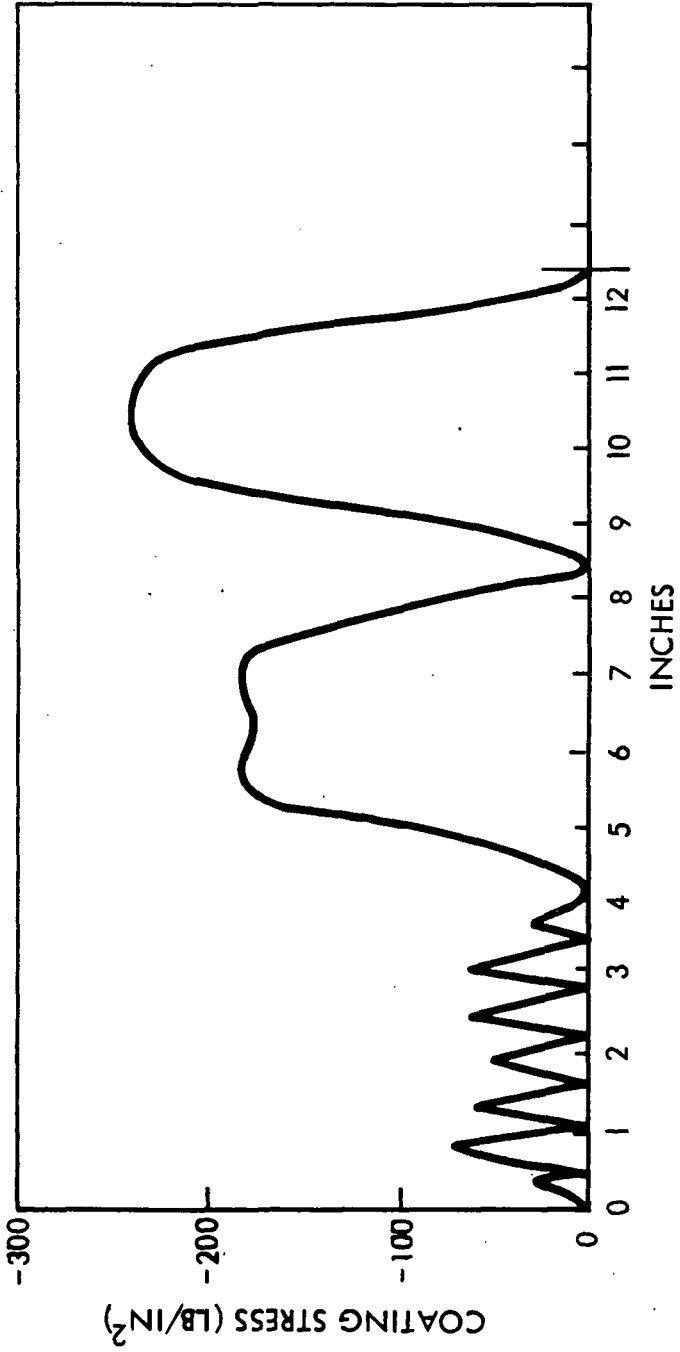
Fig. 3.2-34



VARIATION OF COATING STRESS WITH NUMBER
OF COATING DISCONTINUITIES



LOADING: THERMAL ONLY (AS SHOWN)



D05160

Fig. 3.2-35



Effects of Partial Bonding and Bond Discontinuities on RSI Stress Levels

An investigation was made to evaluate the effects of partial and discontinuous bonding. The effects of partial bonding are summarized in Table 3.2-7; a magnified computer plot of tile and substrate deflection with partial bonding is shown in Fig. 3.2-36. In general, stress levels decrease as the length of bond goes down, and it is noted that a partially bonded 6-in. tile results in the same state of stress as a fully bonded 4-in. tile for an aluminum panel with the loading conditions considered here. Hence, partial bonding can offer some measure of strain isolation from the substrate material. However, dynamic effects must be empirically evaluated before acceptance as a viable attachment method, Figure 3.2-37 shows the results of a study that considers the effects of bond discontinuity at the joints. In essence, a continuous bond allows a considerable in-plane load to develop in the bond; this is transferred into the tiles starting at the corners, thereby raising stress levels over those for a bond discontinuity at tile joints. Similar results are shown for the baseline joint configuration in Table 3.2-8 in which the filler block has been omitted for convenience. Hence, it is concluded that a discontinuity in the bond at tile joints is a desirable design objective.

Mechanical Fastener Study

Two WILSON analyses were conducted to ascertain the influence of a steel screw insert on the stress levels in LI-1500 subjected to the design temperature profile. This profile and related results are shown in Table 3.2-9. Note that high stresses are experienced in the LI-1500 due to the large mismatch in thermal expansion properties of steel and LI-1500. These results indicate that successful use of this method of attachment requires fasteners which have a coefficient of thermal expansion close to that of LI-1500 (e. g., Invar, graphite epoxy, or quartz cloth). Further discussion of this and other mechanical concepts is to be found in Section 5.2.

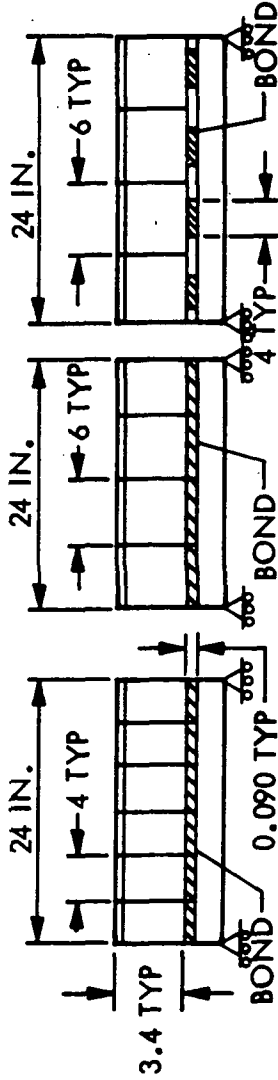
Tile Size Influence on RSI Stress Levels

The general trend of RSI stress levels versus tile length can easily be seen from Table 3.2-10. One major function of the bond is to provide strain isolation between the LI-1500 and the substrate (the other major function, of course, is to hold the tile



Table 3.2-7

EFFECT OF TILE SIZE/BOND AREA ON STRESS INTENSITY



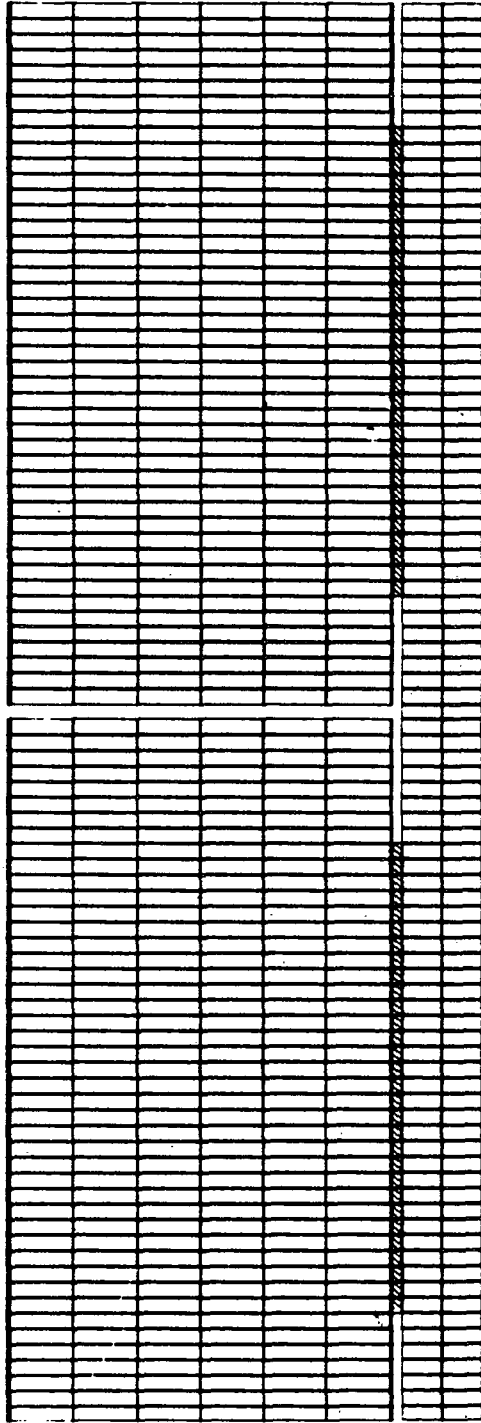
AREA 2 ALUMINUM PANEL ($T_{Al} = 250^{\circ}F$, $T_{COAT} = 75^{\circ}F$)

AXIAL LOAD = 6,000 LB/IN.

PRESSURE = 1.5 PSI BURST

STRESS (PSI)	FULL BOND 4 IN. TILE	FULL BOND 6 IN. TILE	PARTIAL BOND 6 IN. TILE
<u>LI-1500</u>			
MAXIMUM	48.9	71.5	44.4
MINIMUM	- 8.7	-10.5	-29.0
SHEAR	15.8	23.5	15.4
LONGITUDINAL	48.9	71.5	44.4
NORMAL	5.6	10.5	3.7
<u>RTV-560</u>			
MAXIMUM	16.9	27.7	15.7
MINIMUM	-14.6	-19.0	-16.2
SHEAR	14.8	21.4	15.3
LONGITUDINAL	- 2.2	- 6.4	- 5.6
NORMAL	- 5.5	10.9	3.3
<u>COATING</u>			
MAXIMUM	20.3	11.8	16.4
MINIMUM	--	-32.6	--

COMPUTER MODEL OF THE PARTIALLY BONDED
ALUMINUM PRIMARY STRUCTURE



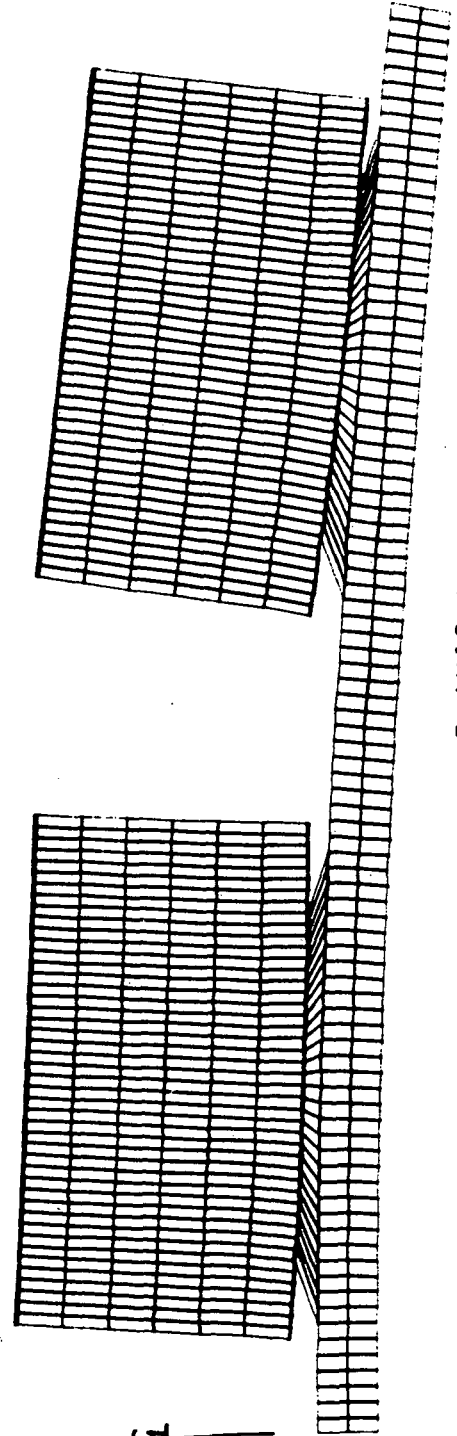
R-AXIS

BEFORE LOADING

151<

3.2-49

DURING LOADING



R-AXIS

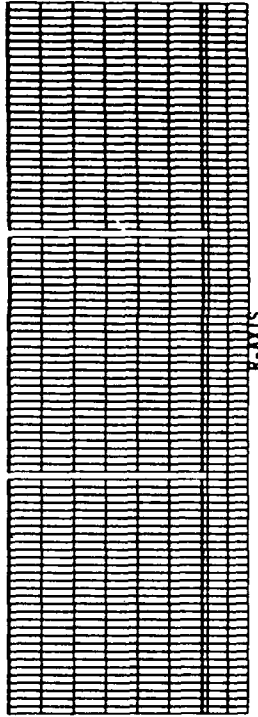
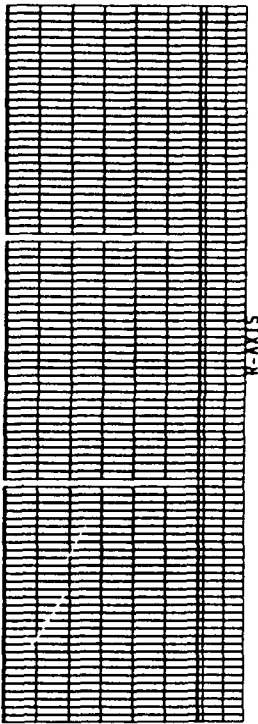
Fig. 3.2-36

DO5020

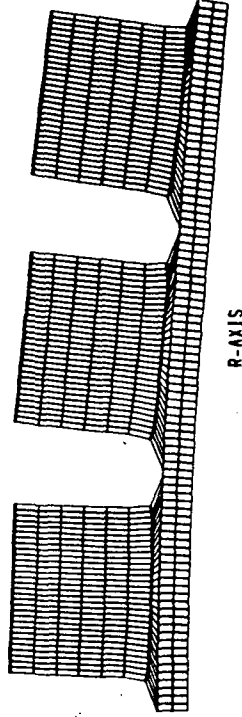
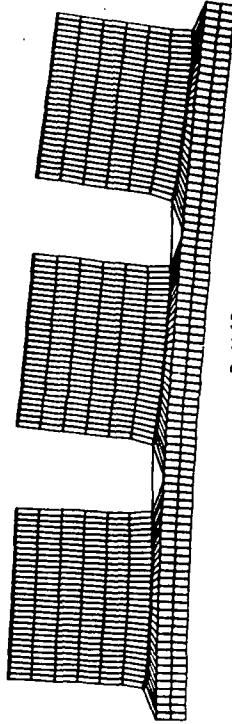


EFFECT OF BOND DISCONTINUITY AT TILE JOINTS ON STRESS INTENSITY

COMPUTER MODEL



DEFLECTED SHAPE



3.2-50

152

STRESS PSI	BOND CONTINUOUS AT TILE JOINTS	BOND DELETED AT TILE JOINTS
ALUMINUM PANEL AT AREA 2 - P = 1.5 PSI, 6000 PPI TENSION		
LI-1500		
MAXIMUM	93.6	58.1
MINIMUM	-10.5	-10.5
SHEAR	31.9	18.2
LONGITUDINAL	82.3	58.1
NORMAL	6.5	6.1
RTV-560		
MAXIMUM	31.0	19.0
MINIMUM	-17.7	-17.2
SHEAR STRESS	17.8	17.4
LONGITUDINAL	31.0	-5.4
NORMAL	15.3	5.4
COATING		
MAXIMUM	18.8	18.8
MINIMUM	-1.6	--

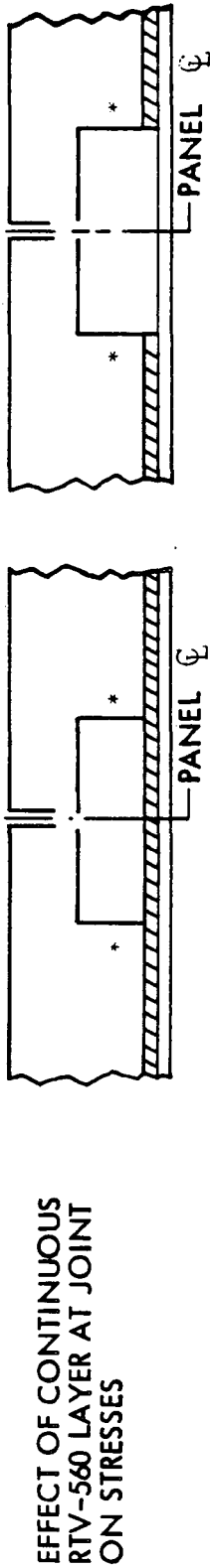
DO5046(1)

Fig. 3.2-37



Table 3.2-8
RTV-560 JOINT STUDY

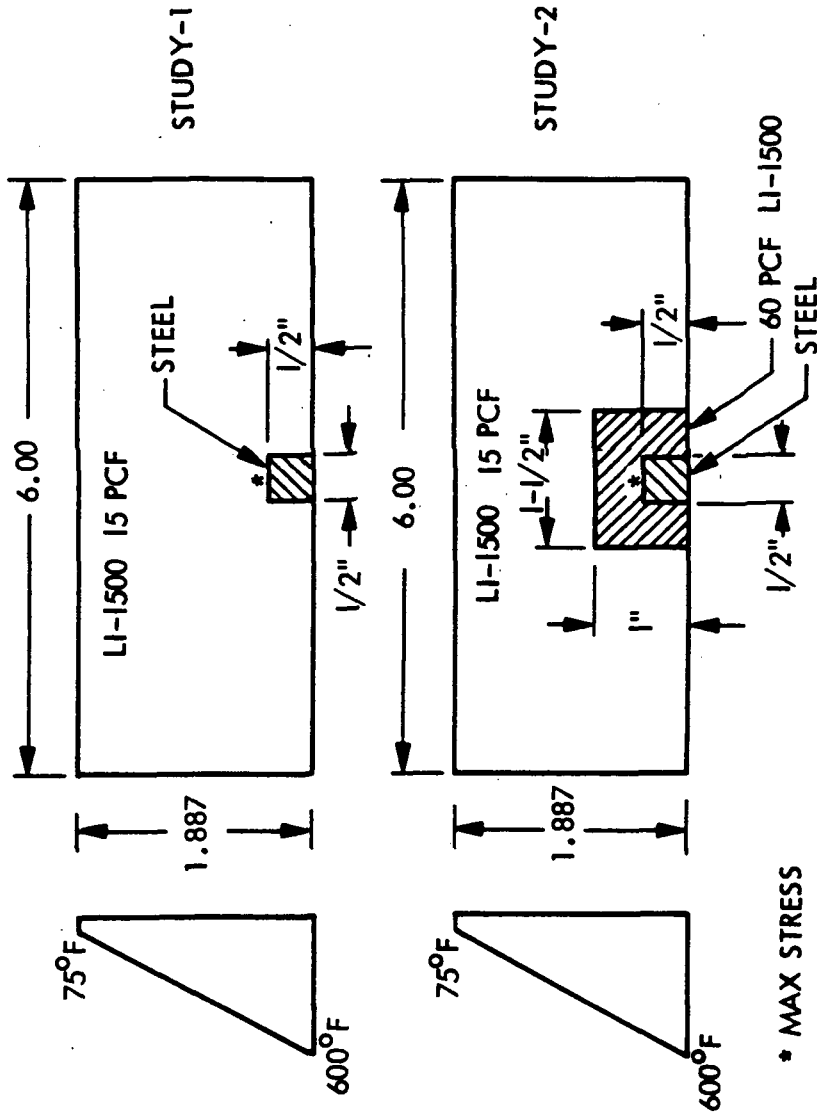
BERYLLIUM PANEL NO. 1 - BURST PRESSURE = 1.5 PSI,
PANEL LENGTH = 24 IN., TILE LENGTH = 12 IN.



LI-1500	74*	42*
PRINCIPAL TENSION	-30	-30
PRINCIPAL COMPRESSION	21	12
RZ-SHEAR	34	21
PRINCIPAL SHEAR	67	38
LONGITUDINAL TENSION	-30	-30
LONGITUDINAL COMPRESSION	14	10
NORMAL TENSION	-3	-3
NORMAL COMPRESSION		
RTV-560		
PRINCIPAL TENSION	16	17
PRINCIPAL COMPRESSION	-15	-15
RZ-SHEAR	11	11
PRINCIPAL SHEAR	14	14
LONGITUDINAL TENSION	2	0
LONGITUDINAL COMPRESSION	-12	-12
NORMAL TENSION	10	11
NORMAL COMPRESSION	-3	-3
COATING		
PRINCIPAL TENSION	1218	1186
PRINCIPAL COMPRESSION	0	0

Table 3.2-9

THREADED FASTENER STUDY - THERMAL STRESSES



	STUDY 1		STUDY 2	
	15 PCF	60 PCF	15 PCF	60 PCF
MAX LI-1500	91	14	395	
MIN LI-1500	-36	-9	-162	
SHEAR LI-1500	17	5	74	
MAX SHEAR LI-1500	47	8	205	
LONG LI-1500	91	14	395	
PEEL LI-1500	15	3	65	



Table 3.2-10



COMPARISON OF STRESSES IN PANELS CUT TO VARIOUS DEPTHS

ALUMINUM TEST PANEL NO. 2 - ORBITER FUSELAGE AREA 2

LOADING: P = 1.5 PSI BURST 6000 LB/IN. TENSION THICKNESSES: LI-1500 = 3.396 IN. RTV-560 = 0.090 IN. COATING = 0.010 IN. ALUMINUM = 0.711 IN.				AT BOND-LINE
STRESSES	AT BOND-LINE *	AT BOND-LINE *	AT BOND-LINE *	AT BOND-LINE
MAXIMUM LI-1500	131.5	132.9	48.9	48.9
MINIMUM LI-1500	-12.7	-11.2	-8.7	-8.7
SHEAR LI-1500	43.6	43.4	15.8	15.8
LONG LI-1500	131.5	132.9	48.9	48.9
PEEL LI-1500	26.9	28.9	5.6	5.6
MAXIMUM RTV-560	59.0	60.4	16.9	16.9
MINIMUM RTV-560	-30.5	-29.3	-14.6	-14.6
SHEAR RTV-560	38.4	38.3	14.8	14.8
LONG RTV-560	9.6	10.6	-2.2	-2.2
PEEL RTV-560	29.0	31.0	5.5	5.5
MAXIMUM COATING	6.1	11.2	20.3	20.3
MINIMUM COATING	-530.4	-26.0	-1.0	-1.0

155 A

onto the vehicle). The longer the tile the more nearly the strain in the tile must conform to the substrate; the gaps between the tiles provide essential strain relief which allows the bond to act more effectively as a strain isolator. Observe that no relief to maximum LI-1500 stresses results by partially cutting through the tiles, although coating stresses are reduced.

Quantitative relationships for both aluminum and titanium primary structure panels are established in Figs. 3.2-38 through 3.2-46 for critical RSI system stress levels as a function of tile length. It is seen that all these curves display a monotonically increasing stress with increasing tile length.

Effects of Different Coating Configurations on RSI Stress Levels

A series of coating studies, summarized in the following figures, considers the two basic cases of (1) local densification of LI-1500 to 60 pcf, and (2) an add-on coating, alone or in combination with densification. In the studies, the effects of two different add-on coatings were modeled: A 0.010-in. thick chrome-oxide coating used alone and a 0.004-in. thick silicon-carbide coating used alone or with a 0.010-in. thick 60-pcf LI-1500 densified layer. Typical beryllium subpanel configurations under thermal loading (surface at +75°F, substrate at +600°F) have been studied and results are presented in Fig. 3.2-47 through Fig. 3.2-52. In Fig. 3.2-52 is shown the shear stress variation through the panel at the location of the critical shear stress in the LI-1500, for a chrome-oxide coating alone. As might be expected, the shear stress is maximum at the bondline and rapidly decays with distance from the bond. In Figs. 3.2-49 and 3.2-50 are shown, qualitatively, the same type of behavior for an all-around 60-pcf densified layer of LI-1500 with a 15-pcf core. However, as noted, the maximum stress in the LI-1500 has dropped about 30 percent. These two figures can be compared with Figs. 3.2-51 and 3.2-52, in which the core density was reduced to 10 pcf. From these curves, it appears that core density in this range does not have any significant influence on shear stress in the LI-1500. From Table 3.2-11, it is noted that this lack of core density influence is also carried over to other stresses of interest.

Another series of similar curves is presented in Figs. 3.2-53 and 3.2-54, which also summarizes maximum core and coating shear stresses for a silicon-carbide add-on

3.2-54



VARIATION OF LI-1500 MAXIMUM PRINCIPAL TENSION STRESS WITH LI-1500 TILE BOND LENGTH

ALUMINUM PRIMARY STRUCTURE PANEL NO. 2
(FUSELAGE AREA NO. 2)

ORTHOTROPIC ANALYSIS

- $T_{COATING}$ = 0.010 IN
- $T_{LI-1500}$ = 3.396 IN
- $T_{RTV-560}$ = 0.080 IN
- $T_{ALUMINUM}$ = 0.711 IN
- $E_{COATING}$ = 10.6×10^6 PSI
- $E_{LI-1500}$ = 60,000 PSI (L)
6,000 PSI (T)
- $G_{LI-1500}$ = 4,150 PSI
- $E_{RTV-560}$ = 300 PSI

LOADING:

$P = 1.5$ PSI BURST
6,000 LB/IN AXIAL TENSION

SURFACE ALUMINUM: $T = 100^\circ F$
 $T = 250^\circ F$

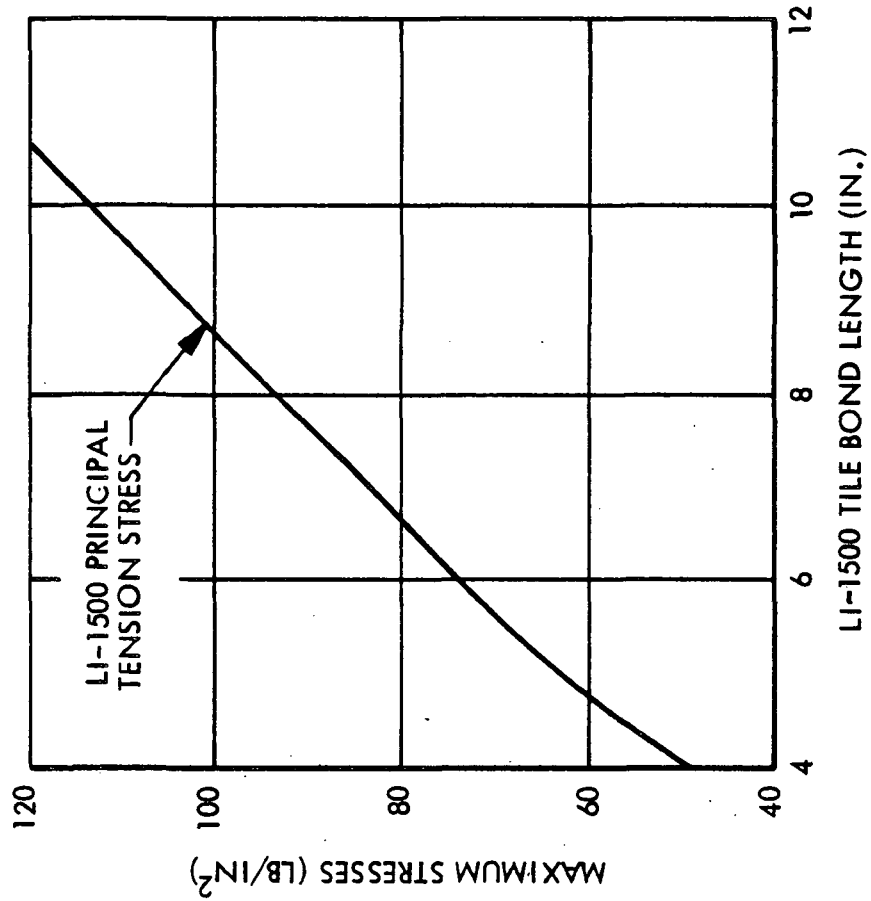


Fig. 3.2-38



VARIATION OF LI-1500 MINIMUM PRINCIPAL COMPRESSION STRESS AND NORMAL COMPRESSION STRESS WITH LI-1500 TILE LENGTH

ALUMINUM PRIMARY STRUCTURE PANEL NO. 2
(FUSELAGE AREA NO. 2)
ORTHOTROPIC ANALYSIS

- $T_{COATING} = 0.010$ IN
- $T_{LI-1500} = 3.396$ IN
- $T_{RTV-560} = 0.090$ IN
- $T_{ALUMINUM} = 0.711$ IN
- $E_{COATING} = 10.6 \times 10^6$ PSI

LOADING:

$P = 1.5$ PSI BURST
6,000 LB/IN AXIAL TENSION

- $E_{LI-1500} = 60,000$ PSI (L)
6,000 PSI (T)
- $G_{LI-1500} = 4,150$ PSI
- $E_{RTV-560} = 300$ PSI
- SURFACE $T = 100^\circ F$
- ALUMINUM $T = 250^\circ F$

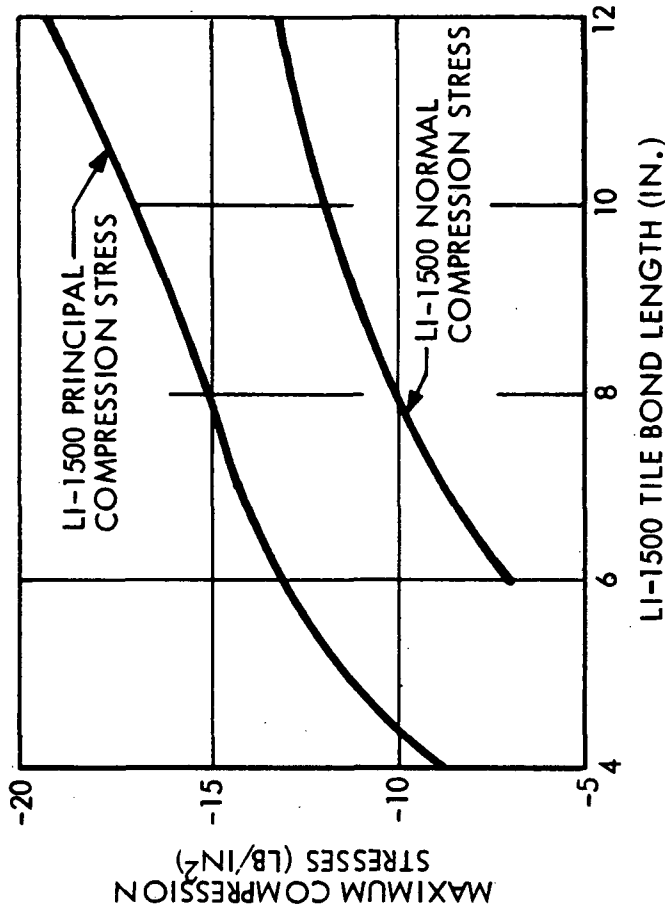


Fig. 3.2-39

DO5978 (1)



VARIATION OF LI-1500 MAXIMUM SHEAR STRESS AND
MAXIMUM PEEL STRESS WITH LI-1500 TILE LENGTH

ALUMINUM PRIMARY STRUCTURE PANEL NO. 2
(FUSELAGE AREA NO. 2)
ORTHOTROPIC ANALYSIS

- $T_{COATING} = 0.010$ IN.
- $T_{LI-1500} = 3.396$ IN.
- $T_{RTV-560} = 0.090$ IN.
- $T_{ALUMINUM} = 0.711$ IN.
- $E_{COATING} = 10.6 \times 10^6$ PSI
- $E_{LI-1500} = 60,000$ PSI (L)
= 6,000 PSI (T)
- $G_{LI-1500} = 4,150$ PSI
- $E_{RTV-560} = 300$ PSI

LOADING:
P = 1.5 PSI BURST
6000 LB/IN AXIAL TENSION
SURFACE T = 100°F
ALUMINUM T = 250°F

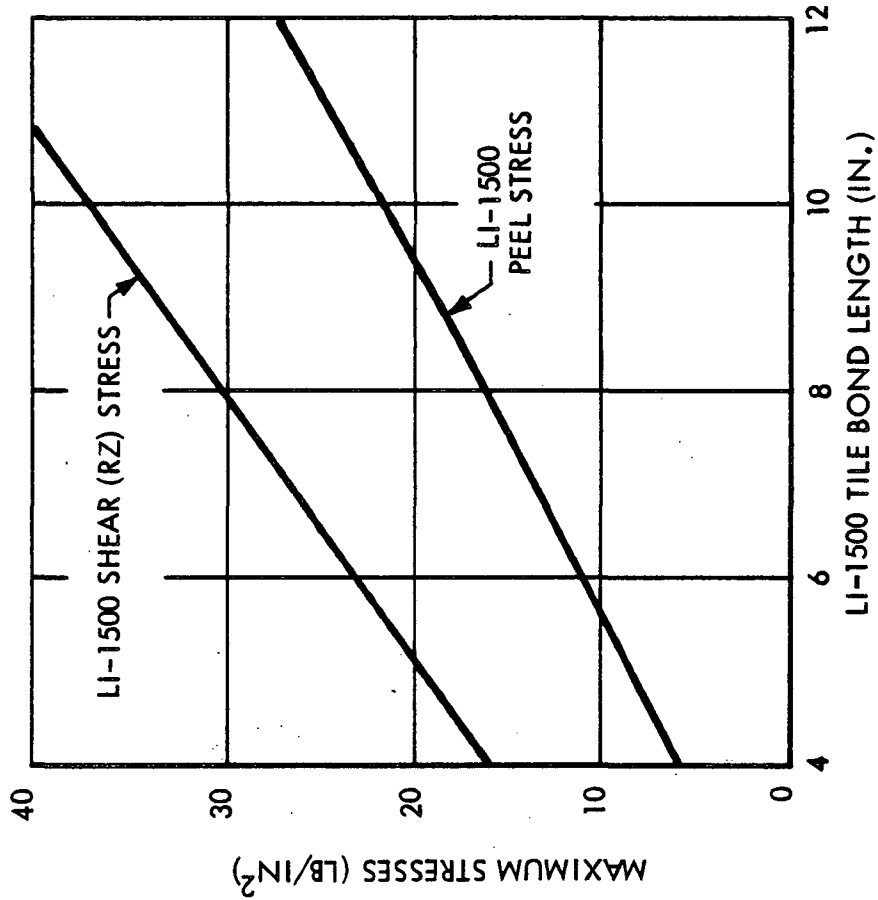


Fig. 3.2-40



VARIATION OF RTV-560 MAXIMUM PRINCIPAL TENSION STRESS, SHEAR STRESS, AND PEEL STRESS WITH LI-1500 TILE LENGTH

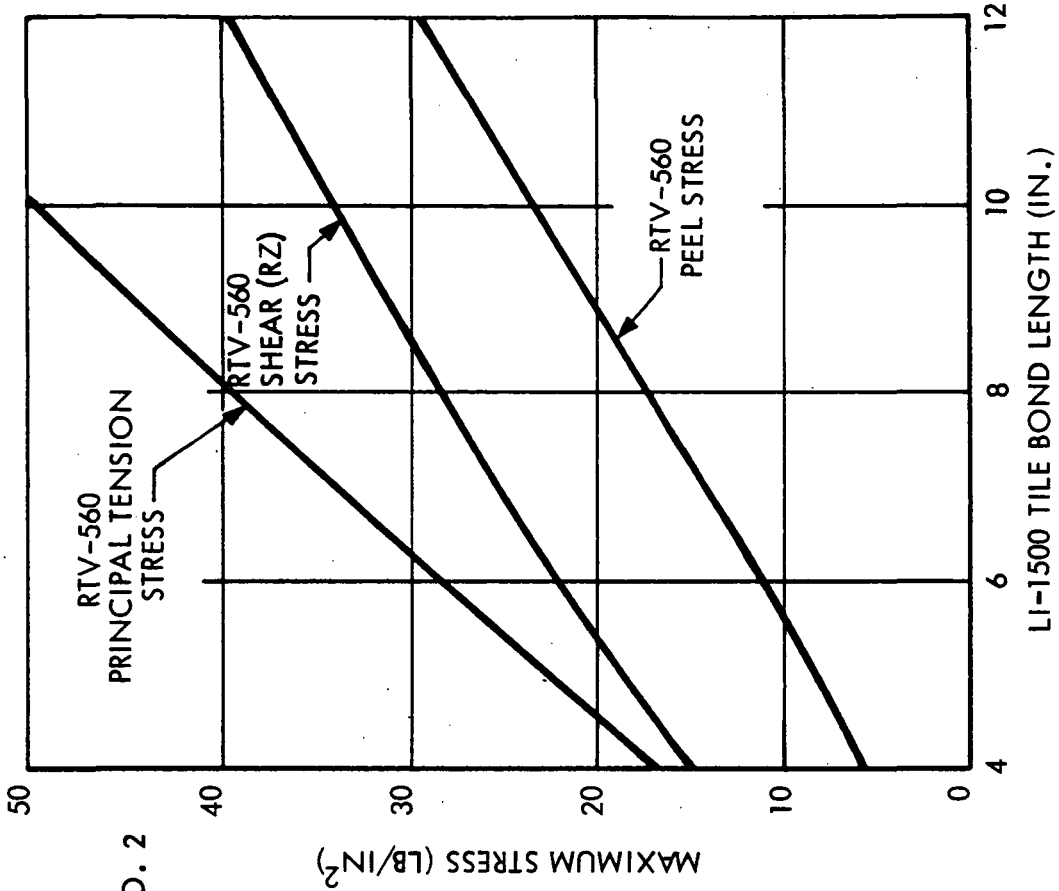


Fig. 3.2-41

ALUMINUM PRIMARY STRUCTURE PANEL NO. 2
(FUSELAGE AREA NO. 2)

ORTHOTROPIC ANALYSIS

- $T_{COATING}$ = 0.010 IN
- $T_{LI-1500}$ = 3.396 IN
- $T_{RTV-560}$ = 0.090 IN
- $T_{ALUMINUM}$ = 0.711 IN
- $E_{COATING}$ = 10.6×10^6 PSI
- $E_{LI-1500}$ = 60,000 PSI (L)
= 6,000 PSI (T)
- $G_{LI-1500}$ = 4,150 PSI
- $E_{RTV-560}$ = 300 PSI

LOADING:
P = 1.5 PSI BURST
6,000 LB/IN AXIAL TENSION

SURFACE T = 100°F
ALUMINUM T = 250°F



VARIATION OF RTV-560 MINIMUM PRINCIPAL COMPRESSIVE STRESS WITH LI-1500 TILE BOND LENGTH

ALUMINUM PRIMARY STRUCTURE PANEL NO. 2
(FUSELAGE AREA NO. 2)

ORTHOTROPIC ANALYSIS

- $T_{COATING} = 0.010$ IN
- $T_{LI-1500} = 3.396$ IN
- $T_{RTV-560} = 0.090$ IN
- $T_{ALUMINUM} = 0.711$ IN
- $E_{COATING} = 10.6 \times 10^6$ PSI
- $E_{LI-1500} = 60,000$ PSI
- $G_{LI-1500} = 6,000$ PSI
- $E_{RTV-560} = 4,150$ PSI
- $F_{RTV-560} = 300$ PSI

LOADING:
 $P = 1.5$ PSI BURST
 6000 LB/IN AXIAL TENSION

SURFACE $T = 100^\circ F$
 ALUMINUM $T = 250^\circ F$

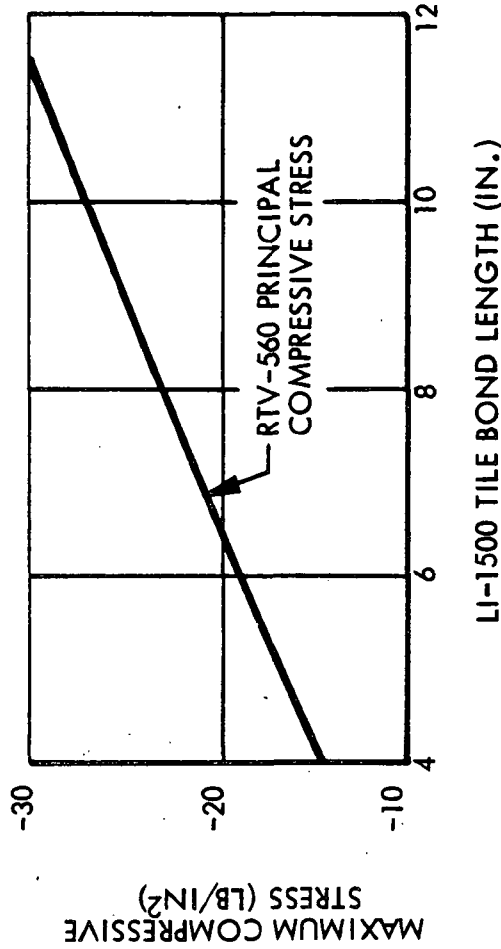


Fig. 3.2-42



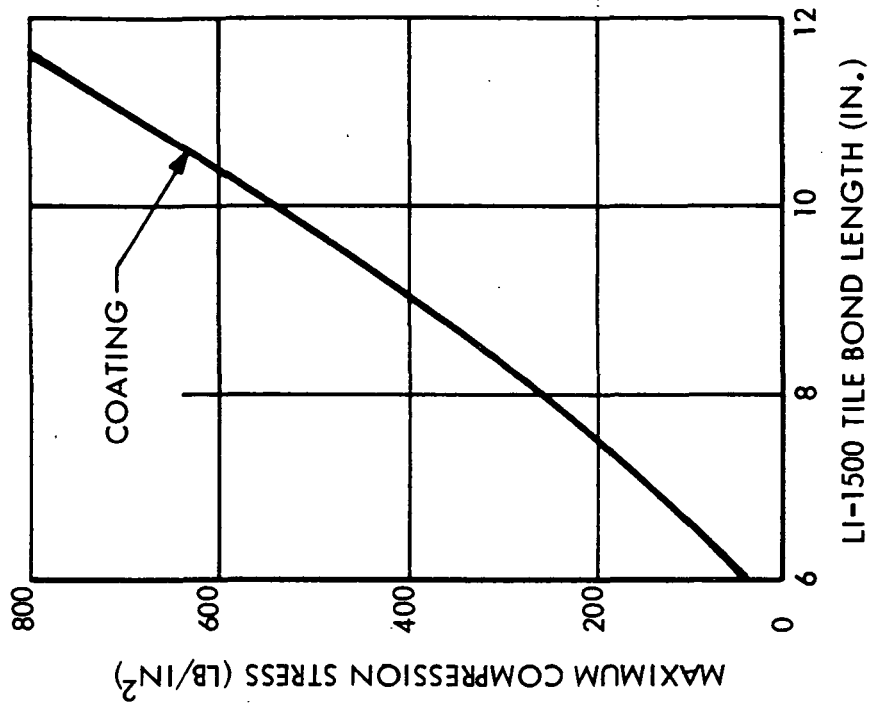
VARIATION OF MAXIMUM COATING COMPRESSION STRESS WITH LI-1500 TILE BOND LENGTH

ALUMINUM PRIMARY STRUCTURE PANEL NO. 2
(FUSELAGE AREA NO. 2)
ORTHOTROPIC ANALYSIS

- $T_{COATING} = 0.010$ IN
- $T_{LI-1500} = 3.396$ IN
- $T_{RTV-560} = 0.090$ IN
- $T_{ALUMINUM} = 0.711$ IN
- $E_{COATING} = 10.6 \times 10^6$ PSI
- $E_{LI-1500} = 60,000$ PSI (L)
6,000 PSI (T)
- $G_{LI-1500} = 4,150$ PSI
- $E_{RTV-560} = 300$ PSI

LOADING:
 $P = 1.5$ PSI BURST
 6000 LB/IN AXIAL TENSION

SURFACE $T = 100^\circ F$
 ALUMINUM $T = 250^\circ F$



DO5977 (1)

Fig. 3.2-43



VARIATION OF LI-1500 MAXIMUM PRINCIPAL TENSILE STRESS WITH LI-1500 TILE LENGTH

TITANIUM PRIMARY STRUCTURE PANEL NO. 4
(FUSELAGE AREA NO. 2)

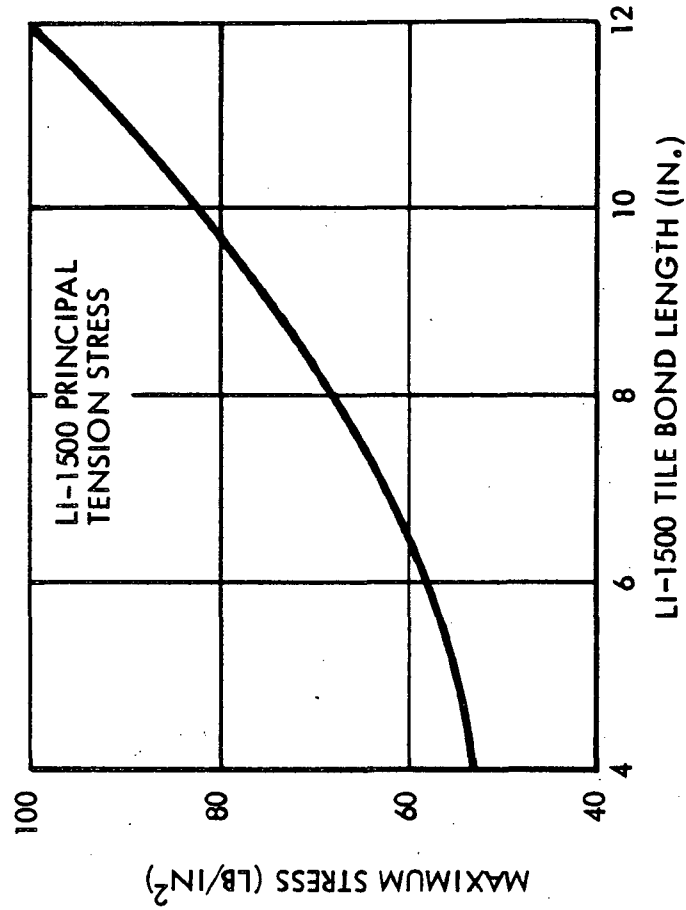
ORTHOTROPIC ANALYSIS

- $T_{COATING} = 0.010$ IN
- $T_{LI-1500} = 2.00$ IN
- $T_{RTV-560} = 0.090$ IN
- $T_{TITANIUM} = 0.628$ IN
- $E_{COATING} = 10.6 \times 10^6$ PSI
- $E_{LI-1500} = 60,000$ PSI (L)
6,000 PSI (T)
- $G_{LI-1500} = 4,150$ PSI
- $E_{RTV-560} = 300$ PSI

LOADING:

- P = 1.5 PSI BURST
- 6000 LB/IN AXIAL TENSION

- SURFACE TITANIUM T = 100°F
- TITANIUM T = 550°F



DO5971 (1)

Fig. 3.2-44



VARIATION OF LI-1500 STRESSES WITH LI-1500 TILE LENGTH

TITANIUM PRIMARY STRUCTURE PANEL NO.4
(FUSELAGE AREA NO.2)

ORTHOTROPIC ANALYSIS

- $T_{COATING}$ = 0.010 IN.
- $T_{LI-1500}$ = 2.00 IN
- $T_{RTV-560}$ = 0.090 IN
- $T_{TITANIUM}$ = 0.628 IN
- $E_{COATING}$ = 10.6×10^6 PSI
- $E_{LI-1500}$ = 60,000 PSI (L)
- = 6,000 PSI (T)
- $G_{LI-1500}$ = 4,150 PSI
- $E_{RTV-560}$ = 300 PSI

LOADING:

- P = 1.5 PSI BURST
- 6000 LB/IN AXIAL TENSION

- SURFACE T = 100°F
- TITANIUM T = 550°F

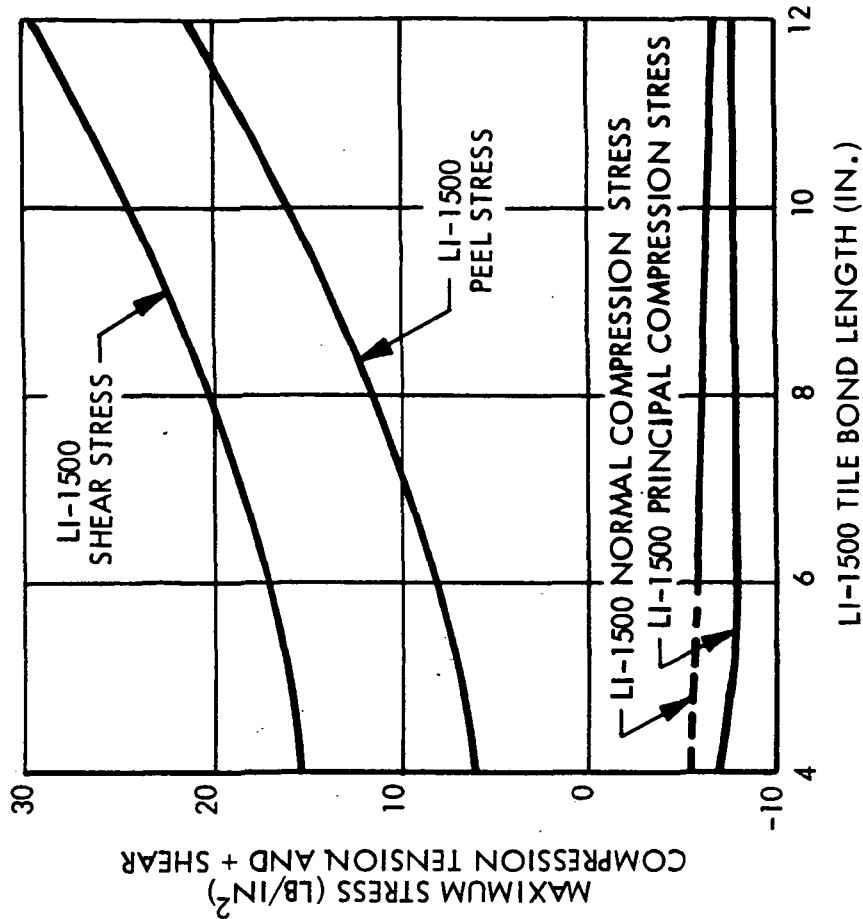


Fig. 3.2-45



VARIATION OF RTV-560 STRESSES WITH LI-1500 TILE LENGTH

TITANIUM PRIMARY STRUCTURE PANEL NO. 4
(FUSELAGE AREA NO. 2)

ORTHOTROPIC ANALYSIS

- $T_{COATING}$ = 0.010 IN
- $T_{LI-1500}$ = 2.00 IN
- $T_{RTV-560}$ = 0.090 IN
- $T_{TITANIUM}$ = 0.628 IN
- $E_{COATING}$ = 10.6×10^6 PSI
- $E_{LI-1500}$ = 60,000 PSI (L)
6,000 PSI (T)
- $G_{LI-1500}$ = 4,150 PSI
- $E_{RTV-560}$ = 300 PSI

LOADING:

$P = 1.5$ PSI BURST
6000 LB/IN AXIAL TENSION

SURFACE TITANIUM $T = 100^\circ F$
 $T = 550^\circ F$

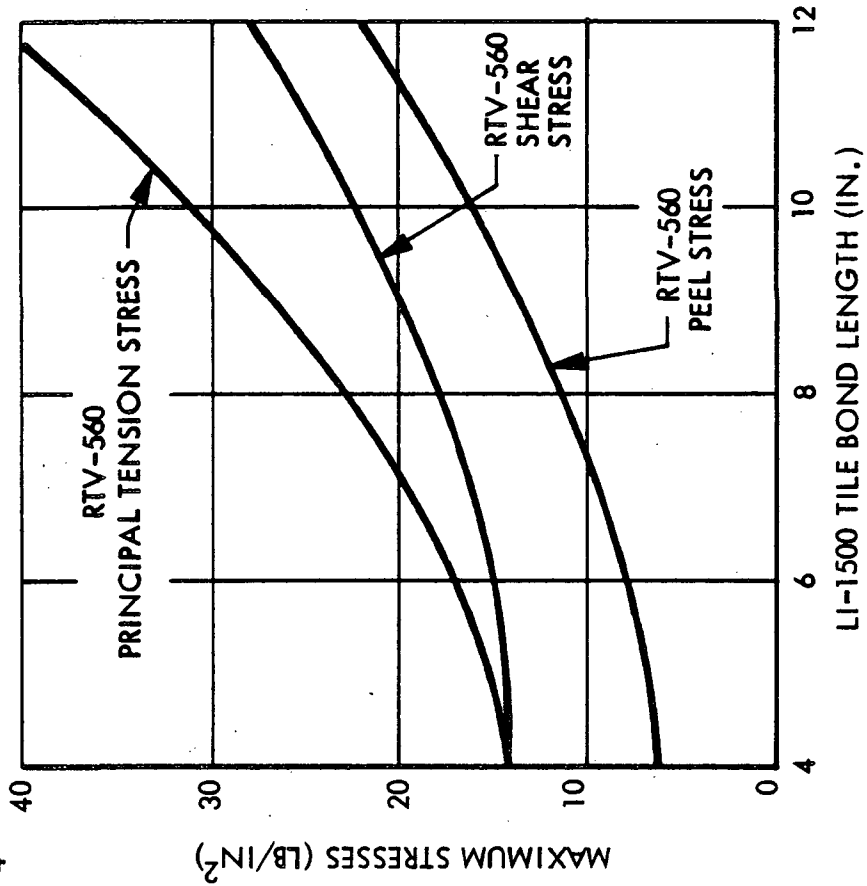


Fig. 3.2-46



SHEAR STRESS PROFILE CONFIGURATIONS

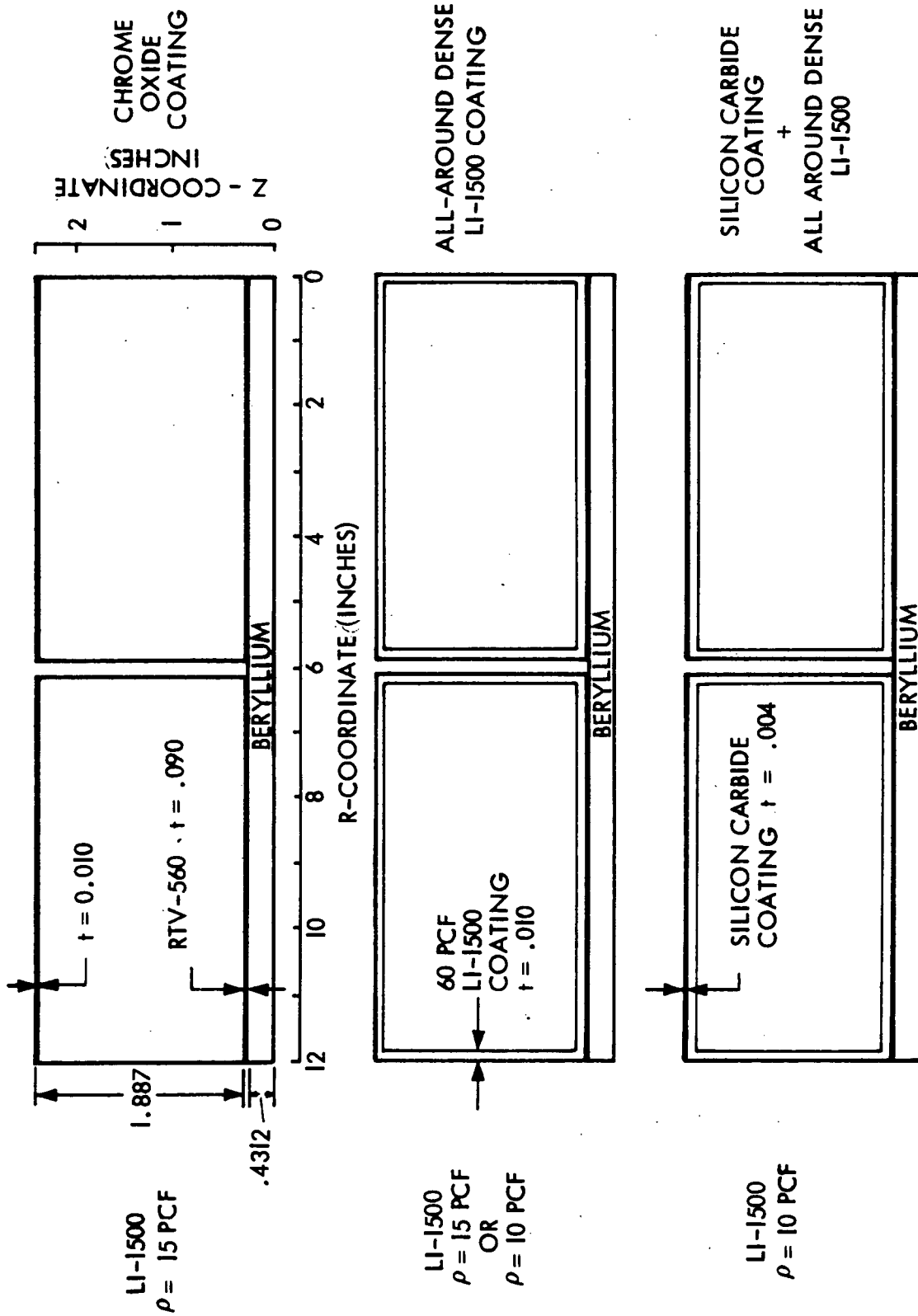


Fig. 3.2-47

STRESS PROFILE AT MAXIMUM LI-1500 SHEAR STRESS
(P LI-1500 = 15 PCF)

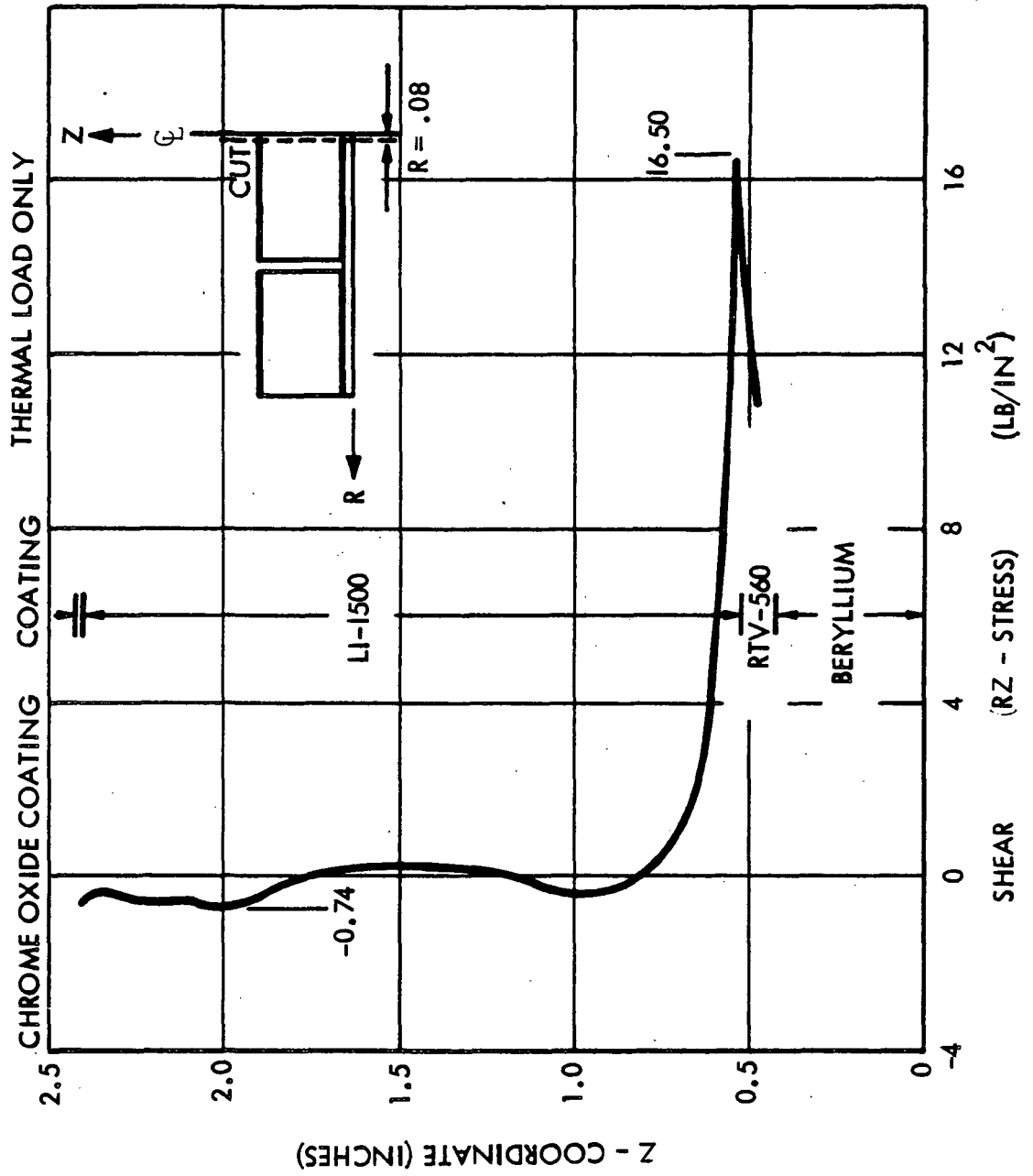


Fig. 3.2-48



STRESS PROFILE AT MAX SHEAR STRESS

(ρ CORE = 15 PCF, ρ COATING = 60 PCF)

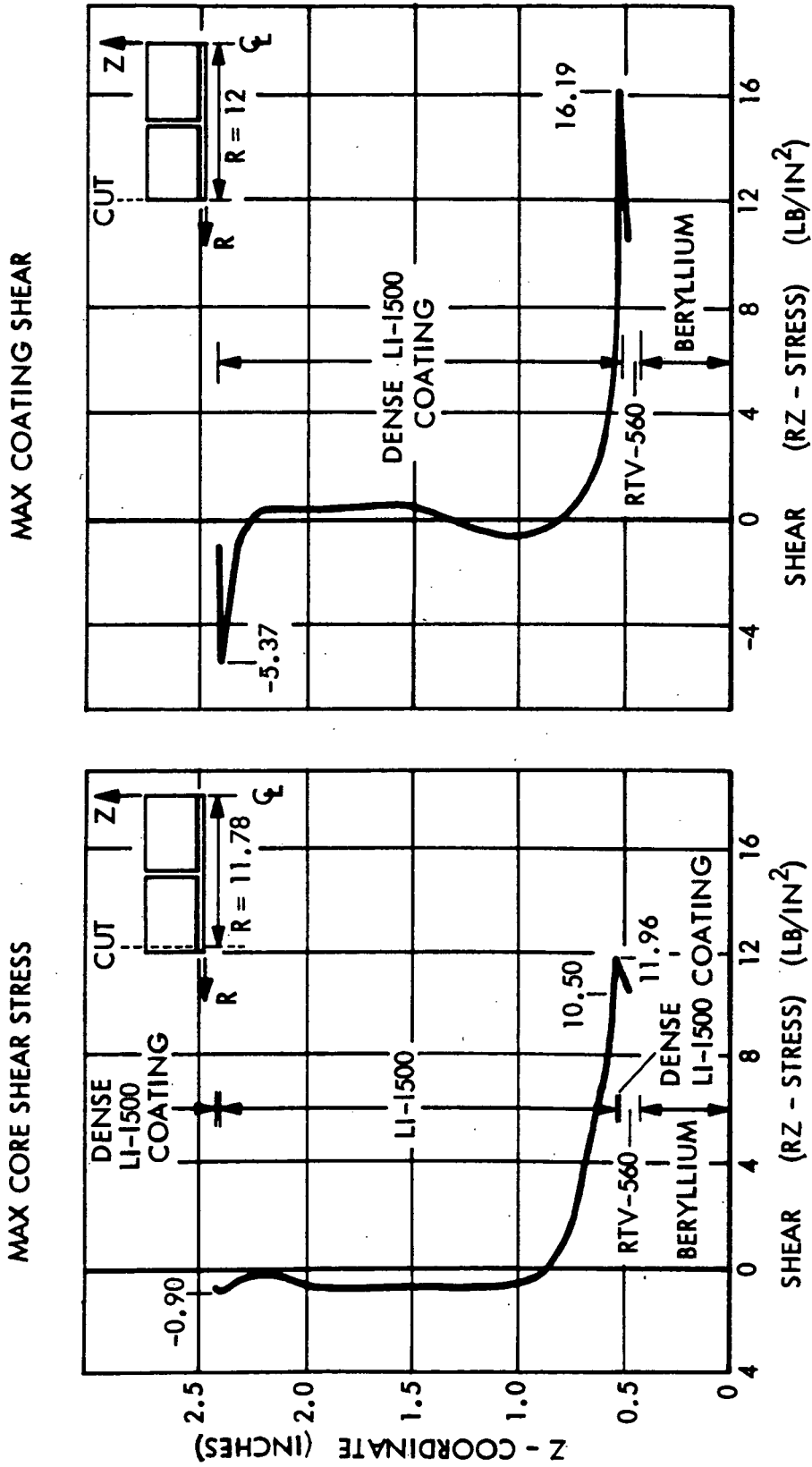


Fig. 3.2-49

Fig. 3.2-50

DO6153 (1)

STRESS PROFILE AT MAX SHEAR STRESS
(ρ CORE = 10 PCF, ρ COATING = 60 PCF)

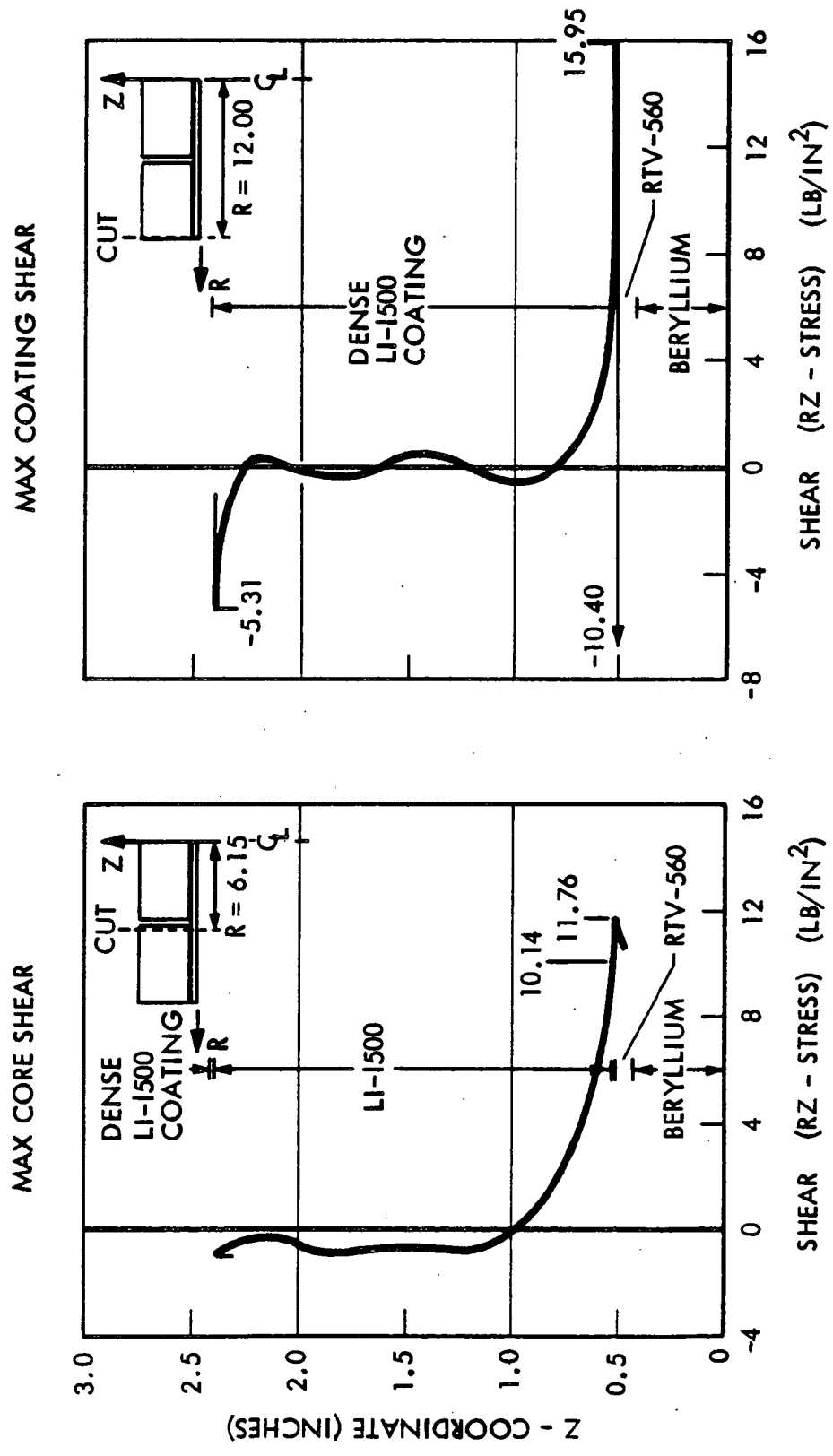


Fig. 3.2-52

Fig. 3.2-51

DO6152(1)

C.4

Table 3.2-11

MAXIMUM STRESS SUMMARY - DENSIFICATION STUDY

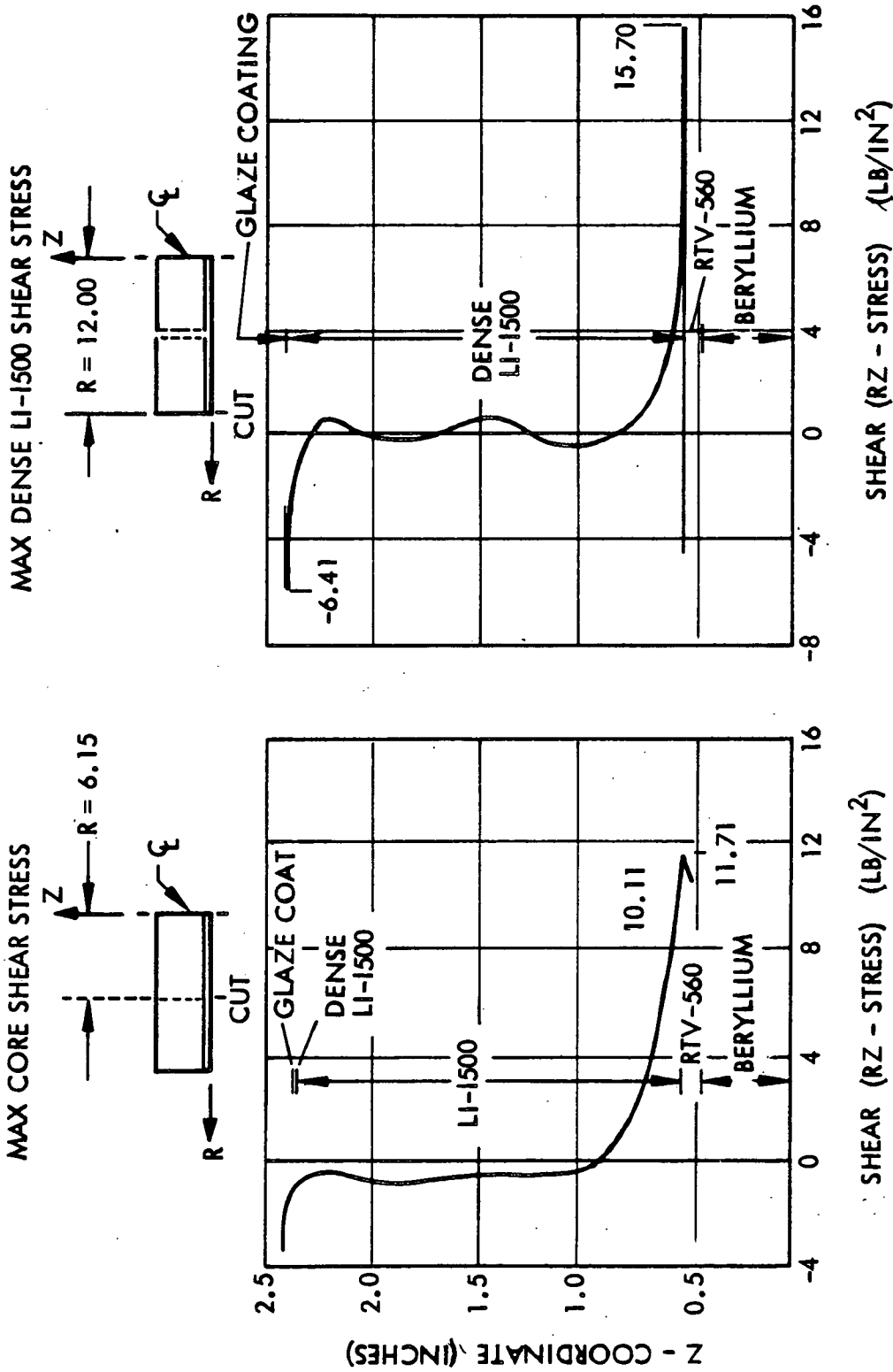
BERYLLIUM PANEL - GROUND CONDITION
(75°F SURFACE TEMP., 600°F SUBSTRATE TEMP).

	15 (LB/FT ³)	15 (LB/FT ³)	10 (LB/FT ³)	10 (LB/FT ³)	10 (LB/FT ³)
DENSITY					
MAX. LI-1500	54	36	35	35	13
MIN. LI-1500	-39	-6	-6	-4	-2
SHEAR LI-1500	17	12	12	12	3
LONG. LI-1500	52	36	35	35	13
PEEL LI-1500	5	5	5	4	2
DENSITY		60 (LB/FT ³)	60 (LB/FT ³)	60 (LB/FT ³)	60 (LB/FT ³)
MAX. LI-1500	-	160	169	167	64
MIN. LI-1500	-	-54	-53	-54	-12
SHEAR LI-1500	-	16	16	16	7
LONG. LI-1500	-	160	169	167	64
PEEL LI-1500	-	-52	-52	-52	2
MAX. RTV-560	11	11	11	11	8
MIN. RTV-560	-20	-20	-20	-20	-22
SHEAR RTV-560	11	11	11	11	12
LONG. RTV-560	-18	-18	-18	-18	-17
PEEL RTV-560	7	6	7	7	2
MAX. COATING	9	-	-	15	3137
MIN. COATING	-156	-	-	-381	-242

11/2/68
NO

STRESS PROFILE AT MAX SHEAR STRESS

(ρ CORE = 10 PCF, ρ DENSE LI-1500 = 60 PCF)



DO6151(2)

coating in conjunction with a 10-mil layer of all-around densified LI-1500. Again, maximum stresses occur in the treated regions while core stresses are small. These results are also summarized in Table 3.2-11.

Another set of similar curves is presented for an aluminum primary structure panel configuration with a 15-pcf LI-1500 core in Figs. 3.2-55 and 3.2-56. Table 3.2-12 is a brief summary of selected results. This study indicates a qualitative similarity with the previous beryllium subpanel results, but quantitatively the effect of the surface densification in this case offers only about a 10-percent reduction in LI-1500 stress levels as compared with the baseline configuration of the add-on coating alone. Local densification is less effective here, due to the fact that the substructure strain is increased. Aluminum at 250^oF experiences nearly as much thermal strain as beryllium does at 600^oF. In addition, the aluminum substructure must carry an in-plane line load, which accounts for mechanical strain of the same order as the thermal strain. Hence, the aluminum panel results correspond to a substrate strain state roughly double that for the beryllium subpanel case.

The conclusion to be drawn from these studies is that all-around densification may be desirable for other reasons such as handling, but it will generally not offer significant stress reduction. In addition, the total system weight will be increased.

RSI Tile Bonded to Corrugated Substrate

Table 3.2-13 is a summary of RSI stress levels that arise due to thermal expansion if a 13-in. LI-1500 tile is directly bonded to a corrugated substrate. The tile is assumed to be 4-in. long in the stiffener direction, and 2-D WILSON stress analysis results are shown for both directions in the tile. It is interesting to note that the RSI stress levels are of the same order in both directions, primarily since the corrugation imposes a condition of partial bonding on the tile. As discussed earlier, partial bonding acts to reduce stress levels. The corrugation direction results here cannot be applied directly to the actual behavior of a TPS panel as the support of the stiffeners is not incorporated in the 2-D model as discussed in Section 2.3. This additional stiffness would generally act to lower longitudinal stresses in the tile but leads to an increase in peel stress.

STRESS PROFILE AT MAXIMUM SHEAR STRESS

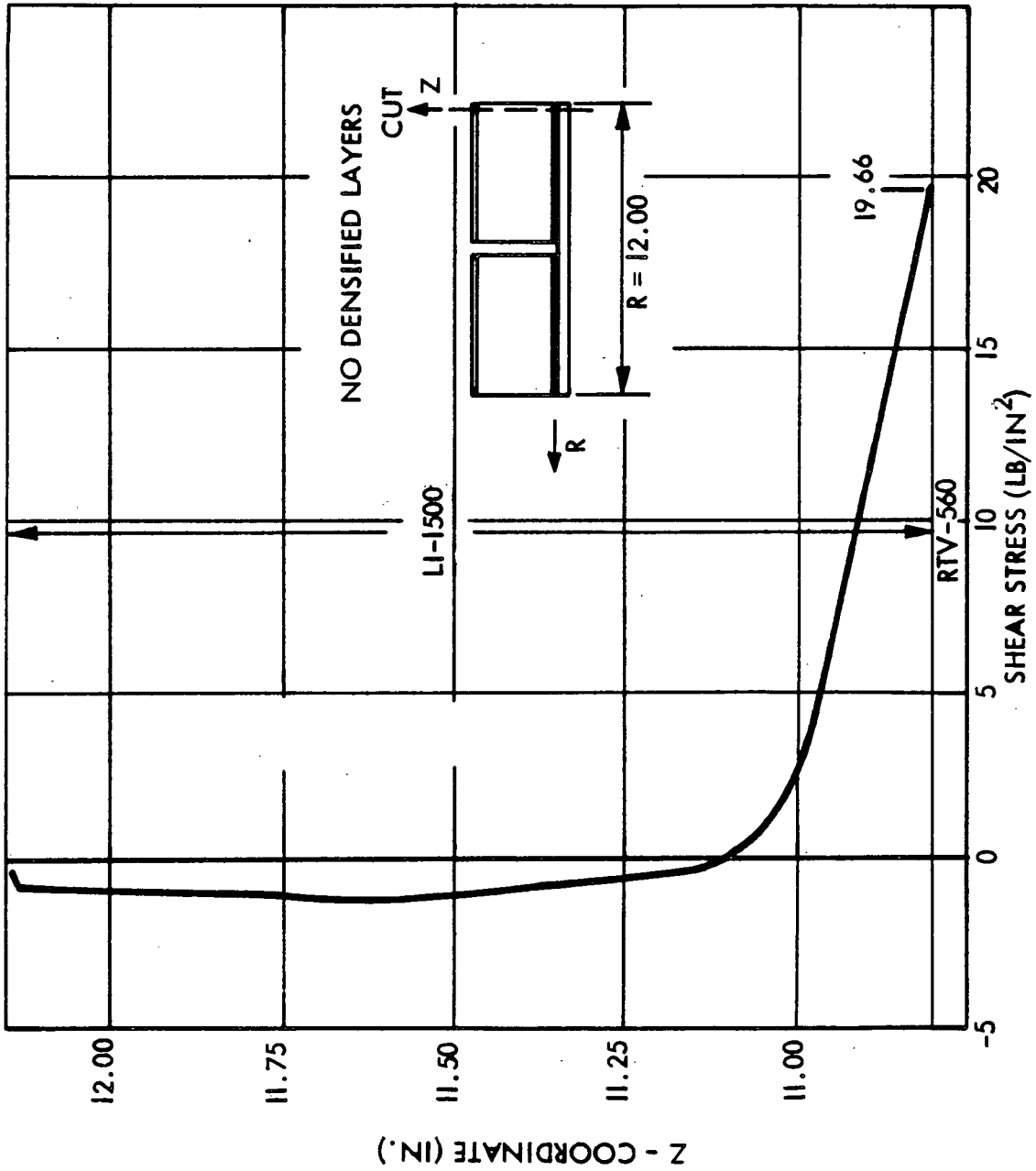


Fig. 3.2-55



STRESS PROFILE AT MAXIMUM SHEAR STRESS

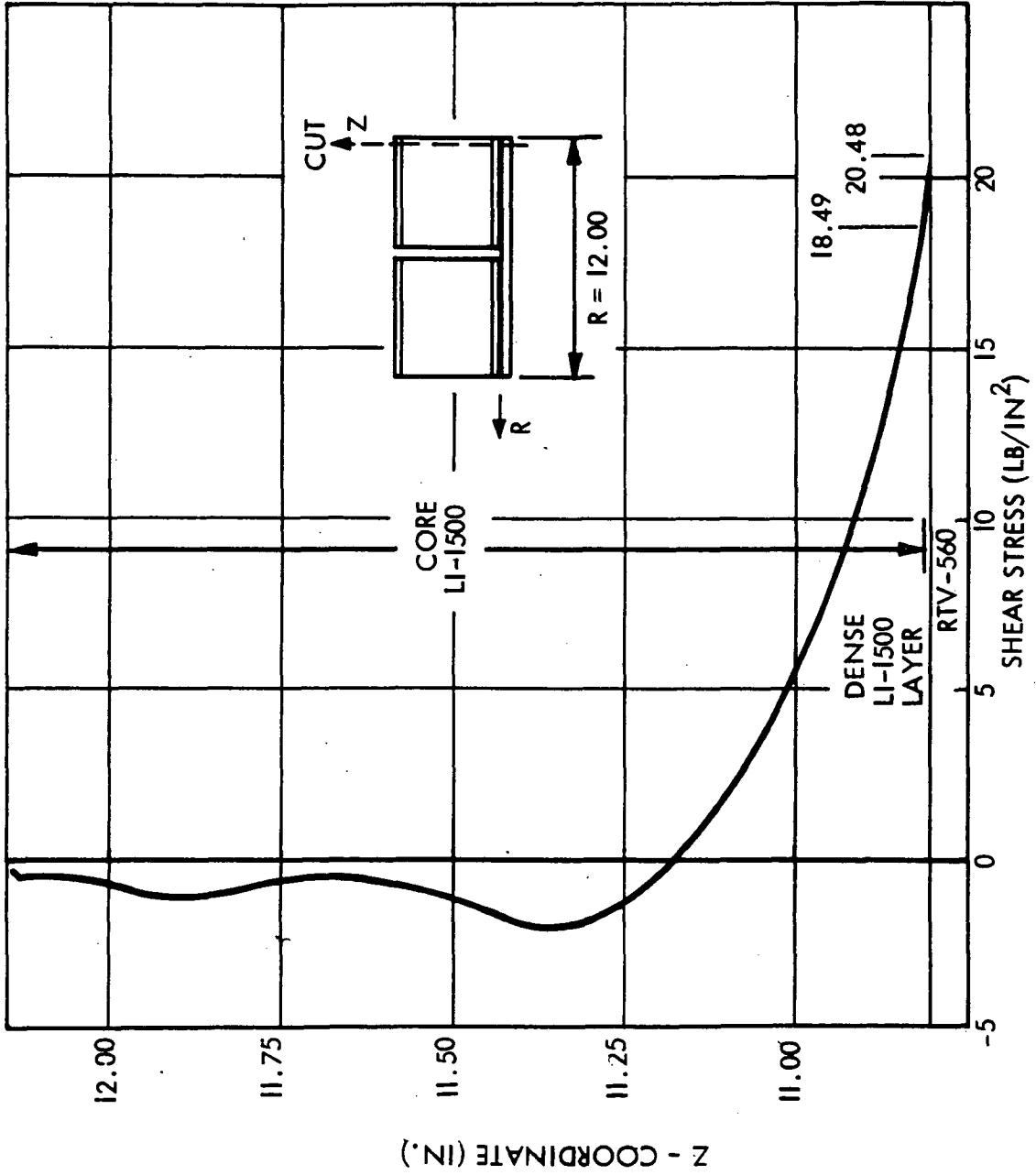


Fig. 3.2-56



3.2-72

174<

D07162 (1)

Table 3.2-12

MAXIMUM STRESS SUMMARY - DENSIFICATION STUDY
ALUMINUM PANEL



1.5 PSI BURST PRESSURE
100°F SURFACE TEMP., 250°F SUBSTRATE TEMP.
6000 PPI LINE LOAD
1.334
.090
.010 SILICON CARBIDE
15 LB/FT³
60 LB/FT³

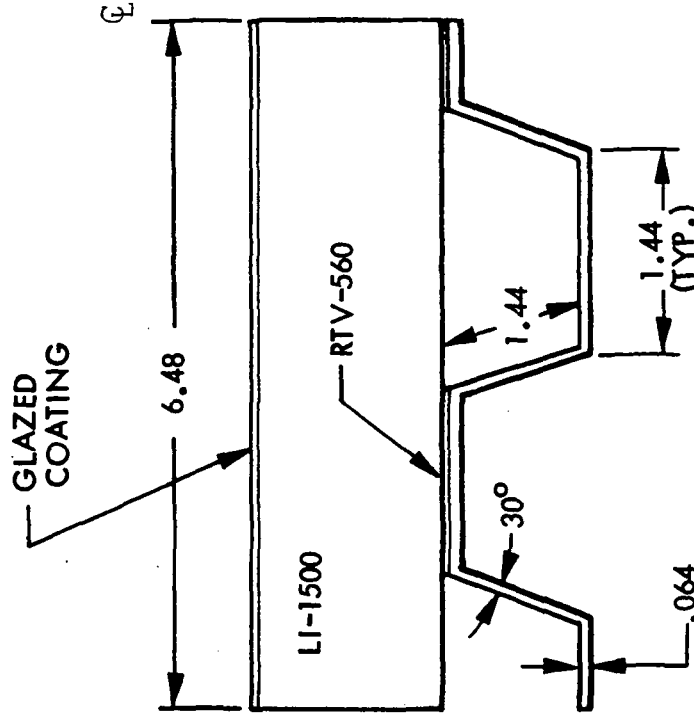
	15 LB/FT ³	15 LB/FT ³	60 LB/FT ³
DENSITY			
MAX. LI-1500	68		83
MIN. LI-1500	-6		-6
SHEAR LI-1500	20		18
LONG. LI-1500	68		63
PEEL LI-1500	11		10
DENSITY			
MAX. LI-1500			280
MIN. LI-1500			-3
SHEAR LI-1500			20
LONG. LI-1500			280
PEEL LI-1500			10
MAX. RTV-560	25		25
MIN. RTV-560	-15		-16
SHEAR RTV-560	18		18
LONG. RTV-560	-7		-7
PEEL RTV-560	12		11
MAX. COATING	0		0
MIN. COATING	-191		-176

Table 3.2-13

ALUMINUM FLIGHT PANEL NO. 2
ORBITER FUSELAGE AREA 2



		CORRUGATION*	4 IN. TILE **
LOADS	PRESSURE AXIAL LOAD	0 PSI 0 LB/IN.	0 PSI 0 LB/IN.
TEMP	SURFACE ALUMINUM	75° 300°	75° 300°
THICK- NESS	COATING LI-1500 RTV-560 ALUMINUM	0.010 2.524 0.090 0.064	0.010 2.524 0.090 0.711
STRESS (PSI)	MAX LI-1500	17	20
	MIN LI-1500	-5	-4
	SHEAR LI-1500	4	7
	LONG LI-1500	17	20
	PEEL LI-1500	3	-2
MAX RTV	10	5	
MIN RTV	-10	-10	
SHEAR RTV	8	5	
LONG RTV	-10	-7	
PEEL RTV	6	2	
MAX COATING	43	1	
MIN COATING	-72	-12	



* GLAZED COATING E = 10.6 x 10⁶
** WITH E = 3.5 x 10⁶ COATING

Effect of Tile Size on Coating Weight

These results are summarized in Fig. 3.2-57 which applies to both the 0025 and 0042 coating systems. As would be expected, the number of joints has a significant effect on coating weight. However, the use of the FI-600 filler strip (discussed in Section 5.3.9 of Volume I) more than compensates for the added coating weight, since this material has a density of 6 pounds per cubic foot. For all cases, the tile weight actually decreases with decreasing tile size. (The filler strip is designed to be 1-inch wide and half the tile thickness in all cases.)

Strain Arrestor Plate

The baseline attachment scheme for RSI panels is direct bonding with a flexible bond such as RTV-560 (baseline for this study) or one of the even more flexible foam bonds. This bond effectively isolates the tile from high substructure strains. It is within the state-of-the-art, however, to use an additional technique in connection with bonding to further reduce tile stresses. This is achieved by placing a high-modulus, high-strength, thin plate between the tile and the substructure (see Fig. 3.2-58). For thermal application, an additional requirement is necessary; i. e., the plate should have a thermal expansion coefficient approximately the same as the RSI tile.

The function of the plate is to act as a barrier between the substructure and the RSI tile. The barrier or arrestor action is accomplished by the high extensional stiffness of the plate. Resulting strains are low even at high stress levels in the substrate.

There are two materials that are readily available for LI-1500 application. These are:

1. Invar Steel
2. Graphite Epoxy Composite
(Thornel 75S/ERLB4617) laminates
Laminate thickness = 0.0025 in.



EFFECT OF TILE SIZE ON COATING WEIGHT

$$\text{COATING WT} = 0.1 \left(1 + \frac{2(t+1)}{a} \right) = W_c$$

$$\text{FI 600 WEIGHT SAVING} = \frac{3}{4} \frac{t}{2} = \Delta W$$

$$\text{NET WT} = W_c - \Delta W$$

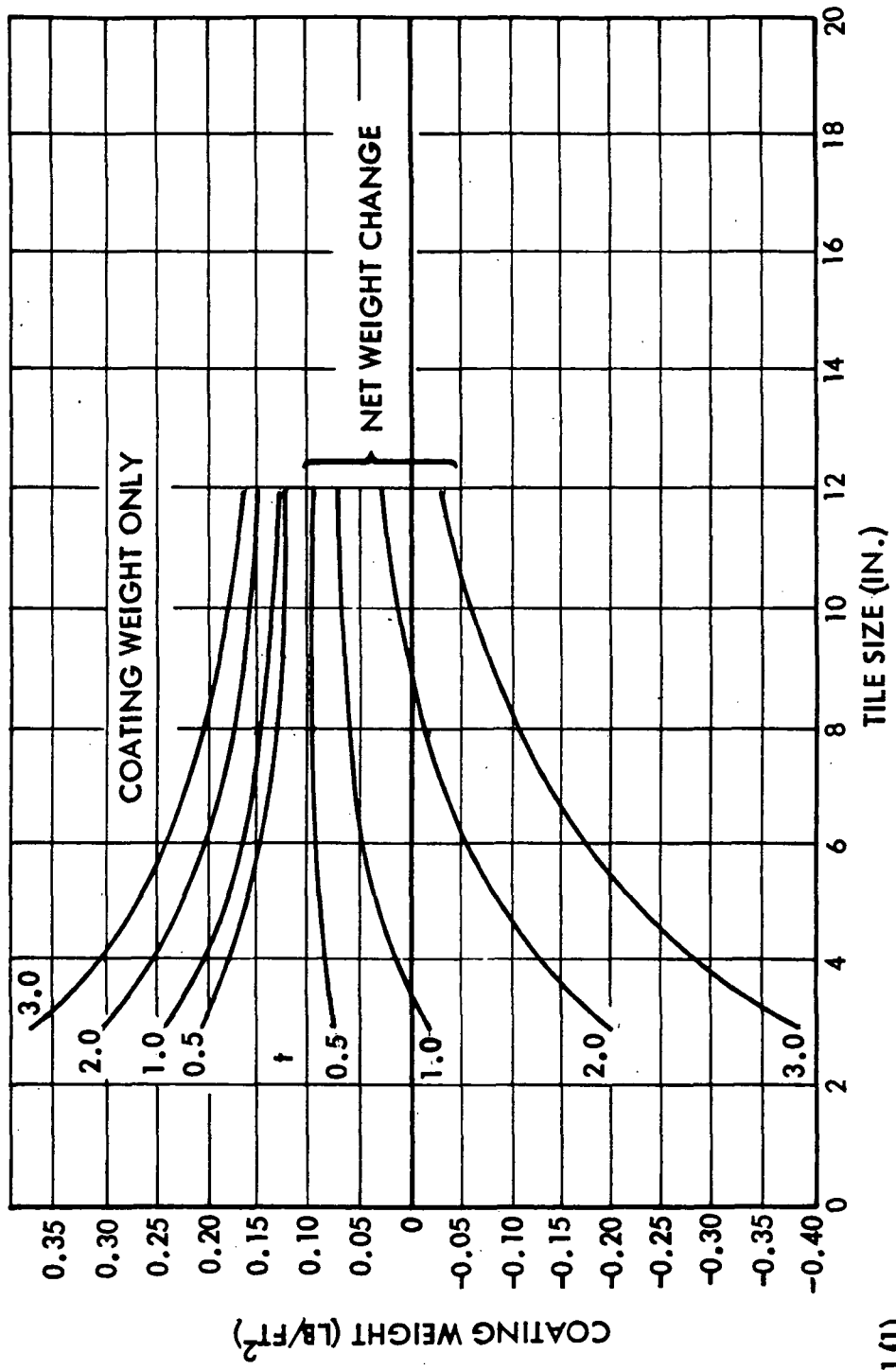
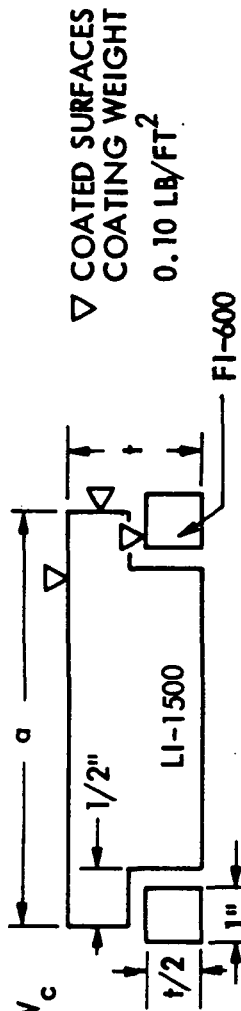


Fig. 3.2-57

D05041 (1)



STRAIN ARRESTOR PLATE

LMSC-D152738
Vol II

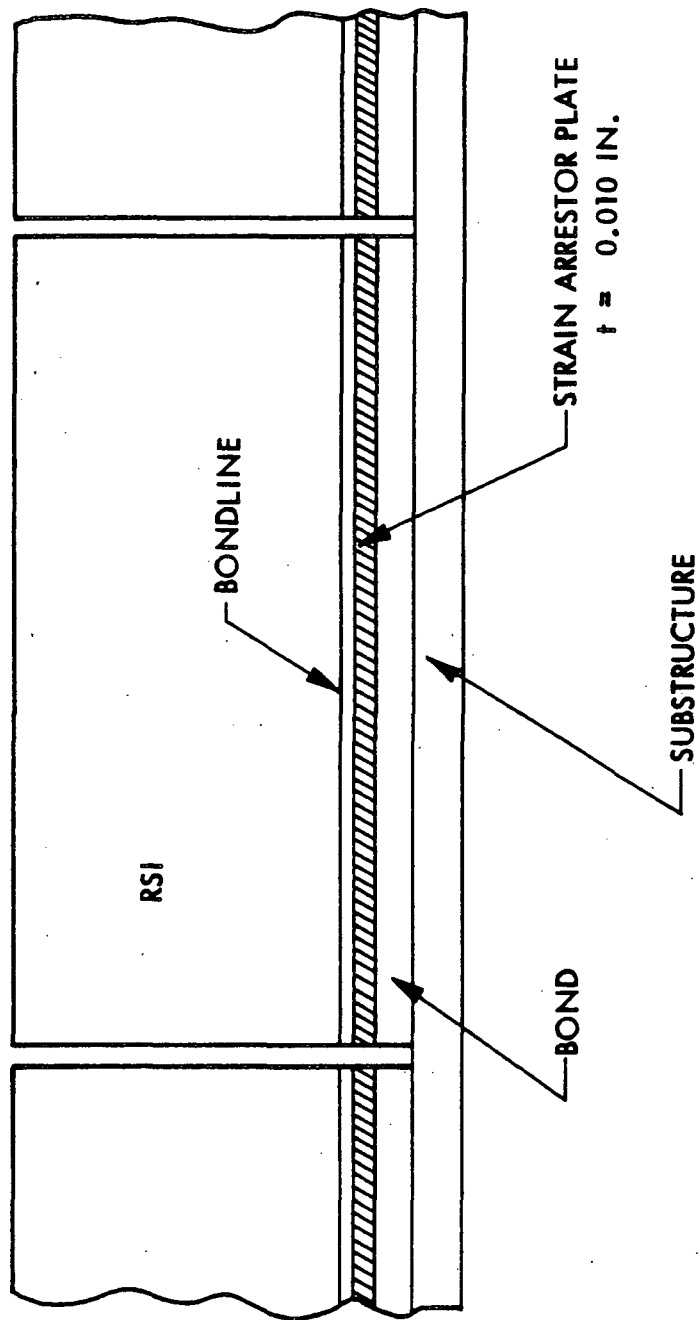


Fig. 3.2-58

Both materials can be manufactured to possess thermal expansion coefficients matching the LI-1500 coefficient. Table 3.2-14 gives readily available material properties for these two materials. Tables 3.2-15 through 3.2-18 show computer results using strain arrestor plates with different panel configurations. Comparisons also are made using models without the arrestor plate.

As noted, LI-1500 stress levels decrease markedly when a strain arrestor plate is used. The results of Table 3.2-18 show a possible orbiter temperature condition in which the substructure is allowed to cool down to -200°F . Since the glassy transition point of the RTV-560 is -165°F , without the strain arrestor plate, it is evident that the LI-1500 would fail. However, usage of this new concept could limit stresses to more tolerable levels. This severe condition is due to the temperature dependence of RTV-560 elastic modulus given in Table 6.2-7, which indicates a value of $E = 67,000$ psi at -200°F , effectively negating the strain isolation properties of RTV-560.

Thermal evaluation of the strain arrestor plate concept indicates that heat sink effects of this additional layer can be utilized and that an overall TPS weight increase of around 2 percent would be expected for the aluminum primary panels and about an 8-percent increase for titanium. However, no weight increase would occur for the beryllium subpanel. These conclusions represent the worst possible upper bound and apply to a graphite-epoxy arrestor plate.

It should be noted that this comparison considers only the orbiter lower surface, and such relationships may not be true for applications in areas with lower heating rates and, hence, smaller LI-1500 thicknesses.

Lightweight Core Concept

This concept is somewhat similar to all-around densification except that, in this case, the LI-1500 core is reduced below that of the surface layer density of 15 lb/ft^3 . One-dimensional thermal models were first constructed to determine the required insulation thickness for test panel No. 2. The models consisted of a 0.75-in. surface layer of baseline LI-1500 over various thickness of 6 lb/ft^3 LI-1500 bonded with 0.090 in. of RTV-560 to 0.114-in. aluminum. The results, shown in Fig. 3.2-59, indicate that

3.2-78

180<



Table 3.2-14

STRAIN ARRESTOR PLATE MATERIAL PROPERTIES

	INVAR*	GRAPHITE EPOXY**
F_{ty}	50,000 LB/IN. ²	50,000 LB/IN. ²
E	21×10^6 LB/IN. ²	11×10^6 LB/IN. ²
G	8.1×10^6 LB/IN. ²	4.4×10^6 LB/IN. ²
α	0.6×10^{-6} IN./IN./°F	0.5×10^{-6} (LOW TEMPERATURE) 0.35×10^{-6} (HIGH TEMPERATURE)
ρ	0.420 LB/FT ³	0.078 LB/FT ³
		ISOTROPIC LAYUP, THORNEL 755/ERLB 4617 LAMINATE

* PROPERTIES OF SOME METALS AND ALLOYS, THE INTERNATIONAL NICKEL COMPANY, INC., N.Y., N.Y.

** ADVANCED COMPOSITE MATERIAL STUDY FOR MILLIMETER WAVELENGTH ANTENNAS, GOODYEAR AEROSPACE CORP, GER-15011, AFML, WPAFB, OHIO, SEPT 1970

Table 3.2-1a

COMPARISON OF ALUMINUM TEST PANEL NO. 2 STRESSES



TILE SIZE = 6 IN.
 LOAD = 6000 PPI
 P = 1.5 PSI BURST
 COAT T = 100°F
 ALT = 250°F
 †COAT = 0.010 IN.
 †LI-1500 = 3.396 IN.
 †RTV-560 = 0.090 IN.
 †AL = 0.711 IN.

STRESSES	WITHOUT ARRESTOR	WITH GRAPHITE ARRESTOR † = 0.010	STRESSES	WITHOUT ARRESTOR	WITH GRAPHITE ARRESTOR † = 0.010
MAX LI-1500 PRINCIPAL TENSION PRINCIPAL COMPRESSION SHEAR (RZ) PRINCIPAL SHEAR LONGITUDINAL NORMAL TENSION	61 -27 19 32 61 8	12 -9 5 6 12 4	MAX COATING PRINCIPAL TENSION PRINCIPAL COMPRESSION	32 -1	60 0
MAX RTV-560 PRINCIPAL TENSION PRINCIPAL COMPRESSION SHEAR (RZ) PRINCIPAL SHEAR LONGITUDINAL NORMAL TENSION	22 -17 18 19 -6 8	21 -20 21 21 -6 4	MAX ARRESTOR PLATE PRINCIPAL TENSION PRINCIPAL COMPRESSION SHEAR (RZ) PRINCIPAL SHEAR LONGITUDINAL NORMAL TENSION		2124 -56 24 1062 2124 10

Table 3.2-16

COMPARISON OF BERYLLIUM PANEL STRESSES



STRESSES	WITHOUT ARRESTOR	WITH 0.010 INVAR ARRESTOR	WITH 0.010 GRAPHITE EPOXY ARRESTOR
MAX LI-1500			
PRINCIPAL TENSION	140	39	52
PRINCIPAL COMPRESSION	-100	-44	-52
SHEAR	31	7	14
LONGITUDINAL	140	39	52
NORMAL (TENSION)	3	2	1
MAX RTV-560			
PRINCIPAL TENSION	16	28	26
PRINCIPAL COMPRESSION	-35	-52	-50
SHEAR	24	39	38
LONGITUDINAL	-18	-19	-19
NORMAL (TENSION)	0	1	1
MAX COATING			
PRINCIPAL TENSION	19	4	3
PRINCIPAL COMPRESSION	-2076	-860	-1017
MAX ARRESTOR PLATE			
PRINCIPAL TENSION		10,531	9283
PRINCIPAL COMPRESSION		-162	-156
SHEAR		96	83
LONGITUDINAL		10,531	9283
NORMAL (TENSION)		2	3

TILE SIZE = 12 IN.

LOAD P = 0 PSI

T_{BE} = 0.040 IN.

T_{LI-1500} = 1.6 IN.

E_{COAT} = 3.5 x 10⁶ PSI

E_{LI-1500} = 60,000 PSI (ISOTROPIC)

T_{RTV-560} = 0.060 IN.

T_{COAT} = 75°F

T_{BE} = 600°F

NOTE: THIS IS THE SAME PANEL USED FOR 3-D ANALYSIS (WEAK DIRECTION)

Table 3.2-17

EFFECT OF ARRESTOR PLATE ON FLIGHT PANEL NO. 3 STRESSES



MAXIMUM STRESSES - ALUMINUM FLIGHT PANEL NO. 3
PRESSURE = 1.5 PSI BURST; 6000 PPI TENSION

	6 IN. TILE	12 IN. TILE WITH GRAPHITE ARRESTOR PLATE
LI-1500	57 - 30 17 57 - 29 8 - 4	37 - 8 9 37 - 2 11 - 3
RTV-560	19 - 14 15 0 - 6 8 - 3	42 - 32 36 1 - 7 12 - 3
GRAPHITE ARRESTOR PLATE		6556 -104 44 6556 - 94 21 - 20
COATING	8 -171	736 0

Table 3.2-18

COMPARISON OF ALUMINUM FLIGHT PANEL STRESSES AT -200°F



STRESSES	WITHOUT ARRESTOR	WITH GRAPHITE EPOXY ARRESTOR
MAX LI-1500 (PSI)		
PRINCIPAL TENSION	600	31
PRINCIPAL COMPRESSION	-880	-152
SHEAR	339	81
LONGITUDINAL	573	-152
NORMAL TENSION	18	15
MAX RTV-560		
PRINCIPAL TENSION	1,924	2,068
PRINCIPAL COMPRESSION	-142	-269
SHEAR	279	317
LONGITUDINAL	1,924	2,018
NORMAL TENSION	10	78
MAX COATING		
PRINCIPAL TENSION	202	207
PRINCIPAL COMPRESSION	-27	-23
MAX ARRESTOR PLATE		
PRINCIPAL TENSION		1,093
PRINCIPAL COMPRESSION		-27,913
SHEAR		588
LONGITUDINAL		-27,912
NORMAL TENSION		496

TILE SIZE = 6 IN.
 LOAD = NO MECHANICAL LOAD
 †COAT = 0.010 IN.
 †LI-1500 = 2.524 IN.
 †RTV = 0.090 IN.
 †AL = 0.711 IN.
 E_{RTV-560 @ -200°F} = 67,000 PSI
 E_{RTV -560 @ +70°F} = 300 PSI



LIGHTWEIGHT CORE CONCEPT

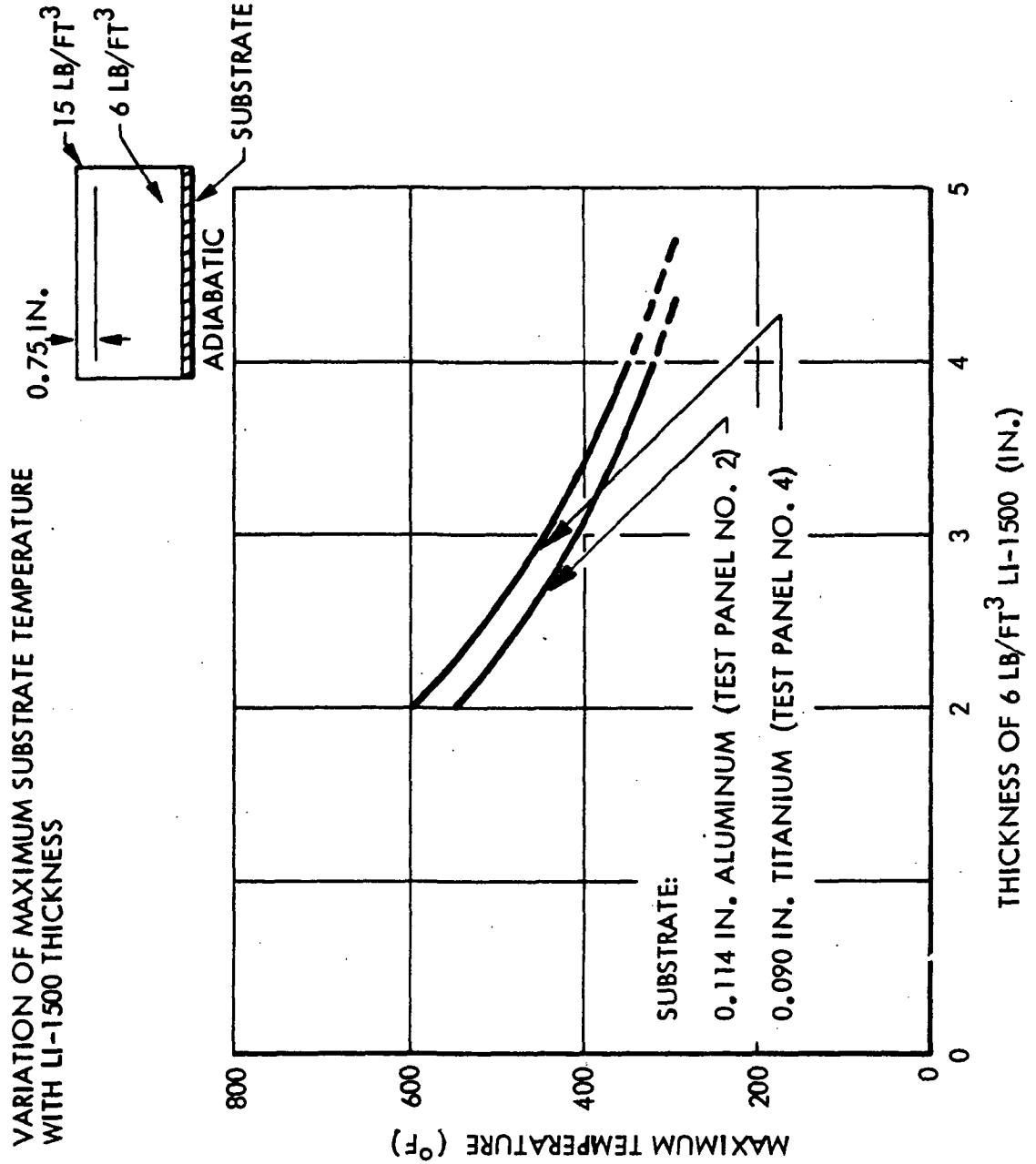


Fig. 3.2-59

4.3 in. of the 6-lb/ft³ LI-1500 is required to restrict the substrate temperature to 300°F. This is an increase of 1.65 in. (including the 0.75-in. surface layer) over the 3.4-in. thickness requirement for the 15-lb/ft³ LI-1500 (see Fig. 3.2-3). The increase in thickness is primarily due to the lower density-specific heat product which tends to increase the temperature of the lower density material at a specified depth from the surface.

Studies given in Tables 3.2-19 and 3.2-20 show that stress levels are reduced in the tile (as indicated by a 2D analysis). However, stresses in the direction perpendicular to the plane of the analysis in the 0.75 in. thick outer layer of the 15 pcf material would still be of the order of the stresses in a solid 15 pcf tile of that length. Thus, tile length is stress limited even though Table 3.2-19 shows a possible weight savings of RSI material of 9 percent by using this concept. On the other hand, stress levels in a 6 in. lightweight core tile would appear to be satisfactory, but Table 3.2-20 indicates that the lightweight core concept for this tile length leads to a heavier TPS system.

Hence, it is tentatively concluded that no apparent advantage is gained from the usage of this concept. Further evaluation of the lightweight core would necessitate the use of 3D studies for both the thermal and stress analyses.

Effect of Contact Conductance on Stiffener Temperatures

Since the fastening method for the titanium panel was riveting, a study was performed to determine the effect of contact conductance upon face sheet and stiffener temperatures at the interface between the face sheet and stiffener. The results for a range of contact conductance values (3-2) and (3-3) are shown in Fig. 3.2-60. For the contact conductance values expected on the titanium panel, 50-500 Btu/ft² hr°F, the maximum temperature difference between the face sheet and titanium stiffener is about 80°F.

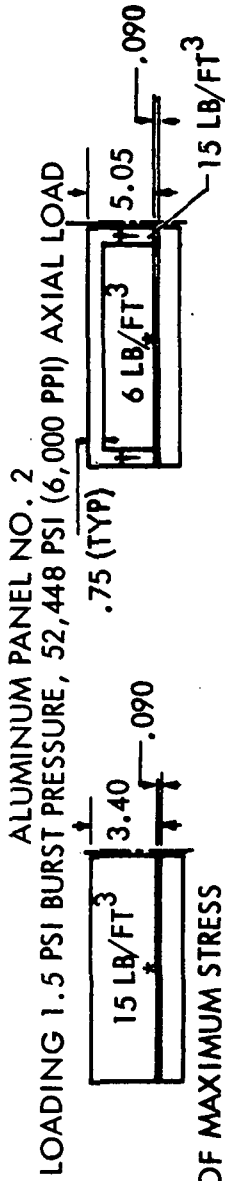
(3-2) "Interface Thermal Conductance of 27 Riveted Aircraft Joints," M. E. Barzelay and G. F. Holloway, NASA TN-3991, July 1957

(3-3) "Range of Interface Thermal Conductance for Aircraft Joints," M. E. Barzelay, NASA TN-D426, May 1960



Table 3.2-19

COMPARISON OF SOLID AND LIGHTWEIGHT CORE TILES
TILE LENGTH = 12 INCHES



*, † LOCATION OF MAXIMUM STRESS

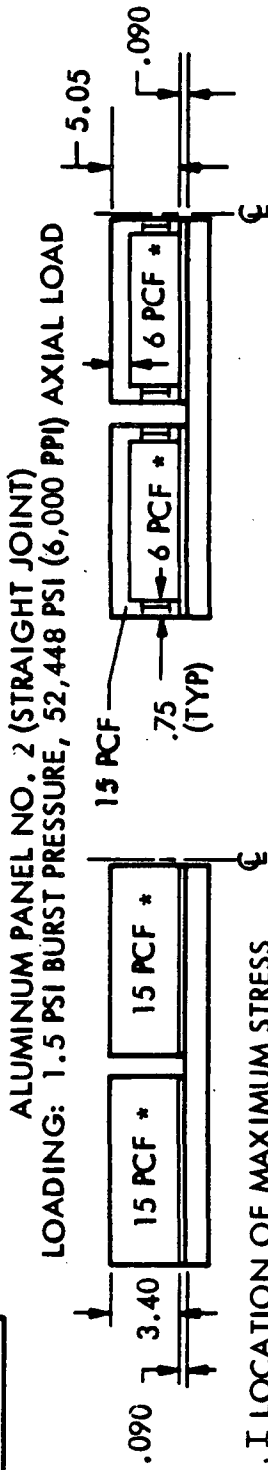
	15 LB/FT ³	6 LB/FT ³ CORE AND 15 LB/FT ³ OUTER LAYER
LI-1500		
MAXIMUM	132*	73†
MINIMUM	-19	-7
SHEAR	44	36
LONGITUDINAL	132	55
PEEL	27	22
RTV-560		
MAXIMUM	59	50
MINIMUM	-31	-25
SHEAR	39	32
PRINCIPAL SHEAR	40	33
LONGITUDINAL	9	9
PEEL	28	25
MAXIMUM COATING	3	9
MINIMUM COATING	-855	-526
TOTAL RSI THICKNESS (IN.)	3.40	5.05
INSULATION WEIGHT	17.0	15.4
COMPARISON (LB)		
(24 IN. X 24 IN. PANEL)		

15 PCF LI-1500 { E = 60,000, 6000 PSI
G = 4150 PSI

6 PCF LI-1500 { E = 40,000, 4000 PSI
G = 2767 PSI



COMPARISON OF SOLID AND LIGHTWEIGHT CORE TILES
TILE LENGTH = 6 INCHES



*. I LOCATION OF MAXIMUM STRESS

	15 LB/FT ³	6 LB/FT ³ CORE AND 15 LB/FT ³ OUTER LAYER												
LI-1500 MAXIMUM MINIMUM SHEAR LONGITUDINAL PEEL	74* -13 23 74 11	<table border="0"> <tr> <td>I</td> <td>58*</td> </tr> <tr> <td>42</td> <td>-4</td> </tr> <tr> <td>-11</td> <td>14</td> </tr> <tr> <td>21</td> <td>58</td> </tr> <tr> <td>38</td> <td>1</td> </tr> <tr> <td>10</td> <td></td> </tr> </table>	I	58*	42	-4	-11	14	21	58	38	1	10	
I	58*													
42	-4													
-11	14													
21	58													
38	1													
10														
RTV-560 MAXIMUM MINIMUM SHEAR PRINCIPAL SHEAR LONGITUDINAL PEEL	28 -19 22 23 -6 11	25 -16 19 19 -4 10												
MAXIMUM COATING MINIMUM COATING	12 -37	10 -37												
TOTAL RSI THICKNESS (IN.) WEIGHT COMPARISON (LB) (24 IN. X 24 IN. PANEL)	3.40 17.0	5.05 18.0												

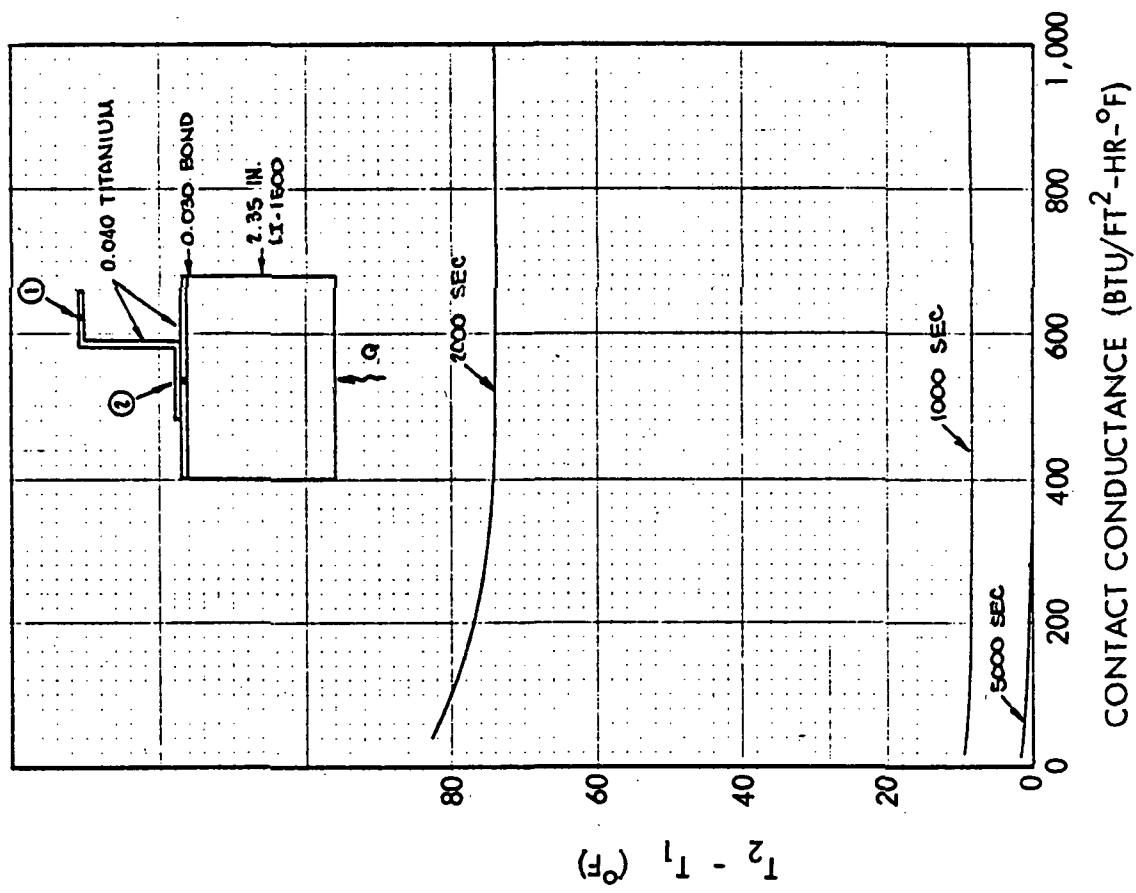
15 PCF { E = 60,000, 6000 PSI
LI-1500 { G = 4150 PSI

6 PCF { E = 40,000, 4000 PSI
LI-1500 { G = 2767 PSI



EFFECT OF CONTACT CONDUCTANCE ON STIFFENER TEMPERATURES

TEST PANEL NO. 4



DO6091

Fig. 3.2-60

For the weldbond technique used to fasten the aluminum panels, contact conductances greater than $1000 \text{ Btu/ft}^2\text{hr}^\circ\text{F}$ are expected. Results for the aluminum test panel No. 2 are shown in Fig. 3.2-61, where values of contact conductance from 50 to $1000 \text{ Btu/ft}^2\text{hr}^\circ\text{F}$ between the face sheet and stiffeners were considered. The maximum temperature difference is about 10°F for the values of contact conductance analyzed. Due to the high thermal conductivity of aluminum and the low rate of heat conducted through the LI-1500 into the panel, the temperature difference between the top and bottom of the stiffener is less than 5°F .

Effect of Discontinuous Bond on Substrate Temperatures

Since a promising method of attachment appeared to be an interrupted bond, which could reduce weight and stresses in the LI-1500, the two-dimensional thermal model was used to show the effect of the adhesive void on the substrate temperatures.

Figure 3.2-62 shows temperature histories for an adhesive void located directly above the location of the stiffener. The results indicate about a 20°F increase in the maximum titanium temperature as compared to the results of Fig. 2.1-15, where a continuous adhesive was used.

The effect of the face-sheet temperature distribution at various reentry times is shown in Fig. 3.2-63 for the continuous and interrupted adhesive. The maximum face-sheet temperature difference occurs at about 4000 sec. The effect of the stiffener heat sink is indicated at earlier times (2000 sec) by the lower temperature in the vicinity of the stiffener.

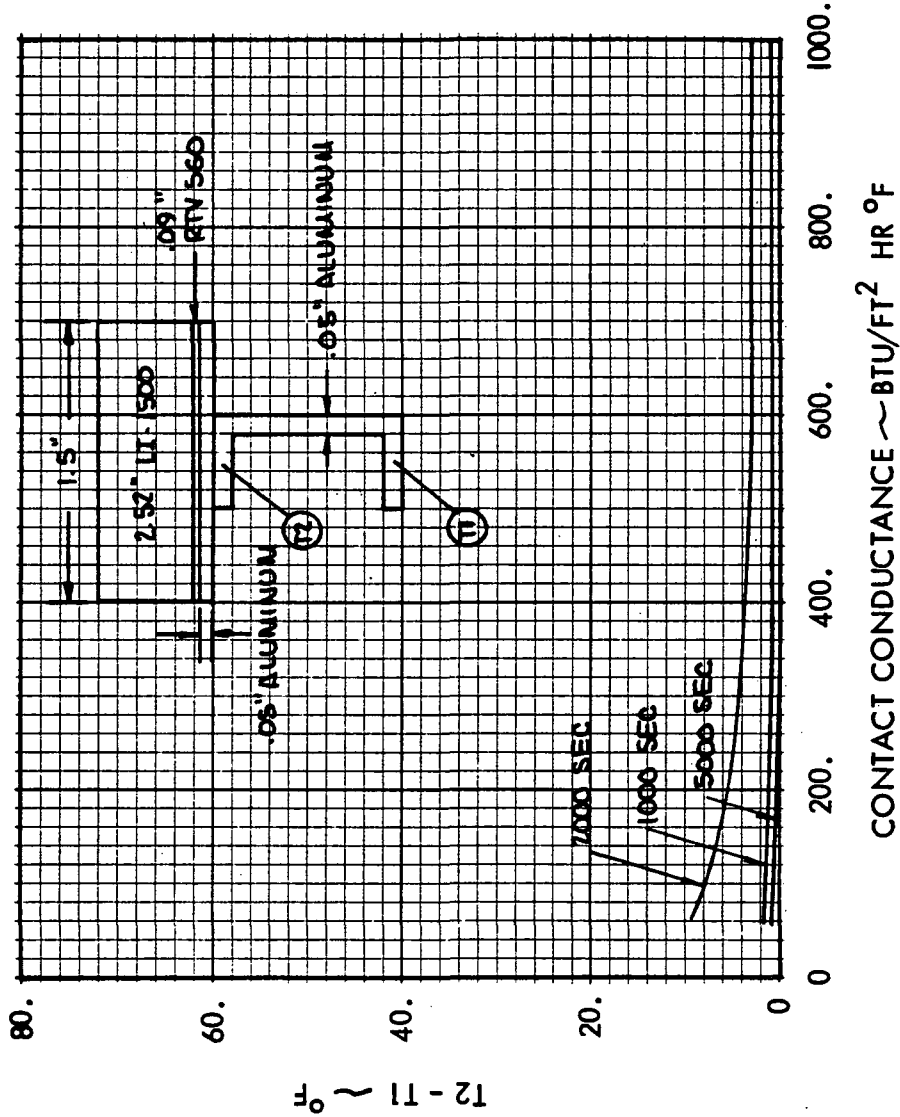
Thermal Analysis of FI-600 Filler Strip

A newly developed (NAS 9-12137) flexible joint filler strip material (FI-600) has been incorporated in the panel designs. To assess the effect of this low density strip a two-dimensional thermal analysis was performed for one half of a 6 in. x 6 in. x 2.5 in. tile for the Aluminum Flight Panel No. 2.



EFFECT OF CONTACT CONDUCTANCE ON TEMPERATURE DIFFERENCE
 BETWEEN FACE SHEET AND BOTTOM OF STIFFENER

TEST PANEL 2



DO6009

Fig. 3.2-61

TEMPERATURE HISTORIES FOR TITANIUM TEST PANEL
WITH ADHESIVE VOID

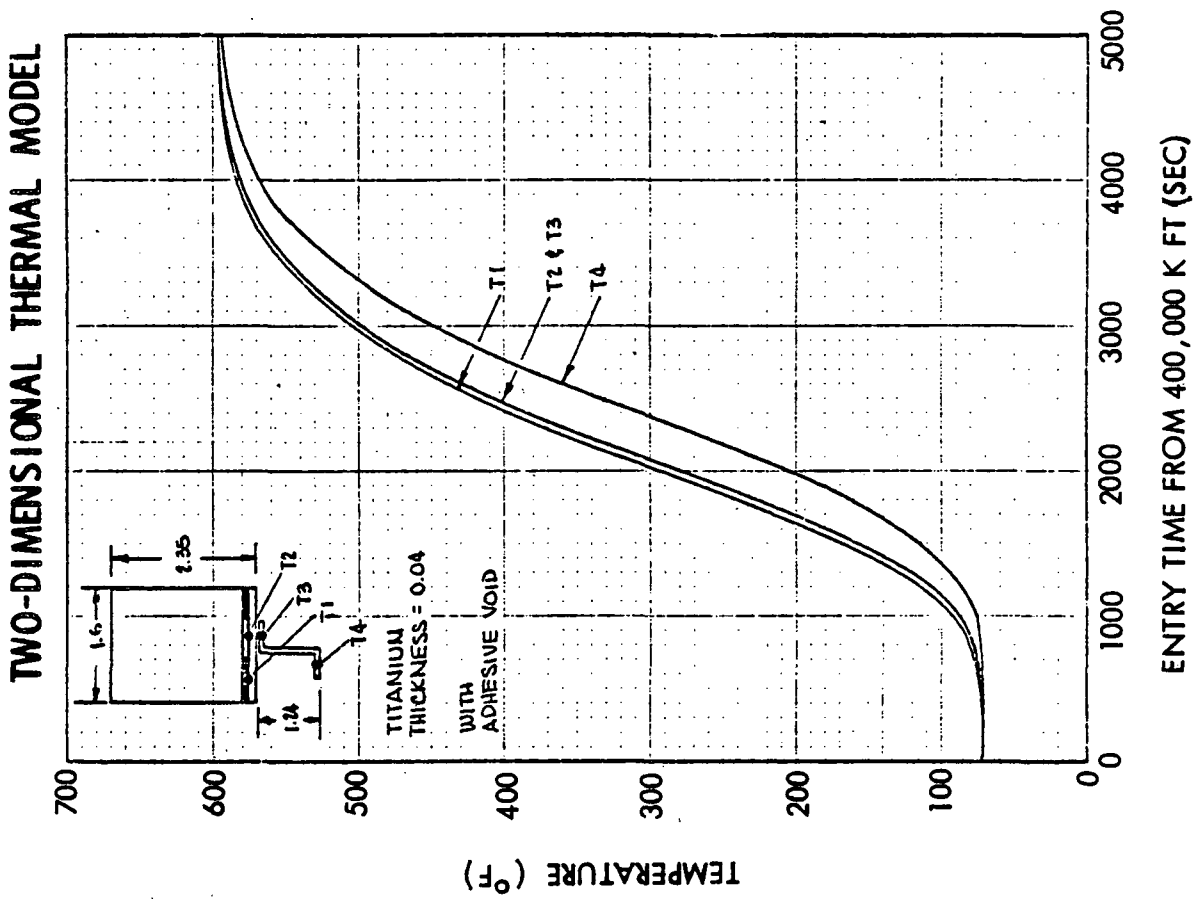


Fig. 3.2-62

DO6101

EFFECT OF ADHESIVE VOID ON TITANIUM FACE SHEET
TEMPERATURE DISTRIBUTION



TEST PANEL NO. 4

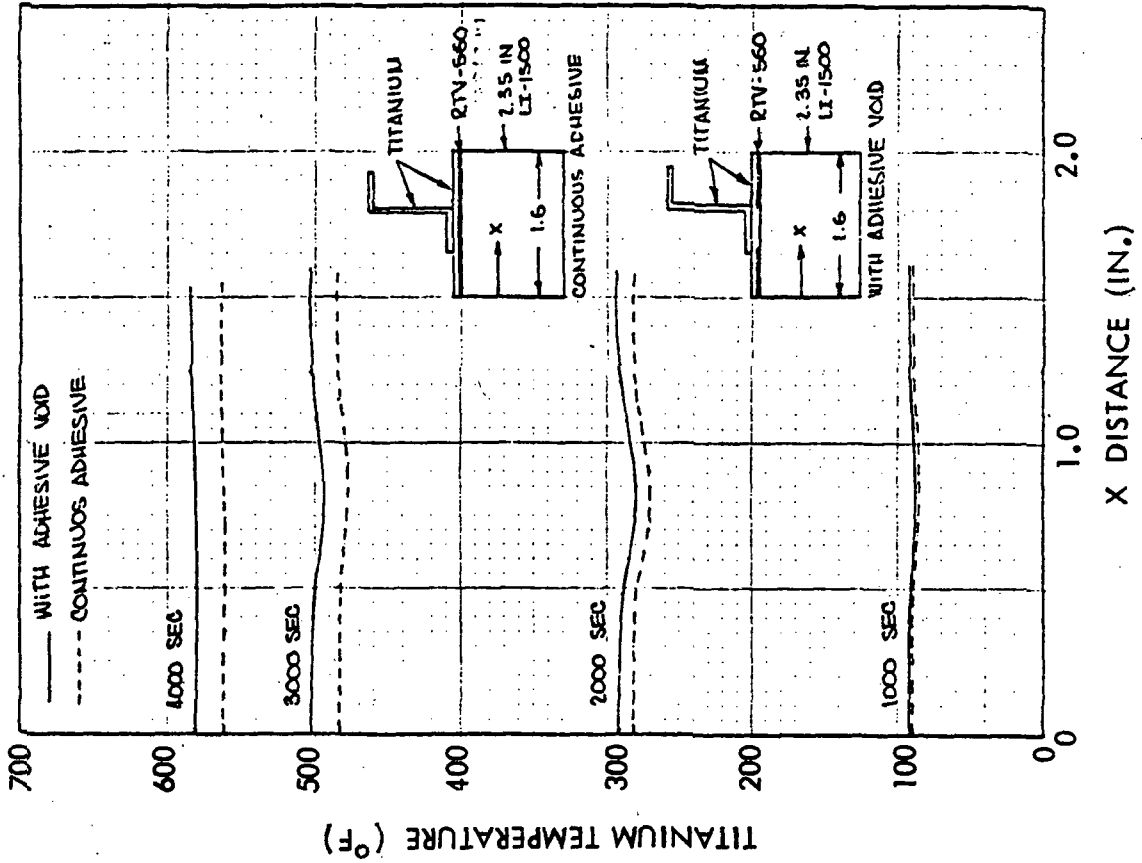


Fig. 3.2-63

DO6090

The results of the analysis indicated a maximum panel temperature of 313^oF for the subpanel under the filler strip as compared with 300^oF for the 15-pcf filler block case. Hence, the usage of a low-density filler has a negligible effect on temperature distributions in LMSC RSI panel designs.

3.3 ENVIRONMENTAL VARIATIONS

Coating Stress During Reentry

Rigidized Surface Insulation (RSI) component stresses have been investigated as a function of reentry time, using design flight loadings and temperatures. Study results are presented in Tables 3.3-1 and 3.3-2 and their companion Figs. 3.3-1 and 3.3-2, where coating stress is plotted as a function of reentry time for both beryllium and aluminum flight panels. Maximum loads and surface temperatures employed are shown in Figs. 3.3-3 and 3.3-4. In addition, the elastic modulus of fused silica, $E = 10.6 \times 10^6$ psi, has been used to simulate the worst possible case of coating modulus. Qualitatively, the coating first experiences compressive stresses, since only the coating is first heated and is restrained from expanding by the LI-1500. Later, as the LI-1500 begins to heat, the coating goes into tension due to the expansion of the LI-1500 being greater than that of the coating*. Finally, as the substrate heats up with the surface cooling, the panel bows, again developing compressive coating stresses. The net effect of this thermal sequence in combination with applied loads results in a final net coating compression for the beryllium panel at 3600 sec. The aluminum panel experiences a relatively low net tensile stress in the coating at this time, due to high in-plane thermal expansion. Variations of other stresses in the RSI system are shown in the tables also as a function of time where it is noted that the ground condition, $t = 3600$ sec, is critical for the LI-1500.

Additional comparative data for 6- and 12-in. tiles with 0025 coating under thermal load only are shown in Table 3.3-3.

Orbital Cold Soak Condition

As per NASA request, a -200° TPS cold soak temperature condition after approximately 10 orbits has been assumed. Such a severe condition could arise due to adverse vehicle

*Coating tests completed just prior to publication of this book indicate that the coefficient of thermal expansion of the coating is 4×10^{-7} in./in./ $^{\circ}$ F which is slightly higher than the value for LI-1500.

orientation in orbit, although only minimal attitude control would be necessary to avoid this situation. The resulting RSI stress levels are shown in Table 3.2-18, and it is noted that these are very severe and would cause failure of the LI-1500. This is primarily due to the high modulus of approximately 67,000 psi for the RTV-560 at -200°F , essentially negating the strain isolation characteristics of RTV-560. However, the usage of the strain arrestor plate concept discussed earlier would act to reduce LI-1500 stresses to tolerable levels as shown in the same table even in this extreme orbit condition.

Without the arrestor plate, additional analysis has indicated that if RTV-560 modulus is restricted to less than 1200 psi (approximately -150°F) then LI-1500 stress levels would not exceed allowables.



Table 3.3-1

BERYLLIUM FLIGHT PANEL #1

TIME (SEC)	500	800	1300	1700	2800	3600
PRESSURE (PSI)	0.0	0.0	0.0	2.25	3.0	3.0
MAX. COAT	104	172	206	133	47	24
MIN. COAT	-134	-175	-172	-141	-386	-560
MAX. LI-1500	5	6	17	35	65	68
MIN. LI-1500	-14	-13	-12	-10	-8	-8
SHEAR LI-1500	2	3	3	6	15	17
LONG. LI-1500	-14	-13	17	35	65	68
PEEL LI-1500	1	1	1	1	6	6
MAX. RTV-560	1	1	0	3	15	18
MIN. RTV-560	-2	-2	-5	-11	-23	-25
SHEAR RTV-560	0	0	2	5	15	17
LONG. RTV-560	-1	-2	-4	-9	-17	-18
PEEL RTV-560	1	1	0	1	8	9

t_{Be} COATING = 0.010 IN.
 $t_{LI-1500}$ = 1.45 IN.
 $t_{RTV-560}$ = 0.050 IN.
 t_{Be} = 0.4312 IN.
 E COATING = 10.6×10^6 PSI
 TILE LENGTH = 6 IN.

LOCKHEED



Table 3.3-2

ALUMINUM FLIGHT PANEL #2

TIME (SEC)	500	800	1300	1700	2500	3600	6700
COLLAPSE PRESSURE (PSI)	0	0	0	2.25	2.25	3.00	0
TENS LOAD (PPI)	450	450	450	2400	2400	6000	0
MAX. COAT	2701	162	285	300	245	94	18
MIN. COAT	3641	-200	-195	-195	-148	-57	-9
MAX. LI-1500	5	3	3	15	21	50	20
MIN. LI-1500	-13	-13	-13	-10	-5	-9	-3
SHEAR LI-1500	1	4	5	4	5	13	7
LONG LI-1500	-13	-12	-11	15	21	50	20
PEEL LI-1500	1	2	2	2	2	3	18
MAX RTV	1	1	1	4	5	13	4
MIN RTV	-1	-1	-1	-4	-6	-14	-9
SHEAR RTV	1	1	1	4	5	13	5
LONG RTV	0	0	0	1	-2	-4	8
PEEL RTV	0	0	0	1	1	3	2

^t COATING - 0.010 IN.
^t LI-1500 - 2.524 IN.
^t RTV-560 - 0.090 IN.
^t AL - 0.711 IN.
^E COATING - 10.6 x 10⁶ PSI
 TILE LENGTH - 4 IN.



COATING STRESS AT VARIOUS TEMPERATURE PROFILES AND LOADS

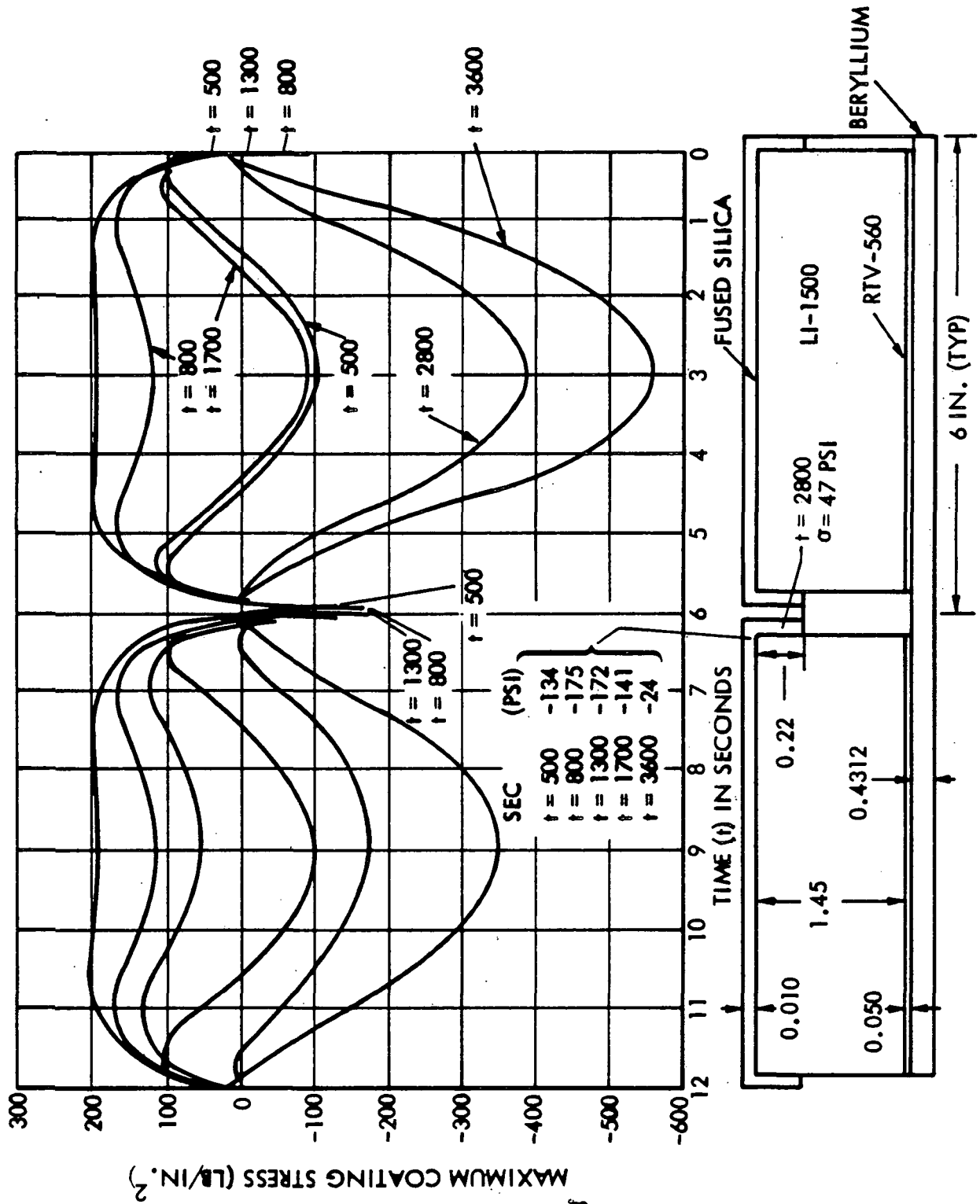
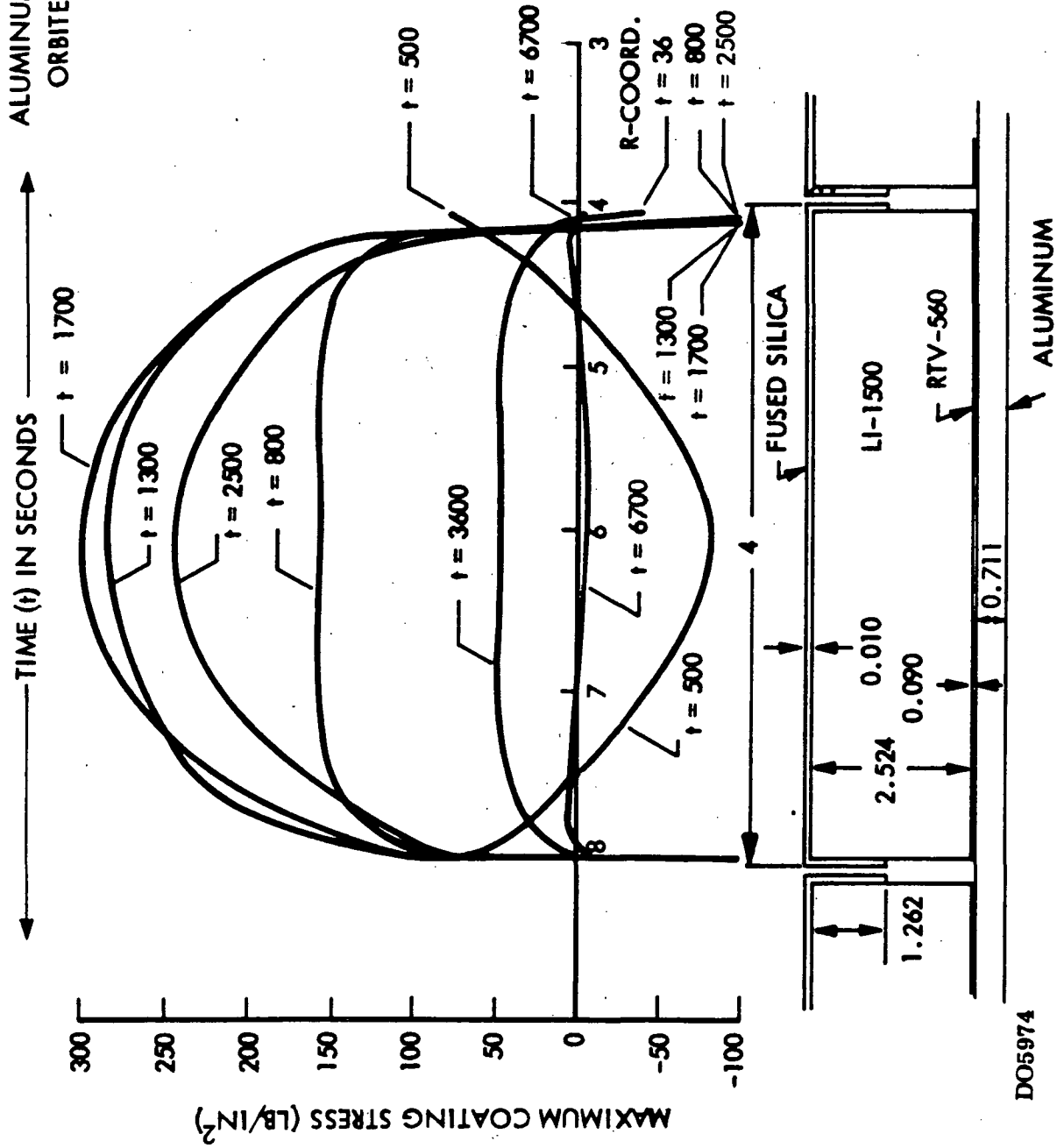


Fig. 3.3-1

COATING STRESS AT VARIOUS TEMPERATURE
PROFILES AND LOADS

ALUMINUM FLIGHT PANEL NO. 2
ORBITER FUSELAGE AREA 2



DO5974

Fig. 3.3-2

LI-1500 TEMPERATURE DISTRIBUTION
BERYLLIUM FLIGHT PANEL NO. I

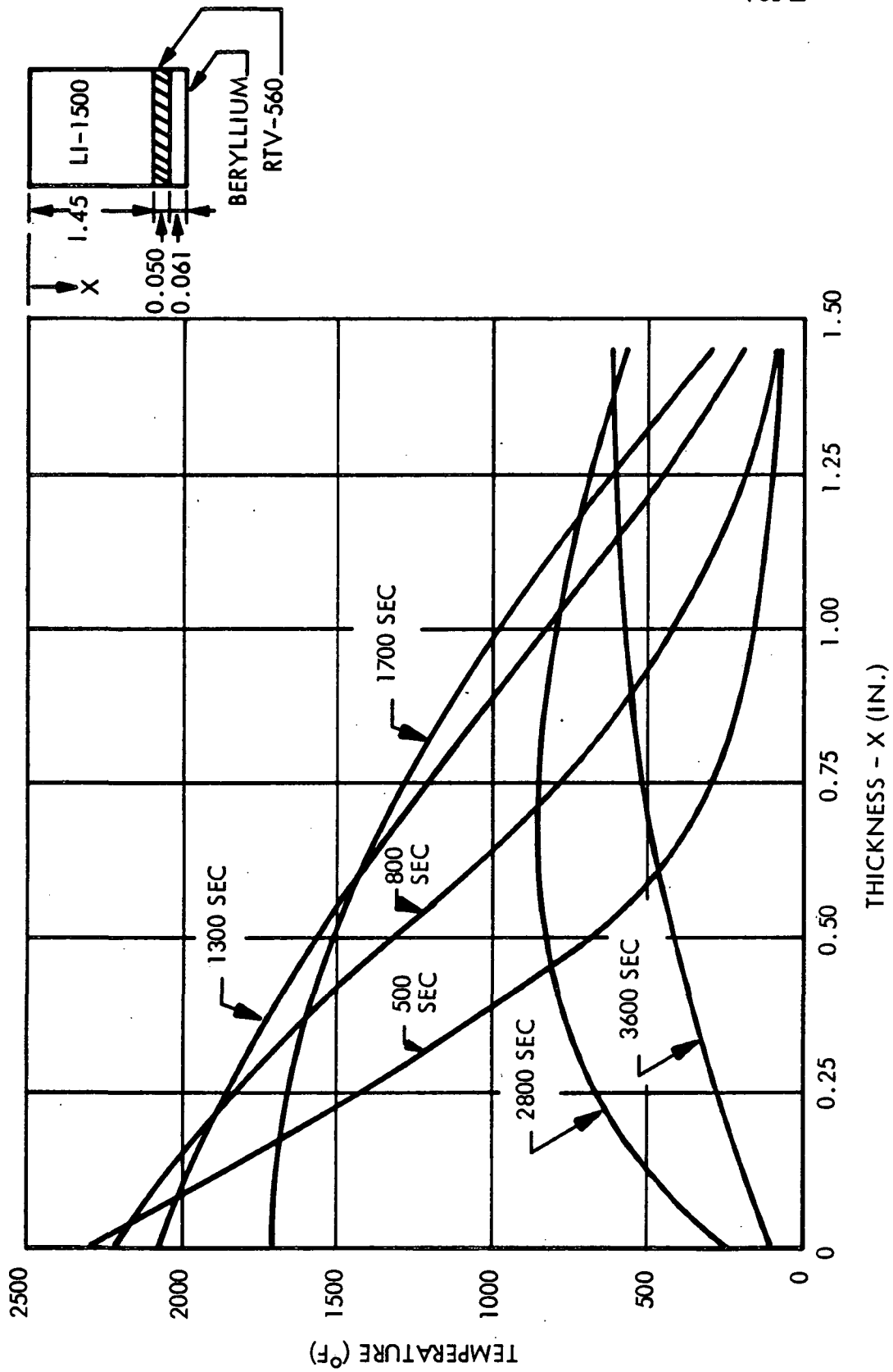


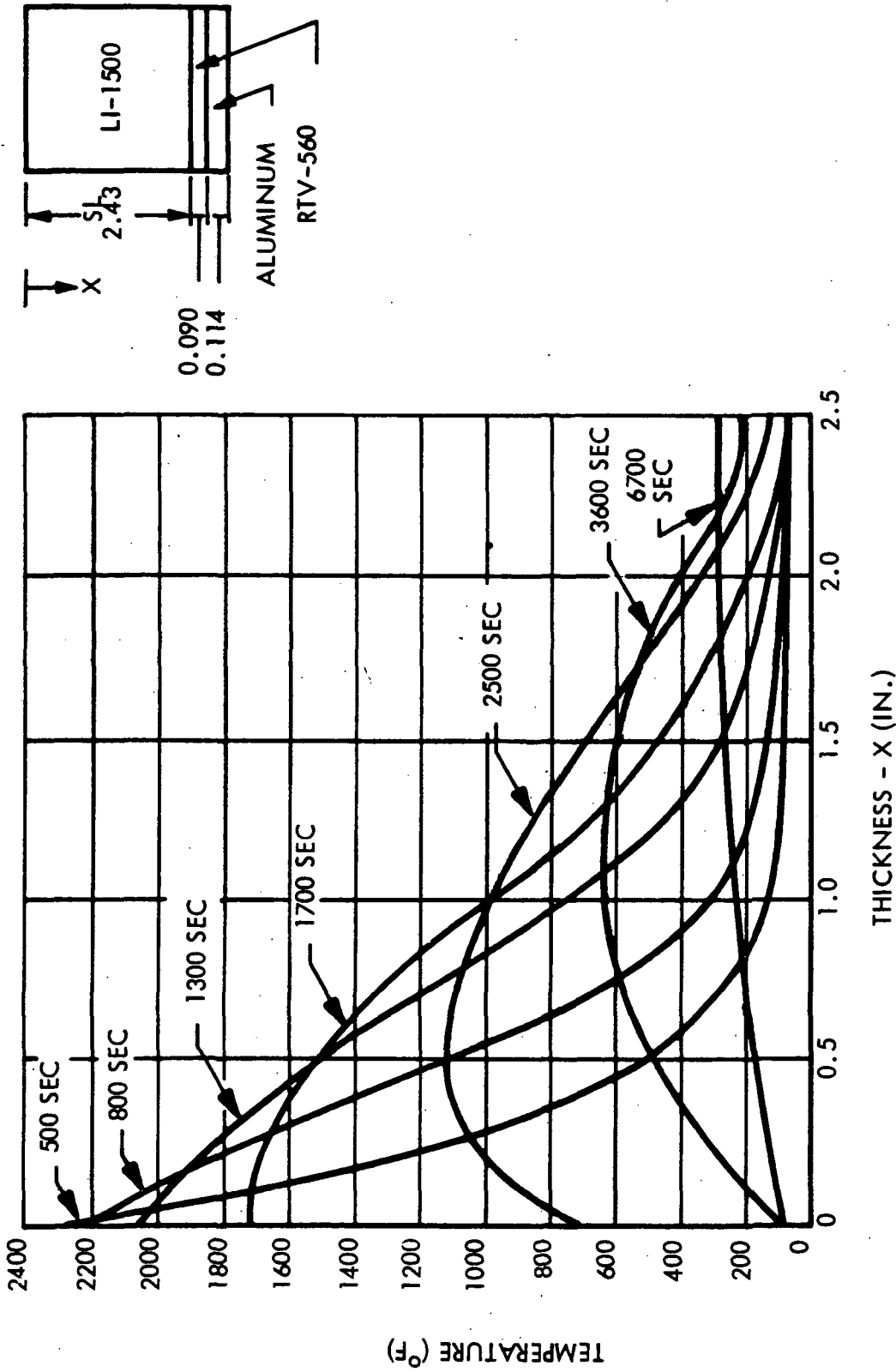
Fig. 3.3-3

3.3-7

202 <

DO5990(1)

LI-1500 TEMPERATURE DISTRIBUTION ALUMINUM FLIGHT PANEL NO. 2



3.3-8

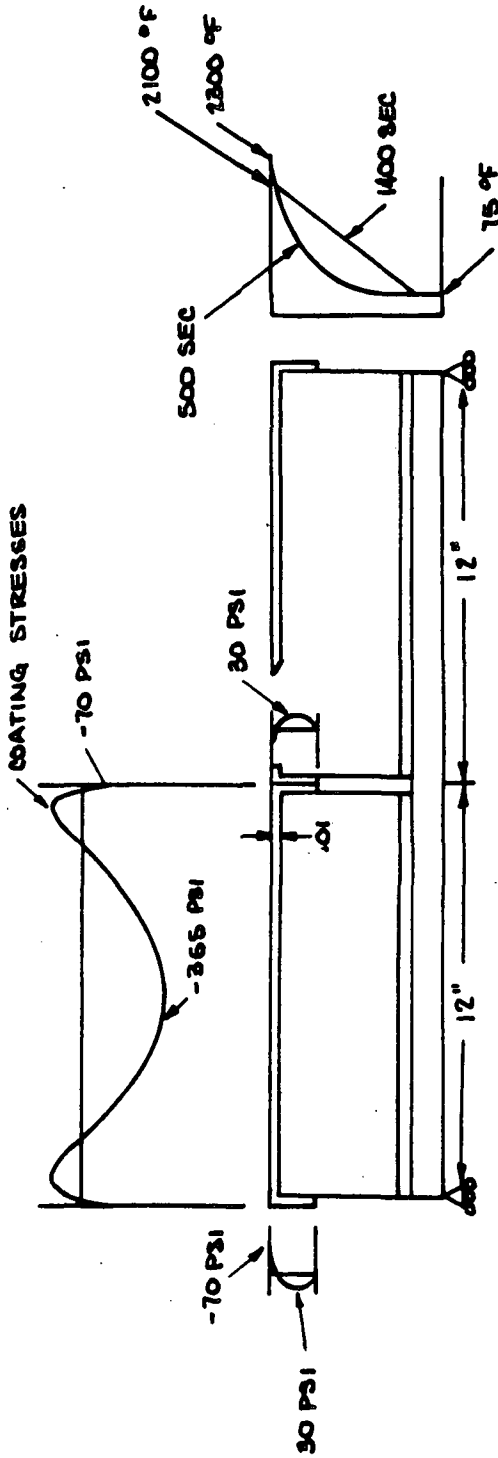
303

Fig. 3.3-4

DO5992(1)

Table 3.3-3

FUSELAGE BERYLLIUM PANEL COATING STRESSES AT
MAXIMUM HEAT IMPULSE - NO MECHANICAL LOAD



MAXIMUM STRESSES IN PANELS (PSI)

QUANTITY	12-IN. TILE TEST PANEL (t = 500 SEC)	6-IN. TILE FLIGHT PANEL (t = 500 SEC)	6-IN. TILE FLIGHT PANEL (t = 1400 SEC)
MAXIMUM COATING	110	80	155
MINIMUM COATING	-365	-140	-75
MAXIMUM LI-1500	7	6	7
MINIMUM LI-1500	-19	-15	-11
SHEAR LI-1500	2	3	3
LONG. LI-1500	-19	-15	-11
PEEL LI-1500	1	1	2
MAXIMUM RTV-560	1	1	1
MINIMUM RTV-560	-4	-2	-3
SHEAR RTV-560	0	0	0
LONG. RTV-560	-2	-1	-1
PEEL RTV-560	1	1	1

$E_{COATING} = 3.5 \times 10^6 \text{ PSI}$



3.4 CONCLUSIONS - PARAMETRIC STUDIES

Parametric relationships have been established between mechanical properties, design details, and environmental conditions with their consequent effects on Rigidized Surface Insulation (RSI) system design. These relationships can be summarized as follows:

- Required LI-1500 thickness varies directly with environmental pressure, surface temperature, and total heat.
- Required LI-1500 thickness varies inversely with bond thickness and substrate thickness.
- RSI system stresses vary directly with tile length.
- RSI system stresses vary inversely with bond thickness.
- RSI stresses vary directly with modulus of elasticity of the material.
- Coating stresses vary inversely with RSI modulus of elasticity.
- Thickness of RSI material does not appreciably alter RSI stresses. However, coating stresses vary inversely with RSI thickness.
- Coating stresses vary inversely with coating thickness. Other stresses in the RSI are not affected.
- Coating stresses vary directly with coating modulus of elasticity.
- Integral coating (densified insulation material) is structurally feasible.
- Reduction in bond modulus of elasticity reduces RSI system stresses.
- Bond discontinuity at tile joints reduces RSI stresses appreciably.
- Textured coatings do not appreciably lower coating stresses.
- Intentional cracks (discontinuities) in the coating decrease coating stresses. However, RSI stresses are increased considerably due to stress concentration effects. Both stresses approach zero as the number of discontinuities in the coating is increased.
- Stresses in the RSI system are mainly due to inplane deformation of the substrate (mechanical and/or thermal loading).
- Common metal mechanical fasteners inserted in LI-1500 induce large stresses due to difference in thermal expansion properties. Use of Invar or graphite-epoxy fasteners avoids such thermal problems.
- Under normal reentry ground condition is the worst case for LI-1500 stresses.
- Use of strain arrestor plate results in large reduction of LI-1500 stresses.
- Lightweight core concept does not appear feasible.

For convenience, some of the more important relationships are presented in Table 3.4-1.

3.4-1

205<



Table 3.4-1

PARAMETRICALLY ESTABLISHED RELATIONSHIPS

LI-1500 MODULUS	↔	LI-1500 SHEAR STRESS RTV-560 PEEL STRESS LI-1500 MAXIMUM STRESS COATING STRESS RTV-560 SHEAR STRESS
LI-1500 THICKNESS	↔	LI-1500 SHEAR STRESS LI-1500 MAXIMUM STRESS RTV-560 PEEL STRESS RTV-560 SHEAR STRESS
RTV-560 THICKNESS	↔	LI-1500 STRESSES RTV-560 STRESSES COATING STRESS
COATING THICKNESS	↔	COATING STRESS RTV-560 STRESSES LI-1500 SHEAR
COATING MODULUS	↔	COATING STRESS
TILE SIZE	↔	LI-1500 SHEAR STRESS LI-1500 MAXIMUM STRESS LI-1500 PEEL STRESS RTV-560 PEEL STRESS RTV-560 SHEAR STRESS COATING WEIGHT
ENVIRONMENTAL PRESSURE AT GIVEN TEMPERATURE RTV-560 THICKNESS SUBSTRATE THICKNESS SURFACE TEMPERATURE TOTAL HEAT		LI-1500 THICKNESS

206

3.4-2

Section 4
OPTIMIZATION STUDIES

This section presents the thermal/structural/weight optimization techniques developed for RSI system design and specifically addresses the following topics:

- Stiffener configuration
- Stiffener material
- Vehicle frame spacing
- Subpanel/primary structure tradeoff
- Heat sink effects/substrate effective thickness
- LI-1500 conductivity (flight vs test panels)
- Panel weight

The studies reported here represent the process by which the deliverable prototype panels have been designed in accordance with load and environmental criteria discussed in Section 6.

4.1 SELECTION OF OPTIMUM SUBPANEL CONFIGURATION

A comparison of several material/configuration combinations, structurally optimized to sustain the design loads for prototype panel No. 1 when utilized as a subpanel, is shown in Fig. 4.1-1. These results were obtained from the SUBPAN computer code which was discussed in Section 2. All designs have been optimized for the burst/collapse pressures shown, which, as noted previously, occur during ascent when the subpanel is at room temperature. The panel span was kept constant at 25 in. and no constraint was placed on the maximum allowable deflection. Note that graphite epoxy is included for comparative purposes even though its acceptability at temperatures approaching the maximum backface temperature of 600^oF is doubtful. Graphite-polyimide was not included, because it is not considered to be a material that is sufficiently developed for the manufacture of panels within the time available on this program.

Most of the designs shown in the figure have been constrained by minimum gage requirements specified in the computer code input. This gage for beryllium is 0.016 in. except in the honeycomb designs where it is 0.010 in. In the conventional constructions, the minimum gage for titanium and graphite-epoxy is 0.012 in. and in honeycomb sandwich construction it is 0.008 in. Because of the thin gages involved, the graphite-epoxy properties have been selected to represent quasi-isotropic layups rather than unidirectional layups. Note also that the attach-flange widths have been assigned fixed, realistic values, and that commercially available honeycomb-sandwich cores have been specified (with the exception of the beryllium honeycomb core). These cores are the lightest which can be handled and utilized without adverse structural effects.

The maximum compressive stresses due to bending are considerably higher for the beryllium designs than for either the titanium or graphite-epoxy designs. This indicates that beryllium satisfies stiffness requirements with less material volume than its competitors. The maximum compressive stress for beryllium is in the range of 44-52 ksi for the four beryllium configurations, generally increasing as weight decreases. This stress is in the range 27-33 ksi for titanium, and 18-24 ksi for graphite epoxy. Referring back to Fig. 3.1-1, observe that the material weight ratios illustrated in this figure are reasonably accurate for a given configuration. Scatter in the ratios is present, but this is due in part to the effect of the constraints in reducing ideal



COMPARISON OF LI-1500 SUBPANELS DESIGNED FOR STRENGTH AND STIFFNESS

COLLAPSE PRESSURE: 4.0 LB/IN.² (LIMIT), 6.0 LB/IN.² (ULTIMATE)

BURST PRESSURE: 3.0 LB/IN.² (LIMIT), 4.5 LB/IN.² (ULTIMATE)

SPAN LENGTH = 25 IN.

DESIGN TEMPERATURE: 70°F

CONFIGURATIONS		WEIGHT (LB/FT ²)	CONFIGURATIONS		WEIGHT (LB/FT ²)
0.387*	<p>Be - 0.020 IN. Be - 0.016 IN. $\bar{t} = 0.039$ 2.754</p>	0.387*	1.325	<p>Ti - 0.030 IN. Ti - 0.016 IN. 2.754</p>	1.325
0.472	<p>Be - 0.025 IN. $\bar{t} = 0.047$ Be - 0.016 IN. 2.39</p>	0.472	0.955	<p>Ti CORE 4.18 LB/FT³ 3/8-IN. CELL SIZE 3.578</p>	0.955
0.409	<p>Be FACE SHEETS 0.010 IN. Be CORE 2.64 LB/FT³ 1/4-IN. CELL SIZE 3.578</p>	0.409	0.721	<p>H/M GRAPHITE EPOXY 0.063 IN. H/M GRAPHITE EPOXY 0.012 3.578</p>	0.721
0.563	<p>Be FACE SHEETS 0.012 IN. Ti CORE 4.18 LB/FT³ 3/8-IN. CELL SIZE 3.578</p>	0.563	0.734	<p>0.016 H/M GRAPHITE EPOXY 3.2 LB/FT³ FIBERGLASS CORE 3/8-IN. CELL SIZE 3.578</p>	0.734
1.186	<p>Ti - 0.025 IN. Ti - 0.012 IN. 3.578</p>	1.186			

*THERMAL OPTIMUM $\bar{t} = 0.06$ IN., OR 0.57 LB/FT² BASED ON 0.10-IN. BOND THICKNESS

D04992 (1)

Fig. 4.1-1

configuration structural efficiency. Whereas Fig. 3.1-1 assumes the same maximum compressive stress in the two materials being compared, this situation does not develop in the comparison presented here. Thus, Fig. 3.1-1 tends to yield conservative weight ratios when the abscissa is entered with the maximum compressive stress of the beryllium. In a similar manner, the configurations comparison shown in Fig. 3.2-1 is also seen to yield reasonably accurate, qualitative projections for a given material.

In summary, this comparison shows that zee-stiffened beryllium construction is the optimum configuration for the substrate of prototype panel No. 1. This configuration, therefore, has been selected as a basis for subsequent steps in the design/analysis process. Other beryllium configurations are competitive; however, these competitors are more difficult to manufacture in addition to being heavier. The present comparison is probably somewhat a function of the loads, constraints, and panel span specified here. Interchanges in the position of various material/configuration combinations may occur for other loads and constraints, but no significant changes are anticipated in the range of orbiter airloads currently cited.

The effect of panel span upon weight may be studied through charts of the type shown in Figs. 4.1-2 and 4.1-3. These charts show total system weight as a function of the sum of the weights of the individual parts. Here the aluminum primary structure has been sized using optimum wide column analysis to carry the in-plane loads in Area 2 as listed in Table 6.1-13. Note the effect of the tension load requirement in overriding the compression load requirement in Fig. 4.1-2. Fuselage frame weights have been calculated⁽⁴⁻¹⁾ for inertia requirements together with web and flange stability criteria for establishing area. These data do not consider curvature effects; in addition, they are dependent upon intermediate support points which for example might be provided by keels, longerons, floors, spars, or struts. In the figures, the assumed support point spacing of 50 in. has been arbitrarily selected to result in a reasonable frame weight while maintaining an acceptably large support point spacing.

Since the above curves show a strong influence of the high design loads (specified for this study) on structural design and weight, additional design trades for the current 040A-L2 delta wing orbiter are shown in Figs. 4.1-4 through 4.1-6.

⁽⁴⁻¹⁾ Emero, D.H. and Spunt, L., "Wing Box Optimization Under Combined Shear and Bending," Journal of Aircraft, March-April 1966, p. 130-141

FRAME SPACING VS TPS/STRUCTURE WEIGHT SUBPANEL CONCEPT - AREA 2 FLIGHT DESIGN

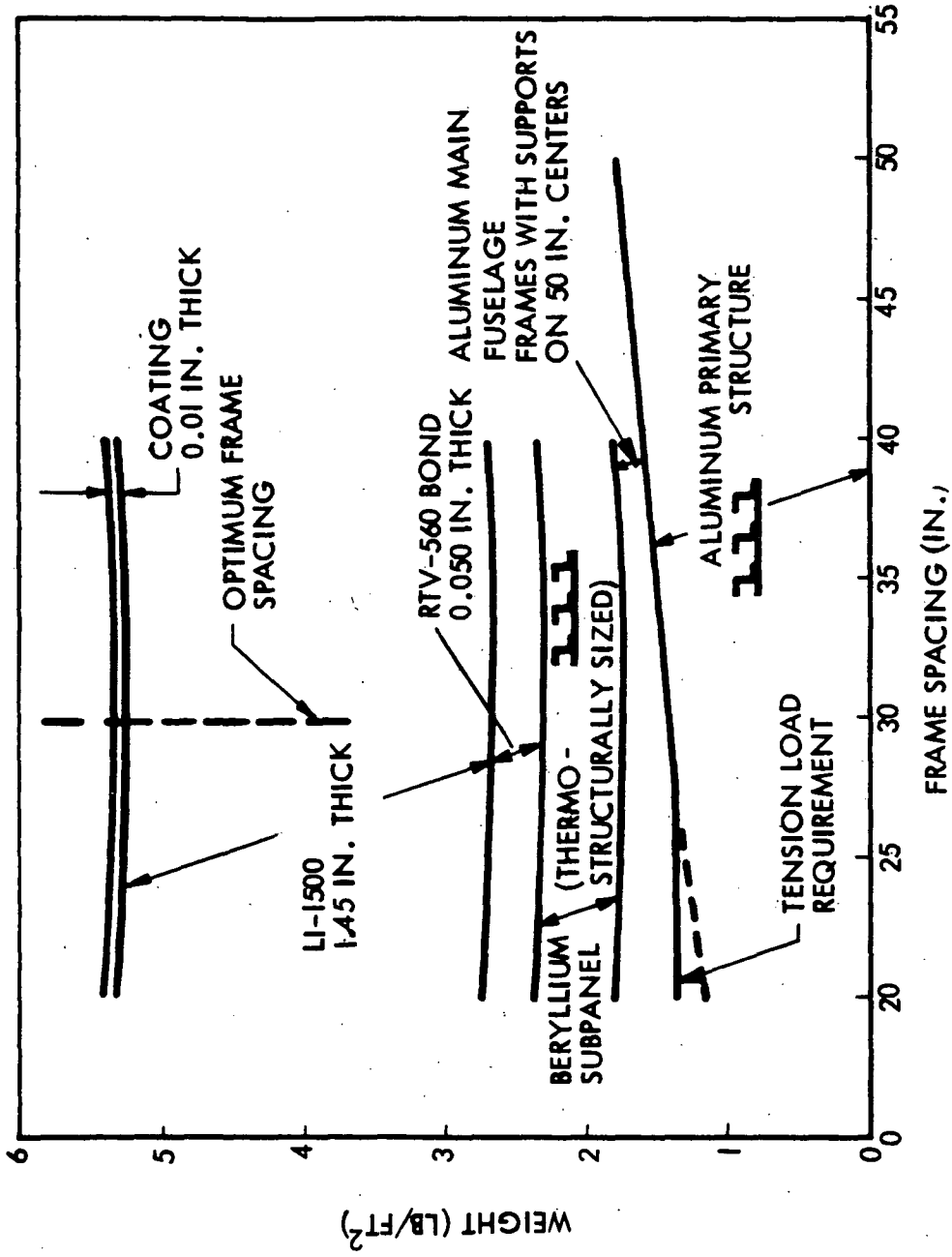


Fig. 4.1-2





FRAME SPACING VS TPS/STRUCTURE WEIGHT SUBPANEL CONCEPT - AREA 2 FLIGHT DESIGN WITH CORRUGATED PRIMARY STRUCTURE

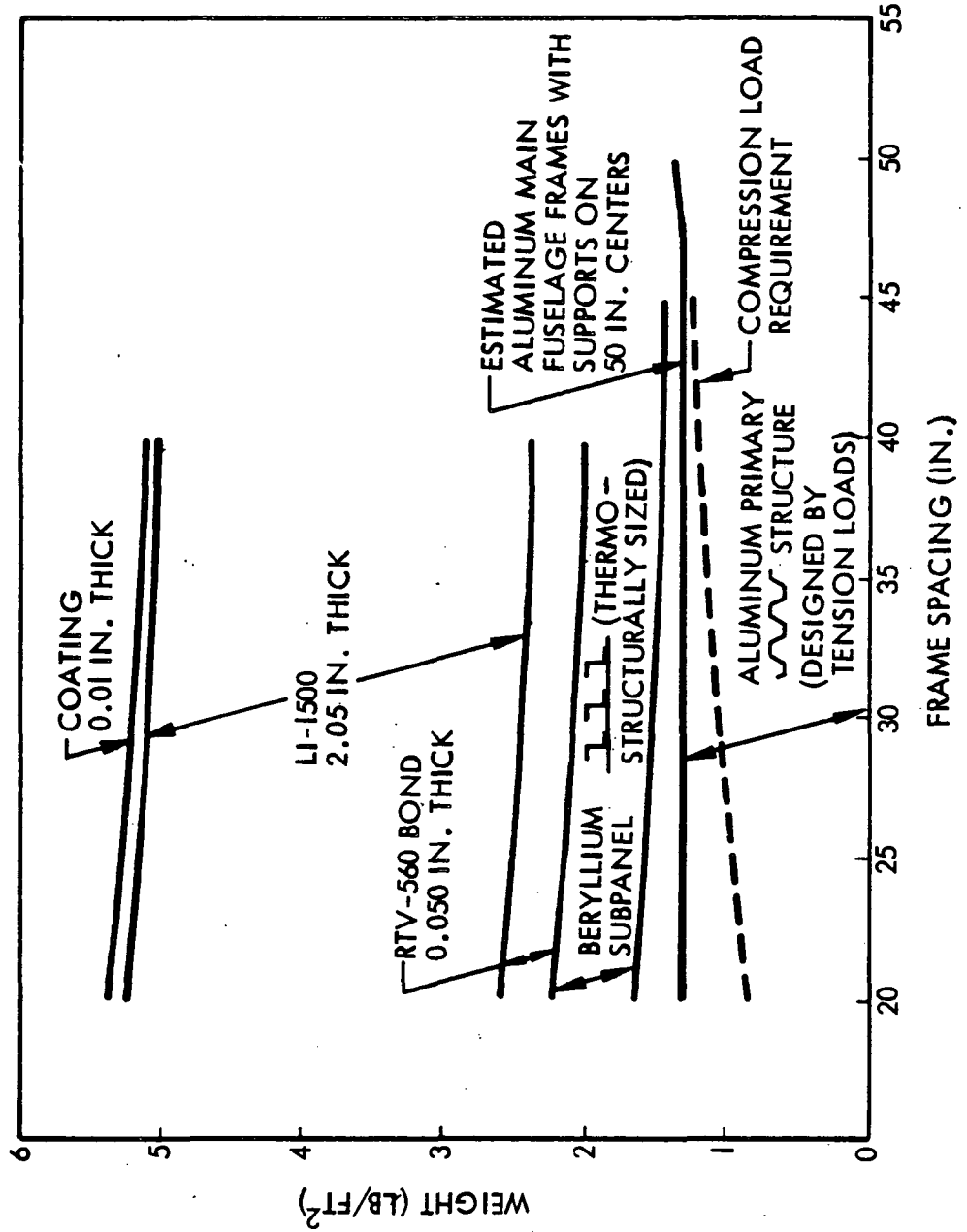


Fig. 4.1-3



FRAME SPACING VS TPS/STRUCTURE WEIGHT
SUBPANEL CONCEPT USING O40-A ORBITER DESIGN LOADS

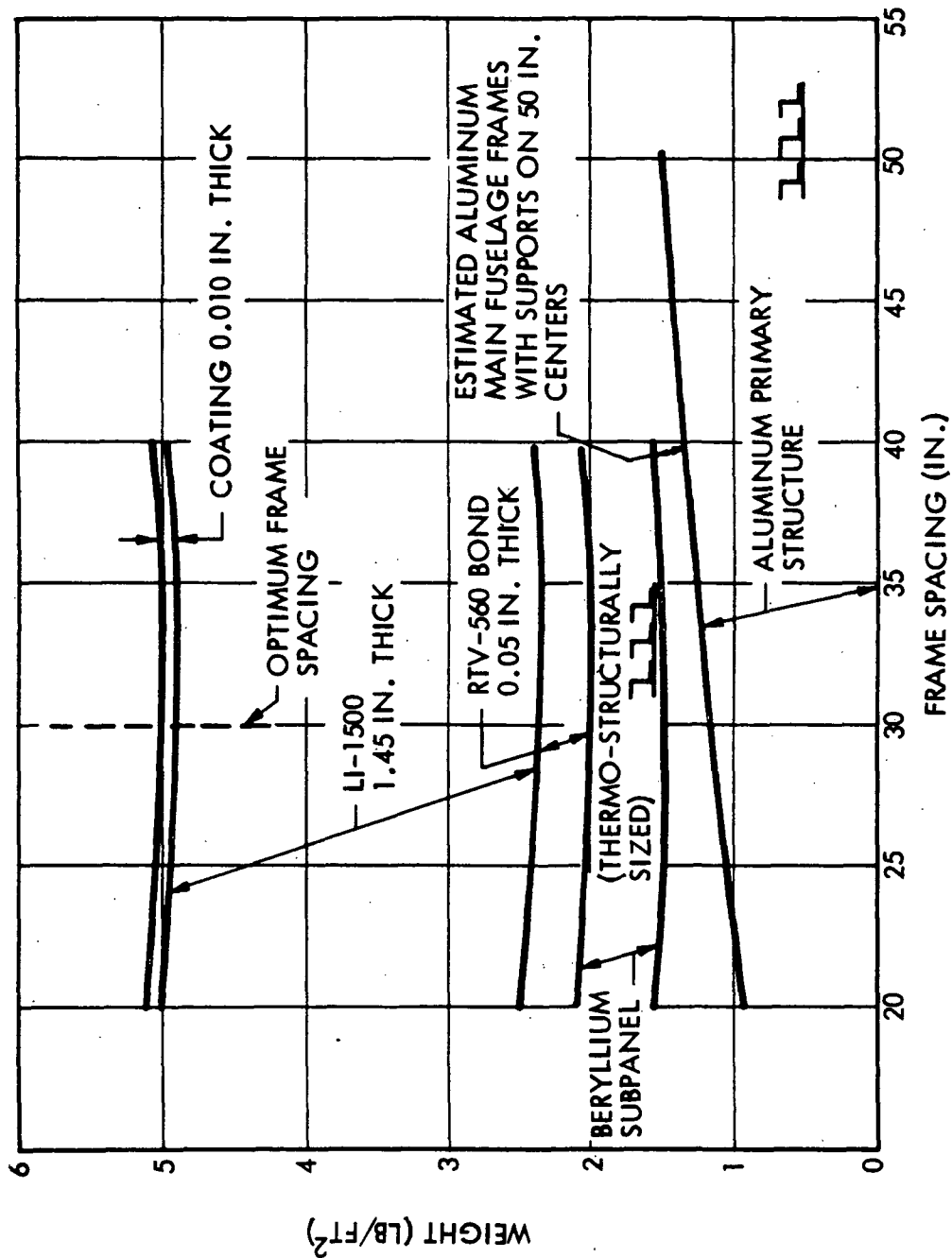
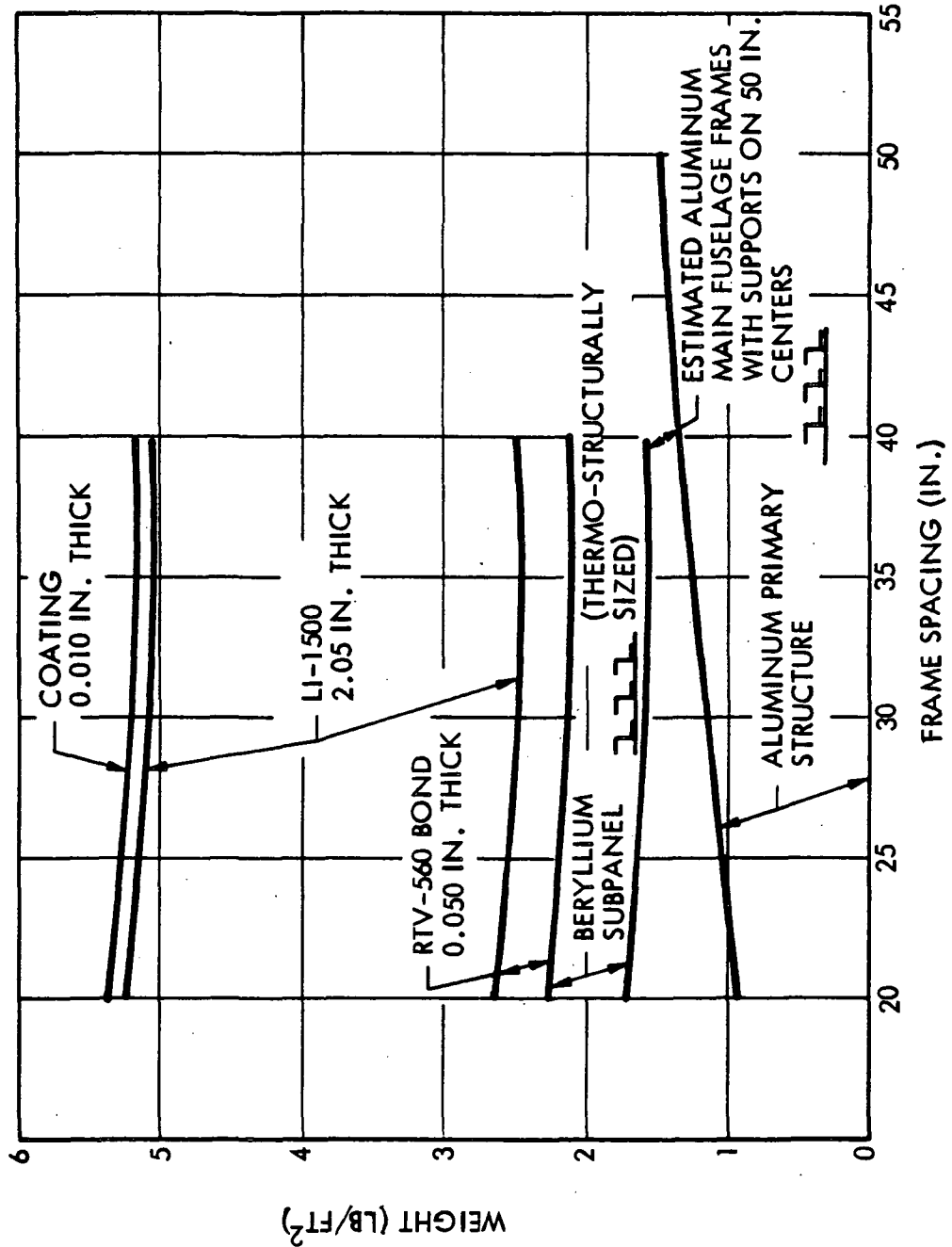


Fig. 4.1-4

FRAME SPACING VS. TPS/STRUCTURE WEIGHT
SUBPANEL CONCEPT USING O40-A ORBITER DESIGN LOADS





FRAME SPACING VS TPS/STRUCTURE WEIGHT
SUBPANEL CONCEPT USING O40-A ORBITER DESIGN LOADS

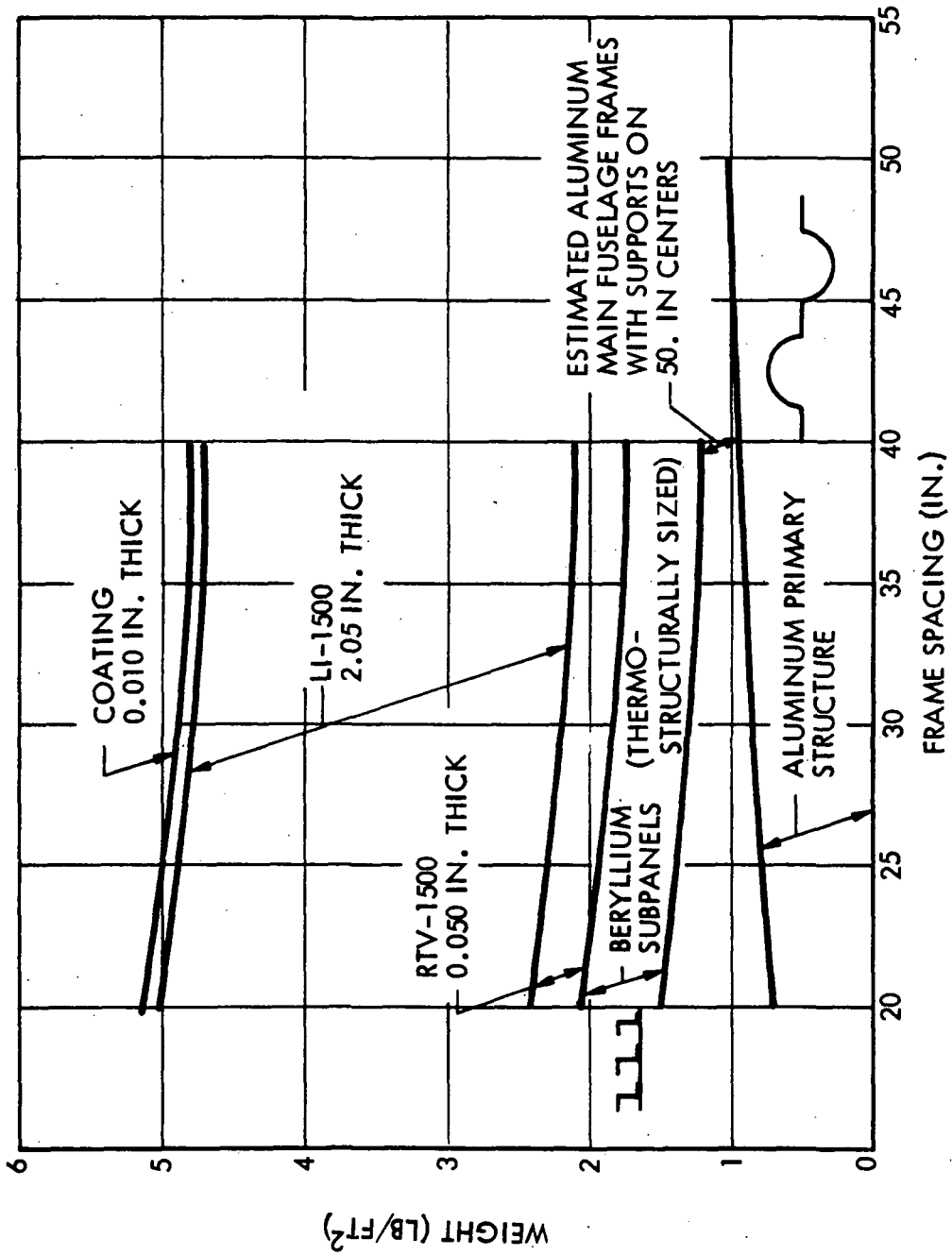


Fig. 4.1-6

The beryllium subpanel weight shown in the figures is constant over the span of frame spacings of interest because it is a thermo-structurally optimized weight. As noted previously and discussed later in this section, lower total system weights are obtained when beryllium in excess of that required for structural purposes is added to the system, used as a heat sink, and traded off against LI-1500 weight. Structural requirements do not exceed the thermo-structural optimization requirement until frame spacings greater than 40 in. are studied.

The LI-1500 thickness shown in Fig. 4.1-2 has been sized to limit the in-flight temperature of the aluminum primary structure to 300°F. The beryllium subpanel, while capable of temperatures to 600°F, does not reach this temperature because of internal radiation between the beryllium subpanel and the aluminum primary structure which causes the aluminum to reach 300°F before the beryllium reaches 600°F.

Figure 4.1-2 shows that the optimum frame spacing is about 30 inches. The total weight curve, however, is rather flat with respect to frame spacing in the range of values shown. Therefore, it is concluded that a span of approximately 25 in. for prototype panel No. 1 is representative of optimum frame spacing under the present design conditions.

In comparing Figs. 4.1-2 and 4.1-3, it is apparent that for the present design conditions, the use of more efficient primary structure configurations does not produce a more efficient design because of the in-plane tension loads. The influence of these loads tilts the total weight curve so that the optimum frame spacing is in excess of 40 inches. Again, however, the total weight curve is rather flat with respect to frame spacing. These charts demonstrate that optimum frame spacing is highly dependent upon the vehicle loads and the character of the parts which compose the system. Note also that the weight of the LI-1500 material is roughly equivalent to the weight of the remaining parts. Thus, efforts to minimize structural weight must be dramatically effective if substantial overall weight reductions are to be obtained.

4.2 SELECTION OF OPTIMUM PRIMARY STRUCTURE CONFIGURATION

Using the analytical techniques described in Section 2, several candidate primary structure configurations were optimized as beam columns. The design loads for vehicle area 2 were used in this study; all configurations were assumed to be fabricated from 7075-T6 aluminum inasmuch as material selection was not an open parameter. Also, a design temperature of 250^oF was used, since this is the maximum temperature that the panels are subjected to in flight (the structure actually reaches a peak temperature of 300^oF about 30 minutes after landing). See Appendix A for the detailed analysis of each configuration.

The results, presented in Fig. 4.2-1, show the zee-stiffened configuration to be the lightest configuration. Again, the relative standing of the four configurations is reasonably well predicted by Fig. 3.2-1. Of interest in Fig. 4.2-1 are the maximum compressive stresses in the various configurations. The trapezoidal corrugation-stiffened configuration maximum stress is apparently the result of the relatively shallow section in bending. Such a section is necessitated by b/t limitations on the greater number of thinner elements making up the section. The high maximum stress in the honeycomb-sandwich configuration is, of course, somewhat misleading, because the core does not sustain any direct load, although it comprises one-third of the weight of the configuration.

The conclusions to be drawn from Fig. 4.2-1 apply specifically to prototype panel No. 2, but they may be applied also to prototype panel Nos. 3 and 4 as well. The stresses may be seen to be essentially elastic; therefore, the same ordering of the configurations may be anticipated for titanium optimum designs for prototype panel No. 4. Prototype panel No. 3, however, must be designed for the considerably higher in-plane compressive line loads in vehicle area 1. As shown in Fig. 3.2-1, these loads result in highly plastic stresses in optimum designs, with the result that weight becomes a function of total available load-carrying material without particular regard to its geometric distribution. In this situation, the honeycomb-sandwich configuration does not improve in standing because of the nonload-carrying status of the core. However, the remaining configurations tend to have equal weights. For reasons of material procurement and simplicity of manufacture, therefore, the zee-stiffened configuration is again selected.



COMPARISON OF CONFIGURATIONS FOR DIRECT-TO-PRIMARY STRUCTURE LI-1500 APPLICATIONS

- RESULTS BASED ON BEAM-COLUMN ANALYSIS (ALL DESIGNS STABLE)
 - ALL DESIGNS USE 7075-T6 ALUMINUM AT 250°F
 - DESIGNS BASED ON AREA 2 VEHICLE LOADS; CRITICAL ULTIMATE LOAD
- FOR MAXIMUM DEFLECTION IN ALL DESIGNS ARE: $N_{X_COMP} = 2250 \text{ PPI}$, $P_{COLLAPSE} = 6 \text{ PSI}$

CONFIGURATION	WT/FT ² (LB)	MAXIMUM DEFLECTION (IN.)		MAX OUTER FIBER STRESS (PSI)
		LINEAR THEORY	BEAM COLUMN	
	1.99	0.093	0.180	38,624*
	1.78	0.120	0.306	43,580*
	2.12	0.104	0.222	44,746*
	1.65	0.089	0.163	39,449*

DO5045

Fig. 4.2-1

* OCCURS UNDER MAXIMUM LINE LOAD CONDITION

Observe that the configurations considered in this comparison have been limited to those with one or more flat surfaces on the premise that such a surface is required for the attachment of LI-1500. This decision may involve an arbitrary weight penalty to the system in those designs that are not critical for in-plane tension loads (see Fig. 3.2-1). In prototype panel Nos. 2-4, the relative magnitudes of the in-plane tension and compression loads result in little or no weight penalty, but there may be other vehicle areas where this situation is not the case. Also, note should be made of the maximum deflections associated with the various configurations in Fig. 4.2-1. Shown are values up to 0.31 in. which appear high for compatibility with LI-1500 tiles. While these values are based on simply-supported edge conditions, and thus may be unrealistically high, it is apparent that some limiting deflection should be considered in primary structure panels with direct-bonded LI-1500 tiles. The zee-stiffened configuration in Fig. 4.2-1, notably, has the lowest maximum deflection of the configurations studied.

Charts of the type of Figs. 4.1-2 and 4.1-3 may be prepared to illustrate the effect of frame spacing upon total system weight when LI-1500 is attached directly to primary structure. An example chart is shown in Fig. 4.2-2. This chart represents a vehicle area 2 design, using aluminum primary structure and frames. The frames have been sized and supported in the same way as described in the previous section. Note that the optimum frame spacing in this case is approximately 25 in. which agrees favorably with the span specified for the prototype panels. The total weight curve is again rather flat, indicating some variation in the frame spacing will not affect system weight significantly.

The LI-1500 thickness shown in Fig. 4.2-2 has been sized to maintain the aluminum primary structure at temperatures of 300⁰F or less. As a result, the weight of the LI-1500 is somewhat in excess of the weight of the rest of the system. Observe that the total system weight in Fig. 4.2-2 is greater than that in comparable designs utilizing subpanels as shown previously in Figs. 4.1-2 and 4.1-3. The difference is due principally to the heat sink capacity of the beryllium subpanel which allows a significant reduction in the LI-1500 thickness (and hence, weight). The combined primary structure/frame/subpanel weight in Figs. 4.1-2 and 4.1-3 is essentially the same as the primary structure/frame weight in Fig. 4.2-2.

4.2-3

219<

Of further interest in Fig. 4.2-2 is the trend in frame weight with frame spacing. The downward trend with increased spacing is due to the fact that the frames are fewer in number and their weight is being distributed over greater surface areas. However, the trend also is influenced by the fact that the frame stiffness requirement is inversely proportional to panel length; i. e., increasing panel stiffness with increasing panel length tends to reduce frame stiffness requirements.



FRAME SPACING VS TPS/STRUCTURE WEIGHT DIRECT-TO-PRIMARY STRUCTURE ATTACH CONCEPT - AREA 2 FLIGHT DESIGN

LMSC-D152738
Vol II

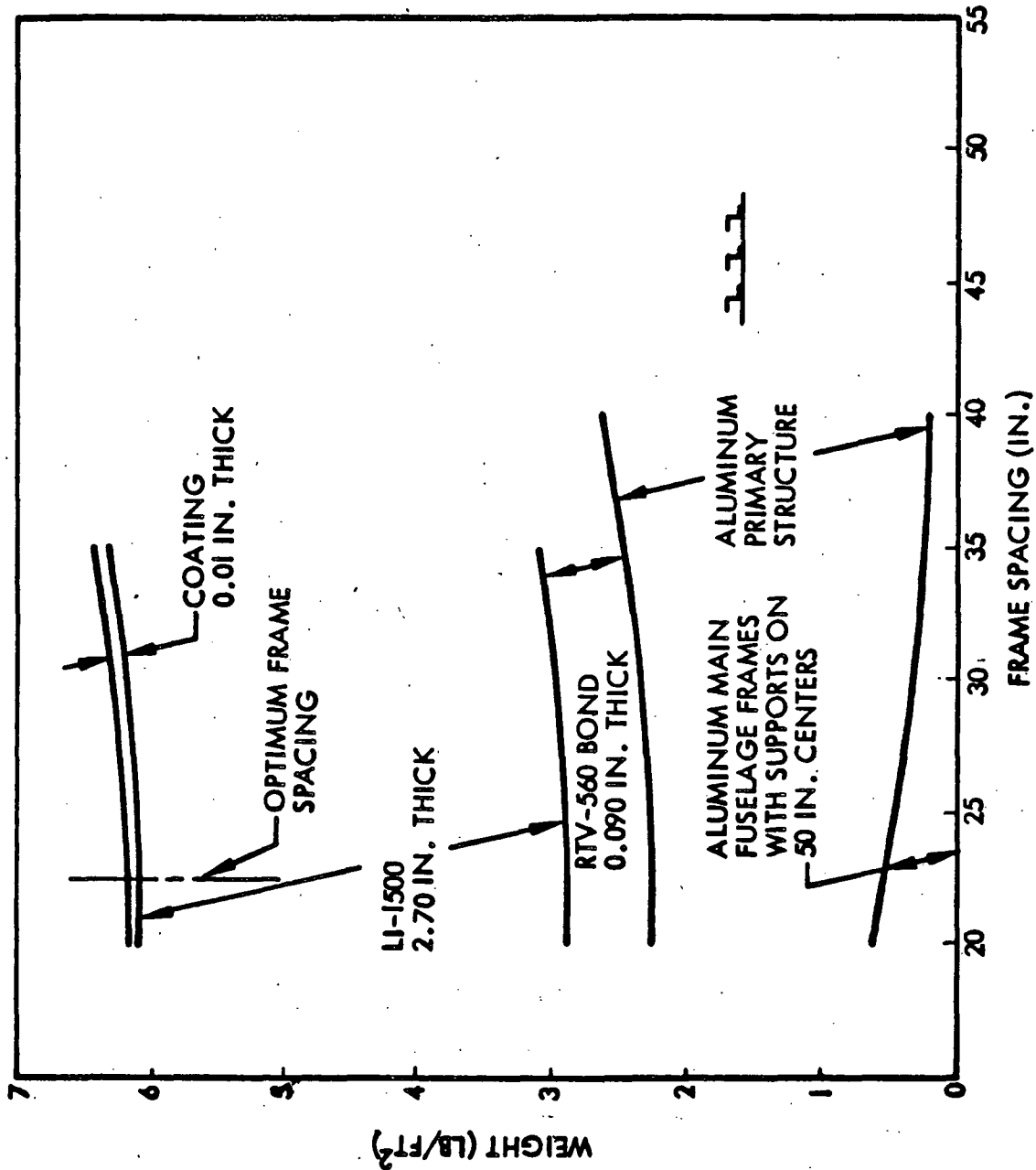


Fig. 4.2-2

4.3 THERMAL/STRUCTURAL OPTIMIZATION OF 1 ATMOSPHERE TEST PANELS

To accomplish the basic insulation sizing for prototype test panels, the thermal properties of LI-1500 at 1 ATM pressure given in Section 6.2 are used. The thermal properties of the panel materials are listed in Table 6.2-2, while the effective substrate thicknesses for the panels are given below.

<u>Panel No.</u>	<u>Material</u>	<u>Area</u>	<u>Max. Surface Temp (°F)</u>	<u>Max. Substrate Temp (°F)</u>	<u>Effective Substrate* Thickness (in.)</u>
1	beryllium	2	2300	600	0.064
2	aluminum	2	2300	300	0.114
3	aluminum	1	1480	300	0.143
4	titanium	2	2300	600	0.090

Typical parametric sizing data for the beryllium panel for a constant adhesive thickness are shown in Fig. 4.3-1. These data indicate the effect of beryllium substrate thickness on the required insulation thickness. Parametric data for the titanium test panel are shown in Fig. 4.3-2.

Data from Fig. 4.3-1 are used as the basis for TPS optimization for the beryllium panel shown in Fig. 4.3-3. The total unit weight, consisting of beryllium, LI-1500, and adhesive, is plotted against the beryllium effective thickness for a maximum beryllium temperature of 600°F. The unit weight of the surface coating and flexible filler strip (approximately 0.02 lb/ft²) is not included in the total unit weight (see Fig. 3.2-51).

While the strength requirement dictates a beryllium thickness of 0.040 in., the minimum weight system occurs at a thickness of about 0.090 in. Although the total unit weight curve is flat, the data indicate that a lower weight system can be achieved at beryllium effective thicknesses up to 0.16 in. Hence, for beryllium, a stronger and lighter TPS is attainable at larger effective thicknesses.

*The effective substrate thicknesses were increased slightly over the values shown here prior to fabrication; however, initial thermal/structural sizing was carried out using the values as shown. See Table 6.5-9 for final panel sizes.

TYPICAL PARAMETRIC SIZING DATA BERYLLIUM FLIGHT PANEL NO. 1

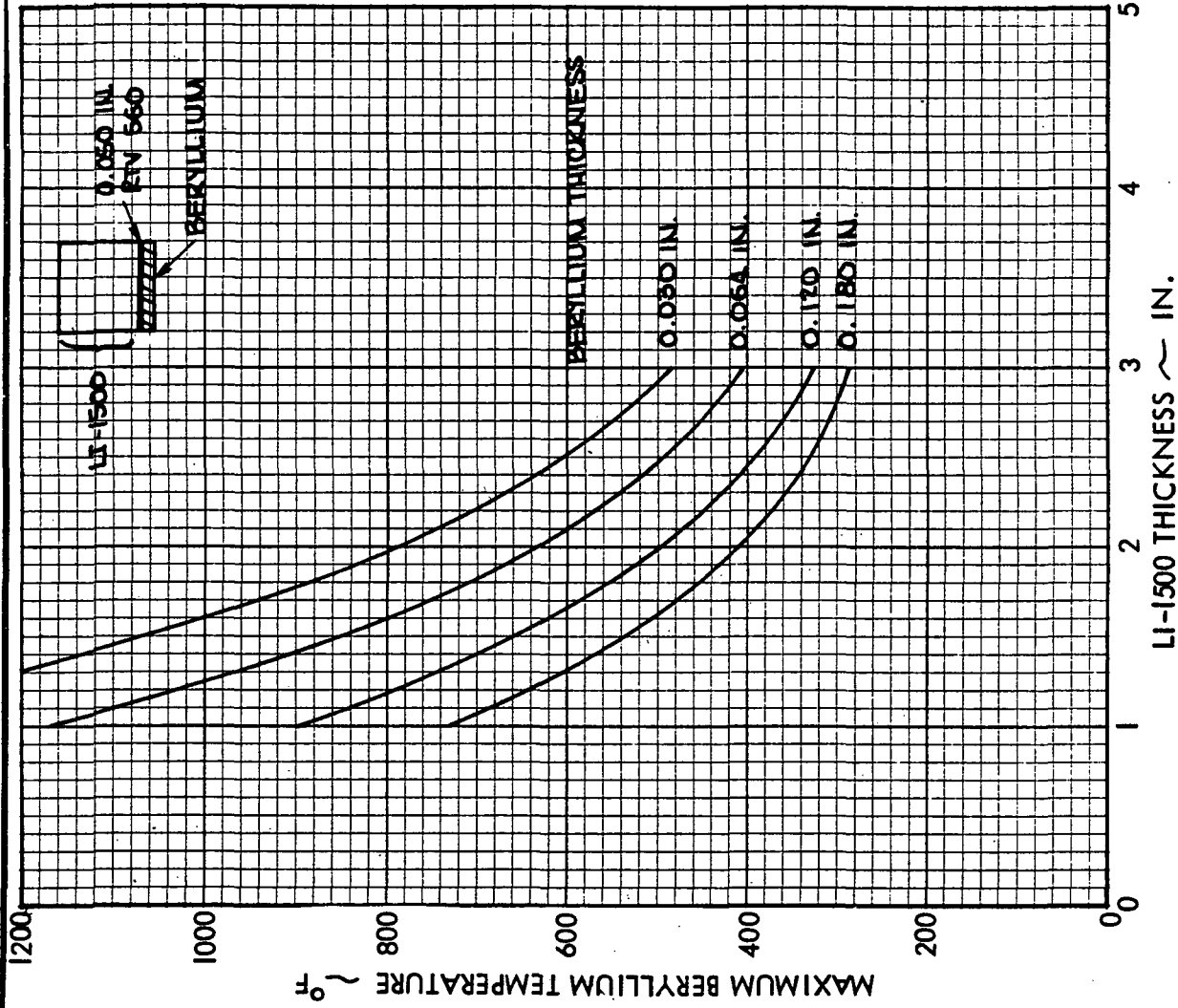


Fig. 4.3-1

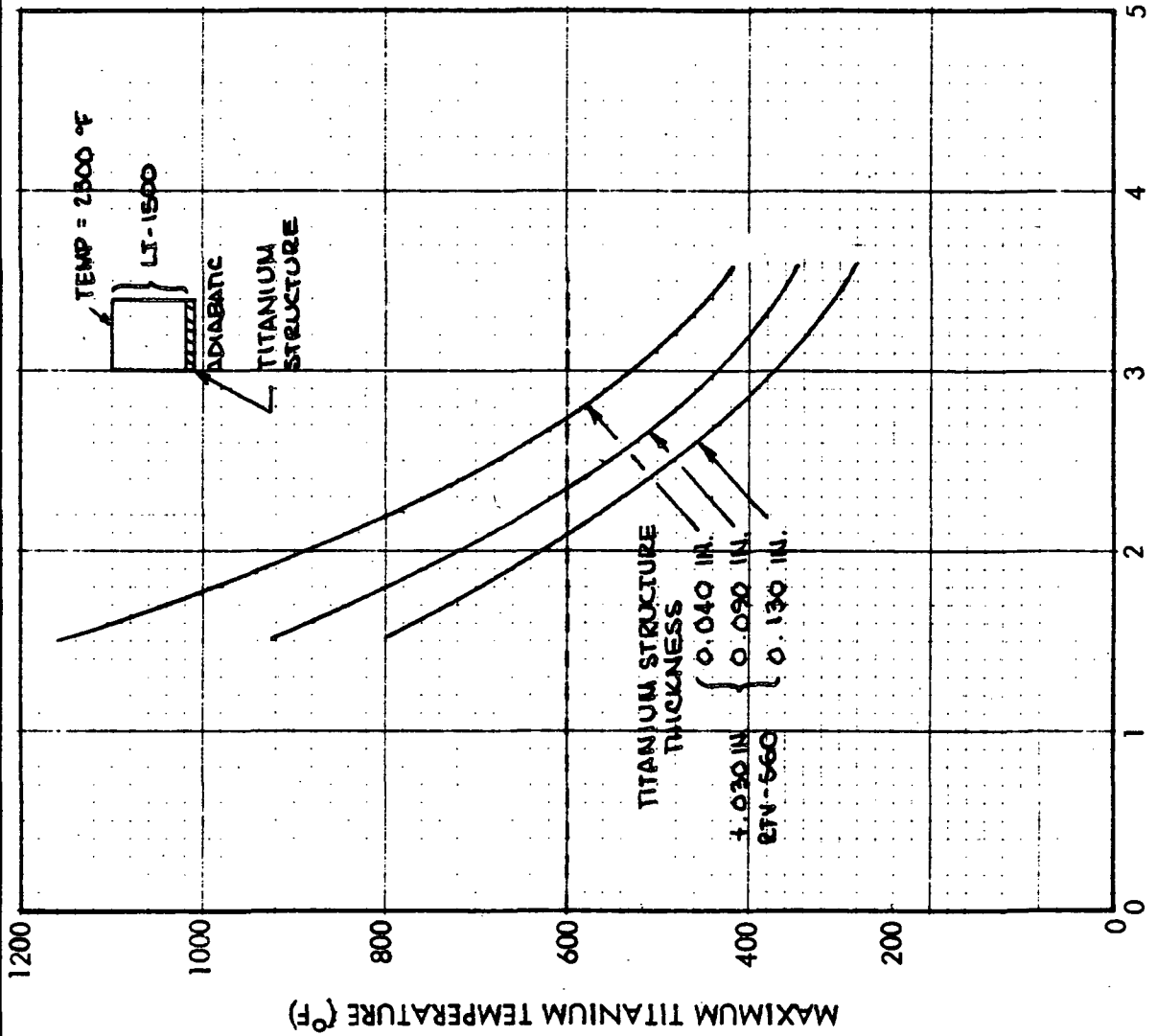


4.3-2

223<

DO6067

TYPICAL LI-1500 PARAMETRIC SIZING DATA
TITANIUM TEST PANEL NO. 4



LI-1500 r (IN.)

Fig. 4.3-2





TPS THERMAL-STRUCTURAL OPTIMIZATION FOR TEST PANEL NO. 1

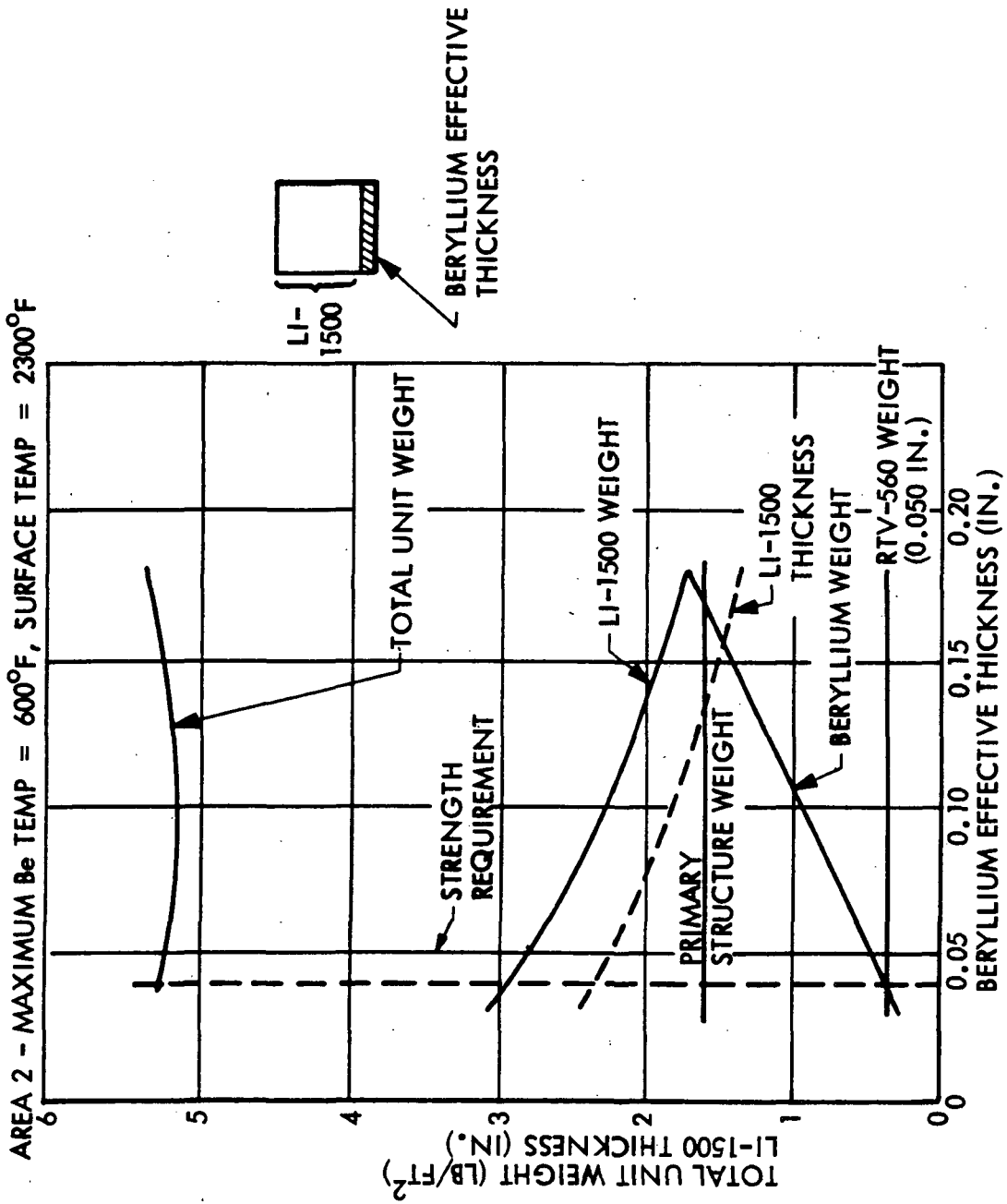


Fig. 4.3-3

D06089

Figure 4.3-4 shows the effect of beryllium effective thickness on the total unit weight for various RTV-560 adhesive thicknesses. Although a highly expanded ordinate is used for total TPS weight, a larger adhesive thickness tends to shift the minimum weight to smaller beryllium effective thicknesses. As adhesive thickness was increased from 0.050 in. to 0.100 in., the minimum weight point shifted from 0.090 in. beryllium to 0.060 in. beryllium. Also, there is an accompanying slight increase in the total unit weight from 3.58 to 3.75 lb/ft², or a 0.17 lb/ft² increment upon changing from 0.050 in. to 0.100 in. of RTV-560 adhesive.

Figure 4.3-5 shows a thermal-structural optimization for the aluminum test panel No. 2 at a maximum temperature of 300^oF. Unlike the beryllium panel, the strength requirement also results in the minimum weight system.

Figure 4.3-6 shows a thermal/structural optimization for Area 1, aluminum test panel No. 3 at a maximum temperature of 300^oF. Again, the strength requirement corresponds to the minimum weight system.

Figure 4.3-7 shows a thermal/structural optimization for the titanium test panel No. 4 at 600^oF. As in the case of the aluminum panels, the strength requirement for the titanium panel corresponds to the minimum weight system.

Hence, because of the high capacity of beryllium, it is the only panel that allows a larger panel thickness than required by strength considerations, while decreasing the total TPS unit weight.



EFFECT OF BERYLLIUM THICKNESS ON TPS THERMAL-STRUCTURAL OPTIMIZATION

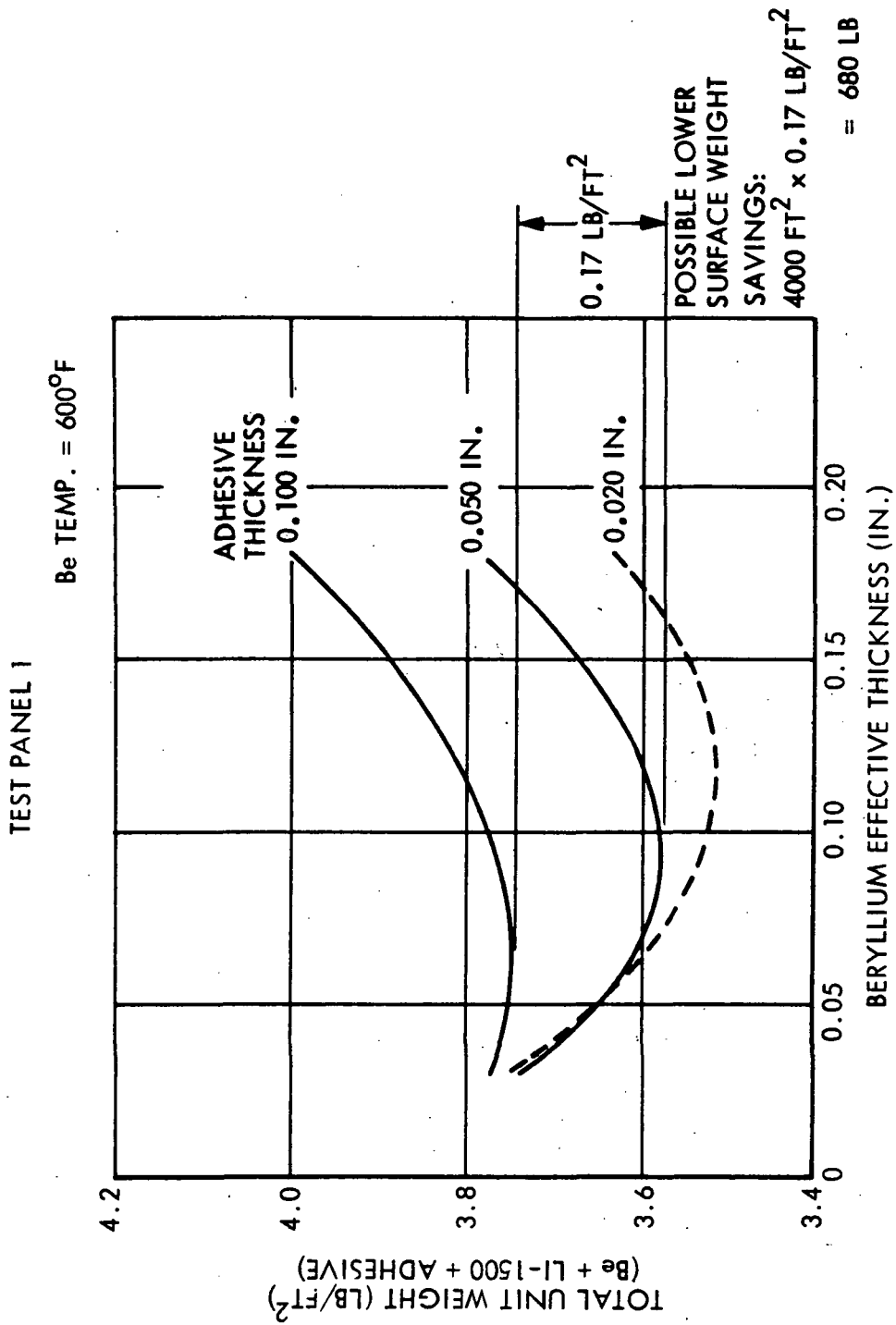


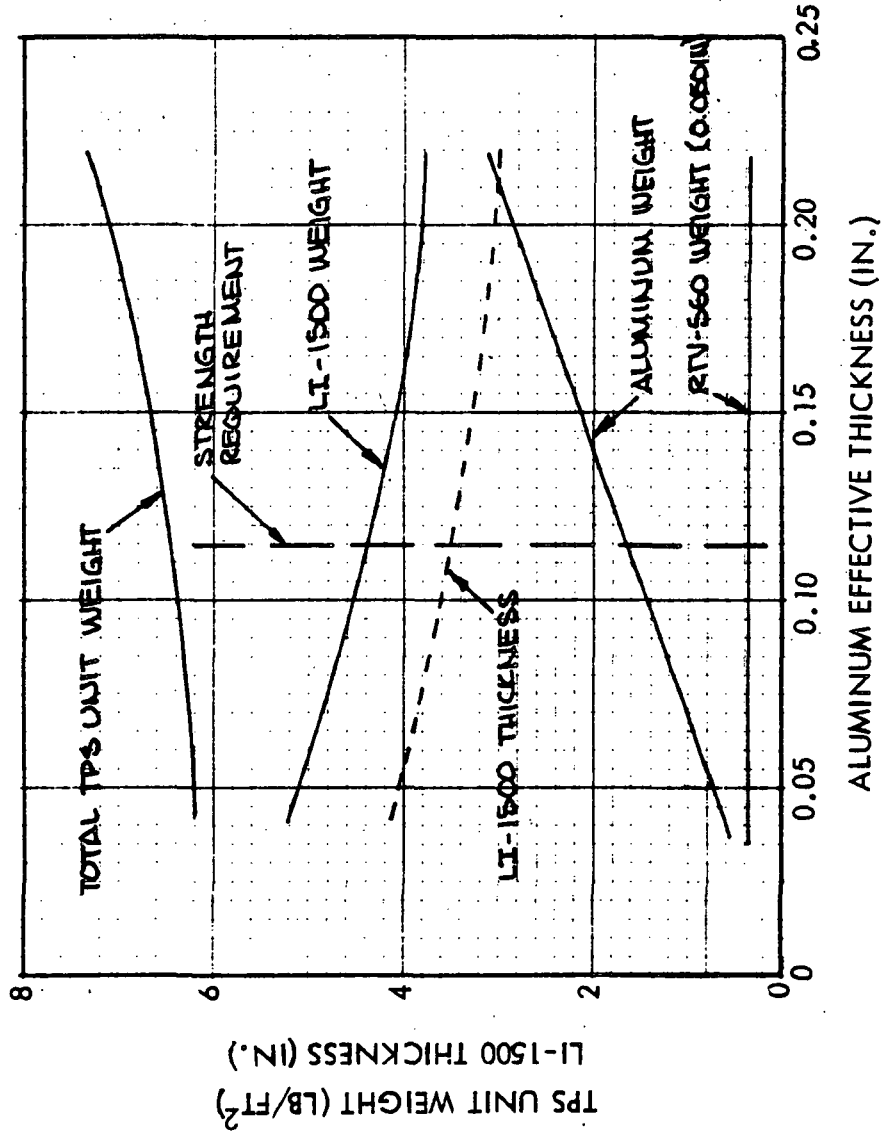
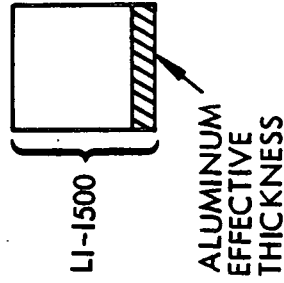
Fig. 4.3-4

DO6006(1)

TPS THERMAL-STRUCTURAL OPTIMIZATION
FOR TEST PANEL NO. 2



AREA 2 MAXIMUM AL. TEMP = 300°F, SURFACE TEMP. = 2300°F



DO6015

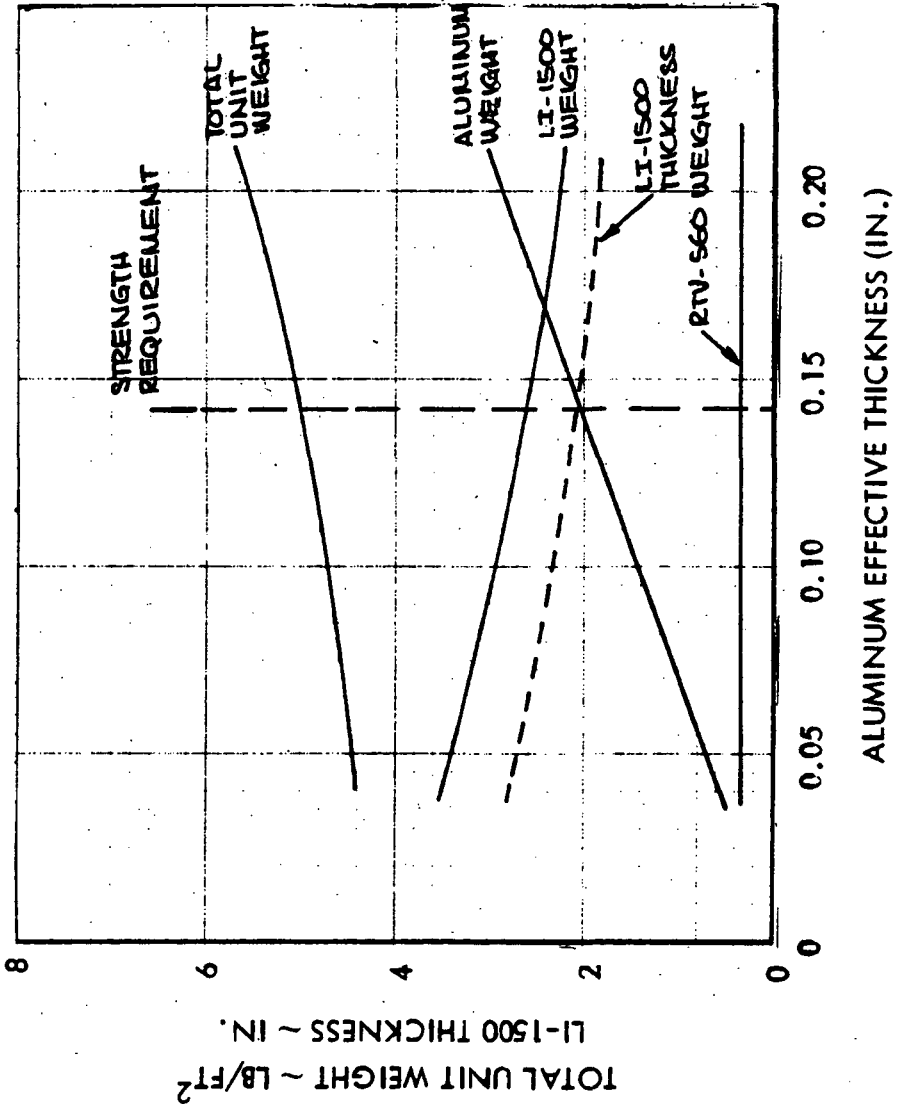
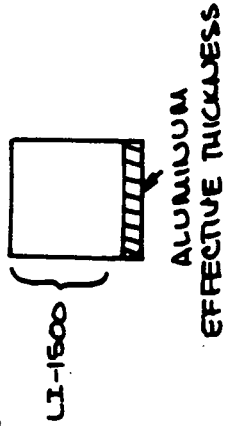
Fig. 4.3-5

C.S.

TPS THERMAL - STRUCTURAL OPTIMIZATION FOR
TEST PANEL NO. 3



AREA 1 - MAXIMUM AI TEMP = 300°F, SURFACE TEMP = 1480°F



TPS THERMAL - STRUCTURAL OPTIMIZATION FOR
TEST PANEL NO. 4



AREA 2 - MAX. Ti TEMP. = 600°F
SURFACE TEMP = 2300°F

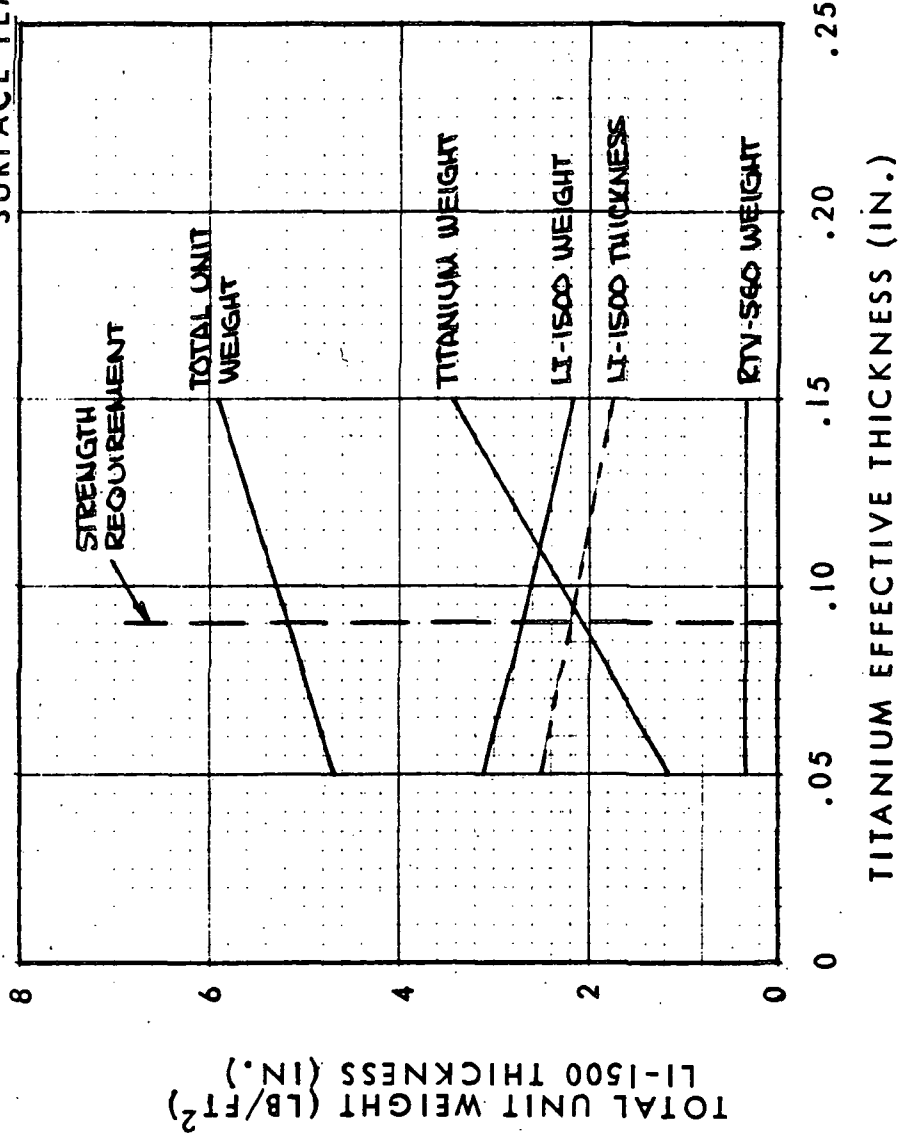
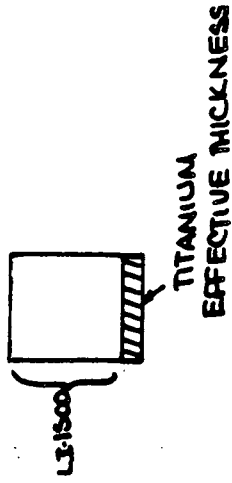


Fig. 4.3-7

4.4 THERMAL/STRUCTURAL OPTIMIZATION FOR FLIGHT PANELS

LI-1500 sizing for flight panels considers the effect of local static pressure on the thermal conductivity of LI-1500. At 2000°F, the vacuum thermal conductivity of LI-1500 is about 45 percent of the 1 ATM value, hence flight panel design assumes that the pressure within the LI-1500 during entry equals the local static pressure at the edge of the boundary layer.

The parametric studies of Fig. 3.1-4 show a comparison of the LI-1500 thickness requirements for a beryllium flight and test panel. These flight panel results were obtained using the temperature and pressure histories for Area 2 (see Section 6) to determine the thermal conductivity of LI-1500. The test panel results utilized the 1-ATM thermal conductivity values.

For a 600°F maximum temperature, the LI-1500 requirements are reduced about 31 percent from 2.1 to 1.45 in. of LI-1500. Similar reductions can be obtained for the other three flight panels.

TPS thermal/structural optimizations are shown for flight panel Nos. 1, 2, 3, and 4 in Figs. 4.4-1 through 4.4-3. As indicated previously for the test panel, the beryllium total unit weight curve is rather flat, and the minimum weight system occurs at a larger beryllium thickness than that dictated by strength requirements. Minimum weight occurs at about 0.090 in. while the strength requirement is at 0.040 in. beryllium (Fig. 4.4-1). For the aluminum and titanium flight panels (Figs. 4.4-2 and 4.4-3), the strength requirement corresponds to the minimum weight system.



TPS THERMAL-STRUCTURAL OPTIMIZATION FOR
FLIGHT PANEL NO. 1

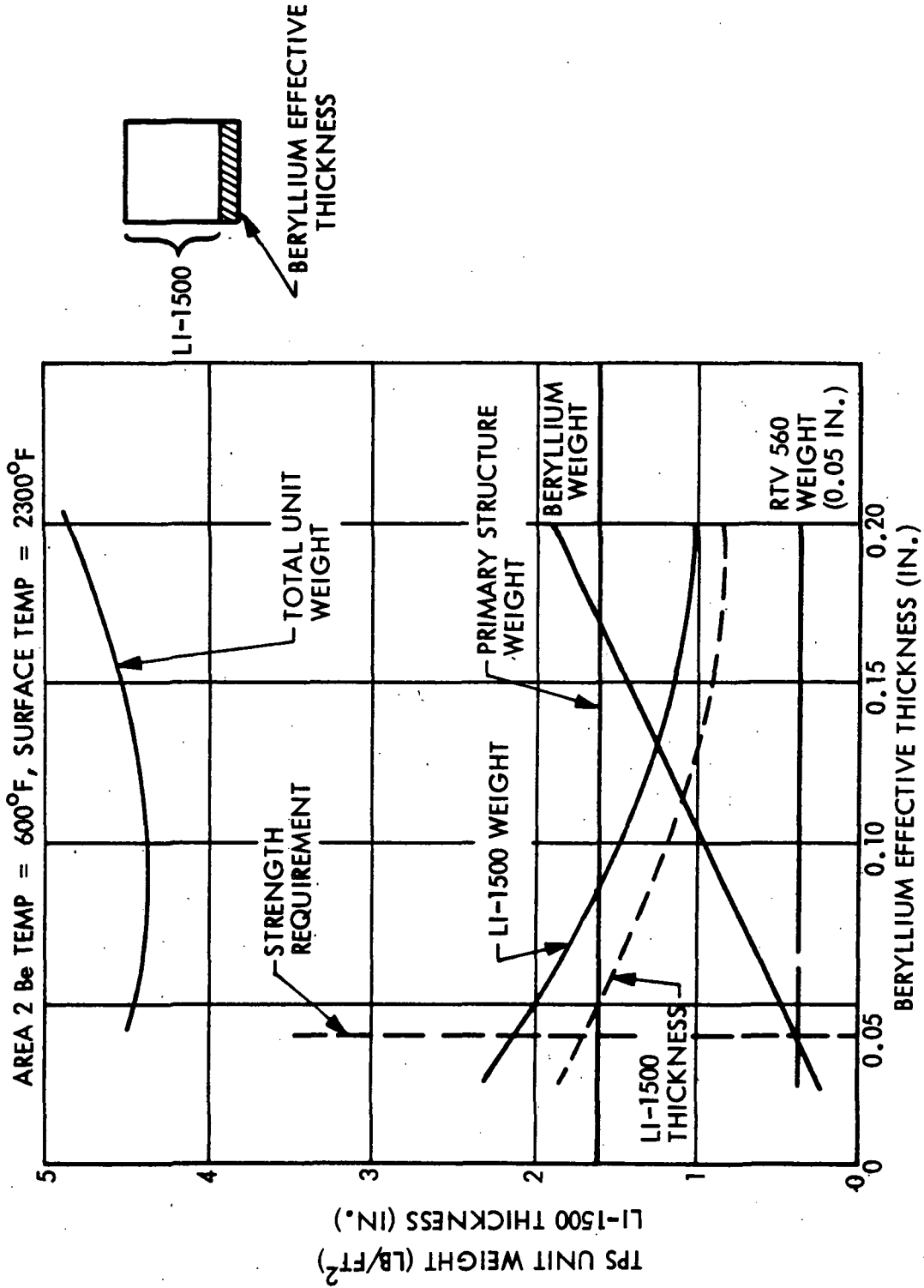
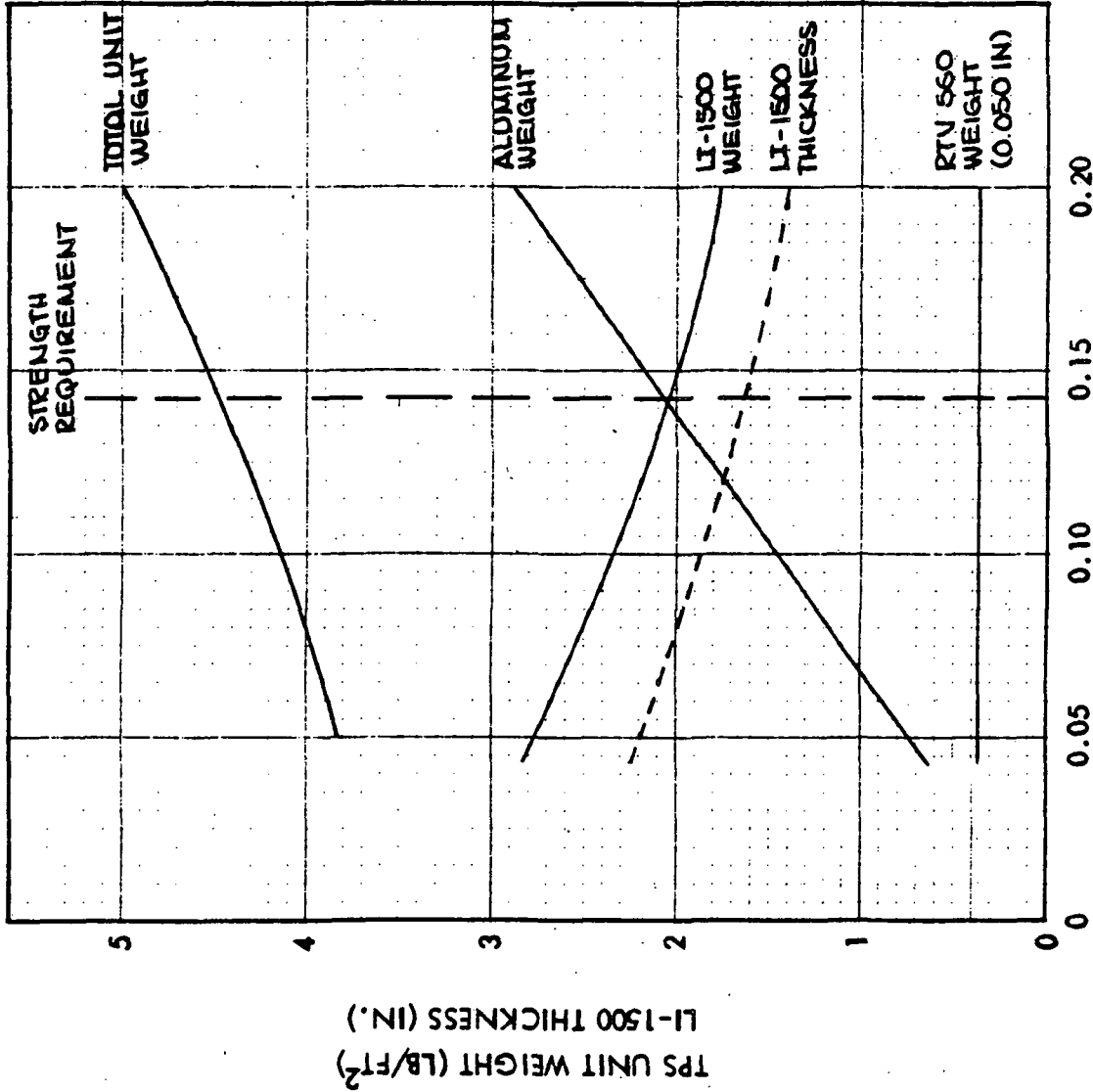


Fig. 4.4-1

TPS THERMAL-STRUCTURAL OPTIMIZATION FOR
FLIGHT PANEL NO. 3



AREA 1 - ALUMINIUM TEMP = 300°F, SURFACE TEMP = 1480°F



ALUMINIUM EFFECTIVE THICKNESS (IN.)

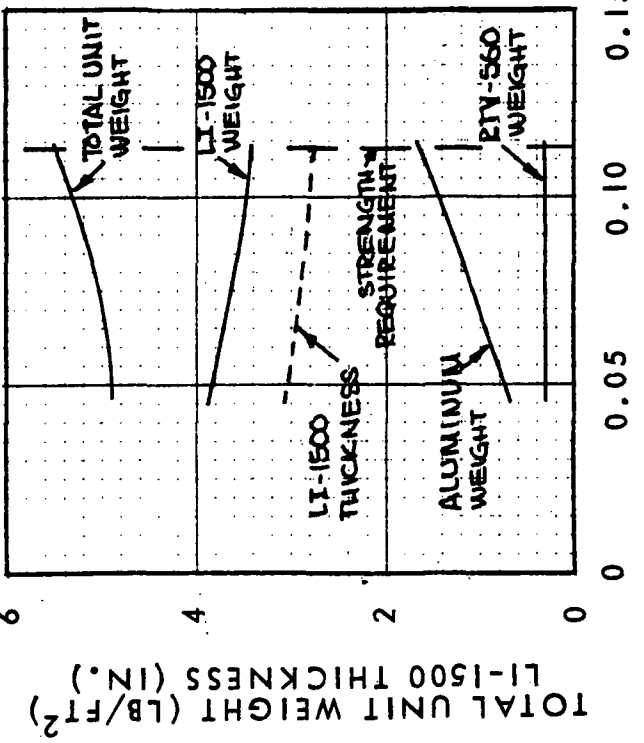
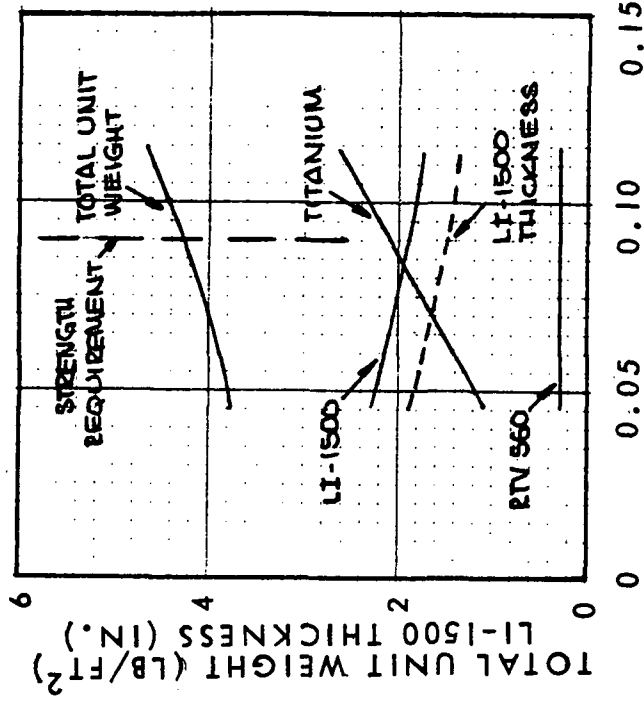
Fig. 4.4-2

TPS THERMAL-STRUCTURAL OPTIMIZATION FOR FLIGHT PANEL 2 AND 4



AREA 2 - MAX Ti TEMP = 600°F

AREA 2 - MAX AL TEMP = 300°F



ALUMINUM EFFECTIVE THICKNESS (IN.) TITANIUM EFFECTIVE THICKNESS (IN.)

DO6007

Fig. 4.4-3

Section 5
ATTACHMENT METHODS

Three attachment methods have been evaluated for the LI-1500 application to the shuttle: direct bonding (with or without a "strain arrestor plate"), mechanical strain-isolation techniques, and partial support of tiles on external vehicle stringers. These methods are discussed in more detail below. One of the best strain-isolation techniques is that used on prototype panel No. 1. The use of the beryllium subpanel isolates the LI-1500 from the high in-plane loadings in the primary structure and results in a lower TPS weight.

5.1 BONDING ATTACHMENT (BASELINE)

Lockheed's baseline attachment method is direct bonding with RTV-560. The bond agent acts as a strain-isolation layer between the tile and substrate. Trade studies on the prototype panel designs (typical of the orbiter lower surface) have shown that as bond thickness increases, only a small portion of its weight is additive to the TPS weights due to the heat sink effect (bond thickness has significant effect on upper surface TPS weights however). Bonded LI-1500 material has been tested both by LMSC and NASA, resulting in confidence in this proven system.

LMSC has considered a number of commercially available adhesives for attaching LI-1500 to substrate materials. The systems considered are shown in Table 5.1-1. RTV-560 has been selected as the baseline adhesive because of its unique characteristics, as follows:

- Relatively low stiffness with high strength
- Temperature range, -150° to 600°F
- Excellent adhesion to LI-1500 and metals
- Thermal stability and oxidation resistance.

BOND SYSTEMS EVALUATED

System	Evaluation
HT-424	Not room curable; high stiffness
DC 96-052	Poor cure under tiles; inconsistent
RTV-30	Low temperature limited (-90°F)
RTV-511	Limited to 500°F
RTV-560 (Sheet)	Lower shear strength than liquid; same stiffness and weight
RTV-560 (Liquid)	Selected as baseline

Foam bonds, which offer even greater strain isolation than the RTV-560, look very promising and are currently under evaluation. If a foam bond is selected to replace the RTV-560, the bond line thickness can be reduced below the present 0.090 in (thereby saving some weight on the upper surface of the orbiter) without increasing the LI-1500 stresses.

A unique way of improving strain isolation of the LI-1500 tile from the thermal and mechanical expansion of the metallic substrate is the "strain arrestor plate" concept, to be used on conjunction with RTV-560 bonding. In this scheme, a thin sheet of

high-modulus/high-strength material is attached to the lower surface of the tile with a thin layer of bond. (Hard, temperature-resistant epoxy bonds such as HT-424 or equivalent can be used.) This "arrestor plate" further must have thermal expansion characteristics similar to LI-1500 so that a minimum of thermal stress can arise due to differential expansion. With this hard undersurface, the tile is bonded with RTV-560 to the panel as in the baseline configuration; as an added feature, the tile handling characteristics prior to installation are improved. The arrestor plate experiences very small strains because of its high modulus, hence strain (and stress) levels in the LI-1500 are much smaller than in the baseline case.

Two materials show promise for this application, Invar sheet and a multi-ply graphite-epoxy composite laminate. At this time, only numerical evaluation is available. Stress comparisons with and without the arrestor plate are presented in Section 3.2, showing a large reduction in LI-1500 stress levels.

Thermal evaluation of this concept indicates that heat sink effects of this additional layer can be utilized and that an overall TPS weight increase of around 2 percent would be expected for the aluminum primary panels and about an 8 percent increase for titanium. However, no weight increase would occur for the beryllium subpanel. These conclusions represent the worst possible upper bound and apply to a graphite-epoxy arrestor plate. Test specimens incorporating this concept are planned.

The influence of bond thickness on overall TPS weight has been studied in connection with the parametric studies reported in Section 3 (see page 3.2-9). Although bond weight increases with increasing thickness, less LI-1500 is necessary to limit the substrate to a specified thickness. These conclusions are summarized in Tables 3.2-2 and 3.2-3.

5.2 MECHANICAL ATTACHMENT

LMSC has considered many strain-relief attachment methods that utilize mechanical fasteners. These methods can be considered in two general categories:

1. Carrier plates the size of each tile, which are mechanically fastened to the structure
2. Fasteners that are tapped into the LI-1500 and attached directly to the structure.

A carrier plate could be either a solid or mesh type of material and should have thermal expansion characteristics matched to those of LI-1500, like the strain arrestor plate concept. Testing of screen materials in this application is currently being conducted under the related Material Development Contract, NAS-9-12137, and will be reported separately.

Various attachments have been designed; weights of selected configurations are compared in Fig. 5.2-1. Designs 1, 2, 3, 6, and 7 are the threaded type (2); design 4, 5, 8, and 9 utilize bonding to the carrier plate type (1).

In Fig. 5.2-2 is shown a fastener concept that could be used in connection with a carrier plate. For each tile, four of these fasteners would be used, one which is rigidly attached to the carrier plate while the other three are free floating to allow for manufacturing tolerances. During installation, the spring stud (3) is pressed into a retainer attached to primary structure. To ensure positive locking, the spring-loaded pin (8) then snaps into the central hole of (3) in its initially undeflected state. To replace a panel with this attachment scheme, the LI-1500 must first be locally removed over the fastener (i. e., a hole drilled through the LI-1500) so that a punch can be inserted in the hole in (3) to dislodge the pin (8).

Figure 5.2-3 shows a concept with a carrier plate that is attached to primary structure by stainless Velcro and Fig. 5.2-4 shows a hybrid concept with rails in LI-1500 which, in turn, are mechanically attached to the structure with quarter-turn fasteners. These last two concepts have been weighed and are compared to the baseline bonded system in Table 5.2-1.



WEIGHT COMPARISON OF MECHANICAL FASTENERS FOR LI-1500

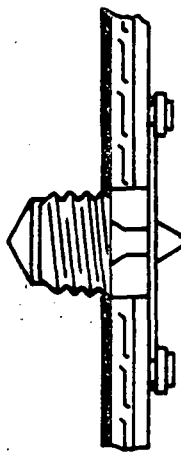
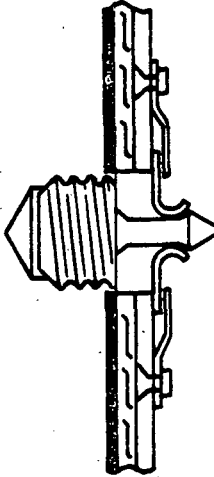
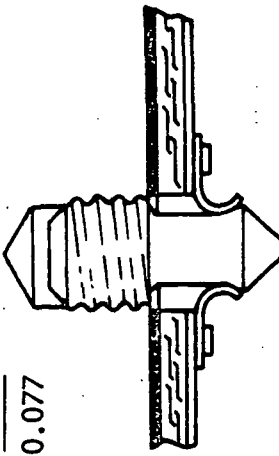
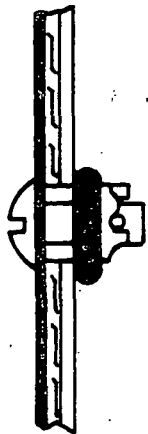
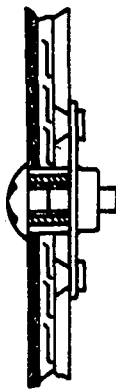
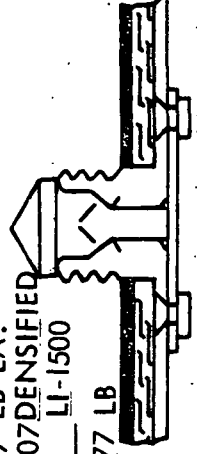
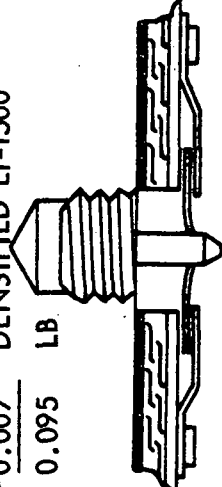
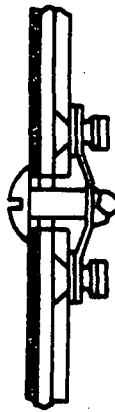
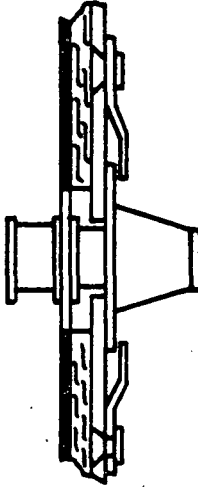
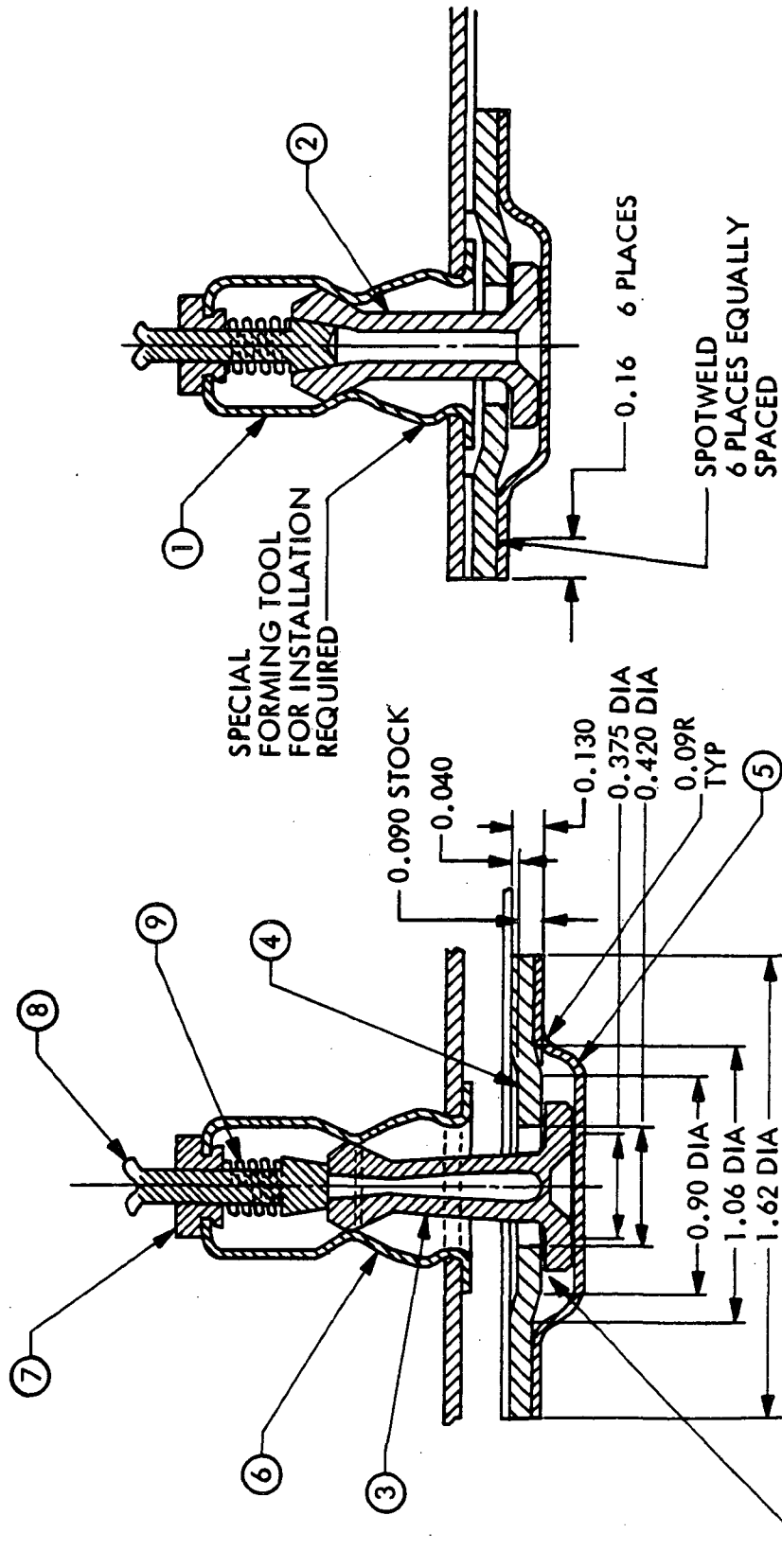
<p>0.06 +0.007 : 0.067 LB</p> <p>LB EA. DENSIFIED LI-1500</p>  <p>SPRING CLIP (1)</p>	<p>0.075 LB EA. +0.007 0.082 LB</p> <p>DENSIFIED LI-1500</p>  <p>FLOATING SPRING CLIP (2)</p>	<p>0.07 LB EA. +0.007 0.077</p> <p>DENSIFIED LI-1500</p>  <p>STATIONARY SPRING CLIP (3)</p>
<p>0.023 LB EA.</p>  <p>VIBREX FASTENER (4)</p>	<p>0.055 LB EA.</p>  <p>FLOATING NUT PLATE (5)</p>	<p>0.07 LB EA. +0.007 0.077 LB</p> <p>DENSIFIED LI-1500</p>  <p>FORMED THREADED SHEET (6)</p>
<p>0.088 LB EA. +0.007 0.095 LB</p> <p>DENSIFIED LI-1500</p>  <p>FLOATING SPRING WASHER (7)</p>	<p>0.017 LB EA.</p>  <p>SOUTHCO FASTENER (8)</p>	<p>0.018 LB EA.</p>  <p>DEUTSCH PRESLOK FASTENER (9)</p>

Fig. 5.2-1



FASTENER ASSEMBLY LI-1500 ATTACHMENT



SPECIAL FORMING TOOL FOR INSTALLATION REQUIRED

0.16 6 PLACES

SPOTWELD 6 PLACES EQUALLY SPACED

0.090 STOCK

0.040

0.130

0.375 DIA

0.420 DIA

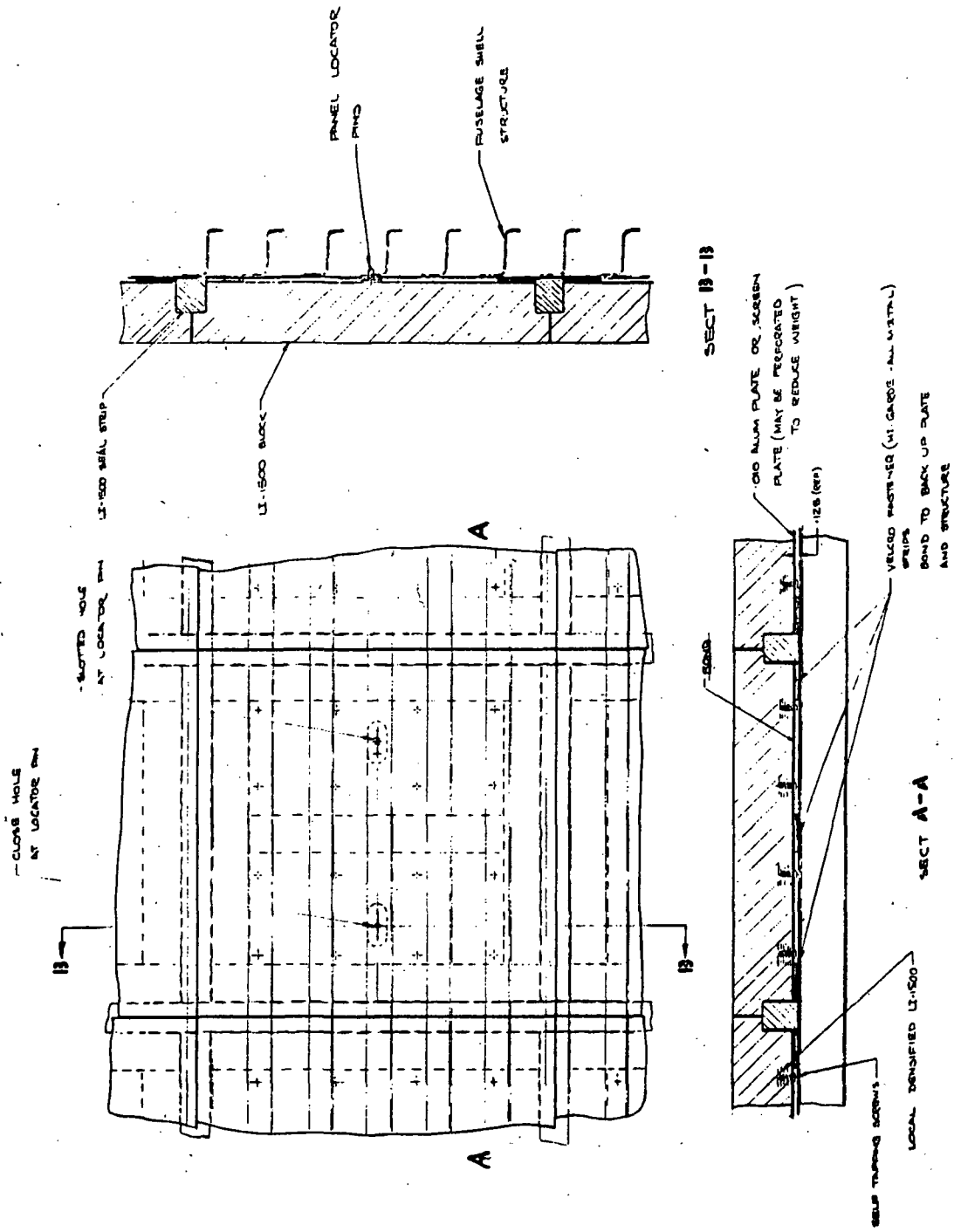
0.099 TYP

ONE FASTENER PER CARRIER PLATE RIGIDLY ATTACHED TO PLATE, OTHERS FREE-FLOATING TO ALLOW FOR MANUFACTURING TOLERANCES

Fig. 5.2-2



VELCRO ATTACHMENT WITH CARRIER PLATE



5.2-4

241<

Fig. 5.2-3

DO6044



RAIL ATTACHMENT SCHEME

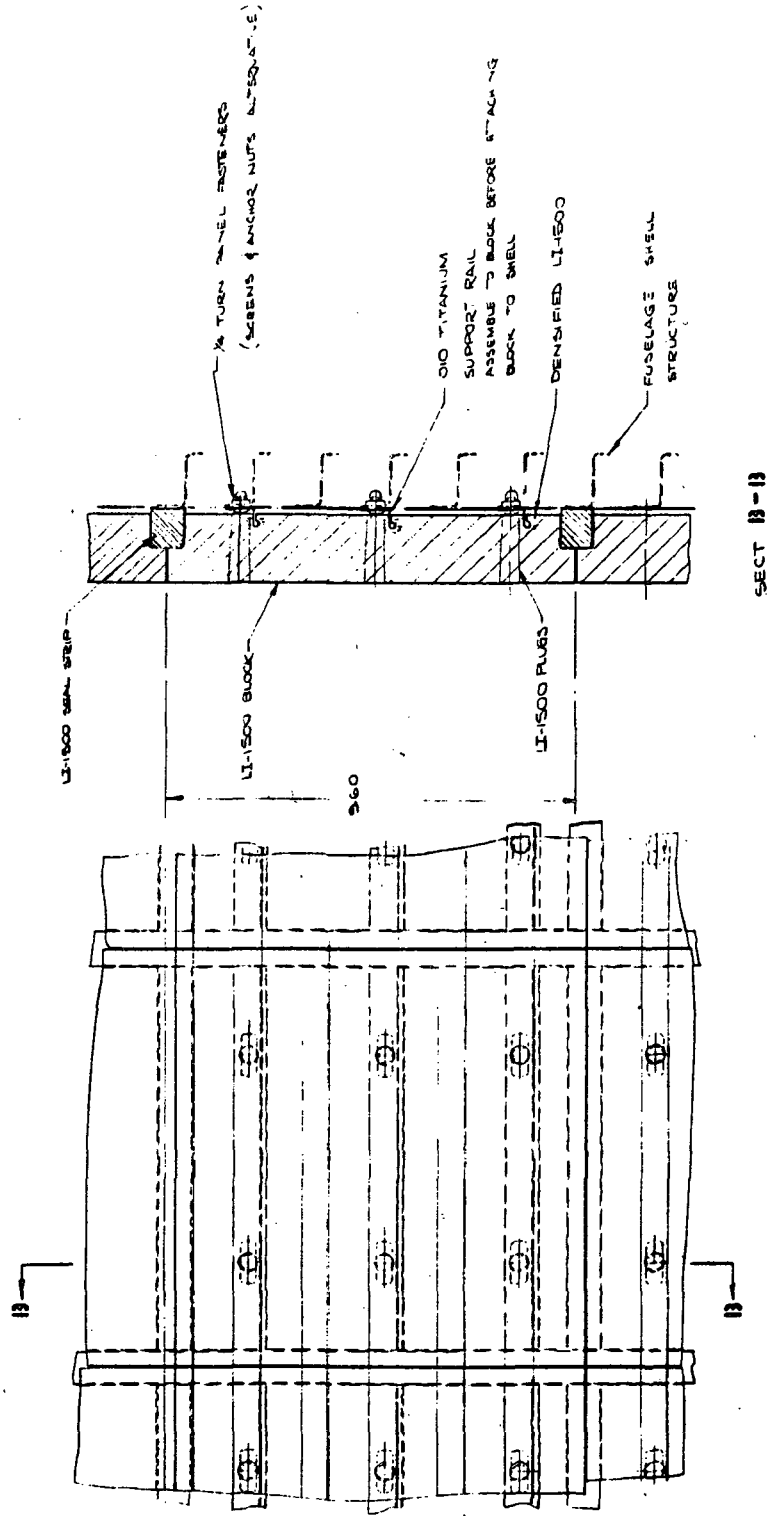


Fig. 5.2-4

Table 5.2-1
WEIGHT OF VARIOUS ATTACHMENT METHODS

Method	Weight (lb/ft ²)		
	Attachment	LI-1500 + Coating *	Total
Velcro	0.48	3.90	4.38
Rail Support	0.41	3.90	4.31
Bonding	0.66	3.53	4.19

* Lower Surface of Vehicle, LI-1500 thickness is 2.50 in.

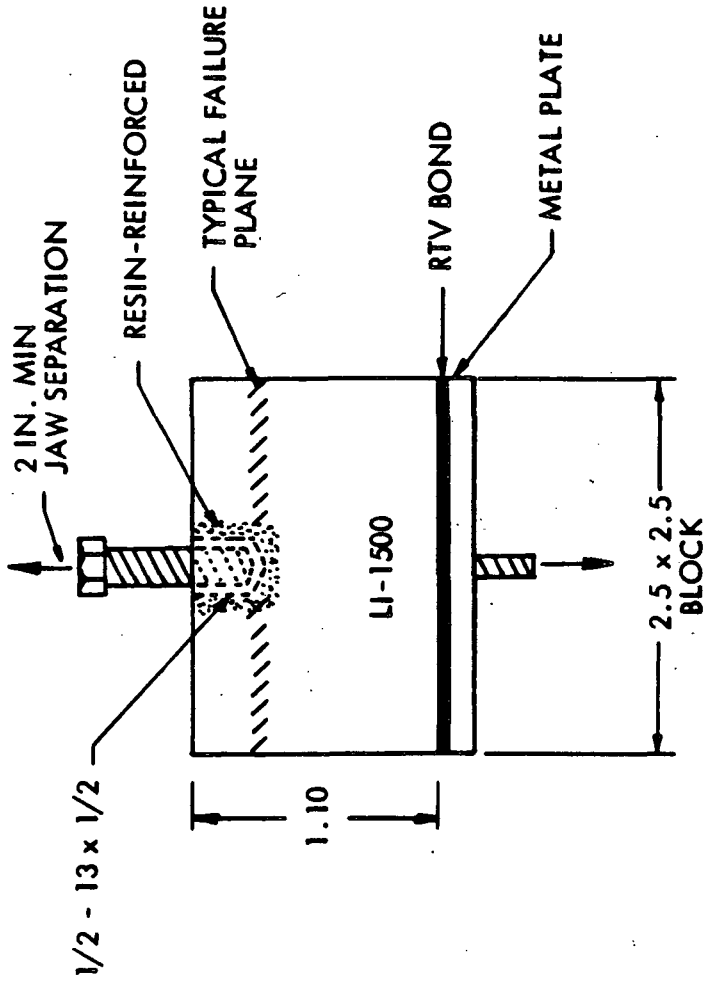
The values displayed show that LI-1500 is lighter for the direct bonding systems as the result of the bond heat sink effect previously noted. These various systems show promise as an effective method of reducing LI-1500 stress levels. However, a considerable test effort is required to evaluate the environmental effects.

Preliminary tests, performed under Contract NAS 9-12137, have shown that to increase strength LI-1500 can be locally densified by either impregnated silica or resin. Figure 5.2-5 summarizes the results of eight pull-out tests on fasteners tapped into LI-1500 with local resin reinforcement; the strength of this type fastener was not truly demonstrated, due to the failure in the weak tensile direction of the specimen.

Some analysis effort has been conducted on this type of mechanical system as related in Section 3.2. These investigations showed that such fasteners when made from common metals are not practical because of the required close tolerance. One metal, Invar, is suited for this type of application. Invar is 35-percent nickel and 65-percent iron with a coefficient of thermal expansion of approximately 1.2×10^{-6} in./in./°F. An analysis has been made for a 0.5-in. diameter Invar insert in undensified LI-1500 at 600°F with negligible resulting stresses.



TEST RESULTS - MECHANICAL FASTENER WITH LOCAL REINFORCEMENT



GRAMS
 ~0.5
 ~0.5
 0

WEIGHT RESIN REINFORCEMENT ADDED
 WEIGHT OF LI-1500 MATERIAL REMOVED
 NET WEIGHT GAIN

LB
 31
 40
 29

8 SPECIMEN - FAILURE LOAD:
 AVERAGE
 MAXIMUM
 MINIMUM

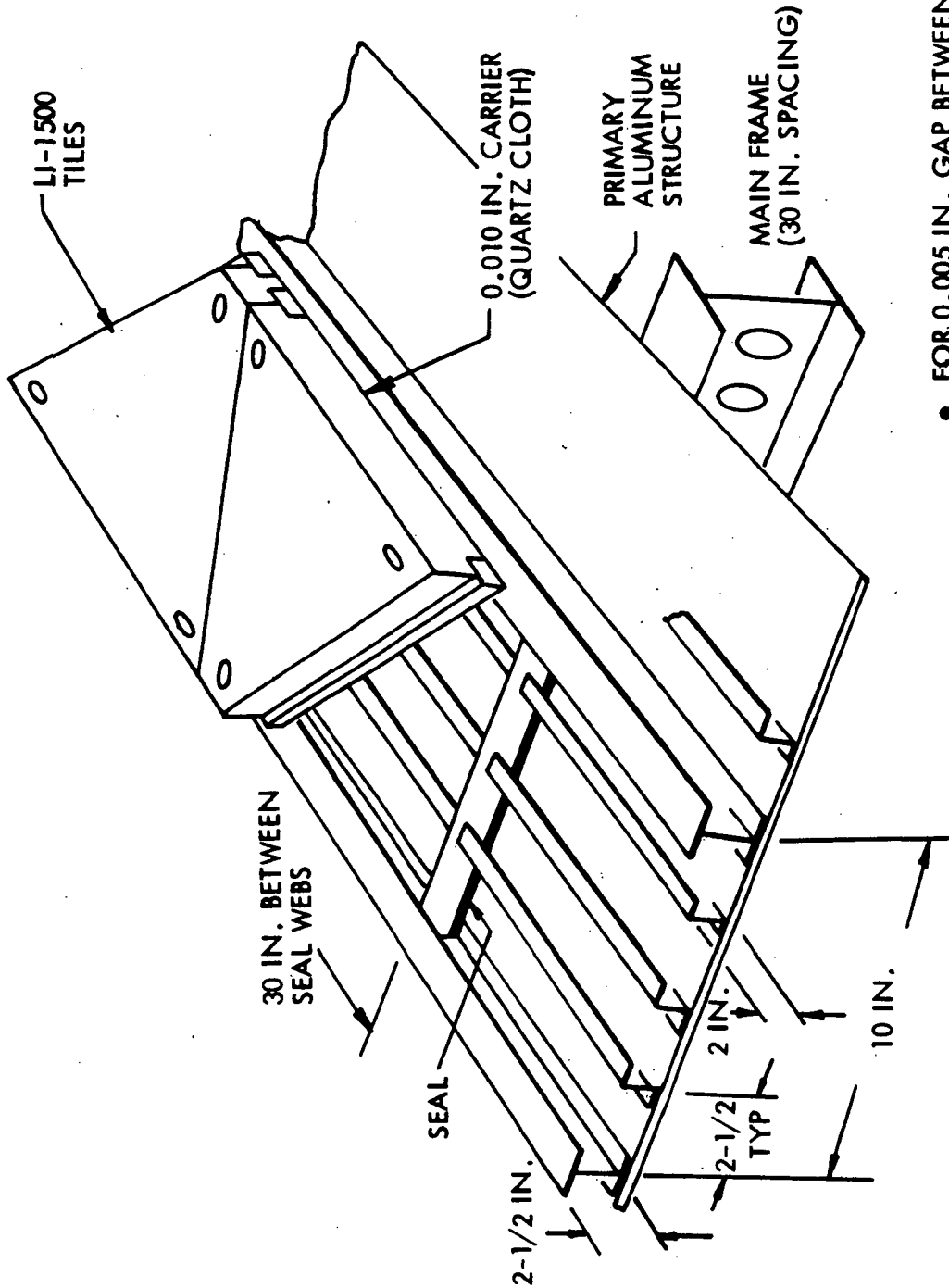
5.3 PARTIAL TILE SUPPORT

The third method of strain isolation considered is that of supporting tiles on external vehicle stringers. Figure 5.3-1 shows such a concept with 10-in. tiles. This concept also can allow venting across the tiles into the chamber below to reduce design pressures. LMSC has performed such a venting analysis, assuming a sealed chamber with a 0.52-cu ft volume.

Various gaps widths were considered with a 10-in. gap length through which all air is vented. For the NASA ascent pressure envelope shown in Section 6.1 and using 0.005- and 0.0025-in. gap widths, the maximum differential pressures are 0.1 and 0.25 psi, respectively. An analysis of rapid external pressure changes are also performed; the resulting differential pressures are quite low. For example, for the recommended design condition with a pressure rate change of 2 psi/sec for 4 sec, a gap of 0.020 in. would vent sufficiently to realize only a 0.175-psi differential pressure. This study has been documented and is included as Appendix E in this report.



DESIGN CONCEPT UTILIZING VENTING ACROSS LI-1500



- FOR 0.005 IN. GAP BETWEEN TILES
 $\Delta P = 0.1$ PSI MAXIMUM IN REENTRY
- FOR 30 IN. X 10 IN. X 2-1/2 IN. CHAMBER
AT $< 1^\circ F$ ON ALUMINUM PRIMARY STRUCTURE
FROM 0-TO-2 PSI (ASSUMING NO MASS FLOW)

Fig. 5.3-1

D05166
rdb

5.4 REMOVAL OF BONDED LI-1500

One means of removing LI-1500, once it has been bonded to a metallic substrate, is shown in Fig. 5.4-1. In this scheme, a powered router is set in place over a tile (or tiles) using tapered pins inserted in holes punched in the LI-1500 at predetermined locations. The cutter is guided and the depth adjusted so that the joint filler blocks are not disturbed during cutting. The remainder of the tile would then be cut away with hand tools. The top portion of the bond line would be removed and a replacement tile bonded in place. LMSC is pursuing evaluation of this type replacement in related in-house efforts.

5.4-1

247<

LI-1500 BLOCK REMOVAL SCHEME

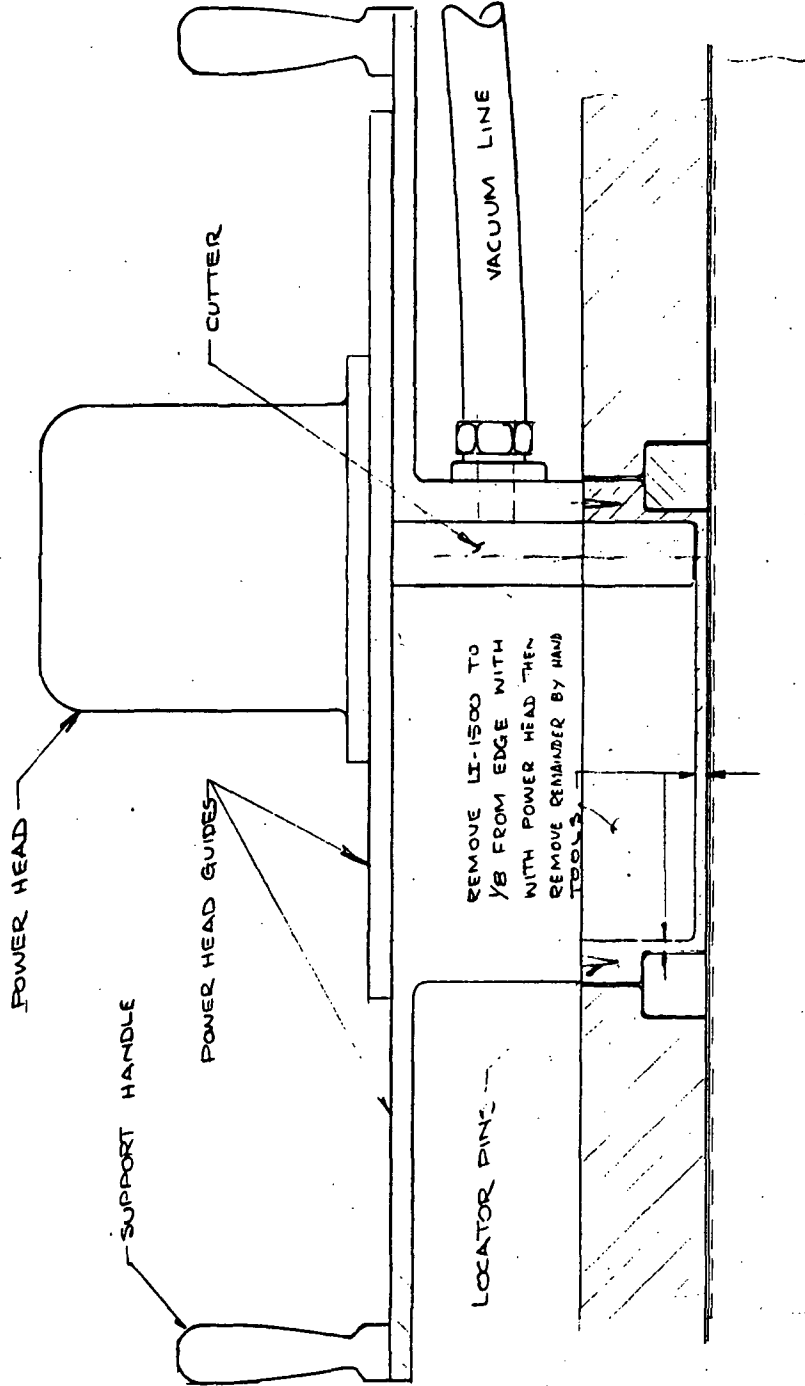


Fig. 5.4-1



DO5059
RDB

Section 6

PROTOTYPE PANEL DESIGN/ANALYSIS

Four prototype panels are to be optimumply designed, analyzed, fabricated, and delivered to NASA/MSC under this program. These panels are to meet the point design requirements specified by NASA/MSC and shown in Section 6.1. In addition, the four panels are to represent the application of LI-1500 to both subpanels and primary structure. The overall size of panels is to be nominally 24 in. x 25 in. in order to be compatible with existing NASA/MSC test fixtures.

The materials to be used in the substrate for each panel, and the applications to be represented by each panel, are shown below. These selections have been based on prior studies performed at LMSC and NASA/MSC with regard to materials and the anticipated usage of reusable surface insulation material on the space shuttle orbiter vehicle:

<u>Prototype Panel No.</u>	<u>Application</u>	<u>Material</u>	<u>Vehicle Area Location *</u>	<u>Maximum Substrate Temperature</u>
1	Subpanel	Beryllium	2	600 ⁰ F
2	Primary Structure	Aluminum	2	300 ⁰ F
3	Primary Structure	Aluminum	1	300 ⁰ F
4	Primary Structure	Titanium	2	600 ⁰ F

* See Fig. 6.1-1

The point design requirements are summarized in Table 6.1-1. Maximum differential pressures occur during ascent while the substrate back-face surface is at room temperature; maximum back-face temperatures noted above are not developed until after landing. The maximum in-plane loads in vehicle Area 2 occur during landing; also, this is true of Area 1 except that maximum compression load occurs during

ascent. Observe that the in-plane tension loads exceed the in-plane compression loads in vehicle Area 2 by a considerable amount; thus, the selection of substrate configuration will probably not have impact upon weight for prototype panel Nos. 2 and 4.

The design/analysis process leading to a completely verified, optimum, LI-1500 substrate system is comprised of a number of specific steps that are interrelated with each other. The logic sequence for this process has already been presented in Fig. 1.1-1. As indicated there, the design/analysis process begins with basic structural optimization (sizing) of the panel substrates, which includes selection of the substrate configuration. These results are preliminary in that they are then used as input to a thermostructural optimization loop for basic sizing of the LI-1500. Included in this loop is a consideration of the heat-sink properties of the substrate. It has been shown in Section 4 that the LI-1500/beryllium subpanel combination for optimum thermostructural design utilizes a beryllium subpanel that is somewhat heavier than the beryllium subpanel developed on the basis of structural optimization principles alone. This situation occurs due to the unique heat-sink properties of beryllium; other materials do not exhibit the same phenomenon.

The last loop of the design cycle is concerned with tile size/bond thickness/RSI stress-level tradeoffs; with a tentative design established, verification is then made of the structural integrity of the bond/LI-1500/coating system under critical loading/environmental conditions. Acoustic and flutter analyses also are presented for the final designs as well as a discussion of panel critical failure modes.

To conclude this section, cost and weight comparisons with competing heatshield concepts are given, which show that an LI-1500 system exhibits clear and distinct advantages over other possible shuttle TPS systems.

6.1 PROTOTYPE PANEL DESIGN CONDITIONS

The point design requirements for the prototype panels have been specified by NASA/MSC. ⁽⁶⁻¹⁾ LMSC has complied with these requirements in the design effort.

Structural Design Requirements

Ultimate Factor-of-Safety:	1.5
Combined Loading:	Summation of ratio of the allowable load to combined limit loads ≥ 1.35
Panel Flutter:	Flutter-free for 1.5 times local dynamic pressures at any flight Mach number

Thermal Design Requirements

Design factors of safety are not applied to the heating rates for the specified vehicle areas shown in Fig. 6.1-1. The heating rate for Area 2 has been perturbed to result in a maximum surface temperature of 2300°F, as shown on Fig. 6.1-2. Adiabatic conditions have been assumed for the panels in insulation sizing efforts.

Environments

Figures 6.1-3 through 6.1-12 show the trajectories, loading, and environments to which the prototype panels have been designed and/or analyzed. The combination of conditions considered and the critical design conditions are summarized in Table 6.1-1.

(6-1) D. J. Tillian, NASA/MSC, to R. D. Buttram, LMSC, "Point Design Requirements for Two Orbiter Design Areas-Reusable Surface Insulation TPS Development, Phase 2, "U.S. Government Two-Way Memo, 21 July 1971

TPS DESIGN AREAS FOR ORBITER LOWER SURFACE

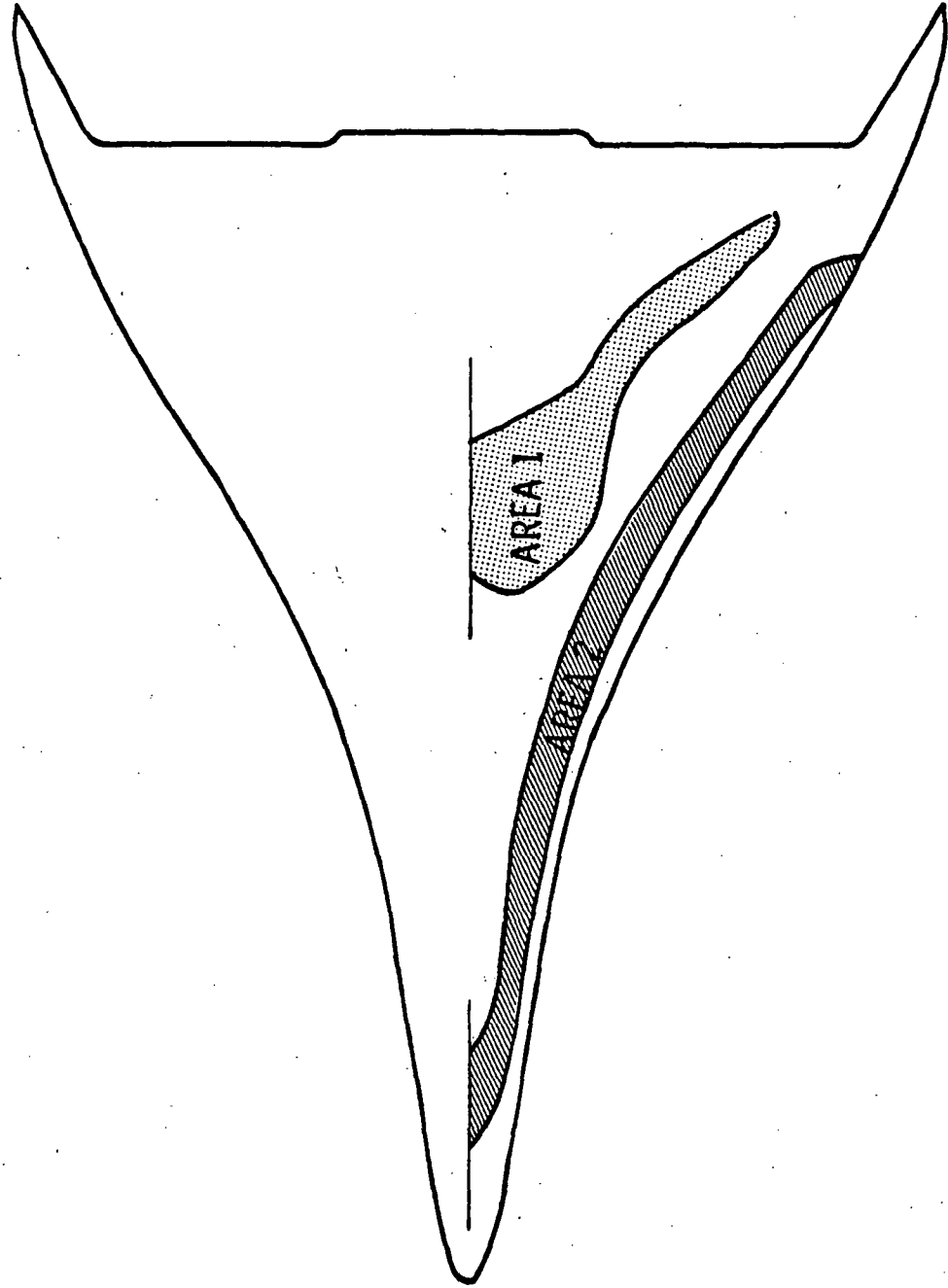


Fig. 6.1-1

D04980



LOCAL HEATING RATE AND STAGNATION TEMPERATURE HISTORIES FOR ORBITER DURING ENTRY

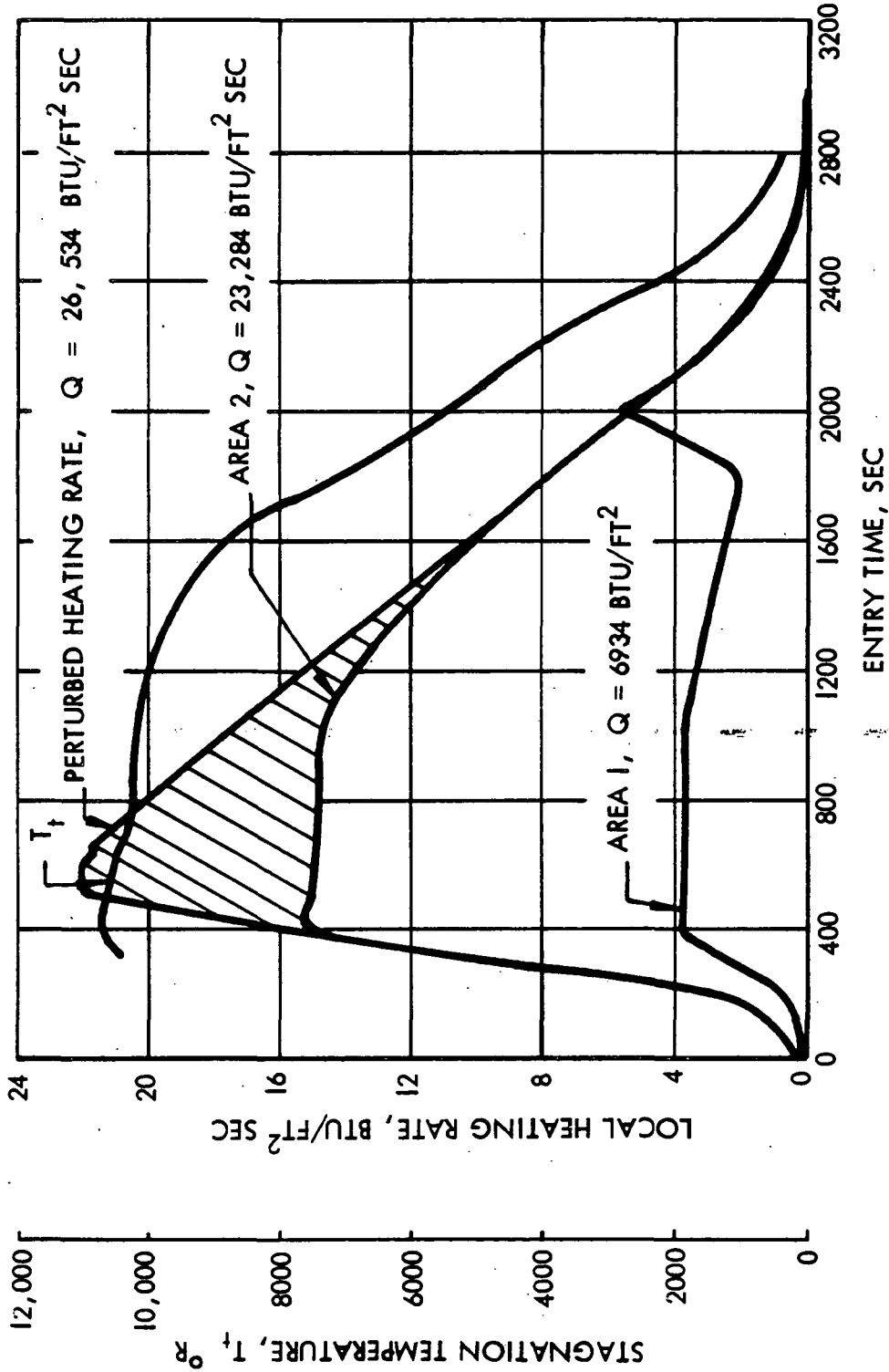
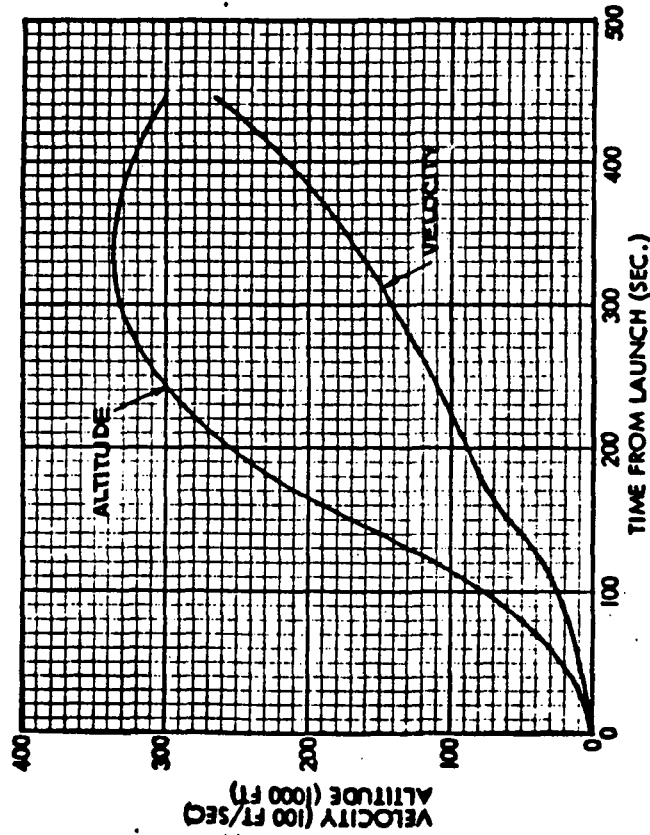
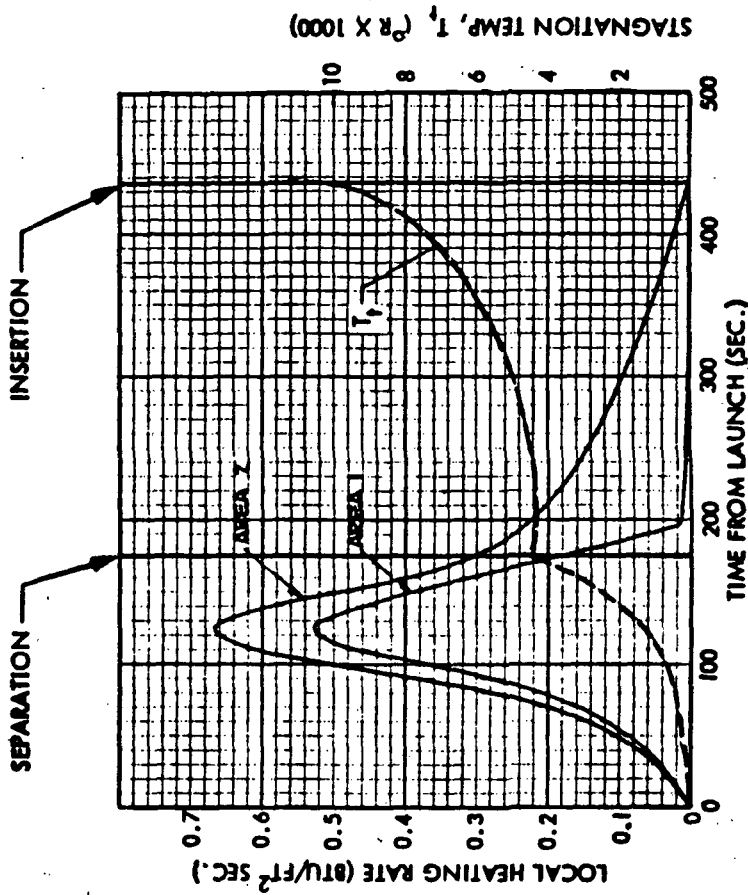


Fig. 6.1-2

ASCENT TRAJECTORY, STAGNATION TEMPERATURE
AND HEAT RATE HISTORIES



DO6150 (1)

Fig. 6.1-3

ENTRY TRAJECTORY

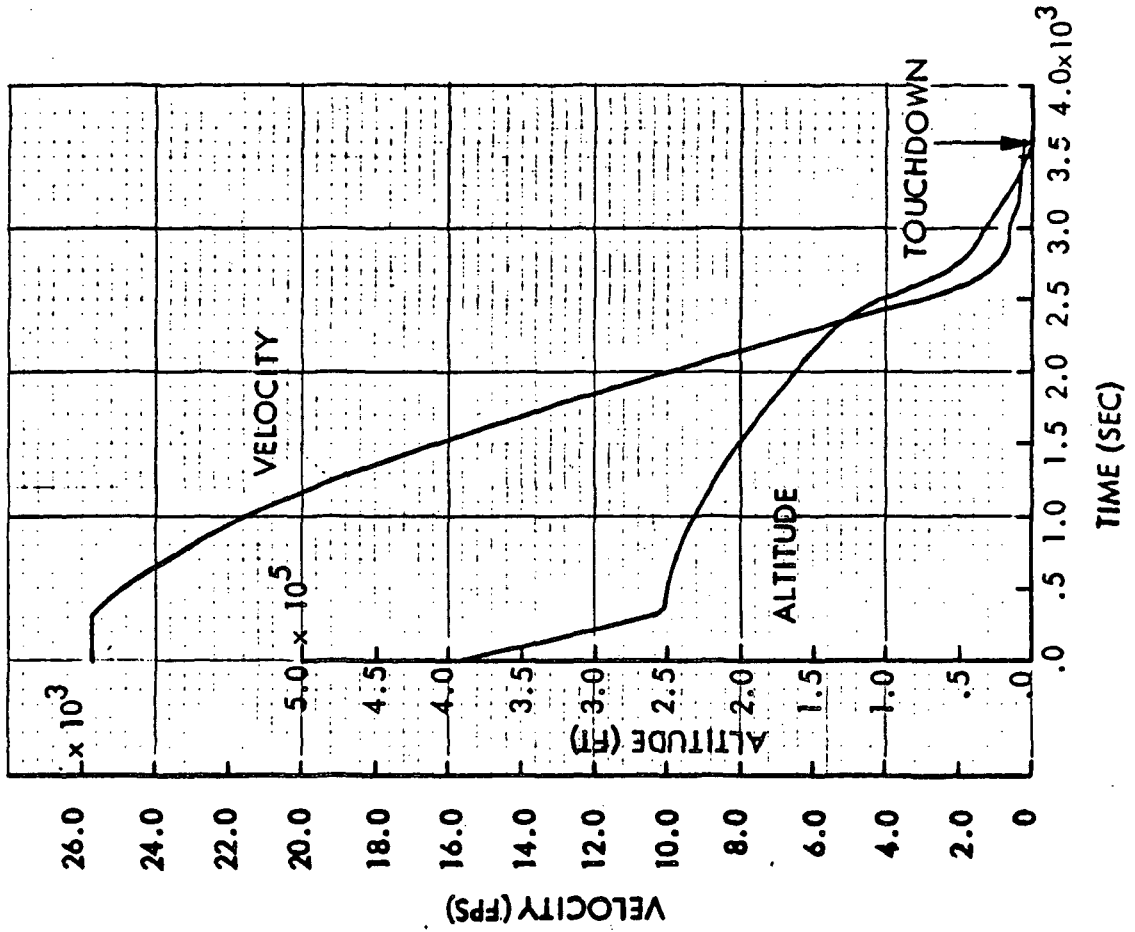
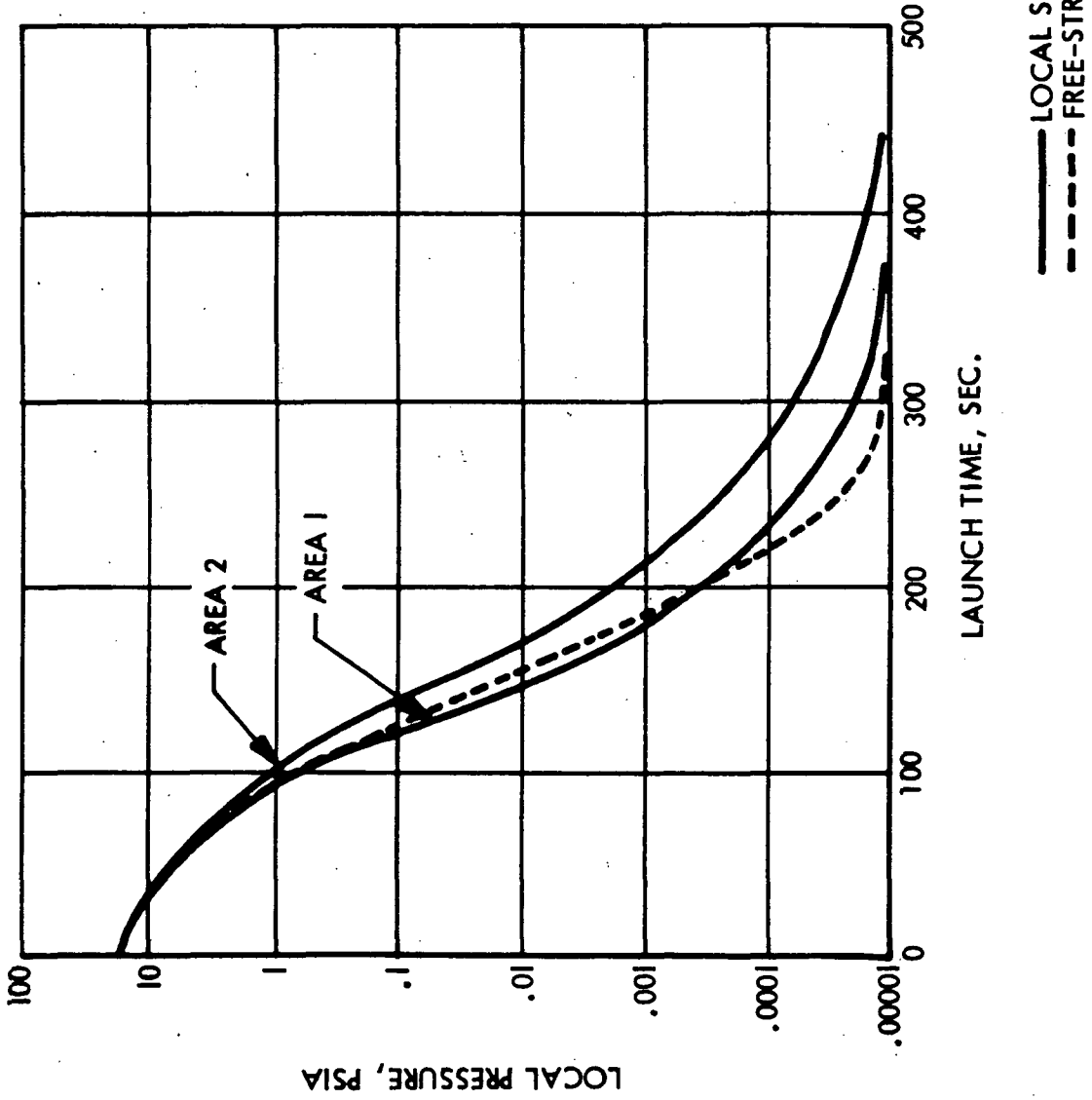


Fig. 6.1-4



LOCAL AND FREE-STREAM STATIC PRESSURE HISTORIES
ON ORBITER FUSELAGE DURING LAUNCH



DO6017

Fig. 6.1-5

FREE-STREAM AND LOCAL PRESSURE HISTORIES ON
ORBITER CENTERLINE DURING ENTRY

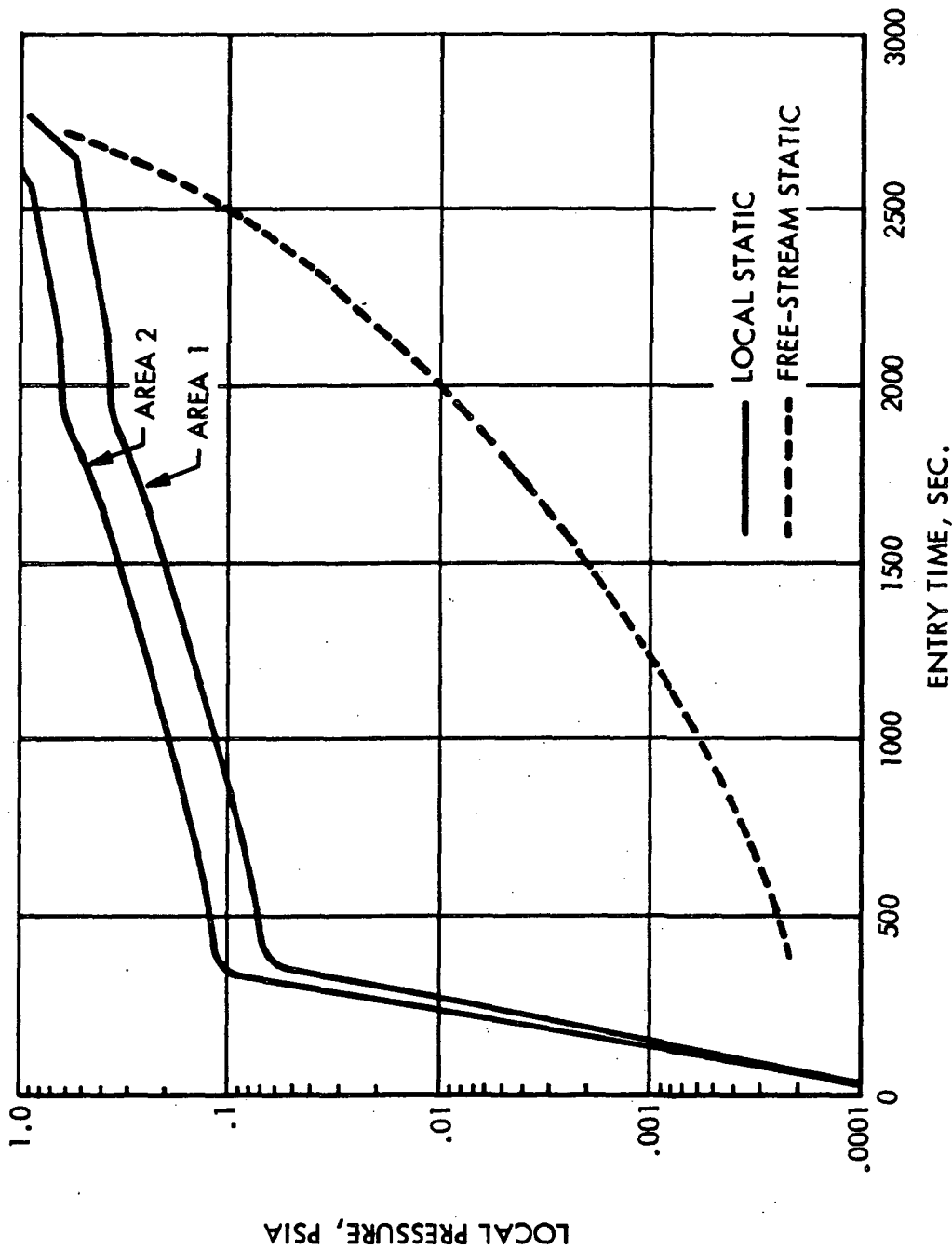


Fig. 6.1-6



LIMIT DIFFERENTIAL PANEL PRESSURES FOR ASCENT

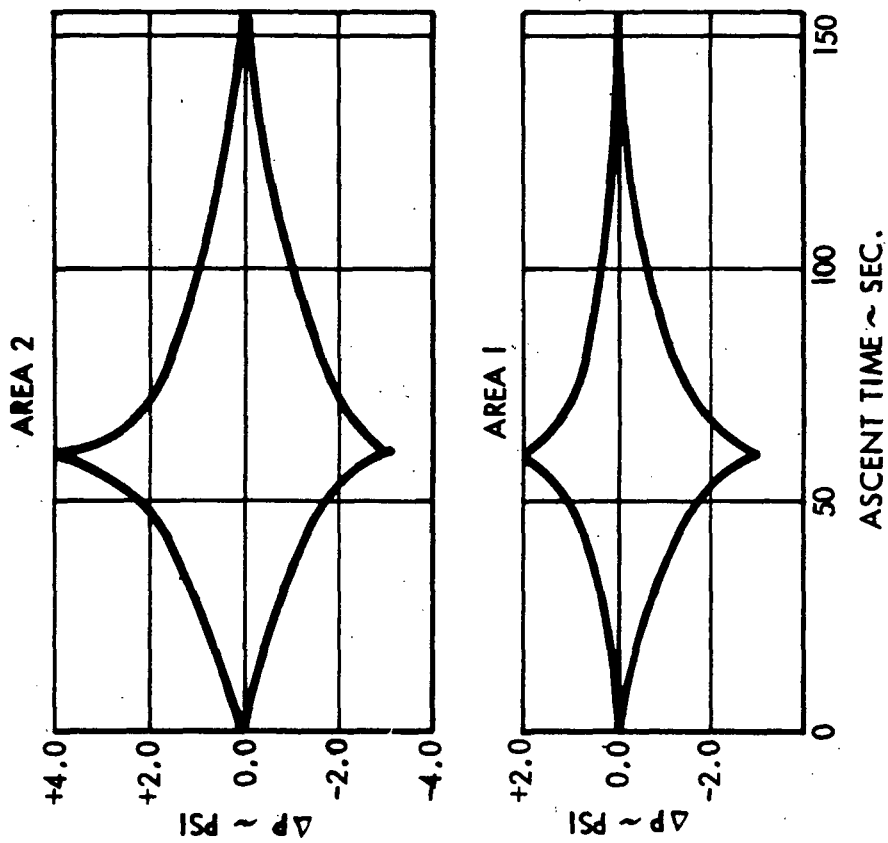


Fig. 6.1-7

DO6019

LIMIT DIFFERENTIAL PANEL PRESSURES FOR ENTRY

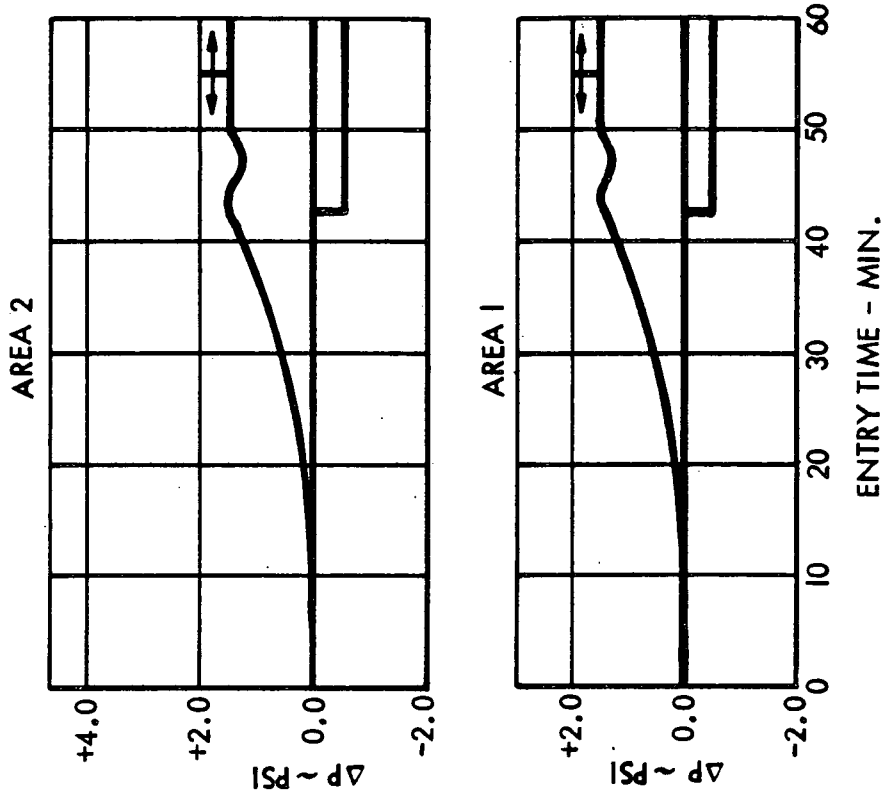


Fig. 6.1-8

ASCENT AND ENTRY DYNAMIC PRESSURES

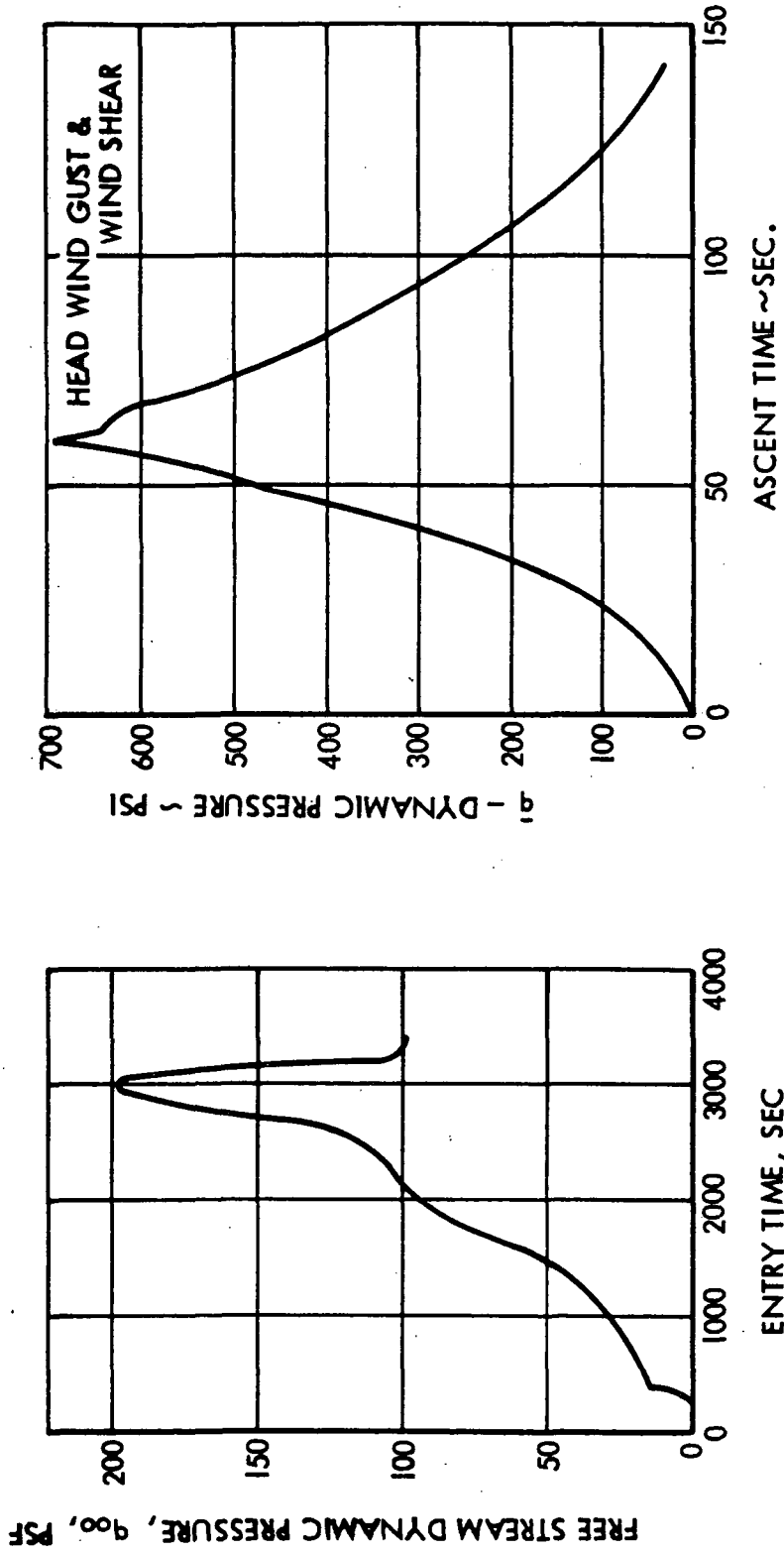


Fig. 6.1-9

DO6132

AREA 1 - ASCENT AND ENTRY LINELOADS

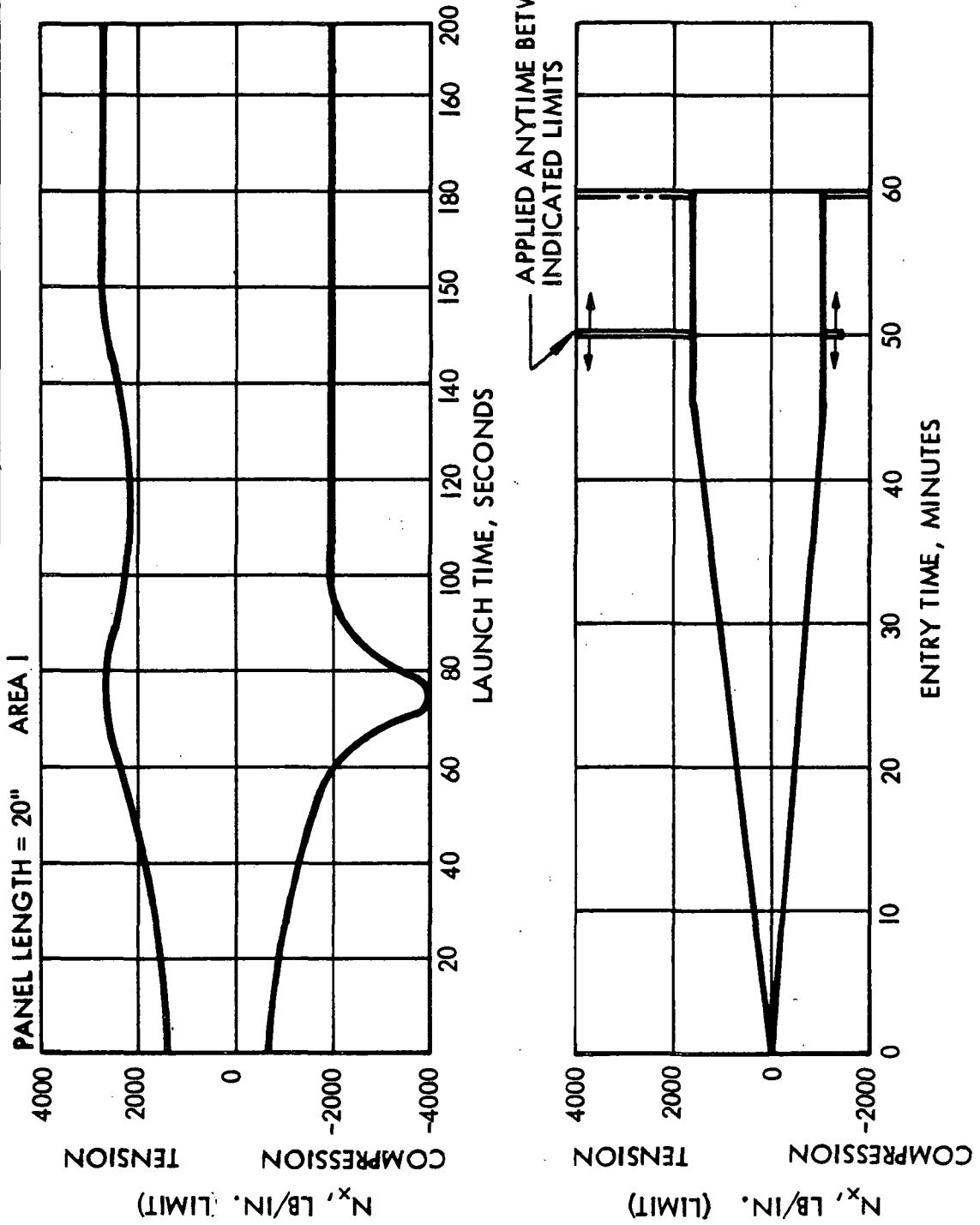
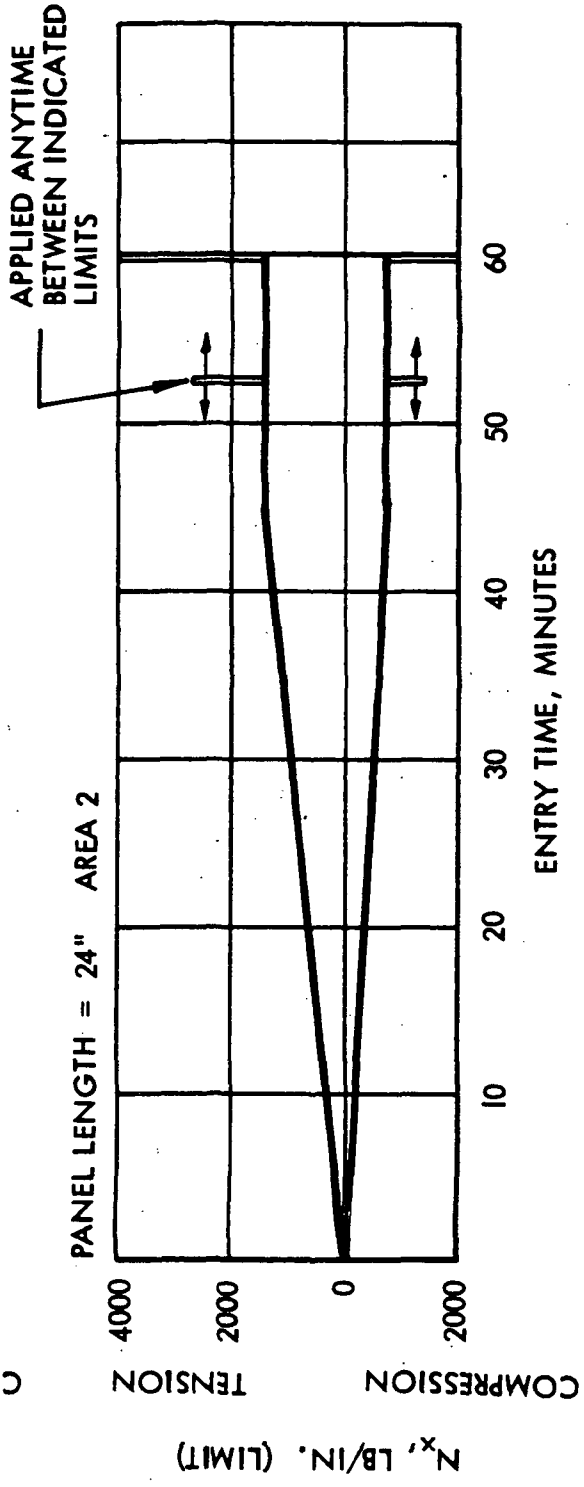
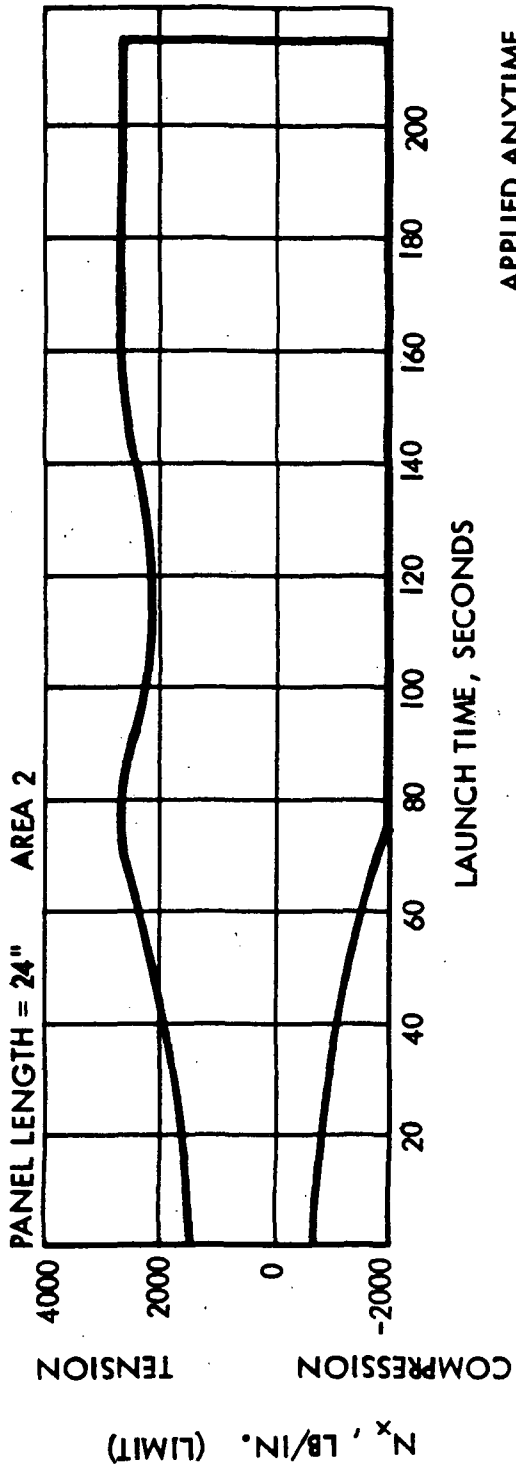


Fig. 6.1-10

AREA 2 - ASCENT AND ENTRY LINELOADS



>292

6.1-12

Fig. 6.1-11



OVERALL SPL VS. TIME - TYPICAL ORBITER MISSION

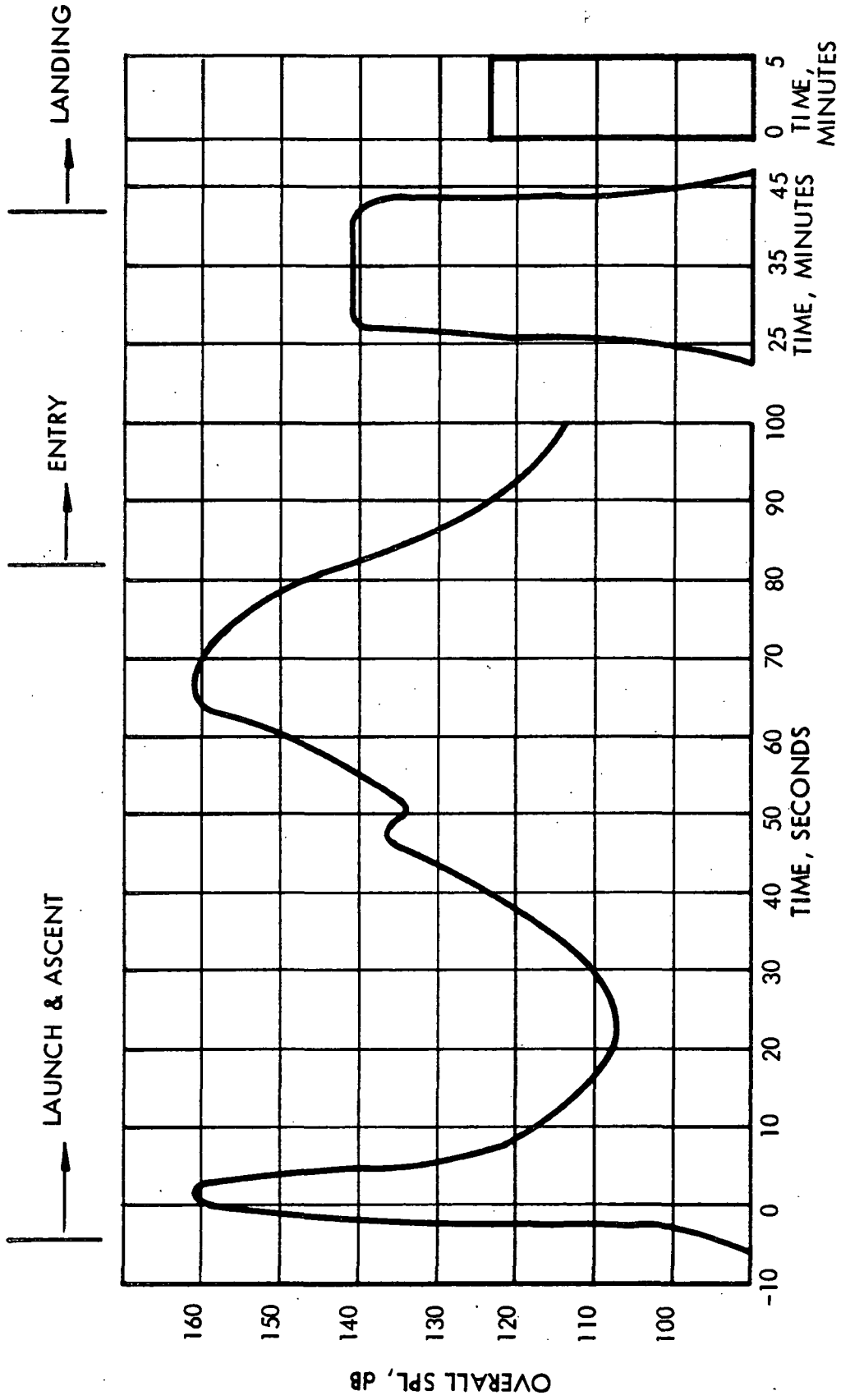
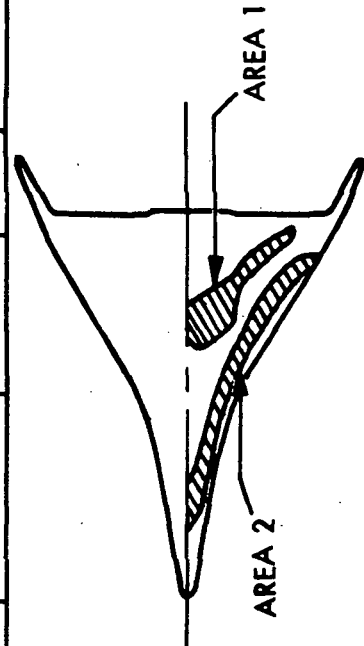


Fig. 6.1-12

Table 6.1-1
ORBITER SHELL DESIGN CONDITIONS

OPERATION	AREA	ELAPSED TIME	DIFFERENTIAL PRESSURE (LIMIT) (PSI)		IN-PLANE LOAD (LIMIT) (PPi)		SPL (dB)	MAX SURFACE TEMP (°F)	MAXIMUM BACKFACE TEMP (AMBIENT) (°F)	
			COLLAPSE	BURST	TENSION	COMP.			ALUMINUM	TITANIUM
LAUNCH	1,2	—	—	—	—	—	160	—	R.T.	R.T.
ASCENT	1	60 SEC	+ 2.0	- 3.0	+ 2400	- 2100	150	≈ 200	R.T.	R.T.
		67 75	+ 0.9	- 1.5	+ 2700	- 4000	161 155		R.T. R.T.	R.T. R.T.
2	2	60	+ 4.0	- 3.0	+ 2300	- 1500	150	≈ 200	R.T.	R.T.
		67 75	+ 1.8	- 1.9	+ 2700	- 2000	161 155		R.T. R.T.	R.T. R.T.
ENTRY	1 2	10 MIN	+ 0.1	- 0.0	+ 300	- 200	—	1480	-150	-150
		10 MIN	+ 0.1	- 0.0	+ 300	- 200	—	2300	-150	-150
POST-ENTRY CRUISE	1 2	25-45 MIN	+ 1.5	- 0.5	+ 1600	- 1000	141	1200 - 400	< 300	< 600
		25-45 MIN	+ 1.5	- 0.5	+ 1400	- 700	141	1850 - 400	< 300	< 600
LANDING	1,2	45-60 MIN	+ 2.0	- 0.5	+ 4000	- 1400	124	≈ 100	< 300	< 600
		45-60 MIN	+ 2.0	- 0.5	+ 2700	- 1400	124	≈ 100	< 300	< 600
DEAD STOP	1,2	60 MIN	+ 0.5	- 0.5	+ 4000	- 2000	124	≈ 100	< 300	< 600
		> 60 MIN	—	—	—	—	—	≈ 100	300	600



- PLUS PRESSURE IS COLLAPSE (VENTING ALLOWANCE INCLUDED)
- PLUS IN-PLANE LOAD IS TENSION
- FACTOR-OF-SAFETY BETWEEN LIMIT AND ULTIMATE IS 1.5

D004947 (1)

6.2 TPS SYSTEM DESIGN PROPERTIES

Table 6.2-1 is a summary of the mechanical and thermal properties of LI-1500 and the two coating systems studied under this contract. The 0042 coating is the one used in the point designs. Thermophysical properties of the metallic substrate materials are given in Table 6.2-2 while the mechanical properties of these materials are listed with the RSI stress analysis summaries presented in Section 6.5. Tables 6.2-3 and 6.2-4 list thermal conductivity values of RTV-560 and the 0042 coating, respectively, whereas in Tables 6.2-5 and 6.2-6, LI-1500 conductivity and specific heat properties are presented. The variation of Young's modulus with temperature for RTV-560 is given in Table 6.2-7.

All LI-1500 and coating design data have been generated by LMSC under this or related contracts while properties for bond and substrate materials have generally been taken from standard references or suppliers' bulletins. In-house material testing is described in Section 4, Vol I of this report.

Note that LI-1500 mechanical properties are shown only for room temperature. The properties do change with temperature as shown in Volume I; however, since the modulus decreases and the strength increases with increasing temperature, the room temperature values shown lead to conservative stress analyses and, hence, have been used in the parametric studies.



LI-1500 INSULATION SYSTEM DESIGN PROPERTIES

Table 6.2-1

(ROOM TEMPERATURE UNLESS OTHERWISE NOTED)

PROPERTY (ULTIMATE)	LI-1500		RTV-560 BOND	LI-0042 COATING	LI-0025 COATING
	STRONG DIRECTION	WEAK DIRECTION			
TENSION (PSI)	70	15	800	> 2000	600
TENSILE MODULUS (PSI)	60,000	6,000	300	<9.1 x 10 ⁶ *	3.5 x 10 ⁶
COMPRESSION (PSI)	150	40	-	> 2000	>>600
COMPRESSION MODULUS (PSI)	50,000	5,000	-	<9.1 x 10 ⁶ *	3.5 x 10 ⁶
SHEAR (PSI)	40	25	400	-	-
SHEAR MODULUS (PSI)	20,000	4,000	100	<3.7 x 10 ⁶	1.4 x 10 ⁶
THERMAL EXPANSION (IN./IN./°F)	PARALLEL TO FIBER	PERPENDICULAR TO FIBER			
	3.0 x 10 ⁻⁷	3.0 x 10 ⁻⁷	1.14 x 10 ⁻⁴	2.0 x 10 ⁻⁷ **	2 x 10 ⁻⁷
HEAT CAPACITY (BTU/LB-°F)	(RT)	0.15	0.30		
	(2000°F)	0.32	-		
THERMAL CONDUCTIVITY (BTU-IN./FT ² -HR-°F) ~1 ATMOSPHERE	(RT)	0.58	2.16	6.5	
	(2000°F)		-	14.2	
THERMAL CONDUCTIVITY (BTU-IN./FT ² HR-°F) ~VACUUM	(RT)	0.31	-	6.5	
	(2000°F)		-	14.2	
EMITTANCE	(RT)	-	-	0.89	0.85
	(2000°F)	-	-	0.93	0.63

* LATEST TEST DATA INDICATE MODULUS VALUES OF APPROXIMATELY 1.9 x 10⁶ PSI. VALUES IN TABLE USED IN ANALYSIS.

**LATEST TEST DATA INDICATE THERMAL EXPANSION COEFFICIENT OF APPROXIMATELY 4.0 x 10⁻⁷ IN./IN./°F VALUES IN TABLE USED IN ANALYSIS, EXCEPT WHERE NOTED.

D05165

Table 6.6-2

THERMOPHYSICAL PROPERTIES OF METALLIC SUBSTRATE MATERIALS

Beryllium $\rho = 115 \text{ lb/ft}^3$			
$T \sim ^\circ\text{F}$	$C_p \sim \text{Btu/lb } ^\circ\text{F}$		$k \sim \text{Btu/ft sec } ^\circ\text{F}$
40	0.425		2.94×10^{-2}
200	0.500		2.750
400	0.570		2.500
600	0.615		2.250
1000	0.675		1.780
1500	0.745		1.250
2200	0.845		0.778
Titanium $\rho = 276 \text{ lb/ft}^3$			
$T \sim ^\circ\text{F}$	$C_p \sim \text{Btu/lb } ^\circ\text{F}$		$k \sim \text{Btu/ft sec } ^\circ\text{F}$
40	0.125		0.116×10^{-2}
200	0.135		0.119
300	0.140		0.153
1000	0.180		0.222
Aluminum 7075 $\rho = 173 \text{ lb/ft}^3$			
$T \sim ^\circ\text{F}$	$C_p \sim \text{Btu/lb } ^\circ\text{F}$		$k \sim \text{Btu/ft sec } ^\circ\text{F}$
0	0.195		2.14×10^{-2}
200	0.218		2.22
400	0.240		2.78
600	0.262		2.84
800	0.288		2.78



Table 6.2-3

THERMAL CONDUCTIVITY OF RTV-560

<u>Temperature (°R)</u>	<u>k</u> <u>(Btu-in./ft²-hr-°R)</u>
530*	1.94
700	1.68
950	1.51

Density = 94 lb/ft³

*Manufacturer's Data at 530°R, k = 2.16 (Btu-in./ft²-hr-°R)

Table 6.2-4

THERMAL CONDUCTIVITY OF 0042 COATING

<u>Temperature (°R)</u>	<u>k</u> <u>(Btu-in./ft²-hr-°R)</u>
460	6.48
860	6.48
1460	10.8
2460	14.2
2960	16.8

Table 6.2.5

LI-1500 DESIGN VALUES - THERMAL CONDUCTIVITY

(Btu-in./ft²-hr-°R)

Pressure (mm Hg)	0.1	1.0	10.0	100.0	760.0
Temp (°R)					
460	0.17	0.19	0.28	0.32	0.35
760	0.21	0.23	0.31	0.34	0.37
1160	0.27	0.29	0.35	0.47	0.52
1860	0.45	0.47	0.60	0.90	1.00
2460	0.67	0.69	1.02	1.40	1.56
2960	0.92	0.94	1.35	1.88	2.09

Table 6.2.6

LI-1500 DESIGN VALUES - SPECIFIC HEAT

(Btu/lb-°R)

Temperature (°R)	C _p (Btu/lb-°R)
360	0.0716
540	0.151
720	0.198
900	0.234
1080	0.263
1260	0.280
1440	0.287
1800	0.294
2160	0.306
2520	0.316
2890	0.320

Table 6.2-7

RTV-560 YOUNG'S MODULUS VS TEMPERATURE

T (°F)	E* (PSI)
-200	67,000
-150	1,200
75	300
300	300
600	100

* Data obtained from ASTM D797 and in-house testing described in Section 3, Vol I of this report.

6.3 THERMAL ANALYSIS

Ascent and Reentry Heating Environment

Ascent and reentry heat rates provided by NASA for Areas 1 and 2 of the delta-wing orbiter, Fig. 6.1-1, are shown in Figs. 6.1-2 and 6.1-3. The perturbed heat rate of Area 2 was used in these analyses. Calculation of ascent temperature histories was based on a surface emittance of 0.8, the LMSC THERM computer code, and a one-dimensional thermal model; results are shown in Figs. 6.3-1 and 6.3-2. Maximum surface temperatures of 495^oF and 565^oF are experienced by Areas 1 and 2, respectively. The ascent heating environment is very mild, as evidenced by the temperature distributions at orbit injection, shown in Fig. 6.3-3. The substrate temperature has not increased from its initial value of 75^oF.

The reentry heating and pressure environment for Areas 1 and 2 are shown in Figs. 6.3-4 and 6.3-5. Radiation equilibrium temperatures, calculated with an emittance of 0.8, and the heat rate histories of Figs. 6.1-2 and 6.1-3 are shown. Maximum surface temperatures are 2300^oF and 1480^oF for Areas 2 and 1, respectively. The difference in the times of peak temperature for Areas 1 and 2 is associated with the occurrence of boundary layer transition for Area 1 at about 2000 sec into the reentry. As noted in Figs. 6.3-4 and 6.3-5, most of the reentry heat pulse occurs while the local static pressure is less than 0.1 ATM. Hence, the pressure dependence of the thermal conductivity of the LI-1500 rigid-surface insulation significantly affects the thermal sizing of the RSI.

Panel Temperature Distribution

Typical temperature histories and temperature distributions for 1 atmosphere for test panel Nos. 1, 2, 3, and 4 are shown in Figs. 6.3-6 through 6.3-9, respectively, as computed using a one-dimensional THERM model. All substrate temperatures reach their maximum values after the assumed touchdown of 3600 sec. For Area 2 where the maximum surface temperature is 2300^oF, the beryllium and titanium panels (Nos. 1 and 4) reach 600^oF at about 5000 sec. The aluminum test panel (No. 3)

reaches 300° F at about 8000 sec. For Area 1, where the maximum surface temperature is 1480° F, the aluminum test panel (No. 2) reaches 300° F at 4500 sec. A nonadiabatic boundary condition for the substrate would result in peak temperatures at earlier times and at lower temperatures for the adiabatically established LI-1500 thicknesses.

Temperature histories and temperature distributions for the flight panels are shown in Figs. 6.3-10 through 6.3-13, respectively. The beryllium and titanium panels (Nos. 1 and 4) reach their design temperature of 600° F at about touchdown (3600 sec), whereas aluminum panels (Nos. 2 and 3) reach their design temperature of 300° at about 6500 sec and 4000 sec, respectively.

The temperature distributions for both flight and test panels indicate that for a 2300° F maximum surface temperature, only about 0.15 in. of the material experiences temperatures greater than 2000° F.

Effect of Adiabatic Substrate on Test Conditions

The effect of an adiabatic boundary condition as specified by NASA, on the maximum attainable backface temperature in a test fixture where the TPS substrate radiates and convects to a 0.375 in. aluminum plate is shown in Fig. 6.3-14. A beryllium panel sized adiabatically for a 600° F maximum temperature requires 2.3 in. of LI-1500. Allowing the panel to radiate and convect energy to a 0.375 in. test fixture will limit the maximum beryllium temperature to 490° F. Hence, to achieve the design temperature on the beryllium panel during the test, the panel should either be sized with a nonadiabatic boundary condition or a piece of low-density insulation (i. e., dynaflex, fiberfrax, or LI-1500) should be attached to the bottom of the test fixture to limit the energy loss.



ASCENT TEMP. HISTORIES FOR AREA I

ASCENT TEMPS. NASA AREA I

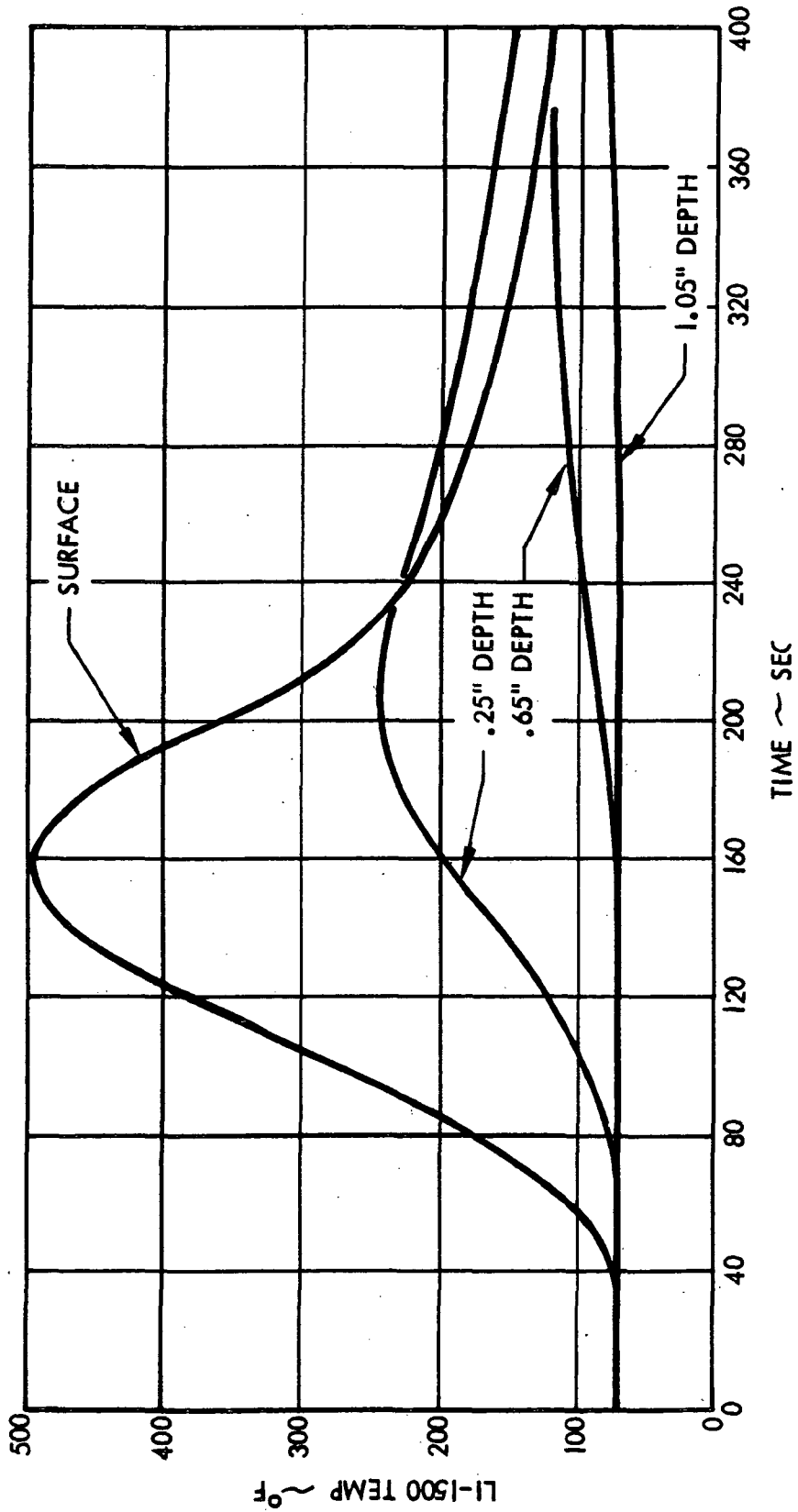
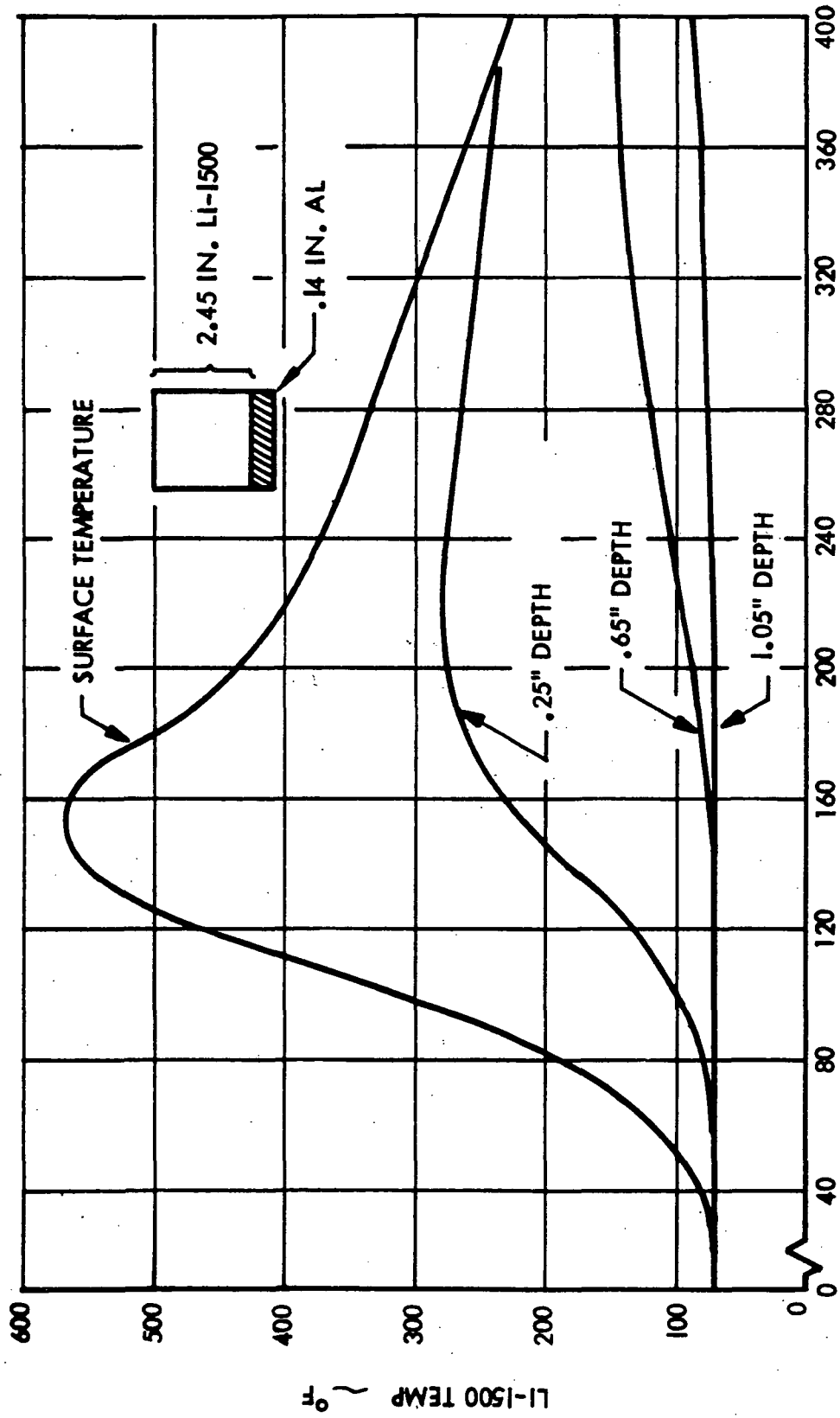


Fig. 6.3-1

6.3-3
273

ASCENT TEMP. HISTORIES FOR AREA 2



TIME ~ SECS.

Fig. 6.3-2



274 <
6.3-4

DO6057

ASCENT TEMPERATURE DISTRIBUTIONS AREA 2

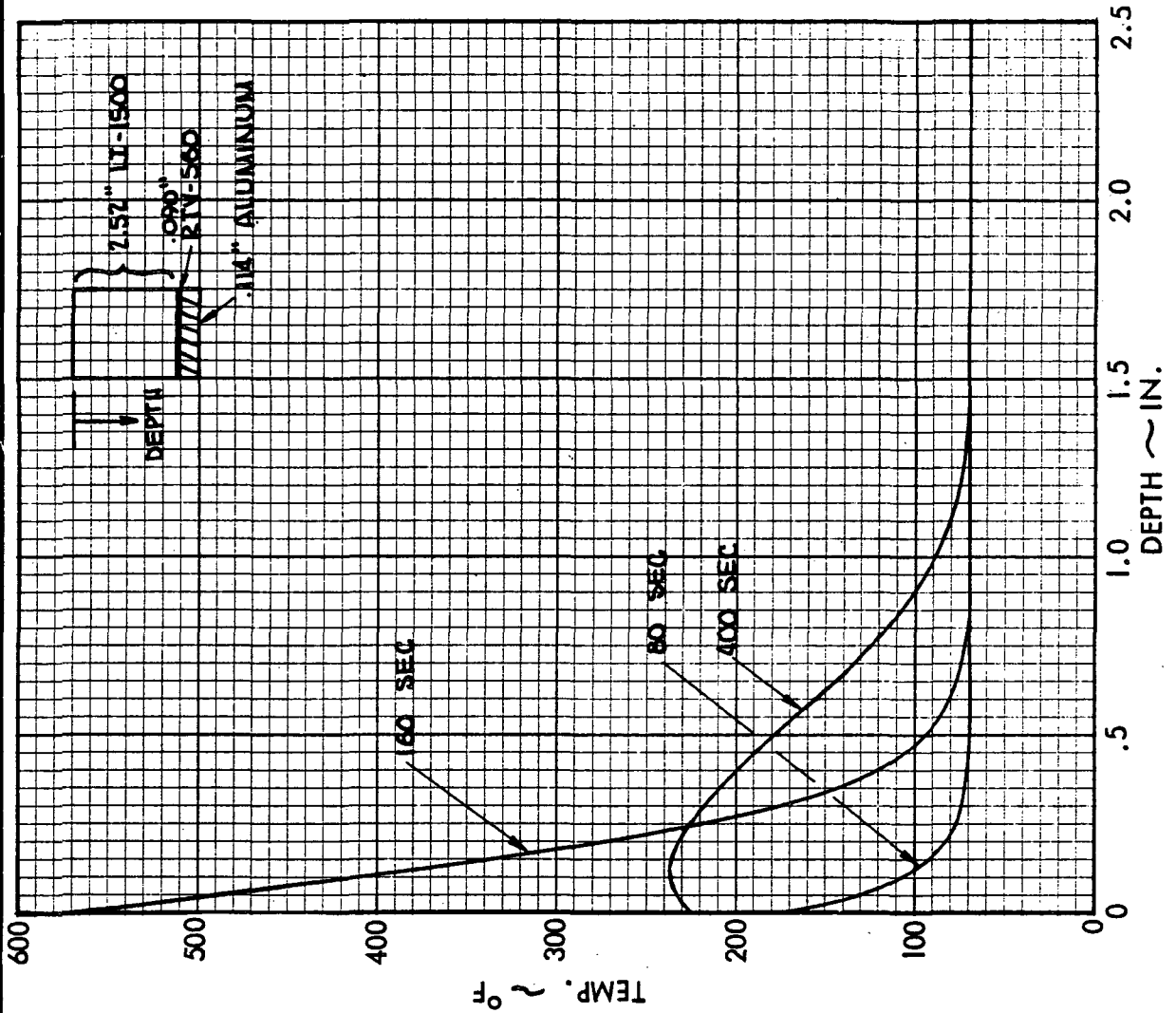


Fig. 6.3-3

DO6064





REENTRY TEMPERATURE AND PRESSURE HISTORIES - AREA I

$\epsilon = 0.8$ - EMITTANCE = 0.8

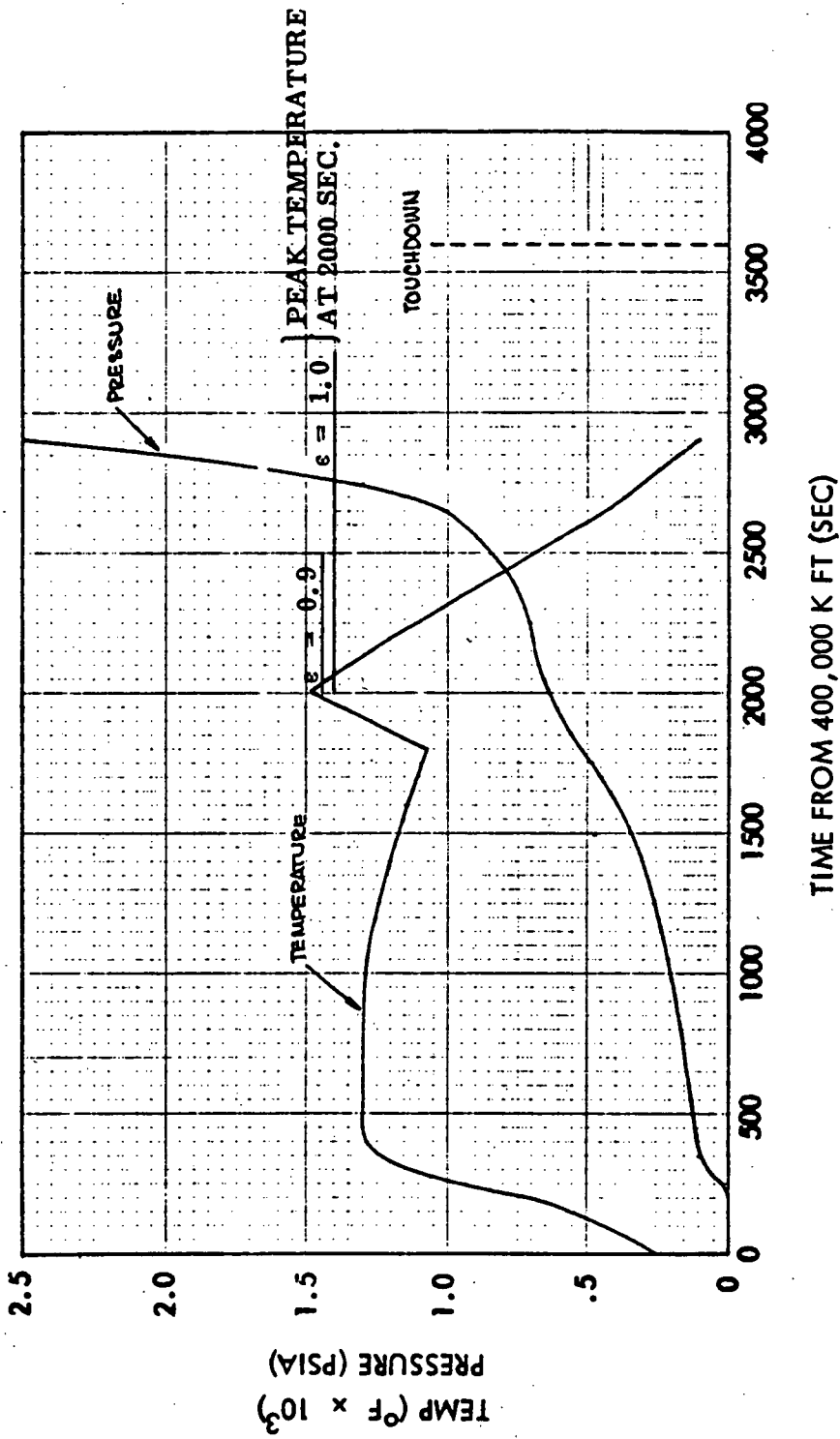


Fig. 6.3-4

DO6102

276 <

6.3-6

REENTRY TEMPERATURE AND PRESSURE HISTORIES
AREA 2



ϵ - EMITTANCE = 0.8

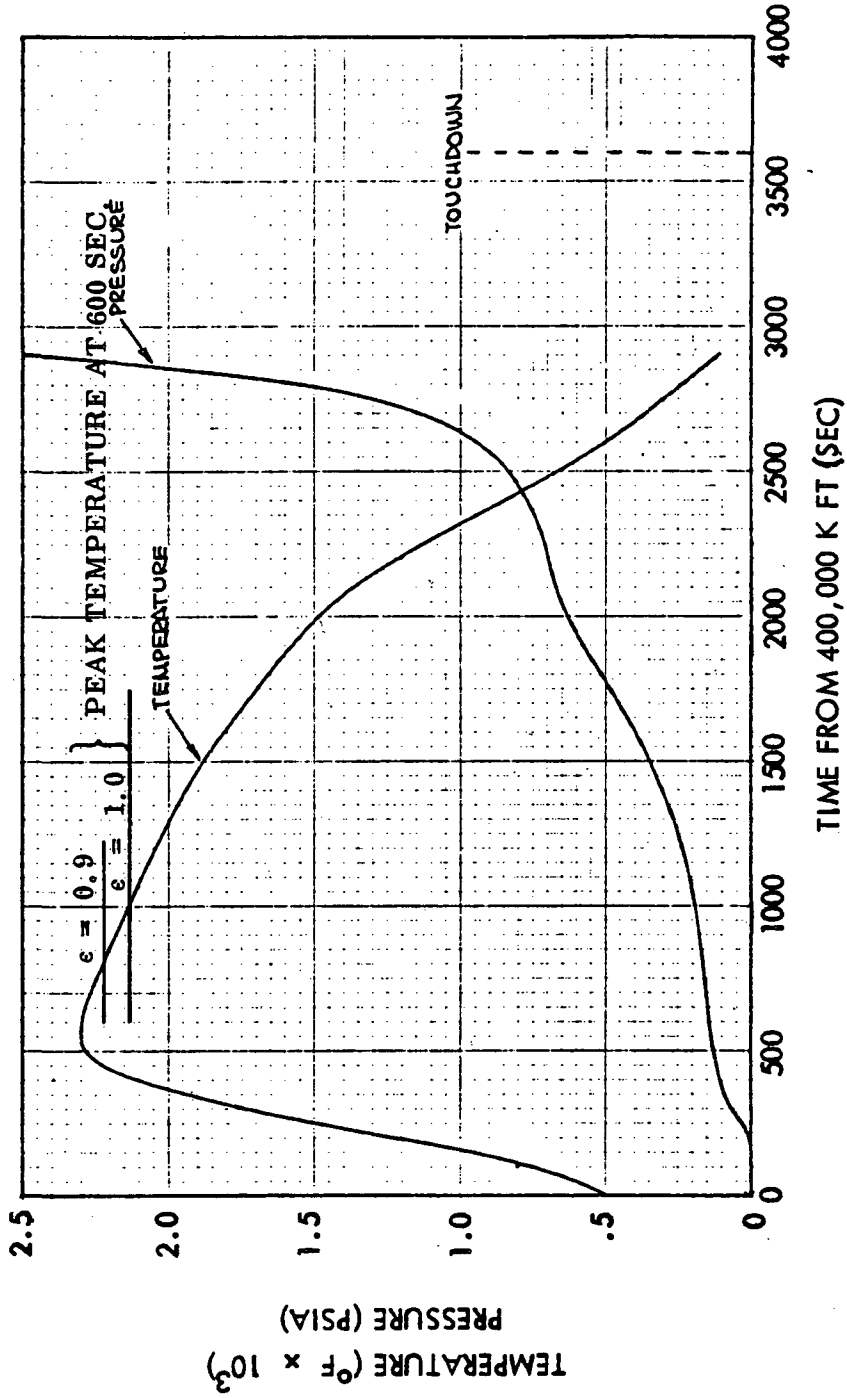
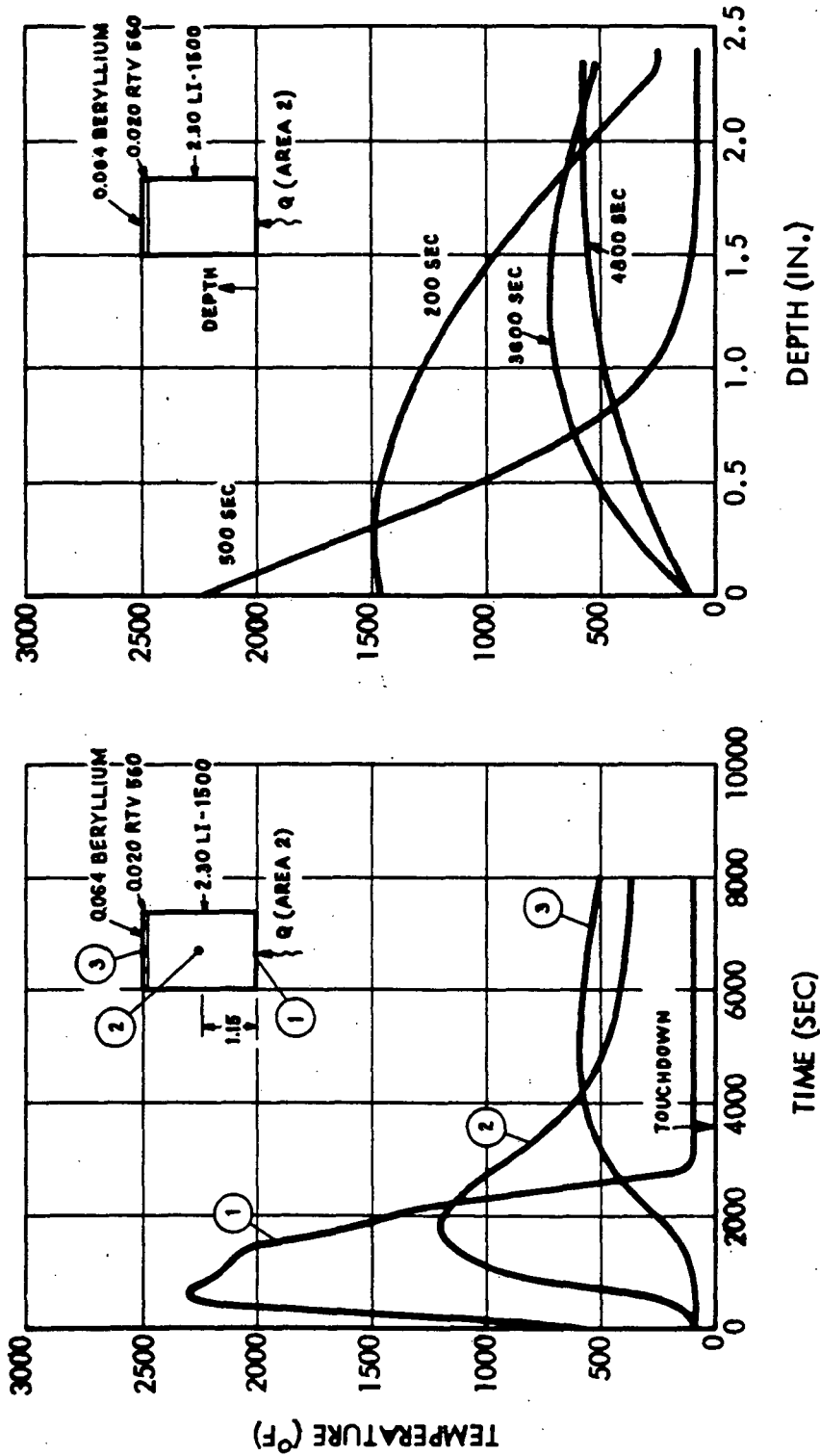


Fig. 6.3-5

6.3-7
277 <



TPS TEMPERATURE HISTORIES AND DISTRIBUTIONS TEST PANEL NO. 1



6.3-8
>822

Fig. 6.3-6

DO6103



TPS TEMPERATURE HISTORIES AND DISTRIBUTIONS TEST PANEL NO. 2

LMSC-D152738
Vol II

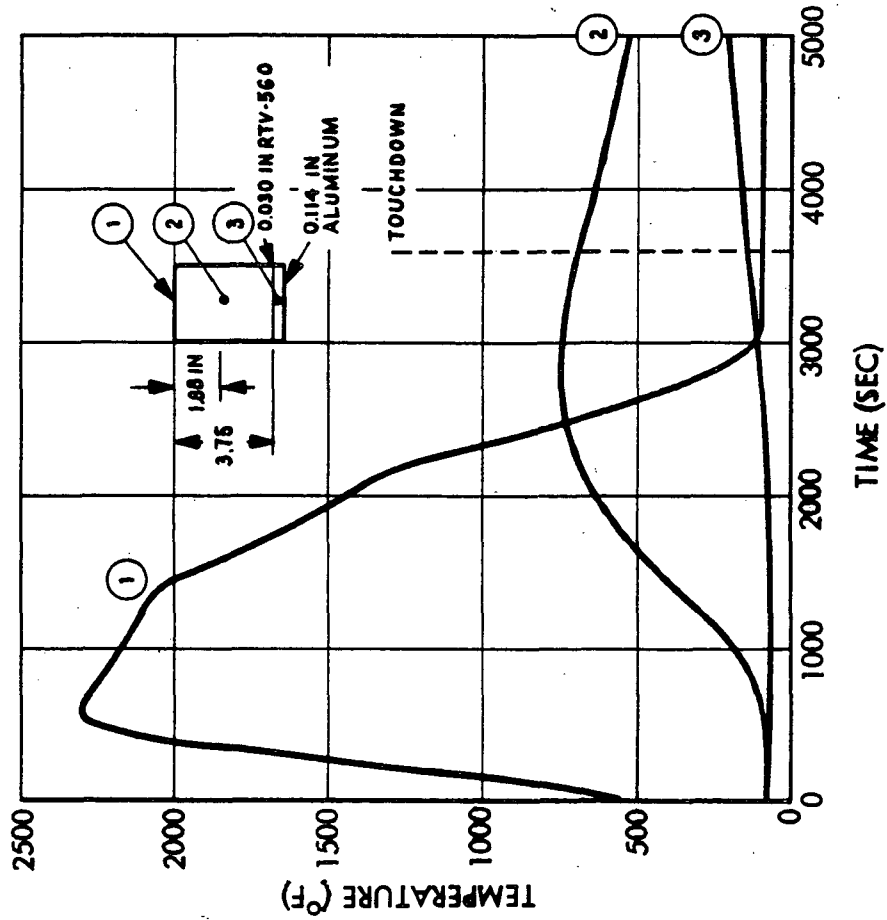
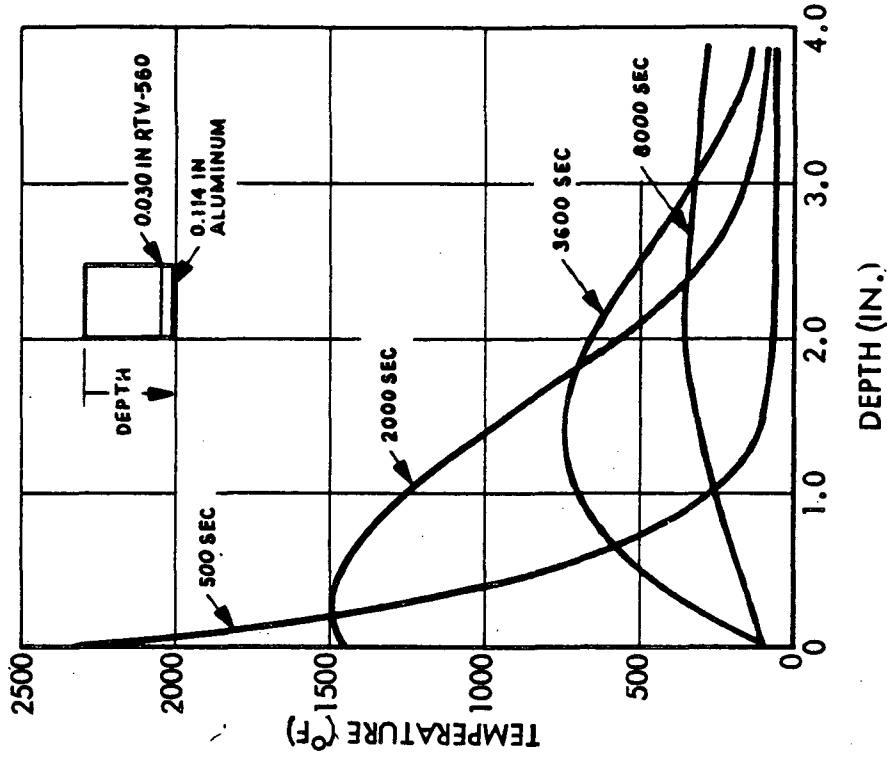
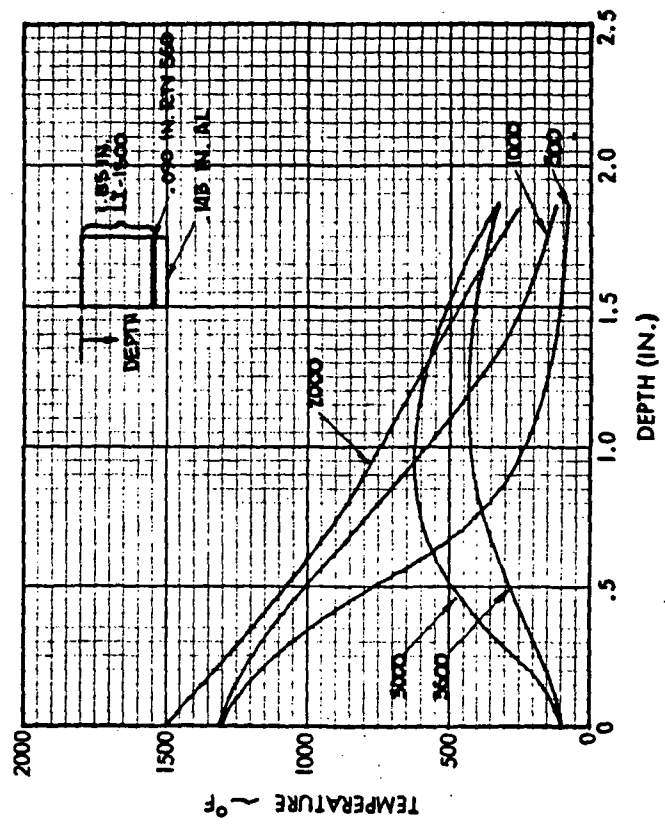
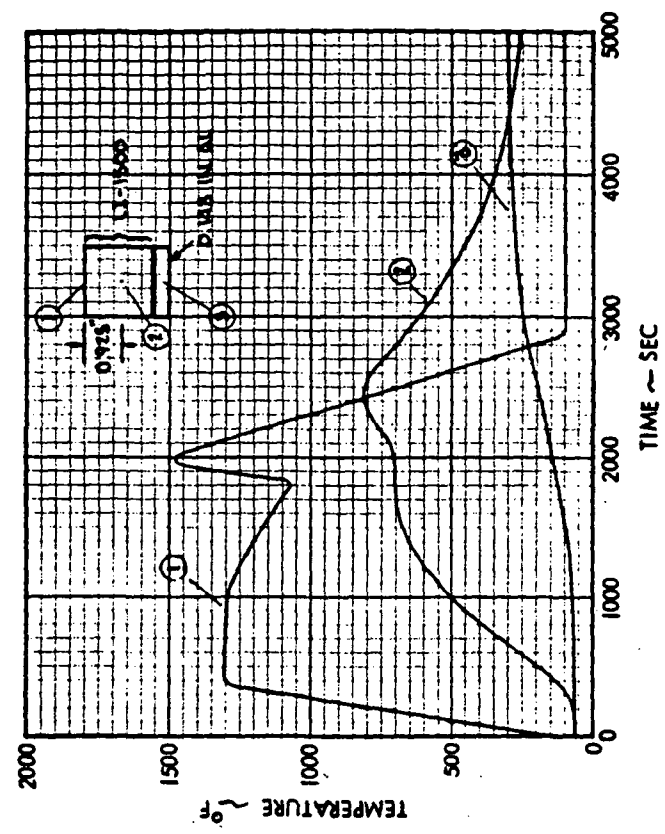


Fig. 6.3-7



TEMPERATURE HISTORIES AND DISTRIBUTIONS FOR TEST PANEL NO. 3

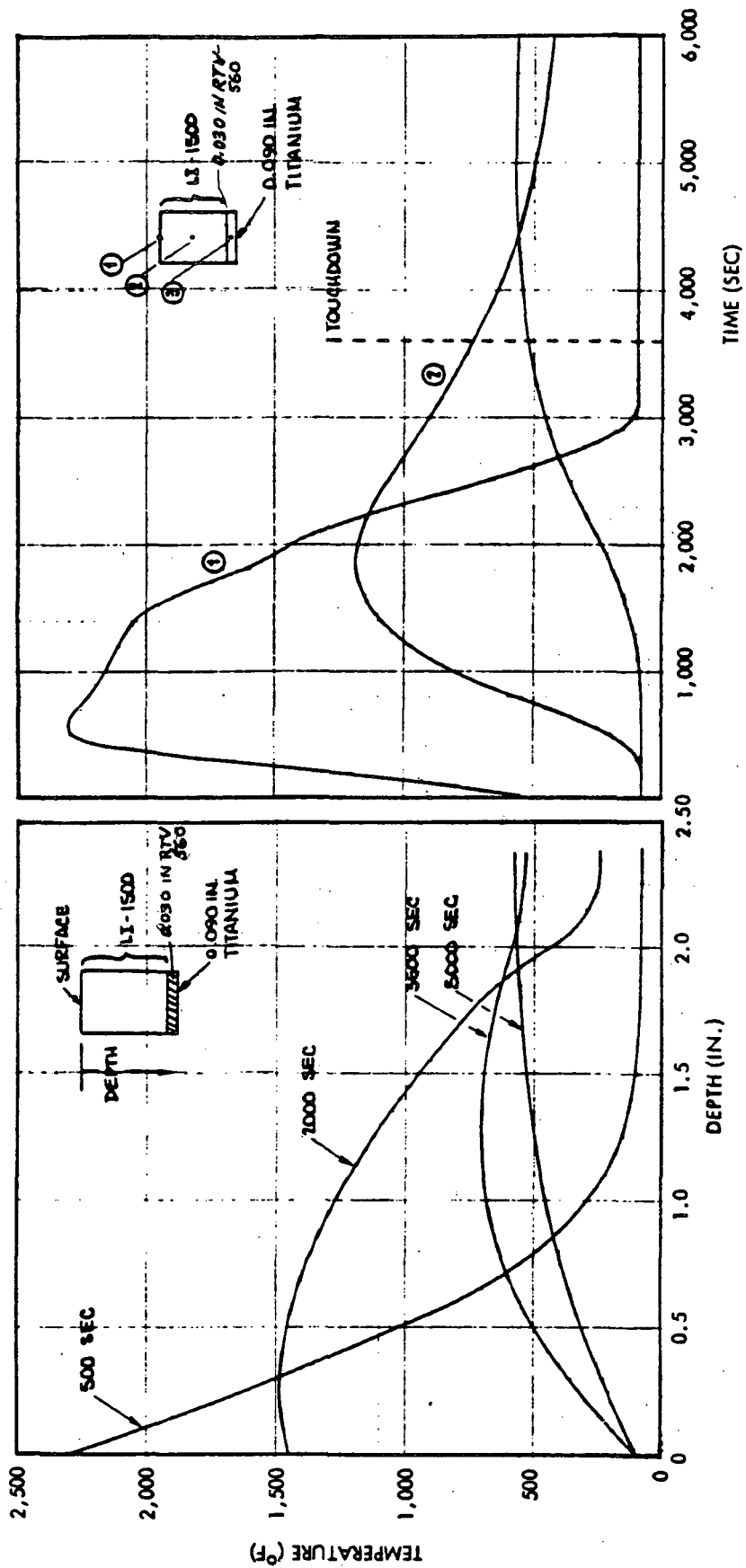


280

Fig. 6.3-8

DO6140

TPS TEMPERATURE HISTORIES & DISTRIBUTIONS TEST PANEL 4

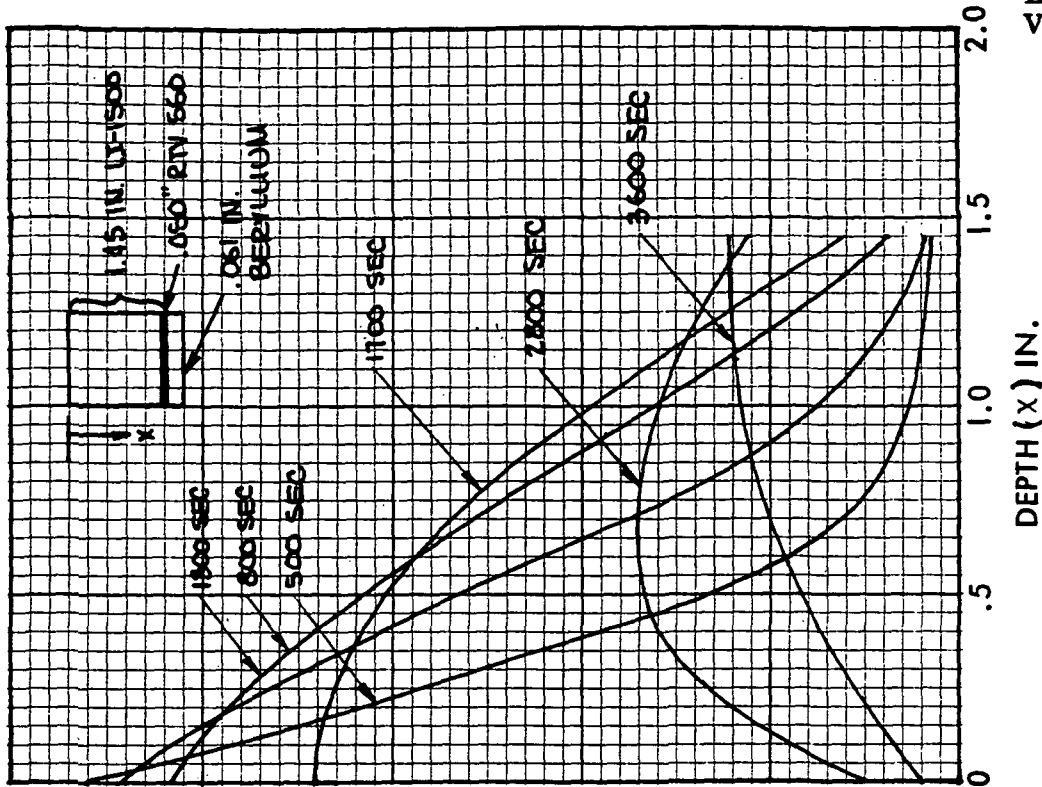
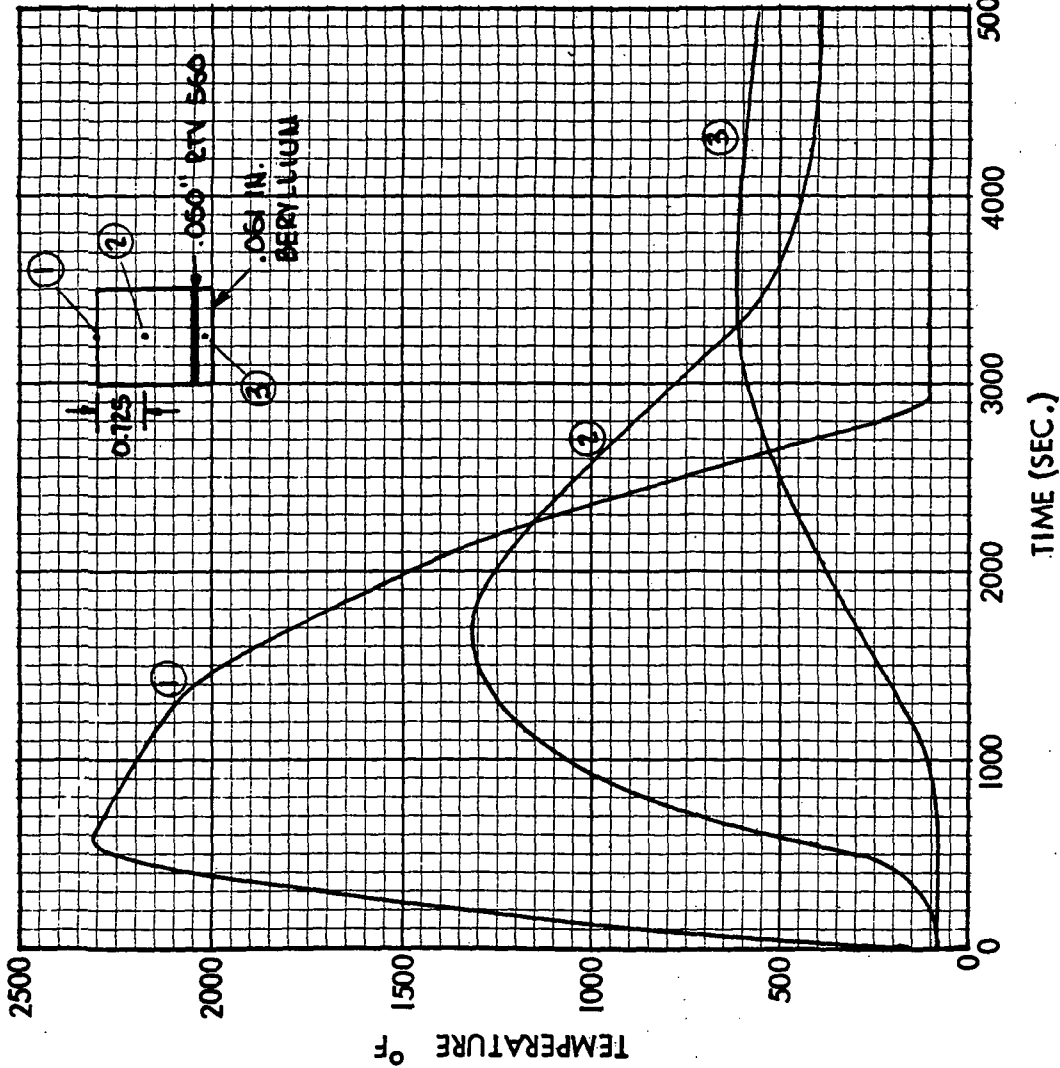


6.3-11
V181

Fig. 6.3-9

D05111

TEMPERATURE HISTORIES AND DISTRIBUTIONS FOR FLIGHT PANEL NO. 1



6.3-12 >282

Fig. 6.3-10



TEMPERATURE HISTORIES AND DISTRIBUTIONS FOR FLIGHT PANEL NO. 2

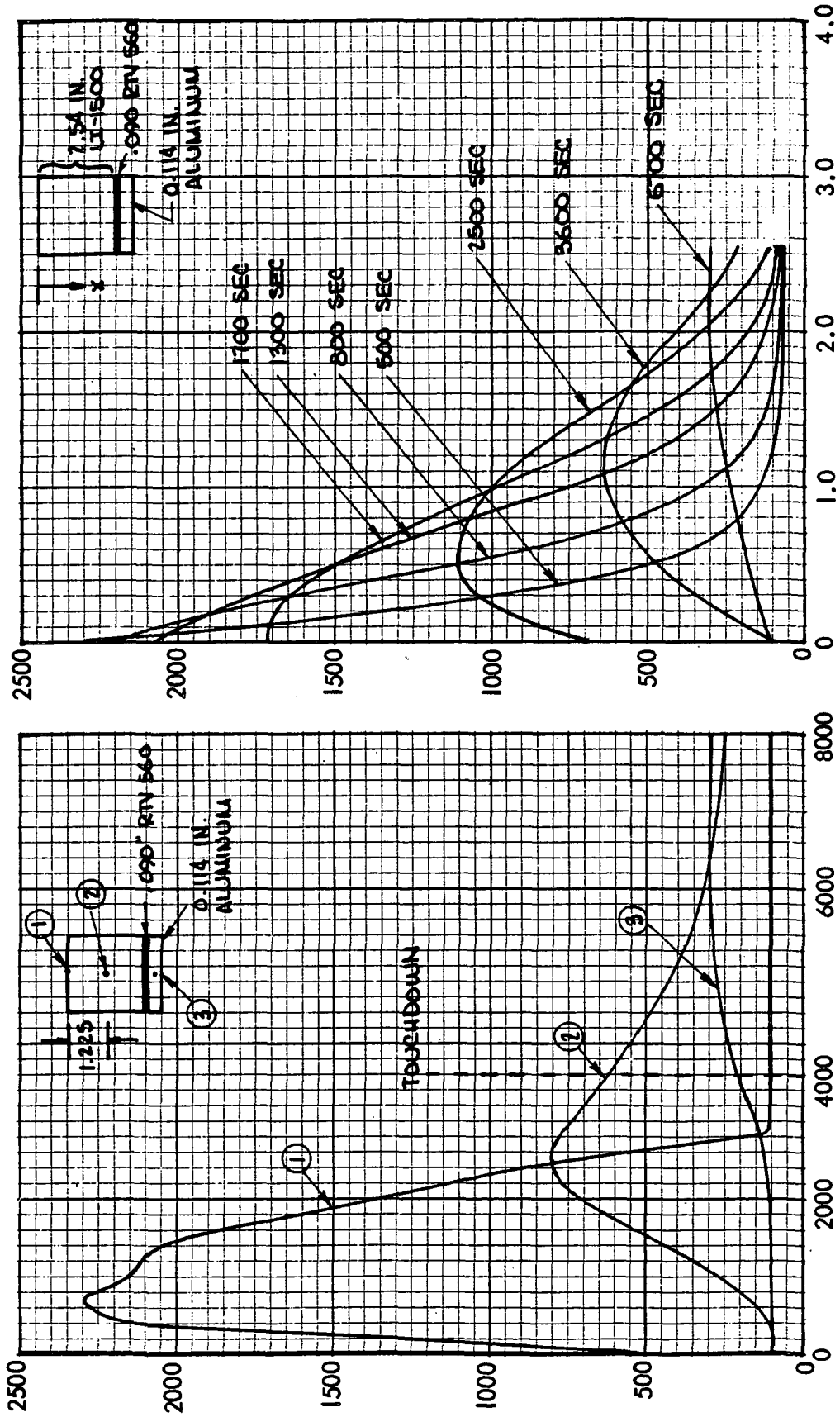
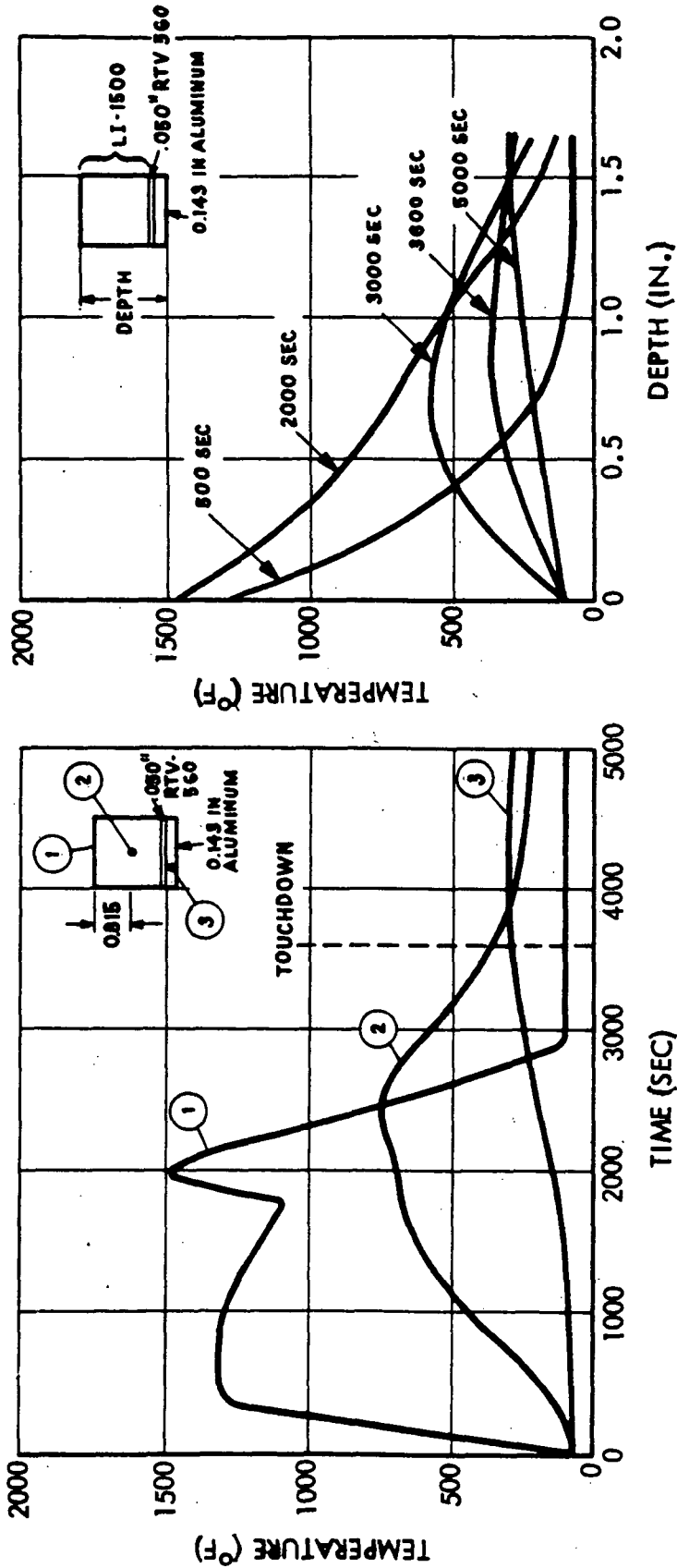


Fig. 6.3-11

DO6047

283
6.3-13

TPS TEMPERATURE HISTORIES AND DISTRIBUTIONS
 FLIGHT PANEL NO; 3



6.3-14
 > 284

Fig. 6.3-12

TPS TEMPERATURE HISTORIES AND DISTRIBUTIONS

FLIGHT PANEL NO. 4

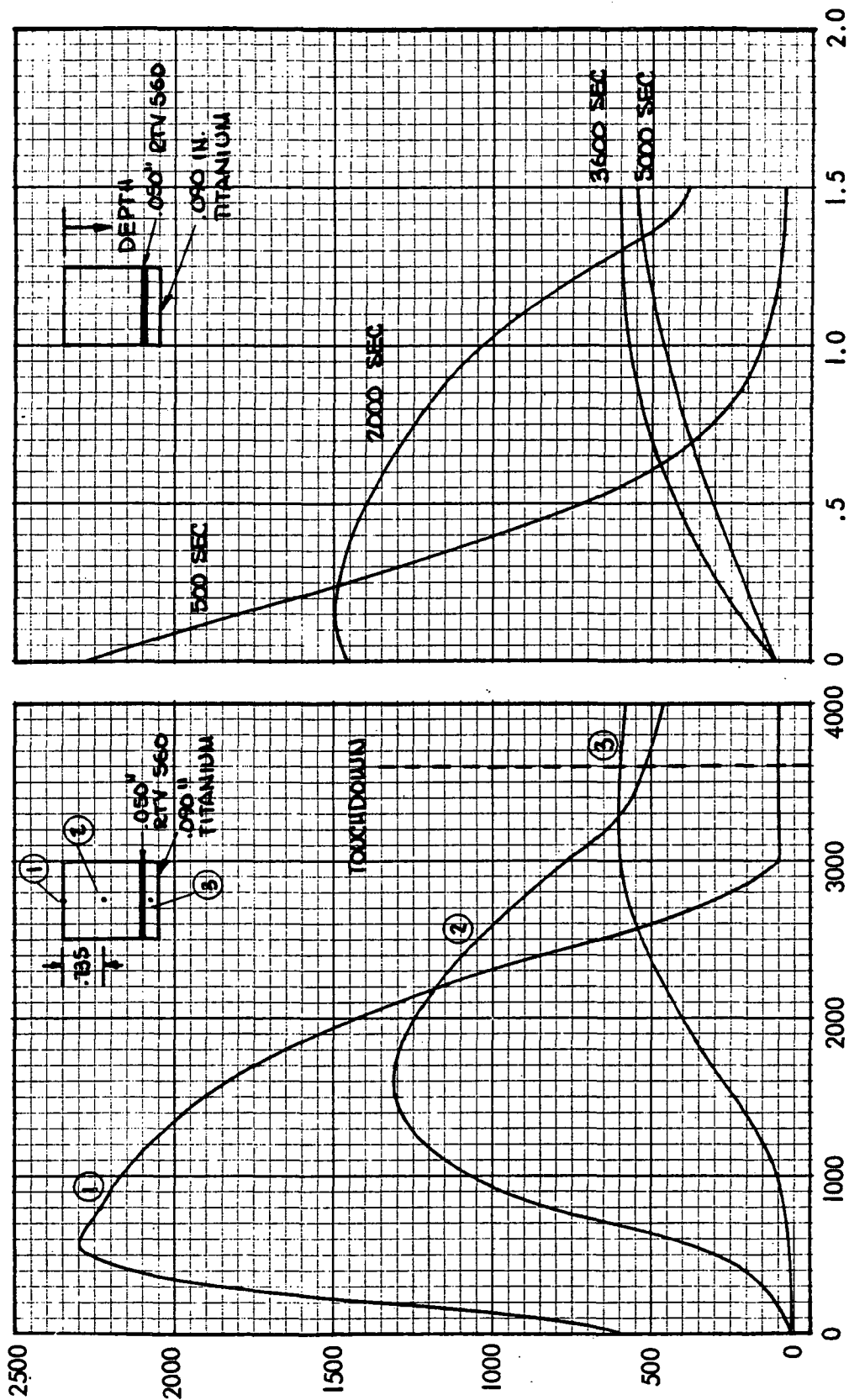


Fig. 6.3-13

DO5996

EFFECT OF SUBSTRATE BOUNDARY CONDITIONS ON
 MAXIMUM BERYLLIUM TEMPERATURE



AREA 2 - $Q_T = 26,534 \text{ BTU/FT}^2$

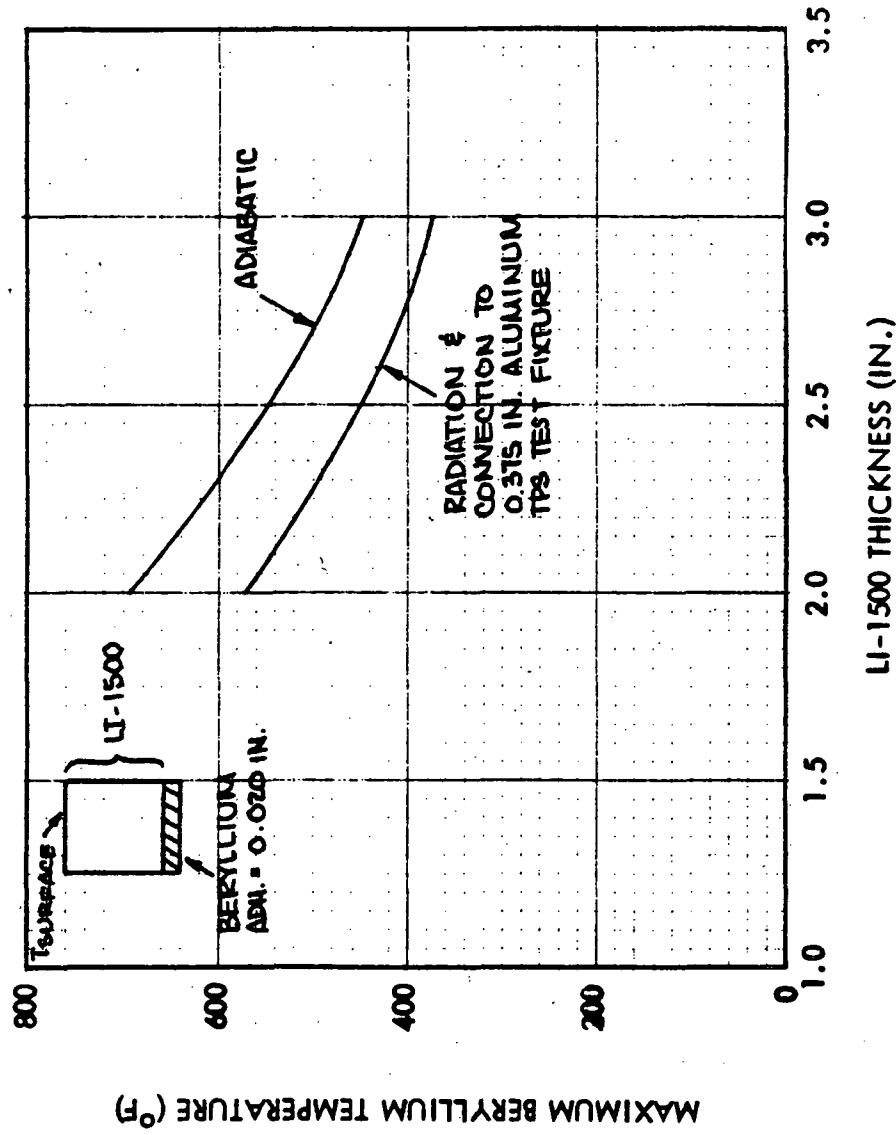


Fig. 6.3-14

DO6008

6.4 DESIGN AND ANALYSIS OF PROTOTYPE PANEL SUBSTRATES

On the basis of the data and results presented in the preceding sections of this report, the following material/configuration selections have been established for the four prototype panels:

Panel No.	Vehicle Area No.	Type	Material	Configuration
1	2	Subpanel	Beryllium	Zee-Stiffened
2	2	Primary Structure	Aluminum	Zee-Stiffened
3	1	Primary Structure	Aluminum	Zee-Stiffened
4	2	Primary Structure	Titanium	Zee-Stiffened

Detailed optimum design and analysis studies for the specific design requirements of NASA/MSD have been performed on each of these selections and are discussed below.

The orbiter design conditions presented in Table 6.1-1 may be summarized for purposes of the present analysis in the form shown in Table 6.4-1. Three load conditions are shown for each vehicle area. Load conditions I and II occur when the substrates are at room temperature, and load condition III occurs when the substrates are at or near the maximum temperatures shown in Note 1 to the figure. It has been conservatively assumed in these studies that any combination of line load and pressure for a given load condition may be applied simultaneously to the panel.

Optimum sizing of the four prototype panels was performed using the structural optimization computer codes previously discussed, followed by perturbations on these proportions as required for thermostructural optimization. The latter optimization produced modifications only to the substrate for prototype panel No. 1. The designs were subsequently subjected to a detailed stress analysis to determine minimum margins-of-safety. These analyses are presented in Appendixes B and C for prototype panel No. 1 and panel Nos. 2 through 4, respectively. Note that panel No. 3, representing Vehicle Area 1, has been sized for a panel span of 20 in., whereas the remaining panels have been sized for a panel span of 24 in.

Q.6

Table 6. 4-1

PROTOTYPE PANELS DESIGN LOADS - SUMMARY



LOAD COND.	IN-PLANE LINE LOAD (LB/IN.)			DIFFERENTIAL PRESSURE (LB/IN. ²)		
	TENSION		COMPRESSION	BURST		COLLAPSE
	LIM	ULT	LIM	LIM	ULT	LIM
AREA 1 PANELS						
I	2400	3600	2100	3150	4.5	3.0
II	2700	4050	4000	6000	2.25	2.0
III	4000	6000	2000	3000	0.75	2.0
AREA 2 PANELS						
I	2300	3450	1500	2250	4.5	6.0
II	2700	4050	2000	3000	2.85	2.7
III	4000	6000	2000	3000	0.75	3.0

NOTES:

1. PROTOTYPE PANEL CONFIGURATION NO.	LOAD AREA NO.	MAX TEMP COND III (°F)	PANEL SPAN (IN.)
1	2	600	24
2	2	250	24
3	1	250	20
4	2	600	24

- LOAD CONDITIONS I AND II AT ROOM TEMPERATURE
- LINE LOADS AND PRESSURES ACT IN ANY COMBINATION ON PANEL CONFIGURATIONS 2, 3, AND 4
- FACTOR OF SAFETY = 1.5
- PRESSURE ONLY ON PANEL I

DO6163

The minimum margins-of-safety for the four panels fall between 1 and 10 percent, as shown in Table 6.4-2. Note that the minimum margin-of-safety for prototype panel No. 1 occurs for loading condition I when the panel is at room temperature. Also, the minimum margin-of-safety for panel No. 2 occurs when the panel is at room temperature, but in the remaining two panels, the minimum margin-of-safety occurs when the panels are at or near the maximum temperature permitted.

Results of the beam-column analysis performed on panels 2 through 4 are summarized in Table 6.4-3. Note that maximum deflections between approximately 0.09 in. and 0.19 in. are predicted. Approximately one-half of the deflection is caused by bending due to airloads in prototype panels 2 and 4, which represent Vehicle Area 2. Panel No. 3, representing Vehicle Area 1, is subject to much higher axial loads over a shorter span; thus, the deflection due to airloads is a much smaller proportion of the total deflection in this panel.

Table 6.4-4 summarizes the zee-stiffener sizes for panels 2, 3 and 4. The results labeled (a) correspond to optimum sizes obtained by the wide-column analysis discussed earlier. However, the weldbond method of attaching the zee-stiffeners to the face sheet requires more flange width than that originally assumed in the optimization process. This additional width allows full development of the spotweld nugget without interference with the flange radius and provides sufficient distance to the edge to preclude cracking. For the titanium riveted panel, a wider flange also is required for manufacturing. The flange widths have been increased to an acceptable dimension and are labeled as (c) in Table 6.4-4. As shown, these increases result in a design slightly heavier than the structural optimum. The panels fabricated for delivery to NASA/MSC utilize these wider flange widths.

Additional analysis were performed using the PRIPAN code (described previously) with the attach flange width held constant at the manufacturing minimum. As shown for the sections labeled as (d), the optimum with this constraint will incorporate a closer zee-spacing. However, the weight differences will be minor and, as discussed earlier, sections with very close zee-spacing must be discounted for manufacturing reasons.

MINIMUM MARGINS OF SAFETY SUMMARY - PROTOTYPE PANELS



CONFIGURATION NO.	ELEMENT	M.S.	FAILURE MODE	CRITICAL LOAD COND
1	PANEL ASSEMBLY	+ 0.34	TENSION - ULTIMATE	I
	STIFFENER ONLY	+ 0.05	LOCAL BUCKLING	I
	FACE SHEET	+ 0.41	BENDING - ULTIMATE	I
	CLOSURE ANGLE	+ 0.12	LOCAL BUCKLING	I
	STIFFENER LEG	+ 0.34	LOCAL BUCKLING	I
2	PANEL ASS'Y	+ 0.82	COLUMN BUCKLING	III
	STIFFENER LEG	+ 0.15	CRIPPLING	II
	STIFFENER LEG	+ 0.06	TENSION - ULTIMATE	III
	STIFFENER LEG	+ 0.28	BEARING - ULTIMATE	III
	FACE SHEET	+ 0.59	LOCAL BUCKLING	III
3	PANEL ASS'Y	+ 0.45	COLUMN BUCKLING	II
	STIFFENER LEG	+ 0.10	CRIPPLING	II
	STIFFENER LEG	+ 0.36	TENSION - ULTIMATE	III
	STIFFENER LEG	+ 0.62	BEARING - ULTIMATE	III
	FACE SHEET	+ 0.49	LOCAL BUCKLING	II
4	PANEL ASS'Y	+ 0.67	COLUMN BUCKLING	III
	STIFFENER LEG	+ 0.18	CRIPPLING	III
	STIFFENER LEG	+ 0.29	TENSION - ULTIMATE	III
	STIFFENER LEG	+ 0.62	BEARING - ULTIMATE	III
	FACE SHEET FASTENERS	+ 0.01	LOCAL BUCKLING	III
		+ 1.2	SHEAR - ULTIMATE	III

M.S. = ALLOWABLE LOAD / ULTIMATE LOAD - 1

Table 6.4-3

BEAM - COLUMN ANALYSIS RESULTS FOR PANELS 2-4

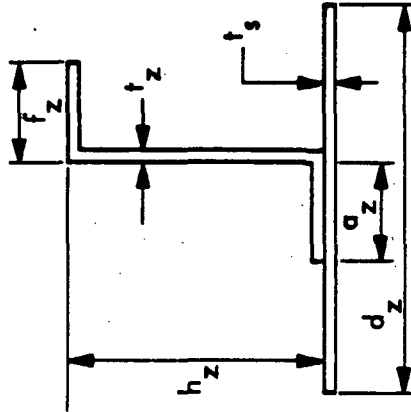


PANEL NO.	MAXIMUM DEFLECTION (IN.)		MAX OUTER FIBER STRESS (PSI)	CRITICAL LOAD CONDITION
	BENDING ALONE	BEAM COLUMN		
2 ($L = 24$ IN.)	0.089	0.163	30,924	I (COLLAPSE PRESSURE)
	0.067	0.122		
3 ($L = 20$ IN.)	0.016	0.087	60,246	I (BURST PRESSURE)
	0.096	0.186		
4 ($L = 24$ IN.)	0.072	0.140	52,561	I (COLLAPSE PRESSURE)

DO5024

Table 6.4-4

ZEE - STIFFENER SIZES - PANELS 2, 3 AND 4



$$\bar{f} = t_s + \frac{t}{d_z} (a_z + h_z + f_z)$$

PANEL	\bar{f}	d_z	t_s	t_z	a_z	h_z	f_z	WEIGHT (lb/ft ²)
2 - a	0.1144	1.60	0.050	0.050	0.40	1.36	0.40	1.83
c	0.1253	1.60	0.050	0.050	0.75	1.36	0.40	
d	0.1298	1.55	0.050	0.050	0.75	1.20	0.52	
d	0.1268	0.99	0.032	0.040	0.75	1.19	0.41	
3 - a	0.1431	1.60	0.063	0.063	0.48	1.20	0.48	2.24
c	0.1537	1.60	0.063	0.063	0.75	1.20	0.48	
d	0.1426	1.34	0.050	0.050	0.75	1.35	0.39	
4 - a	0.0895	1.60	0.040	0.040	0.41	1.24	0.41	2.23
c	0.0970	1.60	0.040	0.040	0.56	1.24	0.56	
d	0.1112	1.08	0.040	0.040	0.56	0.98	0.38	
d	0.1084	1.35	0.050	0.040	0.56	1.03	0.38	



To conclude this subsection, the weights of the metallic portion of all four deliverable panels (with no allowance for fasteners or closeouts) are summarized below:

<u>Panel No.</u>	<u>t (in.)</u>	<u>Panel Wt. (lb/ft²)</u>
1	0.064	0.57
2	0.125	1.83
3	0.154	2.24
4	0.097	2.23

6.5 RSI TILE ANALYSIS

This section summarizes the final design of tile size and bond thickness for the deliverable prototype panels. As shown in Section 6.2, LI-1500 conductivity is a function of environmental pressure; therefore, different LI-1500 thicknesses are required for a "flight" panel as opposed to a 1 atmosphere "test" panel. Eight panel designs are summarized here. Per NASA/MSC direction, the deliverable panels are to correspond to flight environment; hence, only the flight panel designs have been reassessed since the midterm report.

At this point in the design, the metallic substrate already has been determined and LI-1500 thickness/bond thickness requirements have been established in the form of the heat sink tradeoff factor. The final step in the design process then consists of choosing a balanced set of LI-1500 and bond thicknesses in conjunction with a tile length that also satisfies stress allowables.

Final analysis results for the deliverable prototype panels are given in Tables 6.5-1 through 6.5-4. Tables 6.5-5 through 6.5-8 represent previous analysis results of the "test" panels, sized for 1 ATM conductivity values of LI-1500. Table 6.5-9 summarizes required RSI system thicknesses and lists weight comparisons between flight and test prototype panels.

As compared with preliminary designs for the 4 October review (and presented in LMSC-A995708), tile length has been increased for all panels as has been discussed in the midterm report. For the beryllium and titanium panels, bond modulus at elevated temperature (500^oF) is used, which is in contrast to the room temperature properties temporarily assumed previously. Data given in Table 6.2-7 show reduced moduli at temperature; hence, strain isolation of the RSI tile is improved.

For the aluminum panels, room temperature properties of RTV-560 were used (as before) due to lack of data at 250^oF and 300^oF, leading to a degree of conservatism. Increase in tile length for these panels was permissible, since the LI-1500 weak-direction shear allowable is actually larger than previously reported in LMSC-A995708.

of course, this increase in a critical design parameter also contributes to the longer tile lengths selected for the beryllium and titanium panels.

Flight panel designs have been evaluated for stress levels associated with thermal expansion in the direction perpendicular to the stiffeners. To accomplish this, the spring-supported 2-D WILSON model, described in Section 2.3, was used. The results of these calculations have no effect upon panel designs as presented in the midterm report. Although LI-1500 stress levels in the beryllium flight panel are somewhat higher in that direction, they are within allowables. For the other panel designs, transverse direction analysis leads to lower stress levels than in the stiffened direction, due to the lack of an in-plane line load. This is readily seen in Table 6.5-10 for the Aluminum Flight Panel No. 2 comparisons. Similar results hold for other primary structure panels; hence maximum stress levels listed in Tables 6.5-2 through 6.5-4 correspond to 2-D analyses in the stiffener direction.

3-D Coating Stress Analysis

Because of possible cracking of high modulus surface coatings, which extend down the sides of RSI tiles, NASA requested LMSC to determine coating stresses for a typical LI-1500 tile. A two-dimensional thermal model was constructed for a 6 in. x 6 in. tile, which included the 0042 coating, LI-1500, adhesive, and the aluminum substrate for flight panel No. 2. The LI-1500 thermal/mechanical properties were assumed to be isotropic. The temperature distributions at 500 sec into the entry trajectory (see Fig. 6.3-11) are shown for a location at the midpoint of the tile and for the corner of the tile in Figs. 6.5-1. As would be expected, a large temperature gradient is indicated through the LI-1500. This gradient is slightly less in the nodes adjacent to the coating. From these results, the three-dimensional temperature field for the tile shown in Fig. 6.5-2 was estimated.

Based upon Fig. 6.5-2, a 3-D SAP analysis was made of the tile/bond/substrate; the resulting coating stresses are shown in Fig. 6.5-3. These results use the most recent thermal expansion test data for the 0042 coating (reported in Section 4, Vol 1 of this report) which is somewhat higher than that previously used (4×10^{-7} in./in. $^{\circ}$ F as compared with 2×10^{-7} in./in. $^{\circ}$ F). Since the thermal expansion of LI-1500 is 3×10^{-7} in./in. $^{\circ}$ F, the coating in the present analysis is in compression and is well within the allowables shown in Table 6.2-1.

Table 6.5-1

**BERYLLIUM FLIGHT PANEL NO. 1
ORBITER FUSELAGE AREA 2**

COATING THICK = 0.010 IN. LI-1500 THICK = 1.224 IN. RTV-560 THICK = 0.090 IN. TILE LENGTH = 12 IN.

LOADING CONDITIONS	PRESSURE (PSI) AXIAL LOAD	6.75 COLLAPSE	3 COLLAPSE *	1.5 BURST *	0 *
TEMPERATURE	SURFACE (°F) BACKFACE (°F)	75 75	100 550	100 550	75 600
LI-1500	PRIN. TEN.	35	60	64	64
	PRIN. COMP.	- 17	- 32	- 25	- 31
	SHEAR	8	12	12	14
	LONG.	35	60	64	64
RTV-560	NORMAL TEN.	3	5	12	9
	NORMAL COMP.	- 13	- 6	- 5	- 4
	PRIN. TEN.	5	11	19	16
	PRIN. COMP.	- 17	- 17	- 17	- 17
COATING	SHEAR	4	10	10	11
	LONG.	- 7	- 14	- 13	- 13
	PEEL	3	6	14	10
	PRIN. TEN. PRIN. COMP.	0 -2207	6 -310	1283 0	598 - 86
MATERIAL PROPERTIES	E (PSI)	G (PSI)	μ	α (IN./IN./F°)	
COATING LI-1500 RTV-506	9.1 x 10 ⁶ 60,000 (L), 6,000 (T) 300 (RT) - 200 (500°-600° F)	3.9 x 10 ⁶ 4150 100 (RT) - 67 (500°-600° F)	0.17 0.3 0.5	0.2 x 10 ⁻⁶ 0.3 x 10 ⁻⁶ 115.0 x 10 ⁻⁶	
	42 x 10 ⁶ (RT) - 37.2 x 10 ⁶ (600° F)	20 x 10 ⁶ (RT) - 18.8 x 10 ⁶ (600° F)	0.1	5.15 x 10 ⁻⁶ (RT) 7.7 x 10 ⁻⁶ (600° F)	

* EXCEPT FOR COATING STRESS ALL VALUES CORRESPOND TO PANEL EXPANSION
IN DIRECTION PERPENDICULAR TO STIFFENERS

DO7042

25
65
67
7

Table 6.5.2

ALUMINUM FLIGHT PANEL NO. 2
ORBITER FUSELAGE AREA 2

COATING THICK = 0.010 IN. LI-1500 THICK = 2.524 IN. RTV-560 THICK = 0.090 IN. TILE LENGTH = 6 IN.

LOADING CONDITIONS	PRESSURE (PSI) AXIAL/LOAD (PPI)	6.75 COLLAPSE 2250 COMPRESSION	3 COLLAPSE 3000 COMPRESSION	1.5 BURST 6000 TENSION	0 0
TEMPERATURE	SURFACE (°F) BACKFACE (°F)	75 75	100 250	100 250	75 300
LI-1500	PRIN. TEN.	6	13	61	23
	PRIN. COMP.	- 17	- 7	- 32	- 16
	SHEAR	7	3	19	8
	LONG.	- 12	13	61	23
RTV-560	NORMAL TEN.	4	2	8	3
	NORMAL COMP.	- 8	- 3	- 6	- 3
	PRIN. TEN.	4	2	22	6
	PRIN. COMP.	- 13	- 9	- 17	- 10
COATING	SHEAR	6	2	18	7
	LONG.	- 5	- 8	- 6	- 7
	PEEL	4	2	8	3
	PRIN. TEN. PRIN. COMP.	1 - 45	56 0	16 - 44	2 - 50
MATERIAL PROPERTIES	E (PSI)	G (PSI)	μ	α (IN./IN./F°)	
COATING	9.1 x 10 ⁶ 60,000 (L), 6,000 (T) 300 (RT - 300°F) 10.5 x 10 ⁶ (RT) - 9.5 x 10 ⁶ (300°F)	3.9 x 10 ⁶ 4150 100 (RT - 300°F) 4.2 x 10 ⁶ (RT) - 3.66 x 10 ⁶ (300°F)	0.17 0.3 0.5 0.3	0.2 x 10 ⁻⁶ 0.3 x 10 ⁻⁶ 115.0 x 10 ⁻⁶ 13.1 x 10 ⁻⁶ (RT) - 13.5 x 10 ⁻⁶ (300°F)	

DO7043

6.5.4
2021

Table 6.5-3

ALUMINUM FLIGHT PANEL NO. 3
ORBITER FUSELAGE AREA 1

COATING THICK = 0.010 IN. LI-1500 THICK = 1.334 IN. RTV-560 THICK = 0.090 IN. TILE LENGTH = 6 IN.

LOADING CONDITIONS	PRESSURE (PSI) AXIAL LOAD (PPI)	3.75 COLLAPSE 3150 COMPRESSION	3.0 COLLAPSE 3000 COMPRESSION	1.5 BURST 6000 TENSION	0
TEMPERATURE	SURFACE (°F) BACKFACE (°F)	75 75	100 250	100 250	75 300
LI-1500	PRIN. TEN.	8	18	57	26
	PRIN. COMP.	- 18	- 5	- 30	- 20
RTV-560	SHEAR	7	3	17	8
	LONG.	- 14	17	57	24
	NORMAL TEN.	2	1	8	3
	NORMAL COMP.	- 5	- 3	- 4	- 2
COATING	PRIN. TEN.	3	1	19	6
	PRIN. COMP.	- 10	- 8	- 14	- 10
	SHEAR	6	1	15	6
	LONG.	- 3	- 7	- 6	- 8
PEEL	2	1	8	3	
MATERIAL PROPERTIES	E (PSI)	34	34	8	2
		- 66	- 51	- 171	- 127
COATING LI-1500 RTV-560 SUBSTRATE	E (PSI)	G (PSI)		μ	α (IN./IN./F°)
		3.9×10^6			
		4150			
		100 (RT - 300°F)			
		4.2 x 10 ⁶ (RT) -			
SUBSTRATE	E (PSI)	3.16 x 10 ⁶ (300°F)		0.17	0.2 x 10 ⁻⁶
		9.15 x 10 ⁶ (600°F)			
		60,000 (L), 6,000 (T)			
SUBSTRATE	E (PSI)	100 (RT - 300°F)		0.3	0.3 x 10 ⁻⁶
		10.5 x 10 ⁶ (RT) -			
SUBSTRATE	E (PSI)	3.16 x 10 ⁶ (300°F)		0.5	115.0 x 10 ⁻⁶
		9.15 x 10 ⁶ (600°F)			
SUBSTRATE	E (PSI)	4.2 x 10 ⁶ (RT) -		0.3	13.1 x 10 ⁻⁶ (RT) -
		3.16 x 10 ⁶ (300°F)			
SUBSTRATE	E (PSI)	3.16 x 10 ⁶ (300°F)		0.3	13.5 x 10 ⁻⁶ (300°F)
		9.15 x 10 ⁶ (600°F)			



Table 6.5-4

TITANIUM FLIGHT PANEL NO. 4
ORBITER FUSELAGE AREA 2

COATING THICK = 0.010 IN. LI-1500 THICK = 1.234 IN. RTV-560 THICK = 0.090 IN. TILE LENGTH = 6 IN.

LOADING CONDITIONS	PRESSURE (PSI) AXIAL LOAD (PPI)	6.75 COLLAPSE 2250 COMPRESSION	3 COLLAPSE 3000 COMPRESSION	1.5 BURST 6000 TENSION	0 0
TEMPERATURE	SURFACE (°F) BACKFACE (°F)	75 75	100 550	100 550	75 600
LI-1500	PRIN. TEN.	4	21	49	24
	PRIN. COMP.	- 14	- 8	- 22	- 14
RTV-560	SHEAR	6	4	13	7
	LONG.	- 10	20	49	22
	NORMAL TEN.	3	1	6	2
	NORMAL COMP.	- 7	- 2	- 3	- 1
COATING	PRIN. TEN.	4	1	13	4
	PRIN. COMP.	- 12	- 12	- 16	- 12
	SHEAR	5	0	13	5
	LONG.	- 4	- 12	- 12	- 12
MATERIAL PROPERTIES	E (PSI)	G (PSI)	μ	α (IN./IN./°F)	
COATING LI-1500 RTV-560	9.1 x 10 ⁶ 60,000 (L), 6,000 (T) 300 (RT) - 200 (500°-600°F) 16 x 10 ⁶ (RT) - 13.1 x 10 ⁶ (600°F)	3.9 x 10 ⁶ 4150 100 (RT) - 67 (500°-600°F) 6.4 x 10 ⁶ (RT) - 5.2 x 10 ⁶ (600°F)	0.17 0.3 0.5	0.2 x 10 ⁻⁶ 0.3 x 10 ⁻⁶ 115.0 x 10 ⁻⁶	
SUBSTRATE			0.3	5.8 x 10 ⁻⁶ (RT - 600°F)	

Table 6.5-5

**BERYLLIUM TEST PANEL NO. 1
ORBITER FUSELAGE AREA 2**

COATING THICK = 0.010 IN. LI-1500 THICK = 1.887 IN. RTV-560 THICK = 0.090 IN. TILE LENGTH = 12 IN.

LOADING CONDITIONS	PRESSURE (PSI) AXIAL LOAD (PPI)	6.75 COLLAPSE	3 COLLAPSE	1.5 BURST	0
TEMPERATURE	SURFACE (°F) BACKFACE (°F)	75 75	100 550	100 550	75 600
LI-1500	PRIN. TEN.	31			
	PRIN. COMP.	- 21			
RTV-560	SHEAR	8			
	LONG.	31			
	NORMAL TEN.	5			
	NORMAL COMP.	- 17			
COATING	PRIN. TEN.	6			
	PRIN. COMP.	- 20			
	SHEAR	4			
	LONG. PEEL	9 5			
MATERIAL PROPERTIES	PRIN. TEN. PRIN. COMP.	1 -2012			
	E (PSI)		G (PSI)	μ	α (IN./IN./F°)
COATING LI-1500	9.1 x 10 ⁶ 60,000 (L), 6,000 (T)	3.9 x 10 ⁶ 4150	100 (RT) - 67 (500°F-600°F)	0.17 0.3 0.5	0.2 x 10 ⁻⁶ 0.3 x 10 ⁻⁶ 115.0 x 10 ⁻⁶
RTV-560	300 (RT) - 200 (500°F-600°F)	20 x 10 ⁶ (RT) - 18.8 x 10 ⁶ (600°F)	20 x 10 ⁶ (RT) - 18.8 x 10 ⁶ (600°F)	0.1	5.75 x 10 ⁻⁶ (RT) - 7.7 x 10 ⁻⁶ (600°F)
SUBSTRATE	42 x 10 ⁶ (RT) - 37.2 x 10 ⁶ (600°F)				



Table 6.5-6

**ALUMINUM TEST PANEL NO. 2
ORBITER FUSELAGE AREA 2**

COATING THICK = 0.010 IN. LI-1500 THICK = 3.396 IN. RTV-560 THICK = 0.090 IN. TILE LENGTH = 6 IN.

LOADING CONDITIONS	PRESSURE (PSI) AXIAL LOAD (PPI)	6.75 COLLAPSE 2250 COMPRESSION	3 COLLAPSE 3000 COMPRESSION	1.5 BURST 6000 TENSION	0 0
TEMPERATURE	SURFACE (°F) BACKFACE (°F)	75 75	100 250	100 250	75 300
LI-1500	PRIN. TEN.	5	15	61	24
	PRIN. COMP.	- 18	- 10	- 27	- 16
	SHEAR	8	4	19	9
	LONG.	- 12	14	61	24
	NORMAL TEN. NORMAL COMP.	4 - 8	2 - 4	8 - 5	2 - 2
RTV-560	PRIN. TEN.	4	2	22	6
	PRIN. COMP.	- 13	- 9	- 17	- 10
	SHEAR	6	2	18	7
	LONG. PEEL	- 5 4	- 8 2	- 6 8	- 7 3
COATING	PRIN. TEN. PRIN. COMP.	0 - 14	58 0	32 - 1	6 - 5
MATERIAL PROPERTIES	E (PSI)	G (PSI)	μ	α (IN./IN./°F)	
COATING	9.1 x 10 ⁶ 60,000 (L), 6,000 (T) 300 (RT - 300°F)	3.9 x 10 ⁶ 4150 100 (RT - 300°F)	0.17 0.3 0.5	0.2 x 10 ⁻⁶ 0.3 x 10 ⁻⁶ 115.0 x 10 ⁻⁶	
RTV-560	10.5 x 10 ⁶ (RT) - 9.15 x 10 ⁶ (300°F)	4.2 x 10 ⁶ (RT) - 3.66 x 10 ⁶ (300°F)	0.3	13.1 x 10 ⁻⁶ (RT) - 13.5 x 10 ⁻⁶ (300°F)	
SUBSTRATE					

DO7045

301 A

6.5-8

Table 6.5-7

ALUMINUM TEST PANEL NO. 3
ORBITER FUSELAGE AREA I



COATING THICK = 0.010 IN. LI-1500 THICK = 1.846 IN. RTV-560 THICK = 0.090 IN. TILE LENGTH = 6 IN.

LOADING CONDITIONS	PRESSURE (PSI) AXIAL LOAD (PPI)	3.75 COLLAPSE 3150 COMPRESSION	3 COLLAPSE 3000 COMPRESSION	1.5 BURST 6000 TENSION	0	
TEMPERATURE	SURFACE (°F) BACKFACE (°F)	75 75	100 250	100 250	75 300	
MAXIMUM STRESSES (PSI)	LI-1500	PRIN. TEN. PRIN. COMP. SHEAR LONG. NORMAL TEN. NORMAL COMP.	7 - 17 7 - 14 2 - 5	16 - 6 3 16 1 - 3	56 - 27 16 56 7 - 6	25 - 17 9 25 3 - 3
	RTV-560	PRIN. TEN. PRIN. COMP. SHEAR LONG. PEEL	3 - 10 6 - 3 2	1 - 8 1 - 8 1	20 - 14 16 - 6 8	7 - 10 7 - 7 3
	COATING	PRIN. TEN. PRIN. COMP.	27 - 21	49 0	12 - 103	1 - 101
	MATERIAL PROPERTIES	E (PSI)		G (PSI)	μ	α (IN./IN./F°)
		COATING LI-1500 RTV-560 SUBSTRATE	9.1 x 10 ⁶ 60,000 (L), 6,000 (T) 300 (RT - 300°F) 10.5 x 10 ⁶ (RT) - 9.15 x 10 ⁶ (300°F)	3.9 x 10 ⁶ 4150 100 (RT - 300°F) 4.2 x 10 ⁶ (RT) - 3.66 x 10 ⁶ (300°F)	0.17 0.3 0.5 0.3	0.2 x 10 ⁻⁶ 0.3 x 10 ⁻⁶ 115.0 x 10 ⁻⁶ 13.1 x 10 ⁻⁶ (RT) - 13.5 x 10 ⁻⁶ (300°F)

Table 6.5-8

TITANIUM TEST PANEL NO. 4
ORBITER FUSELAGE AREA 2

COATING THICK = 0.010 IN. LI-1500 THICK = 2.000 IN. RTV-560 THICK = 0.090 IN. TILE LENGTH = 6 IN.

LOADING CONDITIONS	PRESSURE (PSI) AXIAL LOAD (PPI)	6.75 COLLAPSE 2250 COMPRESSION	3 COLLAPSE 3000 COMPRESSION	1.5 BURST 6000 TENSION	0
	TEMPERATURE	75 75	100 550	100 550	75 600
LI-1500	SURFACE (°F) BACKFACE (°F)				
	PRIN. TEN.	5	27	48	30
	PRIN. COMP.	- 16	- 11	- 28	- 18
	SHEAR	6	6	15	9
	LONG.	- 12	26	48	27
RTV-560	NORMAL TEN.	3	1	6	2
	NORMAL COMP.	- 7	- 2	- 5	- 2
	PRIN. TEN.	4	1	13	3
	PRIN. COMP.	- 12	- 13	- 16	- 13
	SHEAR	5	0	13	5
COATING	LONG.	- 4	- 13	- 11	- 12
	PEEL	3	1	5	2
	PRIN. TEN. PRIN. COMP.	1 - 93	95 0	37 - 15	3 - 63
MATERIAL PROPERTIES	E (PSI)	G (PSI)		μ	α (IN./IN./F°)
COATING LI-1500 RTV-560	9.1 x 10 ⁶	3.9 x 10 ⁶		0.17	0.2 x 10 ⁻⁶
	60,000 (L), 6,000 (T)	4150		0.3	0.3 x 10 ⁻⁶
SUBSTRATE	300 (RT) -	100 (RT) -		0.5	115.0 x 10 ⁻⁶
	200 (500°-600° F)	67 (500°-600° F)			
	16.0 x 10 ⁶ (RT) -	6.4 x 10 ⁶ (RT) -			
	13.1 x 10 ⁶ (600° F)	5.2 x 10 ⁶ (600° F)		0.3	5.8 x 10 ⁻⁶ (RT - 600° F)

303A



Table 6.5-9
TILE-BOND-COATING SUMMARY CHART

	PANEL							
	BERYLLIUM		ALUMINUM				TITANIUM	
	NO. 1 TEST	NO. 1 FLT	NO. 2 TEST	NO. 2 FLT	NO. 3 TEST	NO. 3 FLT	NO. 4 TEST	NO. 4 FLT
SUBSTRATE †	0.064	0.064	0.125	0.125	0.154	0.154	0.097	0.097
RTV-560 †	0.090	0.090	0.090	0.090	0.090	0.090	0.090	0.090
LI-1500 †	1.89	1.25	3.34	2.52	1.85	1.40	2.00	1.35
COATING †	0.010	0.010	0.010	0.010	0.010	0.010	0.010	0.010
LI-1500 TILE L	12	12	6	6	6	6	6	6
WEIGHT (LB/FT ²)	5.2*	4.6*	6.6	5.7	5.2	4.8	5.4	4.7
Δ WEIGHT (PSF)	+0.84	-	+1.09	-	+0.59	-	+0.96	-

ALL DIMENSIONS IN INCHES

ADIABATIC BACKFACE FOR ALL PANELS

* WT. OF Be PANEL INCLUDES 1.6 LB/FT² FOR PRIMARY STRUCTURE

TEST VS FLIGHT CONDITIONS

- SIMPLE SUPT IN TEST
- CONTINUOUS SPAN IN FLIGHT
- LOAD FITTINGS UNIQUE TO TEST

COMPARISON OF STRONG AND WEAK DIRECTION STRESSES
OF ALUMINUM FLIGHT PANEL NO. 2

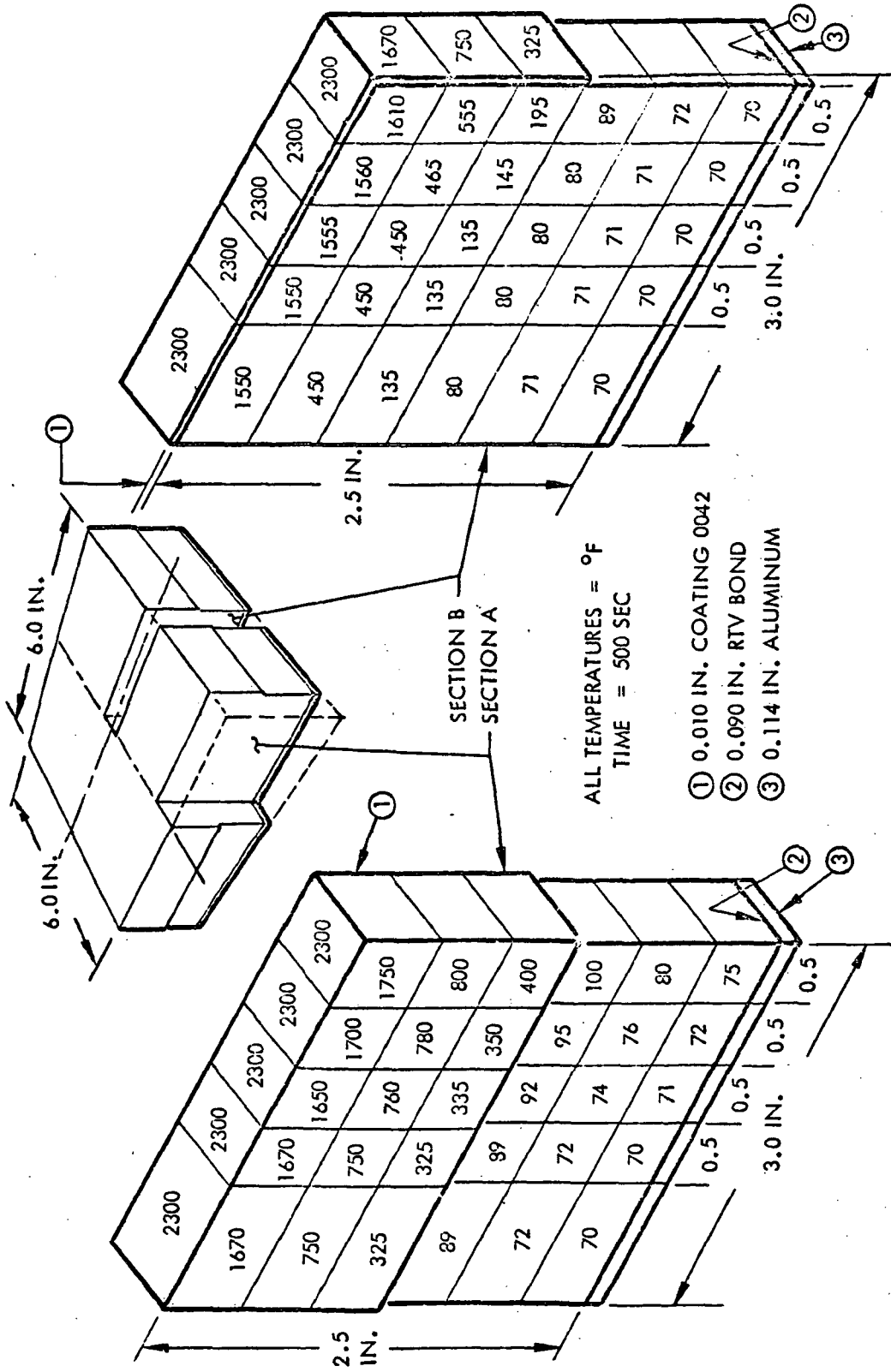


LOADING CONDITIONS	STIFFENER DIRECTION		THICKNESS (IN.)	
	PARALLEL	TRANSVERSE (ON SPRINGS)		
TEMPERATURE	1.5 PSI BURST	1.5 PSI BURST	COATING LI-1500 RTV-560 SUBSTR.	
	6000 PPI TENSION	0		
MAXIMUM STRESSES (PSI)	SURFACE	100°F	0.010 2.524 0.090 0.749 (P) 0.050 (T)	
	BACKFACE	250°F		
	LI-1500	PRINC. TENS.	23	TILE LENGTH = 6 IN.
		PRINC. COMPR.	-16	
		RZ-SHEAR	6	
		PRINC. SHEAR	13	
	LONG. TENS.	21		
	LONG. COMPR.	-16		
	NORMAL TENS.	1		
	NORMAL COMPR.	-3		
RTV-560	PRINC. TENS.	4		
	PRINC. COMPR.	-8		
	RZ-SHEAR	5		
	LONG. TENS.	6		
COATING	LONG. COMPR.	0		
	NORMAL TENS.	-6		
	NORMAL COMPR.	1		
	PRINC. TENS.	0		
MATERIAL PROPERTIES	PRINC. TENS.	39	α (IN./IN./°F)	
	PRINC. COMPR.	0		
	PRINC. SHEAR	20		
COATING LI-1500 RTV-560 SUBSTRATE	E (PSI)	G (PSI)	μ	
	9.1 x 10 ⁶	3.9 x 10 ⁶	0.17	
	60,000 (L), 6000 (T)	4150	0.3	
	300 (R.T.), 200 (600°F)	100 (R.T.), 67 (600°F)	0.5	
	10.5 x 10 ⁶ (R.T.)	4.2 x 10 ⁶ (R.T.)	0.3	
9.15 x 10 ⁶ (300°F)	3.66 x 10 ⁶ (300°F)			



TEMPERATURE DISTRIBUTIONS IN 6 INCH RSI TILE

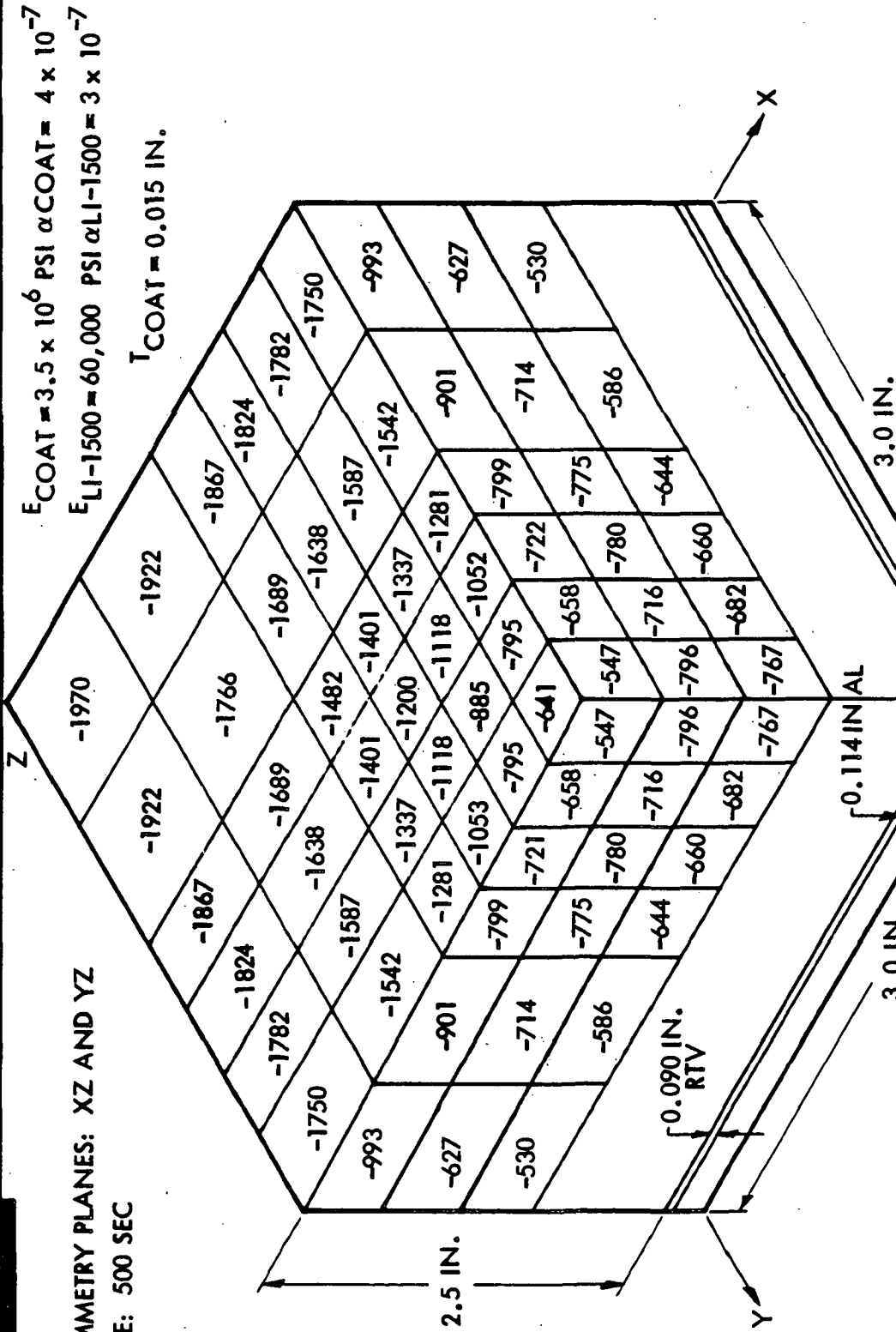
FOR ALUMINUM FLIGHT PANEL NO. 2



306

Fig. 6.5-1

COATING STRESS DISTRIBUTION FOR FLIGHT PANEL NO. 2



ALL STRESSES ARE PRINCIPAL STRESSES IN (PSI). NEGATIVE SIGN INDICATES COMPRESSION

D07047

Fig. 6.5-3

6.6 DYNAMIC ANALYSES

Dynamic analyses were performed on the prototype panels as indicated in the analysis logic sequence diagram of Fig. 1.1-1. These analyses consisted of checks of each panel design for flutter stability and sonic fatigue. Analysis details are presented in Appendix D, and results are summarized in Figs. 6.6-1 and 6.6-2. Figure 6.6-1 shows the interstiffener panel flutter boundary for the weakest prototype panel, which is panel No. 4. Note that this panel is clearly flutter-free when compared to the dynamic pressures expected on the vehicle during launch and reentry. Flutter of the complete panel was also investigated and found to yield significantly higher flutter boundaries for all panels than that shown in Fig. 6.6-1.

Sonic-fatigue analysis results are presented in Fig. 6.6-2. These results are based on an experimentally determined panel damping ratio of 0.02. The data points shown on the figure represent the anticipated life cycle of the panels multiplied by a safe-life margin of four. As may be seen, all four prototype panel points fall below their respective allowable stress curves.



TPS CRITICAL PANEL FLUTTER STABILITY

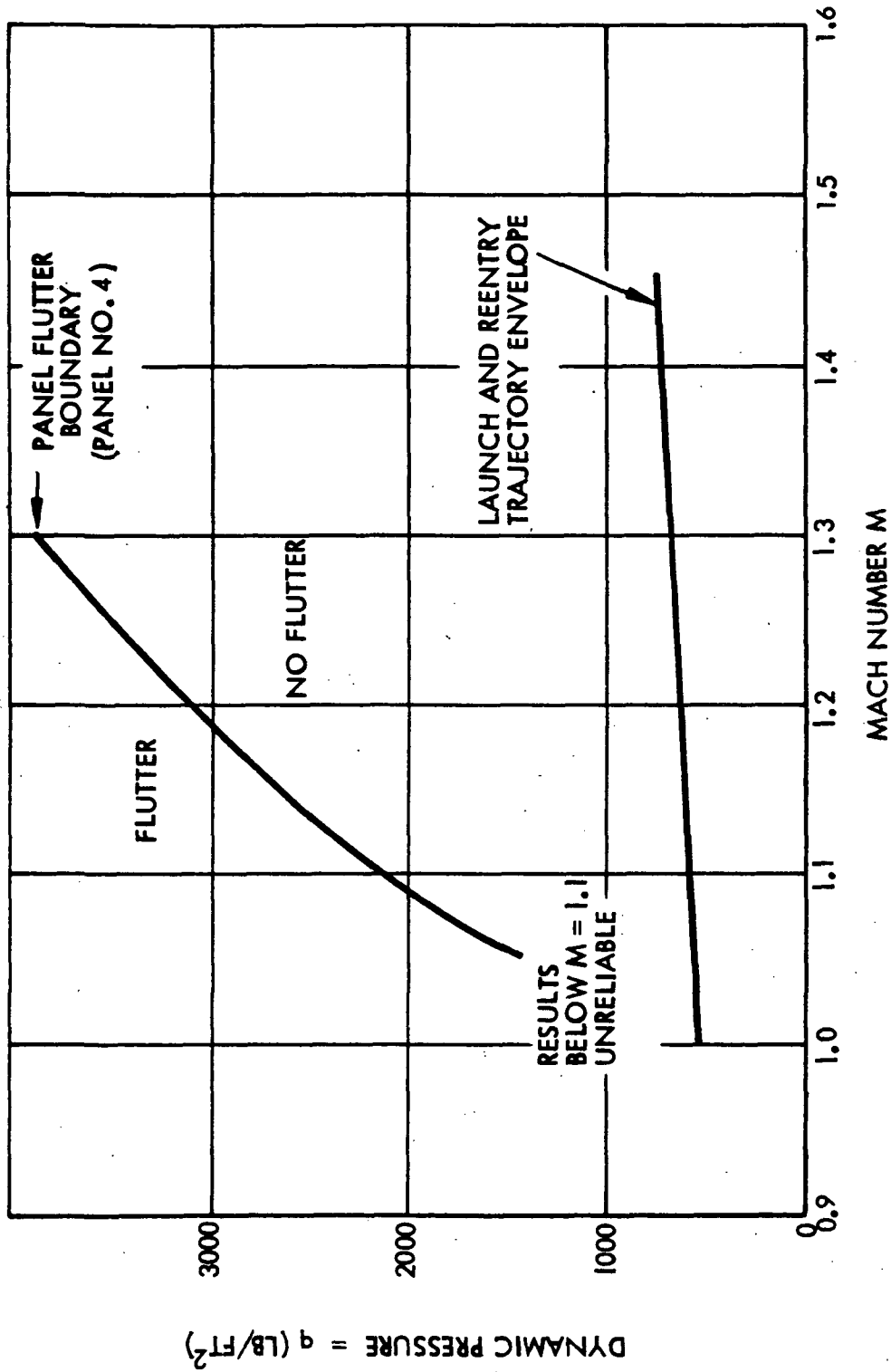
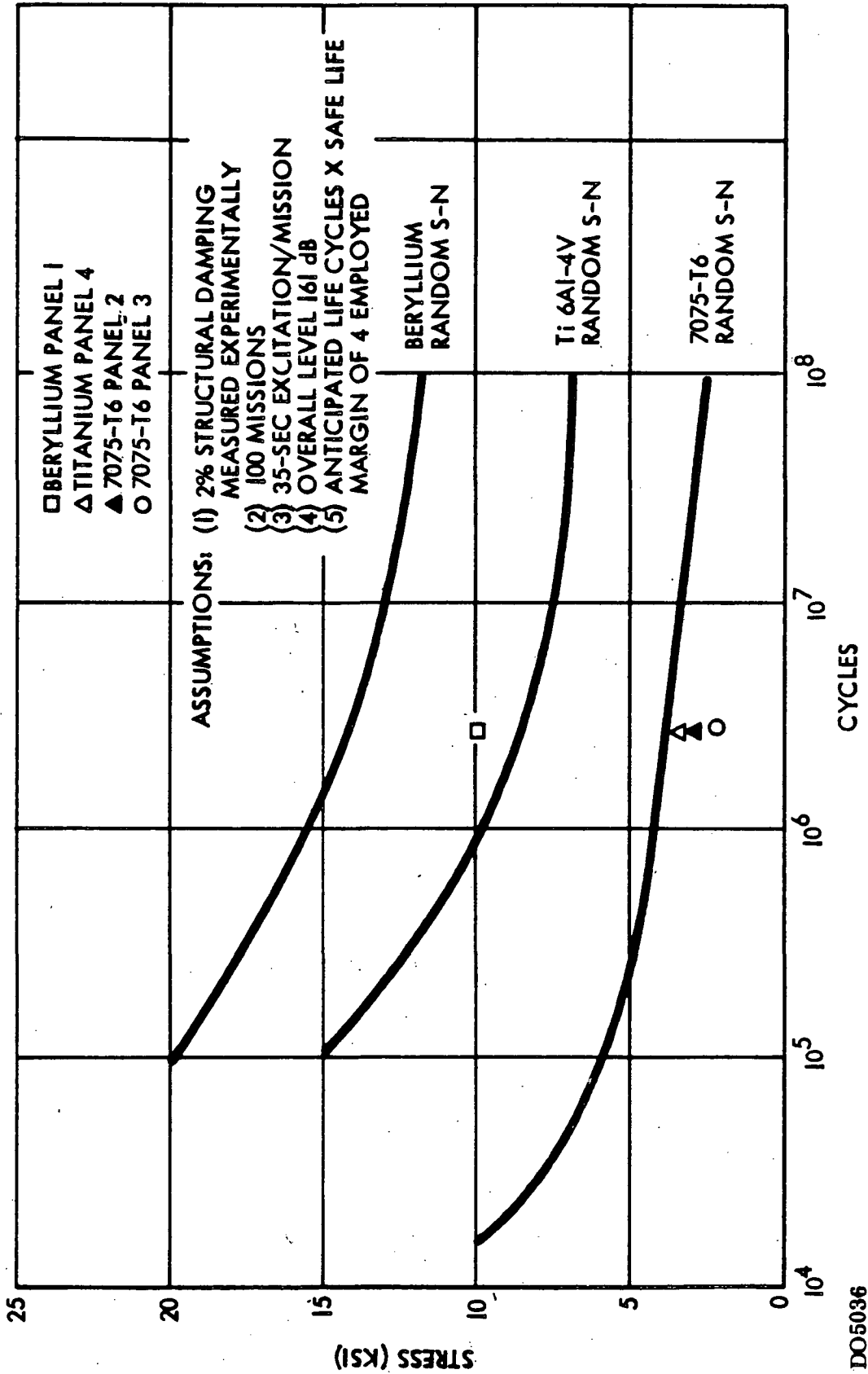


Fig. 6.6-1

DO5042 (1)



SONIC FATIGUE ANALYSIS OF TPS PANELS



311 <
6.6-3

Fig. 6.6-2

6.7 CRITICAL FAILURE MODES

Design validity for substrate configurations under static and dynamic loading conditions has been discussed in Sections 6.3 and 6.6. In this section, brief comments are made concerning RSI stress levels for the deliverable prototype panels summarized in Section 6.5.

For the beryllium subpanel, both coating stress and LI-1500 longitudinal stress represent limitations on the design. For the other three panels, LI-1500 longitudinal stress is the driving variable. In each case, however, the combined normal/shear stress state, which occurs near the ends of a tile, has been compared with the results of preliminary testing described in Section 2.5. It has been found that the critical stress points for panel Nos. 1, 2, and 3 fall somewhat outside the linear interaction curve of Fig. 2.5-5, but well within the rectangular uniaxial allowable criterion. As noted earlier, the linear interaction criterion is the result of very preliminary investigation, and two counterexamples have been demonstrated which question the validity of such a severe restriction. LMSC considers the designs as presented to be sound and assigns high priority in future investigations to the establishment of a more realistic failure condition for this state of combined stress.

6.8 TPS COST STUDY

Unit costs (dollars per pound and dollars per square foot) have been projected for the first orbiter vehicle. These costs are based on extrapolations of present manufacturing experience. During the first few months of 1971, LMSC brought the pilot plant manufacturing facility into full operational status. While the material produced in the first 4 months of 1971 has performed well in arcjet and radiant heat tests, production scale-up problems, combined with variability in raw fiber material, led to relatively expensive processed tiles (approximately \$840/pound). During the past 6 months, the production problems have been resolved and raw material consistency from lot to lot has improved, reducing costs by more than one-third. Furthermore, changing from the pilot plant operation to full-scale production will result in automation of various time-consuming hand operations that are now required and will reduce processing time by more than a factor of 2. Projected manufacturing costs for processed LI-1500 range from \$50 per pound to \$100 per pound. Machining the LI-1500 tiles to size and attaching (bonding) to the vehicle will result in a total installed cost of \$80 to \$135 per pound. Fabrication and installation data are shown in Table 6.8-1. Costs per pound and costs per square foot are shown as a function of tile size and thickness.* The range shown indicates the expected cost bounds; the upper bound is used in all the following cost studies.

Cost estimates for a metallic thermal protection system are generated, using the standard cost complexity factors (C. F.) in Tables 6.8-2 and 6.8-3, which relate the fabricated costs of each metal to that for a stiffened aluminum structure. The metallic heat shield weights for the O4OA delta wing orbiter (using a 2800-second reentry trajectory with peak temperature of 2050⁰F) are shown in Table 6.8-2.

Cost estimating Relationships (CERs) have been used to project the total TPS first unit costs. These data are summarized in Table 6.8-3 for three TPSs: LI-1500, the SLA-561 ablator, and the metallic heatshield. As can be seen, the metallic system is far heavier and most costly than the LI-1500.

*See Figs. 6.8-1 and 6.8-2

Table 6.8-1

LI-1500 TPS UNIT COST VERSUS TILE SIZE

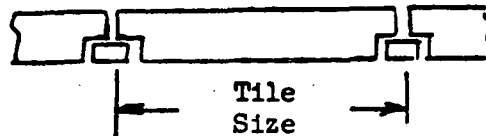
Labor Cost Element	Number and Size of Tiles		
	4 (12 x 12 in.)	16 (6 x 6 in.)	36 (4 x 4 in.)
Saw Cut Tiles to Size	0	0.4	0.8
Grind-Rout Edges	0.8	2.4	4.0
Cut Seal Strips	0.5	1.5	2.5
Bond Tiles to Structure	4.0	6.0	12.0
Labor Hours per Panel	5.3	10.3	19.3
Labor Cost (\$/ft ²)	21.2	41.2	77.2
Total Cost (\$/ft ²)	340	358	390
Total Cost (\$/lb)	135	143	156

NOTES:

1. Estimate is based upon bonding material to primary structure, over an area 2 ft x 2 ft in size, with the LI-1500 material delivered in 12 x 12 x 2 in. tiles shaped and ready for bonding.

$$W/A = 0.24 + 1.25 (t) = 2.74 \text{ lb/ft}^2$$

2. Tile size and assembly is illustrated below.



3. Total costs include basic LI-1500 tile and raw material as well as manufacturing and installation labor.

Table 6.8-2

040A DELTA WING ORBITER - METALLIC TPS SYSTEM - AVERAGE COMPLEXITY FACTOR

Surface Panel Material	Surface Area (ft ²)	Unit Weight (lb/ft ²)	Weight (lb)	C. F.	Weight x C. F.
Cb	90	5.11	460	7.49	3,450
TDNiCrAl	3,513	4.16	14,630	3.37	49,600
Rene 41	722	2.69	1,942	2.75	5,340
Ti	6,713	1.42	9,510	3.25	30,900
Carbon/Carbon	177	3.50	620	7.50	4,150
Σ =	11,215	(2.42)	27,162	(3.44)	93,440

Table 6.8-3

040A DELTA WING ORBITER - TPS COST SUMMARY

TPS	Total System Weight (lb)	System C. F.	First Unit Cost ⁽¹⁾ (\$M)	Cost Per Pound (\$/lb)	Cost Per Sq Ft (\$/ft ²)
LI-1500	21,870	0.8	3.5	144	312
SLA-561	21,650	0.7	3.1	127	276
Metallic	27,162	3.5	16.2	596	1,445

⁽¹⁾ Manufacturing cost of total TPS for first orbiter:

$$c = 2.8 (10^{-2}) (W)^{.5} (C.F.) = \$ \text{ Million}$$



PROJECTED FIRST UNIT COSTS

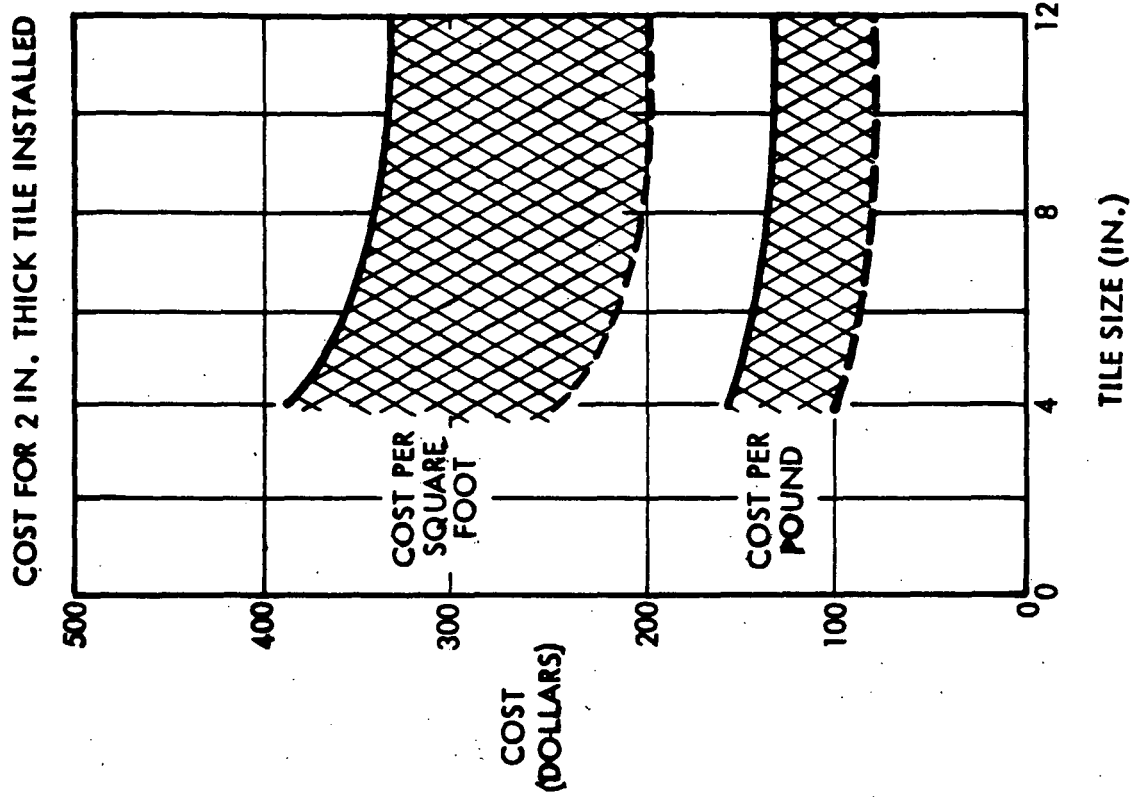


Fig. 6.8-2

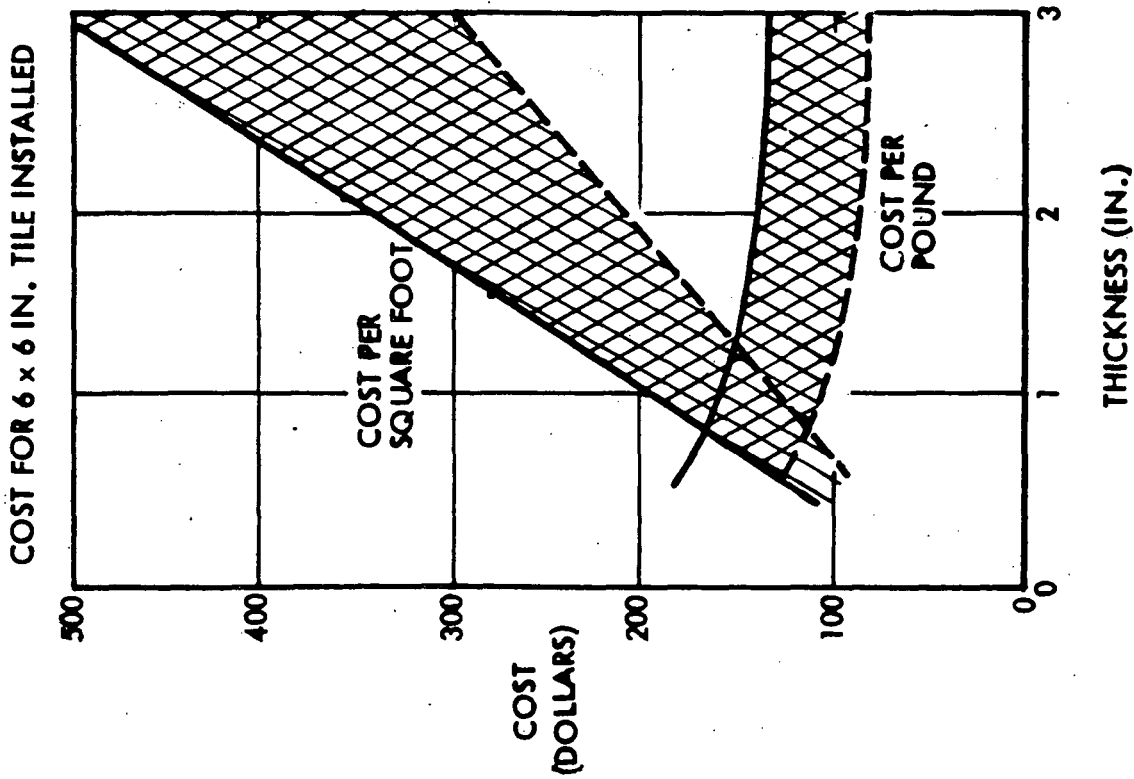


Fig. 6.8-1

A detailed comparison of the ablator and LI-1500 weights and thicknesses is presented in Table 6.8-4 and forms the basis for the system costs projected in Fig. 6.8-3. The DDT&E (Design, Development, Test, and Engineering) and first unit costs are shown on the figure. The total program costs are highly sensitive to the refurbishment rates assumed and, hence, a range is shown. The present design guidelines call for 100-percent replacement of the ablator after every flight (upper bound). It is possible that the ablator can be reused in regions where the maximum temperature is below 600°F. Hence, the lower bound shown in Fig. 6.8-3 is based on replacement over 70 percent of the surface area after every flight.

The LI-1500 rigid surface installation has a demonstrated reuse capability of 100 cycles for trajectories having a peak temperature of 2500°F. In order to project realistic program costs, however, a reasonable refurbishment rate must be estimated. A refurbishment rate of 5 percent of the surface of each flight is shown as the upper bound; a 2 percent refurbishment rate is assumed for the lower bound in Fig. 6.8-3.

One remaining question to be answered is what method of attachment will result in the least cost space shuttle system. Five primary structural materials have been considered for the orbiter (7075-T6 aluminum, 2024-T81 aluminum, magnesium, titanium, and beryllium) in combination with three TPSs: direct bond of LI-1500 to primary structure, LI-1500 bonded to subpanels, and metallic heat shield (titanium or beryllium) for upper surfaces. The all aluminum structure with direct-bond LI-1500 TPS was selected as baseline.

It is interesting that the lightest system (beryllium skin over titanium frames with direct bond of LI-1500 results in 18,000 lb reduction in system weight) is far more expensive than the baseline (\$178 million increase in the total program costs). The least-cost system is obtained by using LI-1500 directly bonded to beryllium subpanels attached to an all aluminum airframe. The system weight is reduced by 7000 lb and total program cost is reduced by \$120 million.

Table 6.8-4

040A ORBITER TPS WEIGHTS

Location	Surface Area (ft ²)	SLA-561 Ablator		LI-1500	
		Thickness (in.)	Weight (lb)	Thickness (in.)	Weight (lb)
Body Lower Surface	1,647	2.05	4,674	2.20	5,528
Body Upper Surface	4,757	1.05	7,257	0.65	6,293
Wing Lower Surface	1,956	2.05	5,550	2.10	6,308
Wing Upper Surface	1,956	0.60	1,829	0.45	2,074
Tail (Sides)	722	1.20	1,244	0.75	1,050
Nose Cap	27	2.40	174	-	95
Wing Leading Edge	126	2.40	812	-	441
Tail Leading Edge	24	1.75	114	-	84
Total	11,215		21,654		21,873

Ablator for nose cap and leading edge is 30 lb/ft³, ESA 3560; for other areas it is 15 lb/ft³.

Ablator weight loss during entry is 1515 lb.

All thicknesses are averages for the surface areas indicated.

Weights include 5 percent non-optimum factor.

Thermal environment is based on LMSC high-crossrange trajectory, RE-230 (2000 sec reentry) (040A delta wing design trajectory).

These studies emphasize the fact that the lightest system is not necessarily the cheapest, and one must consider the entire vehicle in reaching a decision as to which approach to adopt for attaching the TPS to the structure.

TPS COST COMPARISON

O40A DELTA WING ORBITER

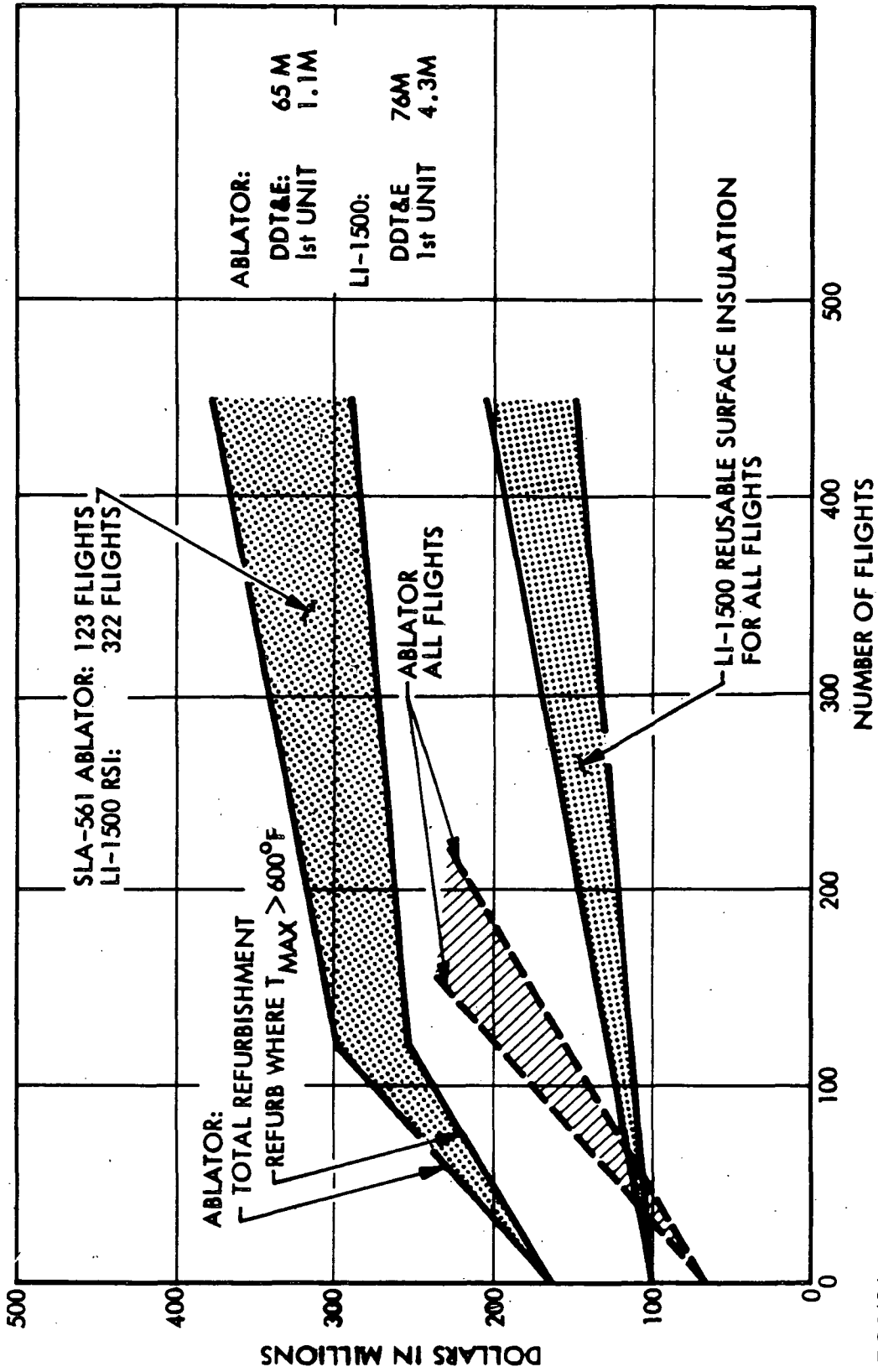


Fig. 6.8-3



6.9 COMPARISON OF LI-1500 PANEL DESIGNS VS METALLIC HEATSHIELD DESIGNS

The LI-1500 prototype TPS panels designed and fabricated under this contract are lighter and more economical than comparable metallic heatshield designs. In this subsection, current LMSC metallic heatshield designs are described and weight comparisons are presented. Two approaches to the design of metallic heatshields have been studied at LMSC. These are as follows:

1. The metallic heatshield is supported by relatively closely spaced standoffs that are attached to a subpanel with span equal to the frame spacing. Flexible insulation is placed between the heatshield and the subpanel; the depth of the standoffs is the optimum derived from a consideration of the materials specified for the design, the design environment, and the insulation properties.
2. The heatshield is designed with sufficient stiffness to span the distance between frames directly; insulation and packaging is placed underneath, between the heatshield and the primary structure.

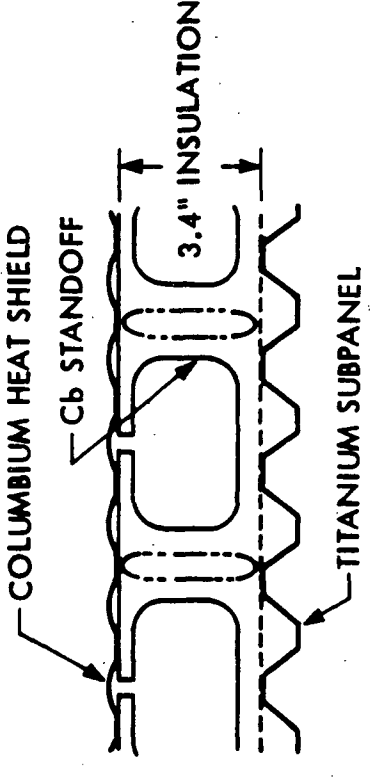
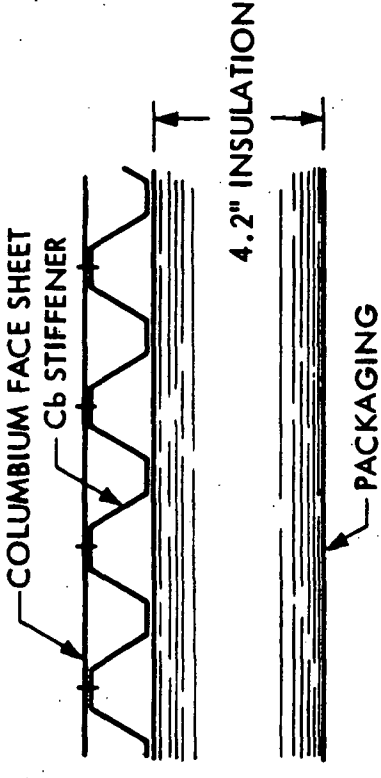
Typical designs utilizing a coated columbium heatshield are shown in Fig. 6.9-1. These designs have been developed for a short-pulse trajectory with maximum temperature of 2300^oF, as utilized in on-going LMSC space shuttle orbiter studies. As shown in the figure, the subpanel approach yields the lightest metallic heatshield weight.

The short-pulse trajectory is characterized by a substantially lower total heat input than the trajectory for which the prototype panels have been designed. Selecting the subpanel approach as the optimum approach, heatshield weights for other total heat inputs have been determined as shown in Fig. 6.9-2. Noted on this figure are total heat inputs for the NASA-MSC trajectory, both perturbed to 2300^oF and unperturbed, for Vehicle Area 2. Weights are shown for LI-1500 panel designs as well as metallic heatshield designs. As a check on these results, a metallic heatshield data point, obtained from a MDAC reference report, also is shown. Good agreement in terms of unit panel weight may be observed. The curves in Fig. 6.9-2 emphasize the weight penalty involved with the longer pulse trajectories as well as the relative efficiency of metallic heatshields vs LI-1500.



METALLIC HEAT SHIELD WEIGHT COMPARISON

(LS 400-7 TWO-STAGE ORBITER WITH FRAME SPACING = 25 IN.
SHORT PULSE TRAJECTORY AT MAXIMUM TEMPERATURE OF 2300°F)

CONCEPTS	DESCRIPTIONS	TPS WEIGHT LB/FT ²
	WEIGHT OF METALLIC HEATSHIELD, STANDOFFS, AND TITANIUM SUBPANEL WEIGHT OF FLEXIBLE INSULATION AND PACKAGING TOTAL WEIGHT	2.361 1.997 <hr/> 4.358
	WEIGHT OF METALLIC HEATSHIELD WITHOUT SUBPANEL WEIGHT OF FLEXIBLE INSULATION AND PACKAGING TOTAL WEIGHT	3.654 2.417 <hr/> 6.071

● LMSC'S BEST METALLIC HEATSHIELD FOR
2300°F APPLICATIONS UTILIZES SUBPANEL CONCEPT

D05172

rdh

Fig. 6.9-1

COMPARISON OF TPS UNIT WEIGHTS

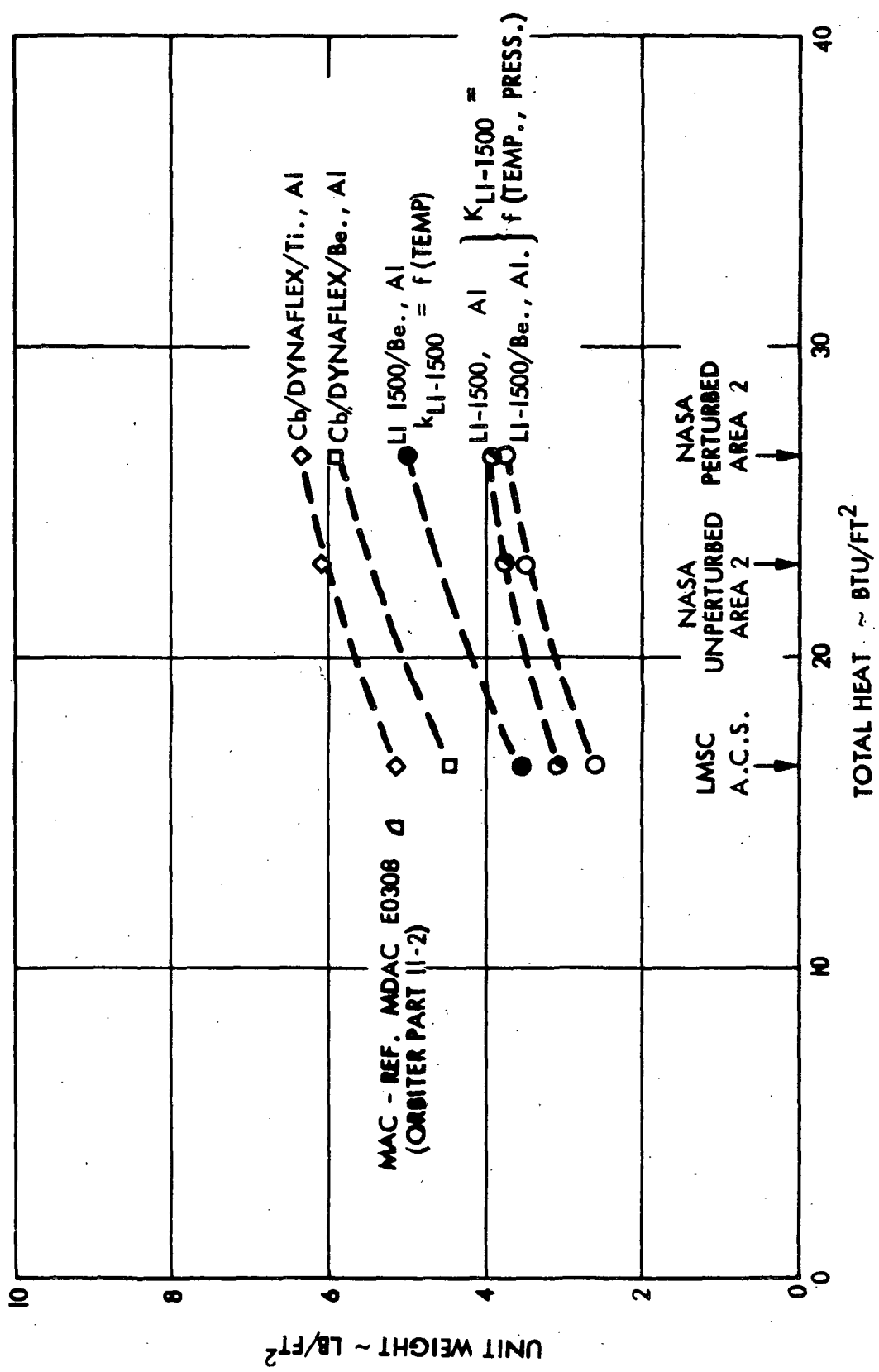


Fig. 6.9-2

It is apparent from Fig. 6.9-2 that care must be exercised to compare TPS designs based on identical heat pulses. Several such comparisons are presented in Fig. 6.9-3; these relate to the heat-pulses presented in Fig. 6.9-4. Heat-pulses are shown in Fig. 6.9-4 for the LMSC delta-wing orbiter protected by LI-1500 and by metallic TPS. Note that the LI-1500 heat pulse is of short duration and peaks at 2300^oF, while the metallic TPS heat pulse is of long duration in order to limit the peak temperature at 2000^oF. The NASA-MSc heat pulse specified for this contract, also shown, is seen to combine the higher maximum temperature with the long duration heat pulse.

The data in Fig. 6.9-3 relate to both Vehicle Areas 1 and 2. Area 2 results are presented for both metallic and LI-1500 TPS designs for the following heat-pulses:

- a. LMSC delta-wing orbiter, 2300^oF maximum temperature flight heat pulse (RE 214)
- b. NASA-MSc unperturbed, 2050^oF maximum temperature flight heat pulse
- c. NASA-MSc perturbed 2300^oF maximum temperature flight heat pulse
- d. NASA-MSc perturbed, 2300^oF maximum temperature test heat pulse (one atmosphere environment)

The significant differences in these heat pulses are: (1) the designs for flight heat pulses account for radiation to the primary structure in those designs specifying subpanels, whereas the test heat pulse designs are based on an adiabatic back-face temperature; (2) the flight heat pulse LI-1500 designs utilize the lower thermal conductivity of LI-1500 in vacuum, whereas the test heat pulse designs do not; and (3) the LMSC-RE214 heat pulse involves significantly lower total heat input. Because Area 1 experiences a much lower maximum surface temperature, only two heat pulses are considered; these correspond to the NASA-MSc flight and test heat pulses specified for this contract.



COMPARISON OF METALLIC TPS VS LI-1500 TPS

CONCEPT	DESCRIPTION	COLUMBIUM VS LI-1500				RENE 41 VS LI-1500	
		2300°F LMSC RE 24 FLIGHT	2050°F NASA FLIGHT	2300°F NASA 2 FLIGHT	2000°F 1 ATM TEST	1480°F NASA 1 FLIGHT	1480°F 1 ATM TEST
 COLUMBIUM HEAT SHIELD INSULATION Ti SUBPANEL Al PRIMARY STRUCTURE LIMITED TO 300°F	METALLIC	COLLAPSE = 6 LB/IN. ² , BURST = 4.5 LB/IN. ² , + N ₂ = 6000 LB/IN. ² , -N ₂ = 3000 LB/IN. ² , PANEL LENGTH = 24 IN.					
	HEAT SHIELD/Ti SUBPANEL FLEXIBLE INSULATION HEAT SHIELD + INSULATION *Z* STIFFENED ALUMINUM PRIMARY STRUCTURE* TOTAL UNIT WEIGHT LB/FT ² MAX. SUBPANEL TEMP. INSULATION THICKNESS	2.5 2.7 5.2 1.5	2.6 3.3 4.1 1.5	2.6 3.6 6.2 1.5	2.5 2.9 5.4 1.5	1.6 2.1 3.7 1.7	1.6 1.8 3.4 1.7
 LI-1500 Ti SUBPANEL Al PRIMARY STRUCTURE LIMITED TO 300°F	RSI WITH SUBPANEL	COLLAPSE = 3 LB/IN. ² , BURST = 4.5 LB/IN. ² , N ₂ = 6000 LB/IN. ² , PANEL LENGTH = 20 IN.					
	BERYLLIUM SUBPANEL LI-1500 & BOND LI-1500 + BOND + SUBPANEL CORRUGATED ALUMINUM PRIMARY STRUCTURE TOTAL UNIT WEIGHT LB/FT ² MAX. SUBPANEL TEMP. INSULATION THICKNESS	0.6 2.2 2.8 1.5	0.6 2.9 3.5 1.5	0.6 3.1 3.7 1.5	0.6 3.2 3.8 1.5	0.6 1.8 2.4 1.6	0.6 2.0 2.6 1.6
 LI-1500 Al PRIMARY STRUCTURE LIMITED TO 300°F	RSI ATTACHED DIRECTLY TO PRIMARY STRUCTURE	COLLAPSE = 6 LB/IN. ² , BURST = 4.5 LB/IN. ² , + N ₂ = 6000 LB/IN. ² , -N ₂ = 3000 LB/IN. ² , PANEL LENGTH = 24 IN.					
	LI-1500 + BOND *Z* STIFFENED ALUMINUM PRIMARY STRUCTURE TOTAL UNIT WEIGHT LB/FT ² INSULATION THICKNESS	3.1 1.7 4.8 2.1	3.7 1.7 5.4 2.6	3.9 1.8 5.7 2.7	5.0 1.7 6.7 3.6	2.7 2.2 4.9 1.8	3.2 2.2 5.4 2.1

* DESIGNED BY TENSION LOADS; CORRUGATED
 PRIMARY STRUCTURE 0.13 LB/FT² LIGHTER WHERE
 COMPRESSION LOADS GOVERN. (AREA I)

NO GROUND COOLING

Fig. 6.9-3

D05181 (1)

COMPARISON OF LMSC - MSC RADIANT - HEAT PULSES FOR 1100 - NM CROSSRANGE TRAJECTORY

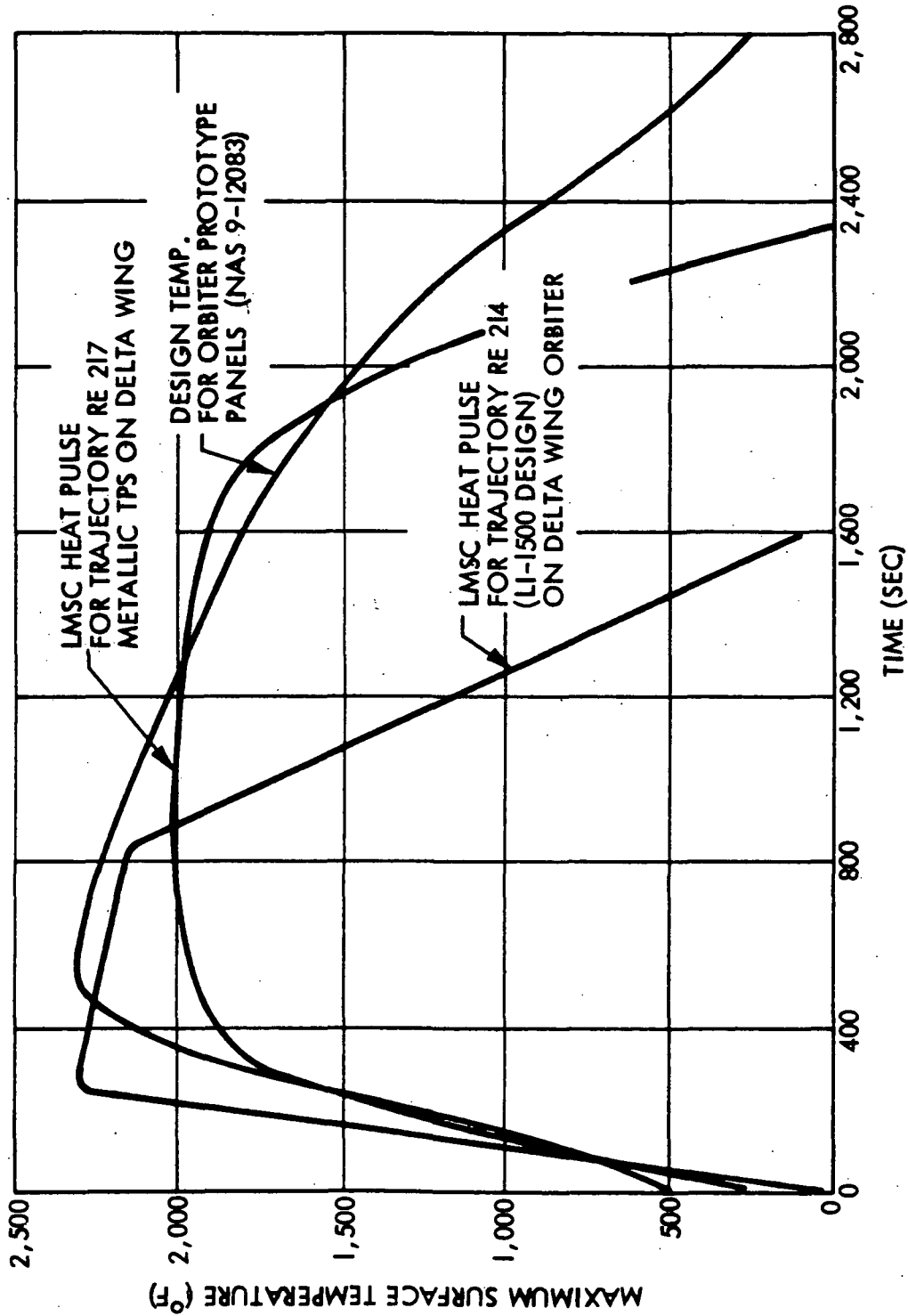


Fig. 6.9-4



In Vehicle Area 2, it can be seen that the adiabatic back-face temperature stipulation for test at one atmosphere is advantageous for the metallic TPS designs but disadvantageous for the LI-1500 TPS designs. In the latter designs, the lower thermal conductivity of LI-1500 in vacuum cannot be utilized. The lower thermal conductivity of LI-1500 in vacuum more than compensates for weight penalties in a flight environment in maintaining the aluminum primary structure temperature at or below 300^oF; note that this requirement results in a weight penalty to the metallic TPS flight designs. Thus, the test heat pulse comparison of LI-1500 and metallic TPS designs results in a close comparison that is misleading in terms of the true flight environment. The same phenomenon is observed in the results for Vehicle Area 1.

The NASA-MS 2050^oF and 2300^oF heat pulses yield metallic TPS designs that are not significantly different from the designs for the LMSC-RE214 heat pulse. LI-1500 TPS designs show weight increases due principally to the need for more material to absorb the added heat of the longer heat pulse.

Note, in comparing the data of Figs. 4.1-2, 4.1-3, and 4.2-2 with the data of Fig. 6.9-3, that frame weights have been included in the former but not in the latter. Also, the subpanel and primary structure weights calculated previously have been multiplied by a nonoptimum factor to account for fasteners, closeouts, and other details.

In summary, the data presented here show the LI-1500 TPS designs to be lighter than comparable metallic TPS designs, when both are designed to the same heat pulse. LI-1500 TPS designs based on a 2300^oF maximum temperature flight heat pulse also are lighter than metallic TPS designs based on a 2050^oF maximum temperature flight heat pulse. The desirability of designing and testing LI-1500 TPS designs in the true vacuum environment of flight when maximum temperatures are attained also has been established.

6.10 PROTOTYPE PANELS

LMSC has designed four prototype panels in accordance with contract requirements to point design conditions specified by NASA/MSC. The design effort was accomplished under Task 2.0 as negotiated and reviewed in this report. These panels consist of a metallic structure with 0042-coated LI-1500 bonded to one side with the RTV-560 adhesive system.

Details of the prototype panels are shown in Figs. 6.10-1 through 6.10-4. The materials/applications/design areas for each panel are reviewed in Table 6.10-1. For vehicle application, the beryllium subpanel bolts directly to external vehicle frames. The primary structural panels will attach to frames but will be continuous over many spans. These panel designs utilize 6-pcf filler blocks in the joints, FI-600. Thermal analysis has shown that temperature fields in the substrates are perturbed to a negligible degree relative to those of a total LI-1500 system. The design methodology used to design these panels has been discussed in detail in the preceding sections.

Table 6.10-1

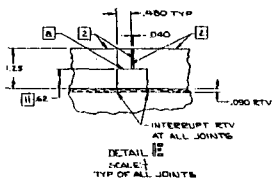
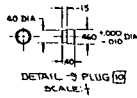
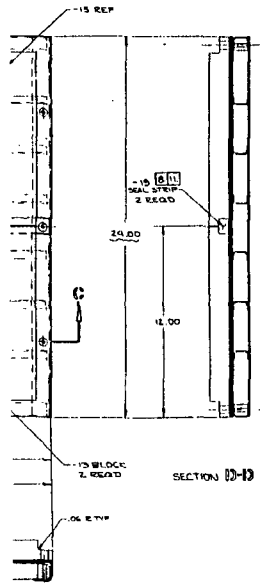
PROTOTYPE PANEL CHARACTERISTICS

Panel No.	Shown in Fig. No.	Substrate Material	Application	Vehicle Area
1	6.10-1	Beryllium	Subpanel	2
2	6.10-2	Aluminum	Primary	2
3	6.10-3	Aluminum	Primary	1
4	6.10-4	Titanium	Primary	2

327<

FOLDOUT FRAME 3

LMSC-D152738
Vol II



REV	CHANGE	DATE APP'D
A	LI-1500 THICKNESS WAS 2.15. TITLE SIZE WAS 0.75. REVISED NOTE (E). ADDED DETAIL 'E'.	
B	LI-1500 THICKNESS WAS 1.90. ADDED PHENOL THRU-PLATE. NOTE B HAD FURNACE BRIDGE WITH 0.03 BRASS ALLOY BUSH. REVISED NOTE 2. ADDED DETAIL '9' PLUG. ADDED NOTE 'D'.	
C	INT. PL. - 1.15 IS 1.00. LI-1500 ADDED. NOTE (C).	

- (1) CUT SEAL STRIPS - IT-15 TO PROVIDE A SLIGHT INTERFERENCE FIT WITH THE LI-1500 (ABOUT .005).
 - (2) ITEMS NOTED ARE TO BE USED WHEN ANY IS INSTALLED IN TEST FIXTURE.
 - (3) BOND WITH RTV-160 PER SPEC. LAC 50-4459.
 - (4) GROUND TOP SURFACE OF SEALING STRIPS .00 THICK PER 0042 COATING SYSTEM.
 - (5) ALL BRASS BUSHES .51 MIN.
 - (6) CLEAN PER SPEC. LAC 0170.
 - (7) PROTECT PER SPEC. LAC-1001.
 - (8) FABRICATE PER LAC. PB-92.
 - (9) HOLD GAP BETWEEN PANELS & 301 FRAME TO .000.
 - (10) GROUND TOP & INSIDE VERTICAL SURFACES. .00 THICK PER 0042 COATING SYSTEM.
 - (11) BOND LI-1500 TO 301 FRAME USING RTV 150 PER SPEC. LAC 50-4459.
- NOTES:

QTY	QTY REQ'D PER SPACE	UNIT	DESCRIPTION	PART OR IDENTIFYING NO.	REMARKS OR DESCRIPTION	MATERIAL SPECIFICATION	REF. SPEC. NO.	ITEM NO.
			AR	M82042HMS	RIVET	MONEL		
			6	2.818553	SCREW	TI 6AL-4V		
			15	ANDROCC10L	WASHER	TI 6AL-4V		
			6	-21	CHANNEL	304 SHEET PERI-LUMID		
			2	-19	SEAL STRIP	FI-600		
			1	-17	SEAL STRIP	TI-600		
			AR	M82042HMS	RIVET	MONEL		
			2	-15	BLOCK	LI-1500		
			3	-13	BLOCK	LI-1500		
			2	-11	CHANNEL	304 SHEET PERI-LUMID		
			15	6	PLUG (C)	LI-1500		
			6	-7	BLOCK	PERI-LUMID		
			2	-5	ANGLE	PERI-LUMID		
			2	-3	ANGLE	PERI-LUMID		
			1	-1	PLATE	PERI-LUMID		
			1	-301	FRAME ASSEMBLY	PERI-LUMID		

PRECEDING PAGE BLANK NOT FILMED
Fig. 6.10-1 Thermal Test Panel No. 1
328<
6.10-3/4

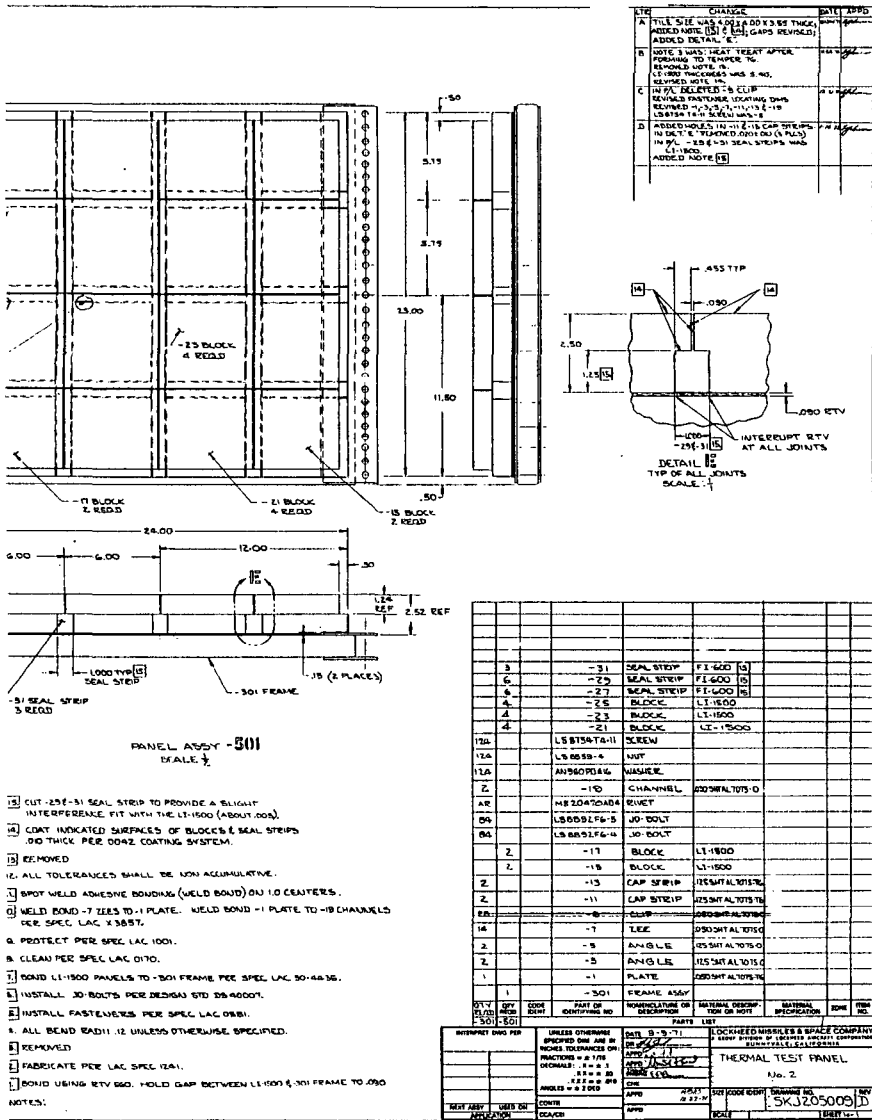
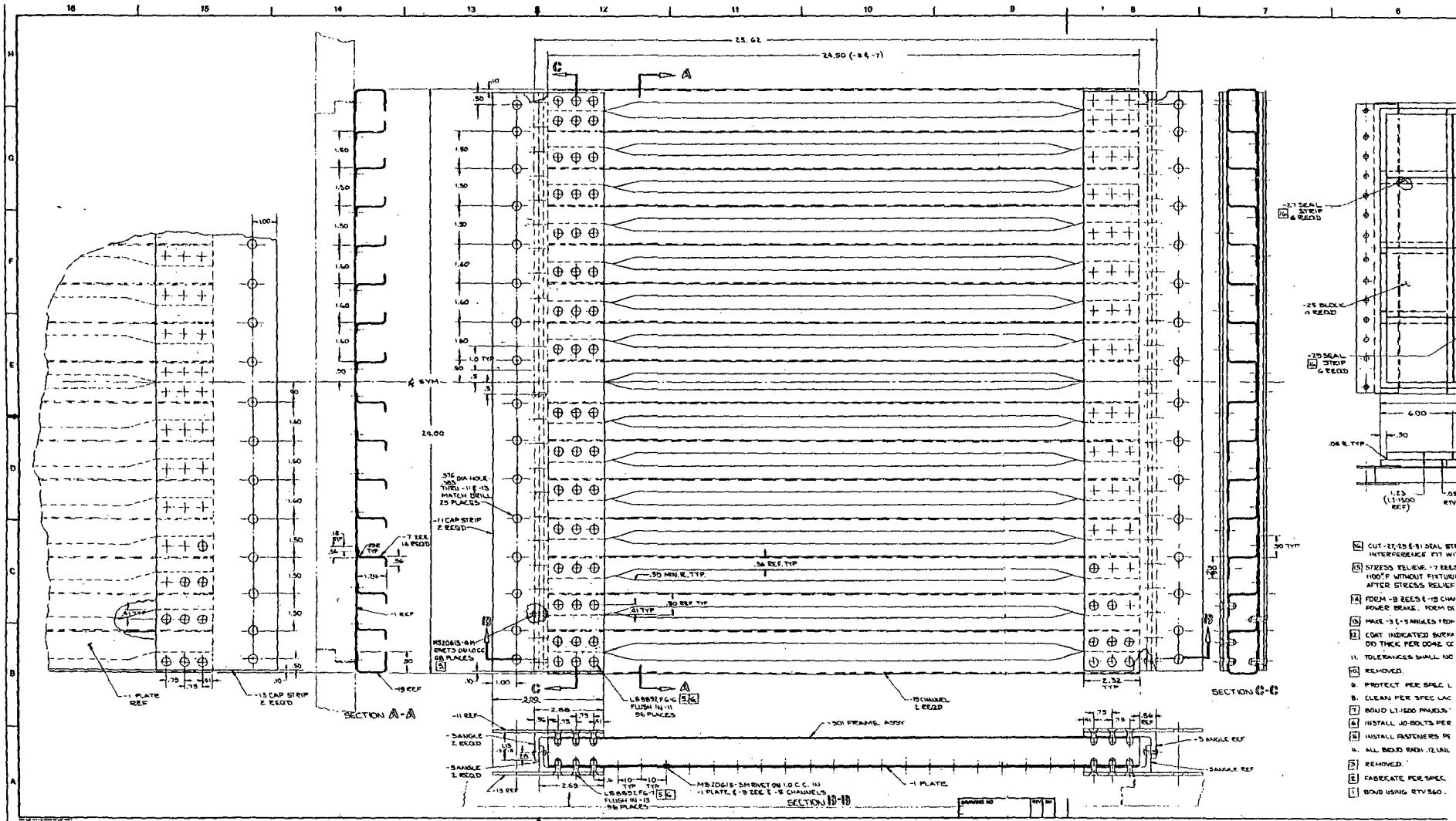


Fig. 6.10-2 Thermal Test Panel No. 2

FOLDOUT FRAME 1

FOLDOUT FRAME 2



- 1 CUT-27-25 6-31 SEAL STR INTERFERENCE FIT W/
- 2 STRESS RELIEVE-7 REE HOOF WITHOUT FIXTURE AFTER STRESS RELIEF
- 3 100M-10 REES 1-15 CHM POWER BRASS, FORM DR
- 4 MAKE-3(1-5)MILES TOP
- 5 COAT INDICATED SURF DO THICK PER DOME CC
- 6 TOLERANCES SHALL NC
- 7 REMOVED
- 8 PROTECT PER SPEC L
- 9 CLEAN PER SPEC LAC
- 10 BOND L/1000 P/ANON
- 11 INSTALL JO-BOLTS PER
- 12 ALL BOND RADI 1/4"AL
- 13 REMOVED
- 14 FABRICATE PER SPEC
- 15 BOND USING RTV SPEC

FOLDOUT FRAME S

LMSC-D152738
Vol II

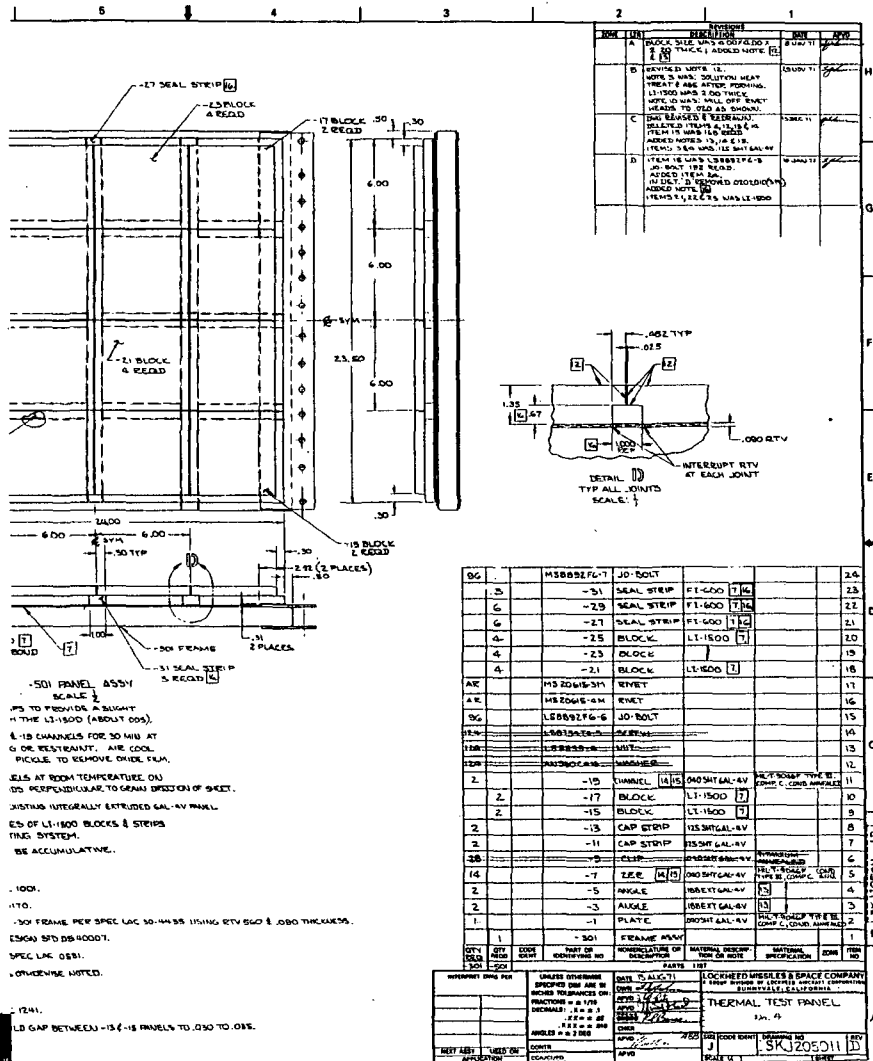


Fig. 6.10-4 Thermal Test Panel No. 4

6.10-9/10

APPENDIX A

DESIGN AND ANALYSIS
OF CANDIDATE PRIMARY
STRUCTURE CONFIGURATIONS

A-1

332<

INTRODUCTION

Three primary structure concepts have been optimized (approximately) and analyzed for Area 2 loads to provide weight (\bar{t}) comparisons for Prototype Panel Configuration No. 2 ($\bar{t} = 0.1144$ in.). The three alternate concepts and their \bar{t} 's are:

- | | |
|-------------------------|------------------------|
| a. Corrugation + Skin | $\bar{t} = 0.1341$ in. |
| b. Honeycomb | $\bar{t} = 0.1472$ in. |
| c. Integrally Stiffened | $\bar{t} = 0.1329$ in. |

Prepared by: <i>J. R. Ritz</i>	Date 10-7-71	LOCKHEED MISSILES & SPACE COMPANY A GROUP DIVISION OF LOCKHEED AIRCRAFT CORPORATION	Page A2
Checked by: <i>G. J. Chinn</i>	Date 11-9-71	Title PROTOTYPE PANELS	Model TPS
Approved by:	Date	DESIGN & ANALYSIS	Report No.

MOMENT AMPLIFICATION FACTORS ~ 2f(u)

$$M_{MAX} = \frac{w l^2}{8} \cdot 2f(u)$$

REF. TIMOSHENKO & GERE,

THEORY OF ELASTIC STABILITY,
2ND ED., ARTICLE 1.5

$$u = \frac{l}{2} \left(\frac{N r_c}{E_c I_o} \right)^{1/2}$$

$$f(u) = \frac{1 - \cos u}{u^2 \cos u}$$

CORR. + SKIN PANELS

$$u_I = \frac{24}{2} \left(\frac{2250}{10.5(22,310)} \right)^{1/2} = 1.176 ; u_I^2 = 1.383 ; u_I (\text{DEG}) = 67^\circ 23'$$

$$u_{II} = \frac{24}{2} \left(\frac{3000}{10.5(22,310)} \right)^{1/2} = 1.358 ; u_{II}^2 = 1.844 ; u_{II} (\text{DEG}) = 77^\circ 48'$$

$$u_{III} = \frac{24}{2} \left(\frac{3000}{9.66(22,310)} \right)^{1/2} = 1.416 ; u_{III}^2 = 2.005 ; u_{III} (\text{DEG}) = 81^\circ 08'$$

COND.	COS u	1-COS u	u ² COS u	f(u)	2f(u)
I	.3846	.6154	.5319	1.157	2.314
II	.2113	.7887	.3896	2.024	4.049
III	.1541	.8459	.3090	2.738	5.475

HONEYCOMB PANELS

$$u_I = \frac{24}{2} \left(\frac{2250}{10.5(25,500)} \right)^{1/2} = 1.100 ; u_I^2 = 1.210 ; u_I (\text{DEG}) = 63^\circ 02'$$

$$u_{II} = \frac{24}{2} \left(\frac{3000}{10.5(25,500)} \right)^{1/2} = 1.270 ; u_{II}^2 = 1.613 ; u_{II} (\text{DEG}) = 72^\circ 46'$$

$$u_{III} = \frac{24}{2} \left(\frac{3000}{9.66(25,500)} \right)^{1/2} = 1.324 ; u_{III}^2 = 1.753 ; u_{III} (\text{DEG}) = 75^\circ 52'$$

COND.	COS u	1-COS u	u ² COS u	f(u)	2f(u)
I	.4535	.5465	.5487	.9960	1.992
II	.2963	.7037	.4779	1.472	2.945
III	.2442	.7558	.4281	1.765	3.531

Prepared by: <i>J. R. Ritz</i>	Date 10-7-71	LOCKHEED MISSILES & SPACE COMPANY A GROUP DIVISION OF LOCKHEED AIRCRAFT CORPORATION	Page A3	Temp.	Perm.
Checked by: <i>G. J. Chwin</i>	Date 11-9-71		Title <u>PROTOTYPE PANELS</u>	Model	
Approved by:	Date	<u>DESIGN & ANALYSIS</u>		Report No.	

MOMENT AMPLIFICATION FACTORS ~ Zf(u)

INTEG. STIFF'D PANELS

$$U_I = 24 \left(\frac{2250}{2 (10.5(28,580))} \right)^{1/2} = 1.039 ; U_I^2 = 1.080 ; U_I (\text{DEG}) = 59^\circ 32'$$

$$U_{II} = 24 \left(\frac{3000}{2 (10.5(28,580))} \right)^{1/2} = 1.200 ; U_{II}^2 = 1.440 ; U_{II} (\text{DEG}) = 63^\circ 45'$$

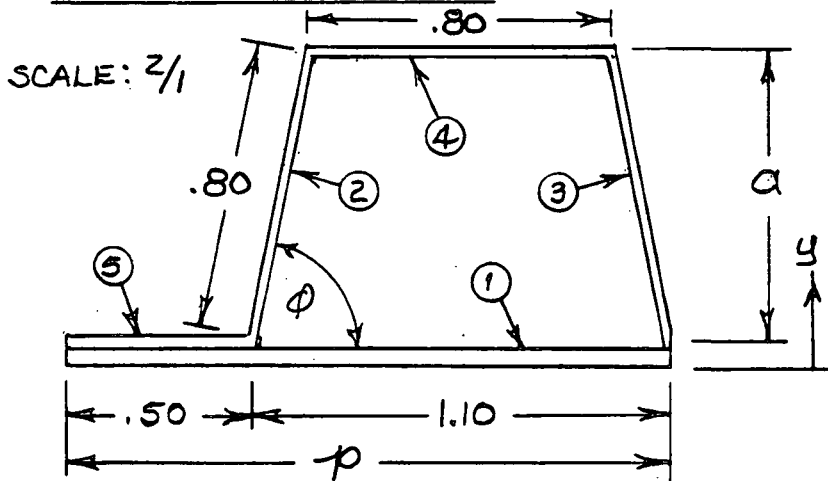
$$U_{III} = 24 \left(\frac{3000}{2 (9.66(28,580))} \right)^{1/2} = 1.251 ; U_{III}^2 = 1.565 ; U_{III} (\text{DEG}) = 71^\circ 41'$$

COND.	cos u	1-cos u	u ² cos u	f(u)	Z f(u)
I	.5070	.4930	.5476	.9003	1.801
II	.3624	.6376	.5219	1.222	2.443
III	.3143	.6857	.4919	1.394	2.788

Prepared by: <i>J. R. Ritz</i>	Date: 9-27-71	LOCKHEED MISSILES & SPACE COMPANY A GROUP DIVISION OF LOCKHEED AIRCRAFT CORPORATION	Page A4
Checked by: <i>A. J. O'Leary</i>	Date: 11-9-71	Title <u>PROTOTYPE PANELS</u>	Model TPS
Approved by:	Date:	<u>DESIGN & ANALYSIS</u>	Report No.

CORR. + SKIN STRUCTURAL PANELS : $l = 24$ in

SECTION! PROPERTIES ~ PER PITCH



$$t_c = .040 \text{ in}$$

$$t_s = .051 \text{ in}$$

$$\cos \phi = .15/.8 = 0.1875$$

$$\phi = 79^\circ 13'$$

$$\sin \phi = 0.9823$$

$$a = .8 \sin \phi = 0.7858 \text{ in}$$

$$p = .50 + 1.10 = 1.60 \text{ in}$$

ELEM.	A	y	Ay	d	Ad ²	I _x
1	.0816	.0255	.002081	.2715	.006015	.000018
2	.0320	.4439	.014205	.1469	.000691	.001647
3	.0320	.4439	.014205	.1469	.000691	.001647
4	.0320	.8368	.026778	.5398	.009324	.000004
5	.0200	.0710	.001420	.2260	.001022	.000003
Σ	.1976		.05869		.01774	.003319

$$\bar{y} = \frac{.05869}{.1976} = 0.2970 \text{ in} ; \bar{E} = \frac{.1976}{1.60} = 0.1235 \text{ in}$$

$$C_{MIN} = 0.2970 \text{ in} ; C_{MAX} = .7858 + .051 - .2970 = 0.5398 \text{ in}$$

$$I_o = .01774 + .003319 = .02106 \text{ in}^4$$

$$\bar{Z}_{OMAX} = \frac{.02106}{.2970} = .07091 \text{ in}^3 ; \bar{Z}_{OMIN} = \frac{.02106}{.5398} = .03901 \text{ in}^3$$

PER INCH OF WIDTH:

$$\bar{I}_o = \frac{.02106}{1.60} = .01316 \text{ in}^4/\text{in} : \text{NOT ADEQUATE ; SEE NEXT PAGE}$$

$$\bar{Z}_{OMAX} = \frac{.07091}{1.60} = .04432 \text{ in}^3/\text{in}$$

$$\bar{Z}_{OMIN} = \frac{.03901}{1.60} = .02438 \text{ in}^3/\text{in}$$

$$R.T. \bar{P}_{CR} = 2602 \text{ lb/in}$$

$$250^\circ \bar{P}_{CR} = 2394 \text{ lb/in}$$

Prepared by: <u>J. R. Ritz</u>	Date: <u>9-27-71</u>	LOCKHEED MISSILES & SPACE COMPANY A GROUP DIVISION OF LOCKHEED AIRCRAFT CORPORATION	Page: <u>A5</u>
Checked by: <u>A. J. Chwin</u>	Date: <u>11-9-71</u>	Title: <u>PROTOTYPE PANELS</u>	Model: <u>TPS</u>
Approved by:	Date:	<u>DESIGN & ANALYSIS</u>	Report No.:

CORR. + SKIN STRUCTURAL PANELS

SECTION PROPERTIES ~ PER PITCH ~ REVISED GEOMETRY

LET $\alpha = 1.00$ & $l_1, l_2,$ & ϕ CHANGE ACCORDINGLY: REST OF GEOMETRY SAME AS ON p. B4.

$\cot \phi = .15/1 = .1500$; $\phi = 81^\circ 28'$; $\sin \phi = 0.9889$; $\cos \phi = 0.1484$
 $l_2 = l_3 = 1/\sin \phi = 1.011$ in

ELEM.	A	y	Ay	d	Ad ²	I _i
1	.08160	.02550	.002081	.3553	.01030	.000018
2	.04044	.5510	.02228	.1702	.00117	.003371
3	.04044	.5510	.02228	.1702	.00117	.003371
4	.03200	1.051	.03363	.6702	.01437	.000004
5	.02000	.07100	.001420	.3098	.00192	.000003
Σ	.2145		.08169		.02893	.006767

$\bar{y} = \frac{.08169}{.2145} = 0.3808$ in; $\bar{z} = \frac{.2145}{1.60} = 0.1341$ in

$C_{MIN} = 0.3808$ in; $C_{MAX} = 1.051 - .3808 = 0.6702$ in

$I_o = .02893 + .006767 = .03570$ in⁴

$\bar{z}_{MAX} = \frac{.03570}{.3808} = .09375$ in³; $\bar{z}_{MIN} = \frac{.03570}{.6702} = .05327$ in³

PER INCH of WIDTH:

$\bar{I}_o = \frac{.03570}{1.60} = .02231$ in⁴/in

$\bar{z}_{MAX} = \frac{.09375}{1.60} = .05859$ in³/in

$\bar{z}_{MIN} = \frac{.05327}{1.60} = .03329$ in³/in

Prepared by: <i>J. R. Ritz</i>	Date: <i>9-28-71</i>	LOCKHEED MISSILES & SPACE COMPANY A GROUP DIVISION OF LOCKHEED AIRCRAFT CORPORATION	Page <i>A6</i>	Temp. <i>A6</i>	Perm.
Checked by: <i>A. J. Chwin</i>	Date: <i>11-9-71</i>	Title <u>PROTOTYPE PANELS</u>	Model <i>TPS</i>		
Approved by:	Date:	<u>DESIGN & ANALYSIS</u>	Report No.		

CORR. + SKIN STRUCTURAL PANELS

MATERIAL ~ ALL 7075-T6, WELDBOND CONSTRUCTION
FROM P. 4, PROTOTYPE PANEL ANALYSIS

	R.T. ~ Ksi	250°F ~ Ksi
F_{tu}	77	63.1
F_{ty}	67	57
F_{cy}	68	60.5
E_c	10.5×10^3	9.66×10^3

LOADS ~ AREA 2 ~ ALL ULTIMATE VALUES
FROM P. 5, PROTOTYPE PANEL ANALYSIS

COND. I: $N_{xT} = 3450$ ppi $p_B = 4.5$ psi
(R.T.) $N_{xc} = 2250$ ppi $p_c = 6$ psi

COND. II: $N_{xT} = 4050$ ppi $p_B = 2.85$ psi
(R.T.) $N_{xc} = 3000$ ppi $p_c = 2.7$ psi

COND. III: $N_{xT} = 6000$ ppi $p_B = 0.75$ psi
(250°F.) $N_{xc} = 3000$ ppi $p_c = 3$ psi

ALLOWABLE COLUMN LOADS ~ EULER

$$\bar{P}_{CR} = \frac{\pi^2 E_c \bar{I}_o}{(1-\nu^2) l^2} = \frac{\pi^2 E_c (.02231)}{.91 (24)^2} = \frac{E_c}{2380}$$

AT R.T.:

$$\bar{P}_{CR} = \frac{10,500}{2.380} = 4412 \text{ lb/in} ; \sigma_{CR} = \frac{4412}{.1341} = 32,900 \text{ psi}$$

AT 250°F.:

$$\bar{P}_{CR} = \frac{9660}{2.380} = 4059 \text{ lb/in} ; \sigma_{CR} = \frac{4059}{.1341} = 30,270 \text{ psi}$$

Prepared by: J. R. Ritz	Date 9-28-71	LOCKHEED MISSILES & SPACE COMPANY A GROUP DIVISION OF LOCKHEED AIRCRAFT CORPORATION	Page A7	Temp. A7	Perm.
Checked by: A. J. Chinn	Date 11-9-71	Title PROTOTYPE PANELS	Model TP5		
Approved by: REV. J. R. R.	Date 10-11-71	DESIGN & ANALYSIS		Report No.	

CORR. + SKIN STRUCTURAL PANELS

MAX. STRESSES ON SECTION ~ ULTIMATE

1. COMPRESSION : COMBINE $N_{\gamma c}$ & P_B ~ BEAM-COLUMN ANALYSIS

$$\sigma_{c \max} = \frac{N_{\gamma c}}{E} + \frac{M_{\max}}{Z_{\min}} = \frac{N_{\gamma c}}{.1341} + \frac{72 P_B z f(u)}{.03329} = 7.457 N_{\gamma c} + 2163 P_B z f(u)$$

COND. I: $\sigma_{c \max} = 7.457(2250) + 2163(4.5)(2.314) = 16,780 + 22,520 = 39,300$ psi

COND. II: $\sigma_{c \max} = 7.457(3000) + 2163(2.85)(4.049) = 22,370 + 24,960 = 47,330$ psi

COND. III: $\sigma_{c \max} = 7.457(3000) + 2163(0.75)(5.475) = 22,370 + 8882 = 31,250$ psi

2. TENSION : COMBINE $N_{\gamma t}$ & P_c ~ DIRECT SUPERPOSITION

$$\sigma_{t \max} = \frac{N_{\gamma t}}{E} + \frac{M_{\max}}{Z_{\min}} = 7.457 N_{\gamma t} + 2163 P_c$$

COND. I: $\sigma_{t \max} = 7.457(3450) + 2163(6) = 25,730 + 12,980 = 38,710$ psi

COND. II: $\sigma_{t \max} = 7.457(4050) + 2163(2.7) = 30,200 + 5840 = 36,040$ psi

COND. III: $\sigma_{t \max} = 7.457(6000) + 2163(3) = 44,740 + 6489 = 51,230$ psi

LOCAL BUCKLING STRESSES ~ $\sigma_{cr \perp}$, ELEMENT ④
(REF: S.M. 80 C)

AT R.T.: $k_z = .0816$ } $\sqrt{K} = 1.90$ (SIMPLY SUPPORTED)
 $n = 15$ } TAB. Z $b/t = .80 / .04 = 20$
 $F_{0.7} = 70$ Ksi } $(b/t)_e = 20 / 1.9 = 10.53$
 $B = .0816(10.53) = 0.859$
 $F/F_{0.7} = 0.95$ (FIG. 2)

$\sigma_{cr \perp} = .95(70) = 66.5$ Ksi

Prepared by: <i>J. R. Ritz</i>	Date 9-28-71	LOCKHEED MISSILES & SPACE COMPANY A GROUP DIVISION OF LOCKHEED AIRCRAFT CORPORATION	Page A8	Temp. Perm.
Checked by: <i>A. J. Chinn</i>	Date 11-9-71	Title <u>PROTOTYPE PANELS</u>	Model TPS	
Approved by: <i>REV. J. R. R.</i>	Date 10-12-71	<u>DESIGN & ANALYSIS</u>	Report No.	

CORR. + SKIN STRUCTURAL PANELS

MARGINS of SAFETY

1. COMPRESSION ALONE ~ COND. III CRITICAL; T=250°F

$$M.S. = \frac{\bar{P}_{CR}}{N_{fc}} - 1 = \frac{4059}{3000} - 1 = 1.353 - 1 = \underline{\underline{+0.35}}$$

COLUMN BUCKLING

2. COMBINED TENSION & COLLAPSE PRESSURE ~ COND. III CRITICAL

$$M.S. = \frac{F_{cu}}{\sigma_{III MAX}} - 1 = \frac{63.1}{51.23} - 1 = 1.232 - 1 = \underline{\underline{+0.23}}$$

TENS.-ULT.

3. COMBINED COMP. & BURST PRESSURE ~ COND. II CRITICAL

$$M.S. = \frac{\sigma_{CR I}}{\sigma_{II MAX}} - 1 = \frac{66.5}{47.33} - 1 = 1.405 - 1 = \underline{\underline{+0.40}}$$

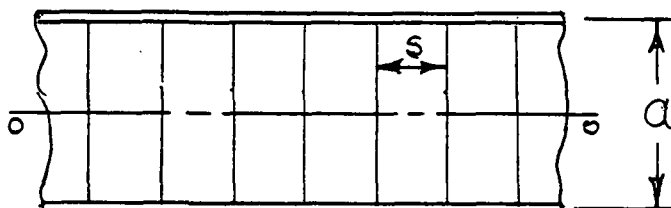
LOCAL BUCKLING

Prepared by: <i>R. Ritz</i>	Date 9-27-71	LOCKHEED MISSILES & SPACE COMPANY A GROUP DIVISION OF LOCKHEED AIRCRAFT CORPORATION	Page A9	Temp. Perm.
Checked by: <i>G. J. Chiu</i>	Date 11-9-71	Title PROTOTYPE PANELS	Model TPS	
Approved by:	Date	DESIGN & ANALYSIS	Report No.	

HONEYCOMB STRUCTURAL PANELS : $l = 24$ in

SECTION PROPERTIES

FULL SCALE



$t_f = .051$ in
 $a = 1.0$ in
 $s = 0.375$ in
 $t_c = .004$ in (S.4 pcf)

$\bar{t} = 2t_f = 2(.051) = 0.1020$ in (THIS \bar{t} NOT FOR WEIGHT)

$\bar{I}_o = t_f a^2 / 2 = .051 (1.0)^2 / 2 = .02550$ in⁴/in

$\bar{\bar{I}}_o = 2\bar{I}_o / a = 2(.02550) / 1 = .05100$ in³/in

LOADS ~ SAME AS ON p. AG, CORR. + SKIN STR. PANELS
(AREA 2 LOADS)

MATERIAL ~ FACE SHEETS ~ 7075-T6 : PROPERTIES ON
p. AG CITED ABOVE

ALLOWABLE COLUMN LOADS ~ EULER

$$\bar{P}_{cr} = \frac{\pi^2 E_c \bar{I}_o}{(1-\nu^4) l^2} = \frac{\pi^2 E_c (.02550)}{.91 (24)^2} = \frac{E_c}{2083}$$

AT R.T.:

$$\bar{P}_{cr} = \frac{10,500}{2.083} = 5041 \text{ lb/in} ; \sigma_{cr} = \frac{5041}{.1020} = 49,420 \text{ psi}$$

AT 250°F:

$$\bar{P}_{cr} = \frac{9660}{2.083} = 4638 \text{ lb/in} ; \sigma_{cr} = \frac{4638}{.1020} = 45,470 \text{ psi}$$

FACE SHEET DIMPLING STRESS ~ F_{cr0}

$$F_{cr0} = \frac{2\pi E_c (t_f/s)^2}{1-\nu^2} \text{ (REF. MIL-HDBK-23A, EQU 4:1)}$$

AT R.T.: $F_{cr0} = \frac{2\pi (10.5 \times 10^6) (.051)^2}{.91 (.375)^2} = 427\pi \times 10^3$: NOT A FAILURE
 MODE FOR THIS
 PANEL

Prepared by: <u>J.R. Ritz</u>	Date: <u>9-27-71</u>	LOCKHEED MISSILES & SPACE COMPANY A GROUP DIVISION OF LOCKHEED AIRCRAFT CORPORATION	Page: <u>A:10</u> Temp. Perm.
Checked by: <u>G.J. Quinn</u>	Date: <u>11-9-71</u>	Title: <u>PROTOTYPE PANELS</u>	Model: <u>TPS</u>
Approved by: <u>REV. S.R.R.</u>	Date: <u>10-12-71</u>	<u>DESIGN & ANALYSIS</u>	Report No.

HONEYCOMB STRUCTURAL PANELS

MAX. STRESSES ON SECTION ~ ULTIMATE

$$\sigma_{\text{max}} = \frac{N_{yc}}{\bar{I}} + \frac{M_{\text{max}}}{\bar{I}_o} = \frac{N_{yc}}{.1020} + \frac{72 P_{\text{max}} \cdot Z_f(u)}{.05100} = 9.804 N_{yc} + 1412 P_{\text{max}} \cdot Z_f(u)$$

$$\sigma_{\text{Tmax}} = \frac{N_{yt}}{\bar{I}} + \frac{M_{\text{max}}}{\bar{I}_o} = \frac{N_{yt}}{.1020} + \frac{72 P_{\text{max}}}{.05100} = 9.804 N_{yt} + 1412 P_{\text{max}}$$

	σ_u	σ_p	$\sigma_{\text{max}} \sim \text{psi}$
<u>COND. I</u> : TENS.	+33,820	+8470	+42,290
COMP.	-22,060	-16,880	-38,940
<u>COND. II</u> : TENS.	+39,710	+4020	+43,730
COMP.	-29,410	-11,850	-41,260
<u>COND. III</u> : TENS.	+58,820	+4240	+63,060
COMP.	-29,410	-14,960	-44,370

MARGINS of SAFETY ~ COND. III CRITICAL ; T = 250°F.

1. COMPRESSION ALONE

$$M.S. = \frac{\bar{P}_{CR}}{N_{yc}} - 1 = \frac{4638}{3000} - 1 = 1.546 - 1 = \underline{\underline{+ 0.55}} \quad \text{COLUMN BUCKLING}$$

2. COMBINED TENSION & PRESSURE

$$M.S. = \frac{F_{tu}}{\sigma_{\text{Tmax}}} - 1 = \frac{63.1}{63.06} - 1 = 1.001 - 1 = \underline{\underline{+ 0.0}} \quad \text{TENS. - ULT.}$$

UNIT WEIGHT ~ W_T & WEIGHT BAR "t" ~ t_w

$$\begin{aligned} W_T &= W_T (\text{FACES}) + W_T (\text{CORE}) + W_T (\text{BOND}) \\ &= (0.1 \text{ lb/in}^3)(.1020 \text{ in})(144 \text{ in}^2/\text{ft}^2) + (5A \text{ lb/ft}^3)(\frac{1}{2} \text{ ft}) + 2(0.1 \text{ lb/ft}^2) \\ &= 1.469 + 0.450 + 0.200 \end{aligned}$$

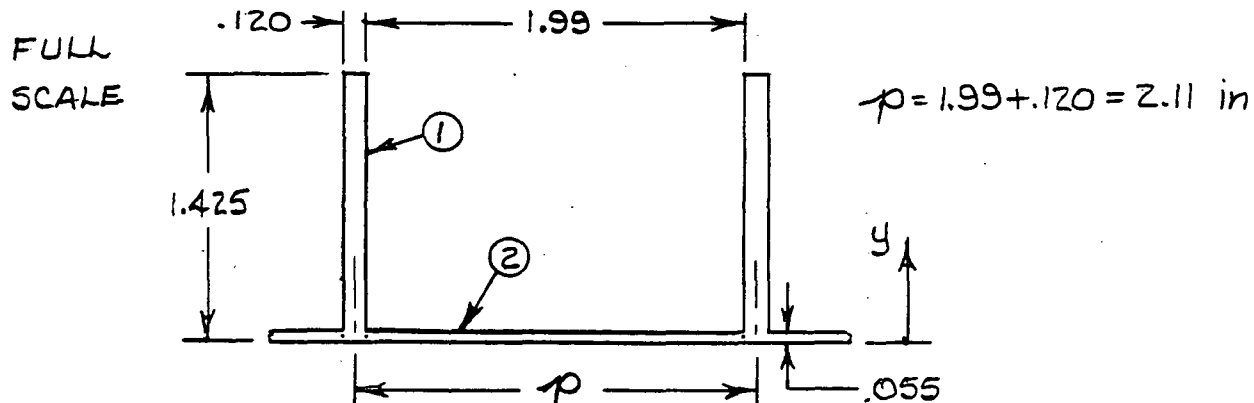
$$W_T = 2.119 \text{ lb/ft}^2$$

$$t_w = \frac{2.119 \text{ lb/ft}^2}{(0.1 \text{ lb/in}^3)(144 \text{ in}^2/\text{ft}^2)} = 0.1472 \text{ in. WEIGHT EQUIVALENT AVERAGE THICKNESS IN ALUMINUM}$$

Prepared by: <u>J. R. Ritz</u>	Date: <u>9-28-71</u>	LOCKHEED MISSILES & SPACE COMPANY A GROUP DIVISION OF LOCKHEED AIRCRAFT CORPORATION	Page: <u>A11</u> Temp. Perm.
Checked by: <u>G. J. Chwin</u>	Date: <u>11-9-71</u>	Title: <u>PROTOTYPE PANELS</u>	Model: <u>TPS</u>
Approved by:	Date:	<u>DESIGN & ANALYSIS</u>	Report No.

INTEG. STIFF'D STRUCTURAL PANELS : $l = 24$ in

SECTION PROPERTIES ~ PER PITCH



ELEM.	A	y	Ay	d	Ad ²	I _i
1	.1710	.7125	.1218	.2674	.01223	.02894
2	.1094	.0275	.0030	.4176	.01910	.00003
Σ	.2804		.1248		.03133	.02897

$$\bar{y} = \frac{.1248}{.2804} = 0.4451 \text{ in} ; \bar{I} = \frac{.2804}{2.11} = 0.1329 \text{ in}$$

$$C_{\text{MIN}} = 0.4451 \text{ in} ; C_{\text{MAX}} = 1.425 - .4451 = 0.9799 \text{ in}$$

$$I_o = .03133 + .02879 = .06030 \text{ in}^4$$

$$Z_{\text{O MAX}} = \frac{.06030}{.4451} = 0.1355 \text{ in}^3 ; Z_{\text{O MIN}} = \frac{.06030}{.9799} = 0.06154 \text{ in}^3$$

PER INCH of WIDTH :

$$\bar{I}_o = \frac{.06030}{2.11} = .02858 \text{ in}^4/\text{in}$$

$$\bar{Z}_{\text{O MAX}} = \frac{.1355}{2.11} = .06422 \text{ in}^4/\text{in}$$

$$\bar{Z}_{\text{O MIN}} = \frac{.06154}{2.11} = .02917 \text{ in}^4/\text{in}$$

Prepared by: J. P. Ritz	Date 9-28-71	LOCKHEED MISSILES & SPACE COMPANY A GROUP DIVISION OF LOCKHEED AIRCRAFT CORPORATION	Page A12	Temp. Perms.
Checked by: G. J. Chinn	Date 11-9-71	Title PROTOTYPE PANELS	Model TPS	
Approved by: REV. J. P. R.	Date 10-12-71	DESIGN & ANALYSIS	Report No.	

INTEG. STIFFENED STRUCTURAL PANELS

LOADS & MATERIAL : ALL AS GIVEN ON P. AG,
CORR. + SKIN PANELS
(AREA 2 LOADS ; 7075-T6 MAT'R'L)

ALLOWABLE COLUMN LOADS ~ EULER

$$\bar{P}_{CR} = \frac{\pi^2 E_c \bar{I}_o}{(1-\nu^2) l^2} = \frac{\pi^2 E_c (.02858)}{.91 (576)} = \frac{E_c}{1858}$$

AT R.T.:

$$\bar{P}_{CR} = \frac{10,500}{1.858} = 5651 \text{ lb/in} ; \sigma_{CR} = \frac{5651}{.1329} = 42,520 \text{ psi}$$

AT 250°F:

$$\bar{P}_{CR} = \frac{9660}{1.858} = 5199 \text{ lb/in} ; \sigma_{CR} = \frac{5199}{.1329} = 39,120 \text{ psi}$$

LOCAL BUCKLING STRESSES ~ σ_{CRl}

ELEMENT ① : REF. S. TANG REPORT

ASSUME $\alpha = 0.5$; THEN $k_c = 1.4$; $(t/b)^2 = (.12/1.425)^2 = 1/141.0$

$$\sigma_{CRl} = \frac{k_c \pi^2 E_c \left(\frac{t}{b}\right)^2}{12(1-\nu^2)} = \frac{1.4 \pi^2 E_c}{12(.91)(141.0)} = \frac{E_c}{111.4} \text{ ; NOT A FAILURE MODE ~ THIS SECTION}$$

ELEMENT ② : ASSUME SIMPLE SUPPORTS

$$\sigma_{CRl} = 3.6 E_c \left(\frac{t}{b}\right)^2 = 3.6 E_c \left(\frac{.055}{1.99}\right)^2 = \frac{E_c}{363.6}$$

$$\text{AT R.T. : } \sigma_{CRl} = \frac{10.5 \times 10^6}{363.6} = 28,880 \text{ psi}$$

$$\text{AT 250°F : } \sigma_{CRl} = \frac{9.66 \times 10^6}{363.6} = 26,570 \text{ psi}$$

Prepared by: <u>J. R. Ritz</u>	Date: <u>9-28-71</u>	LOCKHEED MISSILES & SPACE COMPANY A GROUP DIVISION OF LOCKHEED AIRCRAFT CORPORATION	Page: <u>A 13</u>	Temp.:	Perm.:
Checked by: <u>A. J. Chinn</u>	Date: <u>11-9-71</u>	Title: <u>PROTOTYPE PANELS</u>	Model: <u>TPS</u>		
Approved by: <u>REV. J. R. R.</u>	Date: <u>10-12-72</u>	<u>DESIGN & ANALYSIS</u>	Report No.:		

INTEGRALLY STIFFENED STRUCTURAL PANELS

CRITICAL STRESSES ON SECTION ~ ULTIMATE

1. COMPRESSION ON ELEM. ②: COND. III CRITICAL
(COMP. N_x & COLLAPSE p)

$$\sigma_{c, \max} = \frac{N_{xc}}{F} + \frac{M_{\max}}{Z_{o, \max}} = \frac{3000}{.1329} + \frac{72(3)}{.06422} = 22,570 + 3363 (2.788)$$

$$\sigma_{c, \max} = 22,570 + 9377 = 31,950 \text{ psi}$$

2. TENSION ON ELEM. ①: COND. III CRITICAL
(TENS. N_x & COLLAPSE p)

$$\sigma_{t, \max} = \frac{N_{xt}}{F} + \frac{M_{\max}}{Z_{o, \min}} = \frac{6000}{.1329} + \frac{72(3)}{.02917} = 45,140 + 7404$$

$$\sigma_{t, \max} = 52,540 \text{ psi}$$

MARGINS OF SAFETY ~ COND. III CRITICAL; T = 250 °F.

1. COMPRESSION ALONE

$$M.S. = \frac{\bar{P}_{cr}}{N_{xc}} - 1 = \frac{5199}{3000} - 1 = 1.733 - 1 = \underline{+ 0.73}$$

COLUMN BUCKLING

2. COMBINED COMPRESSION & COLLAPSE PRESSURE

$$M.S. = \frac{\sigma_{cr, l}}{\sigma_{c, \max}} - 1 = \frac{26.57}{31.91} - 1 = 0.833 - 1 = \underline{- 0.17}^*$$

LOCAL BUCKLING

3. COMBINED TENSION & COLLAPSE PRESSURE

$$M.S. = \frac{F_{tu}}{\sigma_{t, \max}} - 1 = \frac{63.1}{52.45} - 1 = 1.203 - 1 = \underline{+ 0.20}$$

TENS. - UJT.

* THE GEOMETRY SELECTED (p. A11) IS NOT ADEQUATE FOR THE DESIGN LOADS; HOWEVER, THE POINT IS MADE THAT THIS CONFIGURATION IS NOT MORE EFFICIENT THAN THE Z-STIFFENED PANELS.

Appendix B
STRESS ANALYSIS OF SUBSTRATE
FOR PROTOTYPE PANEL No. 1

B-1

346<

Prepared by:
A. J. CHINN

Date
9-1-71

LOCKHEED MISSILES & SPACE COMPANY
A GROUP DIVISION OF LOCKHEED AIRCRAFT CORPORATION

Page Temp. Perm.
81

Checked by:
J. R. Ritz

Date
9-13-71

Title
TASK 6: PROTOTYPE PANELS

Model

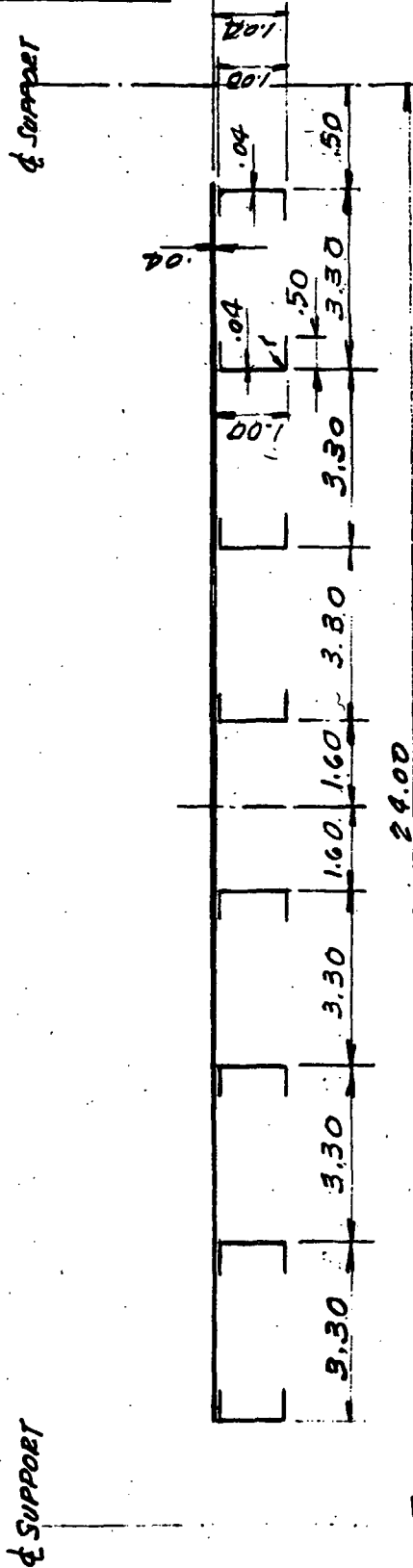
Approved by:

Date

DESIGN & ANALYSIS

Report No.

Bc SUBPANEL #1



SECTION - TYPICAL

MATERIAL: BERYLLIUM X-ROLLED SHEET

BRAZING MAT: B18A9 ALLOY 60A9-30Ca-10Sr 0.003 THICK

$r = 5t = 5 \times .040 = .200$

D/N SK 90371

Prepared by: A. J. CHINN	Date 9-1-71	LOCKHEED MISSILES & SPACE COMPANY A GROUP DIVISION OF LOCKHEED AIRCRAFT CORPORATION	Page B2	Temp. 	Perm.
Checked by: J. L. Ritz	Date 9-13-71	Title TASK 6: PROTOTYPE PANELS	Model		
Approved by: REV. J. R. R.	Date 9-26-71	DESIGN & ANALYSIS	Report No.		

Be SUBPANEL #1

THIS PANEL WILL BE DESIGNED FOR PRESSURE ONLY

LOADS

ASCENT $P_{COLLAPSE} = 4.0 \text{ psi LIMIT @ R.T., } 6.0 \text{ psi ULT.}$

$P_{BURST} = 3.0 \text{ psi LIMIT @ R.T., } 4.5 \text{ psi ULT.}$

REENTRY $P_{COLLAPSE} = 2.0 \text{ psi LIMIT @ } 600^{\circ}\text{F } 3.0 \text{ psi ULT.}$

$P_{BURST} = 0.5 \text{ psi LIMIT @ } 600^{\circ}\text{F } 0.75 \text{ psi ULT}$

BY INSPECTION - ASCENT LOADINGS ARE CRITICAL FOR DESIGN

MATERIAL PROPERTIES

	<u>@ R.T.</u>	<u>@ 600°F</u>
F_{CU}	$75,000 \text{ #/IN}^2$	$46,000 \text{ #/IN}^2$
F_{CY}	$57,800 \text{ #/IN}^2$	$43,000 \text{ #/IN}^2$
E	$42.5 \times 10^6 \text{ #/IN}^2$	$39.3 \times 10^6 \text{ #/IN}^2$

CRITICAL STRESSES

$$F_{CR} = K \eta E_c \left(\frac{t}{b}\right)^2$$

FOR FIXED EDGES $K = 6.3$

FOR FREE EDGES $K = 0.395$

$$\eta = \sqrt{\frac{E_T}{E}}$$

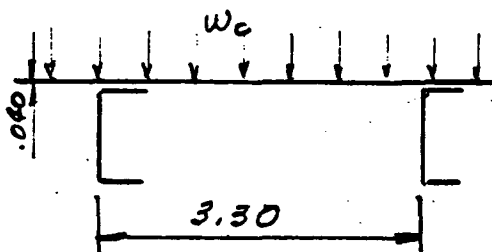
REFERENCE

- 348<
- 1 BERYLLIUM MECHANICAL PROPERTY DATA AFML MAR 67
 - 2 "STRENGTH OF MATERIALS" BY SHANLEY, PAGE 611

Prepared by: A. J. CHINN	Date 9-1-71	LOCKHEED MISSILES & SPACE COMPANY A GROUP DIVISION OF LOCKHEED AIRCRAFT CORPORATION	Page 33	Temp. Perm.
Checked by: J. R. Ritz	Date 9-13-71	Title TASK G. PROTOTYPE PANELS	Model	
Approved by: REV. J. R. R.	Date 9-26-71	DESIGN & ANALYSIS.	Report No.	

BE SUBPANEL #1

FACE SHEET



CONSIDER THE FACE SHEET AS CONTINUOUS AND SPANNING OVER A NUMBER OF SUPPORTS

LOADING = 6.0 #/IN^2 (ULT.) @ RT.

FOR CONSERVATIVE REASONS, LET $M = \frac{w_0 l^2}{10}$

$$M = \frac{6.0 \times 3.30^2}{10} = 6.534 \text{ #/IN}$$

$$f_b = \frac{6M}{t_s^3} = \frac{6 \times 6.534}{.040 \times .040} = 24,500 \text{ #/IN}^2$$

$$\frac{F_{cr}}{A} = K E_c \left(\frac{t_s}{b}\right)^2 = 6.3 \times 42.5 \times 10^6 \left(\frac{.040}{3.30}\right)^2 = 39,340 \text{ #/IN}^2$$

$$V = \frac{w_0 l}{2} = \frac{6.0 \times 3.30}{2} = 9.90 \text{ #/IN}$$

$$v = \frac{3}{2} \frac{V}{A} = 1.5 \times \frac{9.90}{.040} = 371 \text{ #/IN}^2$$

$$\Delta_{ult} = \frac{w_0 l^4}{384 E I} = \frac{12 \times 6.0 \times 3.30^4}{384 \times 42.5 \times 10^6 \times .04^3} = .0082'' \text{ etc}$$

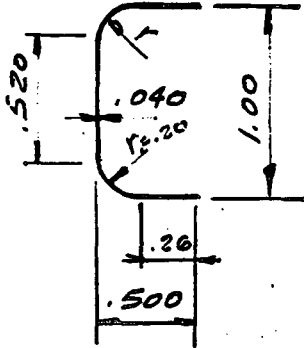
FROM EM B1-M2-1, ENTITLED, "BERYLLIUM CROSS-ROLLED SHEET DESIGN DATA AT ROOM TEMPERATURE AND 600°F" FIG. 12. THE EFFECT OF INELASTIC BUCKLING REDUCES F_{cr} TO $34,500 \text{ #/IN}^2$

$$M.S. = \frac{34,500}{24,500} - 1 = 0.41$$

Prepared by: A. J. CHINN	Date 9-1-71	LOCKHEED MISSILES & SPACE COMPANY A GROUP DIVISION OF LOCKHEED AIRCRAFT CORPORATION	Page 34	Temp.	Perm.
Checked by: J. R. Ritz	Date 9-13-71	Title TASK G: PROTOTYPE PANELS	Model		
Approved by: REV. J. R. R.	Date 9-26-71	DESIGN & ANALYSIS	Report No.		

Be SUBPANEL # 1

STIFFENERS



LOADING = +6.0 #/IN² @ R.T.
- 4.5 #/IN² @ R.T.

$$w_c = 6.0 \times 3.3 = 19.80 \text{ #/IN}$$

$$w_b = 4.5 \times 3.3 = 14.85 \text{ #/IN}$$

b	d	A	y	Ay	y'	A(y') ²	I _o	I _o + A(y') ²
.26	.040	.01040	.020	.000208	.480	.002396		
.26	.040	.01040	.980	.010192	.480	.002396		
π × .22	.040	.02765	.500	.013825	.500	.007424	.000060	
.040	.520	.02080	.500	.010400	-		.000468	
		.06925	.500	.034625				.009744

FOR COLLAPSE PRESSURE

$$l = 23"$$

$$M = \frac{w_b l^2}{8} = \frac{19.80 \times 23^2}{8} = 1309 \text{ "K}$$

$$f_{ULT} = \frac{M c}{I} = \frac{1309 \times .500}{.009744} = 67,170 \text{ #/IN}^2$$

$$m.s. = +0.12$$

$$\frac{F_{cr}}{n} = 0.385 \times 42.5 \times 10^6 \left(\frac{.040}{.380} \right)^2 = 182,000 \text{ #/IN}^2$$

$$F_{cr} = 53,000 \text{ #/IN}^2$$

FOR BURST PRESSURE

$$f_{ULT} = \frac{4.5}{6.0} \times 67,170 = 50,380 \text{ #/IN}^2$$

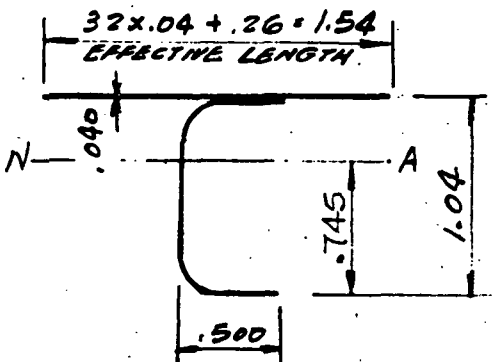
$$m.s. = +0.05$$

$$f_{yield} = \frac{50,380 \times 1.14}{1.5} = 38,290 \text{ #/IN}^2$$

$$m.s. = +0.39$$

13c SUBPANEL #1

STIFFENER & FACE SHEET



$$\bar{t} = \frac{.06925 + 3.30(.040)}{3.30} = .0610 \text{ in}$$

	A	y	Ay	y'	A(y') ²	I _o	I _o + A(y') ²
FACE SHEET 1.54 x .04	.06160	.520	.032032	.275	.004658		
STIFFENER	.06925	0	0	.245	.004157	.009744	
	.13085	.245	.032032		.008815		.01856 ✓

FOR COLLAPSE PRESS:

$$M = 1309 \text{ "lb (PAGE 4)}$$

$$y_1 = .295 \quad y_2 = .745$$

BENDING STRESSES

$$f_{\text{FACE SHEET}} = \frac{My_1}{I} = \frac{1309 \times .295}{.01856} = 20,810 \text{ #/IN}^2 \text{ COMP. (ULT.)}$$

$$f_{\text{FLANGE}} = \frac{My_2}{I} = \frac{1309 \times .745}{.01856} = 52,540 \text{ #/IN}^2 \text{ TENSION (ULT.)}$$

$$m.s. = +0.43$$

LONGITUDINAL SHEAR AT JUNCTURE

$$V = \frac{wL}{2} = \frac{19.80 \times 23}{2} = 228 \text{ #}$$

$$\tau = \frac{VQ}{I} = \frac{228 \times .06160 \times .275}{.01856} = 208 \text{ #/IN (ULT.)}$$

DEFLECTION FOR LIMIT LOAD, $w = \frac{19.80}{1.5}$

$$\Delta = \frac{5wl^4}{384EI} = \frac{5 \times 19.80 \times 23^4}{1.5 \times 384 \times 42.5 \times 10^6 \times .01856} = 0.061 \text{ "}$$

FOR BURST PRESSURE, $f_{\text{FLANGE}} = \frac{4.5}{6.0} \times 52,540 = 39,400 \text{ #/IN}^2$

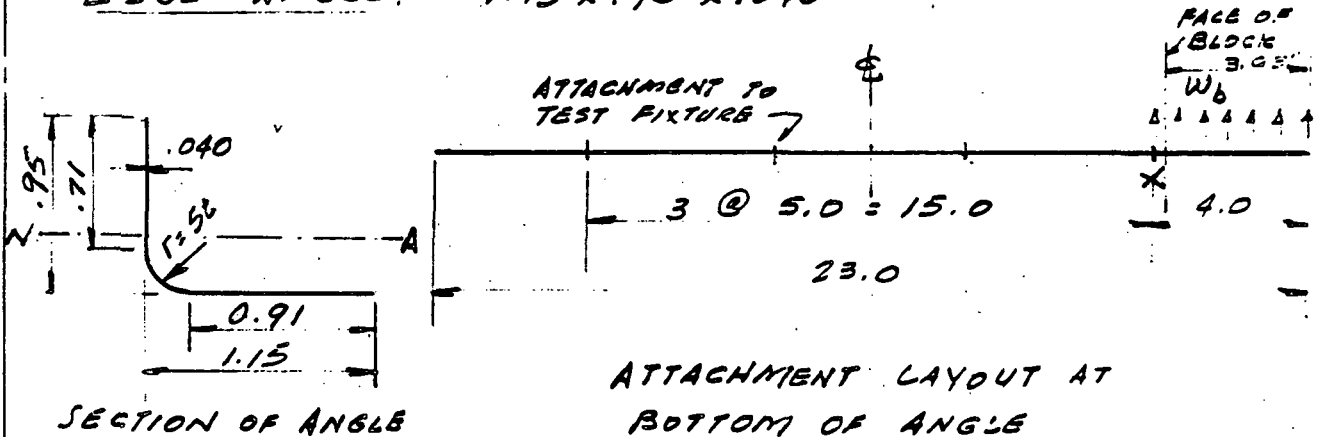
351 < B-6

$$m.s. = +0.34$$

Prepared by: <i>G. J. CHINN</i>	Date: <i>9-2-71</i>	LOCKHEED MISSILES & SPACE COMPANY A GROUP DIVISION OF LOCKHEED AIRCRAFT CORPORATION	Page <i>36</i>	Temp.	Perm.
Checked by: <i>J. R. Ritz</i>	Date: <i>9-16-71</i>	Title <i>TASK G: PROTOTYPE PANELS</i>	Model		
Approved by: <i>REV. J. R. R.</i>	Date: <i>9-26-71</i>	<i>DESIGN & ANALYSIS</i>	Report No.		

Bc SUBPANEL #1

EDGE ANGLE. 1.15 x .95 x .040 Bc



b	d	A	y	Ay	y'	A(y') ²	I _o	I _o + A(y') ²
0.910	0.040	.03640	.020	.000728	.222	.001794	.000005	
$\frac{\pi}{4} \times .220$	0.040	.01382	.100	.001382	.142	.000279	.000060	
0.040	0.710	.02840	.595	.016898	.353	.003539	.001193	
		.078620	.242	.019005		.005612		.006870

$$W_b = 12 \times 4.5 = 54 \text{ #/IN Burst Press (ULT.)}$$

$$M_{\text{FACE OF BLOCK}} = \frac{W_b l^2}{2} = \frac{54 \times 3.63^2}{2} = 356 \text{ "#}$$

$$f_{\text{BOTTOM FLANGE}} = \frac{My_1}{I} = \frac{356 \times .242}{.00687} = 12,530 \text{ #/IN}^2 \text{ (TENSION)}$$

$$f_{\text{VERT. LEG}} = \frac{My_2}{I} = \frac{356 \times .708}{.00687} = 36,690 \text{ #/IN}^2 \text{ (COMP.)}$$

$$\frac{FCR}{\eta} = 0.385 \times 92.5 \times 10^6 \left(\frac{.040}{.71} \right)^2 = 52,000 \text{ #/IN}^2$$

CORRECTED FOR INELASTIC REDUCTION.

$$FCR = 41,000 \text{ #/IN}^2 \text{ ALLOWED}$$

$$M.S. = \frac{41,000}{36,690} - 1 = 0.12$$

352<

B-7

Appendix C

STRESS ANALYSIS OF SUBSTRATES
FOR PROTOTYPE PANEL Nos. 2 THROUGH 4

C-1

353<

Prepared by: <i>J. P. Ritz</i>	Date 10-11-71	LOCKHEED MISSILES & SPACE COMPANY A GROUP DIVISION OF LOCKHEED AIRCRAFT CORPORATION	Page c1	Temp.	Perm.
Checked by:	Date	Title <u>PROTOTYPE PANELS</u>	Model TPS		
Approved by:	Date	<u>DESIGN & ANALYSIS</u>	Report No.		

TABLE of CONTENTS

1. INTRODUCTION	2
2. DESIGN LOADS ~ SUMMIARY	3
3. CONFIGURATION No. 2 ANALYSIS	4
4. CONFIGURATION No. 3 ANALYSIS	11
5. CONFIGURATION No. 4 ANALYSIS	17
6. MAXIMUM STRESSES ~ SUMMARY ~ LINEAR ANALYSIS	24
7. REFERENCES	25

Prepared by: <i>J. R. Ritz</i>	Date <i>10-5-71</i>	LOCKHEED MISSILES & SPACE COMPANY A GROUP DIVISION OF LOCKHEED AIRCRAFT CORPORATION	Page <i>C2</i>	Temp.	Perm.
Checked by: <i>E. Davis</i>	Date <i>10-12-71</i>	Title <u>PROTOTYPE PANELS</u> <u>DESIGN & ANALYSIS</u>	Model <i>TPS</i>		
Approved by:	Date		Report No.		

Reproduced from
best available copy. 

INTRODUCTION

THE STRUCTURAL PROTOTYPE PANELS, CONFIGURATION NO'S. 2, 3, & 4, WERE OPTIMALLY SIZED FOR THE DESIGN LOAD CONDITIONS BY USE OF THE DIGITAL COMPUTER. THE FOLLOWING ANALYSIS OF THESE PANELS IS, THEREFORE, BASICALLY AN INDEPENDENT CHECK OF THE COMPUTER ANALYSIS. THE PRESSURE LOADS USED IN THIS ANALYSIS ARE, IN MOST CASES, SLIGHTLY LESS THAN THE VALUES WHICH WERE USED IN SIZING THE PANELS; THE SIZING, HOWEVER, HAS NOT BEEN ALTERED.

THE PORTIONS OF THIS WORK, WHICH RELATE TO BEARING, FASTENER STRENGTH, AND RIVET SPACING, WERE NOT INCLUDED IN THE COMPUTER ANALYSIS.

THESE PANELS HAVE BEEN FURTHER EVALUATED, AND DEFLECTIONS DETERMINED, UNDER COMBINED PRESSURE & COMPRESSIVE LINE LOAD, BY USE OF THE "BEAM-COLUMN" COMPUTER CODE.

355<

Prepared by: <i>R. Ritz</i>	Date 9-29-71	LOCKHEED MISSILES & SPACE COMPANY A GROUP DIVISION OF LOCKHEED AIRCRAFT CORPORATION	Page C3	Temp. Form.
Checked by: <i>E. J. Davis</i>	Date 10-12-71	Title <u>PROTOTYPE PANELS</u>	Model TPS	
Approved by:	Date		Report No.	

DESIGN LOADS ~ SUMMARY (REF. No. 5)

LOAD COND.	IN PLANE LINE LOAD ~ lb/in				DIFFERENTIAL PRESSURE ~ lb/in ²			
	TENSION		COMPRESSION		BURST		COLLAPSE	
	LIM.	ULT.	LIM.	ULT.	LIM.	ULT.	LIM.	ULT.
<u>AREA 1 PANELS</u>								
I	2400	3600	2100	3150	3.0	4.5	2.0	3.0
II	2700	4050	4000	6000	1.5	2.25	0.9	1.35
III	4000	6000	2000	3000	0.5	0.75	2.0	3.0
<u>AREA 2 PANELS</u>								
I	2300	3450	1500	2250	3.0	4.5	4.0	6.0
II	2700	4050	2000	3000	1.9	2.85	1.8	2.7
III	4000	6000	2000	3000	0.5	0.75	2.0	3.0

NOTES:

1.	PROTOTYPE PANEL CONFIGURATION No.	LOAD AREA No.	MAX. TEMP. COND. III ~°F.
	1	2-PRESSURE PANEL	600
	2	2	250
	3	1	250
	4	2	600

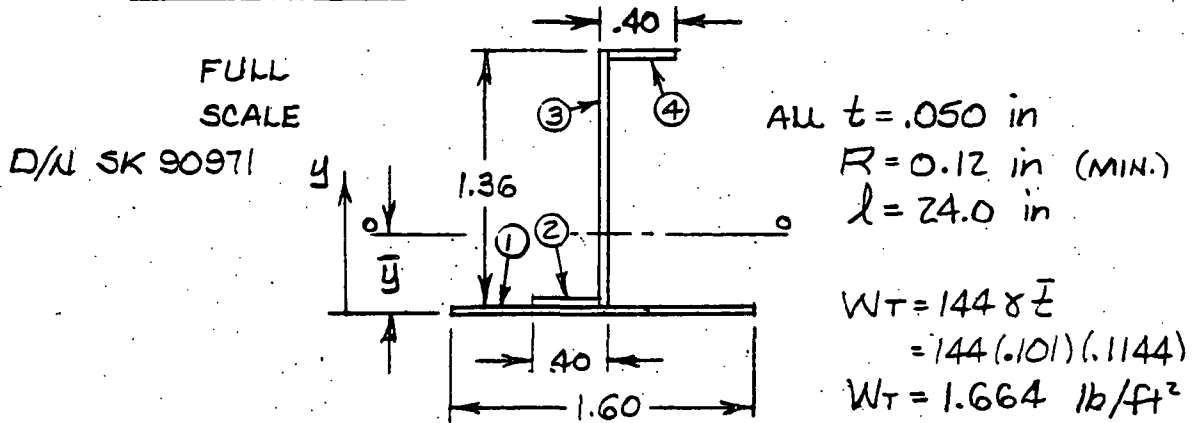
2. LOAD CONDITIONS I, II AT ROOM TEMPERATURE

3. LINE LOADS AND PRESSURES AND IN ANY COMBINATION ON PANEL CONFIGURATIONS 2, 3 & 4

4. FACTOR OF SAFETY 1.6

Prepared by: <i>J. R. Ritz</i>	Date 9-4-71	LOCKHEED MISSILES & SPACE COMPANY A GROUP DIVISION OF LOCKHEED AIRCRAFT CORPORATION	Page Temp. Perm. 64
Checked by: <i>E. F. Lamb</i>	Date 10-12-71	Title <u>PROTOTYPE PANELS</u>	Model TPS
Approved by:	Date	<u>DESIGN & ANALYSIS</u>	Report No.

CONFIGURATION No. 2
SECTION PROPERTIES



ELEM.	A	y	Ay	d	Ad ²	I _i
1	.0800	.025	.00200	.3968	.01260	.00002
2	.0175	.075	.00131	.3468	.00210	—
3	.0680	.730	.04964	.3082	.00646	.01048
4	.0175	1.385	.02424	.9632	.01624	—
Σ	.1830		.07719		.03740	.01050

$$\bar{y} = \frac{.07719}{.1830} = 0.4218 \text{ in} ; \bar{z} = \frac{.1830}{1.60} = 0.1144 \text{ in}$$

$$I_o = .03740 + .01050 = .04790 \text{ in}^4 ; \bar{I}_o = \frac{.04790}{1.60} = .02994$$

$$\bar{I}_o = \frac{.04790}{1.60} = 0.2994 \text{ in}^4/\text{in}$$

$$e = (.2617)^{1/2} = 0.5116 \text{ in} \left\{ \begin{array}{l} \bar{z}_{o \max} = .02994 / .4218 = .07098 \text{ in}^3/\text{in} \\ \bar{z}_{o \min} = .02994 / .9822 = .03048 \text{ in}^3/\text{in} \end{array} \right.$$

MATERIAL ~ 7075-T6 - ALUMINUM ALLOY : REF. MIL-HDBK-5A, SECT. 3.2.7

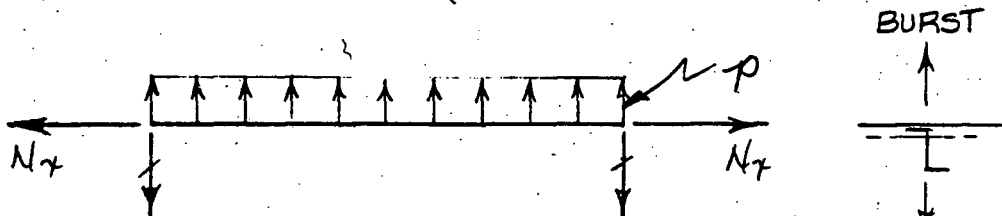
	R.T. (TAB. 3.2.7.0 (b))	250 °F (5 HRS. EXPOSURE)
F_{tu}	77 Ksi (.82)	63.1 Ksi (FIG. 3.2.7.1.1 (a))
F_{ty}	67 Ksi (.85)	57.0 Ksi (FIG. 3.2.7.1.1 (b))
F_{cy}	68 Ksi (.89)	60.5 Ksi (FIG. 3.2.7.1.2 (a))
E	10.3×10^3 Ksi (.92)	9.47×10^3 Ksi (FIG. 3.2.7.1.4)
E_c	10.5×10^3 Ksi (.92)	9.66×10^3 Ksi (FIG. 3.2.7.1.4)
F_{brx}	146 Ksi (.83)	121 Ksi (FIG. 3.2.7.1.3 (a))
F_{by}	107 Ksi (.91)	97.4 Ksi (FIG. 3.2.7.1.3 (b))
$\chi = 0.101 \text{ lb/in}^3$		

Prepared by: <i>J.R. Ritz</i>	Date 9-4-71	LOCKHEED MISSILES & SPACE COMPANY A GROUP DIVISION OF LOCKHEED AIRCRAFT CORPORATION	Page C5	Temp. Perm.
Checked by: <i>E.F. Davis</i>	Date 10-12-71		Title PROTOTYPE PANELS	
Approved by: REV. <i>J.R.R.</i>	Date 9-26-71		Model TPS	
Title DESIGN & ANALYSIS			Report No.	

CONFIGURATION No. 2

DESIGN LOADS (AREA 2) (REF. No. 5)

COND.	$N_x \sim \text{ppi}$		$p \sim \text{psi}$	
	LIMIT	ULT.	LIMIT	ULT.
I (R.T.)	2300 -1500	3450 -2250	3.0 -4.0	4.5 -6.0
II (R.T.)	2700 -2000	4050 -3000	1.9 -1.8	2.85 -2.7
III (250°F)	4000 -2000	6000 -3000	0.5 -2.0	0.75 -3.0



+ $N_x \sim$ TENSION ; - $N_x \sim$ COMPRESSION
+ $p \sim$ BURST ; - $p \sim$ COLLAPSE

ALLOW. COLUMN LOADS \sim EULER

$$\bar{P}_{cr} = \frac{\pi^2 E_c \bar{I}_o}{(1-\nu^2) l^2} = \frac{\pi^2 E_c (.02994)}{.91 (24)^2} = \frac{E_c}{1774}$$

AT R.T.:

$$\bar{P}_{cr} = \frac{10,500}{1.774} = 5919 \text{ lb/in}$$

$$\sigma_{cr} = \frac{\bar{P}_{cr}}{t} = \frac{5919}{.1144} = 51,740 \text{ psi}$$

AT 250°F:

$$\bar{P}_{cr} = \frac{9660}{1.774} = 5445 \text{ lb/in}$$

$$\sigma_{cr} = \frac{5445}{.1144} = 47,600 \text{ psi}$$

358<

Prepared by: J. R. Ritz	Date 9-7-71	LOCKHEED MISSILES & SPACE COMPANY A GROUP DIVISION OF LOCKHEED AIRCRAFT CORPORATION	Page 66	Temp. Perm.
Checked by: E. F. Davis	Date 10-12-71	Title PROTOTYPE PANELS	Model TPS	
Approved by: REV. J. R. R.	Date 9-26-71	DESIGN & ANALYSIS	Report No.	

CONFIGURATION No. 2

MAX. ULTIMATE STRESSES ~ APPLIED

1. COMPRESSIVE N_c & BURST P ~ MAX. σ_c ON FREE LEG

REF.: TIMOSHENKO, THEORY OF ELASTIC STABILITY, 2ND ED.,
CHAPTER 1

$$\sigma_{c \max} = \frac{N_c}{I} + \frac{M_{\max}}{Z_{\min}}$$

$$M_{\max} = \frac{P l^2}{8} \cdot \frac{2(1 - \cos u)}{u^2 \cos u} = 144 P_B \cdot f(u) \quad (\text{EQN 1-23, REF.})$$

$$u = \frac{l}{2} \sqrt{\frac{N_c}{E_c I}} \quad (\text{EQN 1-13, REF.}) ; f(u) = \frac{1 - \cos u}{u^2 \cos u}$$

$$u = \frac{l}{2 (I \times 10^6)^{1/2}} \left(\frac{N_c}{E_c \times 10^6} \right)^{1/2} = \frac{24}{2(29,940)^{1/2}} \left(\frac{N_c}{E_c \times 10^6} \right)^{1/2} = \frac{1}{14.42} \left(\frac{N_c}{E_c \times 10^6} \right)^{1/2}$$

$$u_I = \frac{1}{14.42} \left(\frac{2250}{10.5} \right)^{1/2} = 1.015 ; u_I^2 = 1.030$$

$$u_{II} = \frac{1}{14.42} \left(\frac{3000}{10.5} \right)^{1/2} = 1.172 ; u_{II}^2 = 1.374$$

$$u_{III} = \frac{1}{14.42} \left(\frac{3000}{9.66} \right)^{1/2} = 1.222 ; u_{III}^2 = 1.493$$

LOAD COND.	u RAD.	u DEG.	$\cos u$	$1 - \cos u$	$u^2 \cos u$	$f(u)$
I	1.015	58°09'	.5277	.4723	.5435	0.8690
II	1.172	67°09'	.3883	.6117	.5335	1.147
III	1.222	70°01'	.3418	.6582	.5103	1.290

$$M_{I \max} = 144 (4.5) (0.8690) = 563.1 \text{ in-lb/in (ULT.)}$$

$$M_{II \max} = 144 (2.85) (1.147) = 470.7 \text{ in-lb/in (ULT.)}$$

$$M_{III \max} = 144 (0.75) (1.290) = 139.3 \text{ in-lb/in (ULT.)}$$

Prepared by: J. R. Ritz	Date: 9-7-71	LOCKHEED MISSILES & SPACE COMPANY A GROUP DIVISION OF LOCKHEED AIRCRAFT CORPORATION	Page 07	Temp. Per.
Checked by: E. F. Davis	Date: 10-12-71	Title: PROTOTYPE PANELS	Model TPS	
Approved by: REV. J. R. R.	Date: 9-26-71	DESIGN & ANALYSIS	Report No.	

CONFIGURATION No. 2

MAX. ULTIMATE STRESSES ~ APPLIED ~ STIFFENER FREE LEG

1. COMPRESSIVE N_x & BURST P ~ MAX. σ_c ON FREE LEG

COND. I: $\sigma_{I \max} = \frac{2250}{.1144} + \frac{563.1}{.03048} = 19,670 + 18,470 = 38,140$ psi (ULT.)

COND. II: $\sigma_{II \max} = \frac{3000}{.1144} + \frac{470.7}{.03048} = 26,220 + 15,440 = 41,660$ psi (ULT.)

COND. III: $\sigma_{III \max} = \frac{3000}{.1144} + \frac{139.3}{.03048} = 26,220 + 4,570 = 30,790$ psi (ULT.)

2. TENSILE N_x & COLLAPSE P ~ MAX. σ_T ON FREE LEG

USE DIRECT SUPERPOSITION OF TENSION & BENDING

$$\sigma_{T \max} = \frac{N_{xT}}{E} + \frac{M_{\max}}{Z_{\min}} = \frac{N_{xT}}{E} + \frac{P_{\max} l^2}{8 Z_{\min}} = \frac{N_{xT}}{E} + \frac{72 P_{\max}}{8 Z_{\min}}$$

COND. I: $\sigma_{I \max} = \frac{3450}{.1144} + \frac{72(6.0)}{.03048} = 30,160 + 14,170 = 44,330$ psi (ULT.)

COND. II: $\sigma_{II \max} = \frac{4050}{.1144} + \frac{72(2.7)}{.03048} = 35,400 + 6,378 = 41,780$ psi (ULT.)

COND. III: $\sigma_{III \max} = \frac{6000}{.1144} + \frac{72(3.0)}{.03048} = 52,450 + 7,087 = 59,540$ psi (ULT.)

ALLOWABLE CRIPPLING STRESSES ~ STIFFENER FREE LEG

REF. STRESS MEMO NO. 126: $b/t = (40-.12)/.05 = 5.6$

$F_{cc} = 37$ (FIG. 12, REF.) (CONSERVATIVE: t IN b)

MCF

AT R.T.: $F_{cy}/E_c = 68/10,500 = .00648$

$K_m = .0190$ (FIG. 15, REF.)

$MCF = .0190(68) = 1.292$

$F_{cc} = 1.292(37) = 47.8$ Ksi

AT 250°F: $F_{cy}/E_c = 60.5/9660 = .00626$

$K_m = .0195$ (FIG. 15, REF.)

$MCF = .0195(60.5) = 1.180$

$F_{cc} = 1.180(37) = 43.7$ Ksi

360 <

Prepared by: <i>J. R. Ritz</i>	Date 9-7-71	LOCKHEED MISSILES & SPACE COMPANY A GROUP DIVISION OF LOCKHEED AIRCRAFT CORPORATION	Page 28	Temp.	Perm.
Checked by: <i>E. F. Davis</i>	Date 10-12-71	Title PROTOTYPE PANELS	Model TPS		
Approved by: REV. <i>J. R. R.</i>	Date 9-26-71	DESIGN & ANALYSIS	Report No.		

CONFIGURATION No. 2

MARGINS of SAFETY ~ ULTIMATE

1. MAX. COMPRESSION ON STIFFENER FREE LEG

$$M.S. = \frac{F_{cc}}{\sigma_{cmax}(ULT)} - 1$$

$$COND. I: M.S. = \frac{47.8}{38.14} - 1 = 1.253 - 1 = \underline{\underline{+ 0.25}} \\ \text{CRIPPLING-ULT.}$$

$$COND. II: M.S. = \frac{47.8}{41.66} - 1 = 1.147 - 1 = \underline{\underline{+ 0.15}} \\ \text{CRIPPLING-ULT.}$$

$$COND. III: M.S. = \frac{43.7}{30.79} - 1 = 1.419 - 1 = \underline{\underline{+ 0.42}} \\ \text{CRIPPLING-ULT.}$$

2. MAX. TENSION ON STIFFENER FREE LEG

$$M.S. = \frac{F_{tu}}{\sigma_{Tmax}(ULT)} - 1$$

$$COND. I: M.S. = \frac{77}{44.33} - 1 = 1.737 - 1 = \underline{\underline{+ 0.74}} \\ \text{TENS.-ULT.}$$

$$COND. II: M.S. = \frac{77}{41.78} - 1 = 1.843 - 1 = \underline{\underline{+ 0.84}} \\ \text{TENS.-ULT.}$$

$$COND. III: M.S. = \frac{63.1}{59.54} - 1 = 1.060 - 1 = \underline{\underline{+ 0.06}} \\ \text{TENS.-ULT.}$$

Prepared by: <i>J. R. Ritz</i>	Date <i>9-30-71</i>	LOCKHEED MISSILES & SPACE COMPANY A GROUP DIVISION OF LOCKHEED AIRCRAFT CORPORATION	Page <i>09</i>	Temp.	Perm.
Checked by: <i>E. F. Davis</i>	Date <i>10-12-71</i>	Title <u>PROTOTYPE PANELS</u>	Model <i>TFS</i>		
Approved by:	Date	<u>DESIGN & ANALYSIS</u>	Report No.		

CONFIGURATION No. 2

MAX. FACE SHEET COMP. STRESSES ~ ULTIMATE

COMBINE COMP. N_x & COLLAPSE P

BEAM-COLUMN ANALYSIS (REF. P. 6)

$$\sigma_{c_{MAX}} = \frac{N_x c}{I} + \frac{M_{MAX}}{Z_{O_{MAX}}} ; M_{MAX} = 72 p_c \cdot z f(u)$$

$$\text{COND. I: } \sigma_{c_{MAX}} = \frac{2250}{.1144} + \frac{72(6)(1.738)}{.07098} = 19,670 + 10,580 = 30,250 \text{ psi (ULT.)}$$

$$\text{COND. II: } \sigma_{c_{MAX}} = \frac{3000}{.1144} + \frac{72(2.7)(1.294)}{.07098} = 26,220 + 3544 = 29,760 \text{ psi (ULT.)}$$

$$\text{COND. III: } \sigma_{c_{MAX}} = \frac{3000}{.1144} + \frac{72(3)(2.580)}{.07098} = 26,220 + 7852 = 34,070 \text{ psi (ULT.)}$$

Prepared by: J. R. Ritz	Date 9-18-71	LOCKHEED MISSILES & SPACE COMPANY A GROUP DIVISION OF LOCKHEED AIRCRAFT CORPORATION	Page C10	Temp. Perm.
Checked by: E. F. Owen	Date 10-12-71	Title PROTOTYPE PANELS	Model TPS	
Approved by: REV. J. R. R.	Date 9-26-71	DESIGN & ANALYSIS	Report No.	

CONFIGURATION No. 2

BEARING IN STRINGER ENDS: 6 No. 10 JO-BOLTS PER END

MAX. STRINGER LOAD ~ P_{MAX} : COND. III CRITICAL (REF. p. 7)

AT 250°F: $P_{MAX} = C_{MAX} A_{STR} = 52,450 (1030) = 5402 \text{ lb (ULT)}$

ALLOW. BEARING LOAD ~ PER END

$A_{br} = 6 (.190) (.050) = .05700 \text{ in}^2$

AT 250°F: $P_{brall} = A_{br} F_{brall} = .05700 (121 \times 10^3) = 6897 \text{ lb (ULT.)}$

MARGIN of SAFETY

$M.S. = \frac{P_{brall}}{P_{MAX}} - 1 = \frac{6897}{5402} - 1 = 1.277 - 1 = \underline{+ 0.28}$
BEARING-ULT.

SKIN STABILITY ANALYSIS: COND. III CRITICAL; T = 250°F

MAX. COMP. STRESS, $\sigma_{cmax} = 34,070 \text{ psi (ULT.)}$ (FROM p. 9)

SKIN BUCKLING STRESS ~ F_{CCR} ; REF. S.M. 80 c

AT R.T.: $b/t = .0816$; $n = 15$; $F_{0.7} = 70 \text{ Ksi}$ (TAB. II, REF.)

$b/t = 1.60 / .050 = 32$; $\sqrt{K} = 2.51$ (FIG. 3, CASE @, REF.)

$(b/t)_e = 32 / 2.51 = 12.75$

$B = .0816 (12.75) = 1.040$

$F/F_{0.7} = 0.84$ (FIG. 2, REF.)

$F_{CCR} = 0.84 (70) = 58.8 \text{ Ksi}$

AT 250°F: ASSUME $F_{CCR 250} = F_{CCR R.T.} \frac{E_{CRT}}{E_{c250}} = 58.8 (.92) = 54.1 \text{ Ksi}$
(REF. p. 4)

MARGIN of SAFETY

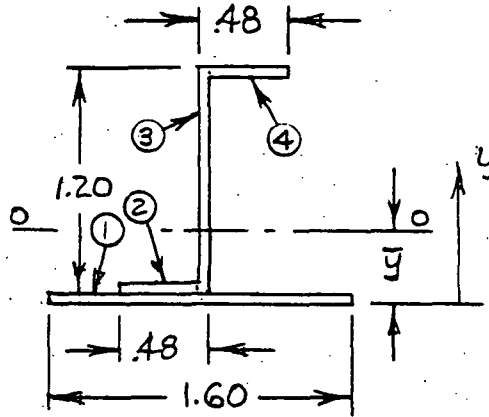
$M.S. = \frac{F_{CCR}}{\sigma_{cmax}} - 1 = \frac{54.1}{34.07} - 1 = 1.588 - 1 = \underline{+ 0.59}$
BUCKLING-ULT.

Prepared by: <i>J. R. Ritz</i>	Date: 9-7-71	LOCKHEED MISSILES & SPACE COMPANY A GROUP DIVISION OF LOCKHEED AIRCRAFT CORPORATION	Page Temp. Perm. C 111
Checked by: <i>E. F. Davis</i>	Date: 10-12-71	Title: <u>PROTOTYPE PANELS</u>	Model: TPS
Approved by:	Date:	<u>DESIGN & ANALYSIS</u>	Report No.

CONFIGURATION No. 3

SECTION PROPERTIES

FULL SCALE
D/N SK 91071



ALL $t = .063$ in
 $R = 0.16$ in (MIN.)
 $l = 20.0$ in

WT = $144(.101)(.1431)$
WT = 2.081 lb/ft²

ELEM.	A	y	Ay	d	Ad ²	I _x
1	.1008	.0315	.00318	.3563	.01280	.00003
2	.0263	.0945	.00249	.2906	.00222	—
3	.0756	.663	.05012	.2779	.00584	.00907
4	.0263	1.232	.03240	.8469	.01886	—
Σ	.2290		.08819		.03972	.00910

$$\bar{y} = \frac{.08819}{.2290} = 0.3851 \text{ in} ; \bar{z} = \frac{.2290}{1.60} = 0.1431 \text{ in}$$

$$C_1 = \bar{y} = 0.3851 \text{ in} ; C_2 = 1.263 - \bar{y} = 0.8779 \text{ in}$$

$$I_o = .03972 + .00910 = .04882 \text{ in}^4$$

$$\bar{I}_o = \frac{.04882}{1.60} = .03051 \text{ in}^4/\text{in}$$

$$\bar{I}_{o \text{ MAX}} = \frac{.03051}{.3851} = .07923 \text{ in}^3/\text{in}$$

$$\bar{I}_{o \text{ MIN}} = \frac{.03051}{.8779} = .03475 \text{ in}^3/\text{in}$$

MATERIAL ~ 7075-T6

PROPERTIES GIVEN ON p.4 FOR ROOM TEMP. & 250°F.

Prepared by: <i>J. R. Ritz</i>	Date 9-7-71	LOCKHEED MISSILES & SPACE COMPANY A GROUP DIVISION OF LOCKHEED AIRCRAFT CORPORATION	Page C 12	Temp. Perm.
Checked by: <i>E. F. Davis</i>	Date 10-12-71	Title <u>PROTOTYPE PANELS</u>	Model TPS	
Approved by: <i>REV. J. R. R.</i>	Date 9-26-71	<u>DESIGN & ANALYSIS</u>	Report No.	

CONFIGURATION No. 3

DESIGN LOADS (AREA 1) (REF. No. 5)

COND.	N ~ ppi		p ~ psi	
	LIMIT	ULT.	LIMIT	ULT.
I (R.T.)	2400 -2100	3600 -3150	3.0 -2.0	4.5 -3.0
II (R.T.)	2700 -4000	4050 -6000	1.5 -0.9	2.25 -1.35
III (250°F)	4000 -2000	6000 -3000	0.5 -2.0	0.75 -3.0

SEE p. 2 FOR SIGN CONVENTIONS

ALLOW. COLUMN LOADS ~ EULER (REF. p. 5)

AT R.T. : $\bar{P}_{cr} = \frac{\pi^2 (10.5 \times 10^3) (30.51)}{.91 (400)} = 8687 \text{ lb/in}$

$\sigma_{cr} = \frac{8687}{.1431} = 60,700 \text{ psi}$

AT 250°F : $\bar{P}_{cr} = .92 (8687) = 7905 \text{ lb/in}$

$\sigma_{cr} = \frac{7905}{.1431} = 55,240 \text{ psi}$

ALLOW. CRIPPLING STRESSES ~ STIFFENER FREE LEG

$b = .48 - R - t = .48 - .16 - .063 = .257 \text{ in} ; b/t = .257 / .063 = 4.08$

$F_{cc} = 47.5 \text{ Ksi (REF. S.M. 126, FIG. 12)}$

MCF

AT R.T. : $MCF = 1.292 \text{ (FROM p. 4)}$

$F_{cc} = 1.292 (47.5) = 61.4 \text{ Ksi}$

AT 250°F : $MCF = 1.180 \text{ (FROM p. 4)}$

$F_{cc} = 1.180 (47.5) = 56.0 \text{ Ksi}$

Prepared by: <i>J. R. Ritz</i>	Date 9-30-71	LOCKHEED MISSILES & SPACE COMPANY A GROUP DIVISION OF LOCKHEED AIRCRAFT CORPORATION	Page Temp. Perm. C13
Checked by: <i>E. F. Davis</i>	Date 10-12-71	Title <u>PROTOTYPE PANELS</u>	Model TPS
Approved by:	Date	<u>DESIGN & ANALYSIS</u>	Report No.

CONFIGURATION No. 3

MAX. BENDING MOMENTS ~ FOR COMP. N_x & BURST p
BEAM-COLUMN ANALYSIS (REF. p. 6)

$$M_{max} = \frac{w l^2}{8} \cdot 2f(u) = 50 p_B \cdot 2f(u) ; f(u) = \frac{1 - \cos u}{u^2 \cos u}$$

$$u = \frac{l}{2} \left(\frac{N_{xc}}{E_c I_o} \right)^{1/2} = \frac{20}{2} \cdot \frac{1}{(30,510)^{1/2}} \cdot \left(\frac{N_{xc}}{E_c \cdot 10^6} \right)^{1/2} = \frac{1}{17.47} \left(\frac{N_{xc}}{E_c \cdot 10^6} \right)^{1/2}$$

$$u_I = \frac{1}{17.47} \left(\frac{3150}{10.5} \right)^{1/2} = 0.9914 ; u_I^2 = 0.9830 ; u_I (DEG) = 56^\circ 48'$$

$$u_{II} = \frac{1}{17.47} \left(\frac{6000}{10.5} \right)^{1/2} = 1.368 ; u_{II}^2 = 1.872 ; u_{II} (DEG) = 78^\circ 23'$$

$$u_{III} = \frac{1}{17.47} \left(\frac{3000}{9.66} \right)^{1/2} = 1.009 ; u_{III}^2 = 1.018 ; u_{III} (DEG) = 57^\circ 49'$$

u	$\cos u$	$1 - \cos u$	$u^2 \cos u$	$f(u)$	$2f(u)$
$56^\circ 48'$.5476	.4524	.5383	.8404	1.681
$78^\circ 23'$.2014	.7986	.3770	2.118	4.237
$57^\circ 49'$.5326	.4674	.5422	.8620	1.724

$$M_{I,MAX} = 50 (4.5) (1.681) = 378.2 \text{ in-lb/in (ULT.)}$$

$$M_{II,MAX} = 50 (2.25) (4.237) = 476.7 \text{ in-lb/in (ULT.)}$$

$$M_{III,MAX} = 50 (0.75) (1.724) = 64.6 \text{ in-lb/in (ULT.)}$$

MAX. FACE SHEET COMP. STRESSES ~ COMP. N_x & COLLAPSE p

$$\sigma_{c,MAX} = \frac{N_{xc}}{I} + \frac{M_{max}}{Z_{OMAX}} = \frac{N_{xc}}{.1431} + \frac{50 p_B \cdot 2f(u)}{.07923}$$

$$\text{COND. I: } \sigma_{cI,MAX} = \frac{3150}{.1431} + \frac{50(3)(1.681)}{.07923} = 22,010 + 3183 = 25,190 \text{ psi (ULT.)}$$

$$\text{COND. II: } \sigma_{cII,MAX} = \frac{6000}{.1431} + \frac{50(1.35)(4.237)}{.07923} = 41,930 + 3610 = 45,540 \text{ psi (ULT.)}$$

$$\text{COND. III: } \sigma_{cIII,MAX} = \frac{3000}{.1431} + \frac{50(3)(1.724)}{.07923} = 20,960 + 3264 = 24,220 \text{ psi (ULT.)}$$

366 <

Prepared by: <i>J. R. Ritz</i>	Date 9-8-71	LOCKHEED MISSILES & SPACE COMPANY A GROUP DIVISION OF LOCKHEED AIRCRAFT CORPORATION	Page C14	Temp. Perm.
Checked by: <i>E. F. Davis</i>	Date 10-12-71	Title <u>PROTOTYPE PANELS</u> <u>DESIGN & ANALYSIS</u>	Model TPS	
Approved by: REV. <i>J. R. R.</i>	Date 9-26-71		Report No.	

CONFIGURATION No. 3

MAX. ULTIMATE STRESSES ~ APPLIED ~ STIFFENER FREE LEG

1. MAX. COMPRESSIVE STRESSES ~ σ_{cmax} ~ ON FREE LEG

COMBINE COMP. N_x & BURST P : BEAM-COLUMN ANALYSIS

$$\sigma_{cmax} = \frac{N_{xc}}{\bar{E}} + \frac{M_{max}}{\bar{Z}_{omin}} : M_{max} \text{ FROM p.13}$$

$$\text{COND. I: } \sigma_{cI max} = \frac{3150}{.1431} + \frac{378.2}{.03475} = 22,010 + 10,880 = 32,890 \text{ psi (ULT)}$$

$$\text{COND. II: } \sigma_{cII max} = \frac{6000}{.1431} + \frac{476.7}{.03475} = 41,930 + 13,720 = 55,650 \text{ psi (ULT)}$$

$$\text{COND. III: } \sigma_{cIII max} = \frac{3000}{.1431} + \frac{64.6}{.03475} = 20,960 + 1859 = 22,820 \text{ psi (ULT)}$$

2. MAX. TENSILE STRESSES ~ σ_{Tmax} ~ ON FREE LEG

COMBINE TENS. N_x & COLLAPSE P : DIRECT SUPERPOSITION

$$\sigma_{Tmax} = \frac{N_{Tt}}{\bar{E}} + \frac{50 P_{ca.}}{\bar{Z}_{omin}}$$

$$\text{COND. I: } \sigma_{TI max} = \frac{3600}{.1431} + \frac{50(3.0)}{.03475} = 25,160 + 4317 = 29,480 \text{ psi (ULT)}$$

$$\text{COND. II: } \sigma_{TII max} = \frac{4050}{.1431} + \frac{50(1.35)}{.03475} = 28,300 + 1942 = 30,240 \text{ psi (ULT)}$$

$$\text{COND. III: } \sigma_{TIII max} = \frac{6000}{.1431} + \frac{50(3.0)}{.03475} = 41,930 + 4317 = 46,250 \text{ psi (ULT)}$$

Prepared by: <u>J. R. Ritz</u>	Date <u>9-8-71</u>	LOCKHEED MISSILES & SPACE COMPANY A GROUP DIVISION OF LOCKHEED AIRCRAFT CORPORATION	Page <u>C15</u>	Temp. Perm.
Checked by: <u>E. F. Davis</u>	Date <u>10-12-71</u>	Title <u>PROTOTYPE PANELS</u>	Model <u>TPS</u>	
Approved by: <u>REV. J. R. R.</u>	Date <u>9-26-71</u>	<u>DESIGN & ANALYSIS</u>	Report No.	

CONFIGURATION No. 3

MARGINS of SAFETY ~ ULTIMATE

1. MAX. COMPRESSION ON STIFFENER FREE LEG

$$M.S. = \frac{F_{cc}}{\sigma_{cmax}(ULT)} - 1$$

$$COND. I: M.S. = \frac{61.4}{32.89} - 1 = 1.867 - 1 = \underline{\underline{+0.87}}$$

CRIPPLING-ULT.

$$COND. II: M.S. = \frac{61.4}{55.65} - 1 = 1.103 - 1 = \underline{\underline{+0.10}}$$

CRIPPLING-ULT.

$$COND. III: M.S. = \frac{56.0}{22.82} - 1 = 2.454 - 1 = \underline{\underline{+1.5}}$$

CRIPPLING-ULT.

2. MAX. TENSION ON STIFFENER FREE LEG

$$M.S. = \frac{F_{tu}}{\sigma_{Tmax}(ULT)} - 1$$

$$COND. I: M.S. = \frac{77}{29.48} - 1 = 2.612 - 1 = \underline{\underline{+1.6}}$$

TENS.-ULT.

$$COND. II: M.S. = \frac{77}{30.24} - 1 = 2.546 - 1 = \underline{\underline{+1.5}}$$

TENS.-ULT.

$$COND. III: M.S. = \frac{63.1}{46.25} - 1 = 1.364 - 1 = \underline{\underline{+0.36}}$$

TENS.-ULT.

Prepared by: J. R. Ritz	Date 9-18-71	LOCKHEED MISSILES & SPACE COMPANY A GROUP DIVISION OF LOCKHEED AIRCRAFT CORPORATION	Page C/6	Temp. Perm.
Checked by: E. F. Davis	Date 10-12-71	Title <u>PROTOTYPE PANELS</u>	Model TPS	
Approved by: REV. J. R. R.	Date 9-26-71	<u>DESIGN & ANALYSIS</u>	Report No.	

CONFIGURATION No. 3

BEARING IN STRINGER ENDS

MAX. STRINGER LOAD ~ P_{MAX} : COND. III CRITICAL (REF. p.14)

AT 250°F.: $P_{MAX} = \sigma_{MAX} A_{STR} = 41,930 (.1282) = 5375 \text{ lb (ULT.)}$

ALLOW. BEARING LOAD ~ PER END

$A_{br} = 6 (.190) (.063) = .07182 \text{ in}^2$
 AT 250°F.: $P_{br ALL} = A_{br} F_{br u} = .07182 (121 \times 10^3) = 8690 \text{ lb (ULT.)}$

MARGIN of SAFETY

$M.S. = \frac{P_{br ALL}}{P_{MAX}} - 1 = \frac{8690}{5375} - 1 = 1.617 - 1 = \underline{\underline{+0.62}}$
 BEARING-ULT.

SKIN STABILITY ANALYSIS: COND. II CRITICAL ; T=R.T.

MAX. COMP. STRESS, $\sigma_{c MAX} = 45,540 \text{ psi (ULT)}$ (FROM p. 13)

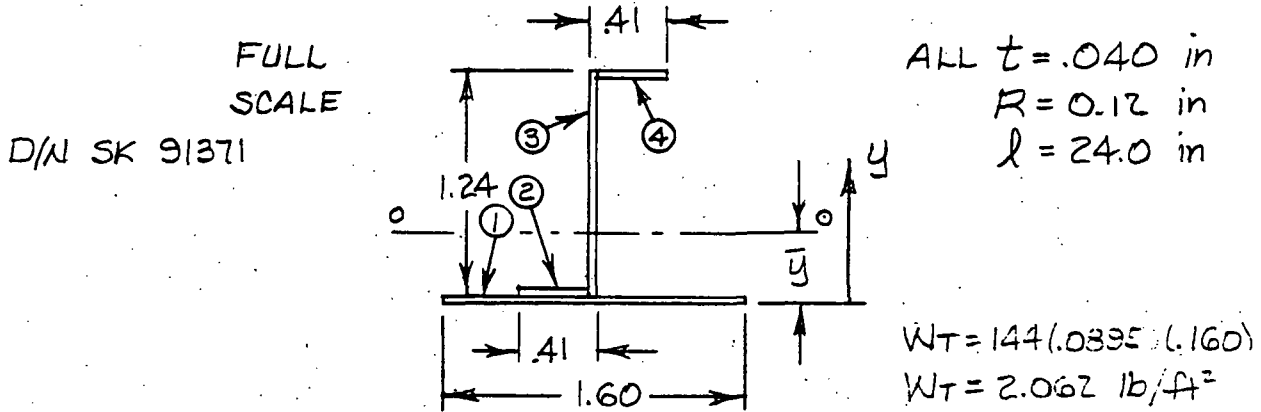
SKIN BUCKLING STRESS ~ F_{CCR} : REF. S.M. 80 c

$k_z = .0816$; $n = 15$; $F_{0.7} = 70 \text{ Ksi (TAB. II, REF.)}$
 $b/t = 1.60 / .063 = 25.4$; $\sqrt{k} = 2.51$ (FIG. 3, CASE @, REF.)
 $(b/t)_e = 25.4 / 2.51 = 10.12$
 $B = .0816 (10.12) = 0.826$
 $F / F_{0.7} = 0.97$ (FIG. 2, REF.)
 $F_{CCR} = 0.97 (70) = 67.9 \text{ Ksi}$

MARGIN of SAFETY

$M.S. = \frac{F_{CCR}}{\sigma_{c MAX}} - 1 = \frac{67.9}{45.54} - 1 = 1.491 - 1 = \underline{\underline{+0.49}}$
 BUCKLING-ULT.

CONFIGURATION No. 4
SECTION PROPERTIES



ELEM.	A	y	Ay	d	Ad ²	I _x
1	.0640	.020	.00128	.3540	.00820	.00001
2	.0148	.060	.00089	.3140	.00146	—
3	.0496	.660	.03274	.2860	.00406	.00636
4	.0148	1.260	.01865	.8860	.01162	—
Σ	.1432		.05356		.02534	.00637

$$\bar{y} = \frac{.05356}{.1432} = 0.3740 \text{ in}; \quad \bar{t} = \frac{.1432}{1.60} = .08950 \text{ in}$$

$$I_o = .03171 \text{ in}^4; \quad \bar{I}_o = .03171 / 1.60 = .01982 \text{ in}^4/\text{in}$$

$$\bar{Z}_{o \max} = .01982 / .3740 = .05299 \text{ in}^3/\text{in}; \quad \bar{Z}_{o \min} = .01982 / .9060 = .02188 \text{ in}^3/\text{in}$$

MATERIAL ~ GAL-4V ANNEALED - TITANIUM ALLOY
REF. MIL-HDBK-5A, SECT. 5.4.6

R.T. (TAB. 5.4.6.1(a))		600°F	
$F_{ty} = 134$ Ksi	(.74)	99.2 Ksi	(FIG. 5.4.6.2.1(a))
$F_{ty} = 126$ Ksi	(.67)	84.4 Ksi	(FIG. 5.4.6.2.1(b))
$F_{cy} = 132$ Ksi	(.68)	89.8 Ksi	(FIG. 5.4.6.2.2(a))
$E = 16.0 \times 10^3$ Ksi	(.82)	13.1×10^3 Ksi	(FIG. 5.4.6.2.4)
$E_c = 16.4 \times 10^3$ Ksi	(.82)	13.4×10^3 Ksi	(FIG. 5.4.6.2.4)
$F_{brx} = 252$ Ksi	} $\frac{e}{D} = 2$ (.75)	189 Ksi	(FIG. 5.4.6.2.3(a))
$F_{bry} = 208$ Ksi		156 Ksi	(FIG. 5.4.6.2.3(b))
$\gamma = 0.160$ lb/in ³			

Prepared by: J. R. Ritz	Date 9-8-71	LOCKHEED MISSILES & SPACE COMPANY A GROUP DIVISION OF LOCKHEED AIRCRAFT CORPORATION	Page C18	Temp. Perm.
Checked by: E. F. Davis	Date 10-12-71	Title PROTOTYPE PANELS	Model TPS	
Approved by: REV. J. R. R.	Date 9-26-71	DESIGN & ANALYSIS	Report No.	

CONFIGURATION No. 4
DESIGN LOADS (AREA 2)

SAME DESIGN LOAD CONDITIONS AS FOR CONFIGURATION NO. 2, GIVEN ON p. 5, EXCEPT THAT FOR LOAD CONDITION II, THE MAX. TEMP. IS 600° F.

ALLOWABLE COLUMN LOADS ~ EULER (REF. p. 5)

AT R.T.: $\bar{P}_{CR} = \frac{\pi^2 (16.4 \times 10^3) (19.82)}{.91(576)} = 6121 \text{ lb/in}$

$\sigma_{CR} = \frac{6121}{.08950} = 68,390 \text{ psi}$

AT 600° F: $\bar{P}_{CR} = .82 (6121) = 5019 \text{ lb/in}$

$\sigma_{CR} = \frac{5019}{.08950} = 56,080 \text{ psi}$

ALLOWABLE CRIPPLING STRESSES ~ STIFFENER FREE LEG

REF. S. M. 126

$b = .41 - .12 = 0.29 \text{ in}; b/t = .29/.04 = 7.25 \text{ (CONSERVATIVE, } t \text{ IN } b)$

$\frac{F_{cc}}{MCF} = 29.0 \text{ Ksi (FIG. 12, REF.)}$

MCF

AT R.T.: $MCF = 2.234 \text{ (TAB. I, REF.)}$

$F_{cc} = 2.234 (29.0) = 64.79 \text{ Ksi}$

AT 600° F: $MCF = 1.659 \text{ (TAB. I, REF.)}$

$F_{cc} = 1.659 (29.0) = 48.11 \text{ Ksi}$

Prepared by: <i>J.R. Ritz</i>	Date 9-30-71	LOCKHEED MISSILES & SPACE COMPANY A GROUP DIVISION OF LOCKHEED AIRCRAFT CORPORATION	Page C 19	Temp. Perm.
Checked by: <i>E. F. Davis</i>	Date 10-12-71	Title <u>PROTOTYPE PANELS</u>	Model TPS	
Approved by:	Date	<u>DESIGN & ANALYSIS</u>	Report No.	

CONFIGURATION No. 4

MAX. BENDING MOMENTS ~ FOR COMP. N_x & BURST P
BEAM-COLUMN ANALYSIS (REF. p. 13)

$$M_{MAX} = \frac{w l^2}{8} \cdot z f(u) = 72 P_c \cdot z f(u); f(u) = \frac{1 - \cos u}{u^2 \cos u}$$

$$u = \frac{l}{z} \left(\frac{N_{xc}}{E_c I_o} \right)^{1/2} = \frac{24}{2} \frac{1}{(19,820)^{1/2}} \left(\frac{N_{xc}}{E_c \cdot 10^{-6}} \right)^{1/2} = \frac{1}{11.73} \left(\frac{N_{xc}}{E_c \cdot 10^{-6}} \right)^{1/2}$$

$$u_I = \frac{1}{11.73} \left(\frac{2250}{16.4} \right)^{1/2} = 0.9986; u_I^2 = 0.9972; u_I (\text{DEG}) = 57^\circ 13'$$

$$u_{II} = \frac{1}{11.73} \left(\frac{3000}{16.4} \right)^{1/2} = 1.153; u_{II}^2 = 1.329; u_{II} (\text{DEG}) = 66^\circ 04'$$

$$u_{III} = \frac{1}{11.73} \left(\frac{3000}{13.4} \right)^{1/2} = 1.276; u_{III}^2 = 1.628; u_{III} (\text{DEG}) = 73^\circ 07'$$

u	$\cos u$	$1 - \cos u$	$u^2 \cos u$	$f(u)$	$z f(u)$
$57^\circ 13'$.5415	.4585	.5400	.8491	1.698
$66^\circ 04'$.4057	.5943	.5392	1.102	2.204
$73^\circ 07'$.2904	.7096	.4728	1.501	3.002

$$M_{I_{MAX}} = 72(4.5)(1.698) = 550.2 \text{ in-lb/in (ULT.)}$$

$$M_{II_{MAX}} = 72(2.85)(2.204) = 452.3 \text{ in-lb/in (ULT.)}$$

$$M_{III_{MAX}} = 72(0.75)(3.002) = 162.1 \text{ in-lb/in (ULT.)}$$

MAX. FACE SHEET COMP. STRESSES ~ COMP. N_x & COLLAPSE P

$$\sigma_{c_{MAX}} = \frac{N_{xc}}{E} + \frac{M_{MAX}}{Z_{OMAX}} = \frac{N_{xc}}{.08950} + \frac{72 P_c z f(u)}{.05299}$$

$$\text{COND. I: } \sigma_{c_{I_{MAX}}} = \frac{2250}{.08950} + \frac{72(6)(1.698)}{.05299} = 25,140 + 13,840 = 38,980 \text{ psi (ULT.)}$$

$$\text{COND. II: } \sigma_{c_{II_{MAX}}} = \frac{3000}{.08950} + \frac{72(2.7)(2.204)}{.05299} = 33,520 + 8086 = 41,610 \text{ psi (ULT.)}$$

$$\text{COND. III: } \sigma_{c_{III_{MAX}}} = \frac{3000}{.08950} + \frac{72(3)(3.002)}{.05299} = 33,520 + 12,240 = 45,760 \text{ psi (ULT.)}$$

372 <

Prepared by: <u>J. R. Ritz</u>	Date: <u>9-9-71</u>	LOCKHEED MISSILES & SPACE COMPANY A GROUP DIVISION OF LOCKHEED AIRCRAFT CORPORATION	Page: <u>C 20</u>	Temp.	Perm.
Checked by: <u>E. F. Davis</u>	Date:	Title: <u>PROTOTYPE PANELS</u>	Model: <u>TPS</u>		
Approved by: <u>REV. J. R. R.</u>	Date: <u>9-26-71</u>	<u>DESIGN & ANALYSIS</u>	Report No.		

CONFIGURATION No. 4

MAX. ULTIMATE STRESSES ~ APPLIED ~ STIFFENER FREE LEG

1. MAX. COMPRESSIVE STRESSES ~ $\sigma_{c \max}$ ~ ON FREE LEG

COMBINE COMP. N_x & BURST p : BEAM-COLUMN ANALYSIS

$$\sigma_{c \max} = \frac{N_{xc}}{E} + \frac{M_{\max}}{Z_{\min}} \quad ; \quad M_{\max} \text{ FROM p. 19}$$

$$\text{COND. I: } \sigma_{cI \max} = \frac{2250}{.08950} + \frac{550.2}{.02188} = 25,140 + 25,150 = 50,290 \text{ psi (ULT)}$$

$$\text{COND. II: } \sigma_{cII \max} = \frac{3000}{.08950} + \frac{452.3}{.02188} = 33,520 + 20,670 = 54,190 \text{ psi (ULT)}$$

$$\text{COND. III: } \sigma_{cIII \max} = \frac{3000}{.08950} + \frac{162.1}{.02188} = 33,520 + 7409 = 40,930 \text{ psi (ULT)}$$

2. MAX. TENSILE STRESSES ~ $\sigma_{t \max}$ ~ ON FREE LEG

COMBINE TENS. N_x & COLLAPSE p : DIRECT SUPERPOSITION

$$\sigma_{t \max} = \frac{N_{xT}}{E} + \frac{M_{\max}}{Z_{\min}} = \frac{N_{xT}}{.08950} + \frac{72 p_{ca.}}{.02188}$$

$$\text{COND. I: } \sigma_{tI \max} = \frac{3450}{.08950} + \frac{72(6.0)}{.02188} = 38,550 + 19,740 = 58,290 \text{ psi (ULT)}$$

$$\text{COND. II: } \sigma_{tII \max} = \frac{4050}{.08950} + \frac{72(2.7)}{.02188} = 45,250 + 8885 = 54,130 \text{ psi (ULT)}$$

$$\text{COND. III: } \sigma_{tIII \max} = \frac{6000}{.08950} + \frac{72(3.0)}{.02188} = 67,040 + 9872 = 76,910 \text{ psi (ULT)}$$

Prepared by: <u>J. R. Ritz</u>	Date <u>9-9-71</u>	LOCKHEED MISSILES & SPACE COMPANY A GROUP DIVISION OF LOCKHEED AIRCRAFT CORPORATION	Page <u>C 21</u>	Temp.	Perm.
Checked by: <u>E. J. Davis</u>	Date <u>10-12-71</u>	Title <u>PROTOTYPE PANELS</u> <u>DESIGN & ANALYSIS</u>	Model <u>TPS</u>		
Approved by: <u>REV. J. R. R.</u>	Date <u>9-26-71</u>		Report No.		

CONFIGURATION No. 4

MARGINS of SAFETY ~ ULTIMATE

1. MAX. COMPRESSION ON STIFFENER FREE LEG

$$M.S. = \frac{F_{cc}}{\sigma_{c \max} (ULT)} - 1$$

$$\text{COND. I: M.S.} = \frac{64.79}{50.29} - 1 = 1.288 - 1 = \underline{\underline{+ 0.29}}$$

CRIPPLING-ULT.

$$\text{COND. II: M.S.} = \frac{64.79}{54.19} - 1 = 1.196 - 1 = \underline{\underline{+ 0.20}}$$

CRIPPLING-ULT.

$$\text{COND. III: M.S.} = \frac{48.11}{40.93} - 1 = 1.175 - 1 = \underline{\underline{+ 0.18}}$$

CRIPPLING-ULT.

2. MAX. TENSION ON STIFFENER FREE LEG

$$M.S. = \frac{F_{tu}}{\sigma_{t \max} (ULT)} - 1$$

$$\text{COND. I: M.S.} = \frac{134}{58.29} - 1 = 2.299 - 1 = \underline{\underline{+ 1.3}}$$

TENS.-ULT.

$$\text{COND. II: M.S.} = \frac{134}{54.13} - 1 = 2.476 - 1 = \underline{\underline{+ 1.5}}$$

TENS.-ULT.

$$\text{COND. III: M.S.} = \frac{99.2}{76.91} - 1 = 1.290 - 1 = \underline{\underline{+ 0.29}}$$

TENS.-ULT.

Prepared by: <i>J. R. Ritz</i>	Date 9-10-71	LOCKHEED MISSILES & SPACE COMPANY A GROUP DIVISION OF LOCKHEED AIRCRAFT CORPORATION	Page C 22	Temp. Perm.
Checked by: <i>E. F. Davis</i>	Date	Title <u>PROTOTYPE PANELS</u>	Model TPS	
Approved by: <i>REV. J. R. R.</i>	Date 9-26-71	<u>DESIGN & ANALYSIS</u>	Report No.	

CONFIGURATION No. 4
FASTENER ANALYSIS

1. INTER-RIVET BUCKLING ~ MAX. ALLOW. SPACING, S

MAX SKIN COMPRESSIVE STRESSES ~ σ_{scmax} (FROM p. 19)

AT R.T. (COND. II): $\sigma_{scmax} = 41,610$ psi (ULT)

AT 600°F. (COND. III): $\sigma_{scmax} = 45,760$ psi (ULT.)

SPACING ~ S : COND. III CRITICAL

$$l'/e = 54 \text{ (REF. S.M. 83 b, FIG. 29, CURVE 6)}$$

$$\frac{S}{t} = .577 \frac{l'}{e} \text{ (REF. S.M. 80 c, p. 8, NOTE 5)}$$

$$S = .577 (54)(.04) = 1.25 \text{ in (MAX.) : USE } S = 1.0 \text{ in ; } \frac{3}{32} \text{ MONEL RIVETS}$$

2. BEARING IN STRINGER ENDS ~ SIX No. 10's PER END: JO-BOLTS

MAX. STRINGER LOADS ~ P_{max} : COND. III CRITICAL (REF p. 20)

$$\text{AT } 600^\circ\text{F : } P_{max} = \sigma_{max} A_{STR} = 67,040 (.0792) = 5310 \text{ lb (ULT.)}$$

ALLOW. BEARING LOAD ~ PER END

$$\text{AT } 600^\circ\text{F : } P_{brall} = A_{br} F_{br} = 6 (.190)(.04)(189 \times 10^3) = 8618 \text{ lb (ULT.)}$$

MARGIN of SAFETY

$$M.S. = \frac{P_{brall}}{P_{max}} - 1 = \frac{8618}{5310} - 1 = 1.623 - 1 = \underline{+0.62} \text{ BEARING-ULT.}$$

3. SHEAR ON JO-BOLTS : LS 889Z FG-2, MAT'L A-286 CRES
D = $\frac{3}{16}$ in (REF: PPH, p. 103)

AT R.T. : ALLOW. SINGLE SHEAR (ULT.), $V_{all} = 2150$ lb (MIL-HDBK-5A, TAB. 8.1.4.2.1(d))

AT 600°F : $V_{all} = .91(2150) = 1956$ lb (M-H-5A, FIG. 8.1.4.2.1(e))

$$M.S. = \frac{6 V_{all}}{P_{max}} - 1 = \frac{6(1956)}{5310} - 1 = 2.210 - 1 = \underline{+1.2} \text{ SHEAR-ULT.}$$

Prepared by: <i>J. R. Ritz</i>	Date 9-18-71	LOCKHEED MISSILES & SPACE COMPANY A GROUP DIVISION OF LOCKHEED AIRCRAFT CORPORATION	Page Temp. Perm. C 23
Checked by: <i>E. F. Davis</i>	Date 10-12-71	Title <u>PROTOTYPE PANELS</u>	Model TPS
Approved by:	Date	<u>DESIGN & ANALYSIS</u>	Report No.

CONFIGURATION No. 4

SKIN STABILITY ANALYSIS : COND. III CRITICAL; $T = 600^\circ F$

MAX. SKIN COMP. STRESS $\sim \sigma_{SCMAX} = 45,760$ psi (ULT) (FROM p.19)

SKIN BUCKLING STRESS $\sim F_{CCR}$ REF. S.M. 30 C

AT $600^\circ F$: $k_z = .0820$
 $n = 30$
 $F_{0.7} = 90.09$ Ksi } TAB II, REF. || $\frac{b}{t} = \frac{1.2}{.04} = 30$

SIMPLE SUPPORT : $\sqrt{K} = 1.90$
 CLAMPED : $\sqrt{K} = 2.51$ } FIG. 3, REF.

ASSUME $\sqrt{K} = 1.90$

$$(b/t)_e = 30/1.90 = 15.78$$

$$B = .0820 (15.78) = 1.292$$

$$\frac{F}{F_{0.7}} = 0.615 \text{ (FIG. 2, REF.)}$$

$$F_{CCR} = 0.615 (90.09) = 46.40 \text{ Ksi}$$

MARGIN of SAFETY

$$M.S. = \frac{F_{CCR}}{\sigma_{SCMAX}} - 1 = \frac{46.40}{45.76} - 1 = 1.014 - 1 = \frac{+0.01}{\text{BUCKLING - ULT.}}$$

Prepared by: <i>J. R. Ritz</i>	Date: 9-20-71	LOCKHEED MISSILES & SPACE COMPANY A GROUP DIVISION OF LOCKHEED AIRCRAFT CORPORATION	Page Temp. Perm. C 24
Checked by: <i>A. J. Chinn</i>	Date: 11-8-71	Title: <u>PROTOTYPE PANELS</u>	Model: TPS
Approved by: <i>REV. J. R. R.</i>	Date: 9-26-71	<u>DESIGN & ANALYSIS</u>	Report No.

SUMMARY ~ MAX. PANEL STRESSES

TABLE BASED ON LINEAR ANALYSIS: DIRECT SUPERPOSITION

CONFIG.	LOADS & MAX. STRESSES ~ STRINGER						EI lb-in ² /in
	N _x ppi	p psi	σ _N psi	σ _p psi	σ psi	T °F	
1	0	+4.5	0	-39,410	-39,410	R.T.	239,000
	0	-6.0	0	+52,540	+52,540	R.T.	239,000
2	-3000	+2.85	-26,220	-6732	-32,950	R.T.	308,400
	+6000	-3.0	+52,450	+7087	+59,630	250	283,500
3	-6000	+2.25	-41,930	-3237	-45,170	R.T.	314,300
	+6000	-3.0	+41,930	+4317	+46,250	250	288,900
4	-3000	+2.85	-33,520	-9378	-42,900	R.T.	317,100
	+6000	-3.0	+67,040	+9872	+76,910	600	259,600
	LOADS & MAX. STRESSES ~ SKIN						
1	0	-6.0	0	-20,810	-20,810	R.T.	239,000
	0	+4.5	0	+15,610	+15,610	R.T.	239,000
2	-3000	-3.0	-26,220	-3043	-29,260	R.T.	308,400
	+6000	+0.75	+52,450	+761	+53,300	250	283,500
3	-6000	-1.35	-41,930	-852	-42,780	R.T.	314,300
	+6000	+0.75	+41,930	+473	+42,400	250	288,900
4	-3000	-3.0	-33,520	-4076	-37,600	R.T.	317,100
	+6000	+0.75	+67,040	+1019	+68,060	250	259,600

SIGN CONVENTIONS : +N_x, +σ TENSION
 -N_x, -σ COMPRESSION
 +p BURST
 -p COLLAPSE

ALL N_x, p, & σ : ULTIMATE VALUES

FACTOR of SAFETY = 1.5

Prepared by: <i>S. R. Ritz</i>	Date <i>10-5-71</i>	LOCKHEED MISSILES & SPACE COMPANY A GROUP DIVISION OF LOCKHEED AIRCRAFT CORPORATION	Page <i>025</i>	Temp.	Perm.
Checked by: <i>E. J. Vain</i>	Date	Title <u>PROTOTYPE PANELS</u>	Model <i>TPS</i>		
Approved by:	Date	<u>DESIGN & ANALYSIS</u>	Report No.		

Reproduced from
best available copy. 

REFERENCES

1. MIL-HDBK-5A, METALLIC MATERIALS AND ELEMENTS FOR AEROSPACE VEHICLE STRUCTURES, JAN. 1970
2. TIMOSHENKO & GERE, THEORY OF ELASTIC STABILITY, 2ND ED., 1961
3. LAC, STRESS MEMO MANUAL
4. LMSC, PREFERRED PARTS HANDBOOK
5. MEMO FROM D. J. TILJIAN, NASA MSC, TO R. D. BUTTRAM, LMSC, "POINT DESIGN REQUIREMENTS FOR Z ORBITER DESIGN AREAS-REUSABLE SURFACE INSULATION TPS DEVELOPMENT, PHASE 2ND, DATED 7-21-71.

Appendix D

**DYNAMIC ANALYSIS
OF PROTOTYPE PANEL
SUBSTRATES**

D1

NASA CONTRACT

ENGINEERING MEMORANDUM

TITLE: DYNAMIC ANALYSIS OF TPS PANELS	EM NO. SSD/451
PREPARED BY: A. D. Houston / F. R. Mason	REF:
CHECKED BY: R. Buttram	DATE: 25 Oct. 1971
	APPROVAL:

- Refs: (1) U. S. Government Two-Way Memo, dated 7/21/71, "Point Design Requirements for 2 Orbiter TPS Design Areas - Reuseable Surface Insulation TPS Development, Phase 2."
- (2) NASA TN-D-451, "Flutter Research on Skin Panels," Kordoos, Tuovilla, and Guy, Sept. 1960.
- (3) LMSC/A814091, SS-1106-5522, "Sonic Fatigue Analysis C-5A Program," D. M. Wong, 28 April 1966.
- (4) Mc Donnell-Douglas Tech Report AFFDL-TR-67-38, "Design Fabrication, and Test of Aerospace Planes Beryllium Wing Box," March 1967.
- (5) Lockheed-California Company, SIM #17, "Structural Life Assurance Manual.

PURPOSE:

To verify by analysis that the four panel designs submitted satisfy the dynamic requirements for sonic fatigue strength and flutter resistance described in Reference (1).

DISCUSSION:

(1) - Panel Flutter Analysis

Two panel flutter modes were examined: complete panel flutter and inter stringer flutter. The experimental data contained in the Reference (2) document was used to demonstrate that the panel flutter requirements of Reference (1) were met.

(a) Complete Panel

The effective stiffness for a stiffened panel is given by:

$$K_{EFF} = \left[12(1-\nu^2) \frac{D_c}{E} \right]^{\frac{1}{3}} \quad (1)$$

380<

Prepared by: A. D. Houston	Date	LOCKHEED MISSILES & SPACE COMPANY A GROUP DIVISION OF LOCKHEED AIRCRAFT CORPORATION	Page	Temp.	Perm.
Checked by: F. R. Mason	Date		2		
Approved by:	Date		Title DYNAMIC ANALYSIS OF TPS PANELS	Model SSD/451	Report No.

DISCUSSION: (continued)

For all of the four panels examined, the length/width ($\frac{l}{w}$) ratio is approximately 1.0. Hence from Figure 2 of Reference (3), we have:

$$\left(\sqrt{M^2-1} \cdot \frac{E}{q}\right)^{\frac{1}{3}} \frac{t_{EFF}}{l} > 0.5 \quad (2)$$

Substituting from (1)

$$\left[\sqrt{M^2-1} \cdot \frac{E}{q} \cdot 12(1-\nu^2) \frac{D_x}{E}\right]^{\frac{1}{3}} \frac{1}{l} > 0.5$$

$$q < \frac{96 \sqrt{M^2-1} (1-\nu^2) I_x E}{l^3}$$

The panel with the lowest value of bending stiffness (I_x) is Panel #1, with a value of 0.01 in.³ Taking Poisson's ratio ν as 0.3, $E = 42 \times 10^6$ lb/in² and length (l) = 24 inches, $q < 380,000 \sqrt{M^2-1}$

Clearly, the panels are flutter free in the complete panel bending mode.

(b) Inter Stiffener Panel Flutter

Panel #1 is the most critical of the four panels in this mode, with a l/w ratio of $(22.5/3.3) = 6.8$. Referring to Figure 2, Reference (2), the following flutter stability criterion applies:

$$\left(\sqrt{M^2-1} \frac{E}{q}\right)^{\frac{1}{3}} \frac{t}{l} > 0.15$$

$$\therefore q < \frac{\sqrt{M^2-1} \cdot E \cdot t^3}{(0.15)^3 l^3}$$

The panel with the minimum Et^3 is panel #4, with a value of 920 lb in. Therefore $q < 3440 \sqrt{M^2-1}$ for no flutter. The flutter stability curve for this

Prepared by: A. D. Houston	Date 10-25-71	LOCKHEED MISSILES & SPACE COMPANY A GROUP DIVISION OF LOCKHEED AIRCRAFT CORPORATION	Page D3	Temp.	Perm.
Checked by:	Date	Title	Model SSD/451		
Approved by:	Date	DYNAMIC ANALYSIS OF TPS PANELS	Report No.		

DISCUSSION: (continued)

mode is plotted in Figure 1, demonstrating that a flutter margin in excess of 1.5 times the maximum dynamic pressure exists at any Mach number along the design trajectories.

(2) - Panel Sonic Fatigue Analysis

The method described in the Reference (3) document was used to evaluate the sonic fatigue characteristics of the four panels. This simplified analysis method developed in Reference (3), provides root mean square stress generated in a panel by acoustic excitation at its fundamental natural vibration mode given by:

$$\sigma = \sigma_0 \sqrt{\frac{\pi}{4\delta}} \sqrt{f_n S_i(f)}$$

where:

- σ = rms stress (psi)
- σ_0 = unit psi stress (psi/psi)
- δ = damping ratio
- f_n = panel primary natural frequency (Hz)
- $S_i(f)$ = pressure power spectral density (p^2/Hz)

From Reference (3),

$$\sqrt{f_n S_i(f)} = 1/3 \text{ octave decibel level} + 6.38 \text{ decibels}$$

From Reference (1), maximum 1/3 octave level is 150 decibels, therefore

$$\begin{aligned} \sqrt{f_n S_i(f)} &= 150 + 6.38 = 156.38 \text{ decibels} \\ &= 0.19 \text{ psi} \end{aligned}$$

From stress analysis of the panels, the following unit pressure stresses are as shown in Table I, together with computed values of RMS stress assuming $\delta = 0.02$.

Prepared by: A. D. Houston	Date: 10-25-71	LOCKHEED MISSILES & SPACE COMPANY A GROUP DIVISION OF LOCKHEED AIRCRAFT CORPORATION	Page D 4	Temp.	Perm.
Checked By: F. R. Mason	Date:	Title DYNAMIC ANALYSIS OF TPS PANELS	Model SSD/451		
Approved by:	Date:		Report No.		

TABLE I - RMS STRESSES GENERATED IN PANELS

Panel #	Unit Pressure Stress (psi/psi) σ_o		RMS Stress (Psi)	
	Stringer	Skin	Stringer	Skin
#1 Beryllium	8800	3460	10,400	4120
#2 7075-T6	2360	1000	2,800	1190
#3 7075-T6	1440	630	1,700	750
#4 Titanium (6Al 4V)	3150	1330	3,750	1580

Discrete frequency S-N curve fatigue data for 7075-T6 (Aluminum) and 6Al 4V Titanium Alloys were obtained from the Reference (5) document and data for Beryllium sheet from the Reference (4) document. A modified Miner cumulative fatigue damage rule is used and the number of cycles to failure N_R is given by:

$$N_R = \frac{1}{\int_0^{\infty} \frac{p(x) dx}{N_i x^2}}$$

where: $p(x) = x e^{-\frac{x^2}{2}}$ is the Rayleigh probability distribution of stress peaks, and x = ratio of peak stress to root mean square stress.

For various values of rms stress, the values of N_R were obtained and random S-N curves constructed from the discrete frequency S-N curves. These are shown in Figures 2, 3 and 4. Estimates of the number of cycles of exposure have been based upon the Reference (1) data, which provided an environment history for a particular mission. For one mission the environment was between the maximum value and 20 decibels below the maximum value for a period of 35 seconds. Assuming 100 missions, a safe life margin of 4 times service life, and an average panel natural frequency of 200 Hz, the design life cycles

Prepared by: A. D. Houston	Date 10-25-71	LOCKHEED MISSILES & SPACE COMPANY A GROUP DIVISION OF LOCKHEED AIRCRAFT CORPORATION	Page 5	Temp.	Perm.
Checked by: F. R. Mason	Date	Title DYNAMIC ANALYSIS OF TPS PANELS	Model SSD/451		
Approved by:	Date		Report No.		

DISCUSSION: (contained)

(N_D) are:

$$N_D = 4 \times 35 \times 200 \times 100 = 2.8 \times 10^6 \text{ cycles}$$

CONCLUSIONS:

Figure 5 shows induced RMS stress plotted for each panel and each are less than allowable random S-N curve allowables.

Therefore, it is concluded that all four panels have adequate fatigue strength to withstand the Reference (1) design environments.

SQUARE 10 X 10 TO THE CENTIMETER 42-8016-01

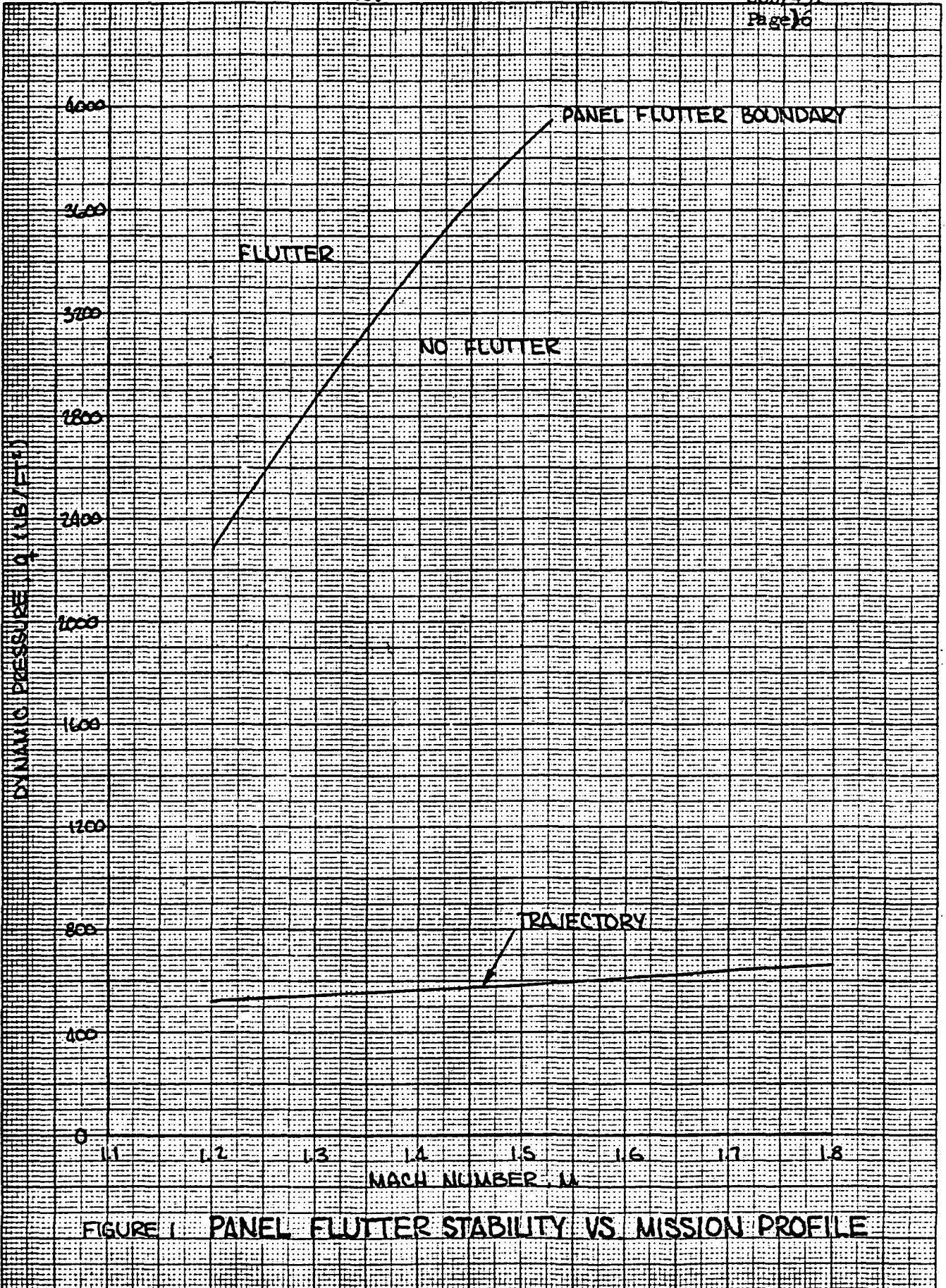
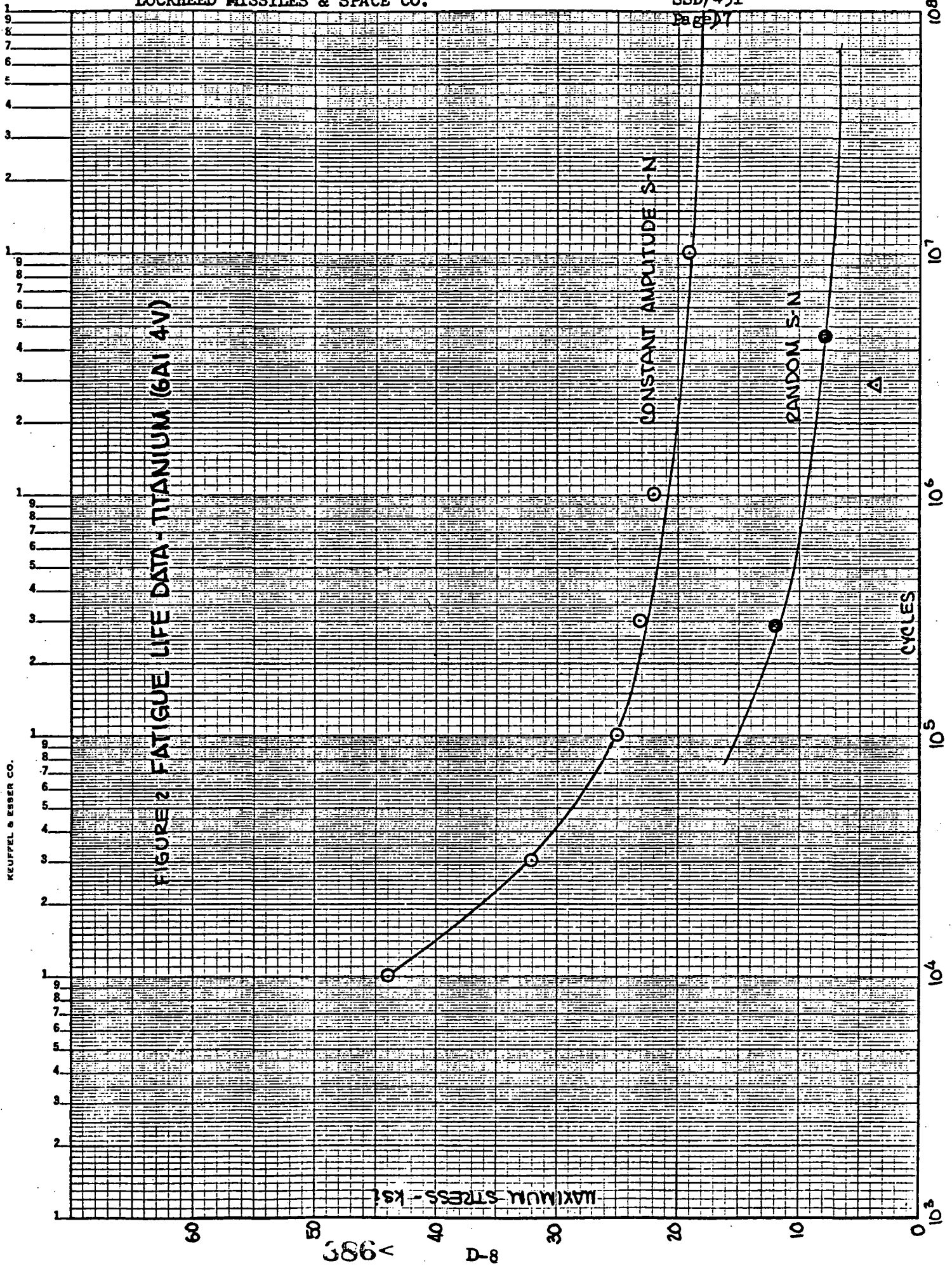


FIGURE 1 PANEL FLUTTER STABILITY VS MISSION PROFILE

GRAPHIC PAPERS GRAPHIC CONTROLS CORPORATION Buffalo, New York Printed in U.S.A.

FIGURE 2 FATIGUE LIFE DATA - TITANIUM (6Al 4V)

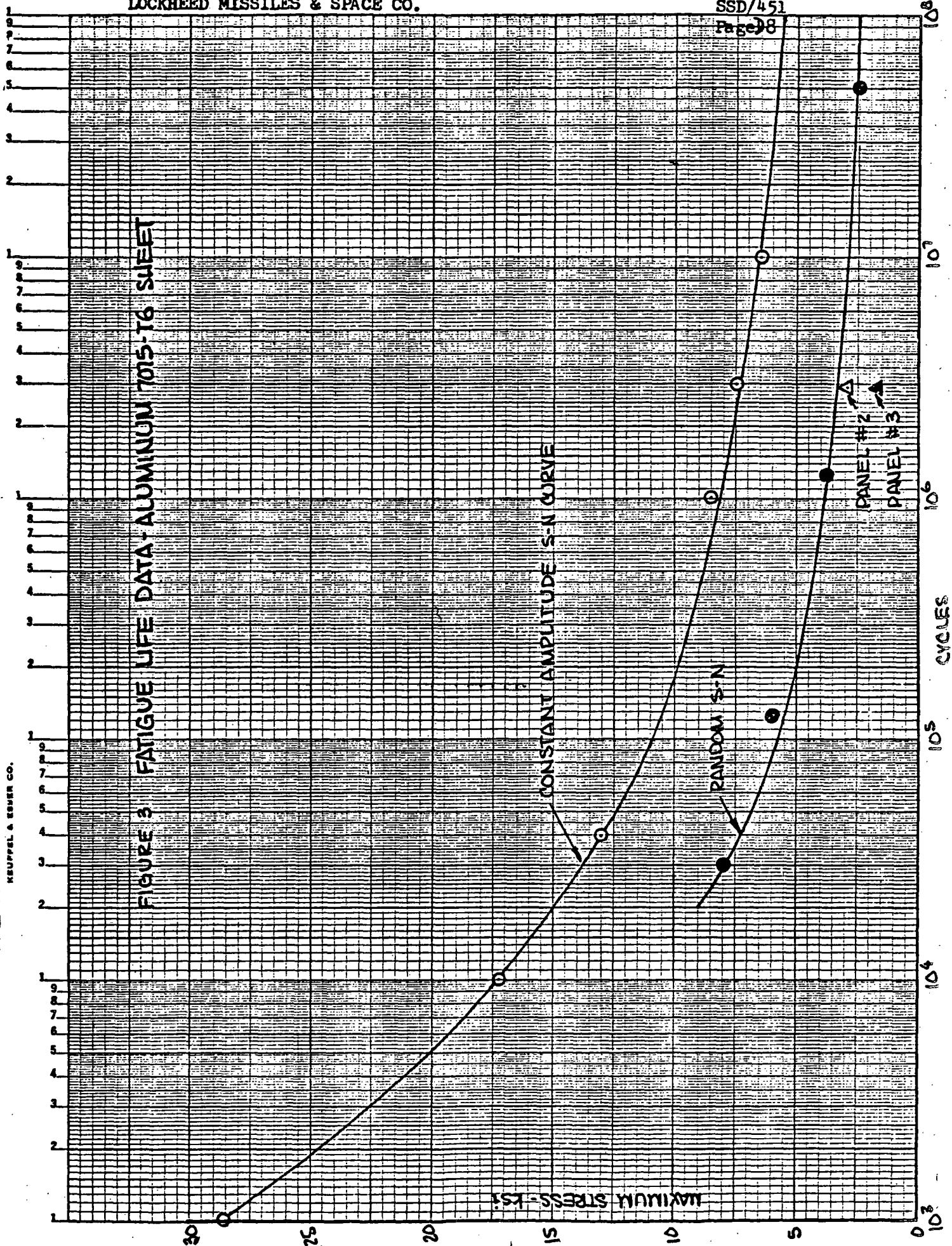


K&E SEMI-LOGARITHMIC 46 6212
5 CYCLES X 70 DIVISIONS MADE IN U.S.A.
KEUFFEL & ESSER CO.

386 < D-8

K&E SEMI-LOGARITHMIC 46 6214
5 CYCLES X 70 DIVISIONS MADE IN U.S.A.
KEUPPEL & EBER CO.

FIGURE 3 FATIGUE LIFE DATA - ALUMINUM 7015-T6 SHEET



K&E SEMI-LOGARITHMIC 46 6212
5 CYCLES X 70 DIVISIONS MADE IN U.S.A.
KEUFFEL & ESSER CO.

FIGURE 4 FATIGUE LIFE DATA - BERYLLIUM SHEET

CONSTANT AMPLITUDE S-N CURVE

RANDOM S-N

PANEL #1

MAXIMUM STRESS - KSI

CYCLES

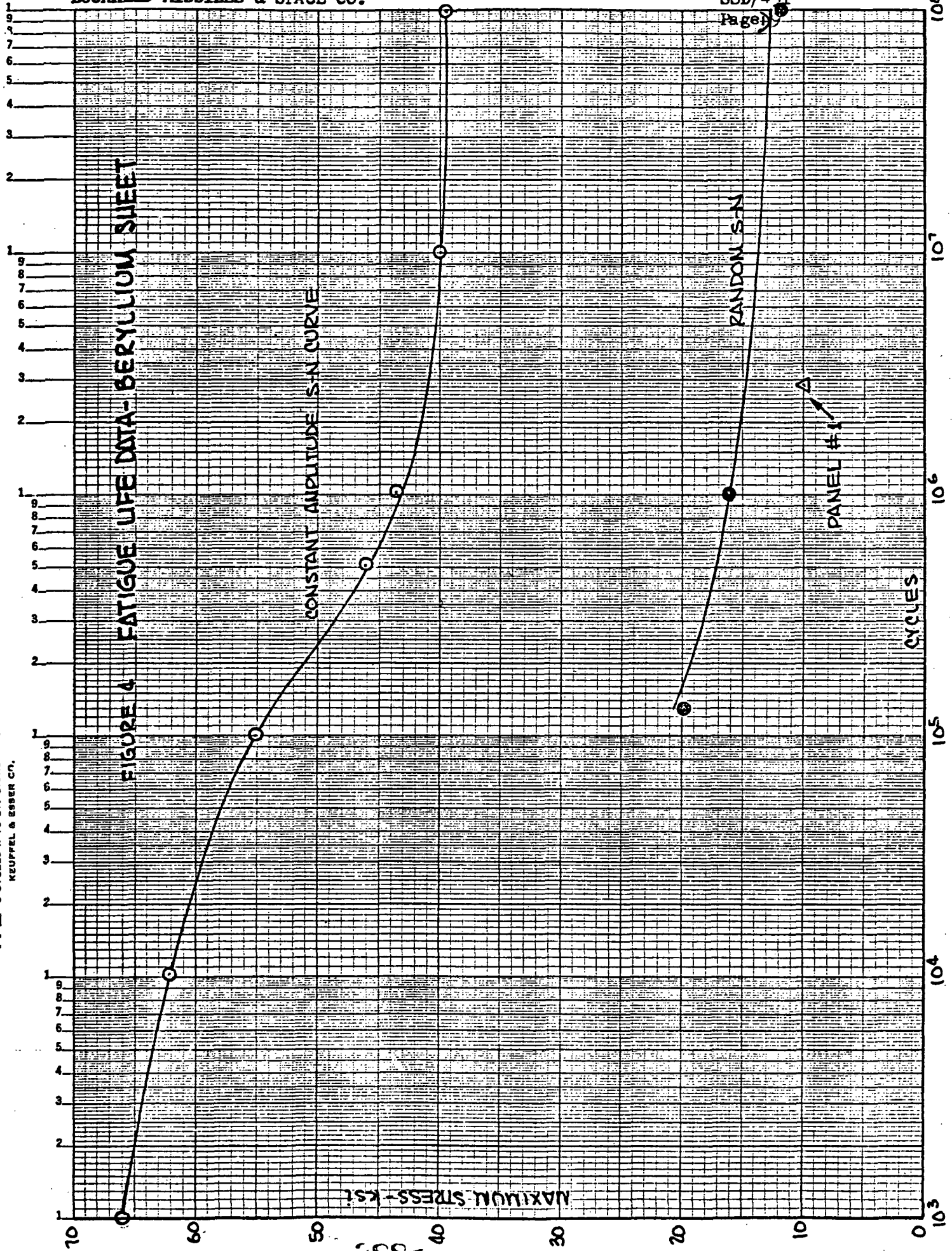
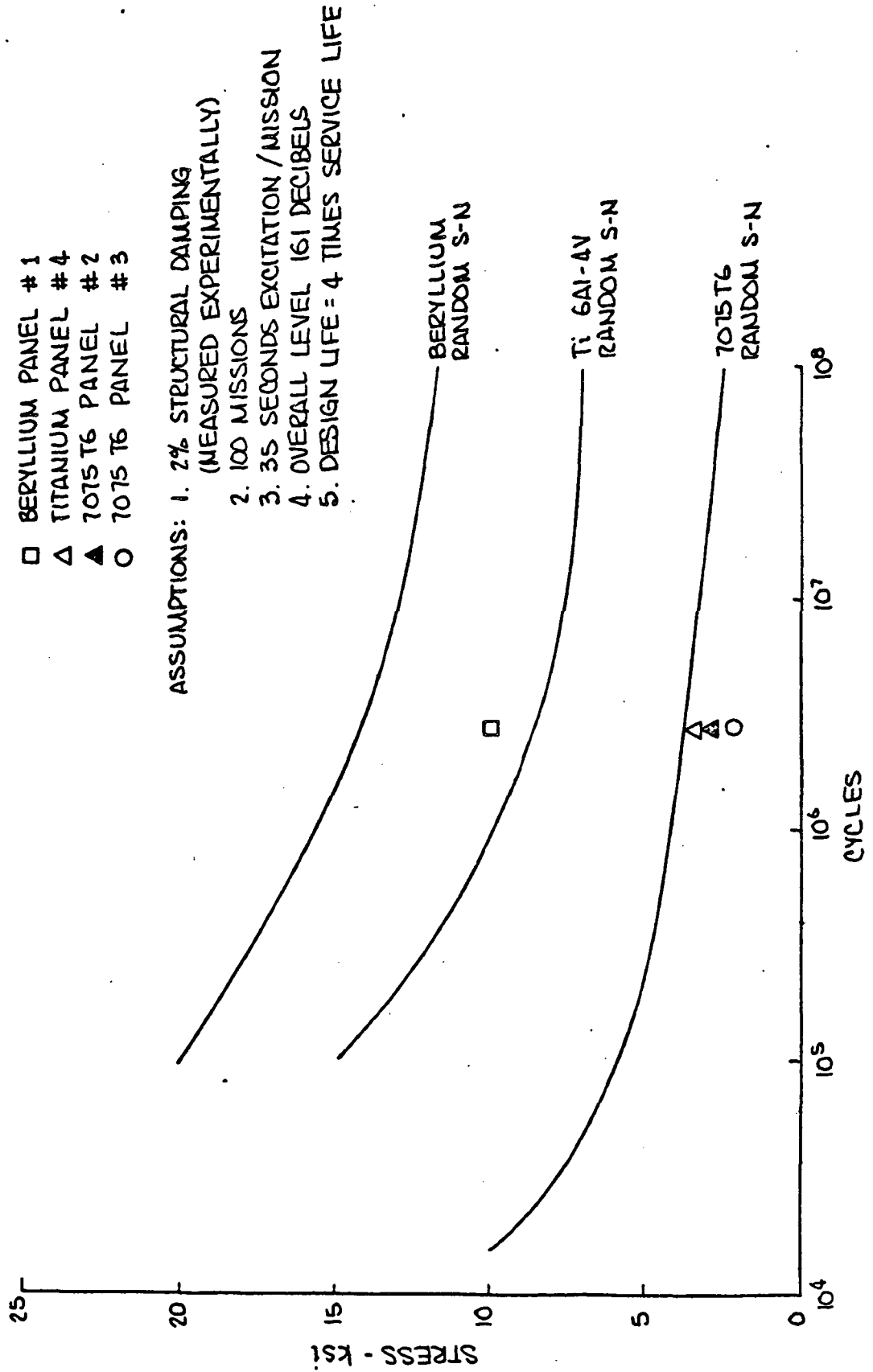


FIGURE 5 RANDOM S-N CURVES VS ACOUSTICALLY INDUCED RMS STRESSES IN PANELS



Appendix E

**VENTING CHARACTERISTICS OF
LI-1500 TILES WITH
STRAIN ISOLATION**

ENGINEERING MEMORANDUM

TITLE: VENTING CHARACTERISTICS OF LI-1500 TILES WITH STRAIN ISOLATION	EM NO: REF: DATE: 15 October 1971
AUTHORS: R. Diggins	APPROVAL: ENGINEERING SYSTEM ENGRG

REFERENCES

1. Drawing No. SKJ-205007, "TPS Mechanical Attachment for LI-1500 Tiles With Strain Insulation," 27 September 1971.
2. U.S. Government Two-Way Memo, "Point Design Requirements for Two Orbiter TPS Design Areas - Reusable Surface Insulation TPS Development, Phase 2," Tillian to LMSC, 21 July 1971.

PURPOSE:

To investigate the venting characteristics of the thermal protection system (TPS) configuration shown on Reference 1. Specifically, as requested, the analysis was performed to determine maximum differential pressures across the TPS tiles, under the assumption that each panel assembly (approximately 10 in. by 30 in.) is hermetically sealed from adjacent panels.

TECHNICAL DISCUSSION:

It has been established that the maximum differential pressures on vented compartments occur during the transonic phase of ascent, rather than during reentry. An ascent venting analysis has been performed, using the digital computer program "VENTRX". In this program, a venting model is set up to describe the volume(s) of air to be vented, orifice areas (external and/or between compartments), and external pressure fields for all external orifices. Sharp-edged, circular orifice flow coefficients are used, as modified to account for the effects of an external velocity field.

The calculated volume of air under each panel assembly is 0.52 cu ft, and the external vent area (in square inches) is 37 times the average gap width (in inches) between TPS tiles. External pressures have been taken from the Area 2 data of Reference 2, and these pressure histories (in envelope form) are shown in Fig. 1. For this analysis, it has been assumed that these pressures (identified as differential pressures in Reference 2), represent the difference between the external surface pressure (p_0) and local ambient pressure (p_∞). Ascent venting simulations were run for both the positive and negative pressures shown in Fig. 1, using average gap widths of 0.005 and 0.0025 in. The maximum resultant differential pressures are 0.1 and 0.25 psi, respectively. However, with this venting configuration (individual panels sealed off), since the internal air pressure very nearly follows the external surface pressure, the primary load-carrying structure in "Area 2" must withstand differential pressures similar to (within 1.0 psi) those shown in Fig. 1. Also, the supporting rib structure between adjacent panels must be capable of withstanding up to 8 psi differential in certain locations.

EM NO:
DATE: 15 October 1971

Because high differential pressures are produced by rapid external pressure changes, which are not defined by the pressure envelopes of Fig. 1, an analysis was performed to determine the effects of such changes on maximum differential pressures. In interference regions such as "Area 2," where local surface pressures are affected by the presence of an adjacent body (tank or booster), theoretical techniques during transonic flow are inadequate, and wind-tunnel data are not available to define the maximum rates of change of surface pressures. Therefore, these rates have been analyzed parametrically, using rates of 2 and 4 psi/sec. With each rate, total pressure changes of 4 and 8 psi have been considered. The resulting pressure history for the most severe case (4 psi/sec for 2 sec) is shown in Fig. 2.

The relationship between external, internal, and ambient absolute pressures is shown in Fig. 3, for a gap width of 0.005 in. It is seen that the differential pressure across the thermal-protection surface continues to increase as the external pressure decreases; this is typical for each of the cases examined.

A summary of the maximum differential pressures across the TPS panels is presented in Fig. 4 as a function of gap width, rate of change of external pressure and length of time over which rates are applied. In order to arrive at a maximum differential pressure suitable for design purposes (in lieu of test data), some judgement must be applied. It is considered that 2 psi/sec is a conservative value for change rate; this is approximately twice that used in venting analyses on several SSD programs. Applying this rate for 4 sec reduces the external pressure to less than 1 psi absolute. Thus, the curve noted on Fig. 4 is recommended for use in design analyses. It is emphasized that these pressures apply only for the condition in which it is assumed that each panel assembly is completely sealed from adjacent panels. Should this not be the case, it may be assumed that, for relatively unrestricted flow between panels, the internal pressure (air between TPS and primary structure) will be local ambient ± 1 psi. In that event, the maximum TPS differential pressures (depending on location) will be as given in Fig. 1, plus or minus 1 psi.

CONCLUSIONS:

Design differential pressures on the TPS panels are relatively low (less than 1 psi for an average gap between tiles greater than 0.005 in.) if the entire surface is constructed such that each panel assembly (approximately 10 in. by 30 in.) is hermetically sealed from adjacent panels. This scheme, however, imposes high differential pressures on primary structure (as much as 5 psi) and on support ribs between panels (as much as 8 psi). In addition, high costs would be incurred in manufacture and testing.

Alternatively, if air flow is allowed between panels, differential pressures on primary structure and TPS support ribs would be reduced to less than 1 psi, while differentials across the TPS surface would be increased to as much as 5 psi in certain areas, possibly requiring structural reinforcement in the form of bonded screen or solid subpanels.

Reproduced from
best available copy.

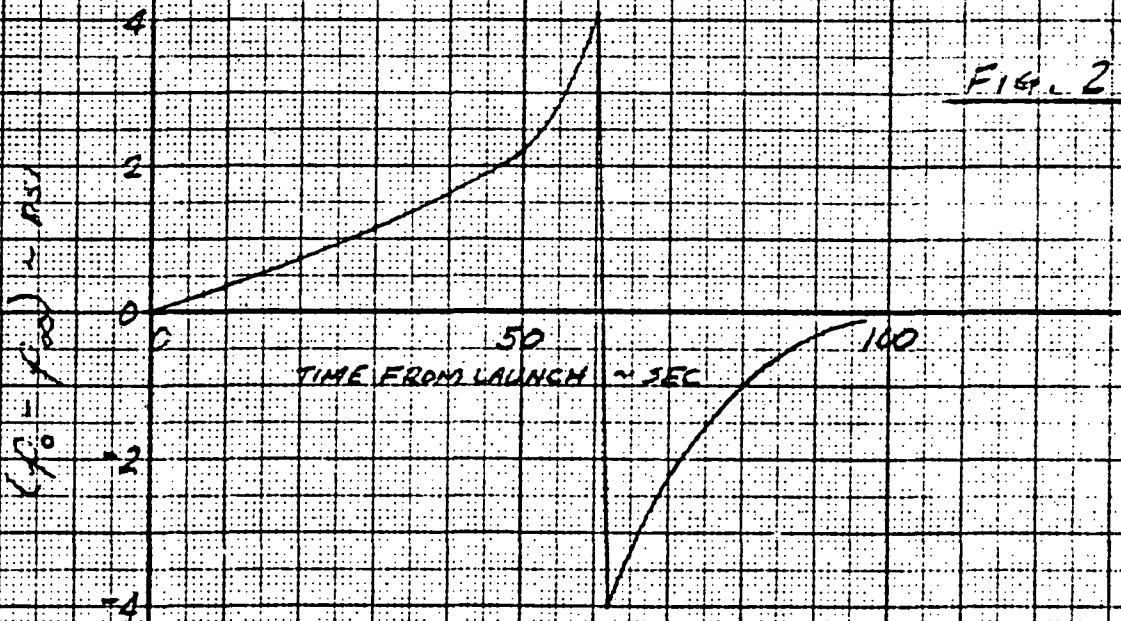
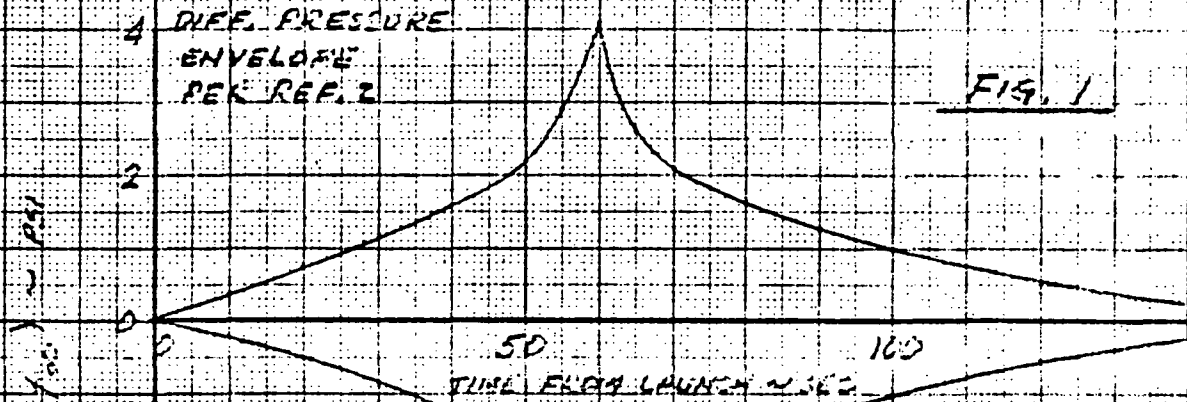


EM NO.

DATE 15 October 1971

PAGE OF

PREPARED BY *R. Diggins*



EM NO.

DATE 15 October 1971

PAGE OF

PREPARED BY *L. DiGiorgio*

TYPICAL PRESSURE HISTORIES

$GAP = .005 IN.$

$\dot{P}_0 = 4 PSI/SEC$

$t = 2 SEC$

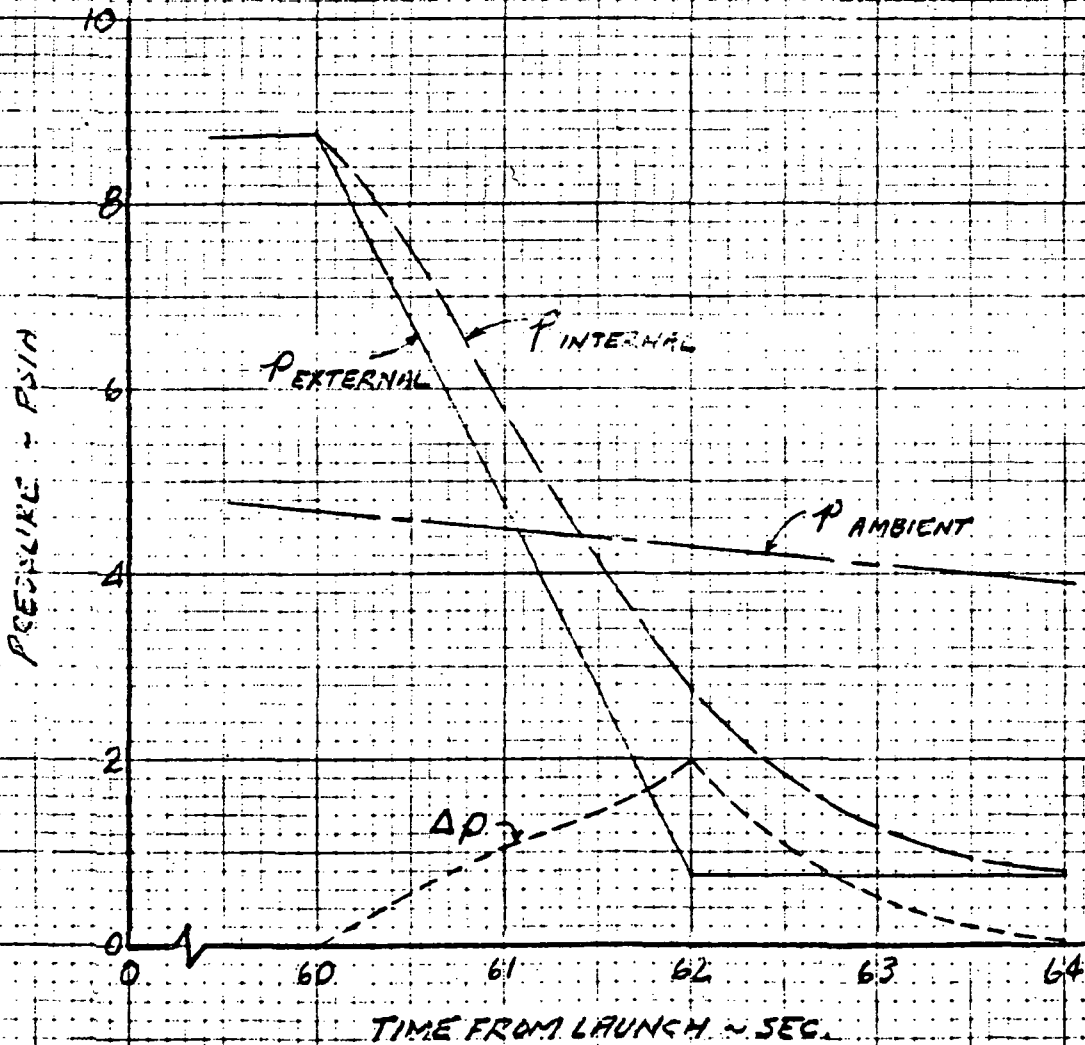


FIG. 3

EM NO:
 DATE: 15 October 1971

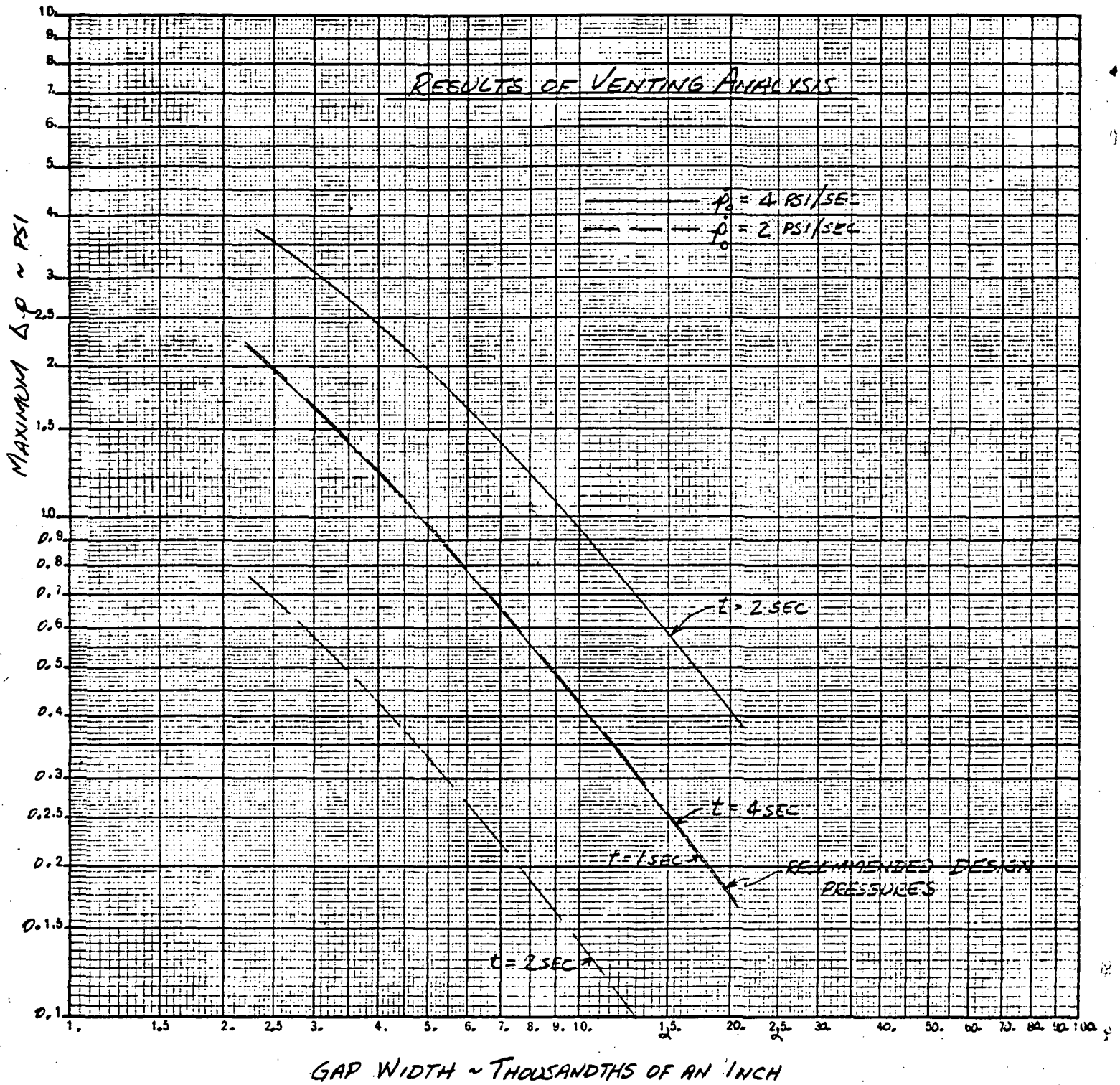


Fig. 4 Results of Venting Analysis